

DOT/FAA/DS-89/19

Advanced System Design Service  
Washington, D.C. 20591

**Windshear Case Study:  
Denver, Colorado,  
July 11, 1988**

**AD-A220 512**

Herbert W. Schlickemaier

Flightcrew Systems Research Branch  
Federal Aviation Administration  
Washington, D.C. 20591

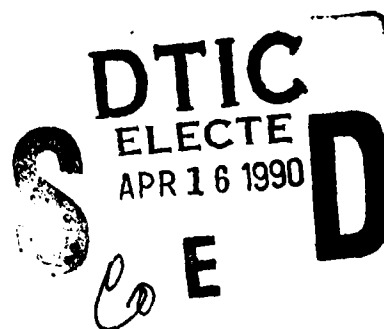
November 1989

Final Report

This document is available to the public  
through the National Technical Information  
Service, Springfield, Virginia 22161.



U.S. Department of Transportation  
Federal Aviation Administration



90 04 13 159

1. Report No. DOT/FAA/DS-89/19		2. Government Accession No.		3. Recipient's Catalog No.	
4. Title and Subtitle Windshear Case Study: Denver, Colorado, July 11, 1988				5. Report Date November 1989	
				6. Performing Organization Code FAA/ADS-210	
				8. Performing Organization Report No.	
7. Author's Herbert W. Schlickemaier				10. Work Unit No. (TRAIS)	
9. Performing Organization Name and Address Flightcrew Systems Research Branch, ADS-210 Federal Aviation Administration 800 Independence Avenue, S.W. Washington, D.C. 20591				11. Contract or Grant No.	
				13. Type of Report and Period Covered Final Report	
				14. Sponsoring Agency Code	
12. Sponsoring Agency Name and Address					
15. Supplementary Note This document contains reprints of five reports: 1. "Microburst Encounter, July 11, 1988, Denver, Colorado," United Airlines Flight Safety Investigation 88-46, February 9, 1989; 2. Proctor, F.H., Bowles, R.L., "Investigation of the Denver 11 July 1988 Microburst Storm with the Three-Dimensional NASA-Langley Windshear Model," (Draft to be Submitted as a NASA Report) July 26, 1989; 3. Coppenbarger, R.A., Wingrove, R.C., "Analysis of Records From Four Airliners in the Denver Microburst, July 11, 1988," AIAA Paper 89-3354, August 14-16, 1989; 4. Campbell, S., Correspondence to Roland Bowles, dated 24 March 1989, containing velocity and shear values from FLOWS for July 11, 1988, at Denver Stapleton Airport, and Isaminger, M. A., "WEEKLY SITE SUMMARY," FL2 Radar Site, Denver, Colorado, both of MIT Lincoln Laboratory; 5. Elmore, K.L., Politovich, M.K., Sand, W.R., "The 11 July 1988 Microburst at Stapleton International Airport, Denver, Colorado," National Center for Atmospheric Research, November 1989. These reprints are included with the explicit permission of the authors to be used as substantiating data for this case study.					
16. Abstract On Monday, July 11, 1988, between 2207 and 2213 UTC (16:07-16:13 MDT), four successive United flights had inadvertent encounters with microburst windshear conditions while on final approach to Denver Stapleton Airport (DEN), each resulting in a missed approach, subsequent delay, and uneventful arrival. A fifth flight executed a missed approach without encountering the phenomena. All of the flight crews were trained utilizing the resources of the Windshear Training Aid. There was no damage to aircraft and no passenger injuries.  At the time the aircraft encountered the microburst, the Terminal Doppler Weather Radar (TDWR) Operations Test and Experiment (OT&E) was in progress and detected divergent flow that intersected the operating zones for the approach runways. The radar used to test the TDWR algorithm was the Massachusetts Institute of Technology Lincoln Laboratory 10 cm Doppler radar. MIT  This Windshear Case Study outlines the technical details of the encounter, as well as describes insights gained from this confrontation that should be applied to future investigations of aircraft encountering windshear. This study summarizes information from several sources including flight crew comments, air traffic control (ATC) operations and surveillance radar data, flight data recorders, data from the TDWR and the Low-Level Wind Shear Alert System (LLWAS), technical details of the event meteorology, and data from the Terminal Area Simulation System (TASS). A. ...					
17. Key Words aircraft safety; air traffic operations; windshear; microburst; flight data recorder; atmospheric modeling; windshear sensors; TDWR; LLWAS			18. Distribution Statement This document is available to the public through the National Technical Information Service, Springfield, Virginia 22161.		
19. Security Classif. (of this report) Unclassified		20. Security Classif. (of this page) Unclassified		21. No. of Pages 552	22. Price

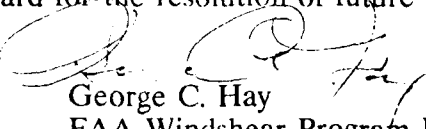
# Prologue

During the first ten days following the July 11, 1988, windshear encounter at Denver, Colorado, I was asked by the Federal Aviation Administration, the National Transportation Safety Board, other government agencies, and representatives of the industry to bring together the necessary resources to examine and document that occurrence. The distribution of this report completes that action.

The objective of this report is to record and evaluate all available data that related to the performance of ground-based windshear detection systems, the flight crews and the aircraft to provide a more thorough understanding of the windshear phenomena.

The opportunity presented by this occurrence allowed a complete review of all of our past and present research efforts regarding the Windshear Training Aid, hazard characterization, airborne warning systems, and the performance of the Terminal Doppler Weather Radar and Low-Level Wind Shear Alert System ground systems by a multi-agency/industry working group.

All parties to this review have provided complete and unrestricted openness and cooperation throughout this writing. The level of cooperation demonstrated could well set a standard for the resolution of future complex issues.

  
George C. Hay  
FAA Windshear Program Manager

Accession For	
NTIS GRA&I	<input checked="" type="checkbox"/>
DTIC TAB	<input type="checkbox"/>
Unannounced	<input type="checkbox"/>
Justification	
By	
Distribution/	
Availability Code	
Dist	Avail and/or Special
A-1	



# Foreword

The events reported in this case study indicate that on July 11, 1988, a severe microburst occurred in Denver, Colorado. Mitigating the trivia of *just another interesting meteorological event* are three facts. One, the microburst was unusual compared to other microbursts that have been studied. Secondly, five airliners' operations were affected by the event, and its detection. Finally, air traffic services at Stapleton International Airport were using an experimental radar that was provisionally commissioned for an operational test just 10 days earlier.

To the credit of the air traffic controllers and the flight crews of the airliners, there was no loss of life, nor damage to property. However, the professionals involved also recognized the potentially lethal event that occurred and the need to document what transpired *and* to document all aspects of it to the future as *lessons learned*. While no one made a mistake -- *it would be a mistake not to learn from the encounter*.

The specialists have compiled invaluable bodies of knowledge based on the windshear that occurred on July 11. Of particular note, the following individuals should be lauded for their participation in developing this case study: Roland Bowles of the National Aeronautics and Space Administration Langley Research Center; Steve Campbell and Mark Isaminger of MIT Lincoln Lab; Bob Ireland of United Airlines Flight Training Center; Bud Laynor of the National Transportation Safety Board, Bureau of Technology; Kim Elmore, Marcia Politovich and Wayne Sand, of the Research Applications Program at National Center for Atmospheric Research; Fred Proctor of MESO, Inc.; and Rod Wingrove and R.A. Coppenbarger of NASA Ames Research Center.

This case study is the focus for their work.



# CONTENTS

	page
1 SYNOPSIS .....	1
2 BACKGROUND .....	3
2.1 Windshear-Related Activities Since 1985 .....	4
2.2 Preparation of this Case Study .....	5
3 FACTUAL MATERIAL .....	9
3.1 General Sequence of Events .....	10
3.2 Radio Communications .....	11
3.3 Aircraft Flight Data Recorders .....	11
3.4 Meteorological Information .....	12
3.5 Ground-Based Sensors .....	13
3.6 Air Traffic Control Observations .....	15
3.7 Flight Crew Observations .....	16
4 ANALYSIS .....	19
4.1 General .....	20
4.2 Meteorological Information .....	21
4.3 Hazard Analysis .....	21
4.4 ARTS III Radar .....	23
4.5 Flight Crew Analysis .....	23
4.6 Aircraft Wind Profile Reconstruction .....	24
4.7 Doppler Radar .....	24
4.8 FLOWS/LLWAS Mesonet .....	25
4.9 Atmospheric Model Analysis .....	25
5 CONCLUSIONS .....	27
5.1 Flight Operations .....	28
5.2 Air Traffic Operations .....	29
5.3 Ground Sensors .....	29
5.4 Flight Data Recorder .....	30
5.5 Terminal Area Simulation System .....	30
6 RECOMMENDATIONS .....	31
6.1 Interaction of Aircraft, Air Traffic, and Ground-Based Sensors .....	32
6.2 The Case Study Process .....	33
7 REFERENCES .....	35
8 SUBSTANTIATING DATA -- Appendices .....	39
APPENDIX 1 -- United Report	
APPENDIX 2 -- NASA Langley Report	
APPENDIX 3 -- NASA Ames Report	
APPENDIX 4 -- MIT Lincoln Lab Report	
APPENDIX 5 -- NCAR Report	

# CONTENTS

page

## Figures

Figure 1 -- Relative locations of the Ground Stations during the TDWR OT&E . . . . .	13
Figure 2 -- Four estimates of maximum F-Factor based on sensed data from the aircraft flight data recorders, TDWR estimate (at 100 m elevation), the TASS model (at 280 m elevation), and the dual-Doppler radar analysis (at 690 m elevation) . . . . .	22

## Table

Table I Compiled Sequence of Events . . . . .	20
---	----

# 1 SYNOPSIS

On Monday, July 11, 1988, between 2207 and 2213 UTC (16:07-16:13 MDT), four successive United flights had inadvertent encounters with microburst windshear conditions while on final approach to Denver Stapleton Airport (DEN), each resulting in a missed approach, subsequent delay, and uneventful arrival. A fifth flight executed a missed approach without encountering the phenomena. All of the flight crews were trained utilizing the resources of the Windshear Training Aid. There was no damage to aircraft and no passenger injuries.

At the time the aircraft encountered the microburst, the Terminal Doppler Weather Radar (TDWR) Operations Test and Experiment (OT&E) was in progress and detected divergent flow that intersected the operating zones for the approach runways. The radar used to test the TDWR algorithm was the Massachusetts Institute of Technology Lincoln Laboratory 10 cm Doppler radar.

This Windshear Case Study outlines the technical details of the encounter, as well as describes insights gained from this confrontation that should be applied to future investigations of aircraft encountering windshear. This study summarizes information from several sources including flight crew comments, air traffic control (ATC) operations and surveillance radar data, flight data recorders, data from the TDWR and the Low-Level Wind Shear Alert System (LLWAS), technical details of the event meteorology, and data from the Terminal Area Simulation System (TASS).

## **2 BACKGROUND**

## BACKGROUND

## 2.1 Windshear-Related Activities Since 1985

On August 2, 1985, Delta Airlines flight 191 crashed while on approach to Dallas-Fort Worth Airport<sup>1</sup>.

On February 26, 1987, the Federal Aviation Administration accepted delivery of a Windshear Training Aid<sup>2</sup>. The Windshear Training Aid describes to flight crews the real threat that windshear can pose. It counsels avoidance of hazardous windshear as the safest avenue for flight crews to follow. The Windshear Training Aid also described precautions for crews to use to improve their chances of escape. For inadvertent encounters, the crews were provided with a Windshear Recovery and Escape Maneuver to maximize their chances of surviving the encounter.

In June 1987, the Federal Aviation Administration published an "Integrated FAA Windshear Program Plan,"<sup>3</sup> that described how the FAA planned to address the threat posed by windshear. The plan addressed five areas: Training and Operating Procedures, Ground Sensors, Airborne Windshear Detection and Avoidance, Terminal Information Systems, and Hazard Characterization. The plan delineated an approach to provide incremental improvements to flight safety. Some areas, like the Windshear Training Aid, could be implemented immediately to all flight crews.

The Ground Sensors program and Airborne Windshear Detection and Avoidance programs required thorough analysis, design and system integration. Some time would have to pass before these aids would be available for the flight crews.

Flight crews would still have to make decisions on how to avoid windshear. As airborne and ground-based systems become fully functional, flight crews must continue to make their own decisions for windshear avoidance. In the meantime, some important questions must be addressed: What is the efficacy of the incremental improvements to the safety of the National Airspace System? How often are crews being exposed to this phenomenon?

Since June 1987, several aircraft have had encounters with low-altitude windshear. The most significant encounter involved an aircraft on approach to Atlanta Hartsfield airport. The aircraft was equipped with airborne windshear alerting equipment, and was being flown by a crew that was trained for the avoidance and recovery procedures contained in the Windshear Training Aid<sup>4</sup>. A report to an SAE meeting described the experience of a number of aircraft that were equipped with certified airborne windshear alerting systems<sup>5</sup>. Some of the aircraft encountered windshear. In all cases, available information concerning these encounters was shared within the

---

<sup>1</sup> "Delta Air Lines, Inc., Lockheed L-1011-385-1, N726DA Dallas/Fort Worth - International Airport, Texas August 2, 1985," Aircraft Accident Report, NTSB/AAR-86/05, National Transportation Safety Board, Washington, DC, August 15, 1986.

<sup>2</sup> "Windshear Training Aid," Federal Aviation Administration, February 1987.

<sup>3</sup> "Integrated FAA Windshear Program Plan," DOT/FAA/DL-VS-AT-88/1, Federal Aviation Administration, June 1987.

<sup>4</sup> Described by Mark E. Kirchner before the Subcommittee on Oversight and Investigations Committee on Public Works and Transportation, United States House of Representatives regarding Windshear, June 30, 1987.

<sup>5</sup> Terry Zweifel, "Flight Experience with Windshear Detection," SAE Aerospace Control and Guidance Systems Committee, Monterey, CA, March 9-11, 1988.

aviation community. To the credit of the industry, improvements were being planned based on these experiences.

## 2.2 Preparation of this Case Study

On July 11, 1988, four United Airlines aircraft experienced inadvertent encounters with microburst-related windshears while approaching runways 26L and 26R at Denver Stapleton International Airport. A fifth flight coordinated a maneuver with ATC to avoid the microburst. The Terminal Doppler Weather Radar Operations Test and Experiment was underway and detected divergent flow that intersected the operating zones for the two runways. The flight crews were all familiar with the Windshear Training Aid.

As a result of this event, technical specialists decided to collaborate and analyze the facts that were available (based on the unique cooperation of organizations represented by these experts). These analyses provide detailed reports of the event from different operational and technical perspectives. The intent of this case study is to integrate the various reports. Therefore, this report not only describes the events that transpired on July 11, but also puts together a reference document that describes the wealth of information that was reported by these technical authorities. This case study will also be the foundation for future investigations of windshear encounters.

A meeting took place in August 1988, to gather all of the technical specialists in one place and share the factual data as it existed. Teams were formed that specialized in atmospheric modeling, flight data recorder, meteorological observation, ground sensor data recording, and operational factors (both flight crew and air traffic).

One team was composed of elements of the FAA/NASA Airborne Windshear Detection and Avoidance program. The objective of the Airborne Windshear Detection and Avoidance program is to develop the system requirements for forward-looking windshear sensors for aircraft. The program is composed of three elements: hazard characterization, flight management, and sensor technology assessment. Of particular interest to this windshear case study is the application of results of the hazard characterization element. Two activities are applicable to this case study: quantifying the windshear hazard in terms of aircraft performance parameters; and the detailed investigation of a microburst at low-altitude.

Quantifying the windshear hazard resulted in a relationship of vertical and longitudinal windshear terms known as the "F-Factor."<sup>6</sup> Although it was developed to be applied to airborne systems, it can be applied to windshear investigations (when its effect on aircraft is of interest) to present a consistent comparison of sensed windshear data.

Investigations into the detailed low-altitude characteristics of the microburst resulted in the development of the TASS<sup>7</sup>. The atmospheric model has been applied to previous windshear microburst cases. However, this case study is unusual in that this is the first time that the products from flight data recorders, weather observations, and ground-based windshear sensors have been

---

<sup>6</sup> Bowles, R.L., "Wind Shear 'Hit'," as presented to the "Wind Shear Detection, Forward-Looking Sensor Technology Conference," February 24 - 25, 1987, Hampton, Virginia; reference NASA CP 10004, DOT/FAA/PS-87/2, October 1987.

<sup>7</sup> Proctor, F.H., "The Terminal Area Simulation System, Volume I: Theoretical Formulation," NASA CR 4046, DOT/FAA/PM-86/50, I, April 1987.

## BACKGROUND

available for comparison on a common time reference. These data provided further support for the model's extensive validation<sup>8</sup>. With the abundance of recorded data available for this case study the TASS was used to manage and focus this effort. Once focused, a consistent data analysis resulted. The case study was simulated with TASS in August 1988, and presented in October 1988. A report of the analysis was drafted in June 1989<sup>9</sup>.

A second team member was United Airlines. United Airlines voluntarily initiated a Flight Safety Incident Investigation that incorporated a thorough operational evaluation (including flight crew and air traffic issues). The results of that investigation were published in early February 1989<sup>10</sup>.

A third team focused on the plethora of ground-based data available through the TDWR OT&E. The National Center for Atmospheric Research contributed an extensive report on the meteorology and ground-based data<sup>11</sup>. The Massachusetts Institute of Technology Lincoln Laboratories contributed a report on the operation of the Terminal Doppler Weather Radar during the Operational Experiment<sup>12,13</sup>. Some comparisons with TASS were also conducted as part of these analyses.

The National Transportation Safety Board (NTSB) voluntarily applied its expertise in interpretation of ARTS III tapes and reducing the data from the flight data recorders for the aircraft that were involved in the windshear encounter. The NTSB data was supplied to all of the team members for their analyses. The NASA Ames Research Center contributed their expertise in analyzing the flight data recorders and extracting and reconstructing the wind profiles<sup>14</sup>.

After the initial meeting in August 1988, the next meeting of the technical specialists took place in February, 1989. All of the technical teams exchanged their data and analyses, after which focused data analyses ensued. By mid-May, draft reports of detailed analyses were combined for use by this case study.

By July 1989, the technical team reviewed a working draft of this case study to ensure

---

<sup>8</sup> Proctor, F.H., "The Terminal Area Simulation System, Volume II: Verification Cases," NASA CR 4047, DOT/FAA/PM-86/50, II, April 1987.

<sup>9</sup> Proctor, F.H., Bowles, R.L., "Investigation of the Denver 11 July 1988 Microburst Storm with the Three-Dimensional NASA-Langley Windshear Model," (Draft to be Submitted as a NASA Report) July 26, 1989.

<sup>10</sup> "Microburst Encounter, July 11, 1988, Denver, Colorado," United Airlines Flight Safety Investigation 88-46, February 9, 1989.

<sup>11</sup> Elmore, K.L., Politovich, M.K., Sand, W.R., "The 11 July 1988 Microburst at Stapleton International Airport, Denver, Colorado," National Center for Atmospheric Research, November 1989.

<sup>12</sup> Isaminger, M. A., "WEEKLY SITE SUMMARY," FL2 Radar Site, Denver, Colorado, MIT Lincoln Laboratory.

<sup>13</sup> Campbell, S., Correspondence to Roland Bowles, dated 24 March 1989, containing velocity and shear values from FLOWS for July 11, 1988, at Denver Stapleton Airport, MIT Lincoln Laboratory.

<sup>14</sup> Coppenbarger, R.A., Wingrove, R.C., "Analysis of Records From Four Airliners in the Denver Microburst, July 11, 1988," Proposed paper for the AIAA Atmospheric Flight Mechanics Conference, August 14-16, 1989, Boston, Massachusetts, AIAA Paper 89-3354, August 14-16, 1989.

## BACKGROUND

7

that it reflected the technical reports. A final draft was circulated to the industry at the end of that month.

The specialists have compiled invaluable bodies of knowledge based on the windshear that occurred on July 11. This case study is the focus for their work.



### **3      FACTUAL MATERIAL**

## FACTUAL MATERIAL

## 3.1 General Sequence of Events

On Monday, July 11, 1988, between 2207 and 2213 UTC (16:07-16:13 MDT), four successive United flights had inadvertent encounters with microburst windshear conditions while on final approach to Denver Stapleton Airport (DEN), each resulting in a missed approach, subsequent delay, and uneventful arrival. A fifth flight executed a missed approach without encountering the phenomenon. There was no damage to aircraft and no passenger injuries were incurred.

The five flights involved were (in approach sequence):

UA395	B-737-291A	AUS/DEN (arriving from Austin)
UA862	B-737-291A	MLI/DEN (arriving from Moline, did not encounter windshear)
UA236	DC-8-71	SEA/DEN (arriving from Seattle)
UA949	B-727-122	IAH/DEN (arriving from Houston)
UA305	B-727-222A	DSM/DEN (arriving from Des Moines)

All five flights were given vectors for an approach to runways 26L and 26R at Stapleton, and were in contact with DEN tower at the time of their respective windshear encounters and/or missed approaches.

UA862 contacted DEN tower approximately two miles outside the ALTUR non-directional beacon (NDB), the final approach fix for runways 26L and 26R. The flight requested a wind report for the airport. The tower gave UA862 clearance to land, and a Microburst Alert with an expected windspeed loss of 40 knots, further characterized as "measured by machine, no pilot reports." The flight executed a missed approach, turning to the north. UA862 did not descend below 8,000 feet above mean sea-level (MSL), and there is no evidence the flight encountered microburst activity.

UA395 contacted the tower inside ALTUR just before UA862 announced its missed approach. It is noted that UA395 was, however, ahead of UA862 in sequence. Because of relative position, the crew of UA395 could not see UA862 but the captain recalls hearing another flight go around on the radio. The tower gave UA395 clearance to land and the same Microburst Alert. The flight continued inbound on glidepath for 83 seconds before beginning to climb and notifying the tower they were abandoning the approach. Radar data shows the flight descended to less than 100 feet above ground level (AGL), or 250 feet below glidepath about one mile from the touchdown zone.

UA236 approached next, contacting the tower about 20 seconds after UA395 went around. Upon initial contact, UA236 was cleared to land and was given a Microburst Alert with an expected airspeed loss of 50 knots on two mile final. The tower did not report the previous missed approaches. UA236 continued inbound for 77 seconds before announcing their missed approach, just after reaching a minimum altitude of 5,800 feet MSL.

UA949 contacted the tower 10 seconds after UA236 announced a missed approach. The tower cautioned of wake turbulence behind the DC-8 going around, and delivered Microburst Alert with an expected loss of 70 knots on three mile final. Clearance to land was not given. About 45 seconds later, the tower broadcast an undirected announcement of Microburst Alert, 80 knots loss expected. The captain recalls a severe downdraft just after the 80 knot loss alert. The windshear recovery technique of 15 degrees pitch and full power was executed while going around.

Stick shaker did not activate. The minimum altitude was about 6,200 feet MSL.

UA305 contacted the tower as UA949 was announcing its missed approach. The Microburst Alert of 80 knots loss was repeated. The crew requested confirmation of the magnitude which they received from the tower and two other airplanes. The crew discontinued the approach, and remained essentially level at 6,100 feet MSL for nearly 1 minute.

### 3.2 Radio Communications

ATIS messages X (2145 UTC), Y (2200 UTC), and A (2203 UTC) were included on the tower voice tape, and are transcribed in the United report (page 48 in Appendix 1). ATIS-X observes a 50°F difference between temperature and dew point, narrowing to a 40 degree difference in ATIS-Y and ATIS-A. The large difference between temperature and dew point is an indication of possible microburst development<sup>15</sup>, and the narrowing is indicative of the approaching rain. Windshear and Microburst Advisories appear in all three reports. ATIS-A notes the development of a thunderstorm at the airport.

A time-based transcript of communications between Denver Tower and the five United flights is contained in the United report<sup>16</sup> (pages 49-50 in Appendix 1). It is not known which ATIS message each flight had last monitored. All communications were clear and readable, and no crew members reported any malfunction of equipment. All radio messages used accepted terminology. Specifically, tower reports pertaining to microburst windshear used standard phraseology. For example: "United 236 heavy, Denver tower. Microburst Alert, threshold wind one four zero at five, expect a five zero knot loss, two mile final..." The "loss" refers to vector wind magnitude along the expected flightpath, not airspeed loss per se. Airspeed loss is impossible to predict with accuracy as it depends on just how the aircraft is flown, how power is modulated, and the distance over which the windspeed change occurs.

All five flights were given a "Microburst Alert" like that quoted above upon initial contact with the tower. UA862, UA395, and UA236 were cleared to land at that time. UA862, although first to contact the tower, was in sequence behind UA395, as sections 3.1 and 3.6.1, 4.4 describe.

None of the four flights encountering the event advised the tower of any reason for declaring missed approaches. Consequently, the tower did not give following crews any such information.

### 3.3 Aircraft Flight Data Recorders

The flight data recorders (FDR) for all five aircraft were removed for data analysis after the windshear encounters and sent to United Airlines' Operations Engineering (SFOEG). All flight recorders were foil medium units with four channels: altitude, airspeed, heading, and

---

<sup>15</sup>"Windshear Training Aid," Federal Aviation Administration, February 1987.

<sup>16</sup> This transcript was provided by United to aid in their analysis of the encounter. There was no formal transcript as is typically provided by the FAA or NTSB in their accident or incident analyses.

## FACTUAL MATERIAL

normal acceleration<sup>17</sup>.

All recorders operated normally. The foil mediums were voluntarily sent to the NTSB for analysis, and to the NASA Ames Research Center for detailed reconstruction of the wind profiles. Graphical data from the NTSB work is included in the United report (pages 56-60 in Appendix 1).

The recorder from UA862 confirms an early missed approach with no apparent abnormal airspeed or altitude fluctuations.

Data from UA395 shows airspeed oscillations during the windshear penetration of up to 9 knots per second. Typical magnitude of the oscillations was plus and minus 20 knots. The minimum altitude was read out to be 5,341 feet MSL. The touchdown zone for runway 26L is at 5,333 feet MSL. ARTS III radar confirmed an altitude of 20 to 70 feet AGL. While these figures disagree, the fact is the flight was at least 250 feet below the glideslope approximately one mile from the touchdown zone.

UA236 was initially stable at approximately 160 knots. Airspeed rose in 20 seconds to 202 knots (about 2.1 knots per second), then fell abruptly to 157 knots (3.5 knots per second), followed by a 27 knot rise at 6.75 knots per second, and a drop of 30 knots at 4.1 knots per second. Minimum altitude was 5,800 feet MSL.

The recorder shows UA949 entered the shear area while stabilized at about 159 knots. Airspeed rose to 171 knots, then dropped 18 knots in three seconds. Subsequent oscillations of plus or minus 20 knots per second occurred and normal accelerations ranged from 0.5 g to 1.3 g. Minimum altitude was recorded as 6,266 feet MSL.

UA305 was steadily bleeding airspeed during approach, reaching 170 knots as it entered the shear. Airspeed rose to 185 knots in 3 seconds (5 knots per second), followed by a 20 knot loss in 1.7 seconds (11.8 knots per second). Other oscillations occurred at rates higher than 10 knots per second. Normal acceleration ranged from -0.19 g to 1.50 g. Minimum altitude recorded was 6,280 feet MSL.

### 3.4 Meteorological Information

The United report (pages 19-27 of Appendix 1) contains a report by United Air Lines Weather Desk (OPBWX) analyzing the weather on July 11, 1988, for landings at Denver. A Low Level Windshear (LLWS) alert was issued by OPBWX at 1516 UTC valid for 2100-0300 UTC and covered the incident period.

Included in pages 28-46 of Appendix 1 are copies of pertinent portions of the Weather Briefing Message (WBM) for each flight. In each case, the LLWS alert appears prominently at the beginning of the WBM. Each contains the DEN terminal forecast of 1818 UTC calling for a slight chance of low clouds and thundershower development with gusts to 40 knots after 2000 UTC.

---

<sup>17</sup> Since the analysis of this encounter was voluntary, certain aircraft parameters (such as specific aircraft weight and balance, as well as moments of inertia) are not available. Analyses conducted that are sensitive to these parameters will be in error. No data has been presented in this report that is affected by those parameters.

A description of the meteorological conditions are contained in the NCAR report (pages 6-8 in Appendix 5).

### 3.5 Ground-Based Sensors

From July 1, 1988, through August 31, 1988, the TDWR OT&E was in progress. The radar was active on July 11, 1988, at the time of the missed approaches and detected divergent flow that intersected the operating zones for the two runways. The Microburst Alerts which were transmitted to each flight were generated by this system.

The radar used to test the TDWR algorithm was the Massachusetts Institute of Technology Lincoln Laboratory (MIT LL) 10 cm Doppler radar (identified as FL2). The University of North Dakota (UND) operated a 5 cm Doppler radar during the project. The radar was located about 11.3 nautical miles (nmi) north of FL2 and radar scans were coordinated to enable dual Doppler analysis.

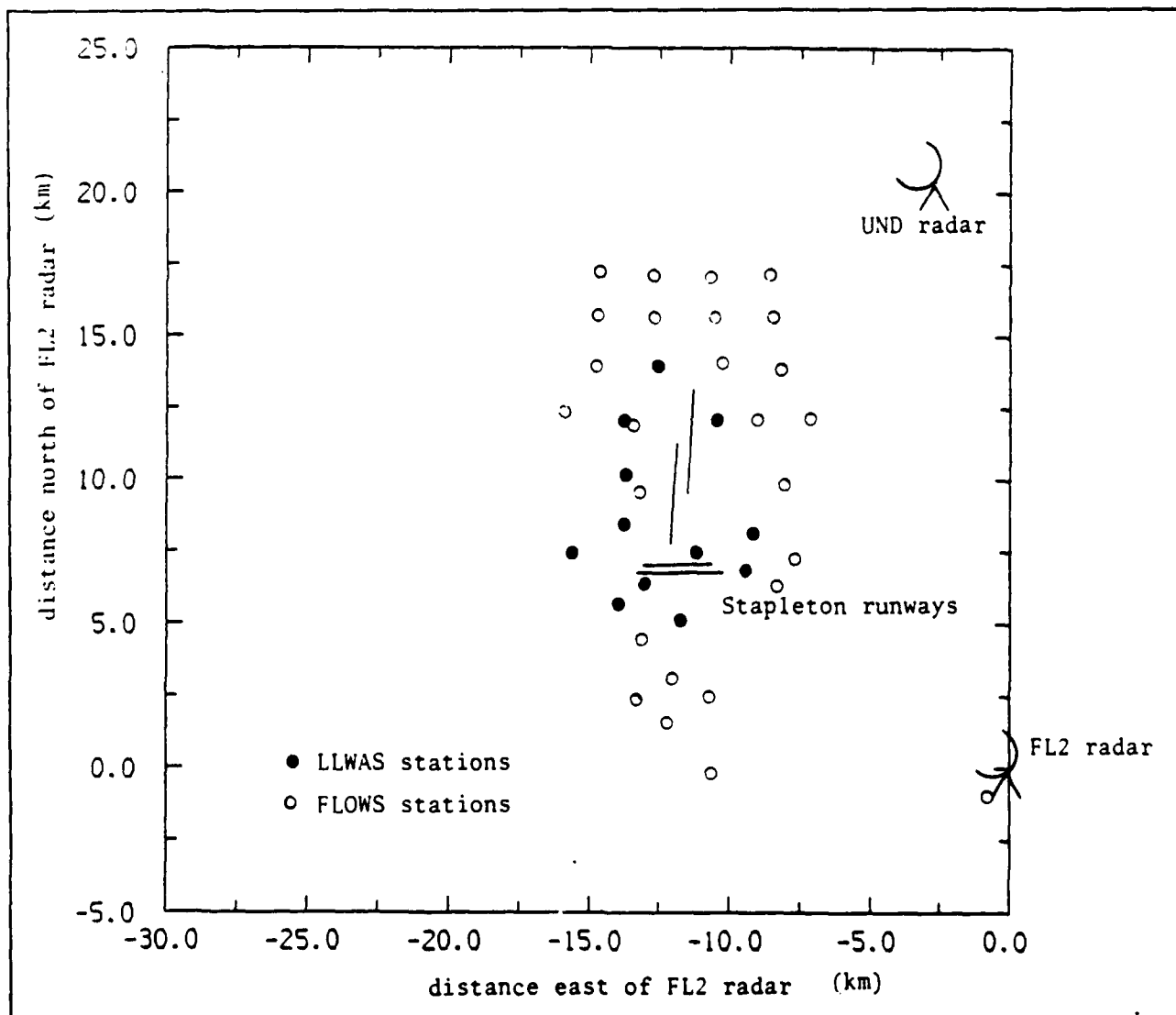


Figure 1 -- Relative locations of the Ground Stations during the TDWR OT&E

The LLWAS is the commissioned facility at Denver Stapleton. During the TDWR OT&E the LLWAS was not displayed to the Air Traffic Service. However, the data was recorded. The FAA-Lincoln Laboratory Operational Weather System (FLOWS) mesonet was in place and operating during the July 11, 1988, microburst. Combining the LLWAS and FLOWS mesonet provided surface wind detection coverage for a total of 42 sensor stations over a 6.5 x 10.8 nmi area around the airport. LLWAS sends data to a central processor and display site every 6 seconds; FLOWS data were available once per minute.

Figure 1 shows the relative location of FL2, the UND radar, the LLWAS stations and the FLOWS stations.

### 3.5.1 Terminal Doppler Weather Radar

The working definition of a microburst for the TDWR OT&E was a 20 knot change in windspeed over a path of 2.2 nmi or less. The radar used to test the TDWR algorithm was the MIT LL 10 cm Doppler radar (identified as FL2). The radar detects only wind components away from and towards the radar. The TDWR algorithm seeks changes in air velocity along each beam which meet the microburst definition and then flags those segments of the beam; adjacent segments are then mapped, a best-fit elliptical shape drawn around them, and the maximum change in radar radial speed is recorded.

In early August, revisions were made to the TDWR microburst detection algorithm to correct a perceived over-warning problem. Changes in the windspeed differences and warning times resulting from these alterations are identified in the analysis section.

If the elliptical shape intersects the operating region for a particular runway, then the position (in increments of 1 mile from the end of the runway) and the windspeed loss is sent to the tower. The exact shape of the ellipse and its windspeed loss is sent to a Graphic Situation Display (GSD). Alerts are generated for events within one-half mile of the approach path, and within three miles of the runway (on approach) or within two miles of the runway (on takeoff).

The GSD diagrams are presented on monitors located in the tower, at the TRACON supervisor's desk, and one other position. The actual display is in color. Microbursts appear as round or elliptical shapes with a number in the center indicating knots of wind differential across the event. Precipitation echoes are irregular, and usually west of the airport in this series of diagrams. The first microburst to appear near runway 26 shows as 35 knots on the diagram labeled as "TIME: 2206". A second microburst was just northwest of Buckley Air National Guard Base, outside the alerting area. As time progresses, the diagram shows up to three events over the runway 26 complex and the approach path. The tower alert gives only the strongest event.

The NCAR report (contained within Appendix B of Appendix 5) contains a list of alarms issued between 22:05 and 22:13 UTC on July 11, 1988, black and white prints of the GSD, and wind vector diagrams from Doppler radar measurements (contained within Appendix A of Appendix 5).

The list of alarms appears in three columns corresponding to the displays in the tower. There are separate sets for the 35R/17L runway, the 35L/17R runway, and the 26/08 complex. The presentation is identical to that which appears on a cathode-ray tube (CRT) in front of the tower controller position for each runway. The list of alerts has been marked to emphasize those alerts issued for the runway 26 approach corridor, confirming the alerts noted in the transcript.

### 3.5.2 University of North Dakota Radar

The University of North Dakota (UND) operated a 5 cm Doppler radar during the project. The radar was located about 11.3 nmi north of FL2 and radar scans were coordinated to enable dual Doppler analysis. This analysis provides a three-dimensional wind field; two-dimensional winds derived from this field in the airport vicinity are shown in Appendix D of Appendix 5.

### 3.5.3 Low-Level Wind Shear Alert System

The LLWAS and the FLOWS mesonet were in place and operating during the July 11, 1988, microburst. These provided surface wind detection coverage for a total of 42 sensor stations over a 6.5 x 10.8 nmi area around the airport. LLWAS sends data to a central processor and display site every 6 seconds; FLOWS data were available once per minute.

The NCAR report (contained within Appendix G of Appendix 5) shows windspeed from the 12 LLWAS stations and from the FL2 and UND radars. East-West windspeeds, U, and North-South windspeeds, V, components are shown for the 6-second LLWAS data in the two upper plots. The lower plots show the radial wind components from each of the two radars, FL2 and UND, with the 1-minute radar data from the gate nearest each LLWAS station, superimposed as asterisks.

### 3.5.4 Combined LLWAS/FLOWS Mesonet

Combining the LLWAS and FLOWS mesonet provided surface wind measurement coverage for a total of 42 sensor stations over a 6.5 x 10.8 nmi area around the airport. Wind vectors (pointing in the direction the wind is blowing toward) are shown in the NCAR report (contained within Appendix E of Appendix 5) for the times pertaining to the microburst. LLWAS stations are labeled with "L," and FLOWS mesonet stations are labeled with "F." The plots are centered at the centerpoint of the runways. The dotted areas indicate approximate areas for microbursts causing divergence levels above threshold value at the approximate TDWR alarm level. The crossed areas indicate stronger divergence levels commensurate with the TDWR microburst alarm level. FLOWS station F13 was not operating correctly throughout the time period.

### 3.5.5 Additional FLOWS Measurements

The NCAR report (contained within Appendix F of Appendix 5) shows the time series of temperature, relative humidity, average and maximum windspeed and wind direction (from true North) for the FLOWS mesonet stations. (Station F30 was located at the FL2 radar.)

## 3.6 Air Traffic Control Observations

Two sets of observations were available. The Automated Radar Terminal System (ARTS III) data that records aircraft position, identification and altitude. The aircraft altitude from ARTS III is periodically data-linked from every aircraft via Mode-C transmission from the aircraft. These data tapes were voluntarily provided by the FAA Air Traffic Service to the NTSB. The second set of observations were the Microburst Alarm messages that were displayed to the tower controllers to be sent to aircraft under their control.

## FACTUAL MATERIAL

## 3.6.1 ARTS III Radar

One minute segment plots of ARTS III radar data are included in the United report (pages 84-89 in Appendix 1). The plots show the geographical position of each aircraft every 5 seconds during the period 2207 through 2213 UTC. Altitude above mean sea-level is indicated each time it changed with resolution to the nearest 100 feet. Runway alignments are shown as well as large crosses indicating the DEN VOR, ALTUR, and the radar installation. Tower communication events are superimposed on the plots.

## 3.6.2 TDWR Microburst Alarm Message

See the NCAR report (contained within Appendix B of Appendix 5) for a list of the Microburst Alarms issued between 2205 and 2213 UTC.

## 3.7 Flight Crew Observations

Flight crew observations in this report are based on the crews' training and their reports after the encounter.

## 3.7.1 Training

All crews received windshear training according to the Advanced Windshear Training Program instituted by United beginning in 1984. United's program is substantially the same as that of the FAA Windshear Training Aid which United personnel helped develop for the FAA. The Pilot Windshear Guide section of the FAA documentation was distributed to all United pilots, and a short test is conducted as a part of Annual Recurrent Training. A table of "Microburst Windshear Probability Guidelines" from this document is included in the United report (page 62 in Appendix 1).

According to bulletins which appear in the Adverse Weather section of each fleet's Flight Manual, and backed by simulator training in conjunction with Annual Recurrent Training, pilots are trained to follow a "Model of Flight Crew Actions" prescribing a systematic approach to detection, avoidance, cautionary practices (called "Prevention"), and recovery from inadvertent encounters with windshear. An example of the bulletin is in the United report (pages 63-67 in Appendix 1).

In addition to the standard training described above, two Flight Manual bulletins were issued for the summer of 1988 in all fleets. The first, a Summer Operations Bulletin (pages 68-75 of Appendix 1) reinforces the windshear training, particularly the Model of Flight Crew Actions. The criteria for beginning a recovery procedure are restated as "uncontrolled changes from normal steady state flight in excess of:

- 15 knots indicated airspeed
- 500 feet per minute vertical speed
- 5 degrees pitch attitude
- one dot displacement from the glideslope"

A second bulletin entitled "Denver Enhanced Low Level Windshear Alert System and Terminal Doppler Weather Radar Operational Demonstration" (pages 76-78 of Appendix 1) describes the TDWR program, its reliability, and the criteria for issuance of a "Microburst Alert." A statement of United policy towards these alerts is included which says, in part, "A FLIGHT



MUST NOT DEPART NOR CONDUCT AN APPROACH THROUGH AN AREA WHERE A MICROBURST ALERT IS IN EFFECT."

### 3.7.2 Captains' Reports

Captains' Reports from each of the involved flights are included in the United report (pages 108-112 in Appendix 1). In addition, available crew members from each flight were interviewed at the United Training Center in Denver (DENTK), on July 22, 1988. Their comments were recorded on videotape for further use in the production of safety and/or training materials.

## **4 ANALYSIS**

## 4.1 General

All data, including TASS modeling, TDWR measurements, crew statements, flight recorders, and radar, substantiate the fact that microburst windshear conditions existed on the final approach path to runways 26L and 26R between 2206 and 2220 UTC on July 11, 1988. The same data confirms that UA862 did not encounter significant windshear, while UA395, UA236, UA949, and UA305 did indeed fly directly through the microburst area.

**Table I** Compiled Sequence of Events

<u>Time (UTC)</u>	<u>Event name</u>
15:16:00	OPBWX issued LLWS alert for 2100-0300
18:00:00	TDWR OT&E On-Line
21:19:00	Real-time reference for the start of the TASS model
22:03:00	Microburst storm maximum strength exceeds F-Factor of 0.10
22:05:56	LLWS Alarm: First windshear alert, runway 26 Approach, 10 knots, on runway
22:06:17	TDWR Alarm: 35 knots, 1 mile final
22:07:00	Microburst storm maximum strength exceeds F-Factor of 0.15
22:07:12	UA862 contacts DEN tower (first reference in United transcript)
22:07:17	TDWR Alarm: 40 knots, 1 mile final
22:07:31	UA395 contacts DEN tower
22:07:55	UA862 declares missed approach
22:08:19	TDWR Alarm: 50 knots, 2 mile final
22:08:35	UA395 exceeds F-Factor of 0.1
22:08:50	UA395 at 5400 feet MSL (100 feet AGL)
22:08:51	UA395 peak F-Factor of 0.12
22:08:53	UA395 exits F-Factor of 0.1
22:09:05	UA395 over the runway
22:09:23	UA236 contacts DEN tower
22:09:35	TDWR Alarm: 60 knots, 3 mile final
22:10:21	UA236 exceeds F-Factor of 0.1
22:10:23	TDWR Alarm: 70 knots, 3 mile final
22:10:30	UA236 stops descent at 5800 feet MSL (500 feet AGL)
22:10:34	UA236 peak F-Factor of 0.15
22:10:39	UA236 exits F-Factor of 0.1
22:10:40	UA236 announces missed approach
22:10:42	LLWS Alarm: First microburst alert, runway 26 Approach, 35 knots, 3 mile final
22:10:50	UA949 contacts DEN tower
22:11:04	UA236 over the runway
22:11:17	TDWR Alarm: 80 knots, 3 mile final
22:11:27	DEN Tower transmits 80 knots loss to all aircraft on frequency
22:11:31	UA949 first exceeds F-Factor of 0.1
22:11:37	UA305 first contacts DEN tower
22:11:40	UA949 declares missed approach
22:11:44	UA949 first peak F-Factor of 0.18
22:11:50	UA949 exits first 0.1 F-Factor
22:12:10	UA305 announces missed approach
22:12:17	UA305 first exceeds F-Factor of 0.1
22:12:24	TDWR Alarm: 80 knots, 3 mile final
22:12:25	UA949 over the runway
22:12:32	UA305 first peak F-Factor of 0.16
22:12:36	UA305 exits from first F-Factor of 0.1
22:12:56	UA305 over the runway
22:13:25	TDWR Alarm: 85 knots, 3 mile final
22:16:00	Microburst storm maximum strength goes below F-Factor of 0.15
22:18:00	Microburst storm maximum strength goes below F-Factor of 0.10
01:00:05	TDWR OT&E Off-Line

Table I contains a listing of the events related to the microburst on July 11, 1988. The TASS results were incorporated into this sequence of events using the following information:

The estimate of each of the aircraft's F-Factor along the respective flight path. This is provided in the NASA Langley report. Figure 22 of Appendix 2 shows the F-Factors as computed from

the TASS model winds.

- The correlation of time and distance provided by the NASA Ames report. In particular, Figure 8 of Appendix 3 shows the correlation between the east-bound distance from the runway and time. The distance and times are correlated through the aircraft flight paths.

#### 4.2 Meteorological Information

The major synoptic scale weather feature was a shallow pressure trough over the western United States, which was moving slowly eastward. This trough was not evident at levels above 700 mb. Westerly winds were present over Wyoming, Colorado, and Utah, which brought warm, moist air into the Denver area throughout the day. Also, two layers of higher windspeeds developed; one centered near 10,800 feet MSL with winds from 295°, and a layer of northwesterly 20-30 knot winds above 22,600 feet MSL.

ATIS-X observed a 50°F difference between temperature and dew point, narrowing to a 40 degree difference in ATIS-Y and ATIS-A. The large difference between temperature and dew point is an indication of possible microburst development, and the narrowing is indicative of approaching rain. Windshear and Microburst Advisories appeared in all three ATIS reports. ATIS-A notes the development of a thunderstorm at the airport.

A line of thunderstorms developed to the west of Stapleton and drifted southeastward. The microburst-producing storm originated from two 60+ dBz cell which formed around 2130 UTC over the mountains 18.4 nmi west of Stapleton. Surface winds were from the north-northwest across the airport, temperatures were 88-90°F across the FLOWS mesonet and the air was fairly dry, with 22-25 percent relative humidity (see Appendix F of Appendix 5). The strongest outflow (which peaked at 80 knots) impacted operations along the east-west runways for approximately 45 minutes. The outflow developed into a line that persisted across the southern periphery of the airport.

#### 4.3 Hazard Analysis

A primary threat of microbursts to aircraft is the single or combined effect of the horizontal velocity shear and downdraft motion. Either of these effects can penalize the performance of an aircraft, and possibly result in a critical loss of altitude for arriving or departing aircraft. A very useful parameter for indicating the severity of the windshear and vertical velocity on aircraft performance is the F-Factor<sup>18</sup>.

$$F = g^{-1} DU/Dt - w/V_{\infty}$$

where  $DU/Dt$  is the rate of change of the horizontal wind component along the aircraft flight path,  $g$  is the acceleration due to gravity,  $w$  is the vertical windspeed, and  $V_{\infty}$  is the airspeed of the aircraft. The first term on the right side represents the contribution of windshear to the performance of the aircraft, while the second term represents the contribution due to the vertical wind. Positive values of  $F$  indicate a performance-decreasing condition, whereas negative values indicate a performance-increasing situation.

---

<sup>18</sup> Bowles, R.L., and Targ, R., "Windshear Detection and Avoidance: Airborne Systems Perspective," 16th Congress of the ICAS, Jerusalem, Israel, 1988.

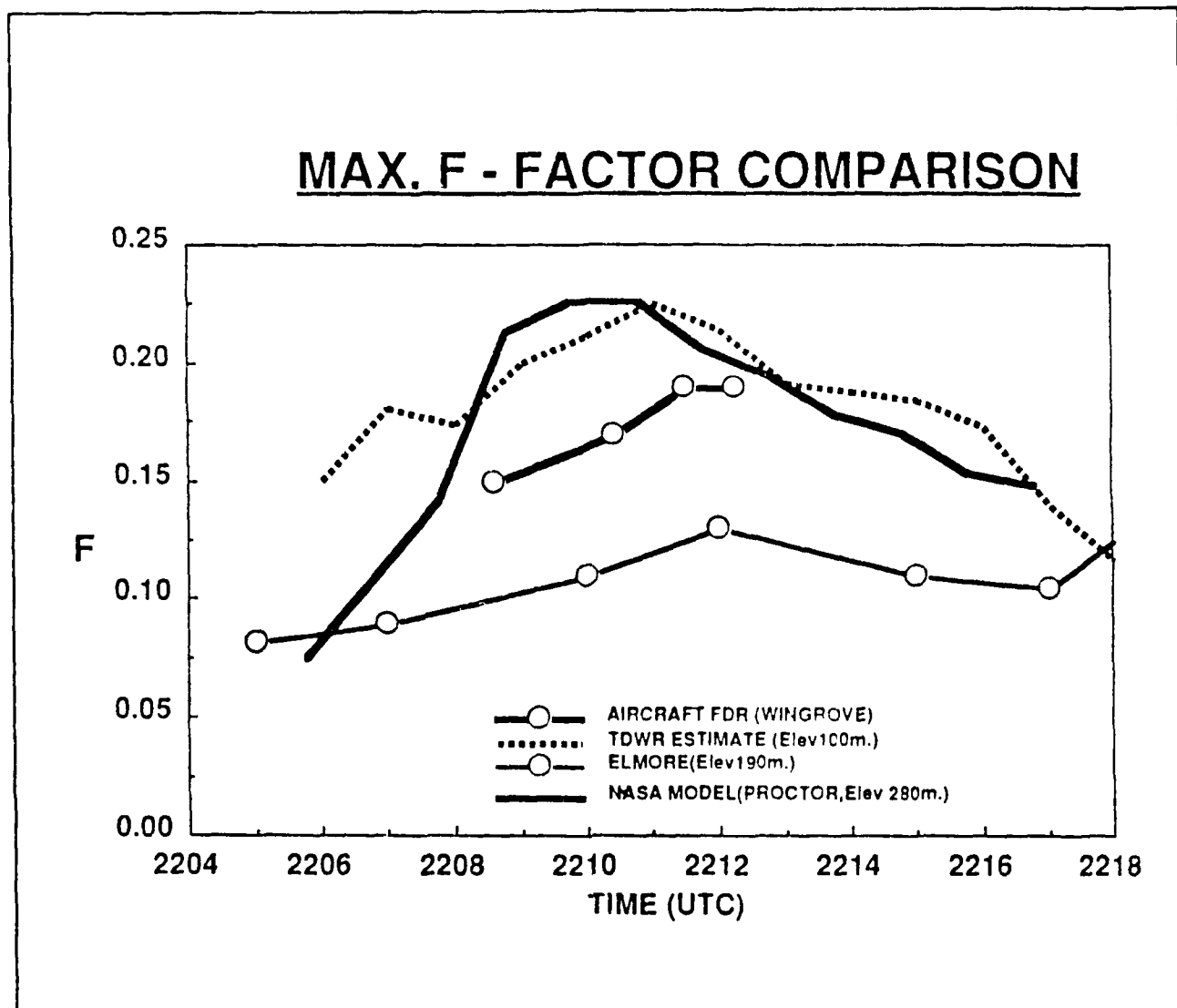


Figure 2 -- Four estimates of maximum F-Factor based on sensed data from the aircraft flight data recorders, TDWR estimate (at 100 m elevation), the TASS model (at 280 m elevation), and the dual-Doppler radar analysis (at 690 m elevation)

F-Factor can be approximated by:

$$F \approx g^{-1} V_r \delta U / \delta R - w / V_r$$

where  $\delta U / \delta R$  is the horizontal velocity shear along the flight path, and  $V_r$  is the aircraft's speed relative to the microburst.

Four estimates of maximum F-Factor, shown in Figure 2, based on sensed data from the aircraft flight data recorders, TDWR estimate (at 328 feet AGL), the TASS model (at 919 feet AGL), and the dual-Doppler radar analysis (at 2,264 feet AGL) showed agreement. The severity of the microburst exceeding an F-Factor of 0.15, for example, started between 2206 and 2207 UTC and lasted until 2216 and 2217 UTC. For an F-Factor of 0.1, the microburst started at 2203 and 2206 UTC and lasted beyond 2218 UTC. The peak maximum F-Factor is 0.25 for the encounter.

#### 4.4 ARTS III Radar

ARTS III radar data are shown in the United Airlines report (pp. 84 - 89, Appendix 1). These are summarized as follows:

2207 to 2208 UTC: UA395 is shown approaching from the southeast and UA862 from the northeast. UA862 enters the chart at 22:07:50 and declares a missed approach abeam ALTUR. UA395 is ahead of UA862 and contacts the tower 1.3 miles inside ALTUR.

2208 to 2209 UTC: UA862 is shown turning to the north and staying above 8,000 feet, well clear of the approach profile. UA395 is shown continuing inbound on the localizer profile to runway 26L. Approximate MSL altitude of the glideslope beam is indicated by numbers in parentheses. UA395 passed below the glidepath at 22:08:35. AT 22:08:50, the ARTS III measurement shows UA395 at 5,400 feet MSL, less than 100 feet AGL, or about 250 feet below the glidepath one mile from the touchdown zone. UA395 maintains 5,400 feet MSL for the remainder of the period.

2209 to 2210 UTC: UA395 begins to climb and turn northward. UA236 enters the area, contacts the tower just inside ALTUR. UA236 is approximately 200 feet below the glidepath.

2210 to 2211 UTC: UA236 continues inbound, staying 200 feet below the glidepath. The flight stops its steady descent at about 22:10:30, at 5,800 feet MSL. The altitude measurement remains 5,800 to 5,900 feet MSL for 45 seconds, during which a missed approach is declared. UA949 enters the area on glidepath and contacts the tower one mile inside ALTUR.

2211 to 2212 UTC: UA236 begins climbing, regaining 6,000 feet MSL at midfield, and thereafter climbing rapidly. UA949 continues inbound and is never below the glidepath. A minimum altitude of 6,200 feet MSL is reached just as the missed approach is declared. UA305 enters the area six hundred feet below the glidepath at ALTUR. UA305 intercepts the glidepath near the end of the period, approximately coincident with tower contact.

2212 to 2213 UTC: UA949 executes a missed approach to the south. UA305 continues on runway heading, declaring a missed approach early in the period but with essentially no climb for another 35 seconds. UA305 was at 6,200 to 6,300 feet MSL for about 50 seconds altogether. The flight continues on approximately runway heading throughout the period.

#### 4.5 Flight Crew Analysis

Each of the flight crews applied the Model of Flight Crew Action depending on their level of information for each decision point. The Model of Flight Crew Action is listed below:

- Search for clues of windshear,
- Avoidance of known windshear,
- Use precautions (when avoidance is not chosen),
- Use of standard operating techniques, and
- Recovery from inadvertent encounters.

The crew of UA862 heard one of the first microburst message, and because of the words "... microburst alert ...," the crew elected not to continue the approach. UA862 received the

message along with the "cleared to land," and the message that the windspeed loss was 40 knots.

The crew of UA395 noted (pages 109 and 110 of the United report, Appendix 1) that "... another aircraft said that they were going missed approach ...."

The crew of UA949 said (page 111 of the United report, Appendix 1) that they were aware of the possibility of windshear, and noted that they "... observed DC-8 execute a go-around and comment maybe it was because of windshear [and] took flaps [to] 25° [and heard tower advise] 'microburst alert'."

The crew of UA305 said (pages 112 of the United report, Appendix 1) "... some aircraft ahead of us were executing go-around's."

No pilots made reports to the tower, and this was contrary to United training. The crews seemed to be aware that aircraft were going around. However, the crews may not have recognized the significance of the cumulative clues and the broadcast Microburst Alert. This combined with the rapid sequence of events that occurred between contacting the tower, receiving the microburst message, encountering the microburst, and executing a windshear escape and recovery maneuver. The rapid dynamics of the encounter may conspire to reduce the overall effectiveness of the pilot report in this particular encounter.

#### 4.6 Aircraft Wind Profile Reconstruction

A detailed analysis the wind profiles based on the flight data recorders is presented in the NASA Ames report (Appendix 3).

#### 4.7 Doppler Radar

The first detection of the microburst affecting the approach for runways 26L and 26R occurred at 2206 UTC. Prior to this time, the radar measurements revealed several cells of moderate (less than 45 dBz) reflectivity to the northwest of the airport. These cells were growing, with strong updrafts that carried precipitation (presumably graupel) upward into the region of strong northwesterly winds. From there, the dual Doppler analyses clearly show that the graupel was carried toward the airport. As it fell out of the updraft regions, it sublimated to produce intense local cooling. The strong downdraft which resulted originated at a level between 11,500 and 12,000 feet MSL.

The TDWR microburst alarm continued until 2248 (the revised alarm began at the same time but ended at 2231). During first 6 min of alarm time, until 2212, the microburst strength as detected by TDWR grew from a windspeed difference of 35 knots to 80 knots (70 knots in the revised version). The dual Doppler analyses indicate a maximum windspeed difference of 68 knots, which makes it the strongest microburst (in terms of windspeed difference) yet analyzed using these techniques.

Additional microbursts developed to the west and northwest of the main feature, but were not as intense. While the microbursts were present, outflow from the main part of the storm which was located to the northwest was encroaching on the airport vicinity. This low level northwesterly flow appears to have distorted the flow patterns of these later-occurring microbursts.

By 2215 the storms from which the microbursts originated was clearly dissipating; downdrafts were present throughout most of the storm's volume and no new cells were observed.

The strong outflows continued for another 20-30 minutes. After 2220, the microburst parent cell dissipated leaving behind only weak, low level divergence. The storm complex developed into a line and moved southeastward while additional outflow from new cells, weaker than that of the main microburst, triggered new convection to the southeast of the airport. As the line of new, although weak, cells moved further southeastward, it became indistinct and precipitation was detected by the radar over a more widespread area.

#### 4.8 FLOWS/LLWAS Mesonet

Prior to the microburst occurrence, surface winds over the FLOWS and LLWAS mesonets were generally light and variable. At around 2200, winds in the northwest part of the domain were beginning to be affected by the outflow from the main storm cell; turning to northwesterly. As compared to the radar-measured winds, surface winds speeds were generally higher throughout the network. This is expected due to surface friction.

Prior to 2209 little evidence of the microburst was evident from the surface measurements. However, between 2209 and 2210, the temperature at station F23, which was near the center of the main microburst (see Appendix F of Appendix 5) dropped 10.8° from 84.2 to 73.4°F, and the windspeed increased from 14 to 30 knots. The relative humidity also increased, from 24 to 43 percent. During the previous minute, windspeed increased from 6 to 14 knots; the winds apparently indicated outflow arrival prior to any temperature or humidity signatures.

From 2210 through 2220, considerable spatial and temporal variations in windspeed are apparent in the LLWAS. This is especially evident in those stations near the edge of the microburst: L1, L2, L7 and L9. Data from these stations showed gustiness which was not resolved by the radar measurements; LLWAS data shows higher maximum microburst windspeeds than those measured by the radars. LLWAS alarms during this time were sporadic and did not maintain a constant strength (windspeed difference of 20 knots) as shown in Figure 11 of Appendix 5.

Temperatures across the FLOWS mesonet slowly declined during the dissipation of the storm. The main microburst actually affected only a few stations, F23, F22, and possibly F21. The rest of the mesonet was affected by multiple outflow centers, which did not produce the equivalent intense winds and temperature falls as did the main microburst. Temperatures decreased 9 - 14.4°F while relative humidity increased by 8 - 21 percent over the mesonet as a result of the microburst and storm outflow.

#### 4.9 Atmospheric Model Analysis

An important aspect of this case study is the reconstruction of the atmosphere using a numerical model. The complete analysis is contained in the NASA Langley report (Appendix 2). The Terminal Area Simulation System model is a time-dependent, non-hydrostatic cloud model which consists of 11 prognostic equations. The model has been applied extensively to the study of microbursts, and has been successfully validated in five case studies of cumulonimbus convection -- ranging from long-lasting supercell hailstorms to short-lived single-cell storms (including the 1985 Dallas-Fort Worth microburst storm).

The model indicates that there were multiple, low to moderate reflectivity microbursts. The strongest of the microbursts came from the anvil. The complete results from the model analysis can be found in the NASA Langley report (Appendix 2).



## **5 CONCLUSIONS**

## CONCLUSIONS

## 5.1 Flight Operations

- 5.1.1 *An aircrew Flight Manual Handbook Bulletin was issued wherein a critical pilot procedural requirement was obscurely located.*

United Flight Standards issued a 3-page aircrew Flight Manual Handbook Bulletin entitled "Denver ... LLWAS and ... TDWR Operational Demonstration" which applied to Denver departures and arrivals only. The Bulletin described the TDWR system, the related test program, and United's policy concerning actions to be taken by flight crews during TDWR Microburst Alerts. Within the Bulletin, a critical pilot procedural requirement which states "A FLIGHT MUST NOT DEPART NOR CONDUCT AN APPROACH THROUGH AN AREA WHERE A MICROBURST ALERT IS IN EFFECT" was obscurely located on page 3 of the Bulletin.

- 5.1.2 *Reports of conditions favorable for the formation of low altitude windshear conditions were available to all flights.*

UA395, UA862, UA236, UA949, and UA305 were issued a Weather Briefing Message prior to departure containing an alert section which forecast conditions favorable for the formation of low altitude windshear. Included were hourly weather observations which revealed temperature and dewpoint spreads of 35 and 39°F, conditions favorable for the formation of low altitude windshear.

- 5.1.3 *UA862 received one of the first "... microburst alert ..." messages from the Tower, and elected to discontinue the approach because of the alert.*

- 5.1.4 *UA395, UA236, and UA949 were all issued landing clearances and a Microburst Alert. All three flights continued inbound, beginning missed approaches after encountering significant altitude and airspeed performance problems.*

At approximate 2-minute intervals, UA395, UA236, and UA949 contacted the Tower from near ALTUR, and all were issued landing clearances and a Microburst Alert with an expected windspeed loss of from 40 to 80 knots. All three flights continued inbound on the Instrument Landing System (ILS) glideslope for 83, 77, and 44 seconds respectively following initial contact, beginning a missed approach only after encountering significant altitude and airspeed performance problems.

- 5.1.5 *UA305 initiated a missed approach after receiving the Microburst Alert and confirming the broadcast windspeed loss.*

UA305 contacted the Tower from near ALTUR approximately 2 minutes after UA949 and slightly after UA949 announced a missed approach to the Tower. A Microburst Alert was issued by the Tower with an expected windspeed loss of 80 knots on final approach. UA305 initiated a missed approach after the Alert and following confirmation of the broadcast windspeed loss.

- 5.1.6 *Individual flight reaction varied from a standard go-around procedure to the use of the windshear recovery procedure.*

UA395, UA236, and UA949 reacted to actual microburst encounters by employing procedures learned during the Advanced Windshear Training Program during initial and

recurrent flight training. Individual flight reaction varied from a standard go-around procedure for UA395, UA862, UA236 to the use of the windshear recovery procedure by UA949 (maximum power and a 15° pitch-up attitude). UA305 reacted to the Microburst Alert broadcast windspeed loss and initiated a missed approach after confirming the information.

- 5.1.7 *UA305 descended to less than 100 feet AGL (250 feet below the glidepath) approximately one mile from the touchdown zone.*

## 5.2 Air Traffic Operations

- 5.2.1 *All flights arrived in the Denver area during a period of time when ATIS broadcasts contained low altitude windshear advisories, microburst advisories, and a statement that a TDWR test was in progress.*
- 5.2.2 *Microburst Alert information was broadcast by the Tower to the flights as part of other routine landing communications and was not used as critical information by all involved pilots.*

UA862 was the first aircraft to contact Denver Tower from a position near ALTUR, the Final Approach Fix. The Tower responded by issuing a landing clearance and a Microburst Alert. UA862 requested an alternate approach from Tower, and subsequently executed a normal missed approach approximately 24 seconds later without encountering microburst activity.

UA395, UA862, UA236, UA949, and UA305 executed what appeared to be go-around maneuvers while encountering microburst conditions.

- 5.2.3 *None of the five flights advised the Tower of the reason for their missed approach; therefore, no pilot reports of windshear could be relayed to subsequent flights by the Tower.*

## 5.3 Ground Sensors

- 5.3.1 *The TDWR detected a microburst along the operating flight path and alarmed at 2206 UTC.*

Dual-Doppler analysis confirmed that the microburst's size and intensity as reported by TDWR were reasonably accurate. The good agreement with the TASS results provide confidence that the inferences used in the radar analysis (see the NCAR report in Appendix 5) are realistic. Further analysis of TDWR data showed that parameters are available within the TDWR to compute F-Factor to use for aircraft hazard determination.

- 5.3.2 *An LLWAS windshear warning occurred at 2206 UTC and indicated a 10 knot windspeed loss on the runway.*
- 5.3.3 *The first LLWAS microburst alarm occurred at 2210:42, indicating a 35 knot windspeed difference.*

A review of LLWAS data (the NCAR report, Appendix 5) shows that an LLWAS windshear warning occurred at 2206 UTC. It indicated a 10 knot windspeed loss

## CONCLUSIONS

located on the runway. The first LLWAS microburst alarm occurred at 2210:42, indicating a 35 knot windspeed difference. This was nearly 5 minutes after the TDWR alarm. There are two main reasons for this discrepancy. First, the radar detected the microburst at 623 m above the ground, prior to its arrival at the surface. Second, the LLWAS network was not in an optimal location for detection of this event, which was situated at the approach to the east-west runways. In fact, one of the LLWAS sensors was located near the center of the microburst; winds there were never very strong. Such a situation effectively removes that sensor from the network for this event. The rest of the sensors were to the west of the microburst. The westward progress of the microburst outflow appears to have been somewhat impeded by the northwesterly outflow from the main part of the storm.

#### 5.4 Flight Data Recorder

5.4.1 *The wind pattern from the flight data recorder analysis agrees with the measurements from the Doppler radar and with the results from the TASS model.*

5.4.2 *Four-channel flight data recorders are able to provide reliable along-flight path windspeed data when complemented with ground-based and analytical atmospheric model data.*

The developing wind pattern from the flight data recorder analysis is in general agreement with the measurements from the Doppler radar and with the analytical results from the numerical TASS model. The aircraft data complement these other findings by providing a detailed analysis of the internal velocity fluctuations. The Doppler data was shown to not only validate the flight data, but also to add insight into the resulting wind profiles by suggesting the presence of a secondary microburst cell. It is possible that the appearance of this second downburst caused the internal fluctuations in horizontal winds observed in the flight data of the latter three aircraft.

#### 5.5 Terminal Area Simulation System

5.5.1 *The multi-dimensional TASS give good quantitative comparisons with observations as well as reconstructed data from Doppler radars and aircraft flight data recorders.*

5.5.2 *The TASS model is a useful tool in aircraft investigations, since it provides useful insight into the storm and microburst structure, and can provide information which is not always apparent from observed data.*

The simulated storm is unusual in structure and produces multiple low-to-moderate-reflectivity microbursts. One of the microburst was unusually intense, containing strong downdrafts, outflow, and windshear; and driven by cooling primarily from sublimating snow. F-Factors in the most intense microburst exceeded 0.2, even before ground contact. This suggests that F-Factors also could be used as a precursor for strong windshear at ground level. The TASS-simulated microburst outflow displays a rough symmetry near the ground, becoming weaker and less symmetrical with altitude above 262 feet AGL. This suggests potential issues to be addressed for Doppler radar analysis of such storms, if the radar beam is too broad, at too high of an elevation, or obstructed at low levels by significant ground clutter.

## **6 RECOMMENDATIONS**

## RECOMMENDATIONS

## 6.1 Interaction of Aircraft, Air Traffic, and Ground-Based Sensors

6.1.1 *It is recommended that procedures be developed for the early, clear, and unambiguous transfer of the microburst message.*

Two points bear careful reexamination, and are: early receipt of microburst message and the context and format of the microburst message.

The first point regards the early receipt of microburst messages. UA862 received its microburst message early in its approach to landing. The early receipt of the message coupled with the flight crew's windshear training, allowed the crew sufficient time to make a decision to go-around and coordinate a maneuver with air traffic to miss the microburst. In this case, the early transfer from Approach Control to Tower frequency allowed the early receipt of the microburst message. If microburst messages are being generated for transmission to flight crews, then aircraft that are under the jurisdiction of radar approach control should be considered as viable candidates to receive terminal area microburst alert messages.

Attaining an unambiguous microburst message implies a coordination between air traffic and the affected flights. The reason for a microburst-related go-around should be relayed back to air traffic from the flight crew. Subsequent flights receiving pilot reports are doubly alerted -- once by the detection technology on the ground and secondly by the pilot report. This double-alert system emphasizes the severity of the situation as strongly as is possible. All training and checking programs must stress the need for timely pilot reporting of windshear and microburst encounters to ensure this emphasis.

The second point regards the context and format of the microburst message. There was no incorrect or misleading information in the microburst messages that were passed to the flight crews. The message format operated as intended. However, the context of the message in the final approach phase of the flight could have been reinforced. There are two areas where this could have been effected. One is to provide microburst messages earlier in the approach. The TDWR provides detection of the microburst to a wider extent than the LLWAS system does (due to its physical layout), and so may allow for microburst messages to be delivered by approach control at airports that have TDWR's installed in them.

6.1.2 *It is recommended that there should be a clear differentiation between windshear and microburst forecasts and real, detected alarms.*6.1.3 *It is recommended that suitable methods for early dissemination of microburst messages should be established to ensure strategic coordination of air traffic to avoid microburst areas.*

The ATIS message should not be considered a replacement for early dissemination of microburst messages. Its role is that of allowing the crew to assess the potential windshear threat along with other signs of windshear.

6.1.4 *It is recommended that policies and methodologies should be established to communicate safety-of-flight information to users operating with the National Airspace System. Differentiation must be made between general information and information related to*

*safety-of-flight matters.*

- 6.1.5 *It is recommended that an examination into the potential implications for windshear data communications should be pursued.*

The three-phase process of terminal area windshear information exchange (sending a microburst message to the aircraft, the flight crew's decision to execute a go-around, and the message back to air traffic that the reason for the go-around is the microburst) should be a candidate for automation. A research program that examines automation is technically feasible. The program should consist of three parts: 1. investigate the transfer of ground-based information to the crew; 2. investigate the flight crew's decision making process based on integrating the ground-based data with airborne information; and 3. examine the automatic transfer of the flight crew's action to the air traffic system.

## 6.2 The Case Study Process

- 6.2.1 *It is recommended that the tools applied to this case study be applied to future investigations of similar microburst encounters.*

Surface wind sensor and Doppler radar data can be analyzed in conjunction with flight data recorder analyses to reconstruct wind profiles from each aircraft. Combining the flight data recorder analyses with TASS-model results, when reconfirmed with observed wind fields, can provide further insight into the wind patterns traversed by the aircraft. The larger-scale atmospheric data and the flight path-derived wind profiles form an understanding of the atmosphere and its interaction with the aircraft that can provide insight for safety briefings and further improvements to windshear systems. Since windshear interaction with aircraft are varied, these kinds of detailed reconstructions allow for further reinforcement of the elements of the model of flight crew action, and insight into the operation of airborne and ground-based sensors and their respective operational issues.

- 6.2.2 *It is recommended that standard investigation techniques can be augmented with the addition of three teams that are responsible for: ground-based windshear data, airborne windshear data, and atmospheric modeling using TASS.*

Standard investigative techniques should be maintained when microburst windshear encounters are suspected. Beyond that which is normally prepared for investigations, the following three teams should be organized:

Ground-based Windshear Data Team: This team should document all sources of ground-based windshear data (LLWAS- and TDWR-data, if available), including basic meteorology, surface wind measurements, and radar data.

Airborne Windshear Data Team: This team should document all sources of airborne windshear data, including aircraft flight data recorder and data from airborne windshear sensors (if available).

Atmospheric Modeling Team: The TASS should be run using data from a special sounding near to the event. Timeliness and proximity must be carefully considered when determining the appropriateness of available sounding data. The nearest National Weather Service Rawinsonde Station should be notified to make a rawinsonde launch within an hour of the event unless earlier, nearby sounding data is already available. Surface measurements from radars, wind sensors and

## RECOMMENDATIONS

National Weather Service stations should be obtained to support the model products. The TASS data should be used to focus data collections and analyses.



## **7 REFERENCES**

## REFERENCES

- Bowles, R.L., "Wind Shear 'Hit'," as presented to the "Wind Shear Detection, Forward-Looking Sensor Technology Conference," February 24 - 25, 1987, Hampton, Virginia; reference NASA CP 10004, DOT/FAA/PS-87/2, October 1987.
- Bowles, R.L., and Targ, R., "Windshear Detection and Avoidance: Airborne Systems Perspective," 16th Congress of the ICAS, Jerusalem, Israel, 1988.
- Campbell, S., Correspondence to Roland Bowles, dated 24 March 1989, containing velocity and shear values from FLOWS for July 11, 1988, at Denver Stapleton Airport, MIT Lincoln Laboratory.
- Coppenbarger, R.A., Wingrove, R.C., "Analysis of Records From Four Airliners in the Denver Microburst, July 11, 1988," AIAA paper 89-3354 for the Atmospheric Flight Mechanics Conference, August 14-16, 1989, Boston, Massachusetts.
- "Delta Air Lines, Inc., Lockheed L-1011-385-1, N726DA Dallas/Fort Worth - International Airport, Texas August 2, 1985," Aircraft Accident Report, NTSB/AAR-86/05, National Transportation Safety Board, Washington, DC, August 15, 1986.
- Elmore, K.L., Politovich, M.K., Sand, W.R., "The 11 July 1988 Microburst at Stapleton International Airport, Denver, Colorado," National Center for Atmospheric Research, November 1989.
- Fujita, T.T., "DFW Microburst on August 2, 1985," University of Chicago, SMRP 217, January 1986.
- Fujita, T.T., "The Downburst: Microburst and Macrobust," University of Chicago, SMRP 210, February 1985.
- "Integrated FAA Windshear Program Plan," DOT/FAA/DL-VS-AT-88/1, Federal Aviation Administration, June 1987.
- Isaminger, M. A., "WEEKLY SITE SUMMARY," FL2 Radar Site, Denver, Colorado, MIT Lincoln Laboratory.
- Kirchner, M., Statement of the Director of Engineering Technology, The Boeing Commercial Airplane Company, before the Subcommittee on Oversight and Investigations Committee on Public Works and Transportation, United States House of Representatives regarding Windshear, June 30, 1987.
- "Microburst Encounter, July 11, 1988, Denver, Colorado," United Airlines Flight Safety Investigation 88-46, February 9, 1989.
- Proctor, F.H., "The Terminal Area Simulation System, Volume I: Theoretical Formulation," NASA CR 4046, DOT/FAA/PM-86/50, I, April 1987.
- Proctor, F.H., "The Terminal Area Simulation System, Volume II: Verification Cases," NASA CR 4047, DOT/FAA/PM-86/50, II, April 1987.
- Proctor, F.H., Bowles, R.L., "Investigation of the Denver 11 July 1988 Microburst Storm with the Three-Dimensional NASA-Langley Windshear Model," (Draft to be Submitted as a

NASA Report) July 26, 1989.

Turnbull, D., et al, "The FAA Terminal Doppler Weather Radar (TDWR) Program," Third International Conference on the Aviation Weather System, 29 January - 3 February, 1989, Anaheim, CA, American Meteorological Society. 414-419.

"Windshear Training Aid," Federal Aviation Administration, February 1987.

Zweifel, T., "Flight Experience with Windshear Detection," SAE Aerospace Control and Guidance Systems Committee, Monterey, CA, March 9-11, 1988.

## **8     SUBSTANTIATING DATA -- Appendices**

The appendices constitute the foundation for the case study. They are duplicated to provide detailed information to the reader. The following reprints are included with the explicit permission of the authors to be used as substantiating data for this case study:

1. "Microburst Encounter, July 11, 1988, Denver, Colorado," United Airlines Flight Safety Investigation 88-46, February 9, 1989.
2. Proctor, F.H., Bowles, R.L., "Investigation of the Denver 11 July 1988 Microburst Storm with the Three-Dimensional NASA-Langley Windshear Model," (Draft to be Submitted as a NASA Report) July 26, 1989.
3. Coppenbarger, R.A., Wingrove, R.C., "Analysis of Records From Four Airliners in the Denver Microburst, July 11, 1988," AIAA Paper 89-3354, August 14-16, 1989.
4. Campbell, S., Correspondence to Roland Bowles, dated 24 March 1989, containing velocity and shear values from FLOWS for July 11, 1988, at Denver Stapleton Airport, and Isaminger, M. A., "WEEKLY SITE SUMMARY," FL2 Radar Site, Denver, Colorado, both of MIT Lincoln Laboratory.
5. Elmore, K.L., Politovich, M.K., Sand, W.R., "The 11 July 1988 Microburst at Stapleton International Airport, Denver, Colorado," National Center for Atmospheric Research, November 1989.

**SUBSTANTIATING DATA -- Appendices**

**APPENDIX 1 -- United Report**

"Microburst Encounter, July 11, 1988, Denver, Colorado," United Airlines Flight Safety  
Investigation 88-46, February 9, 1989.



**UNITED AIRLINES**

Captain David A. Simmon  
Director - Flight Safety

February 9, 1989

TO ALL RECIPIENTS:

Subject: United Airlines Flight  
Safety Investigation

**SYNOPSIS**

On July 11, 1988, at approximately 4:00PM MDT, four successive United flights experienced inadvertent encounters with microburst-related windshear while on final approach to Denver Stapleton Airport. A fifth flight executed a missed approach without encountering the phenomena. There were no injuries or damages to equipment. Worthy of note is the fact that a doppler radar microburst detection system was operational at the time and provided information to crews concerning the intensity of the observed activity.

The listed recommendations have been directed to various UA departments for action. These departments will contact the appropriate industry and government agencies for resolution.

This information is released for your use in the interests of aircraft accident prevention and remedial action and in the spirit of FAR 831.11 (b).

*Dave*

Dave Simmon  
Director of Flight Safety

Att.

MANAGERS OF FLEET OPERATIONS  
MANAGERS OF FLIGHT OPERATIONS

EXOVF - Bill Cotton  
OPBVV - John Dansdill  
SFOEG - Bob Doll  
EXOSW - Paul Green  
EXOVF - Hart Langer  
DENTK - Ed Methot  
EXOFO - John O'Keefe  
SFOFS - Frank Rose  
EXODD - Bob Smith  
DENTK - Bill Traub

EXOFS - Dave Simmon

February 2, 1989

EXOPO - Jim Guyette

FLIGHT SAFETY INCIDENT  
INVESTIGATION 88-46

### MANAGEMENT CONFIDENTIAL

Based on a thorough review of the attached Flight Safety Incident Investigation, the following evaluation and action assignments are provided:

### SYNOPSIS

On July 11, 1988 at approximately 4:00 PM MDT, four successive United flights experienced inadvertent encounters with microburst-related windshear while on final approach to Denver Stapleton Airport. A fifth flight executed a missed approach without encountering the phenomena. There were no injuries or damages to equipment. Worthy of note is the fact that a test doppler radar microburst detection system was operational at the time and provided information to crews concerning the intensity of the observed activity.

The Flight Center was tasked with investigating and documenting the event and that responsibility was carried out by Bob Ireland whose final report is attached.

### CONCLUSIONS

Flight Safety concurs with all findings and recommendations and provides the following action assignments:

Recommendation 1: Action: DENTK/Traub; Due Date: 3/31/89.

Recommendation 2: Action: DENTK/Traub; Due Date: 3/31/89.

Recommendation 3: Action: EXODD/SMITH; Due Date: 3/31/89.



Recommendation 4: Action: EXOVF/Cotton; Due Date:  
3/31/89.

Recommendation 5: Action: DENTK/Traub; Due Date:  
3/31/89.

Recommendation 6: Action: DENTK/Traub; Due Date:  
3/31/89.

Recommendation 7: Action: EXOVF/Cotton; Due Date:  
3/31/89.

Recommendation 8: Action: EXOVF/Cotton; Due Date:  
3/31/89.

Recommendation 9: Action: DENTK/Traub; Due Date:  
3/31/89.

Reviewed by:



Ed Marsey  
Flight Safety Investigator

Atch.

Released by:



Dave Simmon  
Director of Flight Safety

EXOFS - Dave Simmon

DENTK - Bob Ireland

January 27, 1989

FLIGHT SAFETY INCIDENT  
INVESTIGATION 88-46

FACTS

1. General:

On July 11, 1988, between 2207 and 2213 UTC (16:07-16:13 MDT), four successive United flights had inadvertent encounters with microburst windshear conditions while on final approach to Denver Stapleton Airport (DEN), each resulting in a missed approach, subsequent delay, and uneventful arrival. A fifth flight executed a missed approach without encountering the phenomena. There was no damage to aircraft and no passenger injuries were incurred.

The five flights involved were (in approach sequence):

UA395	B-737-291A	AUS/DEN
UA862	B-737-291A	MLI/DEN (did not encounter windshear)
UA236	DC-8-71	SEA/DEN
UA949	B-727-122	IAH/DEN
UA305	B-727-222A	DSM/DEN

All five flights were given vectors for an approach to runways 26L and 26R at Stapleton, and were in contact with DEN tower at the time of their respective windshear encounters and/or missed approaches.

1.1 General Sequence of Events

Flight 862 contacted DEN tower approximately two miles outside the ALTUR NDB, the final approach fix for runways 26L and 26R. The flight requested a wind report for the airport. The tower gave flight 862 clearance to land, and a Microburst Alert with an expected airspeed loss of 40 knots, further characterized as "measured by machine, no pilot reports." The flight executed a missed approach, turning to the north. Flight 862 did not descend below 8000 MSL, and there is no evidence the flight encountered microburst activity.

Flight 395 contacted the tower inside ALTUR just before flight 862 announced its missed approach. It is noted that flight 395 was, however, ahead of flight 862 in

sequence. Because of relative position, the crew of UA395 could not see 862 but the captain recalls hearing another flight go around on the radio. The tower gave flight 395 clearance to land and the same Microburst Alert. The flight continued inbound on glidepath for 83 seconds before beginning to climb and notifying the tower they were abandoning the approach. Radar data shows the flight descended to less than 100 feet AGL (250 feet below glidepath) about one mile from the touchdown zone.

Flight 236 approached next, contacting the tower about 20 seconds after UA395 went around. Upon initial contact, flight 236 was cleared to land and was given a Microburst Alert with expected airspeed loss of 50 knots on two mile final. The tower did not report the previous missed approaches. Flight 236 continued inbound for 77 seconds before announcing their missed approach, just after reaching a minimum altitude of 5,800 MSL. Flight recorder data shows a slow rise in airspeed from 150 to 202 knots followed by a rapid loss back to 150 knots and subsequent oscillations. The climb out was normal.

Flight 949 contacted the tower 10 seconds after flight 236 announced a missed approach. The tower cautioned of wake turbulence behind the DC-8 going around, and delivered a Microburst Alert with an expected loss of 70 knots on three mile final. Clearance to land was not given. About 45 seconds later, the tower broadcast an undirected announcement of Microburst Alert, 80 knots loss expected. The captain recalls a severe downdraft just after the 80 knot loss alert. The windshear recovery technique of 15 degrees pitch and full power was executed while going around. Airspeed rose from 150 to 171 knots, then oscillated sharply to a 130 knot minimum before recovering. Stick shaker did not activate. Minimum altitude was about 6200 MSL.

Flight 305 contacted the tower as 949 was announcing its missed approach. The Microburst Alert of 80 knots loss was repeated. The crew requested confirmation of the magnitude which they received from the tower and two other airplanes. Flight 305 began a missed approach, but remained essentially level at 6,100 MSL, apparently unable to climb, for nearly one minute, at full thrust before climbing.

## 2. Meteorological Data

Appendix 1 contains a report by OPBWX analyzing the weather on July 11, 1988 for landings at Denver. A Low Level Windshear (LLWS) alert was issued by OPBWX at

1516 UTC valid from 2100-0300 UTC and covered the incident period.

Also included in Appendix 1 are copies of pertinent portions of the Weather Briefing Message (WBM) for each flight. In each case, the LLWS alert appears prominently at the beginning of the WBM. Each contains the DEN terminal forecast of 1818 UTC calling for a slight chance of low clouds and thundershower development with gusts to 40 knots after 2000 UTC.

### 3. Radio Communications

ATIS messages X (2145 UTC), Y (2200 UTC), and A (2203 UTC) were included on the tower voice tape, and are transcribed in Appendix 2. ATIS-X observes a 50 degree difference between temperature and dew point, narrowing to a 40 degree difference in ATIS-Y and ATIS-A. The large difference between temperature and dew point is an indication of possible microburst development, and the narrowing is indicative of the approaching rain. Windshear and Microburst Advisories appear in all three reports. ATIS-A notes the development of a thunderstorm at the airport.

A time-based transcript of communications between Denver Tower and the five United flights is contained in Appendix 2. It is not known which ATIS message each flight had last monitored. All communications were clear and readable, and no crewmembers reported any malfunction of equipment. All radio messages used accepted terminology. Specifically, tower reports pertaining to microburst windshear used FAA/NCAR agreed phraseology. For example: "United 236 heavy, Denver tower. Microburst Alert, threshold wind one four zero at five, expect a five zero knot loss two mile final..." The "loss" refers to vector wind magnitude along the expected flightpath, not airspeed loss per se, which is impossible to predict with accuracy as it depends on just how the aircraft is flown and how power is modulated.

All five flights were given a "Microburst Alert" like that quoted above upon initial contact with the tower. Flights 862, 395, and 236 were cleared to land at that time. Flight 862, although first to contact the tower, was in sequence behind flight 395, as sections 1.1 and 6 describe.

None of the four flights encountering the event advised the tower of their reason(s) for declaring missed approaches. Consequently, the tower did not give following crews any such information.

#### 4. Flight Data Recorders

The flight data recorders (FDR) for all five aircraft were removed for data analysis after the windshear encounters and sent to SFOEG - Operations Engineering. All flight recorders were foil medium units with four channels: altitude, airspeed, heading, and normal acceleration.

All recorders operated normally. The foil mediums were voluntarily sent to the NTSB for further analysis. Graphical data from the NTSB work is included in Appendix 3.

The recorder from flight 862 confirms an early missed approach with no apparent abnormal airspeed or altitude fluctuations.

Data from flight 395 shows airspeed oscillations during the windshear penetration of up to 9 knots/sec. Typical magnitude of the oscillations was plus and minus 20 knots. The minimum altitude was read out to be 5341 MSL. The touchdown zone for runway 26L is at 5333 MSL. ARTS III radar confirmed an altitude of 20 to 70 feet AGL. While these figures disagree, the fact is the flight was at least 250 feet below the glideslope approximately one mile from the touchdown zone.

Flight 236 was initially stable at approximately 160 knots. Airspeed rose in 20 seconds to 202 knots (about 2.1 knots/sec), then fell abruptly to 157 knots (3.5 knots/sec), followed by a 27 knot rise at 6.75 knots/sec, and a drop of 30 knots at 4.1 knots/sec. Minimum altitude was 5800 ft. MSL.

The recorder shows flight 949 entered the shear area while stabilized at about 159 knots. Airspeed rose to 171 knots, then dropped 18 knots in three seconds. Subsequent oscillations of plus or minus 20 knots per sec. occurred and normal accelerations ranged from 0.55 G's to 1.3 G's. Minimum altitude was recorded as 6266 ft. MSL.

Flight 305 was steadily bleeding airspeed during approach, reaching 170 knots as it entered the shear. Airspeed rose to 185 knots in three seconds (5 knots/sec.), followed by a 20 knot loss in 1.7 sec (11.8 knots/sec.). Other oscillations occurred at rates higher than 10 knots/sec. Normal acceleration ranged from -0.19 G's to 1.50 G's. Minimum altitude recorded was 6280 MSL.

## 5. Training

All involved crews received windshear training according to the Advanced Windshear Training Program instituted by United beginning in 1984. United's program is substantially the same as that of the FAA Windshear Training Aid which United personnel helped develop for the FAA. The Pilot Windshear Guide section of the FAA documentation was distributed to all UA pilots, and a short test is conducted as part of Annual Recurrent Training. A table of "Microburst Windshear Probability Guidelines" from this document is included in Appendix 4.

According to bulletins which appear in the Adverse Weather section of each fleet's Flight Manual, and backed by simulator training in conjunction with Annual Recurrent Training, pilots are trained to follow a "Model of Flight Crew Actions" prescribing a systematic approach to detection, avoidance, cautionary practices (called "Prevention"), and recovery from inadvertent encounters with windshear. An example of the bulletin is in Appendix 4.

In addition to the standard training described above, two Flight Manual bulletins were issued for the summer of 1988 in all fleets. The first, a Summer Operations Bulletin (example in Appendix 4) reinforces the windshear training, particularly the Model of Flight Crew Actions. The criteria for beginning a recovery procedure are restated as "uncontrolled changes from normal steady state flight in excess of:

- 15 knots indicated airspeed
- 500 fpm vertical speed
- 5 degrees pitch attitude
- 1 dot displacement from the glideslope"

A second bulletin entitled "Denver Enhanced Low Level Windshear Alert System and Terminal Doppler Weather Radar Operational Demonstration" (example in Appendix 4) describes the TDWR program, its reliability, and the criteria for issuance of a "Microburst Alert." A statement of UA policy towards these alerts is included which says, in part, "A FLIGHT MUST NOT DEPART NOR CONDUCT AN APPROACH THROUGH AN AREA WHERE A MICROBURST ALERT IS IN EFFECT."

## 6. ATC/ARTS III Radar

One minute segment plots of ARTS III radar data are included in Appendix 5. The plots show the geographical position of each aircraft every five seconds during the period 22:07 through 22:13 UTC.

Altitude (MSL) is indicated each time it changed with resolution to the nearest 100 feet. Runway alignments are shown as well as large crosses indicating the DEN VOR, ALTUR, and the radar installation. Tower communication events are superimposed on the plots.

During the period 22:07 - 22:08, UA 395 is shown approaching from the southeast and UA 862 from the northeast. UA 862 enters the chart at 22:07:50 and declares a missed approach abeam ALTUR. UA 395 is ahead of UA 862 and contacts the tower 1.3 miles inside ALTUR.

During the period 22:08 - 22:09, UA 862 is shown turning to the north and staying above 8000 ft., well clear of the approach profile. UA 395 is shown continuing inbound on the localizer profile to runway 26L. Approximate MSL altitude of the glideslope beam is indicated by numbers in parentheses. UA 395 passed below the glidepath at 22:08:35. At 22:08:50, the ARTS III measurement shows UA 395 at 5400 MSL, less than 100 feet AGL, or about 250 feet below the glidepath one mile from the touchdown zone. UA 395 maintains 5400 MSL for the remainder of the period.

During the period 22:09 - 22:10, UA 395 begins to climb and turn northward. UA 236 enters the area, contacts the tower just inside ALTUR. UA 236 is approximately 200 feet below the glidepath.

During the period 22:10 - 22:11, UA 236 continues inbound, staying 200 feet below the glidepath. The flight stops its steady descent at about 22:10:30, at 5800 MSL. The altitude measurement remains 5800 - 5900 MSL for 45 seconds, during which a missed approach is declared. UA 949 enters the area on glidepath and contacts the tower one mile inside ALTUR.

During the period 22:11 - 22:12, UA 236 begins climbing, regaining 6000 MSL at midfield, and thereafter climbing rapidly. UA 949 continues inbound and is never below the glidepath. A minimum altitude of 6200 MSL is reached just as the missed approach is declared. UA 305 enters the area six hundred feet below the glidepath at ALTUR. UA 305 climbs to meet the glidepath near the end of the period, approximately coincident with tower contact.

During the period 22:12 - 22:13, UA 949 executes a missed approach to the south. UA 305 continues on runway heading, declaring a missed approach early in the period but with essentially no climb for another 35 seconds. UA 305 was at 6200-6300 MSL for about 50

seconds altogether. The flight continues on approximately runway heading throughout the period.

7. National Center for Atmospheric Research Experiment

During the period from July 1 through August 31, 1988, a demonstration of Terminal Doppler Weather Radar was in progress at Denver. The radar was active on July 11 at the time of the missed approaches. Microburst Alerts transmitted to each flight were generated by this system. Alerts are generated for events within one-half mile of the approach path, and within three miles of the runway (on approach) or within two miles of the runway (on takeoff).

Appendix 6 contains a list of alarms issued between 22:05 and 22:13 UTC on July 11, 1988, black and white prints of the Geographic Situation Display (GSD), and wind vector diagrams from Doppler radar measurements.

The list of alarms appears in three columns corresponding to the displays in the tower. There are separate sets for the 35R/17L runway, the 35L/17R runway, and the 26/08 complex. The presentation is identical to that which appears on a CRT in front of the tower controller position for each runway. The list of alerts has been marked to emphasize those alerts issued for the runway 26 approach corridor, confirming the alerts noted in the transcript.

The GSD diagrams show the display available at one location in the tower and at the TRACON supervisor's desk. The actual display is in color. Microbursts appear as round or "band-aid" shapes with a number in the center indicating knots of wind differential across the event. Precipitation echoes are irregular, and usually west of the airport in this series of diagrams. The first microburst to appear near runway 26 shows as 35 knots on the diagram labeled as "TIME: 2206". A second microburst was just northwest of Buckley ANGB, outside the alerting area. As time progresses, the diagram shows up to three events over the runway 26 complex and the approach path. The tower alert gives only the strongest event.

The "dual Doppler" diagrams give a visualization of the wind patterns derived by two radar facilities simultaneously. The Stapleton runways are at the center. The plots, at about one minute intervals, have arrows indicating local wind direction, with strength given by arrow length. During the period, a large event forms on the approach path somewhat elongated tangentially.



NCAR scientists noted the elongated pattern of the event(s) was unusual in that most would line up north/south rather than east/west as seen here. By lining up east/west the airspeed loss effects were reduced since penetration time was lengthened. Had the aircraft penetrated the event along its minor axis, greater airspeed fluctuations would have been expected.

#### Crew Statements

Captain's Reports from each of the involved flights are included in Appendix 7. In addition, available crewmembers from each flight were interviewed at DENTK on July 22, 1988. Their comments were videotape recorded for further use in the production of safety and/or training materials.

#### ANALYSIS

All data, including TDWR measurements, crew statements, flight recorders, and radar, substantiate the fact that microburst windshear conditions existed on the final approach path to runways 26L and 26R between 2206 and 2220 UTC on July 11, 1988. The same data confirms that flight 862 did not encounter significant windshear, while flights 395, 236, 949, and 305 did indeed fly directly through the microburst area.

Further analysis of events leading to the four encounters with windshear and the one successful avoidance will follow the Model of Flight Crew Actions.

##### 1. Search For Clues of Windshear

The following information was provided to the crews:

- Weather briefing message with LLWS alert and forecast of conditions at DEN conducive to microburst development.
- ATIS report of "windshear advisory and microburst advisory." Windshear advisories are effective during the period of windshear alerts and for 20 minutes afterward. Microburst advisories are in effect during a period of microburst alert and for two hours afterward. ATIS also reported a temperature/dew point spread of 30-40 degrees, a well-known clue of possible windshear.

- Microburst Alert messages were issued by the tower, indicating a divergent flow exceeding 20 knots differential within one half mile of the final approach path. NCAR subsequently changed this criteria to 30 knots after the events of this report.

In addition, crews reported observing:

- Radar echoes of precipitation over/near the airport.
- Convective weather development near the airport.
- Virga or rainfall near the runway.
- Moderate to severe turbulence.

Of the available clues, clearly the strongest is the TDWR-produced Microburst Alert. This single clue means divergent conditions ARE PRESENT at the location detected, with the severity reported, lacking only a report of the altitude of maximum divergence. The Microburst Alert is also treated in a Flight Manual Bulletin as a matter of policy requiring immediate termination of approach.

The other clues are all medium or low probability indicators according to the table on page 36 of the FAA Pilot Windshear Guide (see Appendix 4).

## 2. Avoidance of Known Windshear

Crews are required at this point to make a decision based on the available clues. The FAA Pilot Windshear Guide suggests the clues are cumulative. On this basis, avoidance should have been chosen in all cases.

The crew of flight 862 recognized the significance of the Microburst Alert. This single item caused them to initiate a missed approach. In their interview, the crew also indicated their concern based on the other clues.

The crew of flight 305 also began an avoidance maneuver before their encounter according to voice tapes, radar data, and crew interviews. Their decision was based on the Microburst Alert calling for an 80 knot loss. In the crew interview, however, the captain was clear in stating they understood this to be a pilot report. The words "Microburst Alert" were either not heard or not understood in terms of policy.

It is clear that the crews of flights 395, 236, 949, and 305 either did not hear clearly or did not know the meaning of the term Microburst Alert. None of these crews took action based on hearing this alert, knowing its source (TDWR) and policy implication. Based on the time period between tower broadcast of Microburst Alert and the missed approaches, it is concluded the go-arounds of flights 395, 236, and 949 were not based on the tower report, but rather on conditions encountered. The crews for flights 395, 236, and 949 could not recall that they ever heard "Microburst Alert" upon initial contact with the tower. The crews of flights 395 and 236 did recall their clearance to land from the same transmission. The captain of flight 949 did hear the Microburst Alert which was broadcast as an isolated tower transmission later in his approach. One captain reported that he had not read the associated Flight Manual Bulletin until sometime after the events of July 11.

1. Use Precautions (When Avoidance is Not Chosen)

The four crews which encountered the microburst all indicated they had seen some clues and discussed their significance. The crews of flights 395, 236, and 949 took specific cautionary actions to increase their capability to penetrate an inadvertent encounter with windshear. All flights deliberately held extra airspeed of 10-15 knots. Flight 949 purposely was flown high on the glidepath in a belief that a steeper glidepath might be helpful. It is noted that this is not an appropriate precaution. While extra altitude may be good, the higher descent rates necessary could be quite detrimental.

4. Use of Standard Operating Techniques

Aside from the precautions noted above, all crews appear to have used standard techniques during their approaches and missed approaches. This fact, as intended, aided in the early recognition of inadvertently encountered windshear.

5. Recovery From Inadvertent Encounters

All flights added thrust. Crews from flights 395 and 949 indicated they moved the throttles full forward. Others used only go-around power with which they were satisfied.

All flights raised their pitch attitudes as opposed to chasing airspeed in the decreasing performance part of the windshear. The crew of flight 236 initially lowered the nose during the increasing performance

segment prior to their decision to go around. Only the crew of flight 949 reported specific use of 15 degrees during the go around, and training materials do currently state "towards 15 degrees."

During the recovery phase, flight 395 had a minimum altitude much closer to the ground than the crew thought. Flight recorder data confirms that additional airspeed was available to trade.

Contrary to training, NO crew made a pilot report to the tower about the windshear conditions encountered.

### CONCLUSIONS

Finding 1: Flight Standards issued a 3-page aircrew Flight Manual Handbook Bulletin entitled "Denver Low Level Windshear Alert System (LLWAS) and Terminal Doppler Weather Radar (TDWR) Operational Demonstration" which applied to Denver departures and arrivals only. The Bulletin described the TDWR system, the related test program, and United's policy concerning actions to be taken by flight crews during TDWR Microburst Alerts. Within the Bulletin, a critical pilot procedural requirement which states "A FLIGHT MUST NOT DEPART NOR CONDUCT AN APPROACH THROUGH AN AREA WHERE A MICROBURST ALERT IS IN EFFECT" was obscurely located on page 3. (CONTRIBUTING FACTOR)

Finding 2: Flight 395, 862, 236, 949, and 305 were issued a Weather Briefing Message (WBM) prior to departure containing an \*\*ALERT\*\* section which forecast conditions favorable for the formation of low level windshear. Included were hourly weather observations from 1700 UTC, 1800 UTC, and 1900 UTC which revealed temperature/dewpoint spreads of 35 to 39 degrees F, a condition favorable for the formation of low level windshear.

Finding 3: All flights arrived in the Denver area during a period of time when Airport Terminal Information Service (ATIS) broadcasts contained low level windshear advisories, microburst advisories, and a statement that a Doppler radar windshear demonstration (TDWR) was in progress.

Finding 4: Flight 862 was the first aircraft to contact Denver Tower from a position near ALTUR, the Final Approach Fix. The Tower responded by issuing a landing clearance and a Microburst Alert. Flight 862 executed a normal missed approach approximately 24 seconds later without encountering microburst activity.

Finding 5: At approximate 2 minute intervals, Flights 395, 236, and 949 contacted the Tower from near ALTUR, and all were issued landing clearances and a Microburst Alert with an expected airspeed loss of from 40 to 80 knots. All three flights continued inbound on the ILS glideslope for 83, 77, and 44 seconds respectively following initial contact, beginning a missed approach only after encountering significant altitude and airspeed performance problems. Crews may not have recognized the significance of the cumulative clues and the broadcast Microburst Alert. (PROBABLE CAUSE)

Finding 6: Flight 305 contacted the Tower from near ALTUR approximately 2 minutes after Flight 949 and slightly after Flight 949 announced a missed approach to the Tower. A Microburst Alert was issued by the Tower with an expected airspeed loss of 80 knots on final approach. Flight 305 initiated a missed approach after the Alert and following confirmation of the broadcast airspeed loss. (PROBABLE CAUSE)

Finding 7: Flights 395, 236, and 949 reacted to actual microburst encounters by employing procedures learned during the Advanced Windshear Training Program during initial and recurrent flight training. Individual flight reaction varied from a standard go-around procedure for Flights 395, 862, 236 to the use of the windshear recovery procedure by Flight 949 (maximum power and a 15° pitch-up attitude). Flight 305 reacted to the Microburst Alert broadcast airspeed loss and initiated a missed approach after confirming the information.

Finding 8: Microburst Alert information was broadcast by the Tower to the flights as part of other "routine" landing communications and may not have been perceived as critical information by all involved pilots. (CONTRIBUTING FACTOR)

Finding 9: None of the five flights advised the Tower of the reason for their missed approach; therefore, no

pilot reports of windshear could be relayed to subsequent flights by the Tower. (CONTRIBUTING FACTOR)

Finding 10: Flight 305 descended to less than 100 feet AGL (250 feet below the glidepath) approximately one mile from the touchdown zone.

#### RECOMMENDATIONS

Recommendation 1: Establish a policy and methodology to communicate safety-of-flight information to all pilots. If the Flight Manual Handbook Bulletin is retained for this purpose, differentiation must be made between general information and information relating to safety-of-flight matters. Additionally, bulletins should display critical safety-of-flight information in the same relative position within each bulletin.

Recommendation 2: Clearly differentiate between Windshear Alerts and Microburst Alerts in all written and classroom materials and instruction.

Recommendation 3: Change the Weather Briefing Message phraseology from "Windshear Alert" to "Windshear Forecast."

Recommendation 4: Change ATC procedures so that Microburst Alerts are given as a distinctly separate advisory and not in the same sentence with other information.

Recommendation 5: Establish a standard relative to how low a flight can descend on approach with a Microburst Alert in effect.


Recommendation 6: Insure that all training and checking programs stress the need for timely pilot reporting of windshear and microburst encounters.

Recommendation 7: Assess the feasibility of creating flexibility in the missed approach procedure in order to avoid microburst areas.

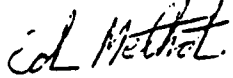
Recommendation 8: Establish a timely system to terminate microburst alerts when the hazard no longer exists.

Recommendation 9: Stress the importance of immediate and positive corrective actions by the Pilot Flying when aircraft performance deteriorates from desired parameters and the responsibility of the Pilot Not Flying to announce aircraft performance and flight path deviations.


Investigated by:

  
Bob Ireland  
Staff Engineer  
Flight Simulators

Reviewed by:

  
Ed Methot  
Manager of  
Flight Standards  
and Training

Approved by:

  
Bill Traub  
Vice President  
Flight Standards  
and Training

Att.

APPENDIX 1 - Meteorological Data

a. Report from OPBW - Carl Knable  
"Denver LLWS - July 11, 1988"

b. Weather Briefing Messages

Flight 395/11

Flight 862/11

Flight 236/11

Flight 940/11

Flight 305/11



# UNITED AIRLINES

TO: EXOFS - Ed Marsey  
EXODD - Dave Rasmussen

FROM: OPBNX - Carl Knable

July 13, 1988

DENVER LLWS - JULY 11, 1988

## INCIDENT

Flights: 395/236/862/949/305

Date/Time: 07-11-88, 2200Z-2232Z

Location: Landing Denver, Runways 26L and 26R

Incident: Microburst LLWS

## WEATHER ANALYSIS

On July 11, a stationary front extended from northwestern Wyoming across Nebraska, and into central Illinois. A weak low pressure trough ran NW-SE across Colorado. Colorado skies were clear during the morning, however an analysis of the 1200Z raob data indicated a strong potential for convective activity during the afternoon.

The first showers began to develop west of Denver around 1700Z, building and drifting at 15 knots to the southeast. By 2100Z, a large area of RW/TRW with tops to FL360 had formed over central Colorado.

Sky conditions at Denver were clear from sunrise to noon. At 1900Z, CB's began to develop over the mountains and the temperature-dew point spread at DEN was nearly 40° (86°/46°). By 2000Z, all LLWS conditions were present: mid level clouds (75 SCT 120 BKN), 40° temperature-dew point spread (86°/46°) and virga/RW being reported (RWU S, VIRGA SW). At 2100Z, CB's were reported SE and SW through N of the airport. Thunder was reported at 2200Z, as some of the cells passed over and close to the field. These cells generated the microbursts and LLWS encountered by the five United flights.

## FORECASTS

The routine OPBNX morning review of all LLWS parameters (moisture aloft, stability, dry layers, and predicted maximum temperatures) indicated a strong potential for LLWS and microbursts at several western terminals including DEN and COS. As a result, OPBNX issued a LLWS Alert for DEN and COS at 1516Z. This Alert was valid from 2100Z through 0300Z.

The DEN terminal forecast issued by both OPBNX and NWS called for TRW during the afternoon.

Both the terminal forecast and LLWS Alert should have been included in each trip's flight papers.

CONCLUSION

July 11 was a typical LLWS day at Denver. Indications of afternoon convective activity were present early in the morning, leading to the issuance of an OPBWX LLWS Alert. Convective activity developed during the afternoon over the mountains and drifted southeast at 15 knots, reaching the airport around 2200Z. The combination of high based CB's and the large temperature-dew point spread was classic, and lead to the formation of dry microbursts and intense shears in and around the airport.



G.R.K.

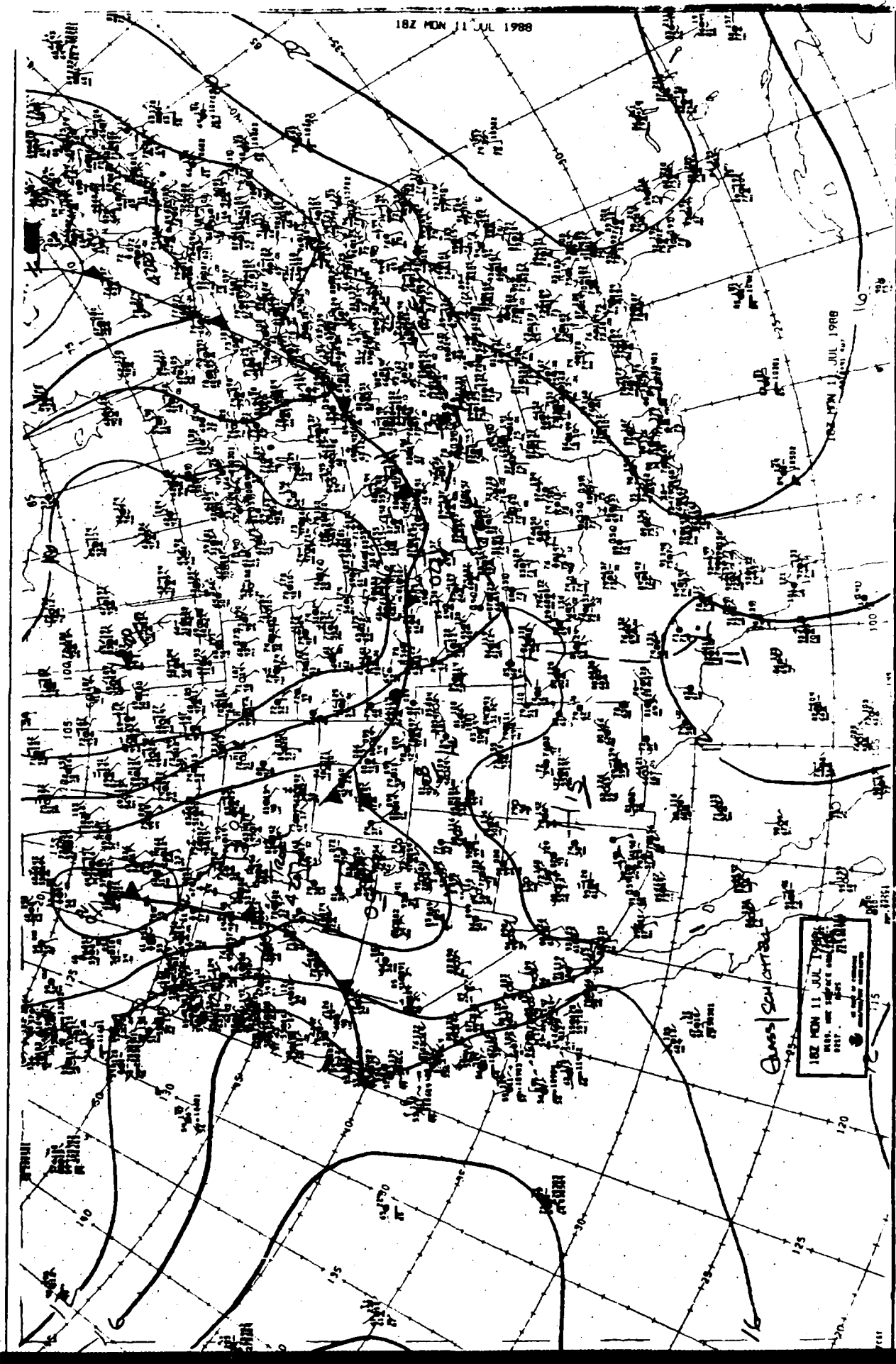
Attachments: Surface Chart 11/1800Z  
Radar Summary Charts 11/1735Z-2235Z  
HICB Work Chart  
Denver Surface Observations  
Denver FI  
OPBWX Wind Shear Alert

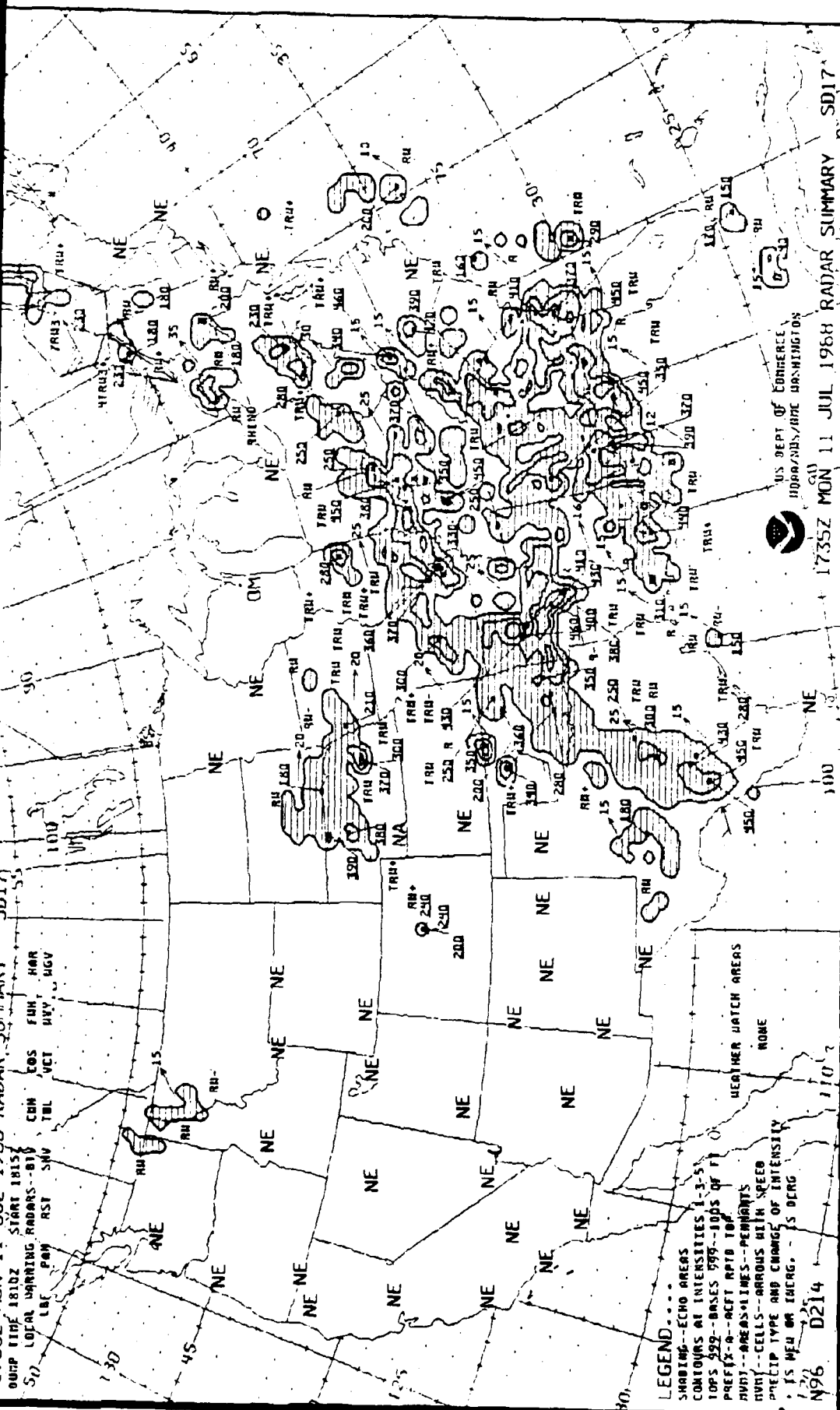
18Z MON 11 JUL 1988

18Z MON 11 JUL 1988

18Z MON 11 JUL 1988  
1800 - 0000 UTC  
0000 - 0600 UTC  
0600 - 1200 UTC  
1200 - 1800 UTC

Quasi-Solar





U.S. DEPT OF COMMERCE  
HARRISON/WHC WASHINGTON

call

1735Z MON 11 JUL 1988 RADAR SUMMARY SD17\*

**N96 D214**

1 FGFND

- SHARING--ECHO AREAS  
CONTOURS AT INTENSITIES 1-3-5  
TOPS 992--BASES 999--TOPS OF P  
PREFIX--A--ACT 997 TO  
HUNT--AREAS--LINES--PERMANENT  
HUNT--CELLS--ARROUS WITH SPEED  
HUNT--HUNT TYPE AND CHANGE OF INTENSITY  
IS NEW ON THERG. - IS BERG



2035Z MON 11 JUL 1988 RADAR SUMMARY

0000Z TIME 2105Z START 2112Z

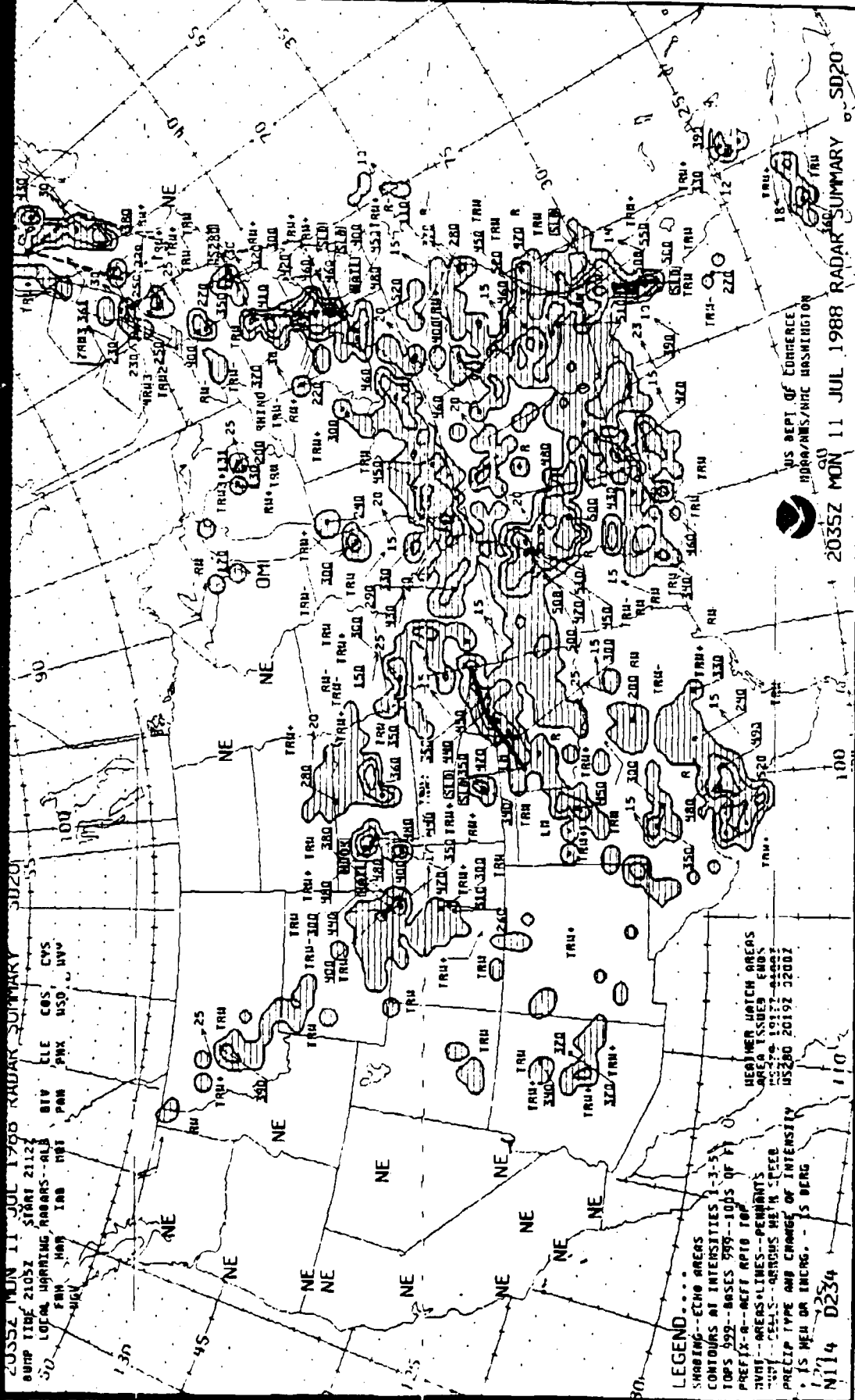
00 LOCAL WARNING RADARS--ALL

00 DIV ELE COS CYS

00 PAN PNK USD UVV

00 FNN HAN IAB HBT

00



LEGEND

SHADING--ECHO AREAS  
 CONTOURS AT INTENSITIES 1-3-5  
 TOPS 500--BASES 500--100S OF 1  
 PREFIX--R--REFL APD 100  
 INT--AREAS--LINES--PERMANENT  
 100--CELLS--AREAS WITH 100  
 PRECIP TYPE AND CHANGE OF INTENSITY  
 15 MEN OR ENCRG. - IS BERG

HEAVY HATCH AREAS  
 AREA ISSUED EMON  
 15 JUL 1988 2105Z  
 US280 20192 2200Z

US DEPT OF COMMERCE  
 NOAA/NWS/NHC WASHINGTON

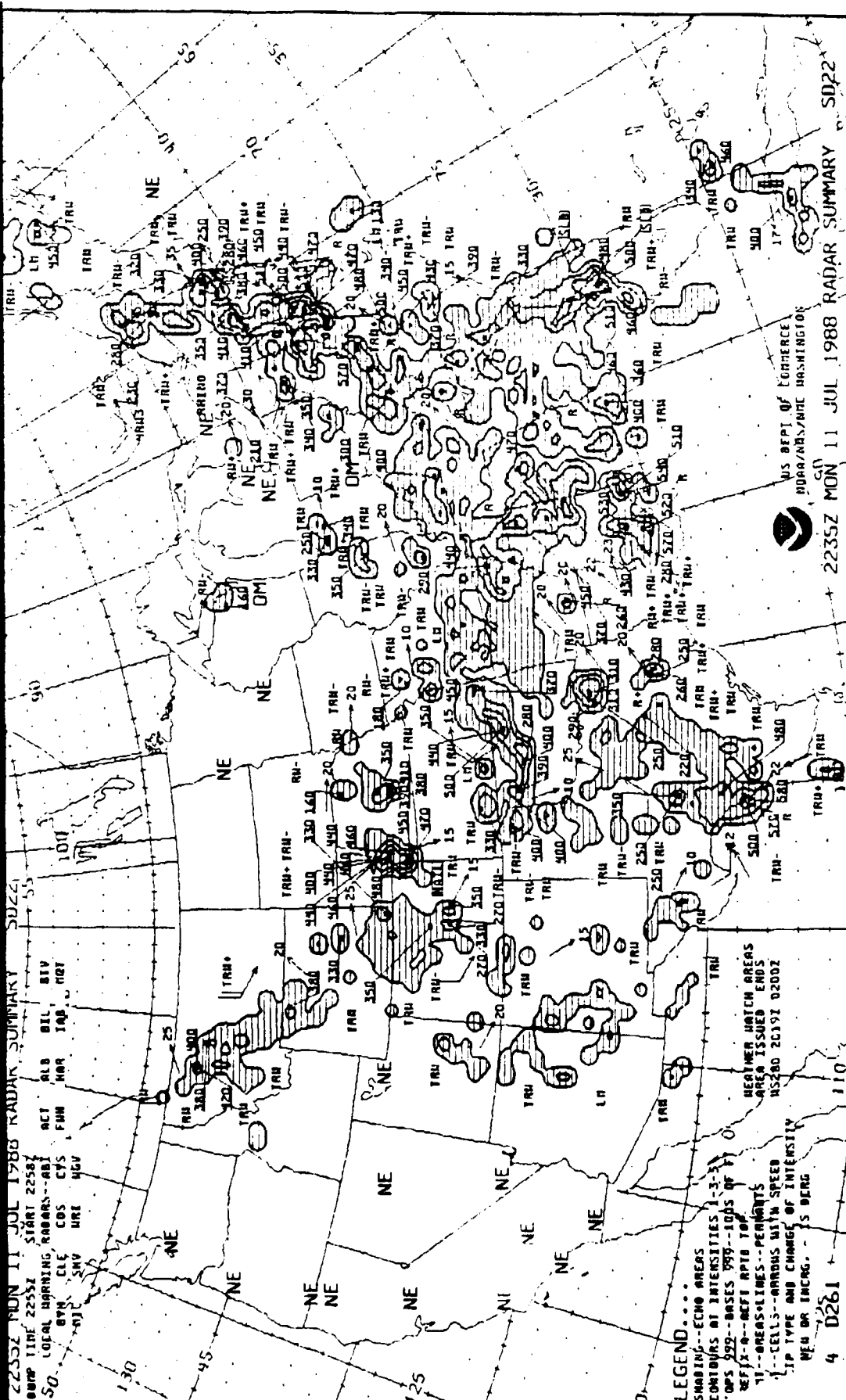
2035Z MON 11 JUL 1988 RADAR SUMMARY SD20

N114 D234



2235Z MON 11 JUL 1988 RADAR SUMMARY 50221

COMP TIME 2255Z START 2258Z  
 SO. LOCAL HARRING, RADARS--ABI  
 BYN CLE COS CYS FWH MNR TAP MGT  
 -01- SNV URE NGV





# 111111 DAILY WORK CHART

DATE 11 Jul 88

SIN	FCS1 HIGH	MIDLEVEL MOISTURE	HIGHLEVEL MOISTURE	FCS1 FROM	VALID TO	ALERT ISSUED AT	VEGETATION
72775 BIF	83	N	Y	22	03	1516Z	
72775 BIL	87	N	Y	22	03	↓	
72681 BUI	83	N	Y	22	03		
72683 BUI	93	N	N				
72775 SUC	96	N	Y?				
72469 DEN	87	N	Y	21	03	1517Z	
72469 COS	96	N	Y	21	03	↓	
72587 LAS	107	N	N				
72565 ABQ	91	Y	Y				
72374 PHX	106	N	Y	22	05	1518Z	
72274 TUS	98	Y	Y	22	05	↓	
72270 ELP	88	Y	Y				

June 7, 1988

07-12-1988 00:11:02

# DAILY SA LOG

XX\*ORD SA 1350 CLR 15 144/79/62/3104/997/ FEW CI  
XX\*ORD SA 1450 250 -SCT 15 147/82/58/2606/998/ 307 1001  
XX\*ORD SP 1529 40 SCT 250 -SCT 15 3610/998/ WSHFT 27 FROPA  
XX\*ORD SA 1550 40 SCT 250 -SCT 15 147/86/54/2408/998  
XX\*ORD SA 1650 250 -SCT 15 145/86/54/3007/997/ CB S WND24VM1  
XX\*ORD SA 1750 40 SCT 250 -SCT 15 141/87/54/2506/996/ CB S/ 907 1901  
XX  
XX\*ORD SA 1750 40 SCT 250 -SCT 15 141/87/54/2506/996/ CB S/ 907 1901  
XX  
XX\*ORD SA 1850 40 SCT 250 SCT 15 137/89/52/2706/995/ CB S WND24V33  
XX  
XX\*ORD SA 1950 40 SCT 250 SCT 15 134/89/52/3206/994/ CB S  
XX\*ORD SA 2050 40 SCT 250 SCT 15 134/89/50/3607/994/ CB S/ 605 1901  
XX\*ORD SA 2150 250 SCT 15 135/86/59/0610/994/ CB SE FEW CU  
XX\*ORD SA 2250 CLR 15 138/82/60/0410/995/ CB SE FEW CU CI  
XX\*ORD SA 2350 CLR 15 138/78/59/0310/995/ CB SE FEW AC CI/ 102 1971 90

YY\*DEN SA 1352 CLR 60 106/66/49/1710/005  
YY\*DEN SA 1450 CLR 70 103/71/48/1809/005/ 000 1001  
YY\*DEN SA 1552 CLR 60 096/76/48/2006/004  
YY\*DEN SA 1652 CLR 60 089/81/46/1308/003/ CU FRMG OMTNS S-NW  
YY\*DEN SA 1750 CLR 60 085/84/46/0809/002/ CB FRMG OMTNS S-NW/ 710 1003 S  
YY\*DEN SA 1851 CLR 50 078/86/47/0406/000/ CB TCU S-N  
YY\*DEN SA 1951 75 SCT E120 BKN 250 BKN 50 076/86/46/1007/999/ CB TCU S-N  
YYRWU S VIRGA SW  
YY\*DEN SA 2051 75 SCT 120 SCT E250 BKN 50 066/89/46/1505/997/ CB SE SW-N/  
YY714 1963  
YY\*DEN RS 2151 75 SCT E120 BKN 250 BKN 50T 070/85/41/0000/997/ TB51 OVHD RWU  
YYOCNL LTGCG W MOVG SE  
YY\*DEN SA 2250 75 SCT E120 BKN 250 BKN 30TRW- 099/71/54/2020/001/ CB OVHD-  
YYSE MOVG SE RB10  
YY\*DEN SP 2302 75 SCT 120 SCT E250 BKN 40 1711/001/TE01 MOVD SE REQ1  
YY\*DEN RS 2351 COR 75 SCT 120 SCT 250 SCT 50 089/79/52/1708/000/TE01 MOVD SE  
YYCB NW-NE-S RWU NE SE REQ1/ 00800 1963 89 RADAR 62149

07-12-1988 00:11:06

# DAILY FT LOG

\*IAD FT 111717 40 SCT 250 -BKN 6H 1806 OCNL 3H SLGT CHC C12 OVC  
 ITRWH G30. 05Z -X 250 -BKN 5H 2006 OCNL 3FH. 11Z MVFR H..  
 \*ORD FT 111717 40 SCT 100 SCT 3110 OCNL C40 BKN 100 BKN. 19Z 40 SCT 3606.  
 00Z CLR. 11Z VFR. 13Z MVFR CIG..  
 \*LGA FT 111717 45 SCT 90 SCT 5H 2414 OCNL C80 BKN 6H CHC C20 OVC  
 ITRW+A G45. 03Z C20 OVC 2F 2608 OCNL C6 X 1/2TRW+F G35. 11Z  
 IFR CIG F. 14Z MVFR H..  
 \*DEN FT 111818 30 SCT 250 SCT 1612 SLGT CHC C70 BKN TRW-A 640 AFT 20Z.  
 04Z 150 SCT 1910. 06Z CLR 1910. 12Z VFR..  
 \*DEN FT 111818 30 SCT 250 SCT 1612 SLGT CHC C70 BKN TRW-A 640 AFT 20Z.  
 04Z 150 SCT 1910. 06Z CLR 1910. 12Z VFR..  
 \*LGA FT 111717 45 SCT 90 SCT 5H 2414 OCNL C80 BKN 6H CHC C20 OVC  
 ITRW+A G45. 03Z C20 OVC 2F 2608 OCNL C6 X 1/2TRW+F G35. 11Z  
 IFR CIG F. 14Z MVFR H..  
 \*IAD FT 111717 40 SCT 250 -BKN 6H 1806 OCNL 3H SLGT CHC C12 OVC  
 ITRWH G30. 05Z -X 250 -BKN 5H 2006 OCNL 3FH. 11Z MVFR H..  
 \*ORD FT 111717 40 SCT 100 SCT 3110 OCNL C40 BKN 100 BKN. 19Z 40 SCT 3606.  
 00Z CLR. 11Z VFR. 13Z MVFR CIG..  
 \*SEA FT 111919 20 SCT C40 OVC 2211 OCNL C15 BKN 30 OVC 5RW-..  
 07Z C15 BKN 25 OVC 2208 CHC RW-.. 13Z MVFR CIG..  
 \*LAX FT 111919 025 BKN 2512 OCNL 25 SCT. 22Z CLR 2512. 02Z C18 BKN 2508  
 OCNL 18 SCT. 05Z C18 OVC. 13Z MVFR CIG..  
 \*IAD FT AMD 1 112117 2040Z 40 SCT 250 -BKN 4H 1606 OCNL C40 BKN CHC  
 C10 X 3/4TRW+A G50. 03Z -X 250 -BKN 5H 2406 OCNL 3FH. 11Z MVFR  
 H..  
 \*LGA FT AMD 1 112117 2125Z -X 45 SCT 90 SCT 3H 1812 OCNL C45 BKN CHC C10  
 OVC ITRW+A G50. 03Z C45 BKN 3H 2608 CHC C6 X 1/2TRW+F G35.  
 11Z IFR CIG F. 14Z MVFR H..  
 \*LGA FT 120024 -X 45 SCT C80 BKN 3H 1915 OCNL C45 BKN CHC C5 X 1/2TRW+A  
 G50. 02Z C45 BKN 3H 2208 OCNL C20 BKN 11/2FH CHC C8 X 1TRW+F G35  
 TIL 10Z. 18Z MVFR H..  
 \*IAD FT 120024 40 SCT C100 BKN 4H 1606 OCNL C40 BKN CHC C12 OVC  
 ITRWH G30. 04Z -X C250 BKN 4H 2506 OCNL C100 BKN CHC C20 BKN  
 2TRW-/RW-.. 08Z -X 250 -BKN 3H OCNL -X 11/2FH. 14Z C250 BKN 4H  
 2508. 18Z MVFR TRWH..  
 \*ORD FT 120024 120 SCT 0408. 04Z CLR OCNL 120 SCT 250 SCT.  
 15Z 100 SCT C250 BKN 0610 OCNL C100 BKN. 18Z VFR..

8  
:5070

BBBWX  
:LLWS ALERT FROM 112200Z TO 120300Z FOR  
GTF BIL 301  
CONDITIONS FAVORABLE FOR DEVELOPMENT OF CONVECTIVE LLWS. IF  
VIRGA, CB'S OR RW ARE OBSERVED OR REPORTED, EXPECT LLWS.  
:07111515 6392 0481

BBBWX  
:LLWS ALERT FROM 112100Z TO 120300Z FOR  
DEN CGS  
CONDITIONS FAVORABLE FOR DEVELOPMENT OF CONVECTIVE LLWS. IF  
VIRGA, CB'S OR RW ARE OBSERVED OR REPORTED, EXPECT LLWS.  
:07111515 6392 0482

BBBWX  
:LLWS ALERT FROM 112200Z TO 120300Z FOR  
PHX TUS  
CONDITIONS FAVORABLE FOR DEVELOPMENT OF CONVECTIVE LLWS. IF  
VIRGA, CB'S OR RW ARE OBSERVED OR REPORTED, EXPECT LLWS.  
:07111517 6392 0483

141524Z FID 2872 ID 075143 RTG KOS

AUSOO

.AUSOOUA 111921 2760/HOL

WBM 395-11 AUS-DEN (2216Z) RT: 1 ALTNT COS  
407-11 DEN-ONT (0127Z) RT: 1 ALTNT LAX  
390-11 ONT-DEN (0405Z) RT: 1 ALTNT NA

\*\*\* PART 01 OF 02 PARTS \*\*\*

\*\*\*\*\*  
\*\*\*\*\* ALERT \*\*\*\*\* ALERT \*\*\*\*\* ALERT \*\*\*\*\*  
\*\*\*\*\*

DEN LLWS ALERT FROM 112100Z TO 120300Z  
CONDITIONS FAVORABLE FOR DEVELOPMENT OF CONVECTIVE LLWS. IF  
VIRGA, CB'S OR RW ARE OBSERVED OR REPORTED, EXPECT LLWS.

COS LLWS ALERT FROM 112100Z TO 120300Z  
CONDITIONS FAVORABLE FOR DEVELOPMENT OF CONVECTIVE LLWS. IF  
VIRGA, CB'S OR RW ARE OBSERVED OR REPORTED, EXPECT LLWS.

\*\*\*\*\*

----- MAP FEATURES -----  
MAP FEATURES: UNITED STATES 111835Z-120600Z  
JET CORES AT 1200Z..FROM SLE(OREG) 350/26075 TO BOI(IDA)  
420/26065..FROM OKC(OK) 380/25080 TO PIA(IL) 420/26065 TO  
BUF(NY) 350/24075..SURFACE AT 1500Z..COLD FRONT SSWD FROM NRN  
IDA TO OFF NRN CALIF COAST, FRONT MOVING EWD AT  
20 KNOTS..LAYERED CLOUDS/R-/F BEHIND FRONT FROM WASH SWD TO NRN  
CALIF.. STRATUS OVER SRN CALIF COASTAL AREAS MOVING OFF-SHORE  
EARLY THEN MOVING BACK ONSHORE NEAR END OF PERIOD. COLD FRONT  
EXTENDS SSWD FROM WRN NY TO NRN IL TO SRN NEB THEN STATIONARY  
NWWD THEN NERN WYO TO NWRN MONT COLD FRONT MOVING EWD AT 15-20  
KNOTS..FEW TO SCATTERED (CHC SEVERE) DEVELOPING VCNTRY  
STATIONARY FROM FRONT FROM MONT SEWD TO NRN NEB. FEW TRW FROM  
AZ/NMEX NEWD INTO SERN WYO..SCATTERED TRW/RW OVER MOST OF AREA  
FROM TX/OK NEWD INTO NEW ENGLAND AND EWD TO NRN FLA.CHC HEAVY  
TO SEVERE TRW FROM SRN NEW ENGLAND TO SCAR BY 00Z.

----- ORIG-DEST-ALTNT-WEATHER -----  
AUS 1849 33 SCT 120 SCT E180 OVC 12 137/85/73/2107/996  
AUS SF 1753 32 SCT E180 OVC 12 140/84/74/1610/997/ 000 152/ 77  
AUS 1651 M29 BKN 43 BKN 140 OVC 12 144/82/73/1705/998  
AUS FT11 AMD 1 111917 1904Z 30 SCT C120 BKN 2010 OCNL C30  
BKN RW CHC C8 OVC 1TRW+. 00Z 40 SCT C120 BKN 2406 SLGT  
CHC TRW. 06Z C12 BKN 1906 SLGT CHC TRW. 11Z MVFR CIG..  
AUS NO 2/6 THR 35 DSPLCD 1200  
AUS NO 2/8 17-35 CLSD EXCP DAY/VFR+12500/BLO  
AUS NO 7/6 ARPT CLSD TO JET TRNG  
AUS NO 13/1 AUS TWR DOES NOT CNTRL THE RAMP AREA.  
PUSHBACK WILL BE AUZD BY UAL TUG OPERATOR. AS A  
COURTESY ADVISE GRND CNTRL ON APPROPRIATE ATC FREQ  
(RWK-DENTK 11 25-87 BY JWS)  
AUS NO 13/2 CONSIDERABLE JET FIGHTER TFC AT BERGSTROM  
A.F.B., LOCATED BTWN ARPT AND COLORADO RIVER. ALT SFC  
TO 3000 FT (PER DICK KRUEGER DENTK 01APR87)  
AUS NO 13/3 POSSIBLE TFC CONFLICT BTWN BERGSTROM  
A.F.B. TRAFFIC CUTTING ACROSS RWY 13R DPTR CORRIDOR.  
TFC AT 3000 FT WHEN NORTH OF CORRIDOR DESCENDS TO 1200  
FT SOUTH OF CORRIDOR. (PER DICK KRUEGER DENTK 01APR88)

AUS NO 13/4 TWY 'P' SOUTHWEST OF TWY 'D' FREQUENTLY  
CLSD FOR EQPT STORAGE.. HARDSTANDS BEHIND GATES 1, 3  
AND 5 USED AT NIGHT BY OTHER AIRCARRIER LAYOVER ACFT  
(DENTK DK CHIDD JWW 4/28/88)

DEN 1851 CLR 50 078/86/47/0406/000/CB TCU S-N  
DEN 1750 CLR 60 085/84/46/0809/002/CB FRMG OMTNS S-NW/ 710 1003  
5

DEN 1652 CLR 60 089/81/46/1308/003/CU FRMG OMTNS S-NW  
DEN FT11 111818 90 SCT 250 SCT 1612 SLGT CHC C70 BKN  
TRW-A G40 AFT 20Z. 04Z 150 SCT 1910. 06Z CLR 1910. 12Z  
VFR..

DEN NO 6/25 LDA LOC 35R OTS  
DEN NO 6/26 ILS DME 35R OTS  
DEN NO 6/38 LDA DME 35R OTS  
DEN NO 7/12 DEN ALS 35R OTS TIL 152000  
DEN NO 13/1 FOR PUSHBACK CLEARANCE AT GATE A-8 CALL  
UA RAMP ON 129.5. DEN PAGE 10-7 WILL BE CHANGED. (DENFO  
PB CHIDD JWW 6/16/88)  
DEN NO 13/2 FDC 8/2040 ILS 35R CRCLG VIS CAT C VIS 2  
3/4. CAT D VIS 3. ALT MINS 900-3  
DEN NO 13/3 CONSTRUCTION AREA - ON RAMP EAST AND  
SOUTHEAST OF THE B CONCOURSE. AREA EXTENDING 300 FT OUT  
FROM THE B CONCOURSE. THE VSR IS LOCATED AT THE EDGE OF  
THE OUTAGE AREA. GATES B19 AND B21 ARE OUT OF SERVICE  
WITH B20 TO BE OUT OF SERVICE BY 6/28/88. AREA IS  
LIGHTED AND BARICADED. TAXI W/CAUTION. DURATION,  
APPROX. 30 DAYS. (CHIDD.GC)

COS 1850 80 SCT 65 104/80/46/1209/008  
COS 1750 70 SCT 65 111/78/47/1307/010/ 705 1100 52  
COS 1650 CLR 65 119/75/45/1406/011/FEW CU SW-NW  
COS FT11 101818 70 SCT 250 SCT 1510 SLGT CHC C60 BKN  
TRW-A G40 AFT 20Z. 05Z 120 SCT 0110. 06Z CLR 0110. 12Z  
VFR..

COS NO 13/1 USE CAUTION TAXIING INTO THE RAMP FROM  
THE SOUTH. TWY A3 SIGN IS LOCATED SOUTH OF TWY A3. THE  
TWY SOUTH OF THE SIGN IS A PRIVATE TWY AND IS NOT AUZD  
FOR UAL ACFT  
COS NO 13/2 COS NOT AUZD FOR PILOT TRAINING FROM  
2300-0600 MDT

ONT 1850 -X 3HK 75/61/1804/002/ HK3  
ONT 1750 M17 BKN 2 1/2FH 69/61/2605/004/FH2  
ONT 1650 -X M13 OVC 21/2FH 65/60/2105/004/ FH2  
ONT FT11 111919 -X C18 BKN 3H 2710 OCNL 18 SCT. 20Z -X  
3H. 23Z -X 5H 2712. 02Z CLR 2712. 05Z CLR. 10Z -X C11 OVC  
3FH. 13Z MVFR CIG FH..  
ONT NO 6/6 ONT ILS GS RY26R UNUSBL BLO 1089 MEL

LAX 1850 M24 OVC 9 171/68/58/2409/004/ CITY 70  
LAX 1754 M24 OVC 9 171/69/59/3105/004/ 108 15// 63/CITY 69  
LAX 1652 M23 OVC 9 170/68/58/1504/003/ CITY 68  
LAX FT11 111919 C25 BKN 2512 OCNL 25 SCT. 22Z CLR 2512.  
02Z C18 BKN 2508 OCNL 18 SCT. 05Z C18 OVC. 13Z MVFR CIG..  
LAX NO 7/2 LAX 6L-24R CLSD 0600-1300 DLY EFF  
7/11-7/15  
LAX NO 13/1 BTWN TRMNLs. IN THE ALLEYS. 180 DEG TURNS  
UNDER PWR ARE NOT PERMITTED. IF A REVERSAL IS RQD.  
SHUT DOWN ENGINES AND REQUEST A TOW. (LAXFO RPS/CHIDD  
JWW 9/15/87)  
LAX NO 13/2 NOTIFY LAX TWR WHEN YOU ARE NUMBER 1 FOR  
TKOF IF YOU SUSPECT THIS WILL HELP ENSURE SEQUENCE  
(EXOVF TG/CHIDD JWW 9/18/87)  
LAX NO 13/3 CONTACT LAX STATION OPERATIONS FOR  
PUSHBACK CLEARANCE AT GATES 70A, 70B, 72A, 72B, 74 AND

80 THRU 84. IF PUSHBACK FROM GATE 74 WILL INTRUDE INTO  
TWY SOUTH OF THE SATELLITE, CALL GRND CNTRL ALSO FOR  
CLEARANCE (01/25/88 JR PER GARY MEERMANS LAXFO)  
LAX NO 13/4 WHEN POSSIBLE, AVOID FLYING OVER OR NEAR  
THE HOLLYWOOD BOWL BETWEEN 1800-2400 PDT, MONDAYS THRU  
SUNDAYS. THE AREA IS LOCATED 5NM SE OF BUR AND 15NM NNE  
OF LAX AND IS VISUALLY DEFINED BY TWIN CROSSED WHITE

\*\*\* END PART 01 OF 02 \*\*\*

EISDR 111924 6977 0634

1415272 AGENT KOS ID 075143 FROM PID 2872 TO PID 6891

141526Z PID 2872 ID 075143 RTG KOS

AUSCO  
LAUSCOUA 111921 2760/HOL

WPM	395-11	AUS-DEN (2216Z)	RT: 1	ALTNT	COS
	407-11	DEN-ONT (0127Z)	RT: 1	ALTNT	LAX
	390-11	ONT-DEN (0405Z)	RT: 1	ALTNT	NA

\*\*\* PART 02 OF 02 PARTS \*\*\*

SEARCHLIGHT BEAMS IN THE SKY AND WHITE STROBE LIGHTS ON  
THE GROUND. EFF THRU 17SEP88.  
(LAXFO-MEERMANS, TOMKO, 27JUN88)  
LAX NO 13/5 FDC 8/937 VOR RWY 7L/R PROC NA  
LAX NO 99/99 WHEN TWY 80V CLSD DUE TO CONSTRUCTION,  
TKOF RWY6L AVBL FM TWY 75V (7000FT AVBL). LDG RWY24R  
LAST EXIT TWY 75V (7000FT AVBL). OBTAIN MEYER WTS  
RWY6LX (7000FT AVBL TKOF) AND RWY24RX (7000FT AVBL LDG)  
FROM CHIDD OR CRT. (EXOVF JP 6/01/88).

----- DRIFTDOWN ALTERNATES -----  
GJT 1850 CLR 70 094/87/45/1208/002/FEW TCU AC CI  
GJT 1750 150 SCT 70 101/85/45/1908/005/ TCU DSNT E/ 114 1280 66  
GJT 1652 150 SCT 70 110/79/48/1209/007  
GJT FT11 111818 80 SCT 250 SCT 1410. 20Z 80 SCT 250 SCT  
2810 SLGT CHC C70 BKN TRW-A 045. 04Z 130 SCT 1109. 06Z  
CLR 1310. 12Z VFR..  
GJT NO 13/1 TOWER CLSD 0400-1200Z (2200-0600MST). WHN  
TWR CLSD/ ALL NAVAIDS MONITORED (04/03/88 JR)  
GJT NO 13/2 SPECIAL TAKEOFF ENGINE OUT PROCEDURE..  
INSURE JNC VOR OPERATING PROPERLY (CHIDD 6/18/86DR)

LAS 1853 CLR 30 092/98/47/1912021/990  
LAS 1751 CLR 30 098/96/49/2016024/991/ 303 83  
LAS 1651 CLR 30 097/94/50/1816024/991/HAZY  
LAS FT11 111919 CLR 2118032. 04Z CLR 2014. 13Z VFR CLR..  
LAS NO 13/2 DUE TO TRAFFIC VOLUMES ATC WILL INCRS USE  
OF RWY 07 DPTRS WHILE ON NORTH FLOW (1R/1L). TO REDUCE  
TAXI COMPLEXITY, EXPECT ATC ROTS FOR RWY 07 DPTRS FM

TWY M OR TWY X (EXOVF JP 4/27/88)

PSP 1846 -X 8 96/M/0908/990/ HK2

PSP 1750 -X 8 95/M/1207/991/ HK2

PSP 1646 CLR 8 94/M/3604/991/ HK ALQDS

PSP FT11 111919 CLR 1212 OCNL 5H. 01Z CLR 3020. 06Z CLR.  
13Z VFR..

PSP NO 13/1 TOWER CLSD 0600-1400Z(2300-0700PDT). WHN  
TWR CLSD/CONTACT WEATHER OBSERVER ON 129.2 FOR WEATHER  
AND TRAFFIC INFORMATION. ALL NAVAIDS MONITORED  
(04/03/88 JR)

PSP NO 13/2 WHEN DPTG AFTER TWR CLSD OBTAIN CLRNC BY  
ONE OF THE FLWG: FM ATC DURING APPCH INTO PSP ..OR..  
TELEPHONE BFR DPTR PSP PHONE NR 805-947-4101 ..OR..  
TRANSMIT ONT RADIO ON 122.1 AND RECEIVE ON 115.5 (PSP  
OMNI - ADJUST VOLUME TO MAX) ..OR.. IF THOSE FAIL  
CONTACT CHIDD FOR FURTHER ASSISTANCE. WHEN DPTG AFTER  
TOWER CLSD BROADCAST ON FREQ 119.7 (25AUG86TJK) IF  
EITHER ONE INACCESSABLE USE 1-800-992-7433 (RIVERSIDE  
FSS).

PSP NO 13/3 ADHERE STRICTLY TO INSTRUMENT APPROACH  
PROCEDURES WHENEVER RADAR GUIDANCE IS NOT AVBL. WHEN  
CLEARED FOR AN APPROACH, IF ON A UNPUBLISHED ROUTE OF  
RADAR VECTOR, MAINTAIN THE LAST ASSIGNED ALTITUDE UNTIL  
ESTABLISHED ON A PUBLISHED ROUTE OR INSTRUMENT APPROACH  
(11/25/86 J. NEFF)

PSP NO 13/4 WHEN ON APPCH TO RWY 30 RQST PSP APPCH TO  
TURN ON VASI AT CATHEDRAL CITY OR WITHIN 3NM (PER PSP  
TWR JPB 02/17/87)

PSP NO 13/5 WIDEBODY DIVERSIONS CAN BE HANDLED ON A  
REFUEL AND GO BASIS ONLY. (NO CARGO LOADERS AVAILABLE)  
(TJF.26JUN87)

PSP NO 13/6 CREW CAN CALL EARLY FOR CLRNC 0650 LCL  
121.9

PSP NO 13/7 ALL PSP OPERATIONS NOW USE GATE 1 (LL  
CHIDD 01/28/88)

PSP NO 13/8 B727 DPTG PSP ON PALM SPRINGS 1 DPTR SET  
CLMB THRUST IN LIEU OF QUIET EPR (02/01/88 JR PER TOM  
WYATT DENTK)

PSP NO 13/9 FDC 8/1281 IFR TKOF MINS RWY 30 3000-2 OR  
STD WITH MIN CLB OF 360 FT PER NM TO 4000. IFR DPTR  
PROC RWY 30 TURN RIGHT DRCT PSP VORTAC. THEN VIA V137  
TO TRM VORTAC. CLB TO MEA OR MCA FOR RTE OF FLT. OR  
HOLD E. RT. 287 INBND

PSP NO 13/10 CRANE OPERATING 75' AGL. LOCATED APPROX  
1500' NE OF THE APPCH END RWY 12. OPERATES MON-FRI  
1300Z-2300Z UNTIL APROX 21JUN88. WILL BE LOWERED WHEN  
NOT OPERATIONAL. (RK..6JUN)

----- DEST AREA WEATHER -----

PUB 1850 CLR 90 090/87/50/1808/999/CB N CU SW-NW

BJC 1848 80 SCT 65 86/48/1110/002

TAD 1850 CLR 60 104/82/42/0605/008/FEW CU

PMD 1846 CLR 20 E2115/997/H ALQDS

WJF 1850 CLR 30 126/86/45/2420/998

RIV 1855 -X 3H 161/78/58/2902/003/H2

SBD 1855 -X 21/2H 154/80/60/3002/H2

----- ENROUTE TERMINAL FORECASTS -----

OKC FT11 111717 40 SCT C100 OVC 1610 CHC C20 OVC 2TRW.

03Z 100 SCT 250 SCT 1508. 11Z VFR..

DFW FT11 111717 12 SCT C25 BKN 1808 OCNL C12 BKN 3R-F CHC  
TRW. 20Z C30 BKN 1808 CHC C10 X 2TRW. 04Z C15 OVC 1808  
CHC TRW. 11Z IFR CIG TRW. 15Z MVFR..

AMA FT11 111717 45 SCT 1808 SLGT CHC TRW AFT 21Z. 02Z 120  
SCT 1608. 11Z VFR..



PUB FT11 111818 90 SCT 250 SCT 1410 SLGT CHC C70 BKN  
TRW-A G40 AFT 20Z. 05Z 120 SCT. 06Z CLR. 12Z VFR..  
CYS FT11 AMD 1 111918 1905Z 50 SCT 100 SCT C250 BKN 1210  
OCNL C50 BKN CHC TRW- G30. 03Z 60 SCT 250 SCT. 12Z VFR NO  
NO CIG..  
PHX FT11 111818 CLR. 22Z 90 SCT 2908. 03Z 120 SCT 2908.  
06Z CLR. 12Z VFR CLR..

----- PIREPS -----  
MLC UA /OV P60 270010/TM 1728/FL310/TP B737/TB LGT RIME  
217 /OV BFF 1916 350 /TA -48/WV 270031/TB SMTH

----- ENROUTE NOTAMS -----  
ENROUTE NOTAM 13 EFF 18APR/1521Z TO  
8/1091 FDC AIRWAY TX. V68 V198 COMFY TX INT TO SAT VORTAC MEA  
4000. (EXODD 18APR88 AR)

ENROUTE NOTAM 04 EFF 02MAY/1951Z TO  
FDC 8/1217 AIRWAYS, TX. V161 BETWEEN MILSAY /MOP/ VORTAC AND  
POLYA INT., TX. MOCA 2500.

ENROUTE NOTAM 25 EFF 01APR/2151Z TO UFN  
FDC 8/967 V74 FROM TULSA, OK VORTAC TO OWETA, OK INT. MOCA TO  
READ 2300FT

ENROUTE NOTAM 31 EFF 29JUN/1459Z TO UFN  
FDC 8/1912 WHEN EL PASO TX FSS IS CLSD THE FLWG AWYS NOT AUTH:  
V280 PINON NM. VORTAC TO EL PASO TX. VORTAC, V19 TRUTH OR  
CONSEQUENCES NM. VORTAC TO NEWMAN TX. VORTAC, V560 NEWMAN TX.  
VORTAC TO CARLSBAD NM. VORTAC.

ENROUTE NOTAM 34 EFF - TO  
CHART LO(09) GLEND INT. REDESIG. LEFT TURNS. 064 DEG INBND

ENROUTE NOTAM 12 EFF - TO  
SNA (SANTA ANA) VOR O/S INDEFINITELY

\*\*\* END PART 02 OF 02 \*\*\*

-  
E13DR 111928 6977 0635

141528Z AGENT KOS ID 075143 FROM PID 2872 TO PID 6891

141530Z AGENT KOS ID 075143 FROM PID 2872 TO PID 6891

141529Z PID 2872 ID 075143 RTG KOS

2  
SEA2Z  
.SEAQUA 111821 3313/KUS

WBM 236-11 SEA-DEN (2214Z) RT: 1 ALTNT COS

\*\*\* PART 01 OF 01 PARTS \*\*\*

\*\*\*\*\*  
\*\*\*\*\* ALERT \*\*\*\*\* ALERT \*\*\*\*\* ALERT \*\*\*\*\*  
\*\*\*\*\*

DEN LLWS ALERT FROM 112100Z TO 120300Z  
CONDITIONS FAVORABLE FOR DEVELOPMENT OF CONVECTIVE LLWS. IF  
VIRGA, CB'S OR RW ARE OBSERVED OR REPORTED, EXPECT LLWS.

COS LLWS ALERT FROM 112100Z TO 120300Z  
CONDITIONS FAVORABLE FOR DEVELOPMENT OF CONVECTIVE LLWS. IF  
VIRGA, CB'S OR RW ARE OBSERVED OR REPORTED, EXPECT LLWS.

\*\*\*\*\*

----- MAP FEATURES -----  
MAP FEATURES UNITED STATES 111103Z-120000Z  
JET CORE AT 11/00Z....NO WINDS GREATER THAN 70KTS OBSERVED WITH  
GENERAL WESTERLY FLOW ACROSS NORTHERN 1/3 OF U.S. AND LIGHT AND  
VARIABLE FLOW SOUTHERN 2/3....SURFACE PATTERN AT 11/06Z....WEAK  
PACIFIC FRONT NEAR IDAHO/WASH BORDER....SECOND FRONT ACROSS  
CENTRAL MICH THRU CHICAGO BECOMING STATIONARY ACROSS  
IOWA/NEBRASKA....ASSOCIATED WX....A.M. STRATUS WEST COASTAL  
STATIONS....WIDESPREAD A.M. HAZE/GF EAST 1/3 OF U.S....CB OTL  
18Z-00Z....ISOLD P.M. CB'S MOST OF EASTERN 2/3 U.S. EXCEPT NONE  
EXPECTED MINN/WISC/MICH/NORTHERN ILL/NORTHERN  
INDIANA....GREATER THAN ISOLD COVERAGE EXPECTED  
SD/NE/WY/MT/ID....SECOND AREA GREATER THAN ISOLD PENN NORTHWARD  
THRU NEW ENGLAND....THIRD AREA GREATER THAN ISOLD ACROSS GULF  
COASTAL STATES....OPBWX/GH

----- ORIG-DEST-ALTNT-WEATHER -----  
SEA 1750 M16 BKN 40 OVC 10R- 140/56/53/2209/995/RB20 21200 15//  
54

SEA 1650 M20 BKN 60 OVC 20 135/58/50/2112/993

SEA 1549 M21 BKN 60 OVC 20 133/56/50/2013/993

SEA FT11 111010 13 SCT C22 OVC 2108 OCNL C13 BKN 5R-F CHC  
C6 BKN 3L-F. 04Z MVFR CIG..

SEA NO 13/1 ALL B-747'S TAXIING TO/FROM GATES N-3 AND  
N-6 MUST TAXI ON THE NORTH AND EAST SIDE OF THE NORTH  
SATELLITE. SEAFO JM (JJD)

DEN 1750 CLR 60 085/84/46/0809/002/CB FRMG OMTNS S-NW/ 710 1003  
5

DEN 1652 CLR 60 089/81/46/1308/003/CU FRMG OMTNS S-NW

DEN 1552 CLR 60 096/76/48/2006/004

DEN FT11 111818 90 SCT 250 SCT 1612 SLGT CHC C70 BKN  
TRW-A G40 AFT 20Z. 04Z 150 SCT 1910. 06Z CLR 1910. 12Z  
VFR..

DEN NO 6/25 LDA LOC 35R QTS  
DEN NO 6/26 ILS DME 35R QTS

DEN NO 6/38 LDA DME 35R QTS  
 DEN NO 7/11 ALS 35R QTS TIL 152000  
 DEN NO 7/12 DEN ALS 35R QTS TIL 152000  
 DEN NO 13/1 FOR PUSHBACK CLEARANCE AT GATE A-8 CALL  
 UA RAMP ON 129.5. DEN PAGE 10-7 WILL BE CHANGED. (DENFO  
 PB CHIDD JWW 6/16/88)  
 DEN NO 13/2 FDC 8/2040 ILS 35R CRCLG VIS CAT C VIS 2  
 3/4. CAT D VIS 3. ALT MINS 900-3  
 DEN NO 13/3 CONSTRUCTION AREA - ON RAMP EAST AND  
 SOUTHEAST OF THE B CONCOURSE. AREA EXTENDING 300 FT OUT  
 FROM THE B CONCOURSE. THE VSR IS LOCATED AT THE EDGE OF  
 THE OUTAGE AREA. GATES B19 AND B21 ARE OUT OF SERVICE  
 WITH B20 TO BE OUT OF SERVICE BY 6/28/88. AREA IS  
 LIGHTED AND BARICADED. TAXI W/CAUTION. DURATION,  
 APPROX. 30 DAYS. (CHIDD.GC)

COB 1750 70 SCT 65 111/78/47/1307/010/ 705 1100 52  
 COB 1650 CLR 65 119/75/45/1406/011/FEW CU SW-NW  
 COB 1550 CLR 65 122/73/51/1007/011/FEW CU SW-W  
 COB FT11 101818 70 SCT 250 SCT 1510 SLGT CHC C60 BKN  
 TRW-A G40 AFT 20Z. 05Z 120 SCT 0110. 06Z CLR 0110. 12Z  
 VFR..  
 COB NO 13/1 USE CAUTION TAXIING INTO THE RAMP FROM  
 THE SOUTH. TWY A3 SIGN IS LOCATED SOUTH OF TWY A3. THE  
 TWY SOUTH OF THE SIGN IS A PRIVATE TWY AND IS NOT AUZD  
 FOR UAL ACFT  
 COB NO 13/2 COB NOT AUZD FOR PILOT TRAINING FROM  
 2300-0600 MDT

----- DEST AREA WEATHER -----  
 GGT 1750 150 SCT 70 101/85/45/1908/005/ TCU DSNT E/ 114 1280 60  
 PUB 1750 CLR 90 100/83/50/1606/001/FEW CU SW-NW MDT CU NW/ 714  
 1200 54  
 BJC 1645 60 SCT 60 79/44/1507/003/ FEW CI NW KH ALDGS  
 TAD 1650 CLR 60 118/76/48/1307/011

----- ENROUTE TERMINAL FORECASTS -----  
 GEG FT11 111010 C250 BKN 2010. 19Z 50 SCT C100 BKN 2214  
 OCNL C50 BKN CHC C40 BKN RW-. 04Z VFR..  
 BDI FT11 111818 100 SCT 200 -BKN 3308. 00Z CFP 60 SCT  
 C100 BKN 3312 SLGT CHC RW-. 06Z 100 SCT C200 BKN 3008.  
 12Z VFR CIG ABV 100..  
 RNO FT11 111010 CLR. 19Z 250 -BKN 2718028. 04Z VFR CLR..  
 IDA FT11 110909 100 SCT 200 SCT 2008. 21Z 60 SCT 100 SCT  
 C200 BKN 2612 SLGT CHC TRW- G35. 10Z CFP 50 SCT C100 BKN  
 2315 SLGT CHC RW-. 12Z VFR CIG ABV 100..  
 SLC FT11 111818 CLR 1815G28. 05Z CLR 1612G19. 12Z VFR  
 WND..  
 CYS FT11 111818 50 SCT 250 -BKN 1710. 21Z 50 SCT 100 SCT  
 C250 BKN 1612 OCNL C50 BKN CHC TRW- G30. 03Z 60 SCT 250  
 SCT. 12Z VFR NO CIG..

----- PIREPS -----  
 GEG UA /OV GEG 180060/TM 1645/FL290/TP MD80/TB MDT...ZSE  
 UA0887 /OV BFF 30S 1650 F310/TB LT-MOD

----- ENROUTE NOTAMS -----  
 ENROUTE NOTAM 01 EFF 11JUL/1230Z TO 12JUL/0200Z  
 A1011/88 FZSE WARNING AREA W570 LOCATED OFF THE COAST OF OREGON  
 ACTIVATED SFC THRU FL500

ENROUTE NOTAM 02 EFF 11JUL/1230Z TO 12JUL/2130Z  
 A1011/88 FZSE WARNING AREA W237A/B LOCATED OFF THE COAST OF  
 WASHINGTON ACTIVATED SFC THRU FL240

ENROUTE NOTAM 34 EFF - TO

CHART LO(09) GLENO INT, REDESIG, LEFT TURNS, 064 DEG INBND

\*\*\* END PART 01 OF 01 \*\*\*

EISDR 111825 7317 0986

141528Z PID 2872 ID 075143 RTG KOS

MLIOG  
.MLIOZUA 111913 187

WBM 862-11 MLI-DEN (2212Z) RT: 1 ALTNT COS

\*\*\* PART 01 OF 01 PARTS \*\*\*

\*\*\*\*\*  
\*\*\*\*\* ALERT \*\*\*\*\* ALERT \*\*\*\*\* ALERT \*\*\*\*\*  
\*\*\*\*\*

DEN LLWS ALERT FROM 112100Z TO 120300Z  
CONDITIONS FAVORABLE FOR DEVELOPMENT OF CONVECTIVE LLWS. IF  
VIRGA, CB'S OR RW ARE OBSERVED OR REPORTED, EXPECT LLWS.

COS LLWS ALERT FROM 112100Z TO 120300Z  
CONDITIONS FAVORABLE FOR DEVELOPMENT OF CONVECTIVE LLWS. IF  
VIRGA, CB'S OR RW ARE OBSERVED OR REPORTED, EXPECT LLWS.

\*\*\*\*\*

----- MAP FEATURES -----  
MAP FEATURES UNITED STATES 111835Z-120600Z  
JET CORES AT 1200Z..FROM SLE(OREG) 350/26075 TO BOI(IDA)  
420/26065..FROM OKC(OK) 380/25080 TO PIA(IL) 420/26065 TO  
BUF(NY) 350/24075..SURFACE AT 1500Z..COLD FRONT SSWD FROM NRN  
IDA TO OFF NRN CALIF COAST. FRONT MOVING EWD AT  
20KNOTS..LAYERED CLOUDS/R-/F BEHIND FRONT FROM WASH SWD TO NRN  
CALIF.. STRATUS OVER SRN CALIF COASTAL AREAS MOVING OFF-SHORE  
EARLY THEN MOVING BACK ONSHORE NEAR END OF PERIOD. COLD FRONT  
EXTENDS SWWD FROM WRN NY TO NRN IL TO SRN NEB THEN STATIONARY  
NWWD THRU NERN WYO TO NWRN MONT COLD FRONT MOVING EWD AT 15-20  
KNOTS..FEW TO SCATTERED (CHC SEVERE) DEVELOPING VCNTY  
STATIONARY FROM FRONT FROM MONT SEWD TO NRN NEB. FEW TRW FROM  
AZ/NMEX NEWD INTO SERN WYO..SCATTERED TRW/RW OVER MOST OF AREA  
FROM TX/OK NEWD INTO NEW ENGLAND AND EWD TO NRN FLA.CHC HEAVY  
TO SEVERE TRW FROM SRN NEW ENGLAND TO SCAR BY 00Z.

----- ORIG-DEST-ALTNT-WEATHER -----  
MLI 1853 250 -SCT 20 139/89/56/3606/996/FEW CU TCU AND CB TOPS  
DSNT E-SE  
MLI 1753 250 -SCT 20 144/88/55/3408/997/TCU E-S FEW CU ALQDS/  
703 1202  
MLI 1652 250 -SCT 20 147/86/56/3208/998/TCU SE HRZN  
MLI FT11 111717 CLR 3606 OCNL 40 SCT. 07Z 25 SCT 80 SCT.  
09Z C25 BKN 80 BKN 1706 CHC C20 OVC 3RW/TRW. 11Z MVFR CIG  
TRW..  
MLI NO 13/1 TOWER CLSD 0400-1100Z(2300-0600CDT). WHN  
TWR CLSD/ CONTACT UA PERSONNEL ON 131.2 FOR TRAFFIC AND  
WEATHER INFORMATION, ILS 9 UNMONITORED (04/03/88 JR)  
MLI NO 13/2 RAMP CONST PHASE-1: NORTH RAMP CLOSED  
FROM TXWY BRAVO TO TXWY ALPHA. TXWY BRAVO OPEN AT ALL  
TIMES. TXWY ALPHA CLSD FROM NORTH RAMP TO RWY 5-23.  
PHASE-1 COMPLETION MID JUNE. RWS 5/16/88.

DEN 1851 CLR 50 078/86/47/0406/000/CB TCU S-N  
DEN 1750 CLR 60 085/84/46/0809/002/CB FRMG OMTNS S-NW/ 710 1003

5  
 DEN 1652 CLR 60 089/81/46/1308/003/CU FRMG OMTNS S-NW  
 DEN FT11 111818 90 SCT 250 SCT 1612 SLGT CHC C70 BKN  
 TRW-A G40 AFT 20Z. 04Z 150 SCT 1910. 06Z CLR 1910. 12Z  
 VFR..  
 DEN NO 6/25 LDA LOC 35R OTS  
 DEN NO 6/26 TLS DME 35R OTS  
 DEN NO 6/38 LDA DME 35R OTS  
 DEN NO 7/12 DEN ALS 35R OTS TIL 152000  
 DEN NO 13/1 FOR PUSHBACK CLEARANCE AT GATE A-8 CALL  
 UA RAMP ON 129.5. DEN PAGE 10-7 WILL BE CHANGED. (DENFO  
 PB CHIDD JWW 6/16/88)  
 DEN NO 13/2 FDC 8/2040 ILS 35R CRCLG VIS CAT C VIS 2  
 3/4. CAT D VIS 3. ALT MINS 900-3  
 DEN NO 13/3 CONSTRUCTION AREA - ON RAMP EAST AND  
 SOUTHEAST OF THE B CONCOURSE. AREA EXTENDING 300 FT OUT  
 FROM THE B CONCOURSE. THE VSR IS LOCATED AT THE EDGE OF  
 THE OUTAGE AREA. GATES B19 AND B21 ARE OUT OF SERVICE  
 WITH B20 TO BE OUT OF SERVICE BY 6/28/88. AREA IS  
 LIGHTED AND BARCADED. TAXI W/CAUTION. DURATION,  
 APPROX. 30 DAYS. (CHIDD.GC)

COS 1850 80 SCT 65 104/80/46/1209/008  
 COS 1750 70 SCT 65 111/78/47/1307/010/ 705 1100 52  
 COS 1650 CLR 65 119/75/45/1406/011/FEW CU SW-NW  
 COS FT11 101818 70 SCT 250 SCT 1510 SLGT CHC C60 BKN  
 TRW-A G40 AFT 20Z. 05Z 120 SCT 0110. 06Z CLR 0110. 12Z  
 VFR..  
 COS NO 13/1 USE CAUTION TAXIING INTO THE RAMP FROM  
 THE SOUTH. TWY A3 SIGN IS LOCATED SOUTH OF TWY A3. THE  
 TWY SOUTH OF THE SIGN IS A PRIVATE TWY AND IS NOT AUZD  
 FOR UAL ACFT  
 COS NO 13/2 COS NOT AUZD FOR PILOT TRAINING FROM  
 2300-0600 MDT

----- DEST AREA WEATHER -----  
 GJT 1850 CLR 70 094/87/45/1208/002/FEW TCU AC CI  
 PUB 1850 CLR 90 090/87/50/1808/999/CB N CU SW-NW  
 BJC 1848 80 SCT 65 86/48/1110/002  
 TAD 1850 CLR 60 104/82/42/0605/008/FEW CU

----- ENROUTE TERMINAL FORECASTS -----  
 ORD FT11 111717 40 SCT 100 SCT 3110 OCNL C40 BKN 100 BKN.  
 19Z 40 SCT 3606. 00Z CLR. 11Z VFR. 13Z MVFR CIG..  
 OMA FT11 111717 80 SCT 250 -BKN 1207 OCNL C80 BKN. 20Z  
 C80 BKN 1007 OCNL C20 OVC CHC C10 OVC 1TRW. 06Z 80 SCT  
 250 SCT 0906. 11Z VFR..  
 MSP FT11 111717 40 SCT 250 SCT. 00Z 100 SCT C250 BKN OCNL  
 C100 BKN. 08Z C80 BKN CHC C40 BKN RW-/TRW-. 11Z VFR TRW..

----- ENROUTE NOTAMS -----  
 ENROUTE NOTAM 50 EFF 30JUN/1988 TO  
 CHART LO(08) PERRY 1A NDB HOLDING DESIG. HOLD NORTHWEST, LEFT  
 TURNS. 130 DEG INBND

ENROUTE NOTAM 34 EFF - TO  
 CHART LO(09) GLENO INT, REDESIG. LEFT TURNS. 064 DEG INBND

\*\*\* END PART 01 OF 01 \*\*\*

EISDR 111916 6417 0798

141526Z PID 2872 ID 075143 RTG KOS

④ IAHOO  
.IAHOOUA 111915 2699/HAL

WBM 949-11 IAH-DEN (2222Z) RT: 1 ALTNT COS

\*\*\* PART 01 OF 01 PARTS \*\*\*

\*\*\*\*\*  
\*\*\*\*\* ALERT \*\*\*\*\* ALERT \*\*\*\*\* ALERT \*\*\*\*\*  
\*\*\*\*\*

DEN LLWS ALERT FROM 112100Z TO 120300Z  
CONDITIONS FAVORABLE FOR DEVELOPMENT OF CONVECTIVE LLWS. IF  
VIRGA, CB'S OR RW ARE OBSERVED OR REPORTED, EXPECT LLWS.

COS LLWS ALERT FROM 112100Z TO 120300Z  
CONDITIONS FAVORABLE FOR DEVELOPMENT OF CONVECTIVE LLWS. IF  
VIRGA, CB'S OR RW ARE OBSERVED OR REPORTED, EXPECT LLWS.

\*\*\*\*\*

----- MAP FEATURES -----

MAP FEATURES UNITED STATES 111835Z-120600Z  
JET CORES AT 1200Z..FROM SLE(OREG) 350/26075 TO BOI(IDA)  
420/26065..FROM OKC(OK) 380/25080 TO PIA(IL) 420/26065 TO  
BUF(NY) 350/24075..SURFACE AT 1500Z..COLD FRONT SSWD FROM NRN  
IDA TO OFF NRN CALIF COAST, FRONT MOVING EWD AT  
20 KNOTS..LAYERED CLOUDS/R-/F BEHIND FRONT FROM WASH SWD TO NRN  
CALIF.. STRATUS OVER SRN CALIF COASTAL AREAS MOVING OFF-SHORE  
EARLY THEN MOVING BACK ONSHORE NEAR END OF PERIOD. COLD FRONT  
EXTENDS SSWD FROM WRN NY TO NRN IL TO SRN NEB THEN STATIONARY  
NWWD THRU NEEN WYO TO NRN MONT COLD FRONT MOVING EWD AT 15-20  
KNOTS..FEW TO SCATTERED (CHC SEVERE) DEVELOPING VCNTY  
STATIONARY FROM FRONT FROM MONT SEWD TO NRN NEB. FEW TRW FROM  
AZ/NMEX NEWD INTO SERN WYO..SCATTERED TRW/RW OVER MOST OF AREA  
FROM TX/OK NEWD INTO NEW ENGLAND AND EWD TO NRN FLA.CH: HEAVY  
TO SEVERE (RW FROM SRN NEW ENGLAND TO SCAR BY 00Z.

----- ORIG-DEST-ALTNT-WEATHER -----

IAH 1852 E30 BKN 250 OVC 12 140/93/74/1809/995/THN SPOTS IOVC  
IAH 1752 30 SCT E250 OVC 12 147/92/74/1812/997/THN SPOTS IOVC/  
00Z 1202 78

IAH 1653 28 SCT E250 OVC 12 149/90/74/1512/998

IAH FT11 111717 30 SCT C80 BKN 1512020 OCNL C30 BKN CHC  
2TRW. 00Z 30 SCT C120 BKN 1608 SLGT CHC TRW. 11Z MVFR F.  
15Z MVFR CIG..

IAH NO 1/20 HIWAS OUTLET 116.6 OTS

IAH NO 6/3 IAH ILS 32R GS OTS

IAH NO 13/1 FDC 8/1004 ILS 8 CHG MISSED APCH

INSTRUCTIONS TO CLB TO 600 THEN CLBG LEFT TURN TO 2000  
HDG 035, FOR RADAR VECTORS TO DAS VORTAC OR AS ASSIGNED  
BY ATC. ILS 9, ILS 14L AND VOR/DME 14L MISSED APCH CLB  
TO 2000 FOR RADAR VECTORS TO DAS VORTAC OR AS ASSIGNED  
BY ATC. ILS 26 MISSED APCH CLB TO 600 THEN CLBG RIGHT  
TURN TO 2000 VIA HDG 305 FOR RADAR VECTORS TO TNV  
VORTAC, OR AS ASSIGNED BY ATC

IAH NO 13/2 FDC 8/1005 ILS 27, ILS 32R, VOR/DME 14L  
AND VOR/DME 32R MSA FROM IAH VORTAC 110-220 3100,  
220-110 2000

DEN 1951 CLR 50 078/86/47/0406/000/CB TCU S-N

DEN 1750 CLR 60 085/84/46/0809/002/CB FRMG OMTNS S-NW/ 710 1003

5

DEN 1652 CLR 60 089/81/46/1308/003/CU FRMG OMTNS S-NW

DEN FT11 111818 90 SCT 250 SCT 1612 SLGT CHC C70 BKN

TRW-A G40 AFT 20Z. 04Z 150 SCT 1910. 06Z CLR 1910. 12Z

VFR..

DEN NO 6/25 LDA LOC 35R OTS

DEN NO 6/26 ILS DME 35R OTS

DEN NO 6/38 LDA DME 35R OTS

DEN NO 7/12 DEN ALS 35R OTS TIL 152000

DEN NO 13/1 FOR PUSHBACK CLEARANCE AT GATE A-8 CALL

UA RAMP ON 129.5. DEN PAGE 10-7 WILL BE CHANGED. (DENFO

PB CHIDD JWW 6/16/88)

DEN NO 13/2 FDC 8/2040 ILS 35R CRCLG VIS CAT C VIS 2

3/4. CAT D VIS 3. ALT MINS 900-3

DEN NO 13/3 CONSTRUCTION AREA - ON RAMP EAST AND

SOUTHEAST OF THE B CONCOURSE. AREA EXTENDING 300 FT OUT

FROM THE B CONCOURSE. THE VSR IS LOCATED AT THE EDGE OF

THE OUTAGE AREA. GATES B19 AND B21 ARE OUT OF SERVICE

WITH B20 TO BE OUT OF SERVICE BY 6/29/88. AREA IS

LIGHTED AND BARACADED. TAXI W/CAUTION. DURATION,

APPROX. 30 DAYS. (CHIDD.GC)

COS 1850 80 SCT 65 104/80/46/1209/008

COS 1750 70 SCT 65 111/78/47/1307/010/ 705 1100 52

COS 1650 CLR 65 119/75/45/1406/011/FEW C' W-NW

COS FT11 101818 70 SCT 250 SCT 1510 SLGT CHC C60 BKN

TRW-A G40 AFT 20Z. 05Z 120 SCT 0110. 06Z CLR 0110. 12Z

VFR..

COS NO 13/1 USE CAUTION TAXIING INTO THE RAMP FROM

THE SOUTH. TWY A3 SIGN IS LOCATED SOUTH OF TWY A3. THE

TWY SOUTH OF THE SIGN IS A PRIVATE TWY AND IS NOT AUZD

FOR UAL ACFT

COS NO 13/2 COS NOT AUZD FOR PILOT TRAINING FROM

2300-0600 MDT

----- DEST AREA WEATHER -----

GJT 1850 CLR 70 094/87/45/1208/002/FEW TCU AC CI

PUB 1850 CLR 90 090/87/50/1808/999/CB N CU SW-NW

BJC 1848 80 SCT 65 86/48/1110/002

TAD 1850 CLR 60 104/82/42/0605/008/FEW CU

----- ENROUTE TERMINAL FORECASTS -----

MSY FT11 111717 20 SCT 100 SCT C250 BKN 2208 OCNL C20 BKN

100 BKN CHC C10 OVC 1TRW 035. 04Z 10 SCT 20 SCT C80 BKN

2106 OCNL C10 BKN C20 BKN 80 OVC CHC C10 OVC 1TRW 035.

11Z 10 SCT C20 BKN 80 OVC 3F OCNL C10 BKN 20 OVC SLGT CHC

TRW. 12Z MVFR. 15Z VFR..

OKC FT11 111717 40 SCT C100 OVC 1610 CHC C20 OVC 2TRW.

03Z 100 SCT 250 SCT 1508. 11Z VFR..

DFW FT11 111717 12 SCT C25 BKN 1808 OCNL C12 BKN 3R-F CHC

TRW. 20Z C30 BKN 1808 CHC C10 X 2TRW. 04Z C15 OVC 1808

CHC TRW. 11Z IFR CIG TRW. 15Z MVFR..

PUB FT11 111818 90 SCT 250 SCT 1410 SLGT CHC C70 BKN

TRW-A G40 AFT 20Z. 05Z 120 SCT. 06Z CLR. 12Z VFR..



----- PIREPS -----  
MLC UA /OV PGO 270010/TM 1728/FL310/TP B737/TB LGT RIME

----- ENROUTE NOTAMS -----  
ENROUTE NOTAM 13 EFF 18APR/1521Z TO  
S/1091 FDC AIRWAY TX. V68 V198 COMFY. TX INT TO SAT VORTAC MEA  
4000. (EXCDD 18APR88 AR)

ENROUTE NOTAM 04 EFF 02MAY/1951Z TO  
FDC 8/1217 AIRWAYS, TX. V161 BETWEEN MILSAY /MOP/ VORTAC AND  
POLKA INT., TX. MOCA 2500.

ENROUTE NOTAM 25 EFF 01APR/2151Z TO UFN  
FDC 8/967 V74 FROM TULSA, OK VORTAC TO OWETA, OK INT. MOCA TO  
READ 2800FT

ENROUTE NOTAM 34 EFF - TO  
CHART LQ(09) GLEND INT, REDESIG, LEFT TURNS, 064 DEG INBND

\*\*\* END PART 01 OF 01 \*\*\*

-  
EISDR 111919 6941 0939

141529Z AGENT LOS ID 075143 FROM PID 2872 TO PID 6891

5

141531Z AGENT KOS ID 075143 FROM PID 2872 TO PID 6891

141531Z PID 2872 ID 075143 RTG KOS

DSMOO  
.DSMOOQA 111907 346

WBM	305-11	DSM-DEN (2213Z)	RT: 1	ALTNT	COS
	403-11	DEN-BIL (0040Z)	RT: 1	ALTNT	GTF
		BIL-GTF (0146Z)	RT: 1	ALTNT	BIL

\*\*\* PART 01 OF 01 PARTS \*\*\*

\*\*\*\*\*  
\*\*\*\*\* ALERT \*\*\*\*\* ALERT \*\*\*\*\* ALERT \*\*\*\*\*  
\*\*\*\*\*

DEN LLWS ALERT FROM 112100Z TO 120300Z  
CONDITIONS FAVORABLE FOR DEVELOPMENT OF CONVECTIVE LLWS. IF  
VIRGA, CB'S OR RW ARE OBSERVED OR REPORTED, EXPECT LLWS.

COS LLWS ALERT FROM 112100Z TO 120300Z  
CONDITIONS FAVORABLE FOR DEVELOPMENT OF CONVECTIVE LLWS. IF  
VIRGA, CB'S OR RW ARE OBSERVED OR REPORTED, EXPECT LLWS.

BIL LLWS ALERT FROM 112200Z TO 120300Z  
CONDITIONS FAVORABLE FOR DEVELOPMENT OF CONVECTIVE LLWS. IF  
VIRGA, CB'S OR RW ARE OBSERVED OR REPORTED, EXPECT LLWS.

GTF LLWS ALERT FROM 112200Z TO 120300Z  
CONDITIONS FAVORABLE FOR DEVELOPMENT OF CONVECTIVE LLWS. IF  
VIRGA, CB'S OR RW ARE OBSERVED OR REPORTED, EXPECT LLWS.

\*\*\*\*\*

----- MAP FEATURES -----  
MAP FEATURES UNITED STATES 111835Z-120600Z  
JET CORES AT 1200Z..FROM SLE(OREG) 350/26075 TO BOI(IDA) 420/26065..FROM OKC(OK) 380/25080 TO PIA(IL) 420/26065 TO  
BUF(NY) 350/24075..SURFACE AT 1500Z..COLD FRONT SSWD FROM NRN  
IDA TO OFF NRN CALIF COAST, FRONT MOVING EWD AT  
20KNOTS..LAYERED CLOUDS/R-/F BEHIND FRONT FROM WASH SWD TO NRN  
CALIF.. STRATUS OVER SRN CALIF COASTAL AREAS MOVING OFF-SHORE  
EARLY THEN MOVING BACK ONSHORE NEAR END OF PERIOD. COLD FRONT  
EXTENDS SSWD FROM WRN NY TO NRN IL TO SRN NEB THEN STATIONARY  
NWD THRU NERN WYO TO NWRN MONT COLD FRONT MOVING EWD AT 15-20  
KNOTS..FEW TO SCATTERED (CHC SEVERE) DEVELOPING VCNTY  
STATIONARY FROM FRONT FROM MONT SEWD TO NRN NEB. FEW TRW FROM  
AZ/NMEX NEWD INTO SERN WYO..SCATTERED TRW/RW OVER MOST OF AREA

FROM TX/OK NEWD INTO NEW ENGLAND AND EWD TO NRN FLA.CHC HEAVY  
TO SEVERE TRW FROM SRN NEW ENGLAND TO SCAR BY 00Z.

----- ORIG-DEST-ALTNT-WEATHER -----  
DSM 1850 80 SCT 250 -BKN 15 156/83/64/3611/001/FEW CU  
DSM 1751 80 SCT 250 -BKN 15 155/86/60/0106/001/FEW CU/ 603 1151

64  
DSM 1651 80 SCT 250 -BKN 15 155/85/59/0306/001  
DSM FT11 111717 80 SCT 250 -BKN 0806 OCNL C80 BKN SLGT  
CHC TRW-. 23Z 60 SCT 250 -BKN 1108 CHC C50 OVC STRW- AFT  
03Z. 11Z VFR..

DSM NO 13/1 EFFECTIVE MAY 31 1988 FROM 1300 UNTIL  
2200 JUL 8 1988 PARTIAL RAMP RECONSTRUCTION ON ELLIOTT  
FLYING SERVICE AND VAN DUSEN FBO APRONS. CAUTION: MEN  
AND EQUIP WORKING ADJACENT ACTIVE TAXI LANES.  
(29JUN88-PAE)

DSM NO 13/2 SOUTH TERMINAL RAMP EXCAVATION WITH 2 FT  
DEPRESSION. TAXI AREA TO GATE A-2 BTWN AREA OF  
CONSTRUCTION AND TERM BUIDLING-TAXI LINE HAS BEEN  
PAINTED.(TIL AUG15 J.P.D.)

DSM NO 13/3 GATE A-4 OUT OF SERVICE UNTIL FURTHER  
NOTICE.(UPD 6/15)

DEN 1851 CLR 50 078/86/47/0406/000/CB TCU S-N  
DEN 1750 CLR 60 085/84/46/0809/002/CB FRMG OMTNS S-NW/ 710 1005

5  
DEN 1652 CLR 60 089/81/46/1308/003/CU FRMG OMTNS S-NW  
DEN FT11 111818 90 SCT 250 SCT 1612 SLGT CHC C70 BKN  
TRW-A G40 AFT 20Z. 04Z 150 SCT 1910. 06Z CLR 1910. 12Z  
VFR..

DEN NO 6/25 LDA LOC 35R OTS  
DEN NO 6/26 ILS DME 35R OTS  
DEN NO 6/28 LDA DME 35R OTS  
DEN NO 7/12 DEN ALS 35R OTS TIL 152000  
DEN NO 13/1 FOR PUSHBACK CLEARANCE AT GATE A-8 CALL  
UA RAMP ON 129.5. DEN PAGE 10-7 WILL BE CHANGED. (DENFO  
PB CHIDD JWW 6/16/88)

DEN NO 13/2 FDC 8/2040 ILS 35R CRCLG VIS CAT C VIS 2  
3/4. CAT D VIS 3. ALT MINS 900-3

DEN NO 13/3 CONSTRUCTION AREA - ON RAMP EAST AND  
SOUTHEAST OF THE B CONCOURSE. AREA EXTENDING 300 FT OUT  
FROM THE B CONCOURSE. THE VSR IS LOCATED AT THE EDGE OF  
THE OUTAGE AREA. GATES B19 AND B21 ARE OUT OF SERVICE  
WITH B20 TO BE OUT OF SERVICE BY 6/28/88. AREA IS  
LIGHTED AND BARACADED. TAXI W/CAUTION. DURATION.  
APPROX. 30 DAYS. (CHIDD.GC)

COS 1850 80 SCT 65 104/80/46/1209/008  
COS 1750 70 SCT 65 111/78/47/1307/010/ 705 1100 52  
COS 1650 CLR 65 119/75/45/1406/011/FEW CU SW-NW  
COS FT11 101818 70 SCT 250 SCT 1510 SLGT CHC C60 BKN  
TRW-A G40 AFT 20Z. 05Z 120 SCT 0110. 06Z CLR 0110. 12Z  
VFR..

COS NO 13/1 USE CAUTION TAXING INTO THE RAMP FROM  
THE SOUTH. TWY A3 SIGN IS LOCATED SOUTH OF TWY A3. THE  
TWY SOUTH OF THE SIGN IS A PRIVATE TWY AND IS NOT AUZD  
FOR UAL ACFT

COS NO 13/2 COS NOT AUZD FOR PILOT TRAINING FROM  
2300-0600 MDT

BIL 1850 120 SCT 250 -BKN 50 052/85/50/1709/980/ DSDNT CU S-NW  
AND NE  
BIL 1751 120 -SCT 250 -SCT 50 065/80/50/1404/983/ TCU SE-SW/619  
1231 61  
BIL 1649 120 SCT 250 -BKN 50 072/77/50/0806/985/ TCU OVR MTNS  
BIL FT11 111818 120 SCT 250 -BKN 0912G22 OCNL 60 SCT 120

SCT. 23Z 60 SCT 120 SCT 091202Z OCNL 60 SCT C120 BKN CHC  
C45 BKN TRW-A G40. 05Z 60 SCT C120 BKN 2807 CHC C45 BKN  
TRW- G30. 12Z VFR TRW..

BIL NO 6/10 9R-27L/16-34 CLSD TIL 122300

BIL NO 7/18 BIL 4-22 CLSD

BIL NO 13/1 TOWER CLSD 0500-1200Z(2300-0600MDT). WHN  
TWR CLSD/CONTACT BIL RADIO(FSS) ON 124.2 FOR TRAFFIC  
AND WEATHER INFORMATION. ALL NAVAIDS MONITORED  
(04/03/88 JR)

GTF 1850 120 SCT 250 -OVC 45 032/83/49/0607/973/TCU SW ACCAS  
NE-E AND SW-NW

GTF 1750 200 -SCT 250 -OVC 45 041/81/48/1306/776/ACCAS NE-E/  
819 1181 62

GTF 1650 120 SCT 200 -SCT 250 -BKN 45 050/77/47/1904/978/ACCAS  
ALQDS VIRGA E

GTF FT11 111818 120 SCT 250 -BKN 201202Z OCNL 60 SCT 120  
SCT. 21Z 60 SCT 120 SCT 271202Z OCNL 60 SCT C120 BKN CHC  
C45 BKN TRW-A G40. 00Z 60 SCT C120 BKN 2614024 OCNL C45  
BKN TRW-A G40. 05Z 60 SCT C120 BKN 2514024 CHC C45 BKN  
TRW- G30. 12Z VFR TRW..

GTF NO 5/2 16-34 CMSN 6350X150 ASPH/HIRL

GTF NO 13/1 TOWER CLSD 0500-1200Z(2300-0600MDT). WHN  
TWR CLSD/ CONTACT GTF RADIO(FSS) ON 118.7 FOR TRAFFIC  
AND WEATHER INFORMATION. ILS 3 AND ILS 34 UNMONITORED.  
ILS 34 OUT OF SVC INDFLY (04/03/88 JR)

----- DEST AREA WEATHER -----

GJT 1850 CLR 70 094/87/45/1208/002/FEW TCU AC C1

PUB 1850 CLR 90 090/87/50/1808/999/CB N CU SW-NW

BJC 1848 80 SCT 65 86/48/1110/002

TAD 1850 CLR 60 104/82/42/0605/008/FEW CU

BIN 1851 120 SCT E250 BKN 30 039/84/47/3507/980

SHR 1850 80 SCT 250 SCT 60 064/87/51/1012/983

RAP 1852 30 SCT 40 118/78/59/1215021/995

BTM 1851 E80 BKN 250 BKN 40 036/80/39/1107/985/RWU NW

MSO 1848 70 SCT 110 SCT 250 -OVC 30 040/81/46/3405/972

HLN 1852 80 SCT 150 SCT 200 SCT 300 -BKN 40 031/87/47/0811/973/  
BLDG CU SW ACCAS E

LWT 1852 100 SCT E200 BKN 50 M/82/49/1110/982/MDT CU ALQDS

FCA 1854 65 SCT 100 SCT 250 SCT 40 036/77/53/3610/969/TCU S-NW

HVR 1852 AMOS 70 SCT 120 SCT 200 SCT 250 -BKN 65 034/ 87/49/  
2104/969 PK WND 9 000 /WSHFT 04 ACCAS S+W RS 1848

----- ENROUTE TERMINAL FORECASTS -----

OMA FT11 111717 80 SCT 250 -BKN 1207 OCNL C80 BKN. 20Z  
C80 BKN 1007 OCNL C20 OVC CHC C10 OVC 1TRW. 06Z 80 SCT  
250 SCT 0906. 11Z VFR..

MSP FT11 111717 40 SCT 250 SCT. 00Z 100 SCT C250 BKN OCNL  
C100 BKN. 08Z C80 BKN CHC C40 BKN RW-/TRW-. 11Z VFR TRW..

PUB FT11 111818 90 SCT 250 SCT 1410 SLGT CHC C70 BKN  
TRW-A G40 AFT 20Z. 05Z 120 SCT. 06Z CLR. 12Z VFR..

CYS FT11 111818 50 SCT 250 -BKN 1710. 21Z 50 SCT 100 SCT  
C250 BKN 1612 OCNL C50 BKN CHC TRW- G30. 03Z 60 SCT 250  
SCT. 12Z VFR NO CIG..

CPR FT11 111818 45 SCT 250 -BKN 2112. 21Z 45 SCT 250 -BKN  
211202Z OCNL C45 BKN SLGT CHC TRW- G30. 03Z 50 SCT 250  
SCT. 12Z VFR NO CIG..

----- ENROUTE NOTAMS -----

ENROUTE NOTAM 50 EFF 30JUN/1988 TO  
CHART LO(08) PERRY IA NDB HOLDING DESIG. HOLD NORTHWEST. LEFT  
TURNS. 130 DEG INBND

ENROUTE NOTAM 34 EFF - TO  
CHART LO(09) GLENO INT. REDESIG. LEFT TURNS. 064 DEG INBND

APPENDIX 2 - Communications

- a. Transcription of ATIS Messages
- b. Transcription of Tower Communications

ATIS-X:

Stapleton Arrival information X-ray, two one four five Zulu  
Temperature 85, dewpoint 44, wind zero nine zero at three  
Altimeter two niner niner five. Expect visual approach runways  
two six left, two six right, runway two five right.  
Notice to Airmen: Use caution for construction on southeast  
corner of the Bravo Concourse. Microburst advisories in effect.  
Low level windshear advisories in effect  
Doppler radar windshear demo in progress. VFR aircraft south  
and east contact Denver approach on 119.3, other VFR aircraft  
126.9. All aircraft advise on initial contact you have  
information X-ray.

ATIS-Y

Stapleton Airport information Yankee. Two two zero zero Zulu.  
Temperature 84, dewpoint 54, wind calm. Altimeter two niner  
niner six. Expect visual approach runway two six left, two six  
right, and two five. Caution for construction southeast corner  
of Bravo concourse. Microburst and low level windshear advisories  
are in effect. Doppler radar windshear demonstration in progress.  
Convective SIGMET three six Charlie is in effect for Nebraska,  
and Eastern Colorado for an area of severe thunderstorms. Contact  
Denver Flight Service for further details. VFR aircraft south  
and southeast, contact Denver Approach on 119.3, other VFR aircraft  
126.9. All aircraft advise on initial contact you have information  
Yankee.

ATIS-A

Stapleton Arrival information Alpha. Two two zero three Zulu.  
Seventy five hundred scattered, estimated ceiling one two thousand  
broken, two five thousand broken, visibility five zero, thunderstorm.  
Temperature 84, dewpoint 54, wind calm. Altimeter two niner niner six.  
Expect visual approach runway two six left, two six right. Runway  
two five may be assigned. Use caution for construction area off southeast  
corner of the Bravo Concourse. Convective SIGMET 36 Charlie is in effect  
for northeast Colorado. Contact Denver Flight Service for details.

Microburst advisories and in effect. Low level windshear advisories are  
in effect. Doppler radar windshear demo in progress. Advise on initial  
contact you have information Alpha.

TRANSCRIPT OF TOWER COMMUNICATIONS, DEN LC-2, 7/11/88

LC-2  
(Denver Tower)

Airborne:

22:07:05  
22:07:06  
22:07:07  
22:07:08  
22:07:09  
22:07:10  
22:07:11  
22:07:12  
22:07:13  
22:07:14  
22:07:15  
22:07:16  
22:07:17  
22:07:18  
22:07:19  
22:07:20  
22:07:21  
22:07:22  
22:07:23  
22:07:24  
22:07:25  
22:07:26  
22:07:27  
22:07:28  
22:07:29  
22:07:30  
22:07:31  
22:07:32  
22:07:33  
22:07:34  
22:07:35  
22:07:36  
22:07:37  
22:07:38  
22:07:39  
22:07:40  
22:07:41  
22:07:42  
22:07:43  
22:07:44  
22:07:45  
22:07:46  
22:07:47  
22:07:48  
22:07:49  
22:07:50  
22:07:51  
22:07:52  
22:07:53  
22:07:54  
22:07:55  
22:07:56  
22:07:57  
22:07:58  
22:07:59

UA862: And Denver tower United 862  
just outside Altur, visual to  
the right, say your winds please  
and we're going to alpha 8

United 862 Denver Tower  
Runway two six right, Cleared  
to land, Microburst Alert,  
center field wind two two zero  
at niner, a four zero knot  
loss final reported by  
machine, no pilot report

UA395: United 395 inside Altur

United 395 Denver Tower. Runway  
two six left, cleared to land.  
Wind two one zero at five, a four  
zero knot loss one mile final,  
Microburst Alert, not substantiated  
by aircraft

UA395: United, uh, 395

United 395, Say your gate

Unknown: Approach, we don't want to  
make the approach with a  
Microburst Alert

Who didn't want to make the  
um who wants to go missed?

UA862: Uh, 862, we'd like to go  
to the right if we can.

22:08:00 United 862, change to runway three  
 22:08:01 five right, cleared to land. I  
 22:08:02 do have a Microburst Alert to that  
 22:08:03 runway, wind three five zero at  
 22:08:04 fifteen, a forty knot loss on  
 22:08:05 three mile final  
 22:08:06  
 22:08:07  
 22:08:08  
 22:08:09  
 22:08:10 UA862: Uh, we don't wanna make any  
 22:08:11 approach. We'd like to go  
 22:08:12 ahead and hold somewhere  
 22:08:13 til you stop gettin' the  
 22:08:14 Microburst Alerts.  
 22:08:15 Standby  
 22:08:16  
 22:08:17  
 22:08:18  
 22:08:19  
 22:08:20  
 22:08:21  
 22:08:22  
 22:08:23  
 22:08:24  
 22:08:25 United 862 turn right heading  
 22:08:26 zero four zero maintain 8000  
 22:08:27  
 22:08:28  
 22:08:29  
 22:08:30  
 22:08:31  
 22:08:32  
 22:08:33  
 22:08:34  
 22:08:35  
 22:08:36  
 22:08:37  
 22:08:38  
 22:08:39  
 22:08:40  
 22:08:41  
 22:08:42  
 22:08:43  
 22:08:44  
 22:08:45  
 22:08:46  
 22:08:47  
 22:08:48  
 22:08:49  
 22:08:50 United 862 contact Denver  
 22:08:51 Approach one two five point  
 22:08:52 three  
 22:08:53  
 22:08:54 UA862: Twenty five three, United 862  
 22:08:55  
 22:08:56  
 22:08:57  
 22:08:58 UA395: and United 395, we're missing  
 22:08:59



22:09:00  
22:09:01  
22:09:02 United 395, roger, fly runway  
22:09:03 heading, climb maintain 7000  
22:09:04  
22:09:05 UA395: 7000  
22:09:06  
22:09:07  
22:09:08  
22:09:09  
22:09:10 United 395, turn right, heading  
22:09:11 zero one zero, climb maintain  
22:09:12 8000  
22:09:13 UA395: Okay, say that heading again  
22:09:14  
22:09:15  
22:09:16 Turn right heading zero one  
22:09:17 zero, climb maintain 8000  
22:09:18 United 395  
22:09:19  
22:09:20 UA395: Zero one zero, 8000, United 395  
22:09:21  
22:09:22  
22:09:23 UA236: United 236 heavy, Sky Ranch  
22:09:24 for the left one, we have  
22:09:25 Buffalo 9 for gate  
22:09:26  
22:09:27  
22:09:28 United 236 heavy, Denver tower,  
22:09:29 Microburst Alert threshold wind  
22:09:30 one four zero at five expect a  
22:09:31 five zero knot loss two mile  
22:09:32 final, runway two six left  
22:09:33 cleared to land  
22:09:34  
22:09:35 UA236: Cleared to land  
22:09:36  
22:09:37  
22:09:38  
22:09:39  
22:09:40  
22:09:41  
22:09:42  
22:09:43  
22:09:44  
22:09:45  
22:09:46  
22:09:47  
22:09:48  
22:09:49  
22:09:50  
22:09:51  
22:09:52  
22:09:53 UA395: And you say 8000 for  
22:09:54 United, uh, 395  
22:09:55  
22:09:56  
22:09:57 Yeah 395, affirmative,  
22:09:58 climb maintain 8000, heading  
22:09:59 zero one zero

22:10:00  
22:10:01  
22:10:02  
22:10:03  
22:10:04  
22:10:05  
22:10:06  
22:10:07  
22:10:08  
22:10:09  
22:10:10  
22:10:11  
22:10:12  
22:10:13  
22:10:14  
22:10:15  
22:10:16  
22:10:17  
22:10:18  
22:10:19  
22:10:20  
22:10:21  
22:10:22  
22:10:23  
22:10:24  
22:10:25  
22:10:26  
22:10:27  
22:10:28  
22:10:29  
22:10:30  
22:10:31  
22:10:32  
22:10:33  
22:10:34  
22:10:35  
22:10:36  
22:10:37  
22:10:38  
22:10:39  
22:10:40  
22:10:41  
22:10:42  
22:10:43  
22:10:44  
22:10:45  
22:10:46  
22:10:47  
22:10:48  
22:10:49  
22:10:50  
22:10:51  
22:10:52  
22:10:53  
22:10:54  
22:10:55  
22:10:56  
22:10:57  
22:10:58  
22:10:59

United 395 fly heading  
zero three zero for right  
now please

UA395: Okay, zero three zero, 395

United 395 contact Denver Approach  
one two eight point zero five

UA395: One two eight zero five

UA236: Uh, we're going around  
United 236 heavy

United 236 heavy, roger, fly  
runway heading climb maintain  
7000

UA236: 7000

UA949: Hey tower, United uh 949  
is marker inbound

United 949 caution wake turbulence  
from the heavy DC-8 going around  
Microburst Alert threshold wind  
zero nine zero at three, expect a  
seven zero knot loss on a three  
mile final.

22:11:00  
 22:11:01  
 22:11:02  
 22:11:03  
 22:11:04 UA949: United 949  
 22:11:05  
 22:11:06  
 22:11:07  
 22:11:08 United uh 236 heavy right  
 22:11:09 turn heading zero one zero  
 22:11:10 climb maintain 8000  
 22:11:11  
 22:11:12  
 22:11:13 UA236: zero one zero roger  
 22:11:14 236 heavy  
 22:11:15  
 22:11:16  
 22:11:17  
 22:11:18  
 22:11:19 \*\* unintelligible\*\*  
 22:11:20  
 22:11:21  
 22:11:22  
 22:11:23  
 22:11:24  
 22:11:25  
 22:11:26  
 22:11:27 Uh, Microburst Alert runway  
 22:11:28 two six, threshold windh one five  
 22:11:29 zero at five, expect an eight zero  
 22:11:30 knot loss on a three mile final  
 22:11:31  
 22:11:32  
 22:11:33  
 22:11:34  
 22:11:35  
 22:11:36  
 22:11:37 UA305: United 30---  
 22:11:38 UA949: And United 949 we're going  
 22:11:39 around  
 22:11:40  
 22:11:41 United 949 fly runway heading  
 22:11:42 climb maintain 7000  
 22:11:43  
 22:11:44 UA949: Climb 7000, United 949  
 22:11:45  
 22:11:46  
 22:11:47  
 22:11:48  
 22:11:49 United 305 Microburst Alert  
 22:11:50 threshold wind one six zero at  
 22:11:51 six, expect an eight zero knot  
 22:11:52 loss on three mile final  
 22:11:53 Say request  
 22:11:54  
 22:11:55  
 22:11:56  
 22:11:57  
 22:11:58 UA305: You say eight zero knots?  
 22:11:59

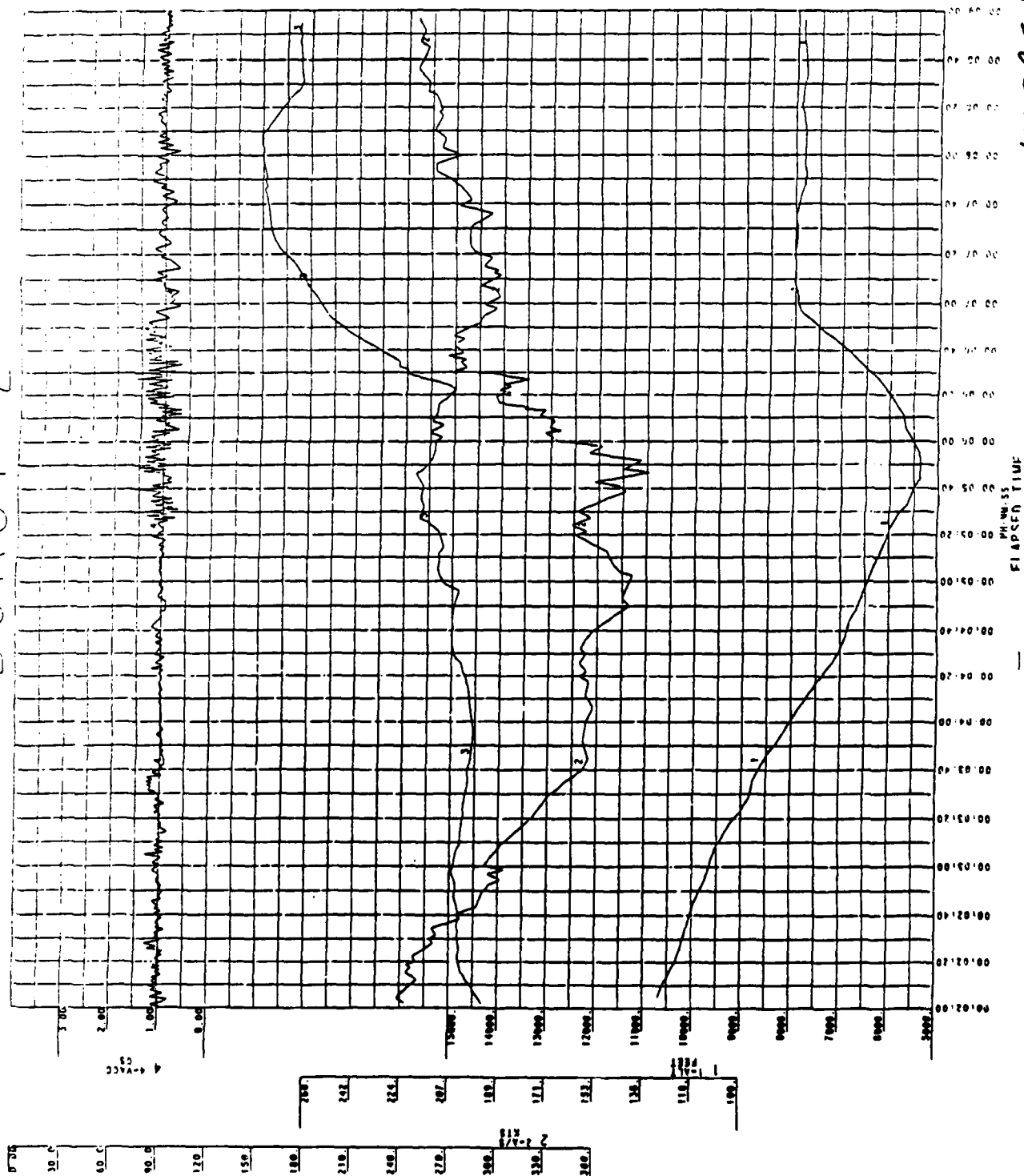
22:12:00 Affirmative  
22:12:01  
22:12:02 Affirmative United 305  
22:12:03  
22:12:04  
22:12:05 Unknown: And he's correct  
22:12:06  
22:12:07 Unknown (different): And we  
22:12:08 can confirm it.  
22:12:09  
22:12:10 United 305 What's your  
22:12:11 request?  
22:12:12 UA395: United 305's going around  
22:12:13  
22:12:14 United 305 roger, fly runway  
22:12:15 heading, climb maintain  
22:12:16 uh 7000 for now  
22:12:17 UA395: runway heading to 7000  
22:12:18 United 305  
22:12:19  
22:12:20

APPENDIX 3 - Flight Data Re orders

- a. FDR data Flight 395/11
- b. FDR data Flight 236/11
- c. FDR data Flight 949/11
- d. FDR data Flight 305/11

\*\*\*\*\*  
To be supplied by addendum at a later date  
\*\*\*\*\*

BUKSI 7



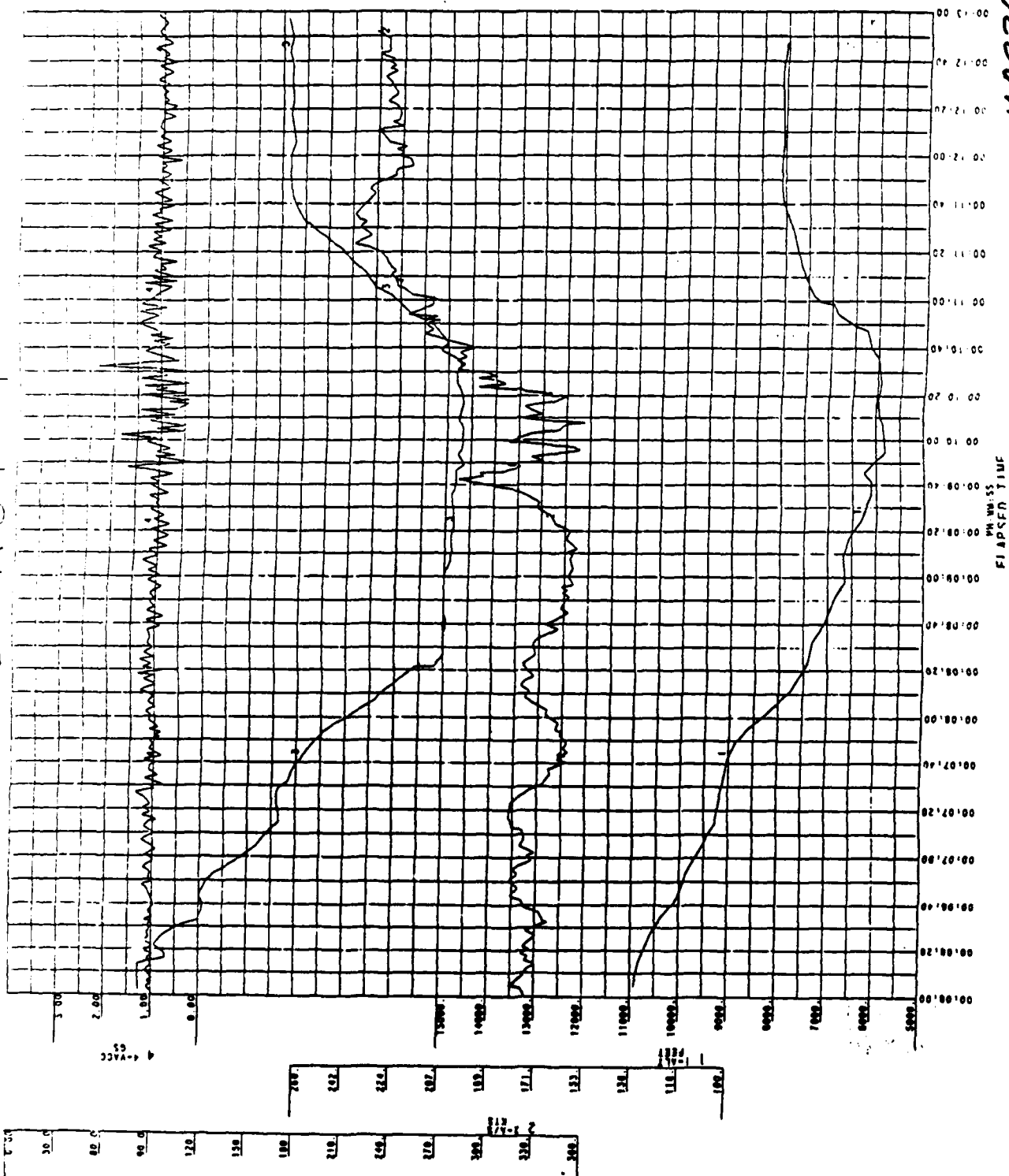
NATIONAL TRANSPORTATION SAFETY BOARD  
BUREAU OF TECHNOLOGY  
WASHINGTON, D. C.  
RECORDED W/M  
IDENT. NO.  
OFFICE  
FLYING 0-737  
DENVER, COLORADO  
DATE 7/11/88  
LOCATION: DENVER, COLORADO  
FLYING 0-737  
OFFICE  
IDENT. NO.  
RECORDED W/M  
IDENT. NO.  
FLYING 0-737  
DENVER, COLORADO  
DATE 7/11/88  
LOCATION: DENVER, COLORADO

UA395/11 July 88

NATIONAL TRANSPORTATION SAFETY BOARD  
BUREAU OF TECHNOLOGY  
WASHINGTON, D. C.

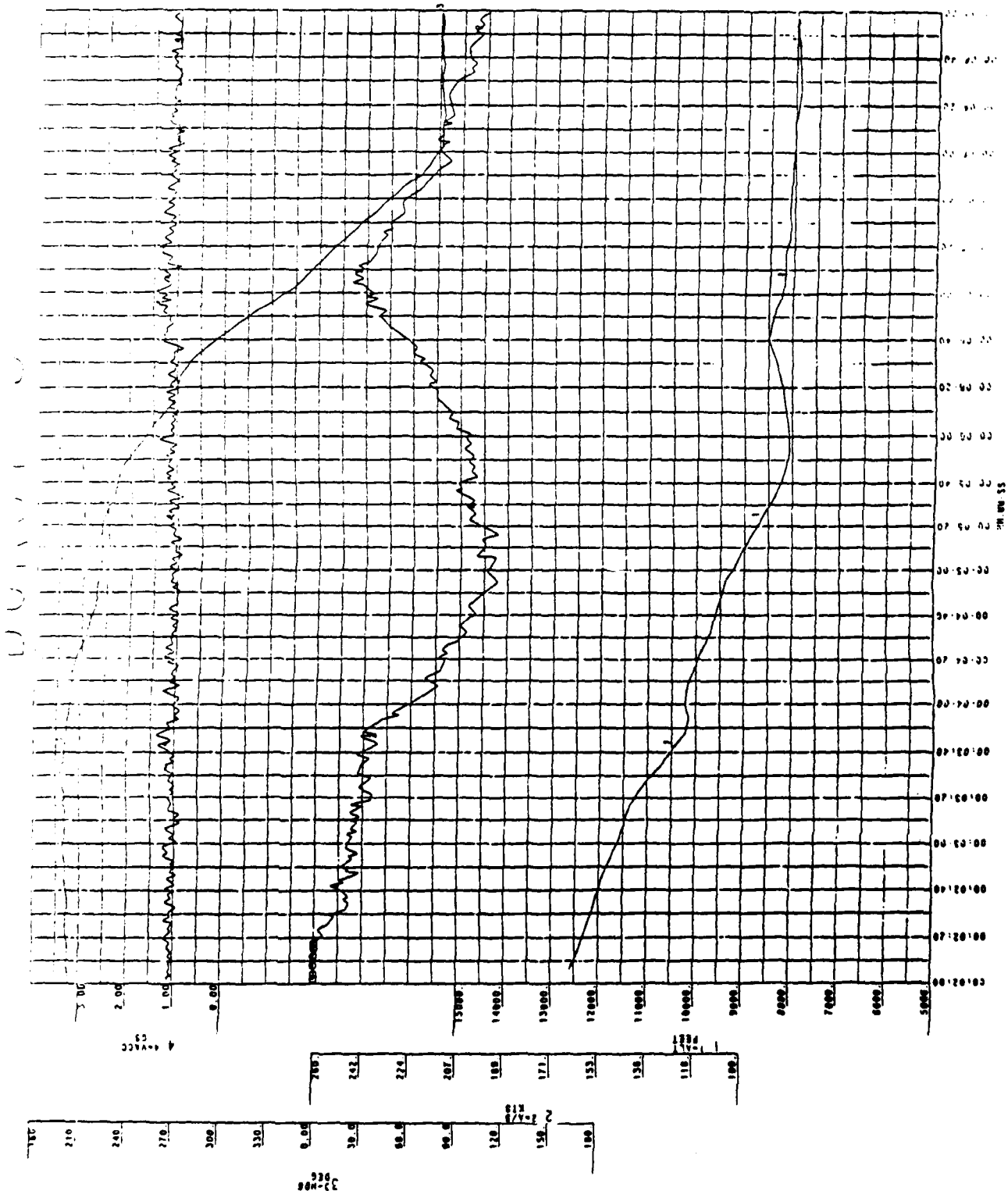
LOCATION: DENVER, COLORADO  
DATE: JULY 11, 1966  
FLIGHT NO.: 634  
OPERATION: UNITED AIRLINES  
RECORDING: S/M  
RECORD NO.: 46-106  
OFFICIAL: 2053

UA236/11 July 68



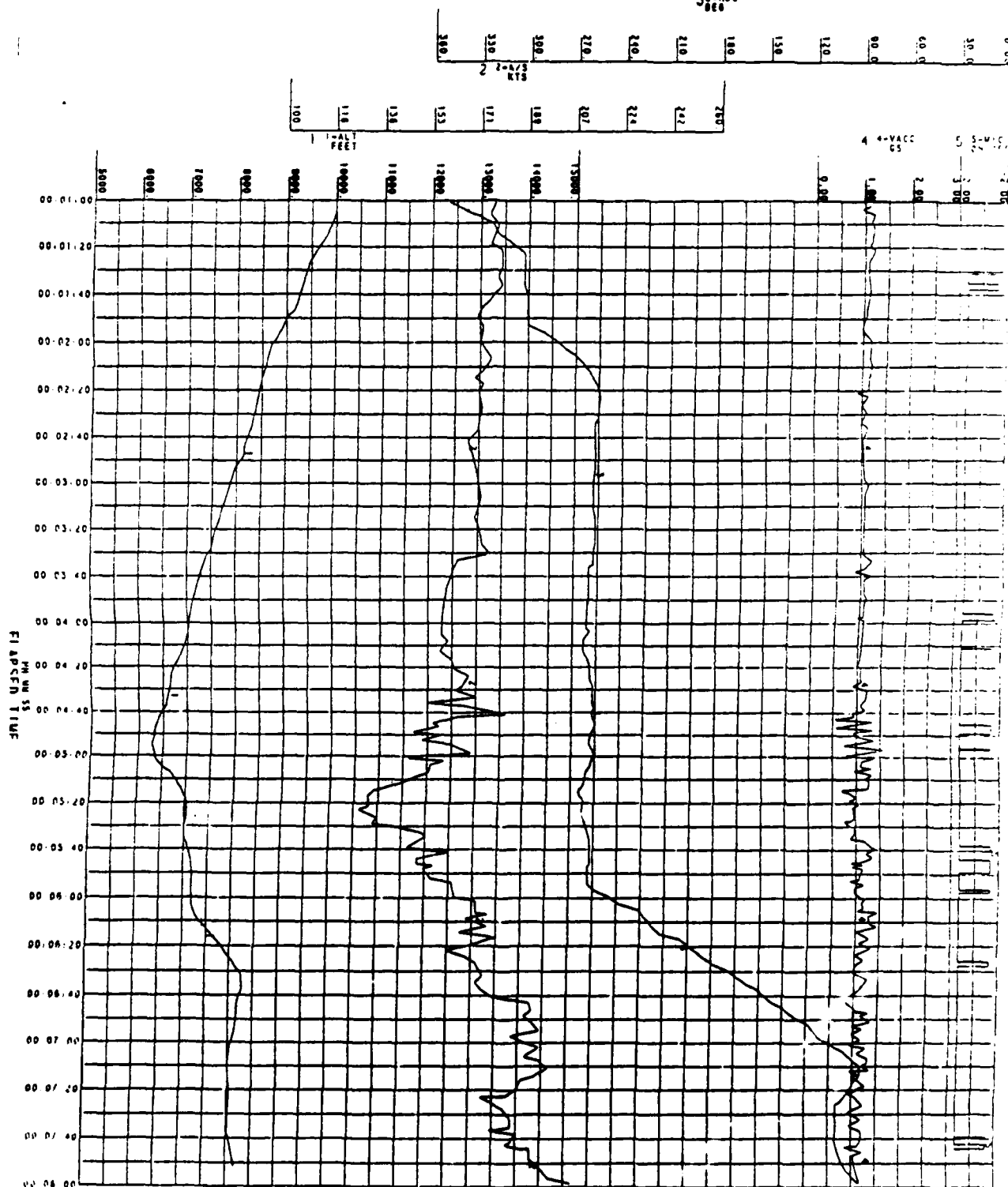
NATIONAL TRANSPORTATION SAFETY BOARD  
BUREAU OF TECHNOLOGY  
WASHINGTON, D. C.

UA862/11 July 88





33-400  
860



4A949/11 July 88

NATIONAL TRANSPORTATION SAFETY BOARD  
BUREAU OF TECHNOLOGY  
WASHINGTON, D. C.

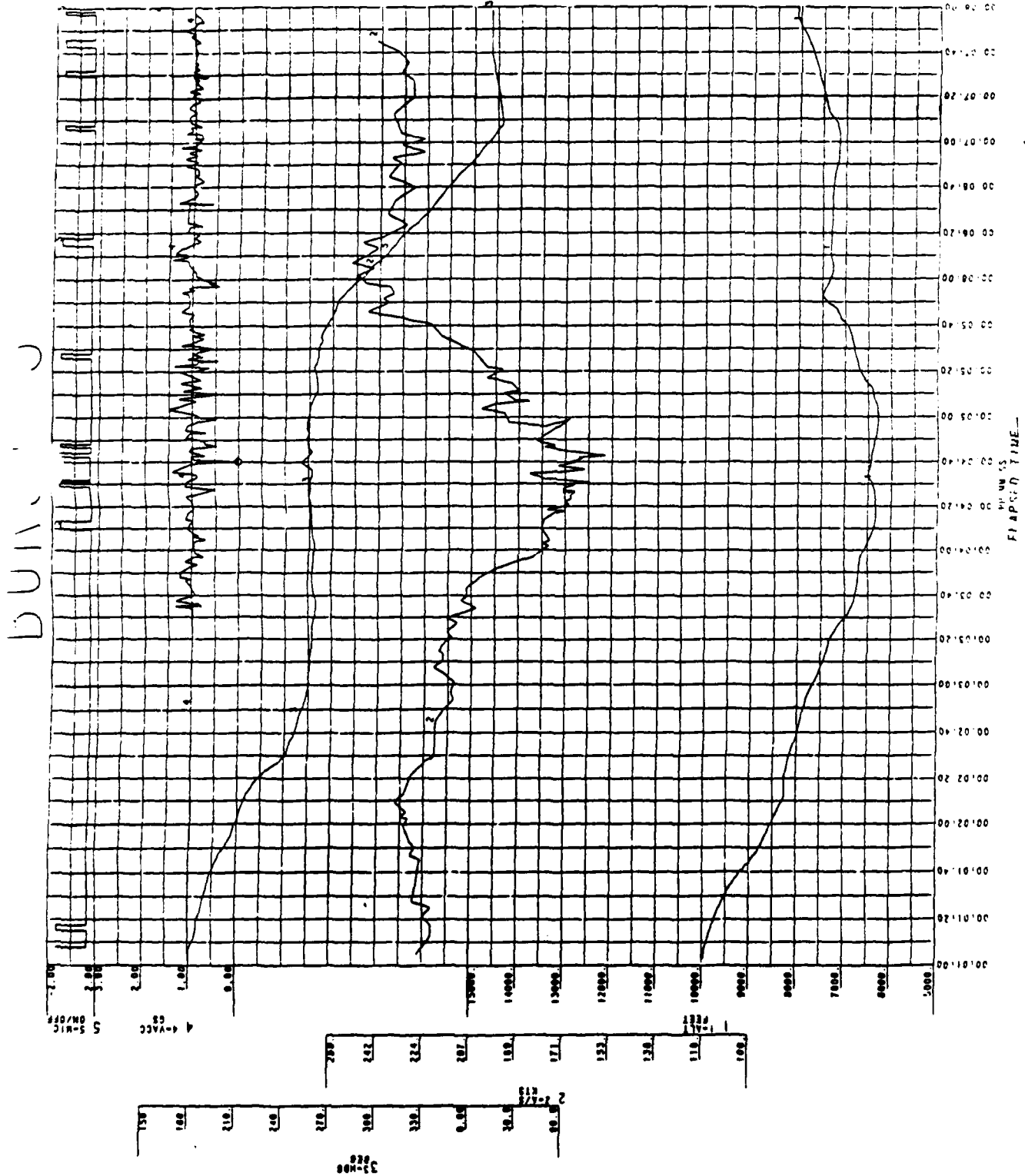
LOCATION: DENVER, CO.  
DATE: JULY 11, 1988  
AIRCRAFT: BOEING 727  
OPERATOR: UNITED AIR LINES  
FLT. NO.: 949

RECORDED BY: FAIRCHILD 5424  
RECORDED BY: UNKNOWN  
IDENT. NO.: SPECIAL  
REPORT NO.: 88-309

NATIONAL TRANSPORTATION SAFETY BOARD  
BUREAU OF TECHNOLOGY  
WASHINGTON, D. C.

LOCATION: DENVER CO.  
DATE: JULY 11, 1988  
FLIGHT NO: 305  
UNIT: 100  
ACCIDENT NO: 28-305  
PILOT: JAMES H. HANCOCK  
RECORDING: SA HANCOCK 5424

61A305 / 11 JULY 88



#### APPENDIX 4 - Training

- a. Microburst Windshear Probability Guidelines  
(from FAA Windshear Training Aid, Section 2)
- b. Adverse Weather Section - Windshear (B-727, typical  
all fleets)  
Issued 15 July 1987, first inserted Summer, 1984
- c. Summer Operations Bulletin (#175, B-727, typical  
all fleets)  
Issued March 15, 1988
- d. Denver Low Level Windshear Alert System and  
Terminal Doppler Weather Radar Operational  
Demonstration (#177, B-727, typical all fleets)  
Issued June 24, 1988

TABLE 1

## MICROBURST WINDSHEAR PROBABILITY GUIDELINES

<u>OBSERVATION</u>	<u>PROBABILITY OF WINDSHEAR</u>
PRESENCE OF CONVECTIVE WEATHER NEAR INTENDED FLIGHT PATH:	
- With localized strong winds (Tower reports or observed blowing dust, rings of dust, tornado-like features, etc.) .....	HIGH
- With heavy precipitation (Observed or radar indications of contour, red or attenuation shadow) ...	HIGH
- With rainshower .....	MEDIUM
- With lightning .....	MEDIUM
- With virga .....	MEDIUM
- With moderate or greater turbulence (reported or radar indications) .....	MEDIUM
- With temperature/dew point spread between 30 and 50 degrees fahrenheit .....	MEDIUM
ONBOARD WINDSHEAR DETECTION SYSTEM ALERT (Reported or observed).....	HIGH
PIREP OF AIRSPEED LOSS OR GAIN:	
- 15 knots or greater .....	HIGH
- Less than 15 knots .....	MEDIUM
LLWAS ALERT/WIND VELOCITY CHANGE	
- 20 knots or greater .....	HIGH
- Less than 20 knots .....	MEDIUM
FORECAST OF CONVECTIVE WEATHER .....	LOW

NOTE: These guidelines apply to operations in the airport vicinity (within 3 miles of the point of takeoff or landing along the intended flight path and below 1000 feet AGL). The clues should be considered cumulative. If more than one is observed the probability weighting should be increased. The hazard increases with proximity to the convective weather. Weather assessment should be made continuously.

CAUTION: CURRENTLY NO QUANTITATIVE MEANS EXISTS FOR DETERMINING THE PRESENCE OR INTENSITY OF MICROBURST WINDSHEAR. PILOTS ARE URGED TO EXERCISE CAUTION IN DETERMINING A COURSE OF ACTION.



## WINDSHEAR

### DEFINITIONS

**WINDSHEAR** - Any rapid change in wind direction or velocity. .

**SEVERE WINDSHEAR** - A rapid change in wind direction or velocity that results in airspeed changes greater than 15 knots, or vertical speed changes greater than 500 fpm.

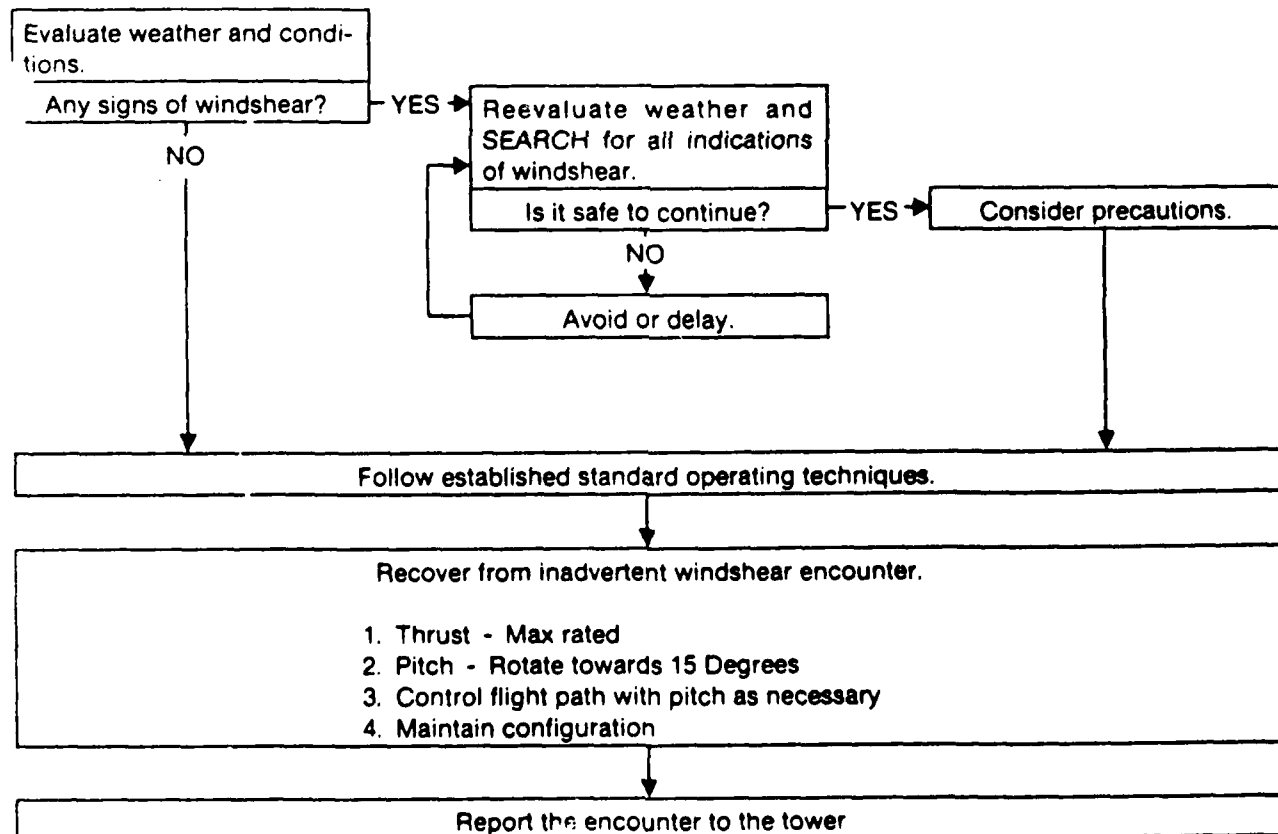
### FLIGHT CREW ACTIONS

Flight crew actions regarding windshear are divided into five areas: Avoidance, evaluation, standard operating techniques, precautions and recovery. The following flow chart summarizes the action items and presents the operational windshear decision from the pilot's viewpoint.

### AVOIDANCE IS THE FIRST PRIORITY

United Airlines policy is to avoid areas of known windshear. Consider one or more of the following actions as appropriate:

- Delay takeoff until conditions improve.
- In flight, divert around the area of known windshear.
- If windshear is indicated during approach, initiate a go-around or hold until conditions improve.



## WEATHER EVALUATION

Detection of windshear is difficult with today's technology. In order for the pilot to successfully avoid windshear, it is necessary to develop an understanding of the **causes** and **danger signals** of windshear. With the exception of a reliable PIREP, there is no single indicator which is conclusive proof of a windshear. Pilots should understand that the most dangerous form of windshear is a convective microburst of either the dry or wet type. Some have been documented with wind changes in excess of 150 knots! Because microbursts intensify for several minutes after they first impact the ground, the severity may be up to twice as much as that which is initially reported. Any airspeed change due to low altitude windshear should be immediately reported to ATC. Dry microbursts are especially insidious since they cannot be detected visually or with conventional radar.

Causes of Windshear	% of Threat
Convective conditions (thunderstorms, rain and snow showers)	65%
Frontal systems	15%
Low altitude jet streams	5%
Strong or gusty surface winds	5%
All other causes: (temperature inversions, mountain waves, sea breeze circulations, unknown causes)	10%

### Danger Signals of Dry Microbursts

- PIREPS: **Actual windshear may be up to twice as severe as the PIREP.**
- LLWAS: **LLWAS sensors are widely spaced and may not detect all microbursts in the airport area, and they are prone to false alarms.**
- VIRGA
- TEMPERATURE/DEW POINT SPREAD of 30° to 50°F.
- LOCALIZED STRONG WINDS: Blowing dust, rings of dust, dust devils, tornado like features, and other evidence of strong local outflow near the surface.

- TURBULENCE: Moderate or greater turbulence may be associated with the outflow from a microburst.
- WEATHER RADAR EVIDENCE: Indications of weak (green) cells with bases 5000-15,000 feet AGL which indicate weak precipitation, usually VIRGA. In addition, in the DOPPLER mode, areas of red (doppler turbulence) surrounding weak precipitation, may indicate microburst windshear conditions in their formative stages aloft.
- WINDSHEAR FORECAST: Potential for convection; mid level moisture; very dry surface conditions; 30°F to 50°F temperature/dew point spread (Windshear advisories are prepared by the UA Weather Center and are included in the weather briefing message.)

### Danger Signals of Wet Thunderstorm Microbursts

- PIREPS: **Actual windshear may be up to twice as severe as the PIREP.**
- LLWAS: **LLWAS sensors are widely spaced may not detect all microbursts in the airport, and they are prone to false alarms.**
- THUNDERSTORMS: In addition to the well known hazards of thunderstorms, an estimated 5% of thunderstorms accompanied by heavy rain and/or lightning, contain embedded microbursts.
- LOCALIZED STRONG WINDS: Heavy rain, blowing dust, rings of dust, dust devils, tornado like features, and other evidence of strong local outflow. **Visual clues may be obscured by low visibilities in wet thunderstorm microburst situations.**
- TURBULENCE: Moderate or greater turbulence may be associated with the outflow from a microburst.
- WEATHER RADAR: Search the area above and along the takeoff and approach paths for heavy precipitation.
- THUNDERSTORM FORECAST: Although no techniques currently exist to forecast wet microbursts, crews should consider the thunderstorm forecasts contained in the terminal forecasts and severe weather advisories as a possible indication of the presence of wet microbursts.



# **MICROBURST WINDSHEAR PROBABILITY GUIDELINES**

The following Table, designed specifically for convective weather conditions, provides a subjective evaluation of various observational clues to aid in making appropriate real time windshear avoidance decisions. The observation weighting is categorized according to the following scale:

## **HIGH PROBABILITY**

Critical attention needs to be given to this observation. A decision to avoid (e.g. divert or delay) is appropriate.

## **MEDIUM PROBABILITY**

Consideration should be given to avoiding. Precautions are appropriate.

## **LOW PROBABILITY**

Consideration should be given to this observation, but a decision to avoid is not generally indicated

OBSERVATION	PROBABILITY OF WINDSHEAR
PRESENCE OF CONVECTIVE WEATHER NEAR INTENDED FLIGHT PATH:	
- With localized strong winds (Tower reports or observed blowing dust, rings of dust, tornado-like features, etc.) . . . . .	HIGH
- With heavy precipitation (Observed or radar indications of contour, red or attenuation shadow) . . . . .	HIGH
- With rainshower . . . . .	MEDIUM
With lightning . . . . .	MEDIUM
With virga . . . . .	MEDIUM
- With moderate or greater turbulence (reported or radar indications) . . . . .	MEDIUM
- With temperature/dew point spread between 30 to 50 degrees Fahrenheit . . . . .	MEDIUM
ONBOARD WINDSHEAR DETECTION SYSTEM ALERT (Reported or observed) . . . . .	HIGH
PIREP OF AIRSPEED LOSS OR GAIN:	
- 15 knots or greater . . . . .	HIGH
- Less than 15 knots . . . . .	MEDIUM
LLWAS ALERT/WIND VELOCITY CHANGE	
- 20 knots or greater . . . . .	HIGH
- Less than 20 knots . . . . .	MEDIUM
FORECAST OF CONVECTIVE WEATHER . . . . .	LOW

### **NOTE**

*These guidelines apply to operations in the airport vicinity (within 3 miles of the point of takeoff or landing along the intended flight path and below 1000 feet altitude). The hazard increases with proximity to the convective weather. Weather assessment should be made continuously.*

*The clues should be considered cumulative. If more than one is observed, the probability weighting should be increased.*

### **CAUTION**

*Currently no quantitative means exists for determining the presence or intensity of microburst windshear. Pilots are urged to exercise caution in determining a course of action.*



## STANDARD OPERATING TECHNIQUES

Certain procedures and techniques can prevent a dangerous flight path situation from developing, even if unexpected windshear is inadvertently encountered. These procedures and techniques are of such importance that they should be incorporated into each pilot's personal standard operating techniques and practiced on every takeoff and landing, whether or not windshear is anticipated. It is important to develop a cockpit atmosphere which encourages awareness and effective crew coordination, particularly at night and during marginal weather conditions.

### Takeoff

- Be alert for any airspeed fluctuations during takeoff and initial climb.
- Know the all-engine initial climb pitch attitude.
- Make a continuous rotation at the normal rotation rate to this target pitch attitude for all non-engine failure takeoffs.
- Minimize reductions from the initial climb pitch attitude until terrain and obstruction clearance is assured.
- Develop an awareness of normal values of airspeed, attitude, vertical speed, and airspeed buildup.
- The pilot not flying should closely monitor the vertical flight path instruments such as vertical speed and altimeters and call out any deviations from normal.

### Landing

- Develop an awareness of normal values of vertical speed, thrust, and pitch.
- Crosscheck flight director commands using the vertical flight path instruments.
- Know the recovery decision criteria and be prepared to execute an immediate recovery if the parameters are exceeded.
- The pilot not flying should closely monitor the vertical flight path instruments such as vertical speed, altimeters and glide slope displacement and should call out any deviations from normal.

### PRECAUTIONS

Whenever the probability of windshear exists, but avoidance action is not considered necessary, the following precautions are recommended:

### Takeoff

- Use maximum takeoff thrust instead of normal (reduced) thrust.
- Use the longest suitable runway.
- Consider using the recommended flap setting, 15°. This flap setting provides the best overall compromise for windshear recovery capability between an on the runway or airborne windshear encounter.
- Consider maximizing available margins between VR and stick shaker through runway selection, flap selection and delayed rotation. The delayed rotation speed must not exceed either: 1) the runway limit VR speed or 2) a 20 knot increase. For example, if the actual gross weight is 150,000 pounds and the runway limit is 160,000 pounds, set the "bugs" for the actual gross weight, but remember to rotate at the VR speed for the runway limit weight. A normal continuous rotation to the target pitch attitude should be used.
- Do not use any pitch mode of the flight director for takeoff.

### Landing

- Achieve a stabilized approach by 1000 feet AGL.
- Consider using the recommended flap setting, 30°.
- Add an appropriate airspeed correction (applied in the same manner as gusts) up to a maximum of 20 knots.
- Avoid large thrust reductions or trim changes in response to sudden airspeed increases, as these may be followed by airspeed decreases.
- Consider use of the autopilot for the approach to provide more monitoring and recognition time.

## RECOVERY FROM INADVERTENT WIND-SHEAR ENCOUNTER

The following action is recommended whenever flight path control becomes marginal below 1000 feet above the ground on takeoff or landing. As a guideline, marginal flight path control may be indicated by **uncontrolled** deviations from normal steady state flight conditions in excess of the following:

- 15 knots indicated airspeed
- 500 fpm vertical speed
- 5 degrees pitch attitude,
- 1 dot displacement from the glide slope, or
- unusual throttle position for a significant period of time.





If flight path control becomes marginal at low altitude, accomplish the following procedure without delay. The first two steps should be accomplished simultaneously.

#### 1. THRUST - MAX RATED

Aggressively position the throttles to ensure maximum rated thrust is attained. Avoid engine overboost unless necessary to avoid ground contact. When airplane safety has been insured, adjust thrust to maintain engine parameters within specified limits.

#### NOTE

*The following is to be used if an overboost is required:*

*If an engine limitation is exceeded, when conditions permit, log maximum indications, if known, and engine indications, after thrust is returned to the normal range. Contact SAMPAC for assistance in evaluating the engine condition.*

#### PITCH - ROTATE TOWARD 15°

Disengage the autopilot and rotate smoothly at a normal rate toward a target pitch attitude of 15 degrees. Stop rotation immediately if stick shaker or buffet should occur.

If a windshear is encountered on the runway during takeoff and an abort is not practical, rotate toward 15° at the normal rate of rotation by no later than 2000 feet of useable runway remaining.

#### 3. CONTROL FLIGHT PATH WITH PITCH AS NECESSARY

Check vertical speed and altitude. If the airplane is descending, adjust pitch attitude smoothly and in small increments to minimize altitude loss. Always respect stick shaker and use **intermittent stick shaker** as the upper limit for pitch attitude. Rapidly changing vertical winds can cause momentary stick shaker actuation at any attitude. Control pitch attitude in a smooth steady manner to avoid overshooting the attitude at which stall warning is initiated. Do not use more pitch than is necessary to control the vertical flight path, since the resulting high drag and inefficient angle of attack will cause a lower recovery altitude. Control column forces necessary to control the flight path may vary from a push force to a heavy pull force. Do **not** follow flight director commands

#### 4. MAINTAIN CONFIGURATION

Do not change flap, gear, or trim position until terrain contact is no longer a factor.

#### Note

*It is recognized that a change in flap position may improve windshear recovery. This procedure however, is not recommended, since the risk of moving the flaps in the wrong direction or amount is considered to be greater than the risk of encountering a shear so great that a flap change is needed for recovery.*

#### REPORT THE ENCOUNTER

Report the airspeed change, location, altitude and aircraft type to ATC as soon as practical.



B-727 FLIGHT MANUAL - HANDBOOK  
BULLETIN #175  
MARCH 15/88  
FROM: DENTK - FLIGHT STANDARDS AND TRAINING

Please insert following the BULLETINS tab. Record on the Bulletin Checklist.

## SUMMER OPERATIONS

### GENERAL

Spring and summer are the times when convective weather presents the greatest problems for United flights, resulting in traffic delays, re-routing, turbulence, turbulence related injuries and less frequent but more critical low level windshear.

Turbulence related incidents causing injury to passengers and/or flight crews from convective weather and CAT were down in 1987 to 68 incidents compared to 87 incidents in 1986. While the trend is down, we must continue to improve in this area.

Turbulence associated with thunderstorms can be detected because of the radar's ability to observe water droplets. The intensity of turbulence, in most cases varies directly with the intensity of precipitation.

Radar will detect various levels of precipitation within the storm. With the non-color radar in the contour mode, heavy rain fall rates are indicated by the well defined black core. On a color radar, strong echos will be displayed by a yellow area or possibly a red area. Plan your deviation path early, and remember, turbulence can extend several thousand feet above a storm and outward more than 20 miles. Refer to the FOM, pp. 109-112 for the suggested margins for avoidance.

### TURBULENCE

Clear Air Turbulence Forms in regions of vertical windshear and temperature discontinuities. One part of the atmosphere that meets the above criteria is the tropopause. The layer at or just below the tropopause becomes a favored location for the development of CAT. Other layers can develop similar wind/temperature profiles that will result in clear air turbulence. Large temperature and/or wind variations, particularly over short distances, or any wave activity, should be viewed as precursors to CAT.

Passenger/Flight Attendant Considerations In Turbulence Whenever possible, advise the First Flight Attendant before or shortly after takeoff of anticipated enroute turbulence so that activities can be planned accordingly.



When Turbulence Is Encountered If light turbulence, turn on the seat belt sign and make a PA announcement to advise passengers of light turbulence, and to request they fasten their seat belts.

If greater than light turbulence, advise the flight attendants on interphone to check seat belts and then be seated.

#### INTERNATIONAL OPERATIONS

International Flight Folder Check the high level significant weather chart for areas of forecast turbulence. This also provides information on tropopause heights and jet core location, altitude and speed.

Check the flight folder to see if any sigmet messages have been included.

Flight Plan Forecast (FPF) Check the FPF for cruise altitude in relationship to the tropopause, and look for any suspect wind/temperature patterns. Large changes in wind speed/direction between fix points are indicative of shears. Large temperature changes are indicative of tropopause penetration.

#### ENROUTE - INTERNATIONAL AND DOMESTIC

Check with ATC for reports of turbulence. Monitor temperature and winds for rapid changes. Treat all wave activity as a possible precursor of CAT.

Forecasts of turbulent activity, CAT and wave action are available from Dispatch and are on the weather briefing message.

High altitude charts also depict areas with the most pronounced exposure to mountain wave turbulence. When mountain wave activity is forecast or reported, alternate tracks should be considered.

The best source for overall domestic thunderstorm information is the automated radar summary chart. They are transmitted 45 minutes after observation time and are available to crews at the major domiciles.

#### WINDSHEAR

The causes of windshear are numerous. It is estimated that 20 aircraft are likely to encounter microbursts at Stapleton Airport below 500 feet AGL in a typical summer. Approximately one half of the microbursts are associated with weak convection, virga and mid-level clouds, characterized by little or no precipitation at the surface. The remainder are associated with thunderstorm convection, characterized by moderate to heavy rain.



## What The Crew Can DO

Crew actions are divided into three areas: **Avoidance, Prevention and Recovery.** Avoidance is common to the takeoff and approach and includes the assessment of conditions that promote the correct decision. Prevention is divided into the takeoff and landing phase and covers recognition and action that will keep a windshear encounter from developing into a more critical situation. Recovery includes specific procedural actions when preventative action is not successful or sudden flight path degradation occurs unexpectedly.

### Avoidance

Carefully access all available information such as pilot reports of windshear or turbulence, low level windshear alerts, and weather reports including thunderstorm and virga activity. If severe windshear is indicated, delay takeoff or do not continue an approach until conditions improve. Severe windshear is that which produces airspeed changes greater than 15 knots or vertical speed changes greater than 500 fpm.

### Prevention-Takeoff

- Use the recommended flap setting and know the runway and performance limits.
- Use max thrust.
- If practical, use the longest suitable runway, provided it is clear of known windshear.
- Know the all engine initial climb pitch attitude.
- Crew coordination and awareness is very important. Be alert for airspeed fluctuations during takeoff and initial climb. Such fluctuations may be the first indication of windshear.
- The pilot not flying should be especially aware of vertical flight path instruments and call out deviations from normal.

### Prevention-Approach and Landing

- Use the minimum landing flap position consistent with field length and an appropriate airspeed wind correction up to the max recommended.
- Avoid large thrust reductions or trim changes in response to sudden airspeed increases, as these may be followed by airspeed decreases.
- Closely monitor vertical flight path instruments.
- Crew coordination and awareness is very important, particularly at night or in marginal weather conditions, to ensure flight path degradation will be recognized immediately.



## Recovery

The flight crew must make the determination of marginal flight path control using all the information available. This determination is subjective and based on the pilots' judgment of the situation. Marginal flight path control may be indicated by uncontrolled changes from normal steady state flight conditions in excess of:

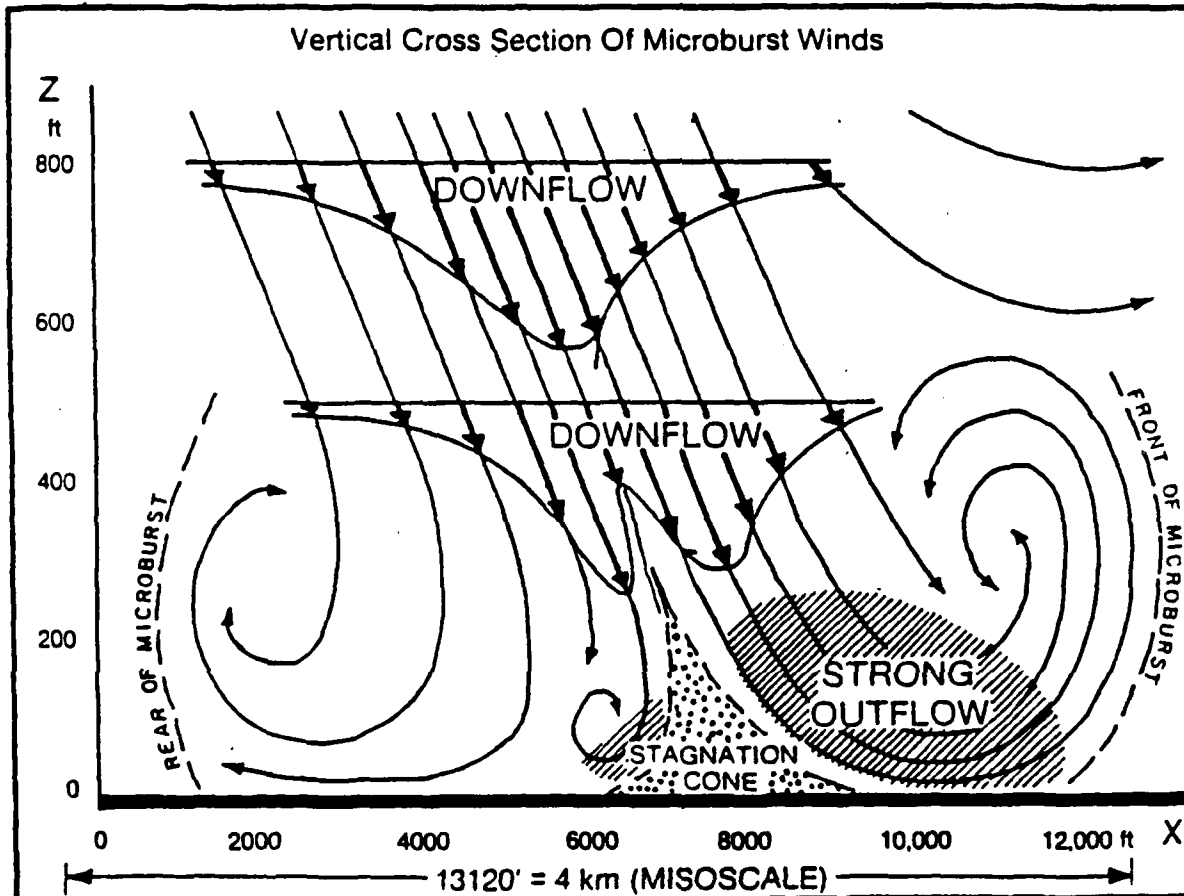
- 15 knots indicated airspeed,
- 500 fpm vertical speed,
- 5 degrees pitch attitude, or
- 1 dot displacement from the glideslope

Accomplish the following procedure without delay whenever flight path control becomes marginal.

Simultaneously:

- Disengage autothrottles and aggressively position thrust levers forward to ensure max rated thrust.
- Disengage the autopilot and rotate toward the target pitch attitude of 15 degrees.
- Control pitch attitude smoothly in small increments to minimize altitude loss while respecting the stick shaker.
- Do not follow flight director commands.
- Do not attempt to regain lost airspeed until terrain contact is no longer a factor.
- Do not change configuration until the vertical flight path is under control. There are enough variables to handle without adding more.
- Assist other pilots by reporting windshear encounters. Accurate pilot reports can be a valuable clue to the severity of a windshear condition.

# MICROBURST WIND SHEAR



ABOVE DIAGRAM 10 to 1 VERTICAL EXAGGERATION

## PREPARATION AND REVIEW

Good preparation, sound flight planning, and heightened awareness are key factors in avoiding summer weather related incidents. Items to consider while operating this spring and summer are:

- Discuss with your crew anticipated weather, turbulence, and delays, and make sure that they are well briefed on their duties.
- Check the POSBD'S and the airport briefing page (SIRD/DD041/STA/Briefing) for your original destination and alternate airports.
- If the runway is wet and considered slippery, consider using slippery runway  $V_1$  speeds.



- Be aware of possible hot starts.
- Consideration needs to be given to minimal use of brakes during taxi. A long taxi in conjunction with a long takeoff roll could cause problems if an abort was necessary. Proper taxi technique and planning is essential.
- Consideration needs to be given to temperature, runway selection, flap settings and thrust applications to assure the best performance.
- Assure that the radar is operating properly during preflight.
- Have the cabin at a comfortable temperature before the passengers board.
- During landing, be aware of possible hazards of landing on wet runways with crosswinds or tailwinds.
- If possible, on landing use minimum braking with more reverse thrust and longer rollouts.

#### REFERENCES

1. Flight Manual
  - 1) Runway clutter adjustments
  - 2) Optional  $V_1$  for slippery runway
  - 3) Additional Procedures/Bulletins
    - Severe Precipitation
    - Severe Turbulence
    - Static Discharge
    - Windshear
    - Weather Radar Operations
2. Operating gross weight manual, wet runway landing weights.
3. FOM

pg. 1	52, 52.1	Pilot Briefing Page
	59	Dispatching to Wet and Slippery Runways
	109-112.2	Weather, Thunderstorms, Turbulence, Radar
	113	Static Discharge
	114.1-.5	Braking Action and Runway Conditions
Far East chapter - Meteorology Section		
4. Video
  - 1) Summer Operations
  - 2) Turbulence
  - 3) Windshear

While the material in this bulletin is not new, it is important that we review all of the procedures associated with Summer Operations. Advance preparation will assist in ensuring an impressive safety record this year.



## B-727 OPERATIONAL CONSIDERATIONS

There is probably nothing more uncomfortable for a passenger than to board an airplane that is too hot. On pushback, wait until the Captain asks for #3 engine to be started before turning off the air conditioning packs. It takes approximately 10 seconds for the duct pressure to come up while keeping the much needed airflow in the cabin for the passengers. This summer let's pay particular attention to passenger comfort in our ongoing effort to give our customers the best possible service.

Tire Pressure - Indications are only valid after tires, wheels and brakes have cooled to ambient temperature. This usually requires at least one hour after the airplane is parked. Considering the way our airplanes are operated, most of the time you will get an accurate reading only before the first flight of the day.

Performance Computations - Check the maximum brake energy (MBE) charts in the flight handbook and see if  $V_1$  should be adjusted or if another flap selection would be better. If the runway is wet, consider clutter corrections in the flight handbook (T-4-6). If there is no clutter, consider the slippery runway  $V_1$  corrections in the bulletins (soon to be moved into the flight handbook, T-6.1). Determine which flap positions are permissible for the gross weight and existing conditions and decide which flap position is most suitable for the particular takeoff and departure. (TR-12-6, FHB A-33).

Ozone - A 727 during April and May is susceptible to high ozone concentrations in the upper atmosphere. The maximum altitude we can fly is FL 390. There are also more restrictions for operations in Canada and Alaska. (FOM pg. 57 and 112.2)

Weather Radar - All of the 727's are equipped with C band radar. Color radar displays show different levels of precipitation by different colors. 3 and 4 color radar indicators are installed on the Advanced and Stretched airplanes. The 4-color sets will display doppler returns as magenta as opposed to the 3-color red display. It does not show dry clear air turbulence. If a magenta turbulence return is displayed, it should be interpreted as a precipitation return with a minimum horizontal component of 10 knots. Color displays do not require a contour mode, as the colors give clear indication of different precipitation levels. On the non-color radars, switching between contour and normal helps in interpreting the shape and density of storm cells. A red area is the equivalent of the black area displayed on the non-color radar screen in the contour mode. With summer operations, we begin to get reports of the radar being left on when the crew leaves the airplane. To ensure an operable radar, sets should be turned off during taxi-in.





Lower Aft Body Overheat - With warmer weather comes an old problem, a lower aft body overheat at the blocks. The problem comes from hot APU air going through the aft airstair area enroute to the packs, and no cool air getting into the area. On a Standard airplane, the aft airstair probably is up, so you can get a ground man to lower it to admit some cooler air. On the long airplane, the airstair should be down already, so you might not have many options. If you can get a ground air conditioning unit, you can unload the APU by turning off the packs. The only other thing you could try is to put someone by the aft entry door to guard it, and then open the door to admit some cool air to the airstair area. Failing that, the light should go out during engine start, when the APU is no longer operating the packs. If it doesn't go out by the completion of engine start, or comes on during taxi out, there is a fault in the system which should be investigated and resolved.

Quick Turnarounds - (L&S-4, N-25) Our high altitude airports such as DEN, ABQ, SLC, and RNO are of particular concern. The 44 minute cooling period is measured block to block (In to Out time) and is completely independent of the amount of braking used. The FAA and Boeing have authorized the redispatching of the airplane without a 44 minute waiting time, if a temperature check confirms that the brakes do not contain enough energy to melt the thermal plugs. You can increase the chances for taking advantage of this method by sending the appropriate MRM code (32480) on ACARS as soon as it is determined that the actual landing weight will exceed the max. turnaround weight. Looking up these weights prior to descent and sending a message prior to landing will assist maintenance in determining if a quicker turn is possible. Be sure and make a writeup in the airplane Flight Log.

#### References

Bulletins or T-6.1  
FHA-1, A-3  
T&R 1-49, 50  
T&R 11-12.1,.2  
FH A-28  
FH A-28  
FH A-29  
FH A-30  
FH A-23  
FH A-22  
FH A-23  
L&S-4, N-25  
T&R 12-6

V<sub>1</sub> for Slippery Runways  
Radar Operation  
Radar Panel (Color)  
Radar Panel (Non-Color)  
Severe Precipitation  
Static Discharge  
Severe Turbulence  
Windshear  
Ozone Reduction  
Cabin Ground Cooling  
Takeoff with A/C Packs Off (ADV.,Str)  
Quick Turnaround  
Takeoff Flap Position



B-727 FLIGHT MANUAL - HANDBOOK  
BULLETIN #177  
JUN 24/88  
FROM: DENTK -FLIGHT STANDARDS AND TRAINING

Please insert following the BULLETINS tab. Record on the Bulletin Checklist.

DENVER LOW LEVEL WINDSHEAR ALERT SYSTEM (LLWAS) AND TERMINAL DOPPLER WEATHER RADAR (TDWR) OPERATIONAL DEMONSTRATION

The Federal Aviation Administration is scheduled to test a Doppler weather radar system at Denver Stapleton International Airport beginning approximately July 1, 1988, and continuing through August. This system is called "Terminal Doppler Weather Radar," or TDWR. The TDWR operational demonstration will provide microburst and windshear alerts identical to the present Denver LLWAS network. These alerts are runway specific and differentiate for "on-the-runway," "approach-zone," and "departure-zone" wind conditions. The departure and approach-zone reports are divided into one-mile segments from the end of the runway.

An expanded LLWAS network is currently in use at Stapleton. This system utilizes 12 sensors, and completed a successful demonstration in the summer of 1987. The system will be used as a backup for the TDWR demonstration during the summer of 1988. The ultimate goal is the complete integration of these two systems to provide comprehensive information to the pilot and controller. During the upcoming TDWR demonstration, the primary windshear alert sensor will be the Doppler radar, while the runway-oriented wind conditions will be provided by the LLWAS. The TDWR demonstration will be between 1200 MDT (1800 GMT) and 1900 MDT (0100 GMT) daily. During hours other than TDWR demonstration, the LLWAS will maintain continuous windshear surveillance.

Under normal conditions, wind information issued to arrival aircraft will be the threshold wind for the runway assigned. Departure aircraft will be issued centerfield wind.

The windshear messages used at Denver will comply with the following format and examples:

FORMAT

1. THRESHOLD WIND (landing aircraft) - The wind from the sensor closest to the runway threshold for arriving aircraft.
2. DEPARTURE WIND (departing aircraft) - The wind from the sensor closest to the departure end of the runway for departing aircraft.
3. TYPE OF WINDSHEAR - If the detection system identifies a windshear event as a microburst, the word "MICROBURST" will be used. All other windshear events will be called "WINDSHEAR".



4. WIND SPEED CHANGE - The maximum wind speed change along the specific runway axis will be reported. Wind speed loss will take precedence over wind speed gain. In the case of microbursts, this corresponds to the total change from the point of peak headwind to peak tailwind. Pilots should be alert to possible microbursts if they encounter increasing headwinds.
5. LOCATION - The approximate location of the windshear event will be given as it applies to each aircraft. Landing aircraft will receive messages for events along the approach path or on the landing runway, while departing aircraft will receive warnings for windshear or microbursts on the departure runway and in the departure zone. All alerts will be specific for each runway.

#### EXAMPLES

1. A microburst event located on the runway will be issued to an arriving aircraft:  
  
"UNITED 226, MICROBURST ALERT, THRESHOLD WIND TWO FOUR ZERO AT FIVE, TWO ZERO KNOT LOSS ON THE RUNWAY."
2. A windshear alert located one mile from the departure end of the runway issued to a departing aircraft:  
  
"UNITED 210, WINDSHEAR ALERT, CENTERFIELD WIND TWO FOUR ZERO AT FIVE, ONE FIVE KNOT GAIN, ONE MILE DEPARTURE."

#### NOTIFICATION OF TDWR DEMONSTRATION ON ATIS

During hours of the TDWR system operational demonstration, notification will be issued on Denver arrival and departure ATIS with the following words:

"DOPPLER RADAR WINDSHEAR DEMONSTRATION IN PROGRESS"

#### LIMITATIONS TO THE SYSTEM

1. The system is not able to detect microbursts before they impact near ground level.
2. The LLWAS cannot detect windshear events that occur outside of the wind measuring network; however, events occurring on the edge of the network which are not able to be distinguished between windshear and microbursts will be issued as "POSSIBLE WINDSHEAR OUTSIDE THE NETWORK." A windshear given to a departing aircraft which is detected on the edge of the network will be issued: "UNITED 22, CENTERFIELD WIND TWO FOUR ZERO AT FIVE, POSSIBLE WINDSHEAR OUTSIDE THE NETWORK."



3. The LLWAS is designed to operate with as many as three sensors inoperative; however, when one or more sensors are out of service and windshear/microburst activity is likely (e.g., frontal activity, thunderstorms, pilot reports), the ATIS will include "LLWAS IMPAIRED FOR MICROBURST DETECTION."
4. The TDWR operational demonstration is designed to test the success of Doppler radar to provide successful windshear alerts. The testing that occurred at Denver during the summer of 1987 predicts that this system will provide greater than 90 percent probability of detection and less than 5 percent false alarm detections of microbursts. To ensure that the highest possible level of safety is maintained during the demonstration, a full-time meteorologist will monitor both the TDWR system and the LLWAS. The meteorologist will be able to insert or delete alert messages when detections are considered to be in error or missing.

#### UA POLICY

During the conduct of this test, as is currently the case, a "Windshear" alert must be given serious consideration by the flight crew. All pertinent factors relating to a planned takeoff or approach must be critically examined before the specific course of action, e.g., normal procedures, precautions, or avoidance action is decided upon. (See Flight Handbook Additional Procedures, Windshear Section)

A "Microburst" alert, however, clearly indicates that avoidance action is required. A FLIGHT MUST NOT DEPART NOR CONDUCT AN APPROACH THROUGH AN AREA WHERE A MICROBURST ALERT IS IN EFFECT. Delay the takeoff or approach until the condition no longer exists along your intended flight path.

#### NCAR QUESTIONNAIRE

Attached to this bulletin is a questionnaire prepared by the National Center for Atmospheric Research (NCAR). Specifically, NCAR is requesting that this questionnaire be completed and forwarded to them, any time a flight encounters windshear below 1,000 ft. AGL in the immediate terminal area or encounters thunderstorm related turbulence within 40 nautical miles of the airport. Your support in this area is necessary to further their research and is encouraged. Extra copies of this questionnaire are available in the FOSR area at DENFO.

**A QUESTIONNAIRE FOR PILOTS OPERATING INTO OR OUT OF  
DENVER STAPLETON INTERNATIONAL AIRPORT  
SUMMER, 1988**

**INTRODUCTION**

During the summer of 1988, several organizations, including the National Center for Atmospheric Research (NCAR) and the Massachusetts Institute of Technology Lincoln Laboratory, will embark on extensive testing of new technology designed to provide improved airport terminal area weather detection capability, with particular emphasis on low-altitude wind shear detection and warnings for air traffic controllers and for pilots. In order to evaluate this new technology, we need the assistance of pilots to provide independent reports of wind shear and thunderstorm-related turbulence encounters in the Denver, Colorado, terminal area. These reports will be instrumental in helping us assess the development of the detection and warning system described below.

The detection system being tested by the Federal Aviation Administration is the Terminal Doppler (wind-measuring) Weather Radar (TDWR) system, which is expected to provide pilots with accurate and timely detection of severe low-altitude wind shear events. The FAA is conducting an operational demonstration of the system after extensive testing at Memphis, Tennessee, Huntsville, Alabama, and last year, at Denver.

The system is particularly capable of detecting the microburst, a dangerous form of wind shear that is caused by a sudden downdraft of air from a thunderstorm or a convective cloud of lesser intensity, which spreads out horizontally near the earth's surface and can cause severe head- and tail-wind changes for landing and departing aircraft.

The 1988 summer operational demonstration follows a successful test of an enhanced version of the FAA Low-Level Wind Shear Alert System (LLWAS) during the summer of 1987. The LLWAS system uses surface wind speed and direction sensing to measure wind shear at the earth's surface. During the 1987 demonstration, pilots were provided with wind shear alerts in a new runway-oriented message format that provided an estimate of wind shear intensity. Because of the high degree of success of the enhanced LLWAS, this system has now been commissioned at Denver. However, during this summer's Doppler weather radar test period, the LLWAS system will stand down as an alerting device to allow for a full and independent test of the more capable Doppler system. The Doppler radar detection system has the advantage of being able to detect wind shears above the surface and over a much wider area than the enhanced LLWAS system.

The TDWR operational demonstration will commence on 1 July and end on 31 August 1988. During this period, the Denver Airport area will be extensively instrumented with Doppler weather radars, numerous automatic ground-based weather stations, and a substantial capability to automatically generate wind shear detection and warning products with the goal of providing this information to pilots.

## **YOUR HELP IS URGENTLY NEEDED**

Critical to the TDWR operational demonstration will be independent substantiation of the presence of significant low-altitude wind shear. In addition, we require identification of any turbulence encounters by aircraft, but only when these encounters occur within 40 nautical miles of Stapleton Airport, and only for turbulence encounters associated with thunderstorm conditions. While the researchers involved in this program will have sensors that will be used to substantiate the quality of the products, feedback from pilots who actually encounter wind shear or thunderstorm-related turbulence is required. Two important benefits will thus be secured: (1) independent verification that significant wind shear or thunderstorm-related turbulence existed, so that a comparison can be made to the automated alert products; and (2) feedback regarding the quality of the operational usefulness of the Doppler-derived runway-oriented wind shear alert messages.

At your earliest convenience following an encounter with wind shear below 1000 ft AGL in the immediate terminal area, or an encounter with thunderstorm-related turbulence within 40 nautical miles of the airport, please fill out the attached questionnaire and drop it into any U.S. mailbox (postage is provided). The completed questionnaires will be delivered to:

Dr. John McCarthy, Manager  
Research Applications Program  
National Center for Atmospheric Research  
P.O. Box 3000  
Boulder, Colorado 80307-3000

## **CONFIDENTIALITY**

The purpose of the attached questionnaire is to obtain pilot feedback on warnings or the absence of warnings of wind shear and turbulence encountered in the Denver Stapleton International Airport area, between 1 July and 31 August 1988. This information will not be used for any other purpose. Thank you for your attention to this critical aviation safety matter.

**PILOT QUESTIONNAIRE**  
**DENVER STAPLETON INTERNATIONAL AIRPORT**  
(For use between 1 July and 31 August 1988)

DATE \_\_\_\_\_ AIRCRAFT TYPE \_\_\_\_\_ FLIGHT NO. \_\_\_\_\_ TAIL NO. \_\_\_\_\_  
TRANSPONDER CODE \_\_\_\_\_ PHASE OF FLIGHT (Circle): ARRIVAL DEPARTURE

WIND SHEAR AND TURBULENCE ENCOUNTER INFORMATION

1. Did you encounter any significant wind shear below 1000 feet AGL during takeoff or approach?  
Yes \_\_\_\_\_ No \_\_\_\_\_

If "Yes", complete: Approximate time of encounter \_\_\_\_\_ (Z)  
Airspeed Loss (-) and/or Gain (+) \_\_\_\_\_ Knots  
Altitude of First Encounter \_\_\_\_\_ Ft MSL  
Altitude Loss (-) or Gain (+) \_\_\_\_\_ Ft  
Location: \_\_\_\_\_ Over the runway  
              \_\_\_\_\_ 0-1 mile from the runway  
              \_\_\_\_\_ 1-2 miles from the runway  
              \_\_\_\_\_ 2-3 miles from the runway  
              \_\_\_\_\_ Beyond 3 miles from the runway

2. Was a microburst or wind shear warning issued to you by ATC at any time during takeoff or approach?  
Yes \_\_\_\_\_ No \_\_\_\_\_ (Circle): Microburst Wind Shear

3. If you answered "Yes" to question 2, please complete the following:

Was the warning useful? Yes \_\_\_\_\_ No \_\_\_\_\_

What windspeed loss or gain value did you receive from ATC as part of the warning?  
\_\_\_\_\_ (-) or (+) Knots (Circle - or +).

What action(s) did you take after receiving the microburst or wind shear alert message (Please mark all appropriate choices):

- \_\_\_\_\_ Made an avoidance decision by performing a go-around or delaying departure.  
\_\_\_\_\_ Took precautionary action such as increasing approach reference speed or departure target speed.  
\_\_\_\_\_ Took no specific action.  
\_\_\_\_\_ Other (Please indicate action in the space provided): \_\_\_\_\_  
\_\_\_\_\_  
\_\_\_\_\_  
\_\_\_\_\_

4. Did you encounter any moderate or greater thunderstorm-related turbulence within 40 nautical miles of Stapleton Airport? Yes \_\_\_\_\_ No \_\_\_\_\_

If "Yes", complete: Time of encounter \_\_\_\_\_ (Z)  
Magnitude: Moderate \_\_\_\_\_ Severe \_\_\_\_\_ Extreme \_\_\_\_\_  
Altitude of encounter \_\_\_\_\_ Ft MSL  
Location (DEN VORTAC) \_\_\_\_\_ Azimuth and Range \_\_\_\_\_

We are attempting to improve real-time low-altitude wind shear alerts. Please use the indicated space on the reverse side for any pertinent comments that you may have (e.g., what additional information would you like to see on alert messages). Remember, the contents of this questionnaire will be treated in confidence. Please fold, seal and return this form to us. Your participation and assistance is greatly appreciated!

SECOND FOLD - SEAL SHUT



NO POSTAGE  
NECESSARY  
IF MAILED  
IN THE  
UNITED STATES

**BUSINESS REPLY MAIL**

FIRST CLASS PERMIT NO 612 BOULDER, CO

POSTAGE WILL BE PAID BY ADDRESSEE

National Center for Atmospheric Research  
Attn: Dr. John McCarthy, Manager  
Research Applications Program  
P. O. Box 3000  
Boulder, CO 80307-9986



FIRST FOLD

ADD COMMENTS BELOW:



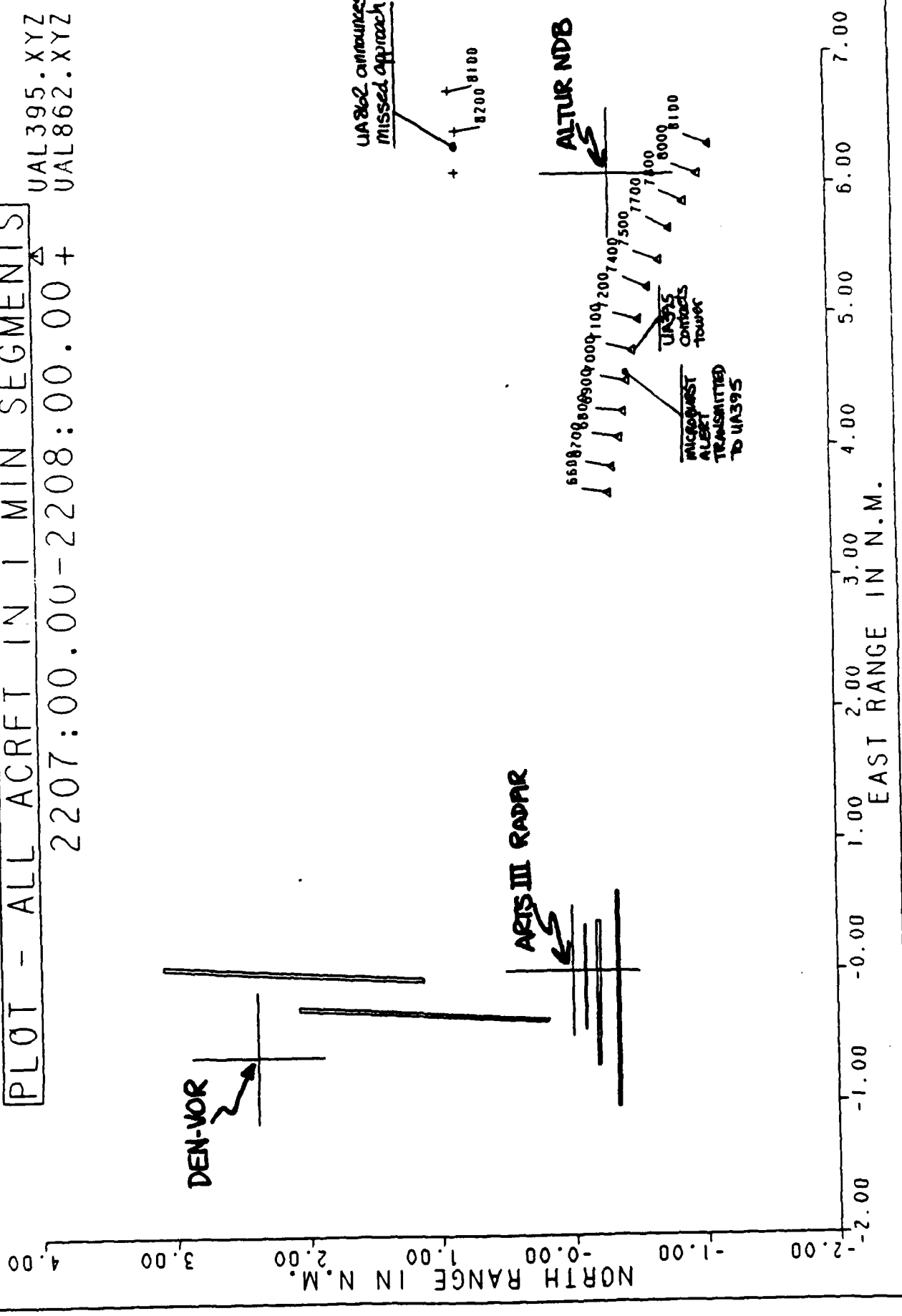
#### APPENDIX 5 - ATC/ARTSIII Radar

- a. All aircraft profile, 22:07 - 22:08 UTC
- b. All aircraft profile, 22:08 - 22:09 UTC
- c. All aircraft profile, 22:09 - 22:10 UTC
- d. All aircraft profile, 22:10 - 22:11 UTC
- e. All aircraft profile, 22:11 - 22:12 UTC
- f. All aircraft profile, 22:12 - 22:13 UTC

# PLOT - ALL ACRFT IN 1 MIN SEGMENTS

UAL395.XYZ  
UAL862.XYZ

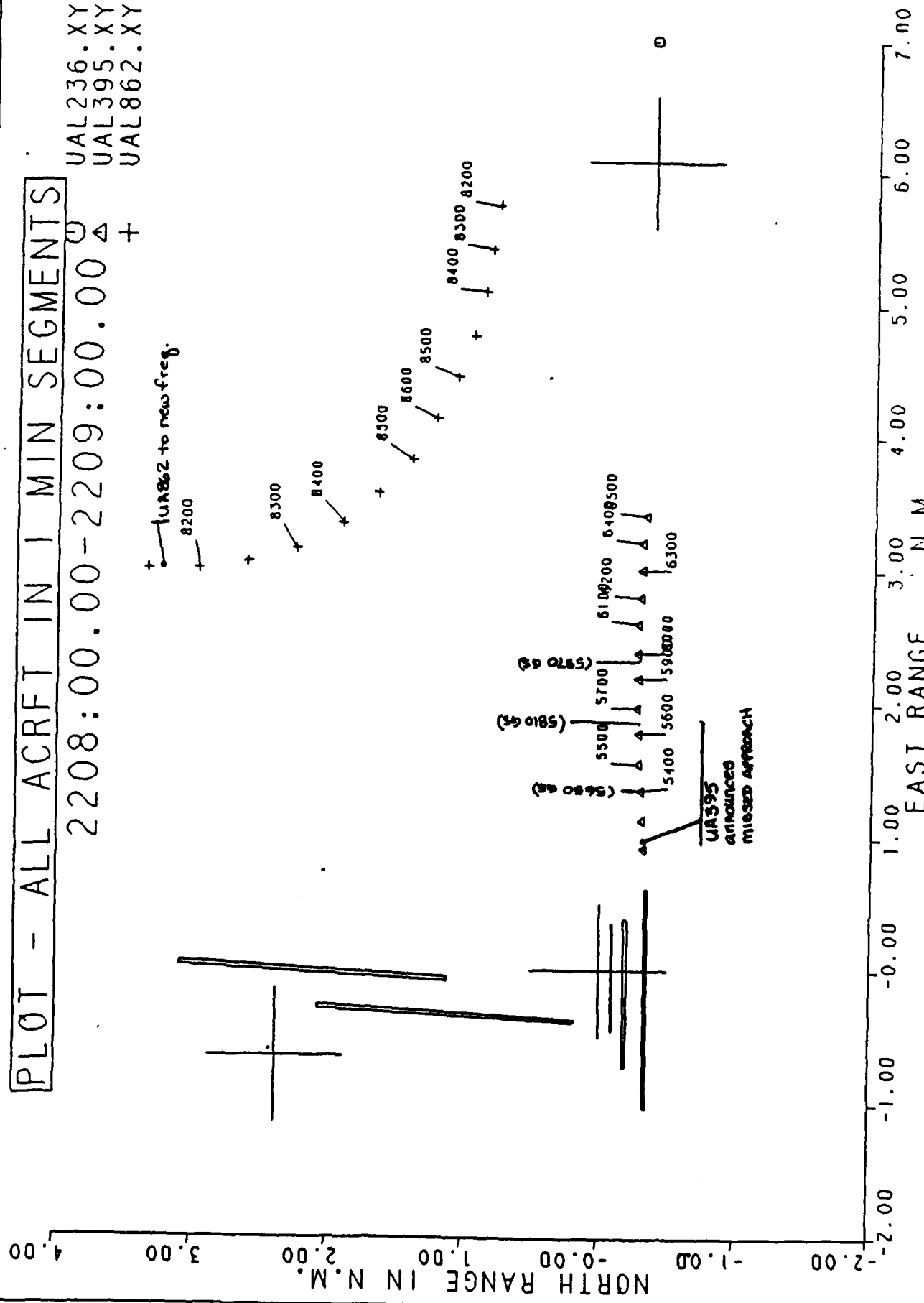
2207:00.00-2208:00.00 +



# PLOT - ALL ACRFT IN 1 MIN SEGMENTS

UAL236.XYZ  
 UAL395.XYZ  
 UAL862.XYZ

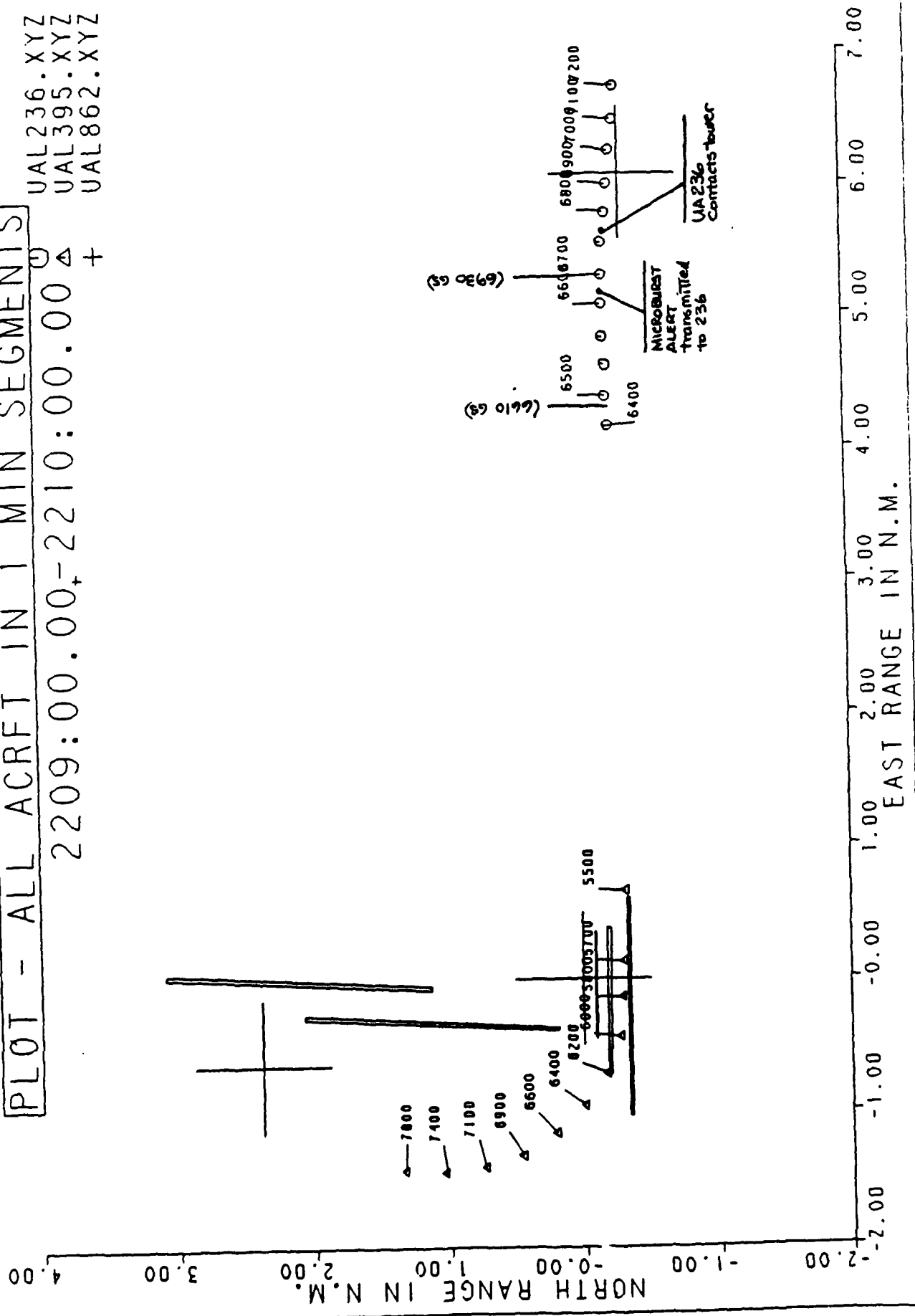
2208:00.00-2209:00.00



# PLOT - ALL ACRFT IN 1 MIN SEGMENTS

UAL236.XYZ  
UAL395.XYZ  
UAL862.XYZ

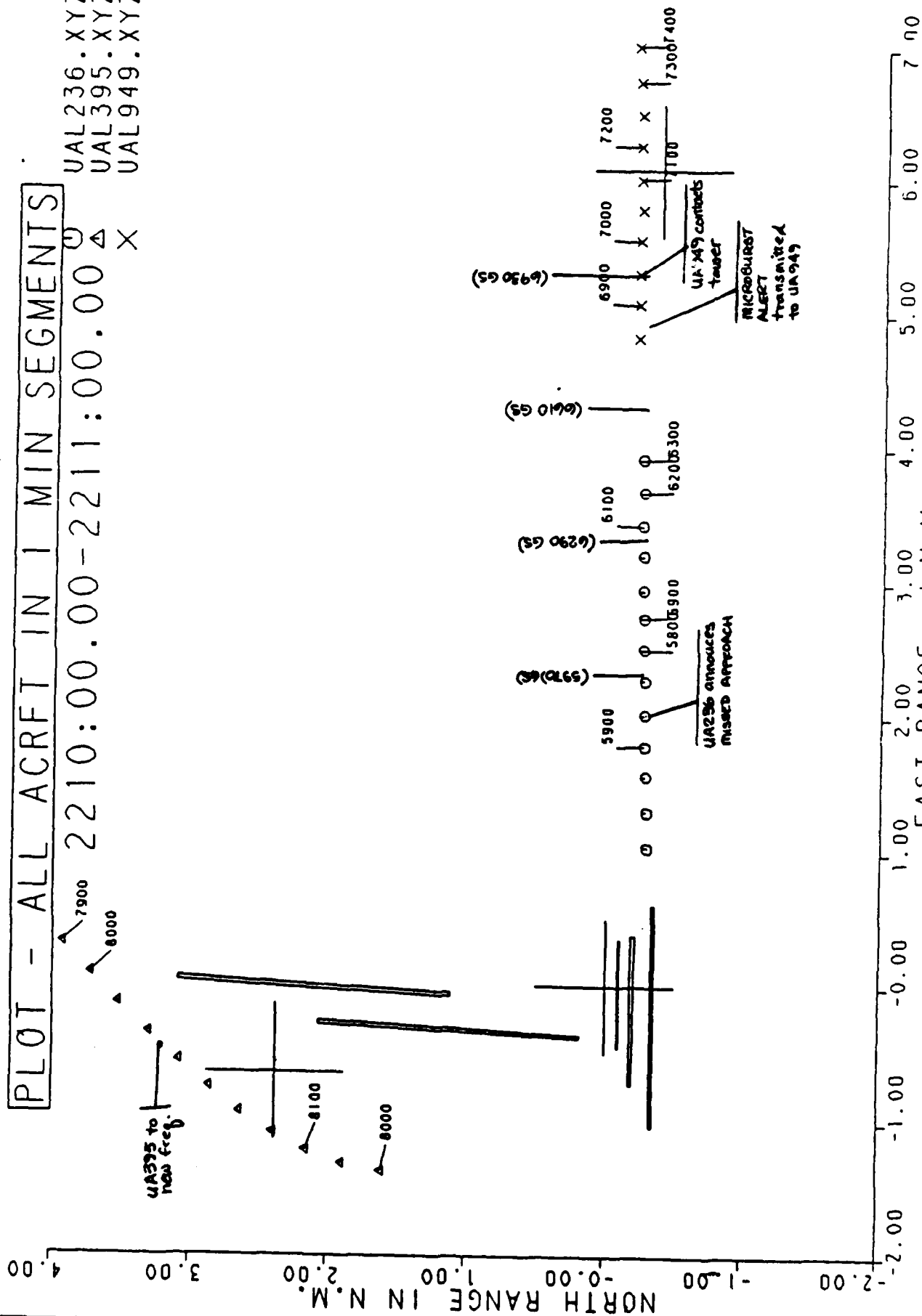
2209:00.00-2210:00.00 +



# PLOT - ALL ACRFT IN 1 MIN SEGMENTS

UAL236.XYZ  
 UAL395.XYZ  
 UAL949.XYZ

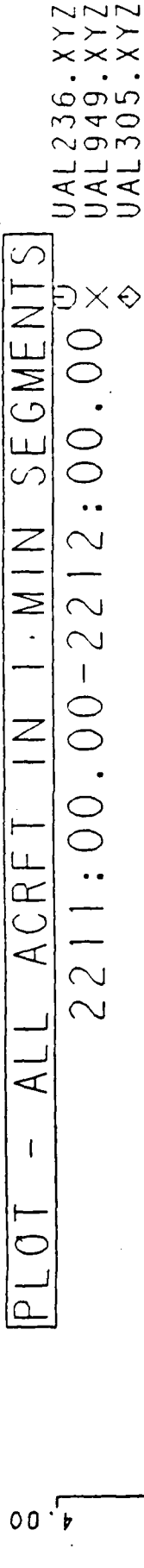
2210:00.00-2211:00.00



# PLOT - ALL ACRFT IN 1 MIN SEGMENTS

UAL236.XYZ  
UAL949.XYZ  
UAL305.XYZ

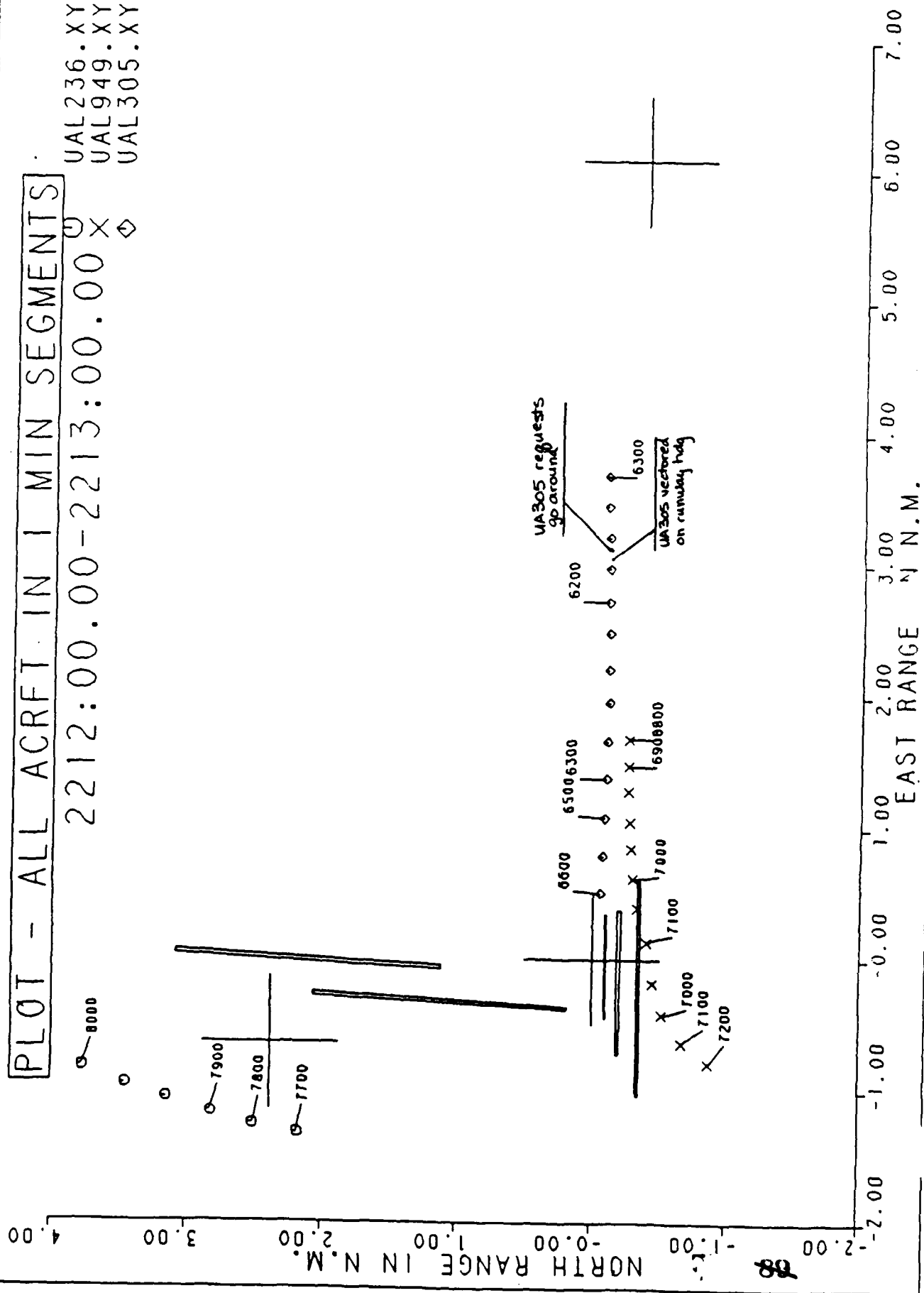
2211:00.00-2212:00.00



# PLOT - ALL ACRFT IN 1 MIN SEGMENTS

UAL236.XYZ  
 UAL949.XYZ  
 UAL305.XYZ

2212:00.00-2213:00.00



APPENDIX 6

a. TDWR Alarms, 22:05 - 22:13 UTC 11 July 1988

b. GSD Depictions (22:10 not available)

22:05

22:06

22:07

22:08

22:09

22:11

22:12

22:13

c. Dual Doppler Radar derived wind vectors

22:06:02

22:06:59

22:08:03

22:09:00

22:10:03

22:11:00

22:11:58



TOWER ALARMS for 11-JUL-88, hour 22

11-JUL-88 22:05:43

WSA 35RA 340 13 10k- 3MF	WSA 35LA 260 3 10k- 3MF	WSA 8A 280 3 10k- RWY
35RD 340 10	35LD 320 8	WSA 8D 240 4 10k- RWY
17LA 340 10	17RA 320 8	WSA 26A 240 4 10k- 1MF
WSA 17LD 340 13 10k- 1MD	WSA 17RD 260 3 10k- 1MD	WSA 26D 280 3 10k- RWY

11-JUL-88 22:06:17

MBA 35RA 330 12 35k- 3MF	MBA 35LA Calm 35k- 2MF	MBA 8A 280 3 35k- RWY
35RD 340 11	35LD 320 11	MBA 8D 230 3 35k- RWY
17LA 340 11	17RA 320 11	MBA 26A 230 3 35k- 1MF ←
MBA 17LD 330 12 35k- 2MD	MBA 17RD Calm 35k- 1MD	MBA 26D 280 3 35k- RWY

11-JUL-88 22:07:17

MBA 35RA 320 13 40k- 3MF	MBA 35LA Calm 40k- 3MF	MBA 8A 240 5 40k- 1MF
35RD 330 12	35LD 320 14	MBA 8D 220 9 40k- RWY
17LA 330 12	17RA 320 14	MBA 26A 220 9 40k- 1MF ←
MBA 17LD 320 13 40k- 2MD	MBA 17RD Calm 40k- 1MD	MBA 26D 240 5 40k- RWY

11-JUL-88 22:08:19

MBA 35RA 360 12 50k- 3MF	MBA 35LA Calm 50k- 2MF	MBA 8A 200 7 50k- 3MF
35RD 320 14	MBA 35LD 300 15 50k- RWY	MBA 8D 220 11 50k- RWY
17LA 320 14	MBA 17RA 300 15 50k- RWY	MBA 26A 220 11 50k- 2MF ←
MBA 17LD 360 12 50k- 1MD	MBA 17RD Calm 50k- RWY	MBA 26D 200 7 50k- RWY

11-JUL-88 22:09:35

MBA 35RA 010 11 60k- 3MF	MBA 35LA 160 7 60k- 3MF	MBA 8A 100 5 60k- 3MF
35RD 320 12	MBA 35LD 310 15 60k- RWY	MBA 8D 110 5 60k- RWY
17LA 320 12	MBA 17RA 310 15 60k- RWY	MBA 26A 110 5 60k- 3MF ←
MBA 17LD 010 11 60k- 1MD	MBA 17RD 160 7 60k- RWY	MBA 26D 100 5 60k- RWY

11-JUL-88 22:10:23

MBA 35RA 360 11 70k- 3MF	MBA 35LA 180 7 70k- 2MF	MBA 8A 040 6 70k- 3MF
MBA 35RD 320 12 70k- RWY	MBA 35LD 320 17 70k- RWY	MBA 8D 070 7 70k- RWY
MBA 17LA 320 12 70k- RWY	MBA 17RA 320 17 70k- RWY	MBA 26A 070 7 70k- 3MF ←
MBA 17LD 360 11 70k- RWY	MBA 17RD 180 7 70k- RWY	MBA 26D 040 6 70k- RWY

11-JUL-88 22:11:17

MBA 35RA 330 8 80k- 3MF	MBA 35LA 140 5 80k- 2MF	MBA 8A 050 4 80k- 3MF
MBA 35RD 310 12 80k- RWY	MBA 35LD 310 13 80k- RWY	MBA 8D 090 3 80k- RWY
MBA 17LA 310 12 80k- RWY	MBA 17RA 310 13 80k- RWY	MBA 26A 090 3 80k- 3MF ←
MBA 17LD 330 8 80k- RWY	MBA 17RD 140 5 80k- RWY	MBA 26D 050 4 80k- RWY

11-JUL-88 22:12:24

MBA 35RA 360 7 80k- 3MF	MBA 35LA Calm 80k- 3MF	MBA 8A 330 14 80k- 3MF
MBA 35RD 310 13 45k- RWY	MBA 35LD 290 14 80k- RWY	MBA 8D 130 3 80k- RWY
MBA 17LA 310 14 45k- RWY	MBA 17RA 290 13 80k- 1MF	MBA 26A 130 3 80k- 3MF ←
MBA 17LD 360 7 80k- RWY	MBA 17RD Calm 80k- RWY	MBA 26D 330 14 80k- RWY

11-JUL-88 22:13:25

MBA 35RA 350 3 85k- 3MF	MBA 35LA 190 3 85k- 3MF	MBA 8A 330 14 85k- 3MF
MBA 35RD 290 13 35k- RWY	MBA 35LD 260 14 85k- RWY	MBA 8D 130 3 85k- RWY
MBA 17LA 290 13 35k- RWY	MBA 17RA 260 14 85k- 1MF	MBA 26A 130 3 85k- 3MF ←
MBA 17LD 350 3 85k- RWY	MBA 17RD 190 3 85k- RWY	MBA 26D 330 14 85k- RWY

NCAR GSD

RANGE

☐ 5m ☒ 15m ☐ 30m ☐ 50m

SCREEN

☒ 1 ☐ 2 ☐ 3 ☐ 4  
☐ 5 ☐ 6 ☐ 7 ☐ 8

MAPS

☐ Vortac & fixes  
☒ ASR rings  
☒ Airports  
☐ Interstates

PRECIPITATION LEVELS

☐ Off ☒ 1-6 ☐ 3-6 ☐ 5-6

WIND SHIFT:

☐ Off ☒ On

PRINT SCREEN:

☒ Yes ☐ No

STATUS:

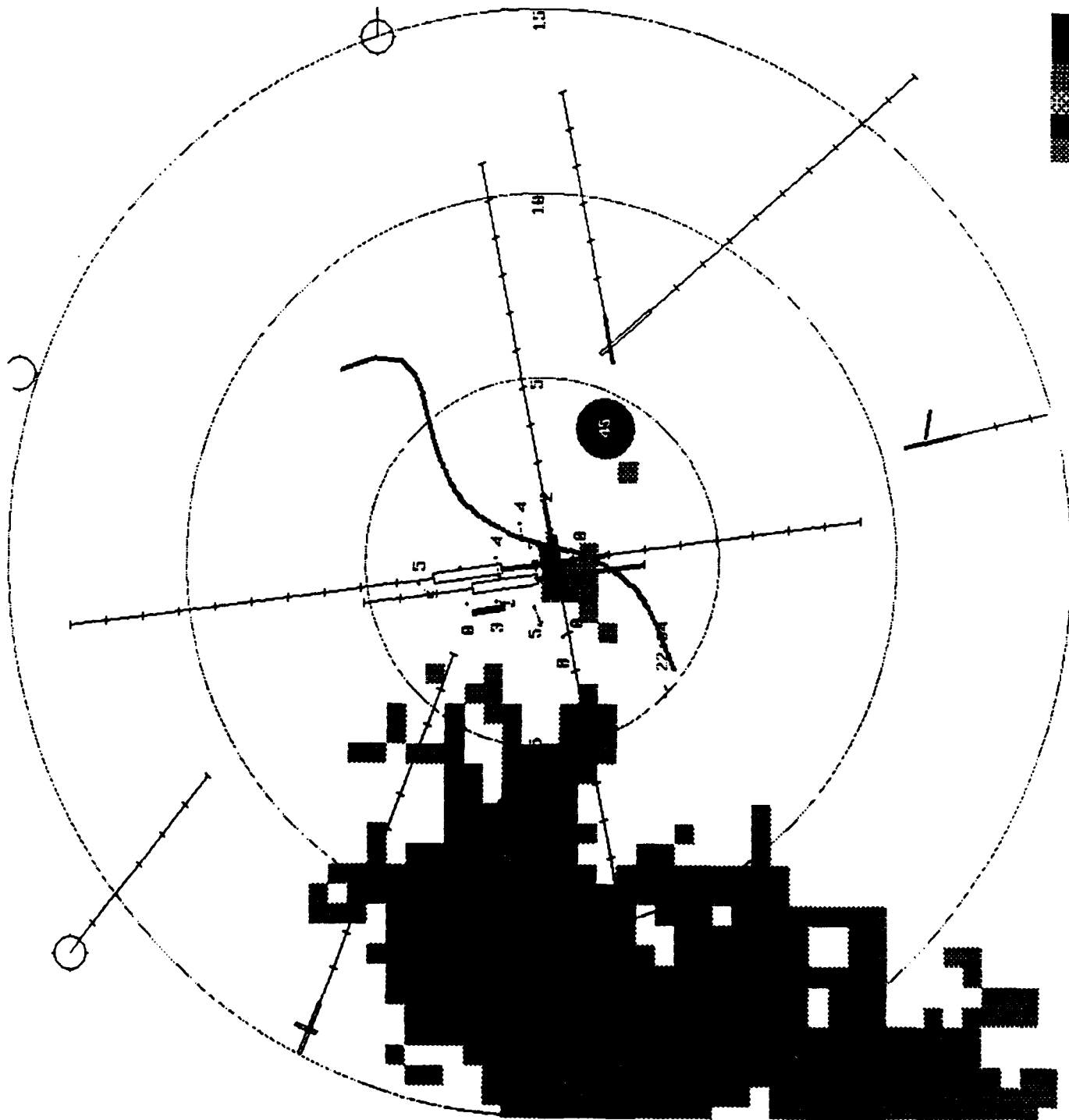
TIME: 22:05

MB: UP

GF: UP

PRECIP: UP

LLWAS: UP



NCAR GSD

RANGE

[5m] [15m] [30m] [50m]

SCREEN

[1] [2] [3] [4]  
[5] [6] [7] [8]

MAPS

- ☐ Vortac & fixes
- ☒ ABR rings
- ☒ Airports
- ☐ Interstates

PRECIPITATION LEVELS

[OFF] [1-6] [3-6] [5-6]

WIND SHIFT:

[OFF] [On]

PRINT SCREEN:

[Print]

STATUS:

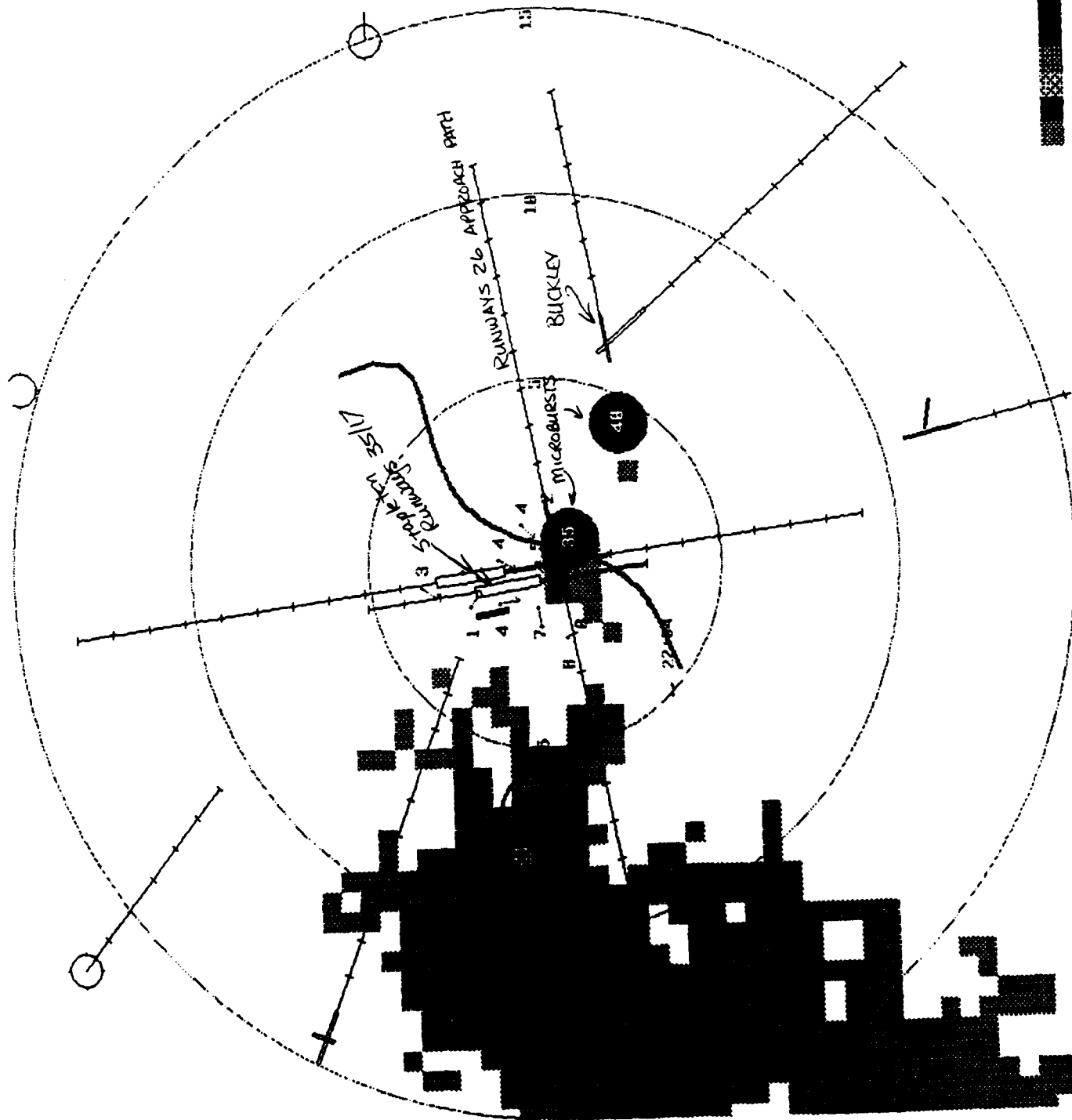
TIME: 2206

MB: UP

GF: UP

PRECIP: UP

LLWAS: UP



NCAR GSD

RANGE

☐ 5m ☒ 15m ☐ 30m ☐ 50m

SCREEN

☒ 1 ☐ 2 ☐ 3 ☐ 4  
☐ 5 ☐ 6 ☐ 7 ☐ 8

MAPS

☐ Vortac & fixes  
☒ ASR rings  
☒ Airports  
☐ Interstates

PRECIPITATION LEVELS

☐ Off ☒ 1-6 ☐ 3-6 ☐ 5-6

WIND SHIFT:

☐ Off ☒ On

PRINT SCREEN:

☒ Print

STATUS:

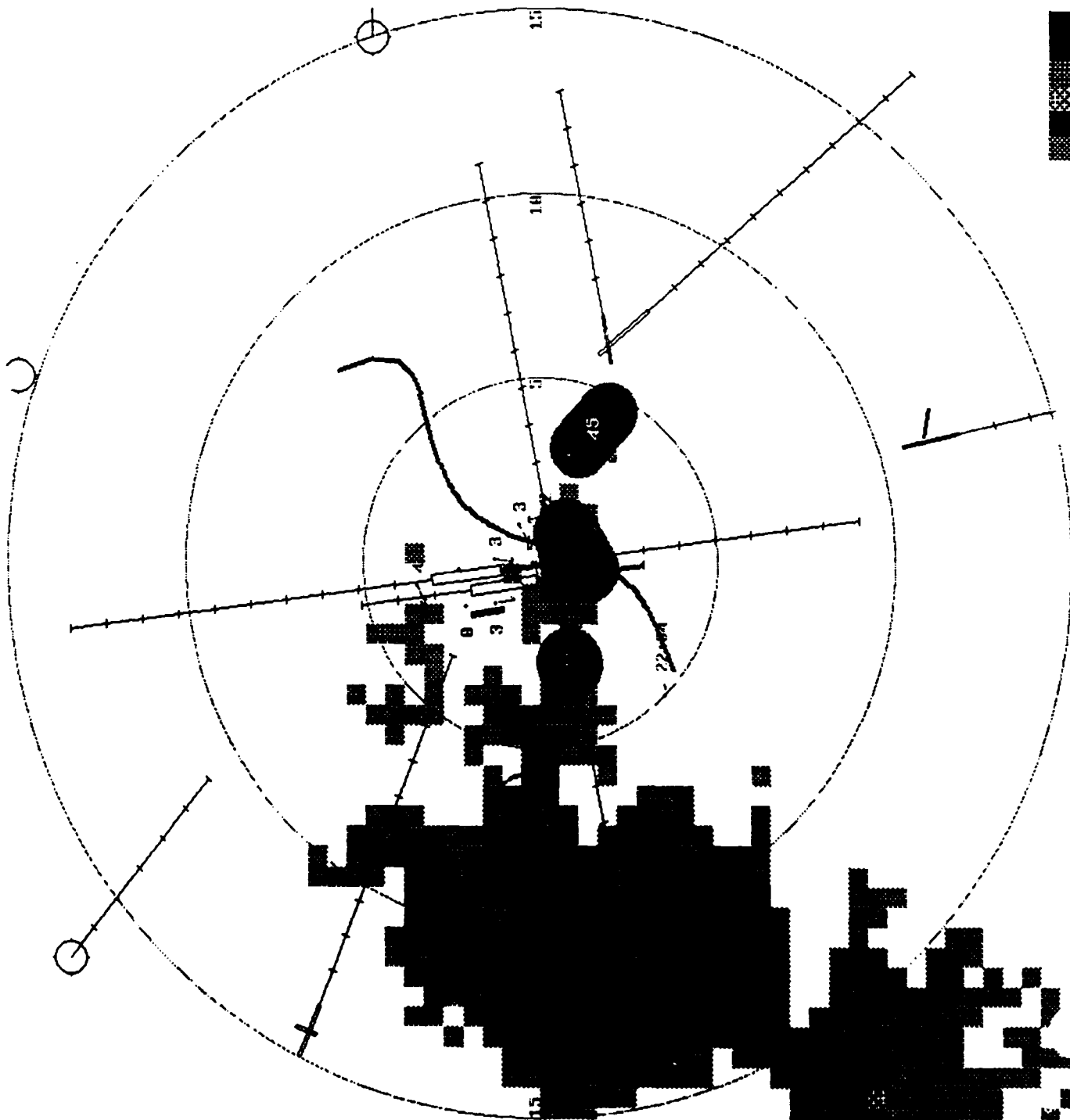
TIME: 2207

MB: UP

GF: UP

PRECIP: UP

LLWAS: UP



**NCAR GSD**

## RANGE

5m 15m 30m 50m

## SCREEN

4	8
3	7
2	6
<b>1</b>	5

## MAPS

- ☐ Vortac & fixes
- ☒ ASR rings
- ☒ Airports
- ☐ Interstates

## PRECIPITATION LEVELS

Off 1-6 3-6 5-6

**WIND SHIFT:**

on  
off

**PRINT SCREEN:**

**STATUS:**

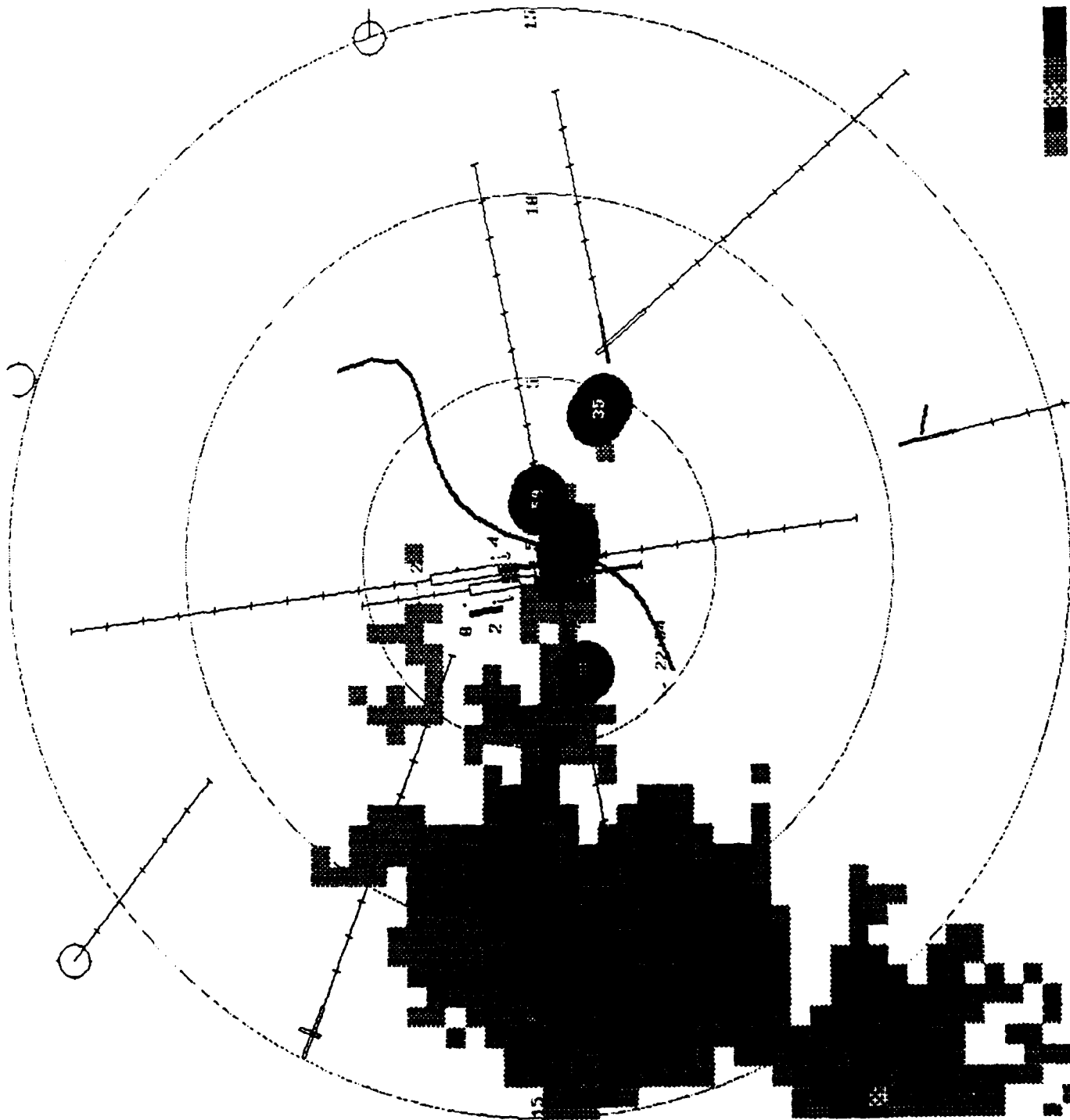
TIME: 2208

UP  
:BA

UP  
: 39

**PRECIP: UP**

**LLWAS: UP**



NCAR GSD

RANGE

☐ 5m ☒ 15m ☐ 30m ☐ 50m

SCREEN

☒ 1 ☐ 2 ☐ 3 ☐ 4  
☐ 5 ☐ 6 ☐ 7 ☐ 8

MAPS

☐ Vortac & fixes  
☒ ASR rings  
☒ Airports  
☐ Interstates

PRECIPITATION LEVELS

☐ Off ☒ 1-6 ☐ 3-6 ☐ 5-6

WIND SHIFT:

☐ Off ☒ On

PRINT SCREEN:

☒ Print

STATUS:

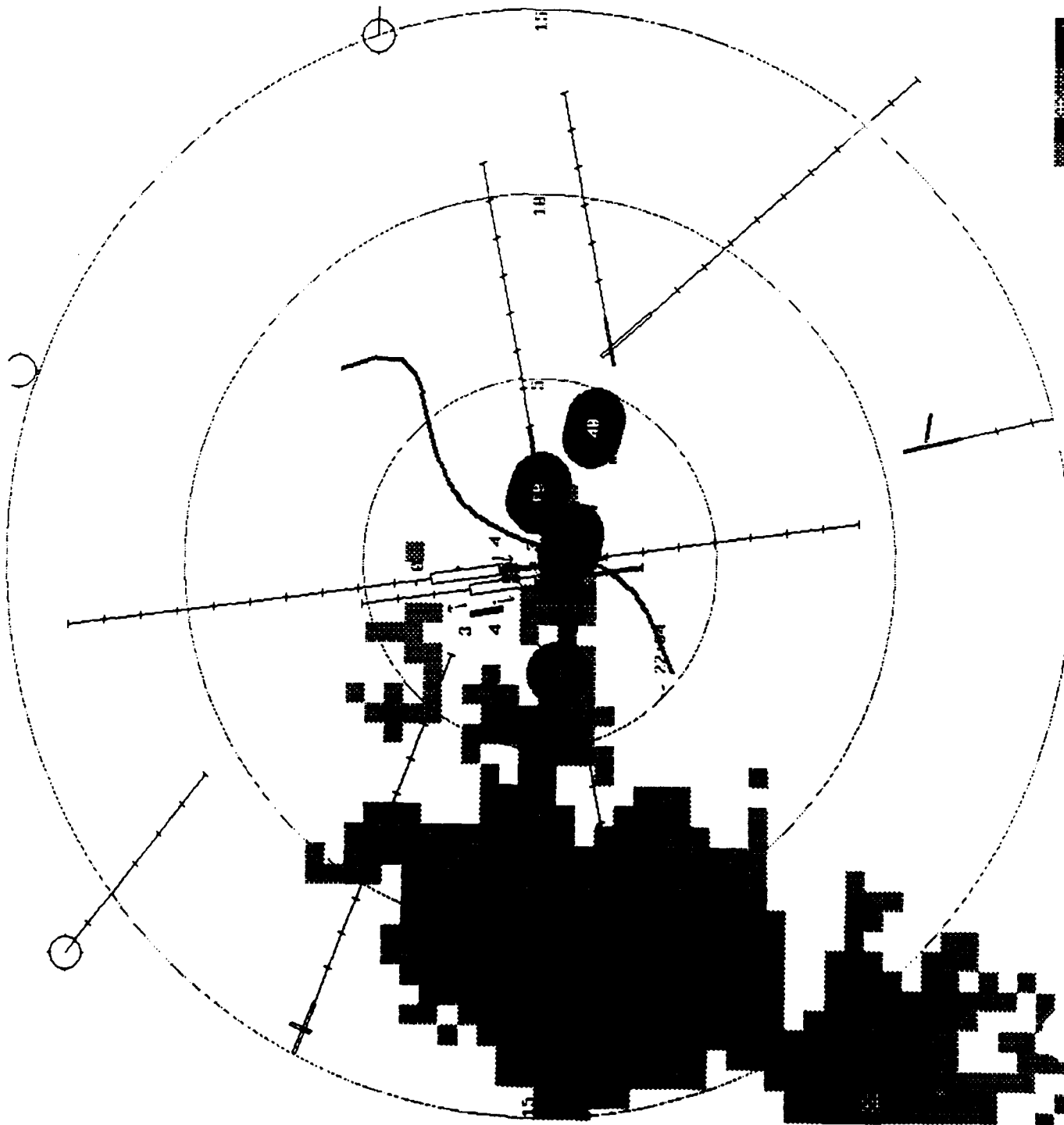
TIME: 2209

MB: UP

GF: UP

PRECIP: UP

LLWAS: UP



NCAR GSD

RANGE

☐ 5m ☒ 15m ☐ 30m ☐ 50m

SCREEN

☒ 1 ☐ 2 ☐ 3 ☐ 4  
☐ 5 ☐ 6 ☐ 7 ☐ 8

MAPS

☐ Vortac & fixes  
☒ ASR rings  
☒ Airports  
☐ Interstates

PRECIPITATION LEVELS

☐ Off ☒ 1-6 ☐ 3-6 ☐ 5-6

WIND SHIFT:

☐ Off ☒ On

PRINT SCREEN:

☒ Print

STATUS:

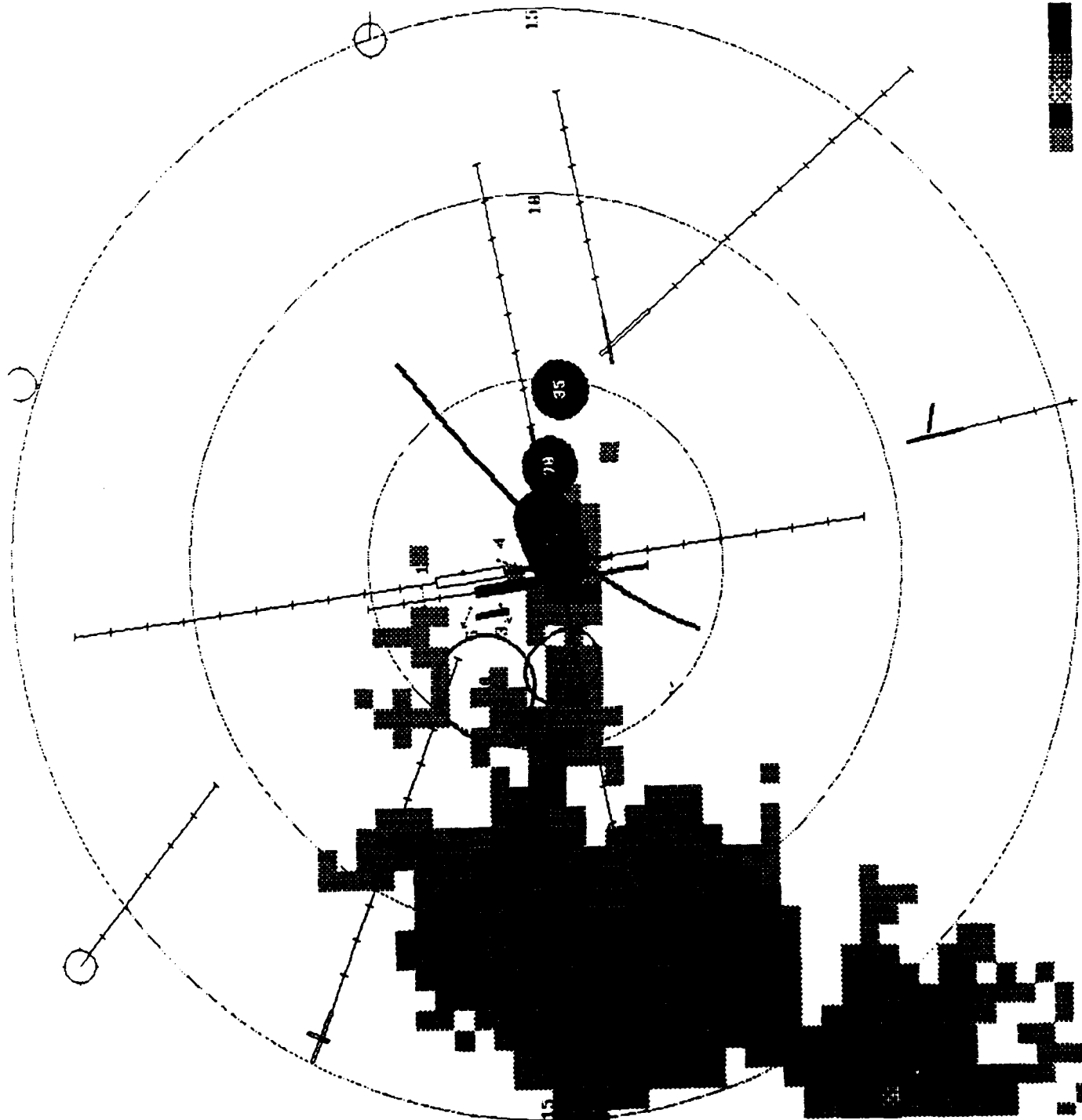
TIME: 2211

MB: UP

GF: UP

PRECIP: UP

LLWAS: UP



NCAR GSD

RANGE

☐ 5m ☒ 15m ☐ 30m ☐ 50m

SCREEN

☒ 1 ☐ 2 ☐ 3 ☐ 4  
☐ 5 ☐ 6 ☐ 7 ☐ 8

MAPS

☐ Vortac & fixes  
☒ ASR rings  
☒ Airports  
☐ Interstates

PRECIPITATION LEVELS

☐ Off ☒ 1-6 ☐ 3-6 ☐ 5-6

WIND SHIFT:

☐ Off ☒ On

PRINT SCREEN:

☒

STATUS:

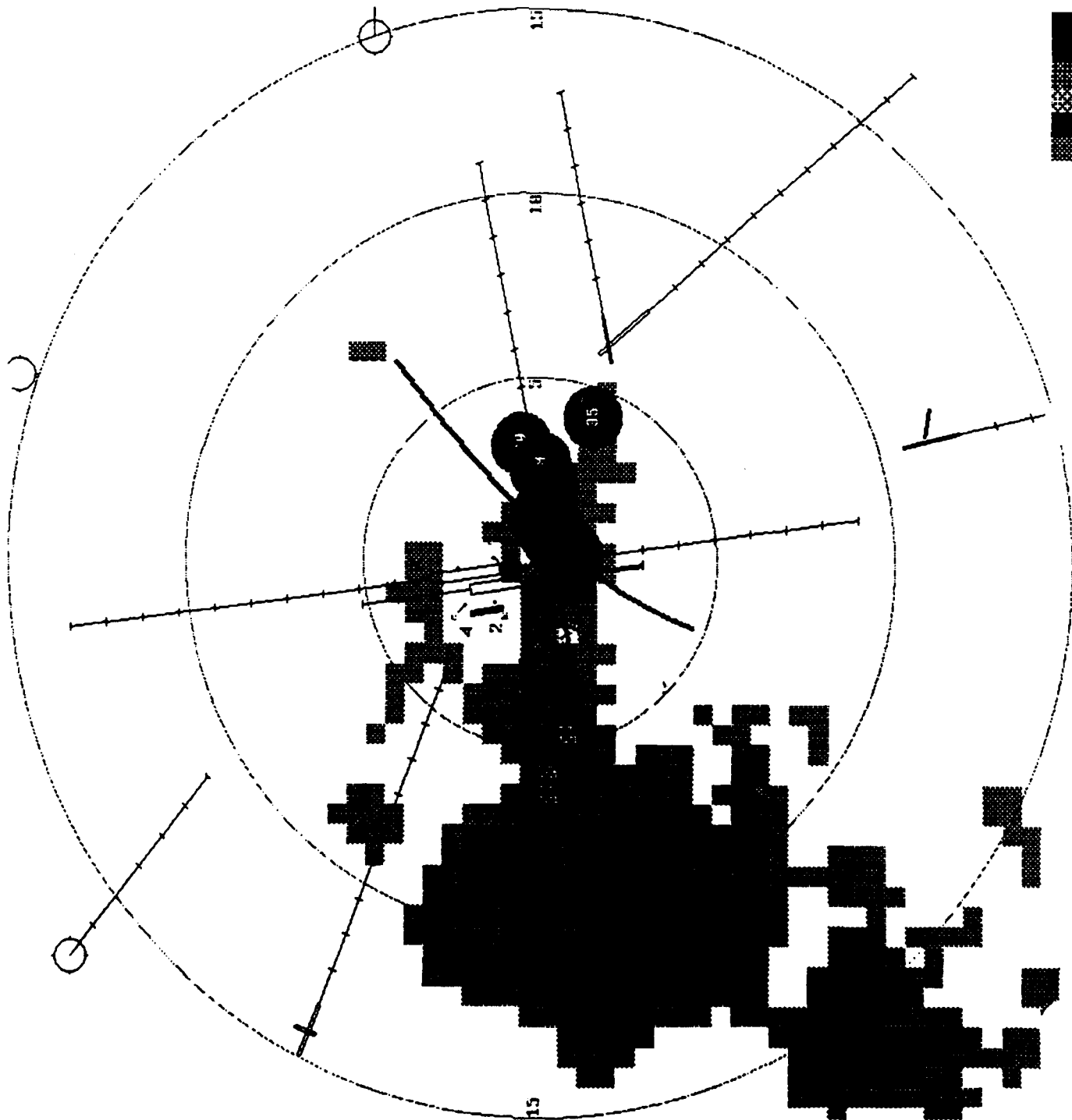
TIME: 2212

MB: UP

GF: UP

PRECIP: UP

LLWAS: UP





NCAR GSD

RANGE

5m 15m 30m 50m

SCREEN

1 2 3 4  
5 6 7 8

MAPS

☐ Vortac & fixes  
☒ ASR rings  
☒ Airports  
☐ Interstates

PRECIPITATION LEVELS

Off 1-6 3-6 5-6

WIND SHIFT:

Off On

PRINT SCREEN:

Print Screen

STATUS:

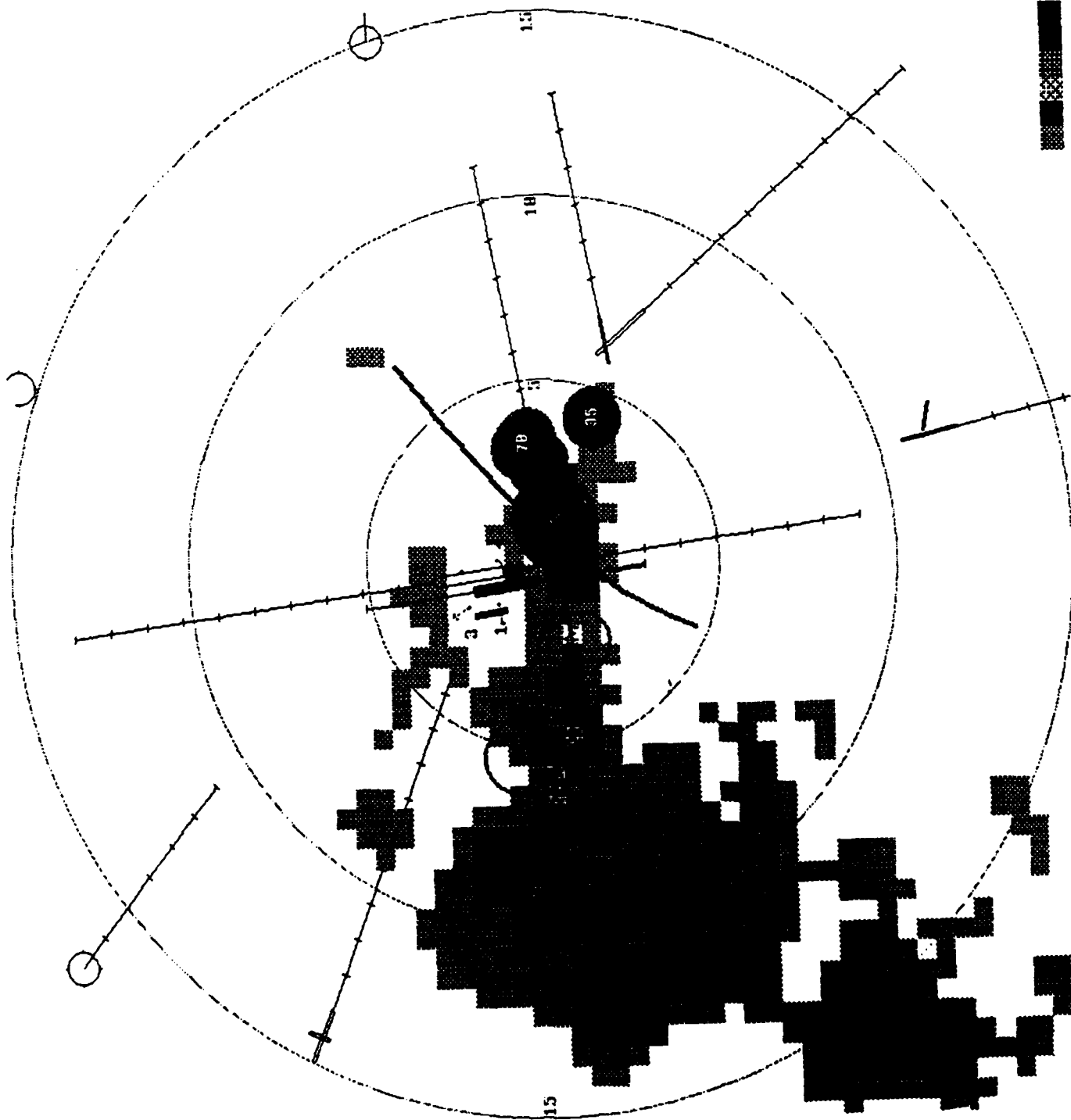
TIME: 2213

MB: UP

GF: UP

PRECIP: UP

LLWAS: UP



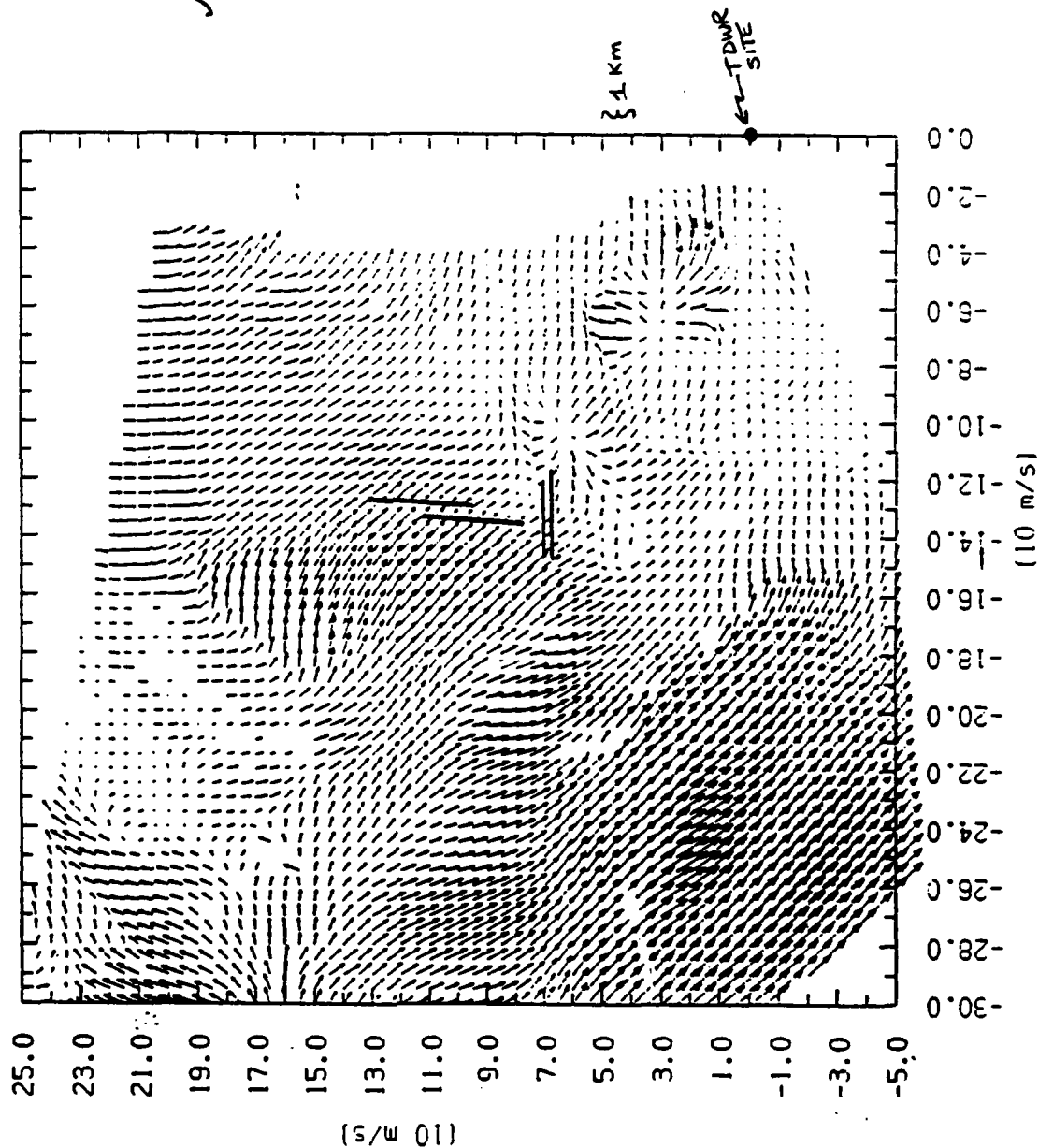
Dun/ Doppler

N ↑

VELOCITY FIELD

FL2 = ( 0.00, 0.00 )      TIME = 88 7 11 (22:6:2)

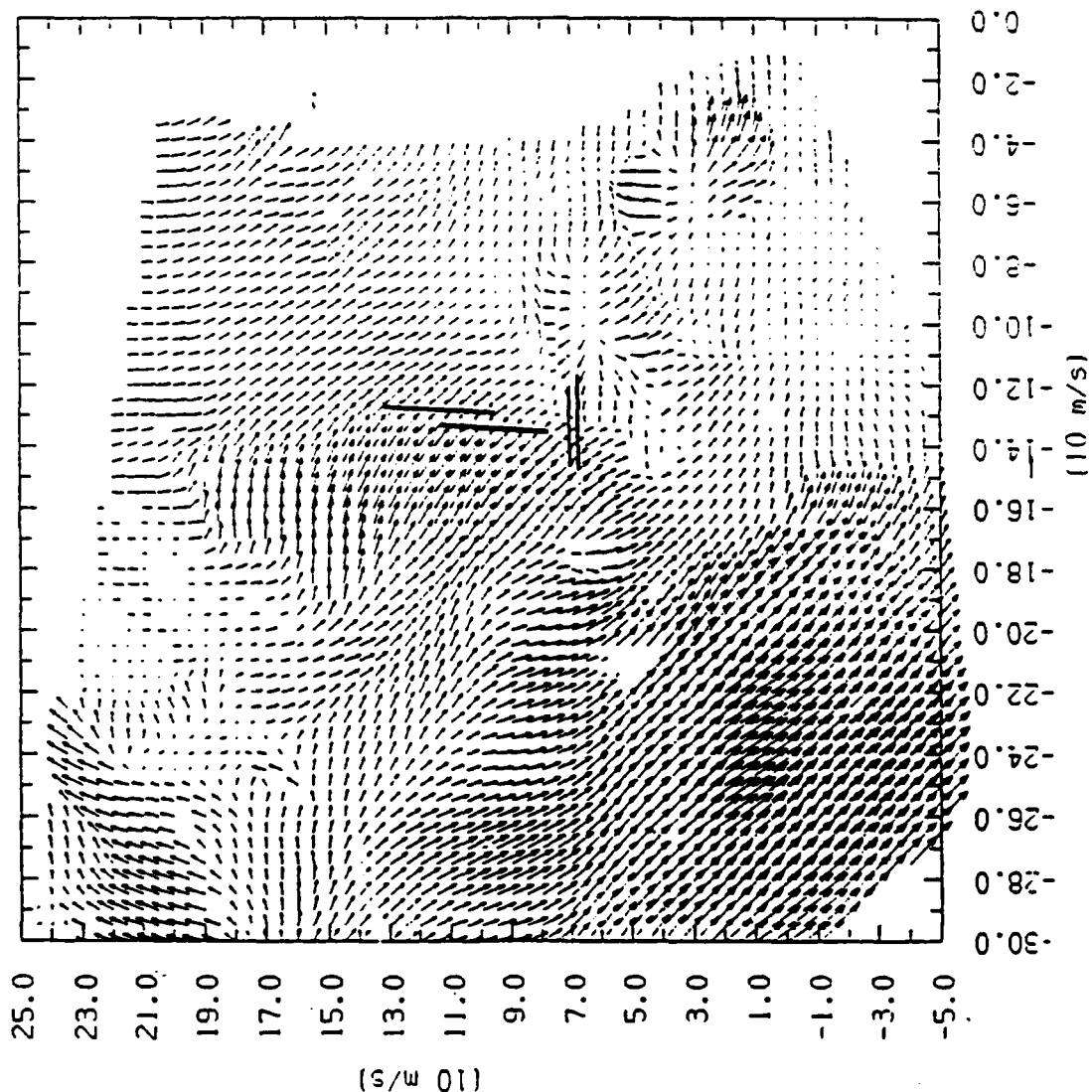
UND = (-2.74, 20.55 )



# VELOCITY FIELD

FL2 = ( 0.00, 0.00 )      TIME = 88   7 11 22: 6:59

UND = (-2.74, 20.55 )

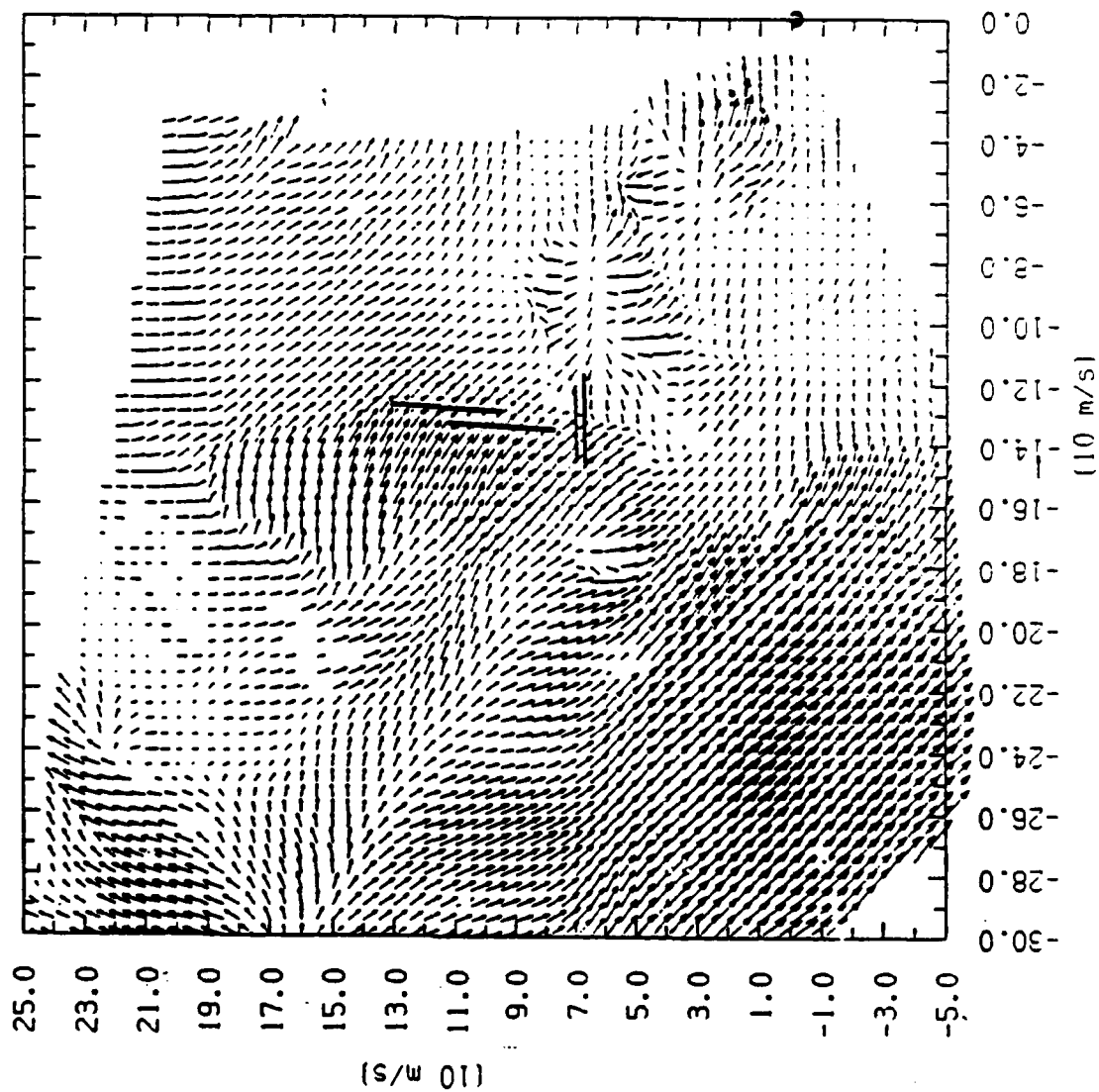


# VELOCITY FIELD

FL2 = ( 0.00, 0.00 )

TIME = 88 7 11 22: 8: 3

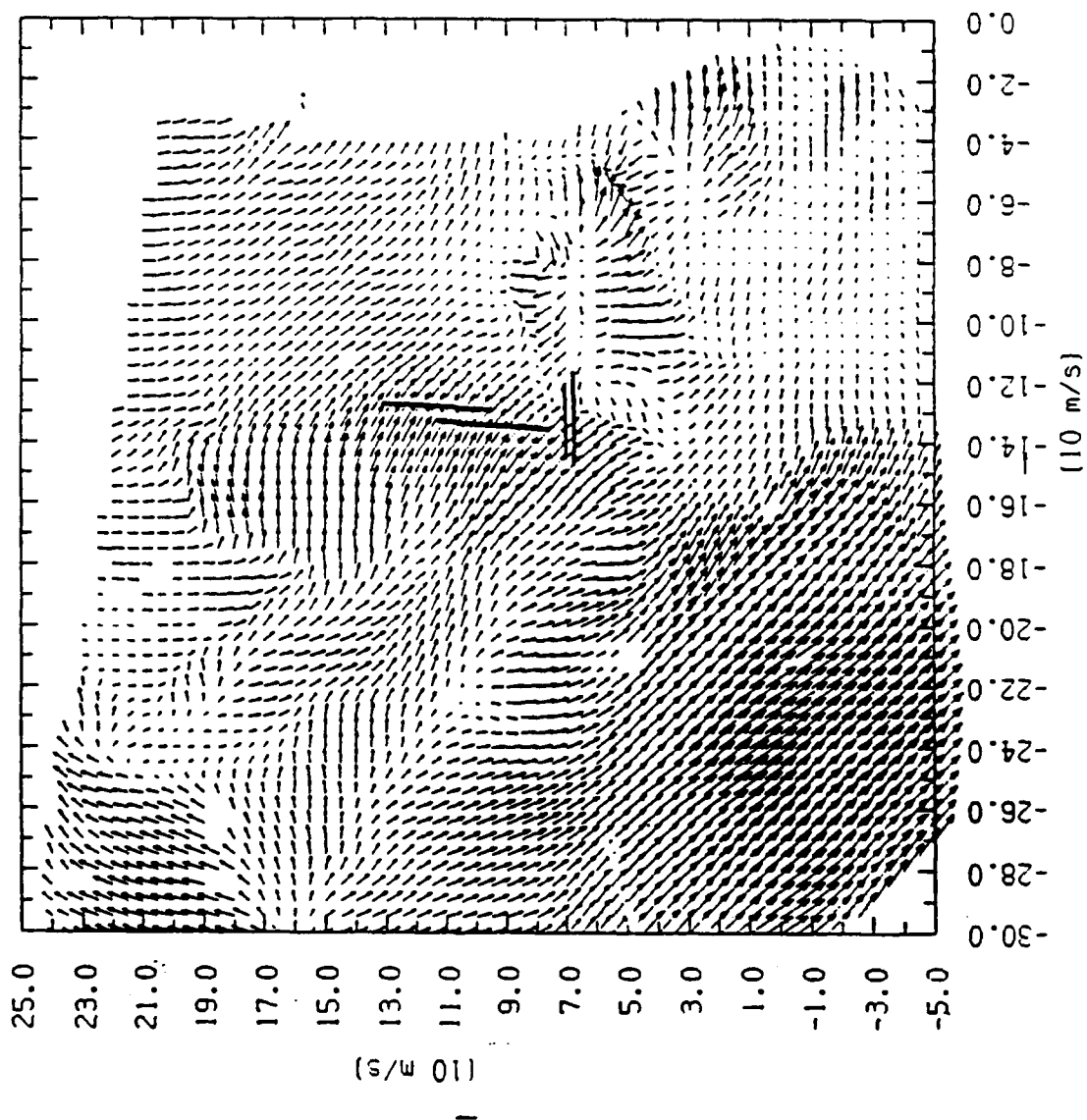
UND = (-2.74, 20.55 )



# VELOCITY FIELD

FL2 = ( 0.00, 0.00 )      TIME = 88 7 11 (22: 9: 0)

UND = (-2.74, 20.55 )



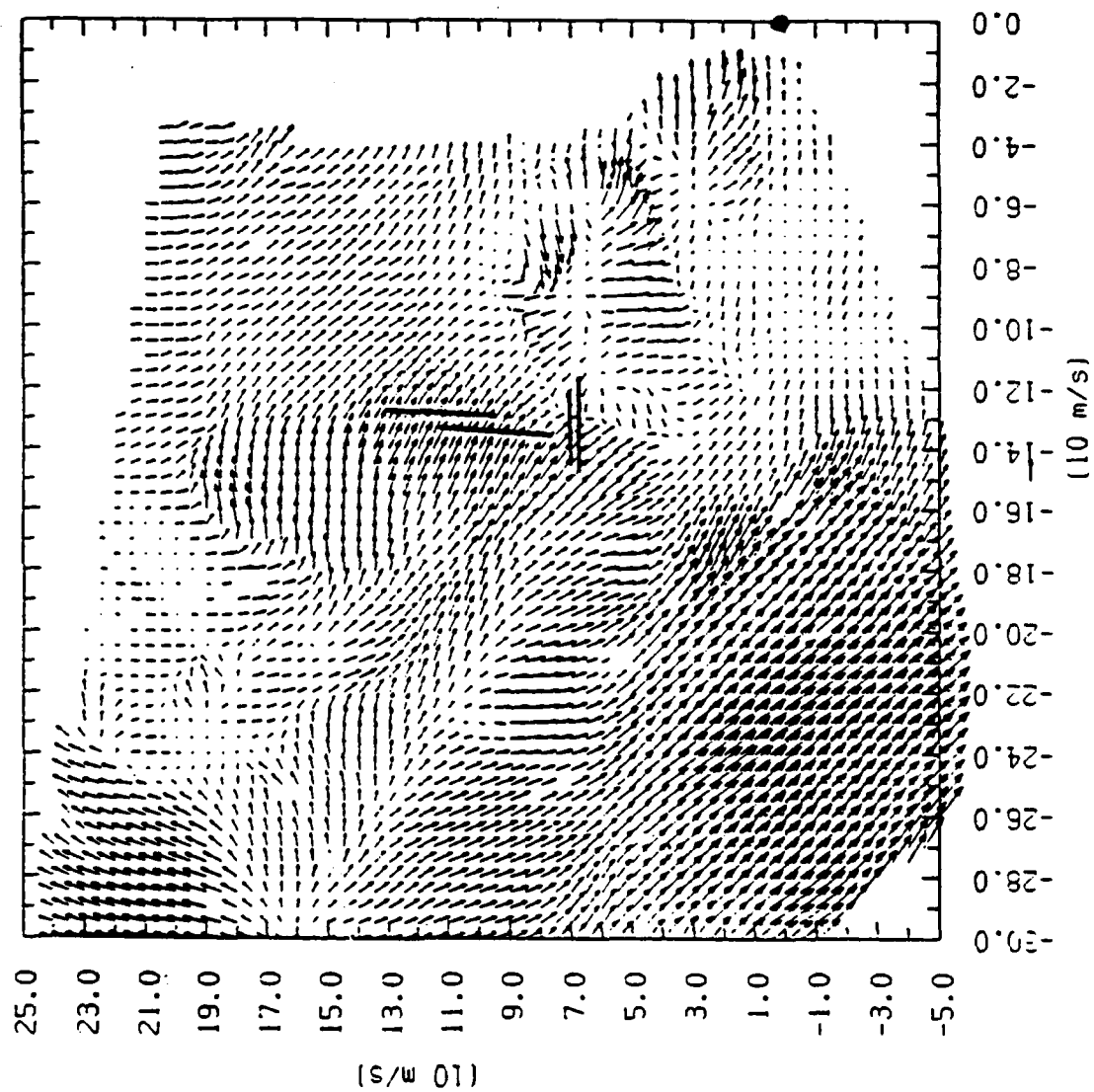
# VELOCITY FIELD

FL2 = ( 0.00, 0.00 )

TIME = 88 7 1

22:10: 3

UND = (-2.74, 20.55 )



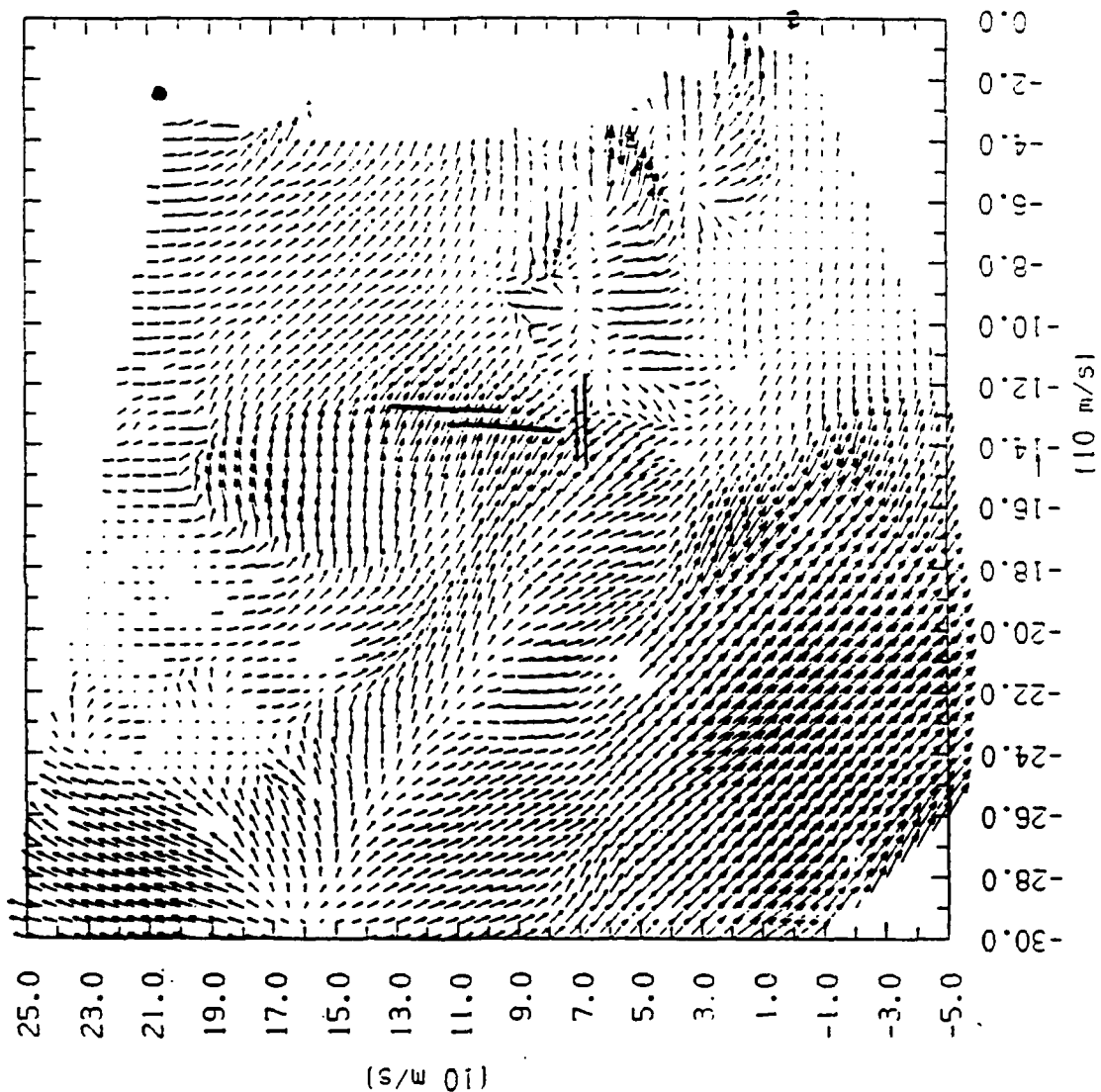
# VELOCITY FIELD

FL2 = ( 0.00, 0.00 )

TIME = 88 7 11

(22:11:0)

UND = (-2.74, 20.55)

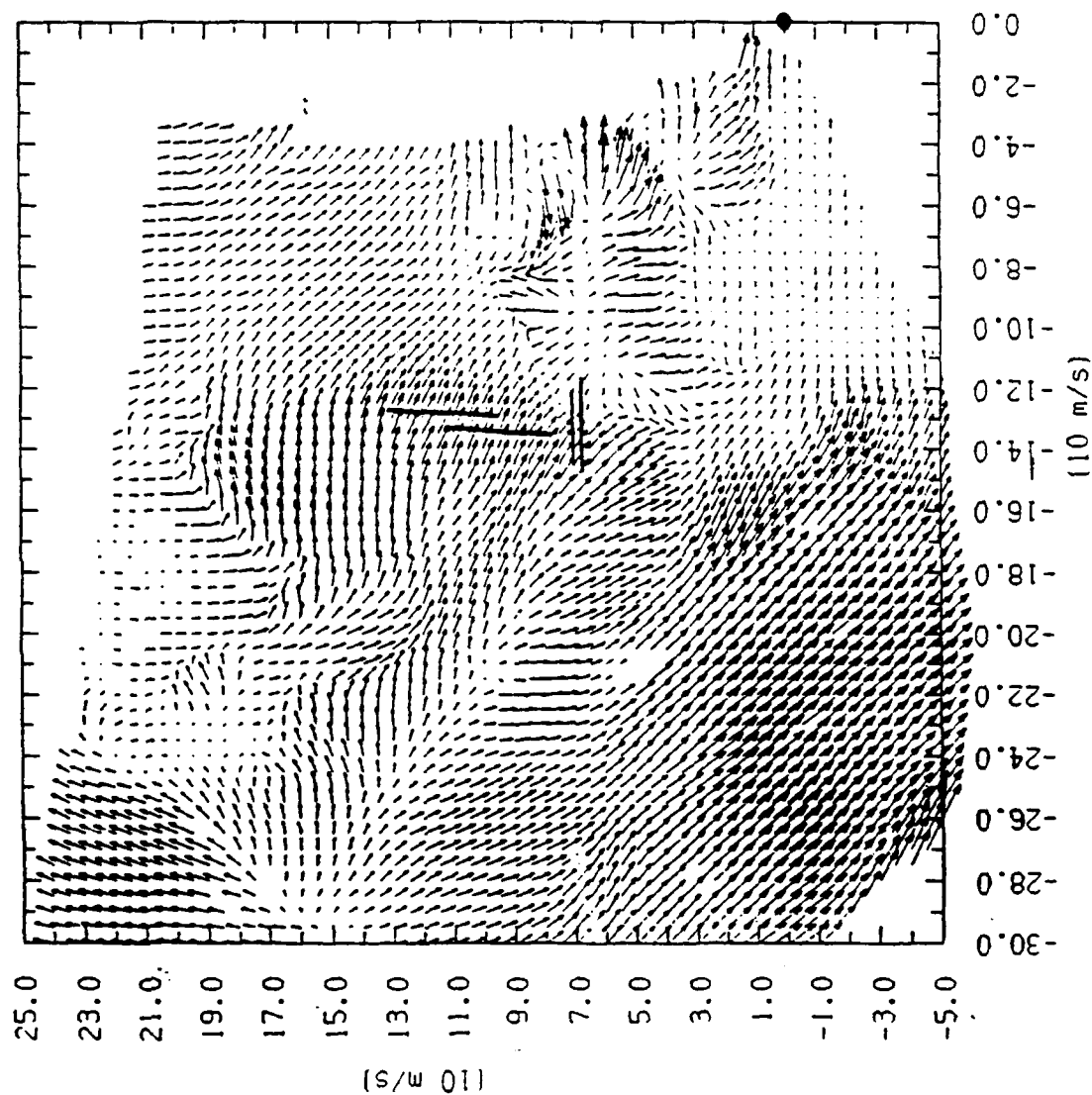


# VELOCITY FIELD

FL2 = ( 0.00, 0.00 )


TIME = 88 7 11 22:11:58

UND = (-2.74, 20.55)





APPENDIX 7 - Crew Statements

- a. Captain's Report, UA862/11 July
  - b. Captain's Report, UA395/11 July
  - c. Supplementary Statement From  
F/O of UA395
  - d. Captain's Report, UA949/11 July
  - e. Captain's Report, UA305/11 July
- 

The following comments were provided by the flight crew of Flight 862 relative to the microburst encounter:

The microburst alert given by Denver Tower when on final approach at approx. 1000' AGL, Rwy. 26R. Visible rain shaft ahead. CB to the SW edge of the airport. Executed a missed approach and held in the clear until weather improved.

The following comments were provided by the flight crew of Flight 395 relative to the microburst encounter:

On a visual approach to 26L at DEN, F/O was flying and we noted and discussed conditions conducive to windshear. Considering these conditions, planned approach to be flown 15-20 kts. above Ref. speed. As we approached 26L in the vicinity of 1000 ft. AGL, the following things happened in very rapid succession: 1) GPWS sounded twice (F/O made slight shallowing of pitch and GPWS warning stopped); 2) tower reported microburst alert with wind speed loss of what sounded like 50 kts., 3) another aircraft on freq. asked about a visual to the 35 runways, 4) another aircraft reported breaking off his approach, and 5) what was virga before was now reaching ground. As I looked over at the 35's to see if that might be a possibility, we almost simultaneously encountered the rain that was now falling at the airport. I called for firewall thrust and flight path, F/O executed windshear encounter SOP. It quickly became apparent aircraft was climbing normally, so executed normal go around SOP. Called tower, told them we were missing on runway 26L, and were given instruction to turn right to 010° and climb to 8000 ft. Approach then vectored us out to the northeast of DEN and cleared us to 14000 ft. Then we were given holding on the DEN 046/20-30. In the holding area I called dispatch to inform them of conditions at the airport and our holding location and LFC time. As we reached 14000 ft., turbulence now reached the level of moderate. Flight attendants called and indicated numerous passengers were experiencing discomfort and airsickness and that they were out of sick sacks. Approach was receiving several complaints as to the turbulence and lightning that was occurring in the holding area, so approach vectored us to the DEN 313/15-25 for holding, which was essentially in the clear with only light chop. Again called dispatch to inform them of our new holding location and our fuel status. Conditions started to improve around 2242Z. After another aircraft started an approach and everything appeared normal, we requested an approach and landed at 2253Z.

We were heavy and the ATIS was indicating a slight tail wind and wind shear alert. Don and I discussed the approach and we decided if anything to stay a little high and keep our speed 15 to 20 knots above ref. I was flying and configured early, but it was still not enough as we were a little higher than I would have liked over Altur. I used flaps 40 for a short time, and as we approached the glide slope I went back to flaps 30 and came in with the power. We could see the cloud and virga over the runways. At some point below 1000 ft the thwer announced that it was raining at the field and then that there were indications of a 50 knot

shear. Another aircraft said they were going missed approach and we got the 'Woop woop, pull up' warning. I pulled up the nose and increased power from about 3000 lbs. to 4000 lbs. The warning ceased but the airspeed began to decrease. Don said, 'Firewall them, let's get out of here.' I did and the aircraft responded immediately. The go-around was completed above 500 feet and at no time did the airspeed decrease to ref.

The following comments were provided by the flight crew of Flight 949 relative to the microburst encounter:

Approach corridor over Kowa. Crossed Kiowa at 15000 ft., 250 kts. Turned to north for vectors to land runway 26L. Cloud over Denver Area with breaks in cloud base, some virga, and observed rain shaft over DEN airport while on north heading. Cleared for visual southeast of Buckley ANG Base to follow a DC-8 by 3-4 miles. Flight conditions - JFR, good vis. and fairly smooth. Briefed crew on possibility of windshear. Took flaps and gear as approaching Altura advised by DEN APP control 'raining at DEN airport.' Rainshower appeared light as you could see through it, seeing runway at all times. Was 200'-300' high on G.S. and carrying flaps 15° and 190 kts. Inside marker, observed DC-8 execute a go-around and comment maybe it was because of windshear. Took flaps 25° smf jrstf ypert sfbodr 'microburst alert'.

The following comments were provided by the flight crew of Flight 305 relative to the microburst encounter:

On downwind to 26L we noticed a rain shower east-southeast of the approach. Turning final we experienced considerable difficulty slowing the aircraft. While still east of the shower, Tower reported wind as calm - later 180/4 then 160/6. Some aircraft ahead of us were executing go-arounds. Tower advised one pilot reported a loss of 80 knots. By this time we were at or just west of the shower about 1100 feet - started our go-around. The go-around was relatively flat and airspeed hard to gain - very choppy. Held north 20-30 min. and landed 17L no problem.

## **APPENDIX 2 -- NASA Langley Report**

Proctor, F.H., Bowles, R.L., "Investigation of the Denver 11 July 1988 Microburst Storm with the Three-Dimensional NASA-Langley Windshear Model," (Draft to be Submitted as a NASA Report) July 26, 1989.

**INVESTIGATION OF THE DENVER 11 JULY 1988  
MICROBURST STORM WITH THE THREE-DIMENSIONAL  
NASA-LANGLEY WINDSHEAR MODEL**

**F. H. Proctor**

**MESO, Inc.**

***Hampton, Virginia***

***and***

**R. L. Bowles**

**NASA Langley**

***Hampton, Virginia***

**DRAFT, TO BE SUBMITTED AS A NASA REPORT**

**July 26, 1989**



## TABLE OF CONTENTS

LIST OF TABLES .....	iii
LIST OF FIGURES .....	iv
ABSTRACT .....	viii
1. INTRODUCTION .....	1
2. MODEL DESCRIPTION .....	2
3. NUMERICAL SPECIFICATIONS AND INITIAL CONDITIONS ..	5
Numerical Domain and Grid Configuration .....	5
Model Constants and Microphysical Parameters .....	6
Initial Sounding .....	6
Initial Impulse .....	7
4. RESULTS .....	8
Storm Characteristics .....	8
<u>Evolution and Storm Structure</u> .....	9
<u>Evolution of Storm Peak Values</u> .....	12
Driving Mechanism for the Intense Overhang Microburst ..	13
Detailed Structure of the Overhang Microburst .....	15
<u>Peak Velocity Differential: Matching of observed and</u>	
<u>model time</u> .....	17
<u>Horizontal and Vertical Structure</u> .....	18
F-Factor Analyses .....	18
Reconstruction of Aircraft Trajectories and Comparison ...	21

5. SUMMARY AND CONCLUSIONS . . . . .	23
ACKNOWLEDGEMENTS . . . . .	25
REFERENCES . . . . .	26

## LIST OF TABLES

Table 1.	Salient Characteristics of TASS.....
Table 2.	Cloud Microphysical Interactions.....
Table 3.	Comparison of Simulated and Observed Storm Characteristics.....
Table 4.	Comparison of Simulated and Observed Characteristics of Most Intense Microburst.....
Table 5.	Axisymmetric Model Experiments - Sensitivity to Cooling and Loading.....
Table 6.	Summary of Simulated Characteristics...

## LIST OF FIGURES

- Fig. 1. Input sounding plotted on Skew T-log p diagram; based on 2000 UTC 11 July 1988, Denver special sounding. Each full wind barb equals 5 m/s or 10 knots.
- Fig. 2. East-West vertical cross sections of radar reflectivity taken near the center of the storm. Time is in minutes after model initialization and x,y coordinates relative to position of initial perturbation.
- Fig. 3. Three dimensional perspectives of the lower 2 km of the storm viewed from the southeast.
- Fig. 4. East-West vertical cross sections of the simulated wind vector field with radar reflectivity superimposed. The cross sections are near the center of the storm at a) 47 min and b) 52 min simulation time. Wind vectors in this and subsequent figures are ground relative.
- Fig. 5. As in Fig. 4a, but for snow field. The contour interval is 0.1 g m<sup>-3</sup>, with peak values slightly greater than 1.6 g m<sup>-3</sup>.
- Fig. 6. Horizontal cross sections of the low-level wind vector field at a) 47 min, b) 52 min, c) 56 min, and d) 60 min simulation time. The horizontal fields are at 80 m AGL and north is in the y direction.
- Fig. 7. As in Fig. 6, but fields are isotachs of horizontal wind speed at a) 52 min and b) 60 min simulation time. The contour interval is 2 m/s.

- Fig. 8. As in Fig. 6 for a) 47 min and b) 52 min simulation time, but at 2.25 km AGL.
- Fig. 9. Time-height cross sections of storm peak values for a) radar reflectivity, b) downdraft velocity, c) updraft velocity. The contour interval is 10 dBZ in a), 4 m/s in b), and 2 m/s in c). Peak values of (vertical component) vorticity greater than  $0.02 \text{ s}^{-1}$  are shaded in a).
- Fig. 10. Time evolution of peak velocity differential in most intense microburst: Comparison between model data, TDWR estimates, and aircraft flight recorder data. Data for TDWR estimates provided by Campbell (1989), and data reconstructed from the four aircraft FDR provided by Wingrove and Coppenbarger (1989).
- Fig. 11. Horizontal cross sections at 180 m of the wind vector field with radar reflectivity superimposed at a) 47 min (2206 UTC), b) 49 min (2208 UTC), c) 50 min (2209 UTC), d) 52 min (2211 UTC) and e) 54 min simulation time (2213 UTC). Area depicted is windowed around most intense microburst. The contour interval for radar reflectivity is 5 dBZ.
- Fig. 12 As in Fig. 11, but for 52 min (2211 UTC) at a) 80 m, b) 280 m, and c) 400 m AGL. Radar reflectivity depicted in a) only.

- Fig. 13. Vertical east-west cross sections near the center of the intense microburst for wind vectors at a) 47 min (2206 UTC), b) 49 min (2208 UTC), c) 50 min (2209 UTC), d) 52 min (2211 UTC), and e) 54 min simulation time (2213 UTC). Area shown is windowed from model domain with the vertical coordinate stretched relative to x coordinate.
- Fig. 14. As in Fig. 13, but for vertical velocity at 52 min. The contour interval is 1 m/s. Contours with negative values are dashed.
- Fig. 15. Comparison of peak low-level F-Factors vs time. Peak east-west F-Factors below 280 m from model data are indicated by thick solid line.
- Fig. 16. As in Fig.15, but includes higher elevations.
- Fig. 17. As in Fig. 13, but for east-west F-Factors at a) 47 min (2206 UTC), b) 49 min (2208 UTC), c) 50 min (2209 UTC), d) 51 min (2210 UTC), e) 52 min (2211 UTC), and f) 54 min simulation time (2213 UTC). The contour interval is 0.05.
- Fig. 18. Horizontal cross section at 80 m AGL of east-west F-Factors at 52 min (2211 UTC).
- Fig. 19. As in Fig. 18, but for north-south F-Factors.
- Fig. 20. Aircraft positions relative to the runway (from Wingrove and Coppenbarger 1989).

- Fig. 21. Horizontal wind profile along the flight path of 4 aircraft (Modified from original figure from Wingrove and Coppenbarger 1989). The dashed lines represent the wind profiles reconstructed from the flight data recorders, whereas the solid lines represent the model x-component winds along the aircraft flight paths.
- Fig. 22. As in Fig. 21, but for model F-Factors computed along the flight paths of the aircraft.

## **ABSTRACT**

Near Denver on July 11, 1988 a moderate reflectivity thunderstorm produced a microburst of unusual intensity during the test operation of the Terminal Doppler Weather Radar (TDWR) system. Several aircraft had inadvertent encounters with the microburst during final approach to Stapleton Airport, but survived with no damage or injuries. This microburst and its parent storm are investigated via simulation with the Terminal Area Simulation System (TASS). Model results show that intense multiple microbursts formed downwind of the main precipitation shaft as sublimating snow fell out of overhanging clouds that were sheared downstream from the main cell. Evolution and structure of the storm and its microbursts, including hazard indices based on F-Factor, are investigated in detail and compared with "observed" data from doppler radar and aircraft flight-data recorders.



## 1. INTRODUCTION

Presented in this report is a numerical simulation of an unusual storm occurring near Denver on July 11, 1988, which was responsible for five successive missed approaches by commercial aircraft. The structure of the storm (as confirmed by doppler radar) is unusual in the sense of previously documented case studies of cumulonimbus storms. The storm was relatively small in vertical extent, long lived, of moderate radar reflectivity, and accompanied by light precipitation amounts. However, the most peculiar aspect of this persistent but benign appearing storm was its generation of uncommonly-intense microbursts some distance downstream from the primary precipitation area. One of these microbursts had near fatal consequences on several of the commercial aircraft attempting to land at Denver Stapleton airport between 2207 and 2213 UTC. Although there were no passenger injuries and no damage to the aircraft, four successive jet airliners experienced inadvertent encounters with an unusually intense wind shear during final approach. The aircraft successfully executed missed approaches with one airliner descending to less than 30 m above ground level (AGL) at a distance of about 1.3 km from the touchdown end of the runway (Ireland 1988). Terminal Doppler Weather Radar (TDWR) at Stapleton was in test operation during the storm and detected dangerous wind shear during the attempted aircraft landings. The peak differential-velocity change detected by TDWR of about 40 m/s (Klass 1989) is unusually strong relative to typical Colorado microbursts and underscores the potential danger that was faced by the approaching aircraft.

This report represents the model investigation of the storm. Parallel reports are being prepared by the National Center for Atmospheric Research (NCAR) concerning the observational and radar analysis of the storm, and by NASA Ames concerning the interpretation of the aircraft flight recorder data.

## 2. MODEL DESCRIPTION

The numerical model used for this simulation is the Terminal Area Simulation System<sup>1</sup> (TASS) which is documented in Proctor (1987a). The TASS model is a time-dependent, nonhydrostatic cloud model which consists of 11 prognostic equations: three equations for momentum, one equation each for pressure deviation and potential temperature, and six coupled equations for continuity of water substance (vapor, cloud droplets, ice crystals, hail/graupel, rain, and snow<sup>2</sup>). Salient characteristics of the TASS model are listed in Table 1.

The TASS model subdivides the precipitating hydrometeors into three bulk categories (hail or graupel, rain, and snow) each governed by its own prognostic equation for continuity. As in Cotton et al. (1982), the hail/graupel category is represented by either high-density hail or moderate-density graupel, depending upon the particle diameter. Parameterizations for numerous microphysical interactions and subsequent latent heat exchanges are included in TASS and listed in Table 2.

The model has been applied extensively to the study of microbursts (Proctor 1988a, 1988c, 1989a, and 1989b), and has been successfully validated in five case studies of cumulonimbus convection -- ranging from longlasting supercell hailstorms to short lived single-cell storms, including the 1985 Dallas-Fort Worth Microburst storm (Proctor 1987b).

---

<sup>1</sup>Also known as the NASA-Langley Windshear Model

<sup>2</sup>Snow in the TASS model is treated as spherical, low-density graupel-like snow particles rather than dendritic flakes; see Proctor (1987a) for details.

**Table 1. Sallent characteristics of TASS**

Compressible nonhydrostatic equation set  
Three-dimensional staggered grid  
Storm-following movable mesh  
Second-order quadratic-conservative space differencing  
Adams-Bashforth time differencing  
Explicit time-splitting method of integration  
Vertical grid-size stretching  
Radiation boundary conditions applied to open lateral boundaries  
Filter and Sponge applied to top four rows in order to diminish gravity wave reflection at top boundary  
No explicit numerical filtering applied to interior points  
Surface friction layer based on Monin-Obukhov Similarity theory  
Smagorinsky subgrid-turbulence closure with Richardson number dependence  
Liquid and ice-phase microphysics  
Inverse-exponential size distributions assumed for rain, hail/graupel, and snow  
Wet and dry hail growth  
Radar reflectivity diagnosed from model rain, snow, and hail/graupel fields  
Accumulated precipitation advected opposite of grid motion, so as to remain ground relative  
Initialization from observed sounding with thermal impulse

**Table 2. Cloud Microphysical Interactions**

Accretion of cloud droplets by rain

Condensation of water vapor into cloud droplets

Berry-Reinhardt formulation for autoconversion of cloud droplet water into rain

Evaporation of rain and cloud droplets

Spontaneous freezing of supercooled cloud droplets and rain

Initiation of cloud ice crystals

Ice crystal and snow growth due to riming

Vapor deposition and sublimation of hail/graupel, snow, and cloud ice crystals

Accretion by hail/graupel of cloud droplets, cloud ice crystals, rain, and snow

Contact freezing of supercooled rain resulting from collisions with cloud ice crystals or snow

Production of hail/graupel from snow riming

Melting of cloud ice crystals, snow, and hail/graupel

Shedding of unfrozen water during hail wet growth

Shedding of water from melting hail/graupel and snow

Conversion of cloud ice crystals into snow

Accretion by snow of cloud droplets, cloud ice crystals, and rain

Evaporation or vapor condensation on melting hail/graupel and snow

### 3. NUMERICAL SPECIFICATIONS AND INITIAL CONDITIONS

The model input conditions were chosen without prior knowledge of the storm structure, and only one high-resolution experiment with the 3-D model was performed. Preliminary analysis of the results from this simulation were presented in October, 1988 (Proctor 1988b), only months after the actual event. The specific input specifications and initial conditions for the numerical experiment are described below.

#### Numerical Domain and Grid Configuration

The dimension of the physical grid domain is 18 km in the west-east direction (x-coordinate), 12 km in the south-north direction (y-coordinate), and 10 km in the vertical direction (z-coordinate). The domain is resolved by 36 vertically-stacked horizontal levels, each separated by a vertical grid spacing stretching from 80 m near the ground to 475 m near the top boundary. Each level is resolved by 92 x 62 grid points with a uniform horizontal grid spacing of 200 m. These specifications should be adequate to resolve most of the major features of the microburst and its parent storm. [A smaller grid size would be preferable, but presently, is limited by computational constraints (i.e., computer time).]

The model internally computes the translation of the storm and correspondingly adjusts the movement of the grid. Thus if the modeled storm changes direction and (or) speed, the translation of the grid is adjusted to keep the storm centered within the domain. This procedure allows a reduction of the domain size and reduces the magnitude of numerical truncation error.

## Model Constants and Microphysical Parameters

In running simulations with the TASS model, it is our philosophy to refrain from readjusting constants so as to "tweak" the simulation and force an *a priori* specification of the storm. However, a few of the model constants are not invariant from case to case and are defined below.

One set of constants important to the cloud microphysics is the cloud droplet number density,  $n_{cd}$ , and their dispersion coefficient,  $\sigma$  (see Proctor 1987a). The values chosen for these two parameters are respectively,  $1000 \text{ cm}^{-3}$  and 0.15; values which are typical of continental clouds and which may be expected in Colorado storms (e.g., Proctor 1987a).

The only other model constants in need of specification are the surface roughness, set at 10 cm; and the latitude (which affects the value of the coriolis parameter) which is chosen as  $39.7^\circ$  north.

## Initial Sounding

The environmental conditions for the experiment (i.e., temperature, humidity, wind speed and direction) are taken from the sounding shown in Fig. 1. The input sounding is only slightly modified from the one observed at Denver Stapleton, at 2000 UTC, just two hours before the occurrence of the microburst. The low-level lapse rates for humidity and temperature in Fig. 1 were slightly adjusted from the original sounding, in order to agree with surface temperatures and cloud-base heights reported just prior to the event.

The input sounding indicates a deep adiabatic layer extending from the ground to about 5 km MSL (3.4 km AGL), dry air near the surface, and high relative humidity near the top of the adiabatic layer. This type

of sounding is not unusual for the Denver area and is similar to other typical "dry-microburst" soundings (e.g., Wakimoto 1985).

The vertical wind profile represented in Fig. 1 indicates light and variable winds below 3.6 km MSL (2 km AGL), and west to northwest winds with speeds greater than 12.5 m/s (25 knots) above 6.1 km MSL (4.5 km AGL).

### Initial Impulse

Cumulonimbus convection is initiated in the simulation by specifying a thermal impulse within a horizontally-uniform, but vertically-varying environment. As in previous case studies with the TASS model (Proctor 1987b), a spheroidal thermal impulse is specified at time zero with a peak amplitude of  $1.5^{\circ}$  C, a diameter of 5 km, and a depth of 2.5 km. The initial impulse is centered at 1.25 km above the ground and horizontally within the domain.

#### 4. RESULTS

The model results produced good quantitative and qualitative agreement with observations of the major storm features. Some of the comparisons are listed in Tables 3 and 4.

**Table 3. Comparison of Simulated and Observed Storm Characteristics**

	<u>Simulated</u>	<u>Observed</u>
Lifetime	Long-lived	Long-lived
Cloud Base (AGL)	3.5 km <sup>a</sup>	3.5 km
Cloud Top (AGL)	7.5 km	9 km
Precipitation	Light	Light
Radar Reflectivity	50 dBZ	Moderate reflectivity
Translation (from)	280° at 8.5 m/s	270° at 10 m/s
Eastern Overhang	Yes	Yes
Rotation Present	Yes	Yes
Microbursts	Multiple	Multiple
<sup>a</sup> An input condition		

#### Storm Characteristics

A persistent but relatively shallow storm develops soon after the initial impulse is imposed. The cloud base of the storm is at 3.5 km AGL



(5.1 km MSL) which is about 300 m above the melting level<sup>3</sup>. The cloud top is at about 7.5 km AGL which is well below the tropopause level. The 4 km thick cloud is composed of ice crystals and supercooled cloud droplets, and generates precipitation mostly in the form of snow and graupel. Rain is produced below the cloud-base level primarily from the melting of falling snow and graupel. Updrafts in the storm are not much greater than 10 m/s with much of the cloud and precipitation carried downstream by the relatively strong winds aloft. The movement of the modeled storm is from the WNW at 8.5 m/s.

#### Evolution and Storm Structure

In Fig. 2 a time sequence of the storm radar reflectivity is depicted in west-east vertical cross sections taken near the center of the storm. [The x,y coordinates indicated in the figure (and subsequent figures) are relative to the position of the initial temperature impulse specified at time zero.] The main precipitation shaft, located on the western side of the storm is persistent with time and has values of radar reflectivity greater than 40 dBZ. An overhang, roughly located between 2 and 7 km AGL, extends eastward from the main precipitation shaft. After 40 min precipitation begins to fall from the overhang, reaching the ground after 47 min and producing an intense microburst with a differential velocity of over 40 m/s. Weaker microbursts are associated with the western precipitation shaft, even though it is associated with higher radar reflectivity. Movement with time of the persistent western precipitation shaft can be noted by the change in the x-coordinate position (Fig. 2). However, note that the precipitation falling from the overhang (at x ~ 15 km) has relatively little eastward movement. The location of the intense overhang microburst, about 7 km to the east of the main cell, compares favorably with observations of the actual event. As confirmed by radar,

---

<sup>3</sup>Height at which the temperature is 273.16 K.

**Table 4. Comparison of Simulated and Observed Characteristics of Most Intense Microburst**

	<u>Simulated</u>	<u>Observed</u>
Maximum Velocity Differential	37 - 42 m/s	34 - 42 m/s <sup>a,b</sup>
Maximum F-Factor	0.24 - 0.27	0.19 - 0.25 <sup>a,b,c</sup>
Maximum Outflow Speed	22.3 m/s	23 m/s <sup>d</sup>
Peak Radar Reflectivity	40 dBZ	38 dBZ
Peak Temperature Drop	5° C	8° C <sup>d</sup>
Peak Pressure Increase	2.64 mb	2.5 mb <sup>d</sup>
Configuration of Radar Echo	Elongated E-W	Elongated E-W
Location	7 km downstream from main echo	8 km downstream from main echo
Precipitation at Ground	Very light rain	Very light rain
Ring Vortex	Yes	Yes <sup>c</sup>
Contains Multiple-Downdraft Centers	Yes	Yes <sup>c</sup>
Expands to Macrobust	Yes	Yes <sup>c</sup>
Source Region of Downdraft (AGL)	3.5 - 4.5 km	3.5 - 4.5 km <sup>c</sup>
<sup>a</sup> From TDWR measurements. <sup>b</sup> From Aircraft FDR. <sup>c</sup> From Dual-Doppler analysis. <sup>d</sup> Measured by PAM surface instruments.		

the microburst (which was encountered by the four aircraft on approach to Stapleton) actually fell from an overhang about 8 km east of the main cell and produced a velocity differential of over 36 m/s! A sequence of 3-dimensional perspectives in Fig. 3 depicts the fallout of precipitation from the overhang as simulated in the model.

The main updraft, which generates much of the storm's precipitation, is located at the rear (western end) of the storm with roots from the southern flank (not shown). Several weaker updrafts exist upstream along the northern flank of the radar echo; however, it is uncertain as to what influence they may have had on the storm.

Figure 4 shows a vertical cross section of the wind vector field prior to the touchdown of the intense microburst (Fig. 4a) and five minutes later at maximum outflow intensity (Fig. 4b)<sup>4</sup>. The snow-field corresponding to Fig. 4a is shown in Fig. 5. It is apparent from these figures that stronger winds aloft are acting to transport precipitation downstream from the western end of the storm. The composition of the precipitation above the melting level is primarily graupel and hail in the western shaft, while being primarily snow in the overhang. The latter is true since snow particles have a relatively slow fall speed compared to either hail, graupel, or rain; and therefore, can be transported more effectively downstream before falling to lower levels. For this reason the downstream microburst is composed mostly of snow particles, which have the potential to rapidly sublime and produce an intense microburst under favorable environmental conditions (e.g., Proctor 1989b). Figure 4 also indicates horizontal convergence between 2.0 - 4.5 km AGL which is within the upper portion of the intense microburst downdraft. In Fig. 4b, several minutes after microburst touchdown, a well developed ring-vortex structure is apparent near ground level.

---

<sup>4</sup>The main storm updraft lies just south of this cross section and is apparent in Fig. 4 only between 5 and 7 km AGL.

The near-surface horizontal-wind field prior to and during the intense microburst is shown in Fig. 6. At 47 min, only weak microbursts associated with the western precipitation shaft are apparent; but several minutes later, a vivid star-burst outflow pattern develops from the intense overhang microburst (located at  $x \sim 15$  km,  $y \sim -5$  km). The outflow from the intense microburst appears roughly symmetric early in its lifetime, but grows more asymmetric as it expands with time. Other microbursts of intermediate intensity are evident also, and their individual outflows appear to coalesce as they expand with time.

The strongest low-level wind speeds are located on the southwest-southern sides of the intense microburst, although strong winds are prevalent on the eastern sides as well (Fig. 7). Peak outflow winds on the western side show the greatest weakening with time, as the intense microburst expands into a macroburst<sup>5</sup> and subsequently interacts with other outflows.

At higher altitudes, horizontal wind vectors indicate the presence of multiple vortices (e.g., Fig. 8). The presence of rotation in the actual storm was inferred from single Doppler radar measurements, and along with mid-level convergence, was used as a precursor for aiding in the detection of the microburst event (Campbell 1989).

#### Evolution of Storm Peak Values

The time-height cross sections of domain-wide peak values are shown in Fig. 9. Precipitation first reaches the ground at 30 min simulation time, 13 min after the first 10 dBZ echo (Fig. 9a). Strong downdrafts do not occur, however, until 50 min in the simulation (Fig. 9b), corresponding to the descent of the strong microburst from the overhang (cf. Fig. 2).

---

<sup>5</sup>A microburst becomes a macroburst if the horizontal distance between diverging outflow peaks exceed 4 km.

Fig. 9c indicates that peak updraft speeds are persistent with time, but do not exceed 11 m/s. An intensification of the upward velocity at low levels after 50 min, is likely due to outflow interactions and the circulation of the microburst ring-vortex.

Shaded areas in Fig. 9a represent peak values of the vertical component of vorticity in excess of  $0.02 \text{ s}^{-1}$ . Downward propagation of peak vorticity from the 4-5 km level coincides with downdraft intensification and the development of the intense microburst (cf. Fig. 9b). Operationally, rotation (about a vertical axis) is used as a possible precursor for microbursts (e.g., Roberts and Wilson 1989); and in the 11 July case, Doppler measurements actually detected the *descent* of rotation from storm mid-levels, just prior to the occurrence of the intense microburst (Campbell 1989).

#### Driving Mechanism for the Intense Overhang Microburst

As noted earlier, the intense overhang microburst is associated with snow, as well as very light rain produced from the melting snow. Physical mechanisms, such as cooling due to sublimating snow, melting snow, and rain evaporation are investigated by conducting additional experiments<sup>6</sup> with the axisymmetric version of TASS<sup>7</sup>

---

<sup>6</sup>The additional experiments are set-up similar to those described in Proctor (1988c, 1989b); i.e., an isolated microburst is initiated by allowing precipitation to fall from the model top boundary located at 5 km AGL. Input conditions for these additional experiments assume: the Denver sounding for environmental temperature and humidity (see Fig. 1); and a distribution of snow (specified at the model top boundary) which is approximated from the time-dependent snow field in the 3-D simulation.

<sup>7</sup>The 3-D version of the model could have been used for these additional experiments, but doing so would have entailed large computation costs.

The baseline case, which is simulated with the axisymmetric model, indicates similar values compared to the 3-D simulation (see Table 5). The remaining experiments listed in Table 5 are conducted identical to the baseline case, except that no cooling (or heating) is allowed for the process being investigated. The integrated effect of each of the physical processes is judged by comparing several of the key parameters (such as KE -- the domain-integrated resolvable kinetic energy) with those of the baseline case.

Table 5 indicates that the dominant process in driving the microburst is cooling due to sublimation of snow. Turning off the cooling due to rain evaporation had only a minor influence, while turning off the cooling from melting had almost no effect. Table 5 also indicates that elimination of all the cooling processes also eliminates the microburst; thus, other processes such as precipitation loading appear to have had little if any influence on driving the microburst.

As discussed in Proctor (1989b), sublimating snow can effectively generate intense microbursts, if within a typical dry-microburst environment -- as is apparently true in this case. Also in Proctor (1989b), it was demonstrated that different types of precipitation can have a varying effect on the intensity of a microburst. This may provide a clue as to the reason why the microbursts associated with the western shaft were weak. These microbursts were composed primarily of graupel and rain which may have been less effective in generating intense downdrafts.

#### Detailed Structure of the Overhang Microburst

This section further examines the structure of the intense microburst which dropped from the overhang. Comparisons of model results with reconstructed and observed data from the actual event suggest strong similarities with the microburst at Denver Stapleton which forced four aircraft to initiate missed approaches.

**TABLE 5. Axisymmetric model experiments - sensitivity to cooling and loading**

EXPERIMENT	Maximum Outflow Speed (m/s)	Maximum Downdraft Speed (m/s)	Maximum Surface Pressure Increase (mb)	$\Delta V$ (m/s)	KE <sup>a</sup> ( $10^{10}$ J)
3-D CASE	22.3	-16.9	2.76	42	---
AXISYMMETRIC EXPERIMENTS					
BASE	22.5	-17.1	2.86	45	263
NO MELTING	22.1	-16.7	2.70	44	262
NO RAIN EVAPORATION	21.3	-16.5	2.36	43	236
NO SUBLIMATION	13.0	-10.9	1.13	26	26
NO COOLING	0.1	-0.4	0.03	0.2	1

<sup>a</sup>Domain-integrated resolvable kinetic energy at time of maximum outflow.

### Peak Velocity Differential: Matching of observed and model time

Fig. 10 shows the temporal distribution of the peak velocity differential associated with the intense microburst. Three curves from the model data are plotted; one each for 1) east-west segments, 2) north-south segments and 3) northeast-southwest segments. The plotted values represent the peak velocity differential,  $\Delta V$ , along any 4 km segment in a specified direction. Also plotted are the values from the TDWR radar (located roughly southeast of the microburst), as well as and peak  $\Delta V$  reconstructed from the flight data recorders (FDR) of the four aircraft which made east-west penetrations of the microburst. By temporally matching the curves, we found that 2210 UTC corresponds to 51.25 min simulation time (see Fig. 10).

Interestingly, data from the model, radar, and flight recorders are in rough quantitative agreement. All show a sudden temporal increase in the magnitude of  $\Delta V$ , followed by a gradual decrease. The aircraft data, however, do show a steeper decrease of  $\Delta V$  following the time of maximum intensity, although this in part may be due to the higher flight trajectory of the last two aircraft which may have carried them above the region of peak outflow. However, the model east-west segments, compared to segments in other directions, do show a relatively steeper decrease of  $\Delta V$  following 52 min (2211 UTC) (Fig. 10).

Differences associated with the direction in which  $\Delta V$  is calculated are apparent in the model data after 50 min, due to flow asymmetries. The strongest magnitudes of velocity differential (42 m/s) are associated with the northeast to southwest segments. The maximum value of  $\Delta V$  along the east-west and the north-south segments are nearly the same as the TDWR estimate of 37 m/s.



### Horizontal and Vertical Structure

Figure 11 shows the detailed horizontal structure of the evolving microburst at 180 m AGL. At 47 min, roughly 3 min before the first encounter by the approaching aircraft, little evidence of outflow is present. By 49 min, a weak radar echo is present at low-levels and outflow is beginning to accelerate. Maximum intensity is reached at about 52 min, roughly the time of the second aircraft encounter. Note that after 50 min, the outflow continues to expand in a roughly symmetrical pattern, even though the radar echo elongates in the east-west direction. Interaction with adjacent microbursts is evident at 54 min.

Figure 12 shows the horizontal flow structure of the microburst at several altitudes above the ground. Note that the wind speeds decrease with altitude, *especially in the east-west direction*. Hence, a Doppler-radar beam which is centered a couple of hundred meters above the ground, would detect a weaker and more asymmetric flow structure than what actually occurred near ground level.

Figure 13 shows a time sequence of vertical west-east cross sections taken near the center of the intense microburst. Note the descent of the downdraft and subsequent intensification of its vortex-ring structure. Other microburst downdrafts are apparent to the west; thus aircraft penetrating the intense microburst from the east would next encounter extreme turbulence.

The vertical velocity field corresponding to Fig. 13d is depicted in Fig. 14. The mature microburst exhibits a double-peak downdraft with upward motion along its eastern side. Peak downdraft speeds with magnitudes of up to 15 m/s are located just below the 1 km level.

## F-Factor Analyses

A primary threat of microbursts to aircraft is the single or combined effect of the horizontal velocity shear and downdraft motion. Either of these effects can penalize the performance of an aircraft, and possibly result in a critical loss of altitude for arriving or departing aircraft. A very useful parameter for indicating the severity of the wind shear and vertical velocity on aircraft performance is the F-Factor (Bowles and Targ 1988):

$$F = g^{-1} DU/Dt - w/V_a,$$

where  $DU/DT$  is the rate of change of the horizontal wind component along the aircraft flight path,  $g$  is the acceleration due to gravity,  $w$  is the vertical wind speed, and  $V_a$  is the air speed of the aircraft. The first term on the right side represents the contribution of wind shear to the performance of the aircraft, while the second term represents the contribution due to the vertical wind. Positive values of  $F$  indicate a performance-decreasing condition, whereas negative values indicate a performance-increasing situation. An F-Factor of 0.1 or greater is considered hazardous for most jet transport aircraft (Targ and Bowles 1988).

The above formula can be approximated for easy application to model data as:

$$F \approx g^{-1} V_g \partial U / \partial R - w/V_a,$$

where  $\partial U / \partial R$  is the horizontal velocity shear along the flight path, and  $V_g$  is the aircraft speed relative to the microburst. The above formula is simplified further by assuming  $V_g \approx V_a = 75$  m/s, a reasonable estimate of the approach and departure speeds of commercial jetliners.

"East-west" F-Factors are computed using the above formula and assuming horizontal east-west trajectories through the model data. Similarly, "north-south" F-Factors are computed assuming horizontal north-south trajectories. In Fig. 15, peak values of model east-west F-Factors are plotted against time and show amazing agreement with F-Factors estimated from both single Doppler radar (TDWR) and aircraft flight recorder data<sup>8</sup>. From the model data, peak values of east-west F-Factor below 280 m AGL, exceed 0.1 after 48 min (2207 UTC) with an overall maximum of 0.24 occurring at 51 min (2210 UTC). The F-Factor values remain large, even at later times in the simulation, when the outflow has expanded to become a macroburst. However, low-level F-Factor values computed from Dual-Doppler radar data (Elmore 1989) appear to underestimate values derived from the model, single Doppler, and aircraft data. But for peak F-Factor at higher elevations, agreement with dual-Doppler radar data is much better (Fig. 16). It may be speculated that the dual-Doppler data analysis is either too coarse or overly smoothed, such that the horizontal shear is underestimated. Thus at higher elevations, where vertical velocity rather than horizontal shear is the contributor to F-Factor, the comparison is much better.

Also, from Fig. 16 it is important to note that peak F-Factor values exceed 0.1, several minutes in advance of strong outflow at the ground. Thus large values of F-Factors below 2 km, but not yet at the surface, may provide a useful precursor to microbursts (cf. Figs. 15 and 16).

A time sequence of east-west F-Factor fields through the center of the evolving microburst are shown in Fig. 17. Note that values of F-Factor greater than 0.2 first occur aloft (about 1 km AGL) early in microburst lifetime. The peak values then descend groundward, and later diminish in magnitude with time as the microburst outflow expands. As

---

<sup>8</sup>The F-Factors derived from aircraft measurements do not include vertical wind, whereas the other curves in Fig. 15 include a vertical wind estimate at the indicated elevation.

suggested above, the descent of large F-Factor values from aloft may provide a useful precursor.

Also in Fig. 17, performance enhancing areas (i.e., negative values of F-Factor) can be found at low-levels along the periphery of the microburst outflow. These areas can contribute to the danger of a microburst encounter, by misleading the pilot and causing him to reduce aircraft thrust levels.

Since microbursts are unlikely to be perfectly symmetric, the magnitude and structure of the F-Factor fields can vary according to the direction in which it is computed. For instance, even though the microburst outflow is roughly symmetric at 52 min (e.g., Fig. 6b), the east-west F-Factor field differs appreciably from the north-south F-Factor field (Figs. 18 and 19).

#### Reconstruction of Aircraft Trajectories and Comparison with Flight Recorder Data

As mentioned earlier, four aircraft had inadvertent encounters with the microburst. For comparison, profiles are interpolated from the model data following the same spatial coordinates as the aircraft (Fig. 20) and at the time when the aircraft was near the center of the microburst [i.e., 50 min (2208.75 UTC) for UAL 395, 52 min (2210.75 UTC) for UAL 236, 53 min (2211.75 UTC) for UAL 949, and 54 min (2212.75 UTC) for UAL 305.]<sup>9</sup> From dual-Doppler radar data of the microburst (Sand 1988), the airport runway is estimated to be 400-600 m north of the microburst center; thus, relative to the model coordinates the runway is chosen at  $y = -4.5$  km (see Figs. 11 and 18).

---

<sup>9</sup>The model profiles are taken at an instant frozen in time, although the aircraft traversed the actual microburst in about 30 to 60 s.

The model profiles show reasonable agreement with the reconstructed aircraft profiles, especially with regard to the diameter between the major outflow peaks (Fig. 21). A strong shift between head and tail winds is indicated for the first two aircraft, which encountered the microburst at somewhat lower elevations than the following two (see Fig. 20). As was true in the TASS simulation of the Dallas-Fort Worth Microburst (Proctor 1987b, 1988a, 1988c), the model simulation captures the expansion rate of the microburst extremely well, but fails to reproduce the high frequency oscillations<sup>10</sup>.

Model F-Factors along the same coordinate positions as the horizontal wind profiles are shown in Fig. 22. The model F-Factors exceed 0.1 for each of the aircraft. The magnitude of F-Factors would have been even larger if the profiles were taken further south, closer to the center of the microburst where stronger downdraft speeds are located.

---

<sup>10</sup>This lack of agreement may be due to the coarseness of the grid mesh. The model experiment assumes a horizontal grid size of 200 m and cannot resolve wavelengths less than 400 m.

## 5. SUMMARY AND CONCLUSIONS

The multi-dimensional Terminal Area Simulation System has been used in the investigation of the Denver, 11 July 1988 Microburst. Results from the model give good quantitative comparisons with observations as well as reconstructed data from Doppler radars and aircraft flight data recorders. Values of some of the parameters from the simulated storm are listed in Table 6.

The model simulation indicates that the storm is of unusual structure and produces multiple low- to moderate-reflectivity microbursts. One of these microbursts was unusually intense, containing strong downdrafts, outflow, and wind shear; and was driven by cooling primarily from sublimating snow. F-Factors in the most intense microburst exceeded 0.2, even before ground contact. This suggests that F-Factors also could be used as a precursor for strong wind shear at ground level. The simulated microburst outflow displayed a rough symmetry near the ground, becoming weaker and less symmetrical with altitude above 80 m. This suggests potential issues for the Doppler analysis of such storms if the radar beam is either 1) too broad, 2) at too high of an elevation, or 3) obstructed at low levels by significant ground clutter.

The model proves to be a useful tool in aircraft investigations, since it provides useful insight into the storm and microburst structure, and can provide information which is not always apparent from observed data.

**Table 6. Summary of Simulated Characteristics**

<u>Storm</u>	
Peak Updraft Speed	11 m/s
Lifetime	Long-lived
Maximum Accumulated Precipitation	0.5 mm
Cloud Base / Top	3.5 km / 7.5 km
Propagation (from)	280° at 8.5 m/s
<u>Microburst</u>	
Maximum Outflow Speed ( $U_{max}$ )	22.3 m/s
Diameter between outflow peaks at time of $U_{max}$	3.75 km
Maximum Velocity Differential	42 m/s
Maximum Radar Reflectivity	40 dBZ
Maximum Temperature Drop at Surface	-5.0° C (-3.5° C, prior to $U_{max}$ )
Maximum Pressure Increase at Surface	2.76 mb
Maximum Rain Rate	3 mm/hr
Maximum Downdraft Speed	-16.8 m/s at 1 km AGL
Maximum F-Fac'	0.24-0.27

## ACKNOWLEDGEMENTS

This report has benefited from informal discussions with several groups involved in the study of the 11 July case. In particular we would like to thank Rod Wingrove and Richard Coppenbarger of NASA Ames for providing data from their analysis of the aircraft flight recorder data; Steve Campbell of MIT Lincoln Laboratory for providing data from his analysis of the TDWR radar; and Kim Elmore, Marcia Politovich, and Wayne Sand of NCAR for providing the Denver 2000 UTC special sounding used in Fig. 1, as well as preliminary analyses from their radar and mesonet network. We also would like to thank Mary Bousquet for her assistance in producing many of the figures.

The work reported herein was supported by the National Aeronautics and Space Administration under contract NAS1-18858. Model computations were carried out on the NASA-Langley Cyber VPS 32.



## REFERENCES

- Bowles, R. L., and R. Targ, 1988: Windshear detection and avoidance: Airborne systems perspective, 16th Congress of the ICAS, Jerusalem, Israel.
- Campbell, S., 1989: Personal communication.
- Cotton, W. R., M. A. Stephens, T. Nehr Korn, and G. J. Tripoli, 1982: The Colorado State University three-dimensional cloud/mesoscale model - 1982. Part II: An ice phase parameterization, J. de Rech. Atmos., 16, 295-320.
- Elmore, K., 1989: Personal communication.
- Ireland, B., 1988: United Airlines flight safety investigation: Microburst encounter July 11, 1988 Denver Colorado. United Airlines internal report 88-46.
- Klass, P. J., 1989: Microburst radar may spur review of tower's role in aborting landings, Aviation Week & Space Technology, 130, No. 18, May, 79-80.
- Proctor, F. H., 1987a: The Terminal Area Simulation System. Volume I: Theoretical formulation, NASA Contractor Rep. 4046, NASA, Washington, DC, 176 pp.
- Proctor, F. H., 1987b: The Terminal Area Simulation System. Volume II: Verification Experiments, NASA Contractor Rep. 4047, NASA, Washington, DC, 112 pp.

- Proctor, F. H., 1988a: Numerical simulation of the 2 August 1985 DFW microburst with the three-dimensional Terminal Area Simulation System, Preprints Joint Session of 15th Conf. on Severe Local Storms and Eighth Conf. on Numerical Weather Pred, Baltimore, Amer. Meteor. Soc., J99-J102.
- Proctor, F. H., 1988b: Numerical simulation of the Denver 11 July 1988 microburst storm, Second Combined Manufacturers' and Technologists' Airborne Wind Shear Review Meeting, Williamsburg, VA, NASA, Washington, DC.
- Proctor, F. H., 1988c: Numerical simulations of an isolated microburst. Part I: Dynamics and structure, J. Atmos. Sci., 45, 3137-3160.
- Proctor, F. H., 1989a: A relation between peak temperature drop and velocity differential in a microburst, Preprints Third International Conf. on the Aviation Wea. System., Anaheim, Amer. Meteor. Soc., 5-8.
- Proctor, F. H., 1989b: Numerical simulations of an isolated microburst. Part II: Sensitivity experiments, J. Atmos. Sci., 46, 2143-2165.
- Roberts, R. D., and J. W. Wilson, 1989: A proposed microburst nowcasting procedure using single-Doppler radar, J. Appl. Meteor., 28, 285-303.
- Sand, W., 1988: 11 July 1988 weather and resulting TDWR alarms at Denver, Colorado, Second Combined Manufacturers' and Technologists' Airborne Wind Shear Review Meeting, Williamsburg, VA, NASA, Washington, DC.

Targ, R., and R. L. Bowles, 1988: Investigation of airborne LIDAR for avoidance of windshear hazards, Second Combined Manufacturers' and Technologists' Airborne Wind Shear Review Meeting, Williamsburg, VA, NASA, Washington, DC.

Wakimoto, R. M., 1985: Forecasting dry microburst activity over the High Plains, Mon. Wea. Rev., 113, 1131-1143.

Wingrove, R., and R. Coppenbarger, 1989: Analysis of records from four airliners in the Denver Microburst, July 11, 1988, Presented at the NASA/FAA July 11th Workshop, Boulder, Co.

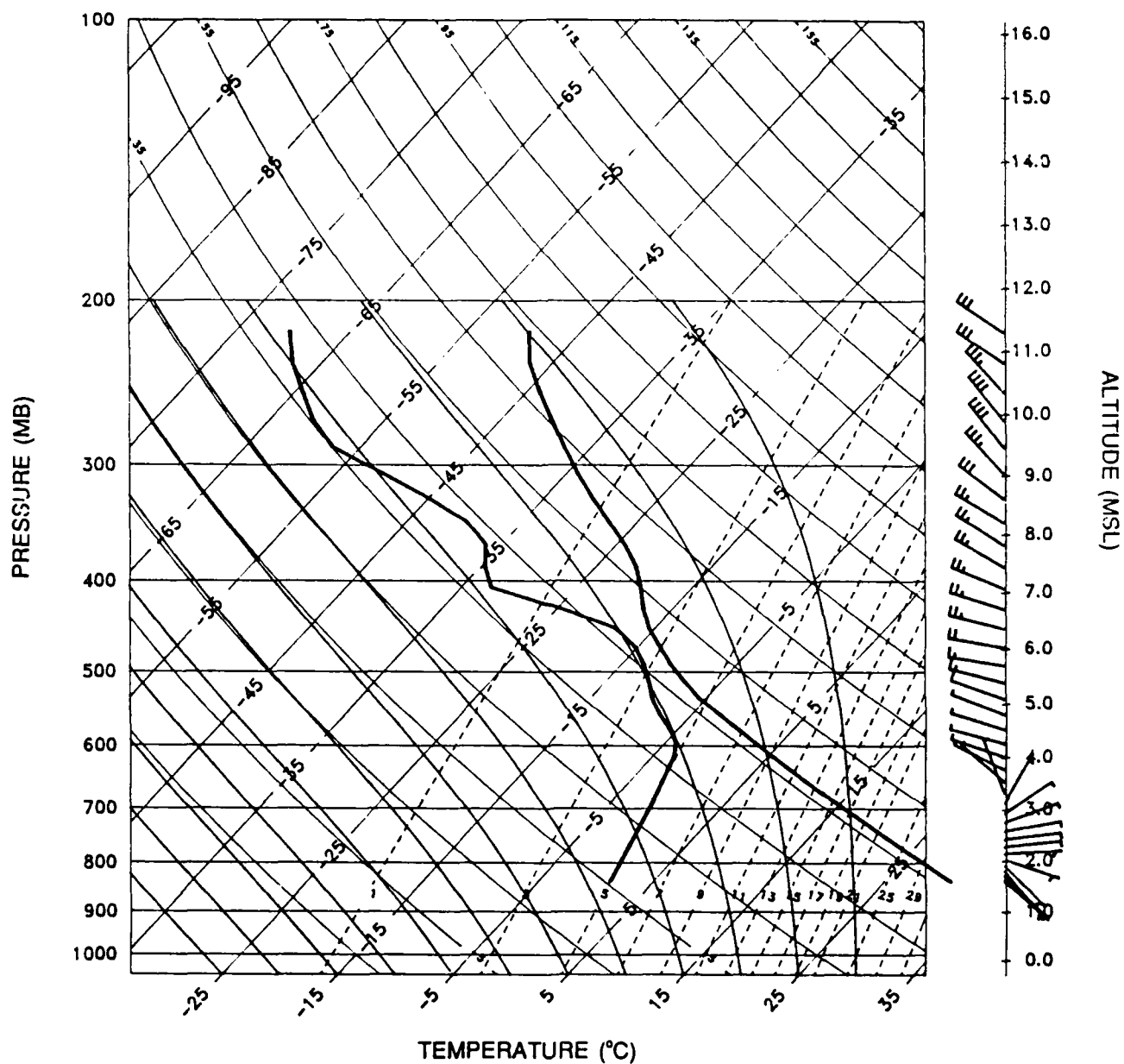


Fig. 1. Input sounding plotted on Skew T-log p diagram; based on 2000 UTC 11 July 1988, Denver special sounding. Each full wind barb equals 5 m/s or 10 knots.

# 11 JULY 1988 DENVER SIMULATION EAST-WEST RADAR-REFLECTIVITY CROSS SECTIONS

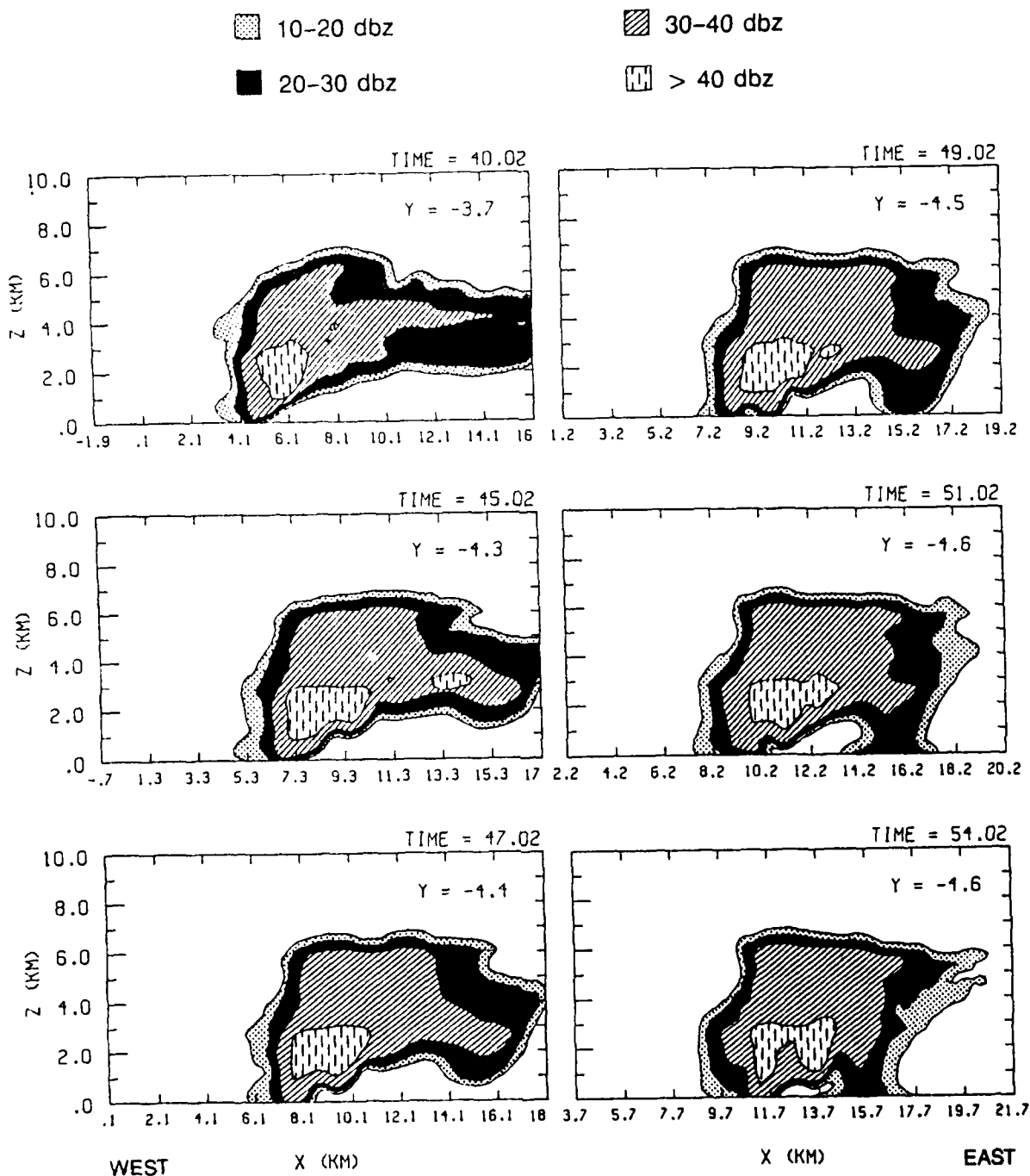


Fig. 2. East-West vertical cross sections of radar reflectivity taken near the center of the storm. Time is in minutes after model initialization and x,y coordinates relative to position of initial perturbation.

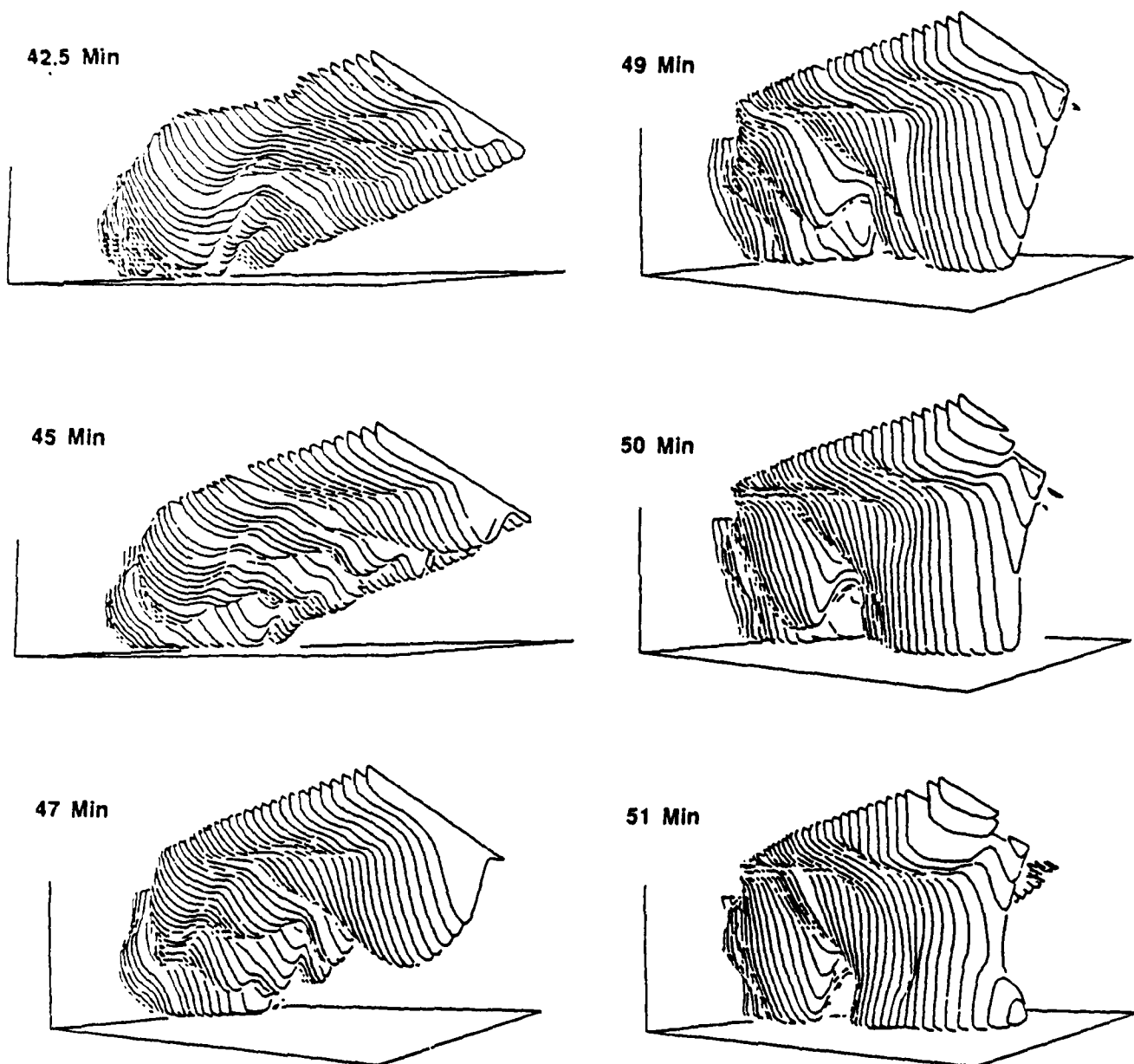


Fig. 3. Three dimensional perspectives of the lower 2 km of the storm viewed from the southeast.

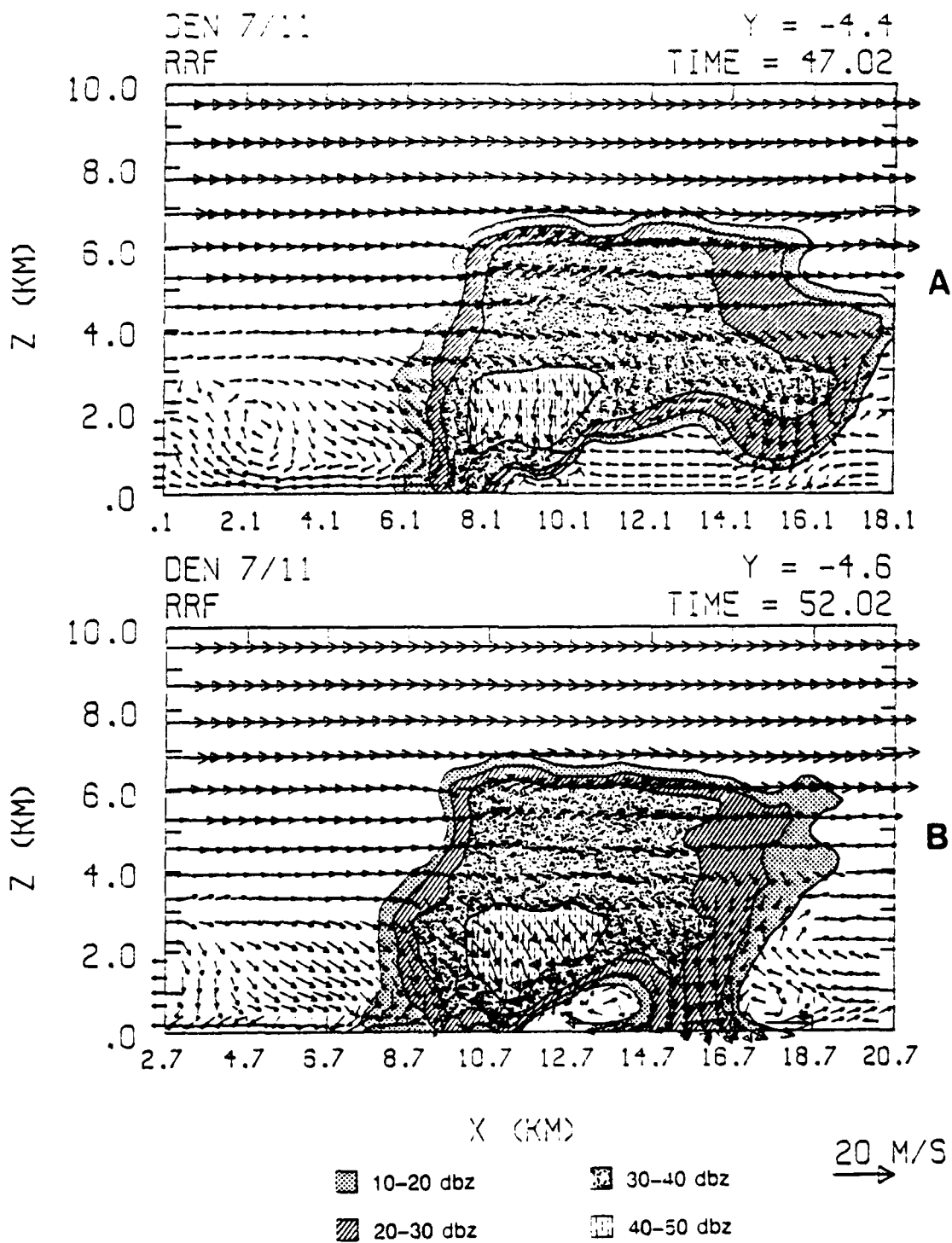


Fig. 4. East-West vertical cross sections of the simulated wind vector field with radar reflectivity superimposed. The cross sections are near the center of the storm at a) 47 min and b) 52 min simulation time. Wind vectors in this and subsequent figures are ground relative.

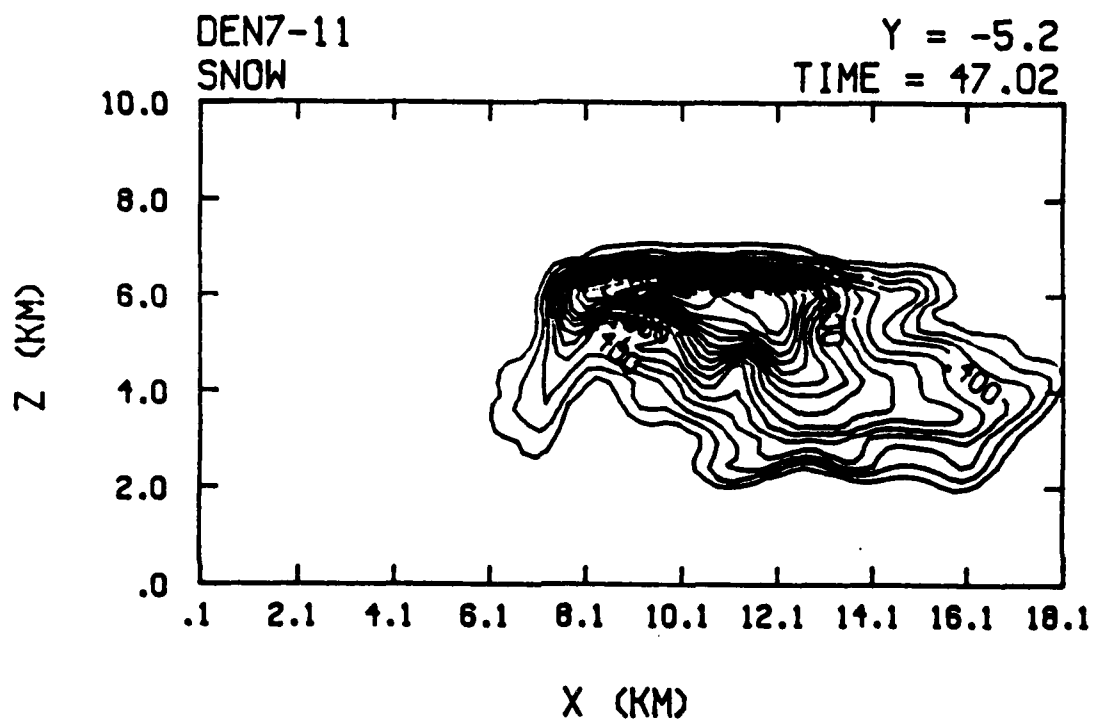


Fig. 5. As in Fig. 4a, but for snow field. The contour interval is  $0.1 \text{ g m}^{-3}$ , with peak values slightly greater than  $1.6 \text{ g m}^{-3}$ .



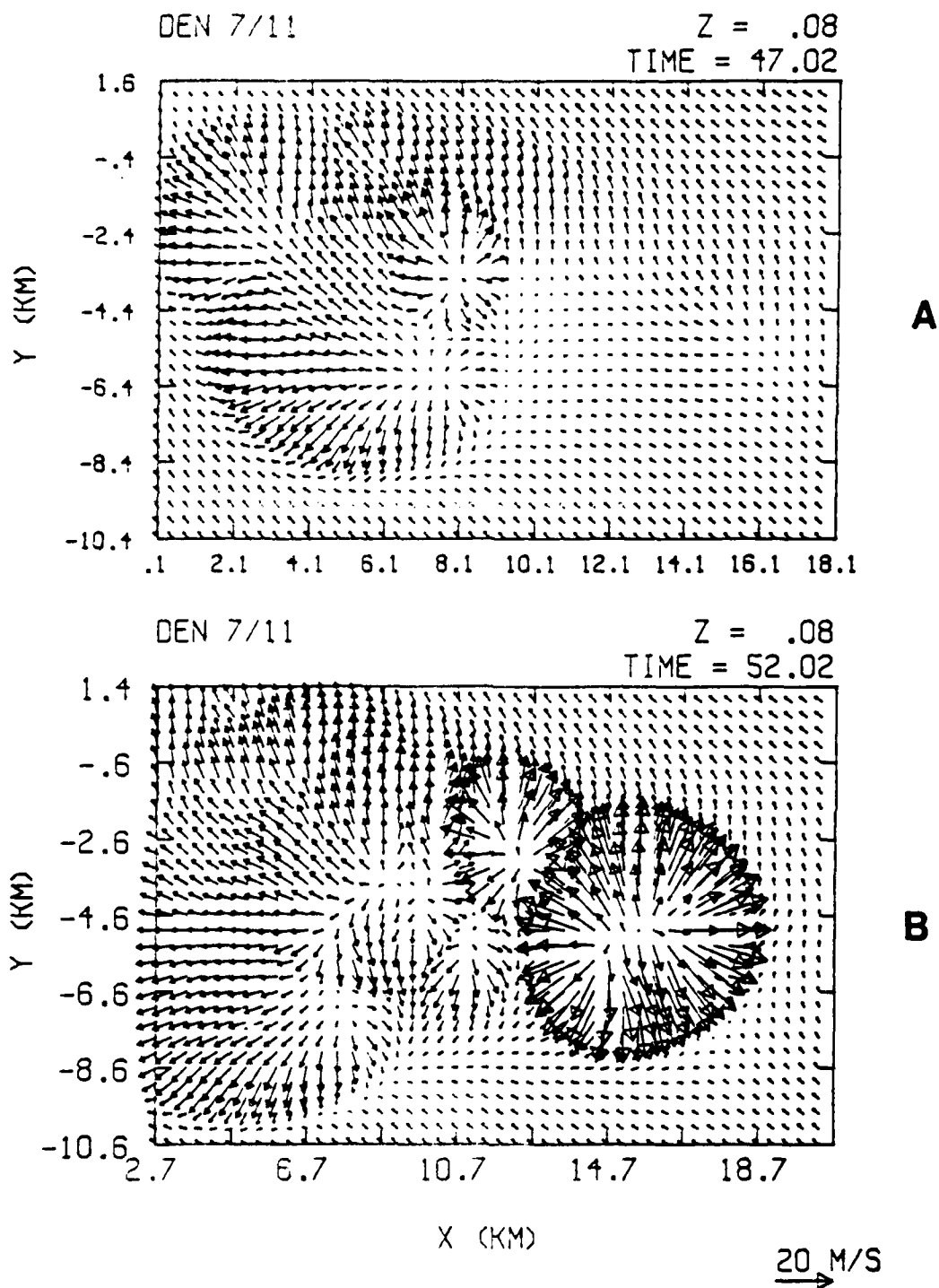


Fig. 6. Horizontal cross sections of the low-level wind vector field at a) 47 min, b) 52 min, c) 56 min, and d) 60 min simulation time. The horizontal fields are at 80 m AGL and north is in the y direction.

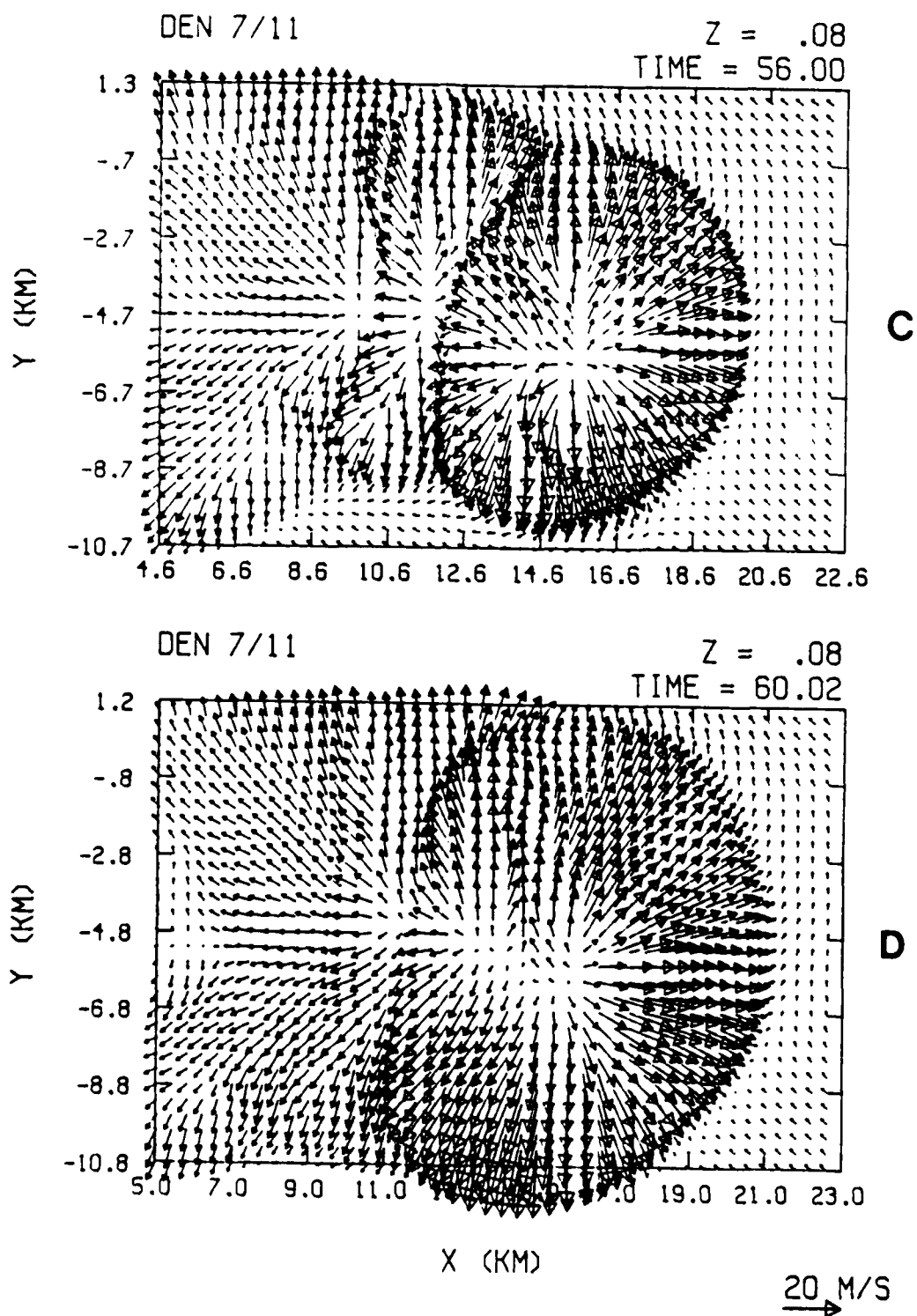


Fig. 6. Continued.

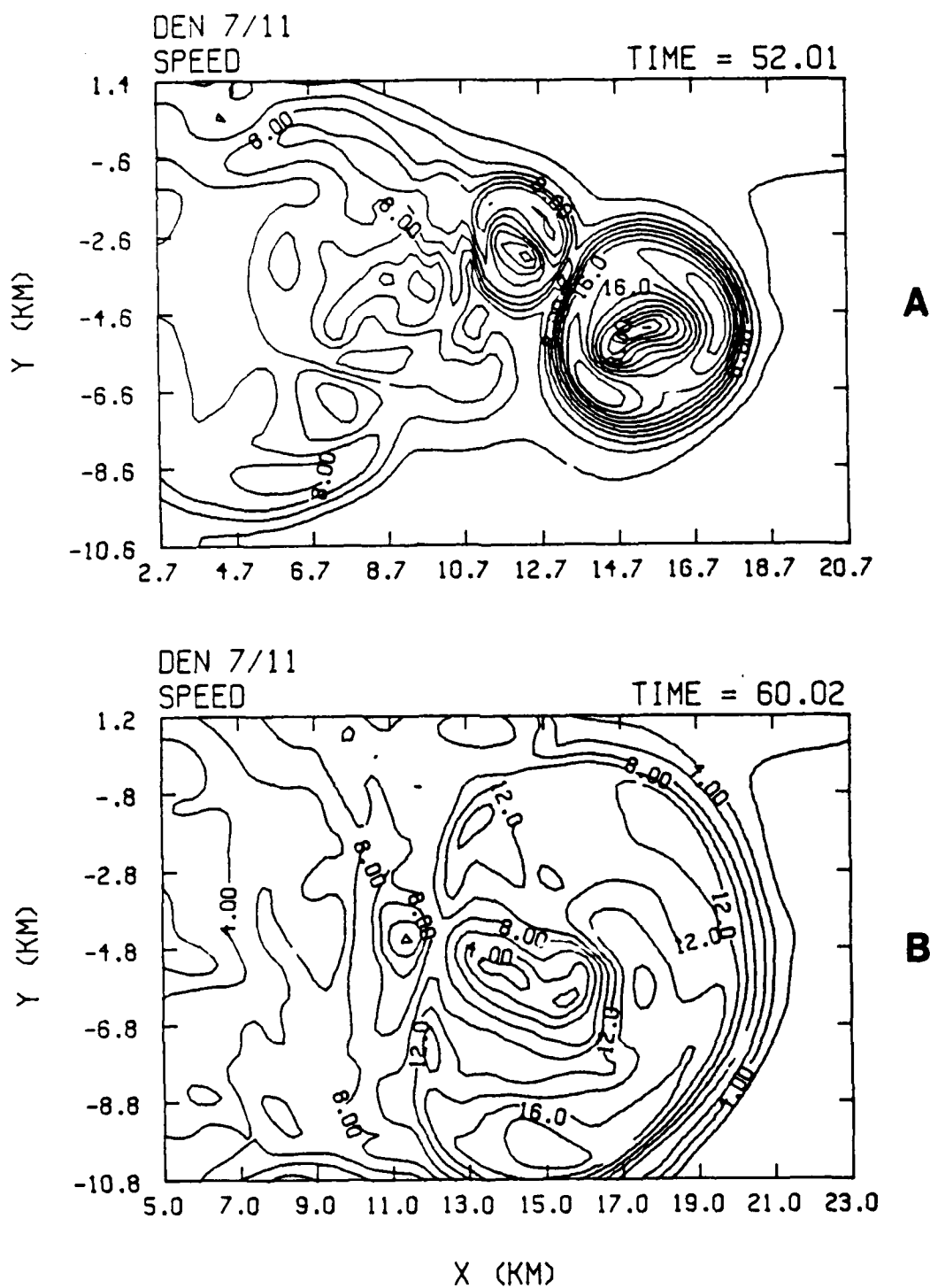


Fig. 7. As in Fig. 6, but fields are isotachs of horizontal wind speed at a) 52 min and b) 60 min simulation time. The contour interval is 2 m/s.

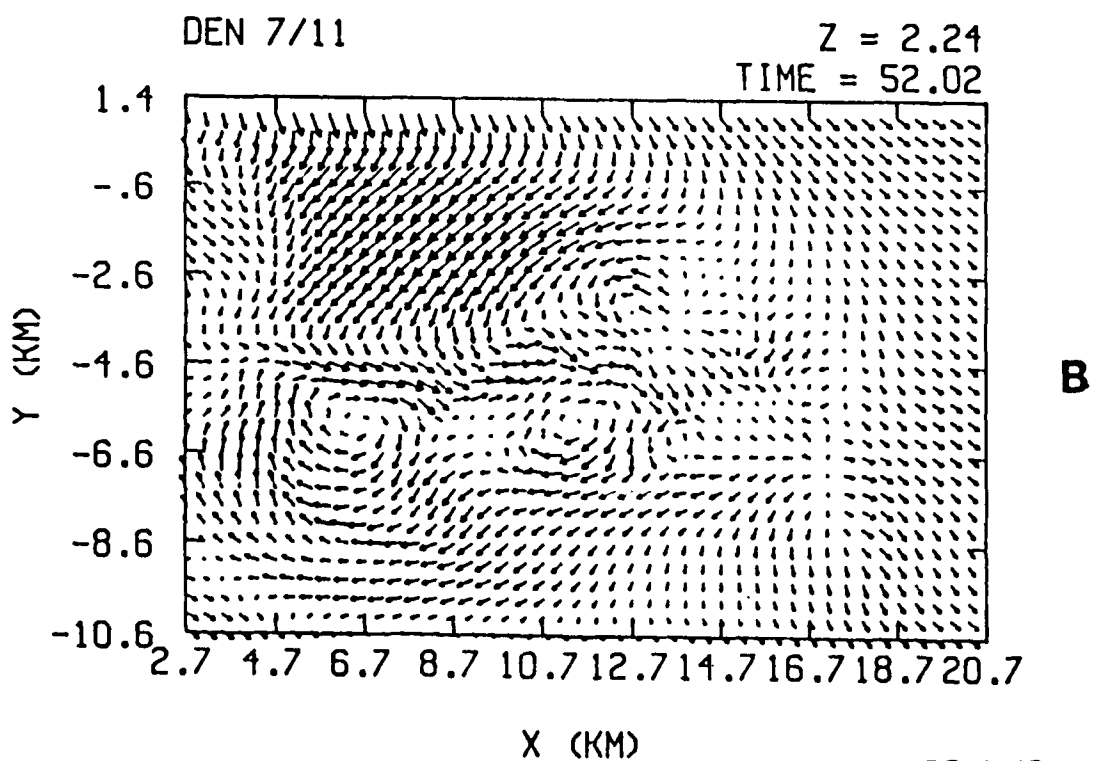
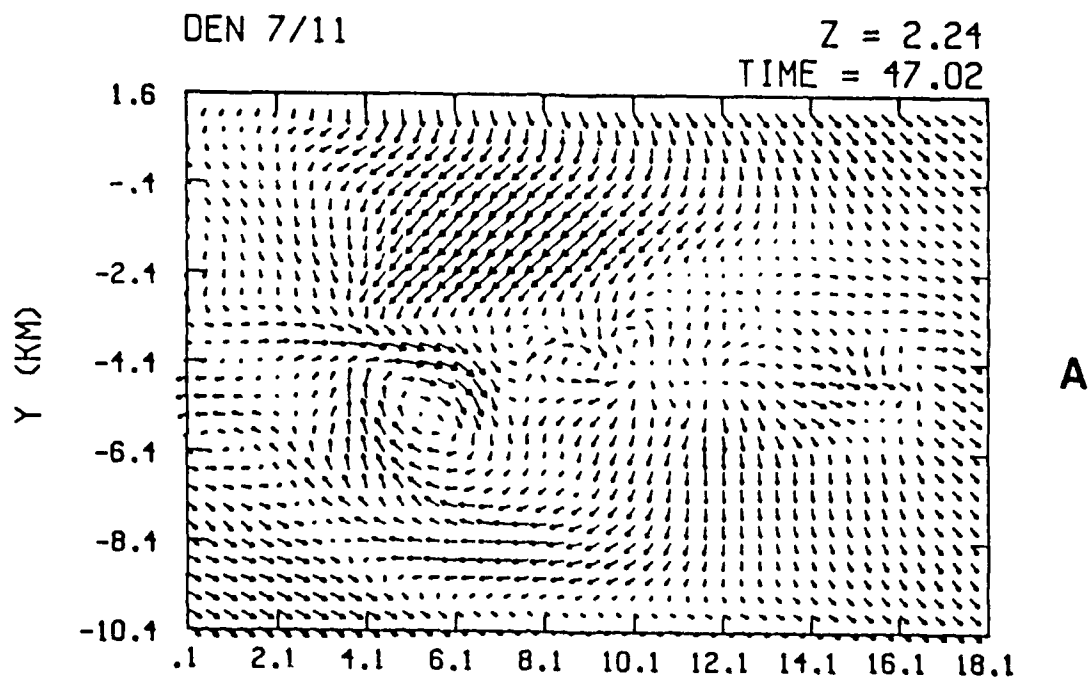


Fig. 8. As in Fig. 6 for a) 47 min and b) 52 min simulation time, but at 2.25 km AGL.



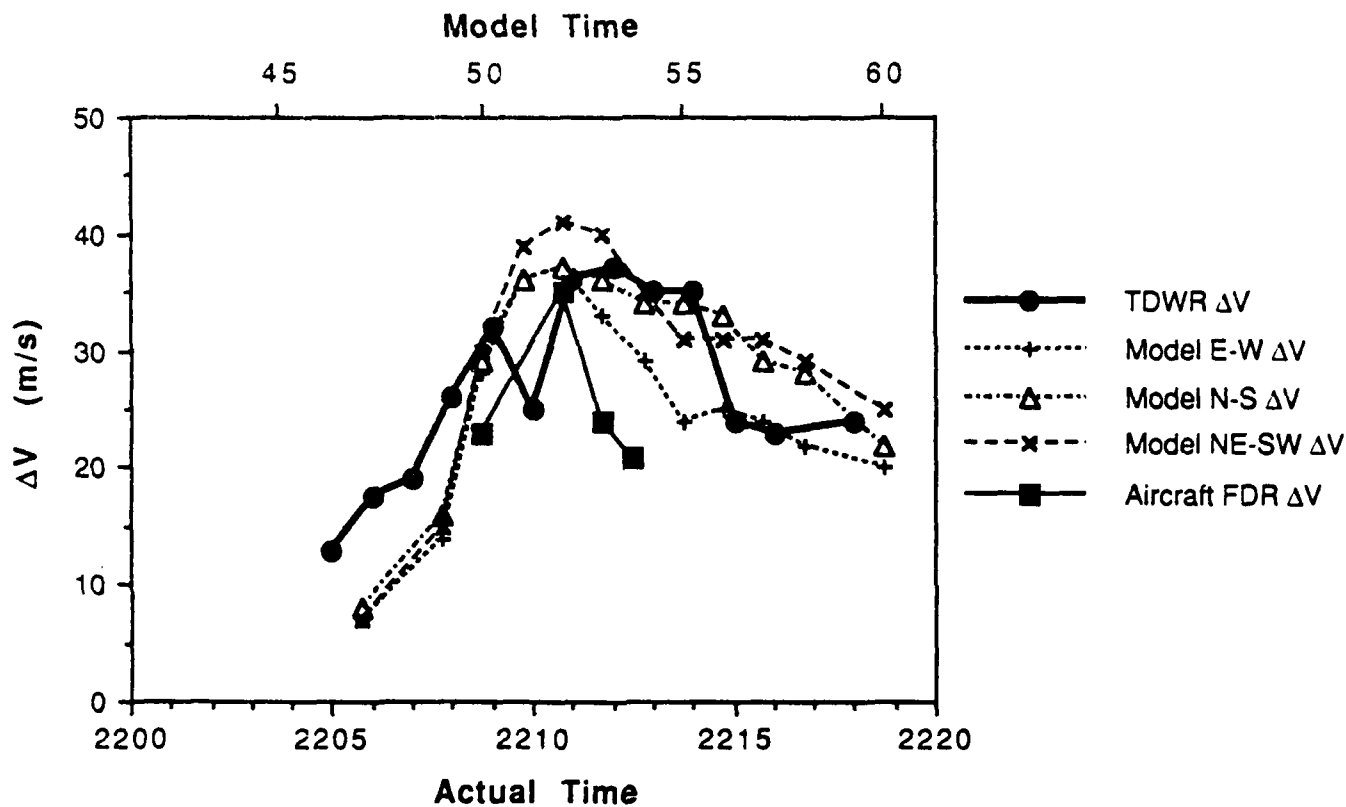
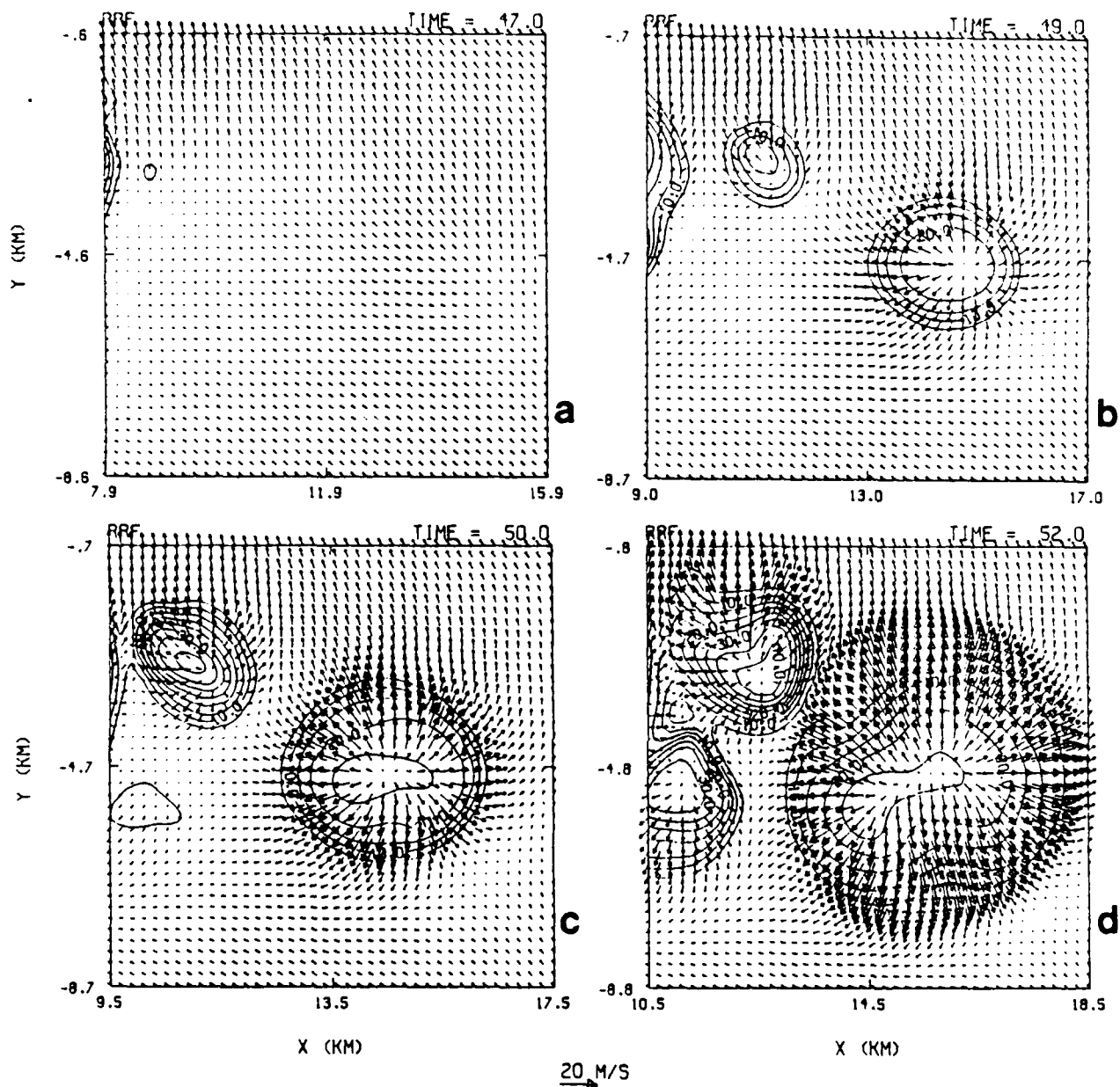


Fig. 10. Time evolution of peak velocity differential in most intense microburst: Comparison between model data, TDWR estimates, and aircraft flight recorder data. Data for TDWR estimates provided by Campbell (1989), and data reconstructed from the four aircraft FDR provided by Wingrove and Coppenbarger (1989).



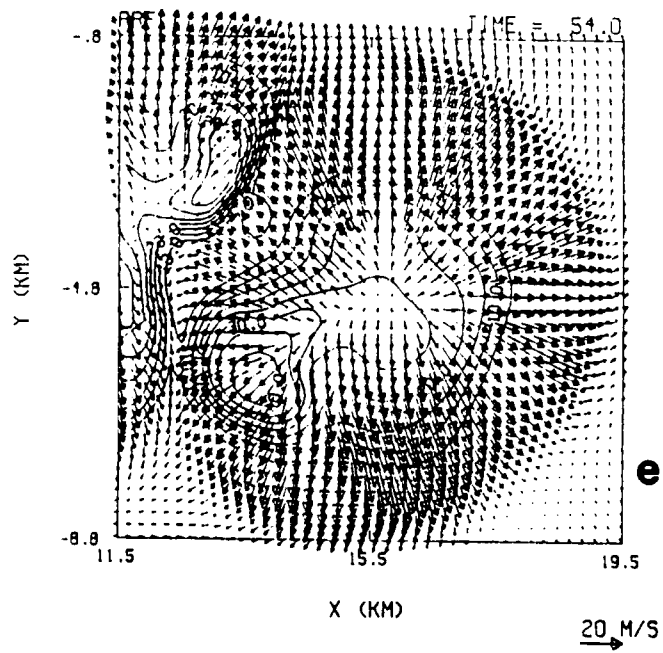


Fig. 11. *Continued.*



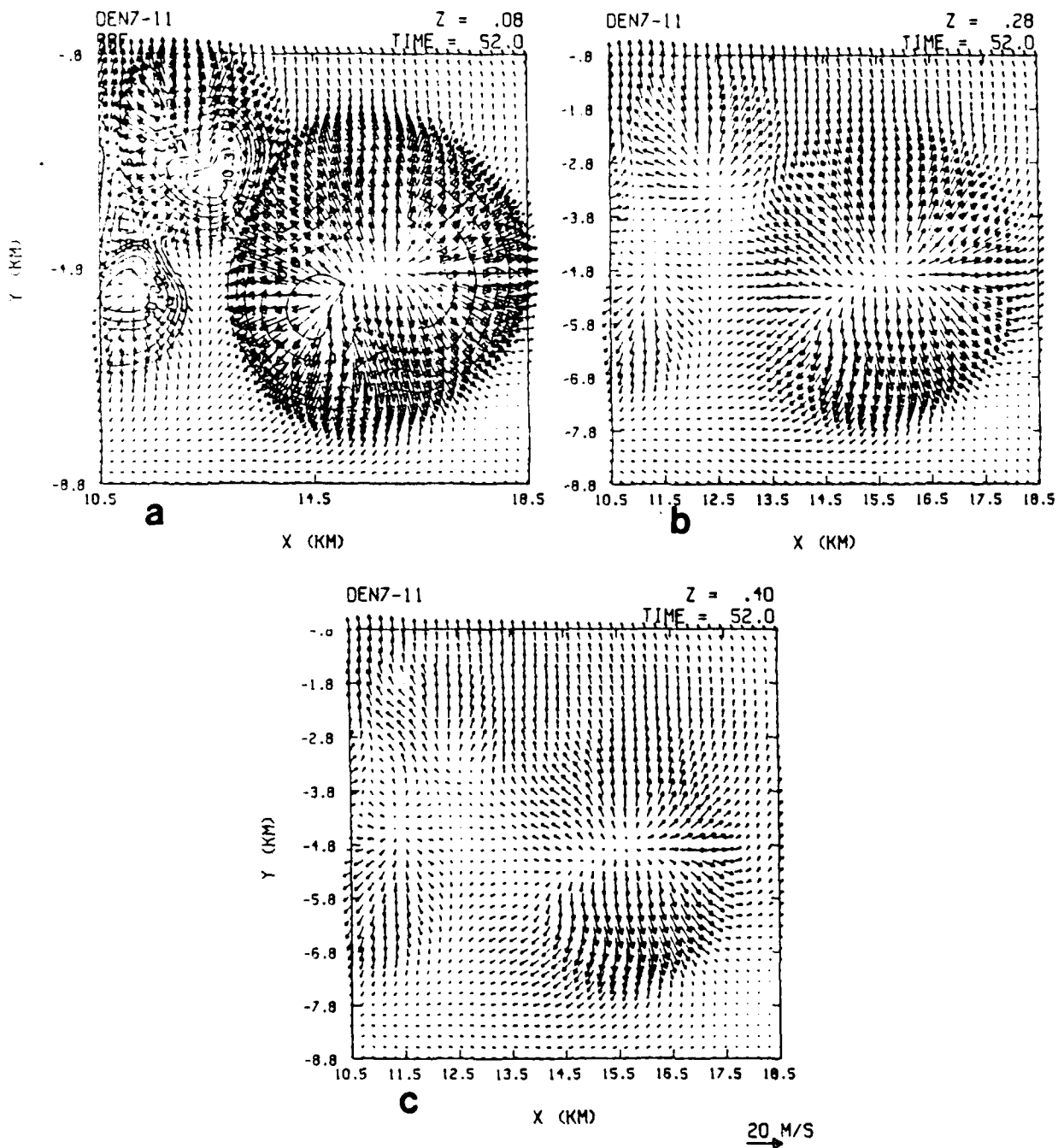


Fig. 12. As in Fig. 11, but for 52 min (2211 UTC) at a) 80 m, b) 280 m, and c) 400 m AGL. Radar reflectivity depicted in a) only.

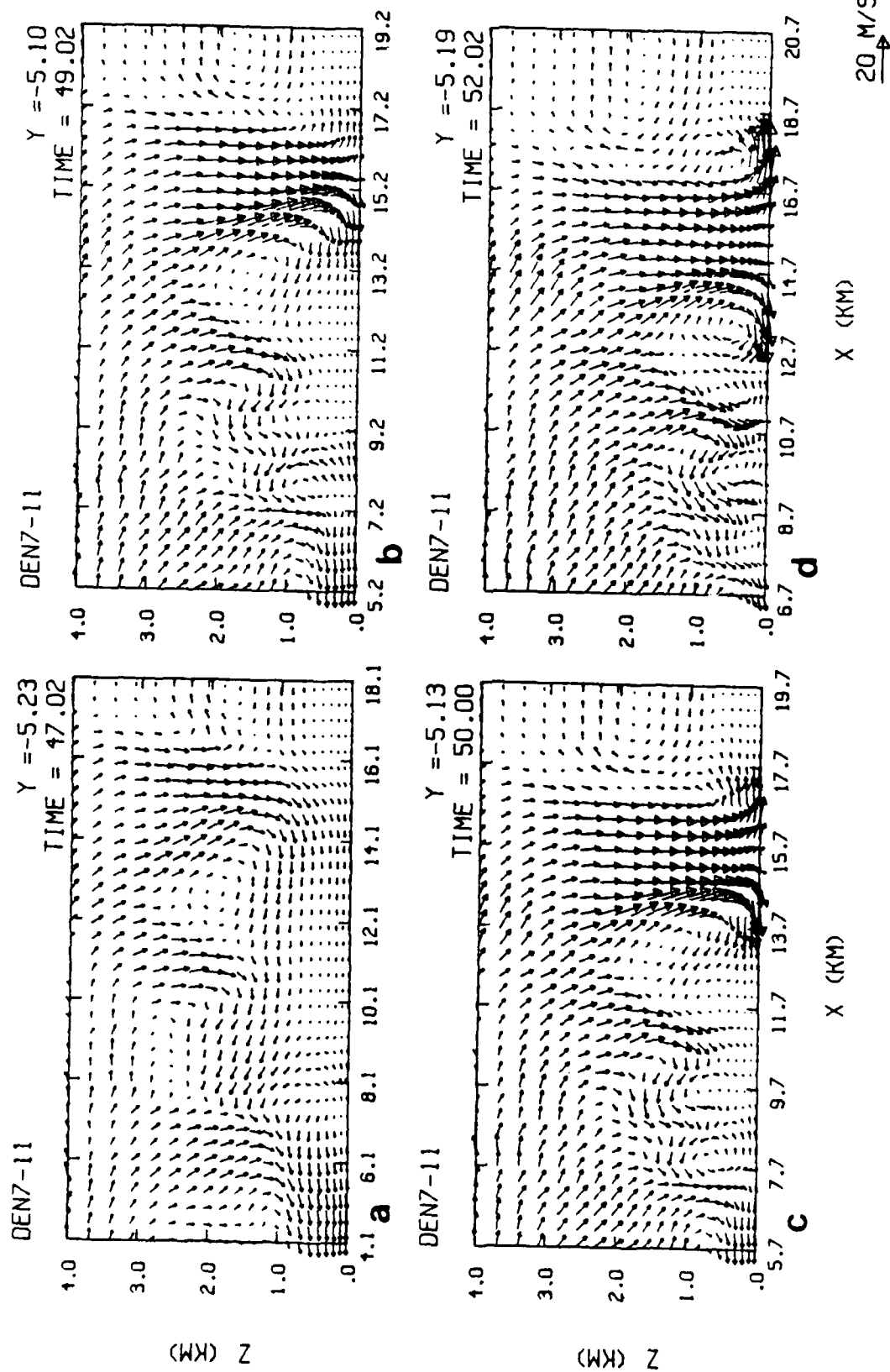


Fig. 13. Vertical east-west cross sections near the center of the intense microburst for wind vectors at a) 47 min (2206 UTC), b) 49 min (2209 UTC), c) 50 min (2211 UTC), d) 52 min (2213 UTC), and e) 54 min simulation time (2213 UTC). Area shown is windowed from model domain with the vertical coordinate stretched relative to  $x$  coordinate.

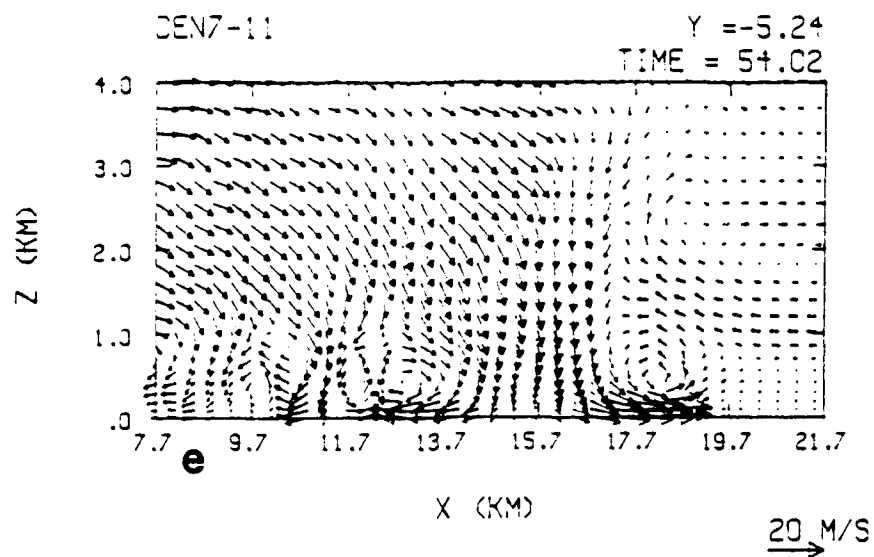


Fig. 13. *Continued.*

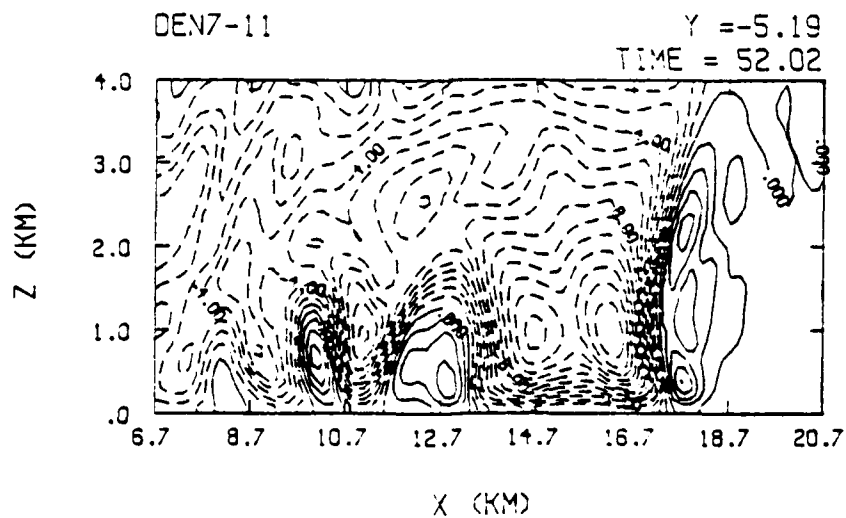


Fig. 14. As in Fig. 13, but for vertical velocity at 52 min. The contour interval is 1 m/s. Contours with negative values are dashed.

## MAX. F - FACTOR COMPARISON

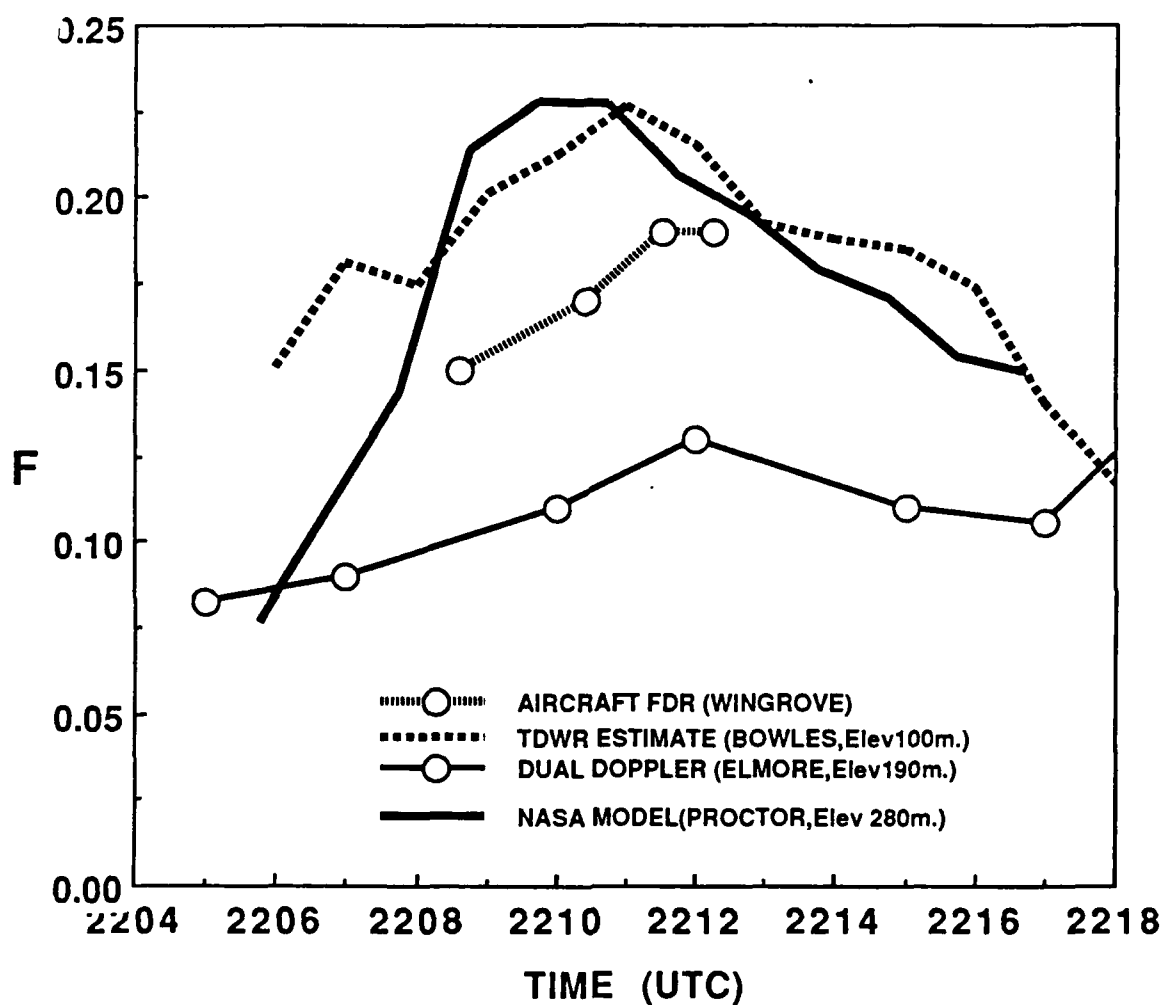


Fig. 15. Comparison of peak low-level F-Factors vs time. Peak east-west F-Factors below 280 m from model data are indicated by thick solid line.

### MAX.F-FACTOR COMPARISON AT HIGHER ELEVATIONS

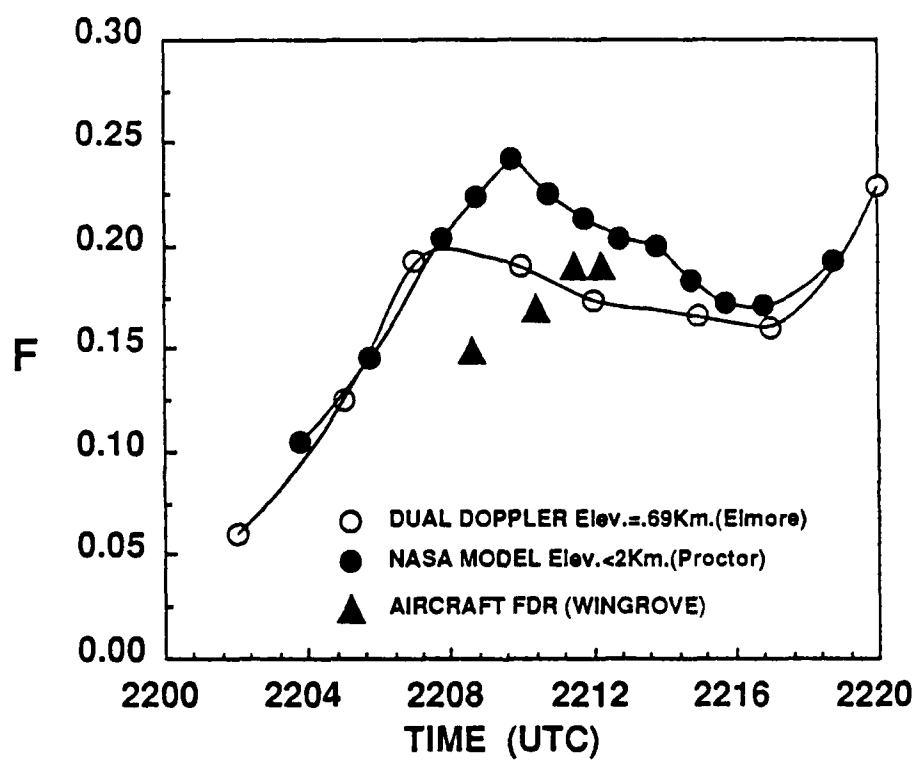


Fig. 16. As in Fig.15, but includes higher elevations.

# VERTICAL WEST-EAST CROSS SECTIONS OF F-FACTOR

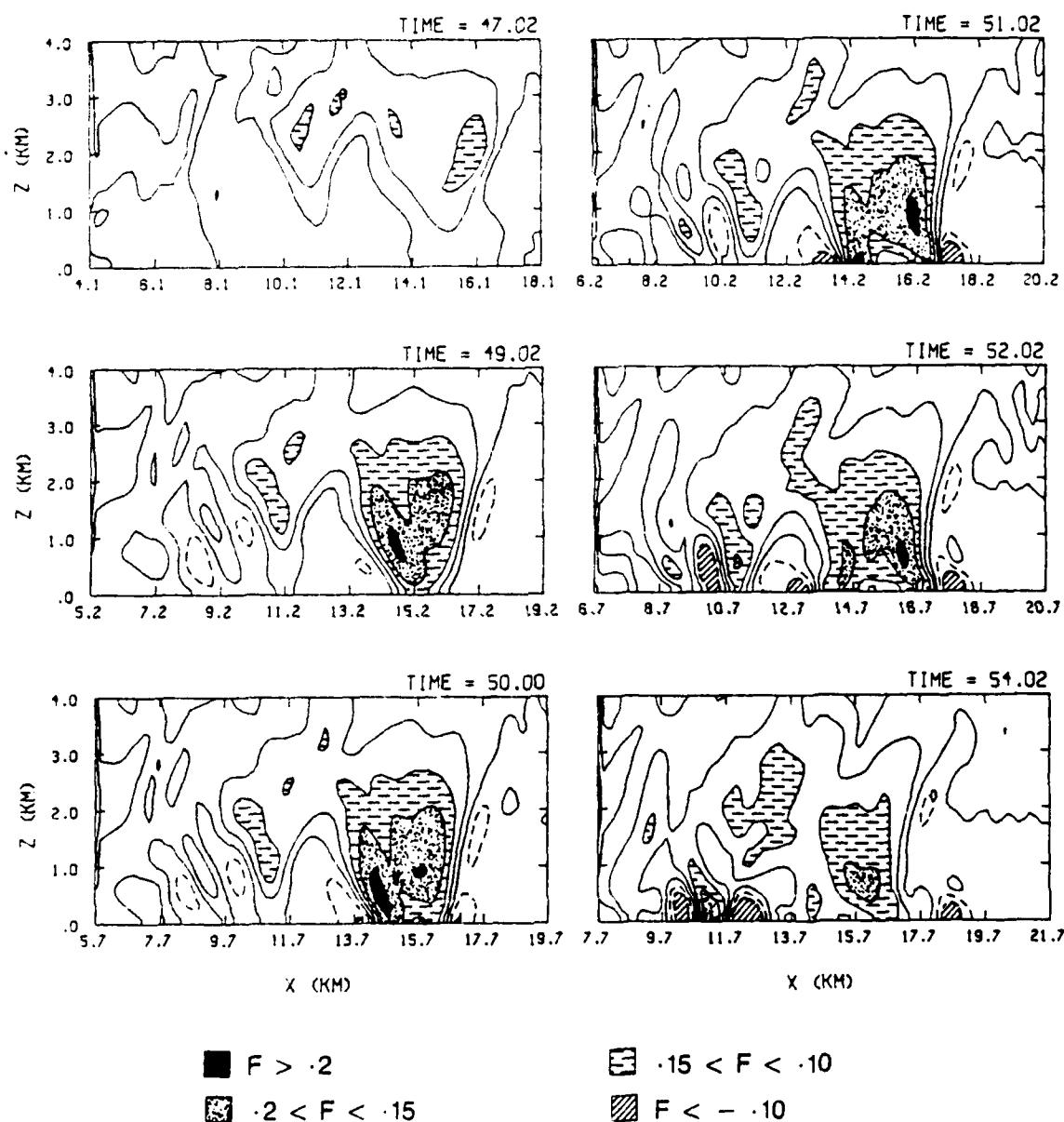


Fig. 17. As in Fig. 13, but for east-west F-Factors at a) 47 min (2206 UTC), b) 49 min (2208 UTC), c) 50 min (2209 UTC), d) 51 min (2210 UTC), e) 52 min (2211 UTC), and f) 54 min simulation time (2213 UTC). The contour interval is 0.05.

DENVER JULY 11, 1988  
EAST - WEST F FACTOR

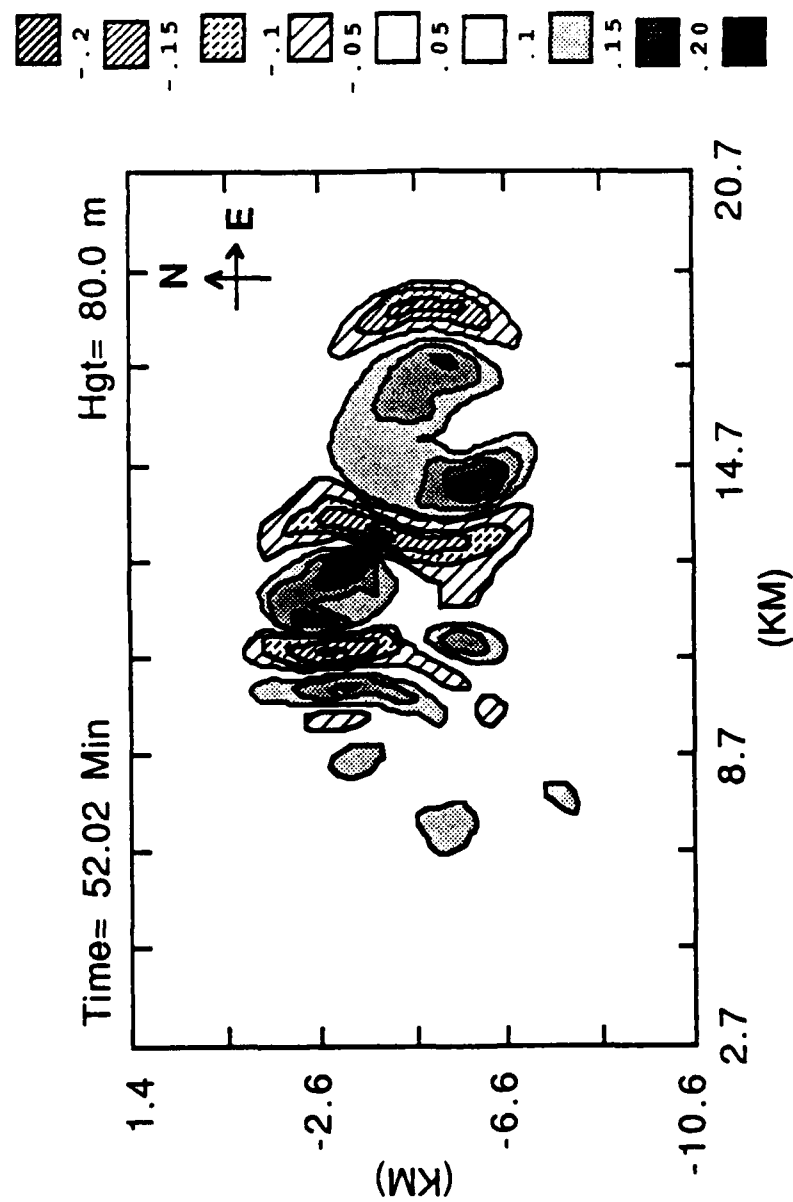


Fig. 18. Horizontal cross section at 80 m AGL of east-west F-Factors at 52 min (2211 UTC).

DENVER JULY 11, 1988  
NORTH - SOUTH F FACTOR

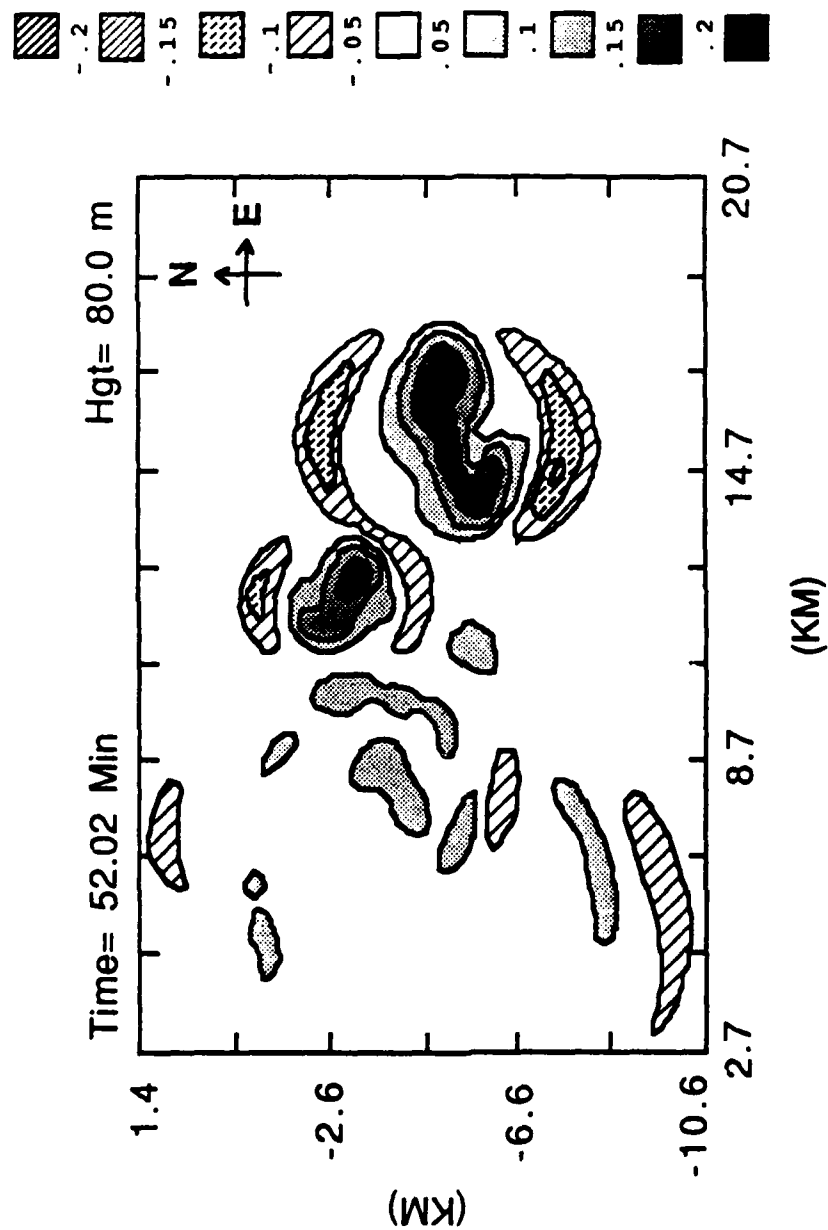


Fig. 19. As in Fig. 18, but for north-south F-Factors.





# COMPARISON OF MODEL WINDS AND HORIZONTAL WINDS RECONSTRUCTED FROM 4 AIRCRAFT

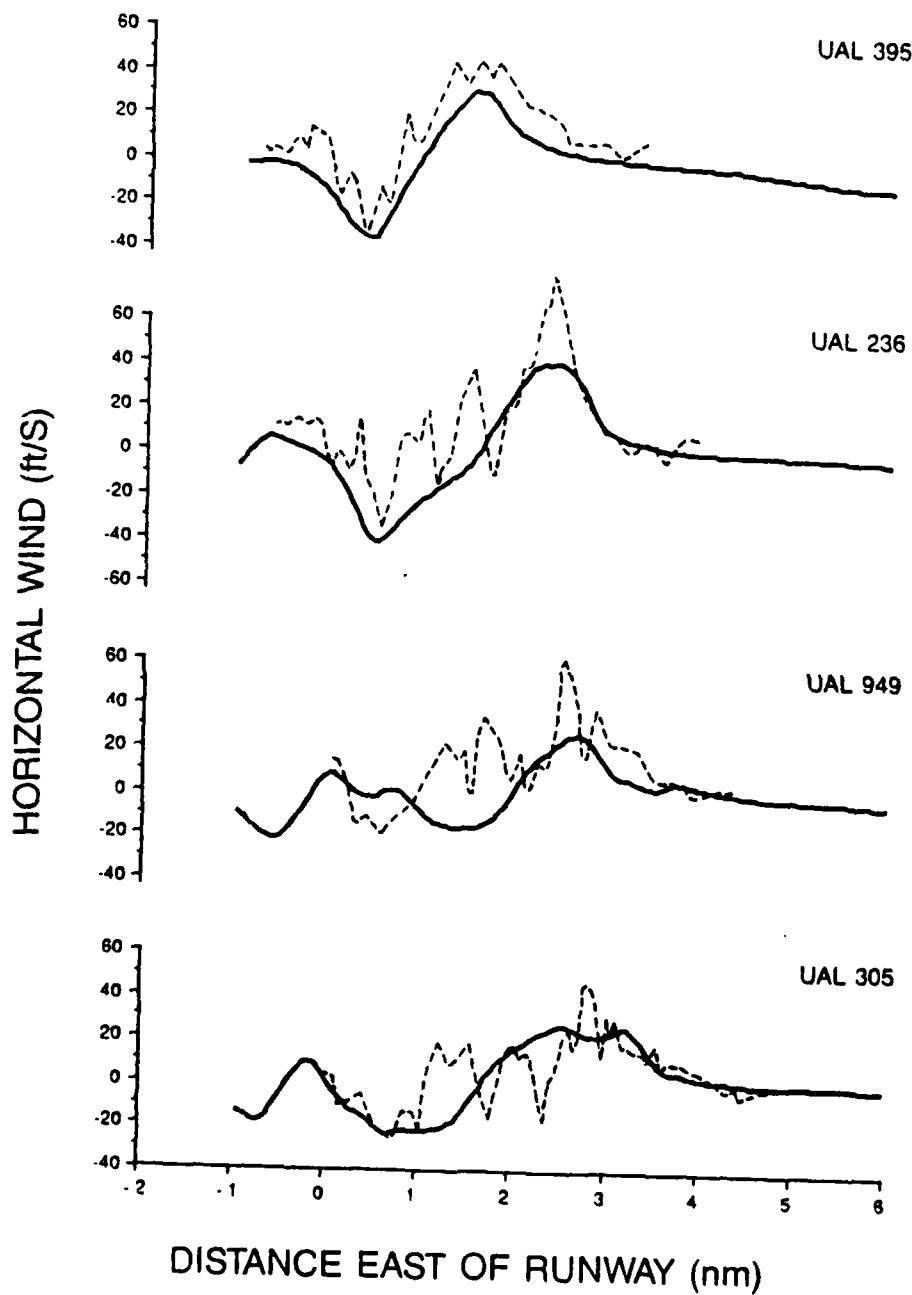


Fig. 21. Horizontal wind profile along the flight path of 4 aircraft (Modified from original figure from Wingrove and Coppenbarger 1989). The dashed lines represent the wind profiles reconstructed from the flight data recorders, whereas the solid lines represent the model x-component winds along the aircraft flight paths.

## MODEL F-FACTORS ALONG RECONSTRUCTED FLIGHT PATHS

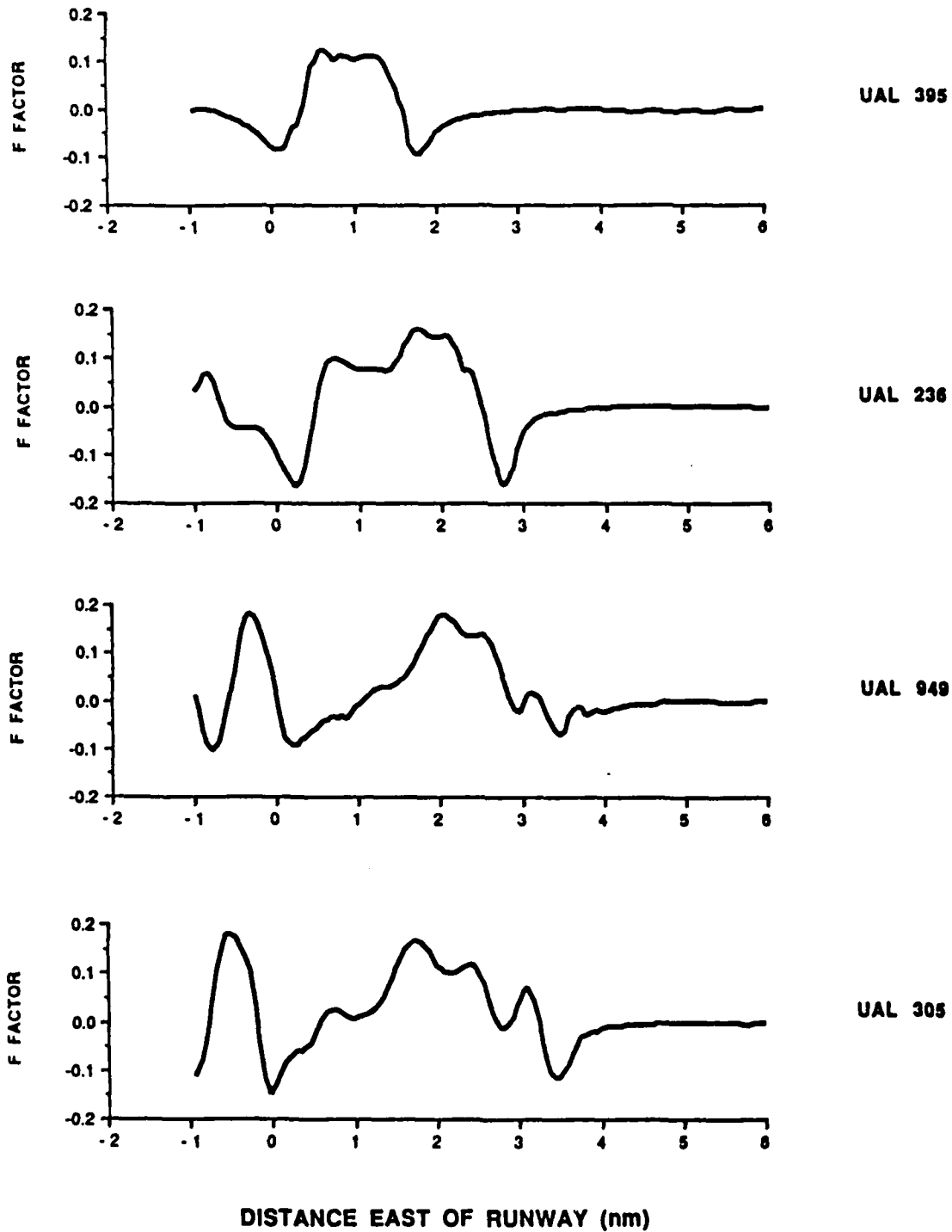


Fig. 22. As in Fig. 21, but for model F-Factors computed along the flight paths of the aircraft.

Windshear Case Study: Denver, Colorado, July 11, 1988  
**SUBSTANTIATING DATA -- Appendices**

## **APPENDIX 3 -- NASA Ames Report**

Coppenbarger, R.A., Wingrove, R.C., "Analysis of Records From Four Airlines in the Denver Microburst, July 11, 1988," AIAA Paper 89-3354, August 14-16, 1989.

BOSTON, MA. AUGUST 14-16, 1989

ANALYSIS OF RECORDS FROM FOUR AIRLINERS IN THE DENVER MICROBURST, JULY 11, 1988

R. A. Coppenbarger\* and R. C. Wingrove\*  
NASA Ames Research Center, Moffett Field, California

**Abstract**

Flight and radar position records are analyzed to determine the winds encountered by four airliners that penetrated a multi-cell microburst on approach to Denver's Stapleton International Airport. The four encounters provide information about the time-varying changes in the strength, size, and location of the microburst phenomenon. The results show significant expansion in the size of the microburst and indicate that there were fluctuations in the internal wind velocity. At its peak strength, as experienced by the second aircraft, the microburst produced a head-wind-to-tail-wind shear of 115 ft/sec. The wind patterns derived from the flight-data analysis are in general agreement with results derived from Doppler weather radar and from a numerical microburst simulation. The data from the four aircraft complement these other findings by providing a more detailed analysis of the turbulent wind environment.

**Introduction**

Low-level microburst wind shear is a continuing problem that must be better understood in the interest of aircraft safety.<sup>1-3</sup> In recent years, research efforts have included 1) the development of ground-based systems for the detection of microburst activity, 2) the development of meteorological models to predict microburst flow fields, and 3) the analysis of airline flight records of actual microburst encounters, to obtain high-resolution wind estimates along flight paths. Although these efforts have proceeded in parallel, there has been no opportunity to apply each approach to a single wind-shear event. Additionally, previous analyses of airline flight records have

been limited to microburst encounters involving single aircraft, which can provide wind estimates only over short time periods and along single trajectories.

Recently, flight records have become available from four airliners that penetrated a multi-cell microburst while approaching Denver's Stapleton International Airport on the afternoon of July 11, 1988. In addition to the availability of multiple flight records, this incident was unique because of the presence of Doppler weather radar that was being evaluated at Denver at the time of the incident. Meteorological soundings were also available before the incident and they were later used as initial conditions for an advanced flow-field simulation of the microburst.

The four aircraft, all operated by United Airlines (UAL), were making visual approaches from the east. As shown in Fig. 1, in the order they approached, the aircraft were UAL 395 (a B-737), UAL 236 (a DC-8), UAL 949 (a B-727), and UAL 305 (a B-727). After encountering the microburst east of the runway threshold, all four aircraft aborted their approaches and initiated go-arounds.<sup>4</sup> Despite the strength of the microburst, there were no injuries to those aboard the airliners and no damage to the aircraft.

During the summer of 1988, Terminal Doppler Weather Radar (TDWR) was in operation at Denver as part of a test and demonstration project, sponsored by the FAA, to detect wind shear in the terminal area.<sup>5</sup> The project was carried out by the National Center for Atmospheric Research (NCAR) and the MIT Lincoln Laboratory. An additional Doppler radar site, operated by the University of North Dakota, together with the TDWR radar, allowed a dual-Doppler analysis of the microburst winds. Wind-velocity fields obtained from both single- and dual-Doppler scans were provided by NCAR for comparison with flight data.<sup>6</sup> Measurements from surface wind sensors, situated in the vicinity of the approach paths, were also available.

\*Aerospace Engineer, Member AIAA.

Copyright © 1989 by the American Institute of Aeronautics and Astronautics, Inc. No copyright is asserted in the United States under Title 17, U.S. Code. The U.S. Government has a royalty-free license to exercise all rights under the copyright claimed herein for Governmental purposes. All other rights are reserved by the copyright owner.

Denver weather soundings, taken about 1 hr before the aircraft encounters with the microburst, were used to initiate the Terminal Area Simulation System (TASS) numerical model.<sup>7</sup> This model, developed through the support of NASA Langley Research Center, provides a three-dimensional prediction of microburst winds.<sup>8</sup>

The purpose of this paper is to present relevant wind information derived from the on-board flight records and compare it with data from the ground-based TDWR and surface wind sensors, and the TASS model. Through this analysis, a detailed history of the structure and development of the microburst is produced. Large-scale characteristics, such as size and shape, are depicted by the Doppler data, whereas small-scale characteristics, such as internal turbulence and peak wind velocities, are shown by the flight data.

The paper first describes the procedure used to calculate wind velocity from the flight data. The aircraft trajectories are then discussed, and the results are presented showing the important physical characteristics of the microburst. Finally, flight-path winds are compared with those obtained from the Doppler radar and the numerical simulation.

### Method of Analysis

The aircraft data, obtained through the National Transportation Safety Board, included both air traffic control (ATC) radar position data and foil flight-recorder data. The radar data included range, azimuth, and mode-C transponded pressure altitude. From these data, the inertial coordinates of each aircraft were reconstructed in a Cartesian frame ( $x, y, h$ ) with its origin at the end of runway 26L at Stapleton. From the foil flight-recorder, pressure altitude, indicated airspeed, heading, and normal acceleration were obtained. The two data sets were synchronized through a time-history comparison of the on-board recorded altitude and the ATC-transponded altitude.

Because of the limited data set, vertical winds were not determined, and it was necessary to calculate horizontal winds using specialized solutions (developed in Ref. 9) as follows. The winds along the aircraft flight path are calculated from

$$W_{fp} = V_i - V_a \quad (1)$$

where the inertial ground speed

$$V_i = \sqrt{\dot{x}^2 + \dot{y}^2}$$

is derived from the ATC radar data, and the true airspeed,  $V_a$ , is determined from the flight data. This equation applies when the flight-path angle is small, and when the difference between the ground-axis heading angle and the wind-axis heading angle is small. This is a very robust solution and applies well along the trajectories considered in this report.

The horizontal wind components are determined as

$$\begin{aligned} W_x &= \dot{x} - V_a \cos \psi_a \\ W_y &= \dot{y} - V_a \sin \psi_a \end{aligned} \quad (2)$$

where the heading angle  $\psi_a$  is measured from the aircraft gyro and obtained from the foil data. This solution applies under the same flight conditions noted for Eq. (1), but is more restrictive since it requires further conditions wherein the roll and sideslip angles are small. These conditions are generally met during the stabilized final approach, but do not hold after the aircraft starts a turn, typically over the approach end of the runway in a go-around maneuver.

### Results and Discussion

#### Aircraft Trajectories and Speeds

The trajectories of the four aircraft, reconstructed from the ATC radar data, are shown in Fig. 2. The upper plot in Fig. 2 shows a plan view ( $x, y$ ), and the lower plot shows a side view ( $h, y$ ). The approximate times at which each aircraft passed over the runway threshold are also indicated in Fig. 2 (in minutes after the hour). Speed and altitude profiles for each aircraft, presented as functions of the distance from the threshold of runway 26L, are shown in Figs. 3-6. In each of these figures, the upper plot shows the true airspeed ( $V_a$ ) and the inertial ground speed ( $V_i$ ). The difference between these two curves is representative of the winds encountered. The lower plots show the altitude above-ground-level from both the flight recorder and the ATC transponder. The microburst winds and subsequent go-around maneuvers, as depicted in Figs. 3-6, are discussed separately below for each of the four aircraft.

**UAL 395.** At approximately 2.5 n. mi. east of runway 26L, UAL 395 began experiencing an increasing head wind (difference between airspeed and ground

speed), indicating its initial encounter with the microburst (Fig. 3). The head wind increased to 40 ft/sec and then began decreasing, eventually transitioning to a peak tail wind of 30 ft/sec. Thus, the resulting head-wind-to-tail-wind shear,  $\Delta V$ , was 70 ft/sec, and occurred over a 25-sec period.

Comments from the crew made after the incident indicate that the airplane was initially flown at a higher-than-normal airspeed and above the glide slope in anticipation of wind-shear conditions. At a distance of about 1 n. mi. from the runway, a ground-proximity warning sounded and the crew, observing that the airspeed had also begun to decrease rapidly, applied takeoff thrust and rotated the airplane to takeoff pitch attitude. The onset of rain was noted at this point, the flaps were reduced to 15°, and the landing gear was raised. During the rest of the go-around, only light turbulence was observed. The flight data show that the airplane came within 100 ft of the ground as the go-around was initiated, near the center of the microburst. Upon the addition of thrust, both airspeed and altitude increased simultaneously and the aircraft recovered normally.

**UAL 236.** The results show that UAL 236 encountered a head wind, at a distance of about 2.8 n. mi. from the threshold, that increased rapidly to 80 ft/sec (Fig. 4). The head wind then decreased to a tail wind of 10 ft/sec within a 15-sec period. During the next 25 sec, fluctuations in wind velocity were experienced before a peak tail wind of 35 ft/sec was reached. The resulting  $\Delta V$  was the largest of all four aircraft—115 ft/sec occurring within 35 sec.

According to the crew, the airplane was initially flown at an airspeed that was about 10 knots faster than normal because of observed cloud activity and virga. Upon entering the microburst, the airspeed suddenly increased and the power was pulled back. At idle thrust, the crew noted that the aircraft appeared to be riding on a smooth wave with increasing airspeed. Anticipating the sudden loss in airspeed, full power was applied. During the recovery, moderate turbulence was encountered with violent jolts that appeared to move the airplane vertically and laterally. The crew noted that the aircraft climbed very slowly at first despite takeoff power and a nose-up pitch attitude. The flight data show that the go-around was initiated at about 2 n. mi. east of runway 26L. During the subsequent recovery, the data show that the aircraft remained near a constant altitude of 700 ft, although its airspeed increased markedly.

**UAL 949.** UAL 949 encountered an increasing head wind at a distance of about 3.5 n. mi. from the runway

threshold (Fig. 5). This head wind increased to 60 ft/sec over a distance of 1 n. mi. and was followed by wind-velocity fluctuations similar to those experienced by UAL 236. UAL 949 encountered a maximum tail wind of 20 ft/sec, resulting in a  $\Delta V$  of 80 ft/sec within a 45-sec period.

The crew, flying the aircraft faster and higher than normal, observed an increase in airspeed at the leading edge of the microburst. The aircraft, as it encountered the downdraft, experienced a strong shock accompanied by a sudden loss in airspeed. In response, full power was applied, and the aircraft was rotated and held at a pitch angle of 15°—in accordance with standard wind-shear recovery procedure.<sup>3</sup> The flight data show that the go-around was initiated at an altitude of about 900 ft, with a sharp pull-up leading to a subsequent gain in altitude to approximately 1700 ft. Unlike UAL 236, airspeed was traded for altitude during the initial part of the go-around.

**UAL 305.** The data in Fig. 6 show that UAL 305 experienced the least severe wind shear, with a maximum head wind of 45 ft/sec that eventually transitioned into a tail wind of 25 ft/sec. This resulted in a  $\Delta V$  of 65 ft/sec within 40 sec. Like the previous two aircraft, UAL 305 also experienced small-scale velocity fluctuations within the core of the microburst.

After experiencing difficulty in slowing the aircraft down for the approach and hearing the prediction of an 80-knot loss by air traffic control, the crew executed a standard go-around procedure. During the go-around, moderate turbulence was encountered and the aircraft did not achieve its expected climb performance. Similar to UAL 236, UAL 305 remained at a fairly constant altitude while traversing the microburst (between 900 and 1,100 ft), while its airspeed increased.

### Microburst Development and Structure

Figure 7 presents a comparison of the flight-path winds for the four aircraft. As indicated in the above discussion, the most intense wind shear was experienced by the second aircraft, UAL 236. The wind profiles suggest that the microburst activity was spreading out during the successive encounters. The distance between velocity peaks (maximum head wind and tail wind) was about 1.3 n. mi. at the time of the first aircraft encounter and grew steadily to over 2 n. mi. by the time of the fourth aircraft encounter. During this period of time, the center of the activity was drifting eastward, moving from approximately 1 n. mi. to 1.7 n. mi. east of the runway threshold. Of greatest significance is the finding of small-scale wind fluctuations that developed between the

time that UAL 395 and UAL 236 traversed the microburst. Comparing the wind profiles of the last three aircraft (Fig. 7), these velocity fluctuations show a similar pattern, with peaks spaced about 0.4 n. mi. apart and occurring near the center of the microburst. Parameters describing the occurrence of these fluctuations are shown in Fig. 8.

Figure 8 shows the primary features of the wind profiles evident in Fig. 7, plotted in temporal and spatial coordinates for each aircraft. The positions, with respect to the runway threshold, of maximum tail and head winds for each encounter are designated by  $D_1$  and  $D_2$ , respectively. Internal peak tail winds, describing the fluctuations observed for UAL 236, UAL 949, and UAL 305, are designated by  $d_1$  and  $d_2$ .

### Comparisons

The maximum  $\Delta V$  encountered by the four aircraft, compared with the maximum  $\Delta V$  measured by the single TDWR Doppler radar, is shown in Fig. 9. As can be seen, the maximum  $\Delta V$ 's from the flight data are somewhat below those measured by the TDWR. This is to be expected, since the maximum  $\Delta V$  reported by the TDWR is the maximum seen in any one direction by the radar. Results suggest that most of the airplanes did not penetrate the center of the microburst cell(s) and thus did not encounter maximum wind changes.

With a single Doppler radar such as the TDWR, only the radial component of the wind velocity can be measured. To provide both components of the wind vectors, along the flight path and in a given altitude plane, data from the additional weather radar site were utilized. The location of the two radar sites with respect to the runways at Stapleton is shown in Fig. 10. Flight-path winds resulting from the dual-Doppler analysis are shown in comparison with those derived from the flight records in Fig. 11. Since the minimum resolution of the Doppler data is 0.25 km, the Doppler-derived winds are naturally more smoothed than those derived from the flight data. Additional filtering results from the combination of data from the two Doppler radars and from the conversion from spherical to Cartesian coordinates. Because of the smoothing involved, the Doppler data do not resolve subtle wind phenomena such as the velocity fluctuations mentioned earlier. Given these considerations, the Doppler data and flight data show good agreement. Figure 11 also shows the flight-path winds predicted by the numerical (TASS) simulation. This model, like the Doppler data, does not show the internal wind fluctuations present in the flight data because of a lack of resolution.

The lowest altitude at which Doppler-derived winds were available was approximately 600 ft AGL. To obtain a comparison of flight-path winds at a lower altitude, data from two surface wind sensors were also compared with the flight data. The surface site closest to the runway was part of the LLWAS already in operation at Stapleton, and the other was part of the FLOWS mesonet. The winds measured by the ground sensors are shown in comparison to those from two aircraft, UAL 949 and UAL 305, in Fig. 12. These two aircraft traversed the microburst at close time intervals but with different trajectories, UAL 305 approaching 26R was about 0.25 n. mi. north of the path on which UAL 949 was approaching 26L. As shown, the flight-data-derived winds compare remarkably well with those from the ground sites.

Dual-Doppler data, constructed at 1-min intervals, suggest that the microburst activity initially involved a single cell with a second cell appearing some time later, aligning with the first in the east-west direction. Both Doppler data and flight data indicate that the second microburst cell reached the surface at some point between the passage of UAL 395 and UAL 236 (about 10.5 min after the hour). In Fig. 13, horizontal wind vectors, measured by the aircraft, are shown in comparison with the cell locations (depicted by circles). These cell locations were construed from the dual-Doppler data.

The pattern of the winds encountered are shown to be dependent on the track of each aircraft with respect to the cells. The first aircraft, UAL 395, encountered a cell with a center located to the south of its track. With two cells developing near the approach path, UAL 236 encountered the edge of the eastmost cell and proceeded to penetrate the center of the cell closest to the runway. By the time the third aircraft, UAL 949, approached, the two cells had drifted slightly in a southeasterly direction. UAL 949 passed through the northern section of the outermost cell and proceeded to pass just north of the center of the innermost cell. The trajectory of the last aircraft, UAL 305, passed well to the north of the center of both microburst cells. Note that this aircraft was approaching 26R, and thus had a track farther north than the previous three aircraft.

The fluctuations in wind velocity seen in the flight data of the last three aircraft may have been the result of either the second microburst cell or secondary ring vortices contacting the ground. As described in Ref. 10, a microburst model based on a multiple-ring vortex structure can predict horizontal wind fluctuations similar to those seen here in the flight data. It appears most probable, however, that the wind phenomenon encountered by



the aircraft resulted from the two adjacent microbursts cells.

### Concluding Remarks

From the resulting wind profiles it is evident that very strong microburst activity was encountered, with a peak head-wind-to-tail-wind shear of 115 ft/sec. Since records from multiple aircraft were available, the time-history development of the microburst phenomenon was evident. The center of the microburst cells moved from 1 n. mi. to 1.7 n. mi. east of the runway threshold during the time of the aircraft encounters. During this time, the size of the microburst (distance between wind velocity peaks) grew from 1.3 n. mi. to over 2 n. mi. A significant result of this analysis is the finding of velocity fluctuations developing within the microburst boundaries. The results for the last three aircraft show that these internal fluctuations exhibited a similar pattern, with peaks spaced about 0.4 n. mi. apart. The developing wind pattern measured from the aircraft is in general agreement with the measurements from the Doppler radar and with the analytical results from the numerical TASS model. The aircraft data complement these other findings by providing a detailed analysis of the internal velocity fluctuations. The Doppler data were shown to not only validate the flight data but also to add insight into the resulting wind profiles by suggesting the presence of a secondary microburst cell. It is very possible that the appearance of this second downburst caused the internal fluctuations in horizontal winds observed in the flight data of the latter three aircraft. Investigation into the behavior of the multi-cell microburst phenomenon is a subject for further research.

This unique incident at Denver offers a wealth of information from both an operational and scientific standpoint. From the experiences of the four aircraft, insight into the warning signs and appropriateness of flight procedures following an inadvertent microburst encounter can be gained. Knowledge gained from flight records and other sources concerning the detailed structure of the microburst phenomenon can be used to create more realistic simulator models and can aid in the development of both ground-based and airborne wind-shear detection systems.

### References

<sup>1</sup>Low-Altitude Wind Shear and Its Hazard to Aviation, National Academy of Sciences, National Academy Press, Washington, D.C., 1983.

<sup>2</sup>Fujita, T. T., "The Downburst," SMRP Research Paper 210, University of Chicago, Chicago Ill., 1985.

<sup>3</sup>"Windshear Training Aid," Federal Aviation Administration, Washington, D.C., 1987.

<sup>4</sup>Ireland, B., "Microburst Encounter, July 11, 1988," United Airlines Flight Safety Investigation 88-46, Denver, Colo., Feb. 1989.

<sup>5</sup>"Terminal Doppler Weather Radar Operational Demonstration," Federal Aviation Administration, Washington, D.C., 1988.

<sup>6</sup>Sand, Wayne, "11 July Weather and Resulting TDWR Alarms at Denver, Colorado," Presented at the Second Combined Manufacturers' and Technology Airborne Wind Shear Review Meeting, Williamsburg, Va., Oct. 1988.

<sup>7</sup>Proctor, Fred H., "Numerical Simulation of the Denver 11 July 1988 Microburst Storm," Presented at the Second Combined Manufacturers' and Technology Airborne Wind Shear Review Meeting, Williamsburg, Va., Oct. 1988.

<sup>8</sup>Proctor, Fred H., "Numerical Simulations of an Isolated Microburst. Part I. Dynamics and Structure," *Journal of Atmospheric Sciences*, Vol. 45, No. 21, Nov. 1988.

<sup>9</sup>Bach, R. E. and Wingrove, R. C., "Equations for Determining Aircraft Motions from Accident Data," NASA TM-78609, 1980.

<sup>10</sup>Schultz, T. A., "A Multiple-Vortex-Ring Model of the DFW Microburst," Presented at the 26th Aerospace Sciences Meeting, Reno, Nev., Jan. 1988.

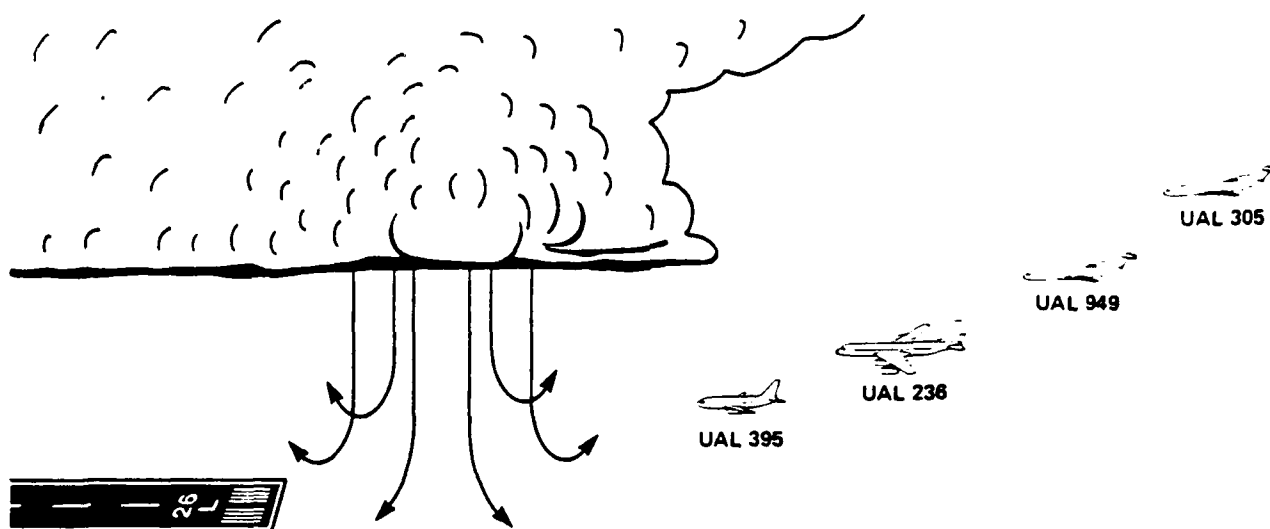


Fig. 1 Overview of the Denver microburst of July 11, 1988.

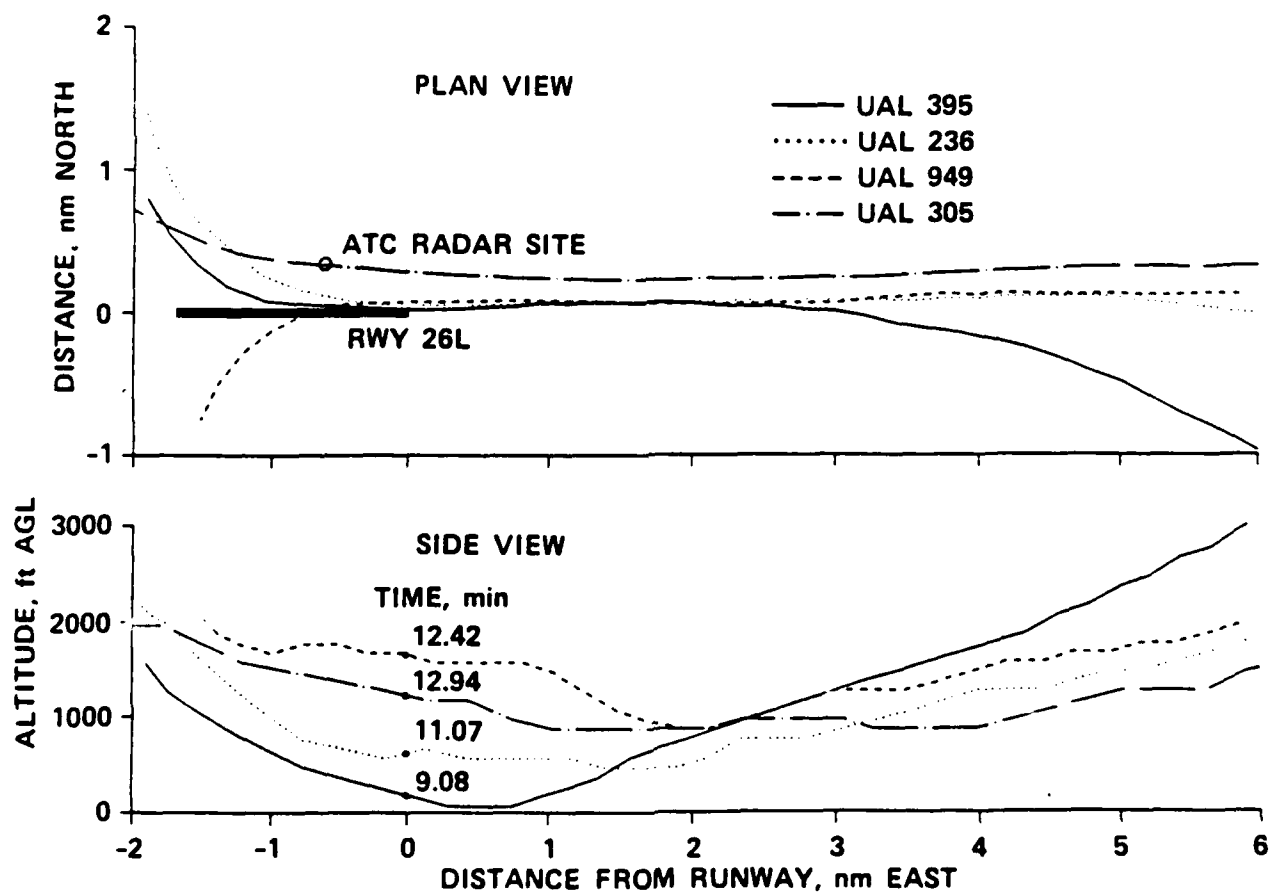


Fig. 2 Airliner trajectories.

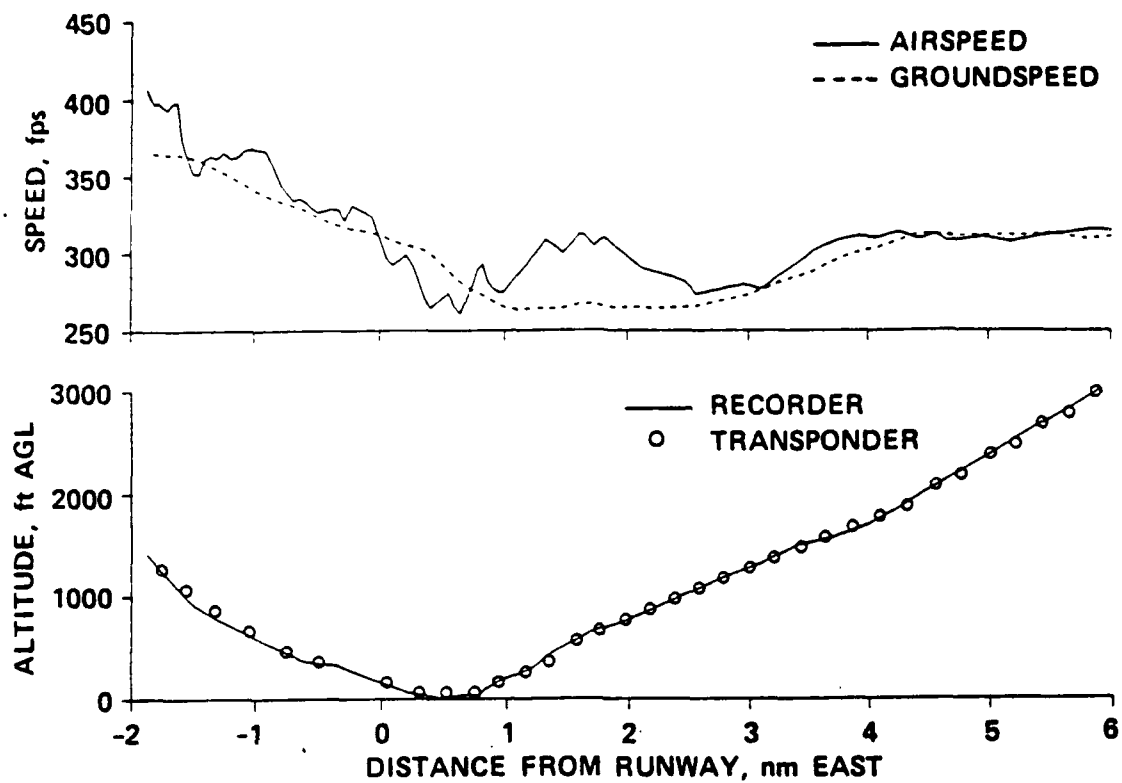


Fig. 3 Speeds and altitude for UAL 395.

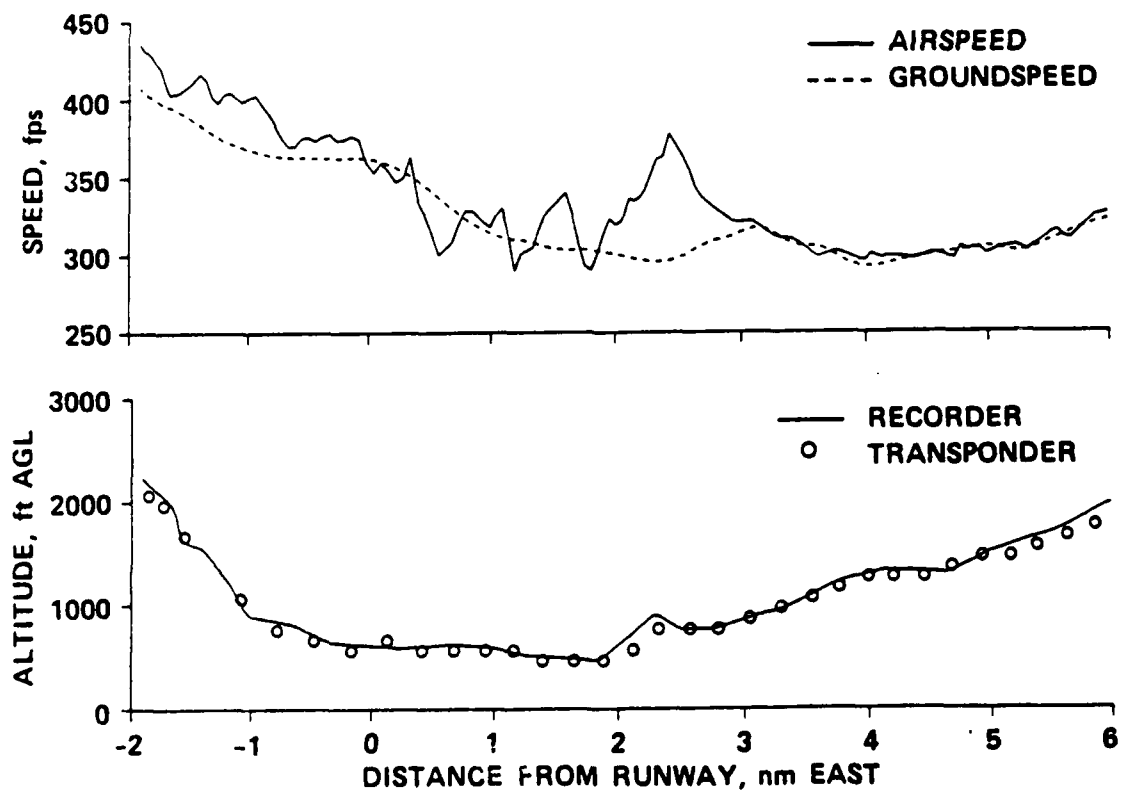


Fig. 4 Speeds and altitude for UAL 236.

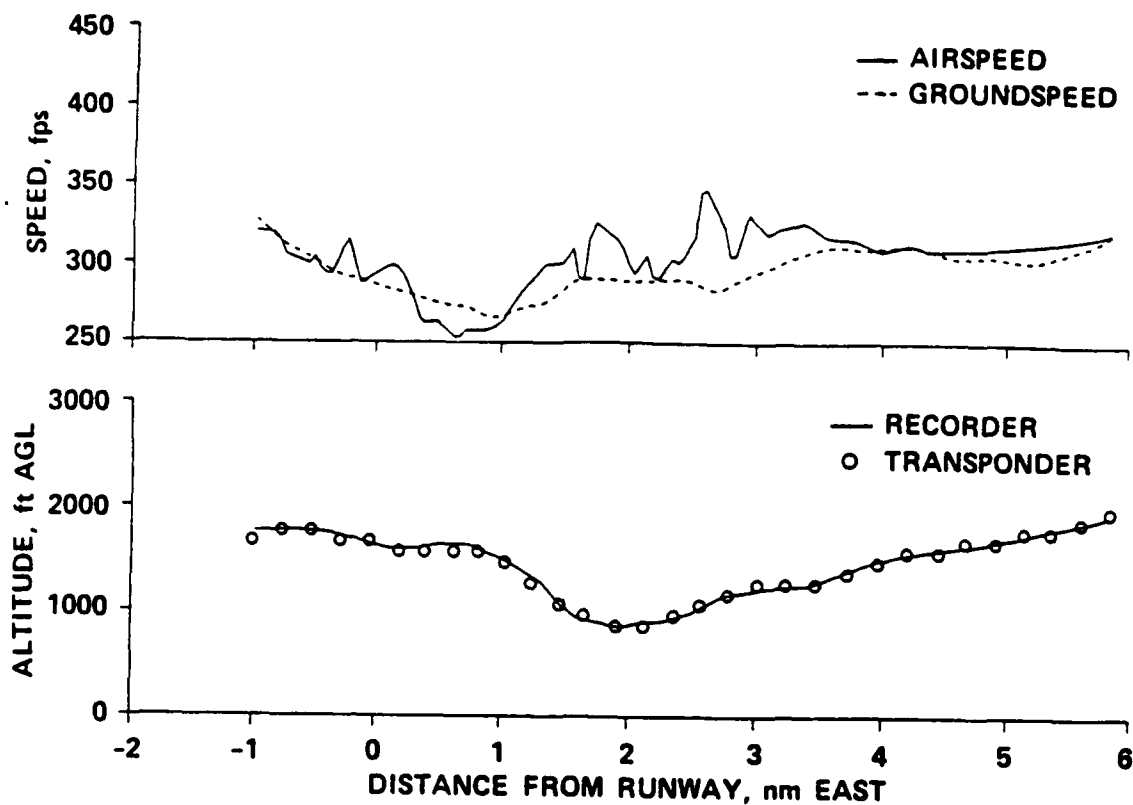


Fig. 5 Speeds and altitude for UAL 949.

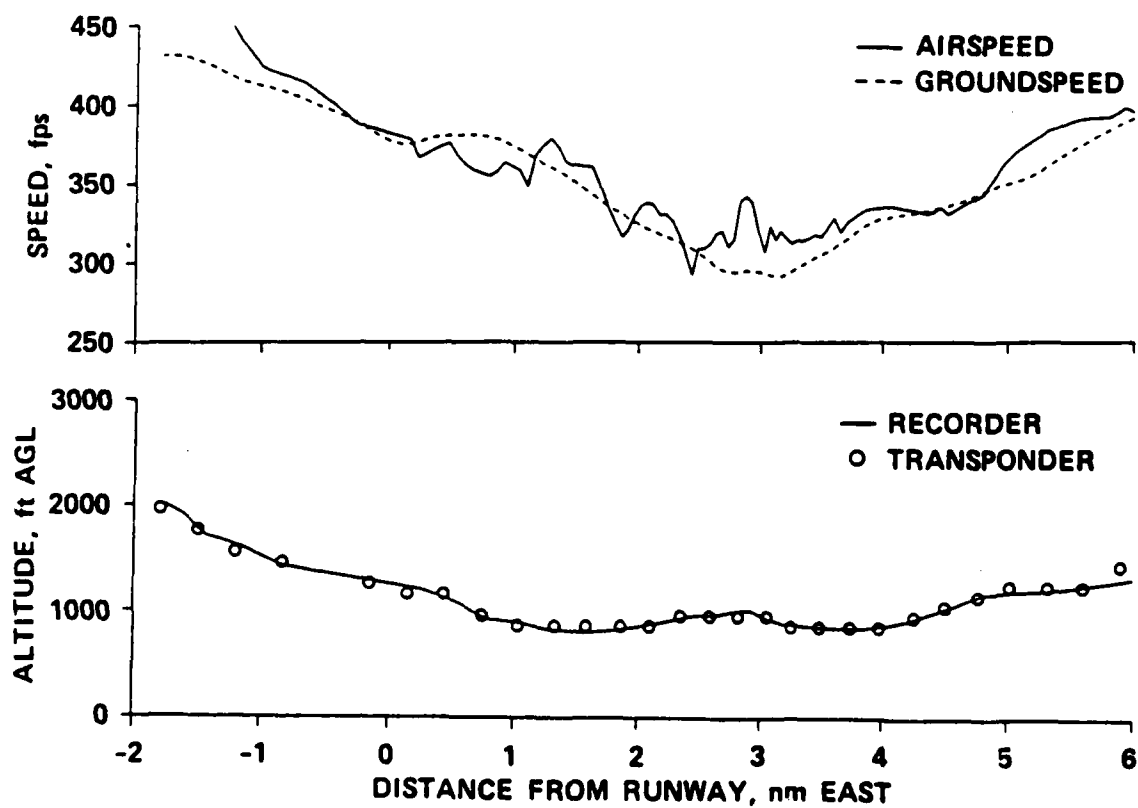


Fig. 6 Speeds and altitude for UAL 305.

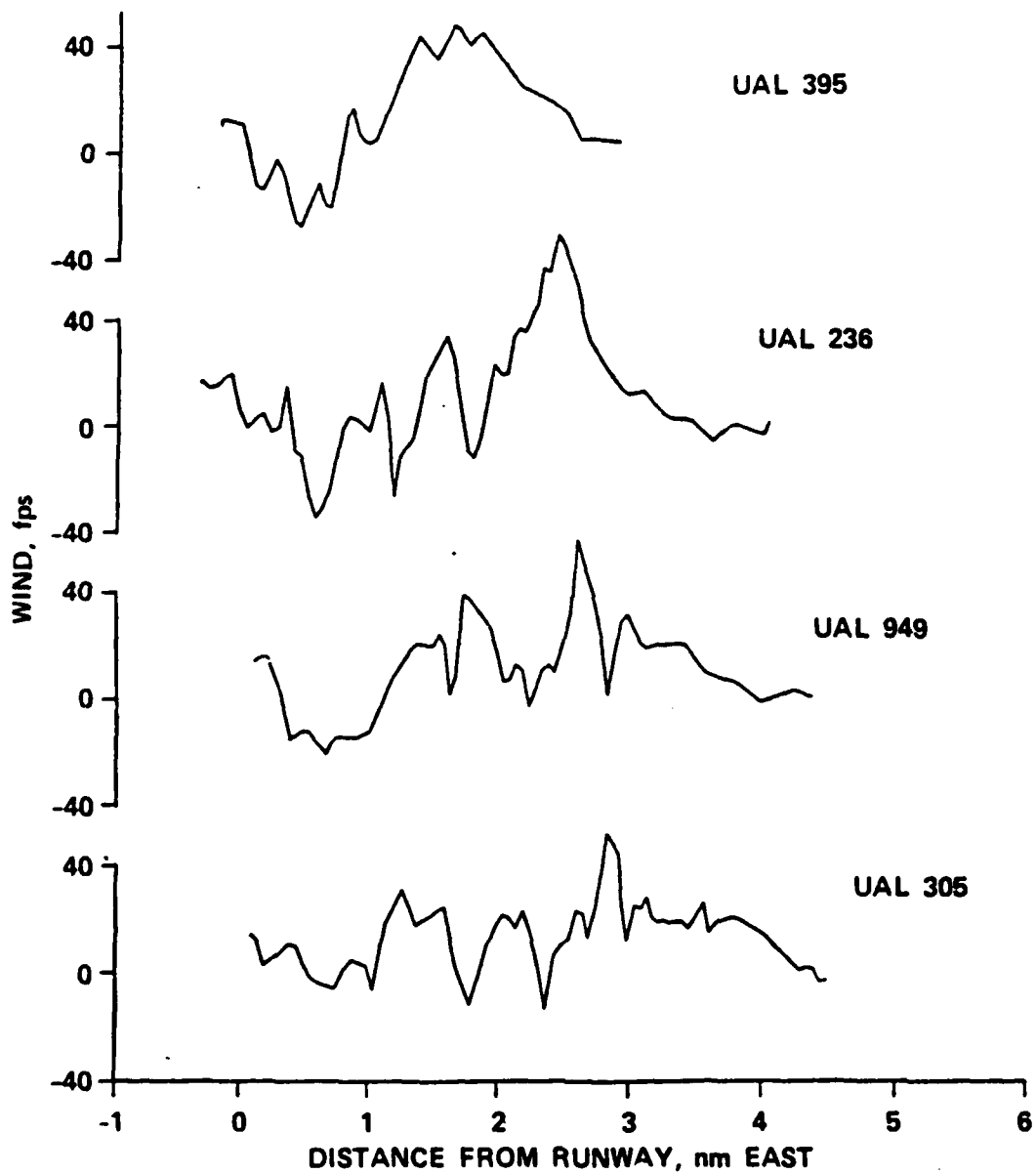


Fig. 7 Flight-path winds.

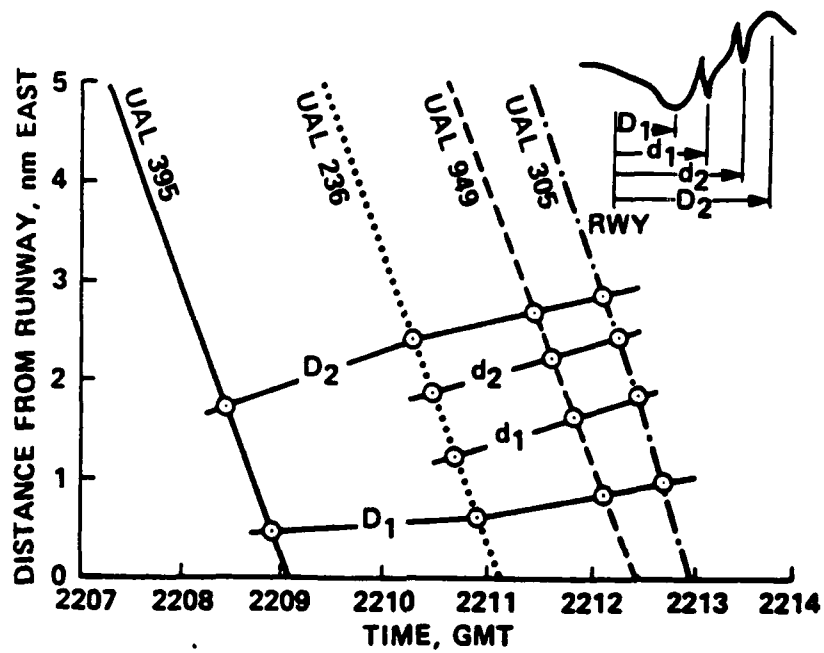


Fig. 8 Time variation of microburst location.

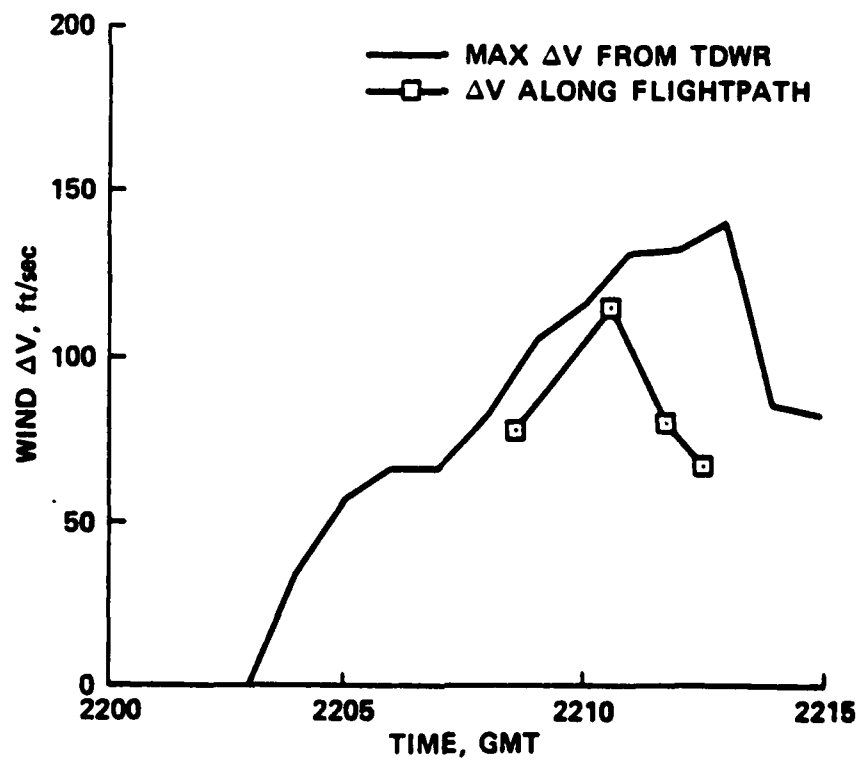


Fig. 9 Maximum ΔV's along flight paths compared with those from TDWR.

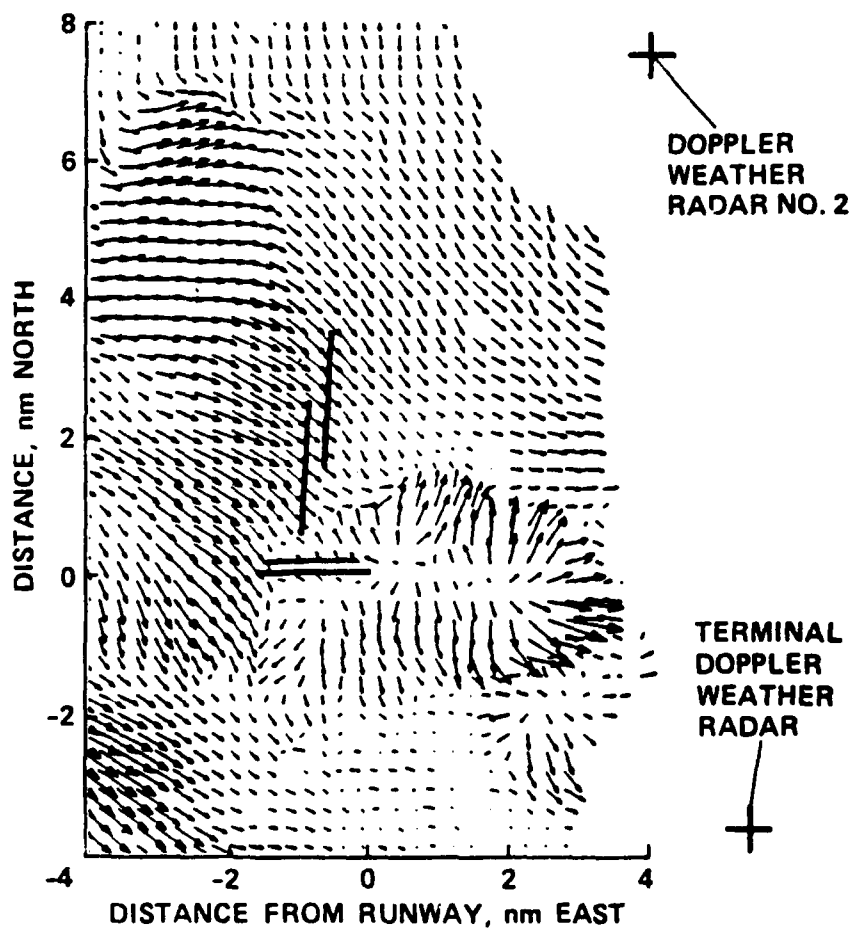


Fig. 10 Location of Doppler radar sites and derived wind pattern at time 2211:00.

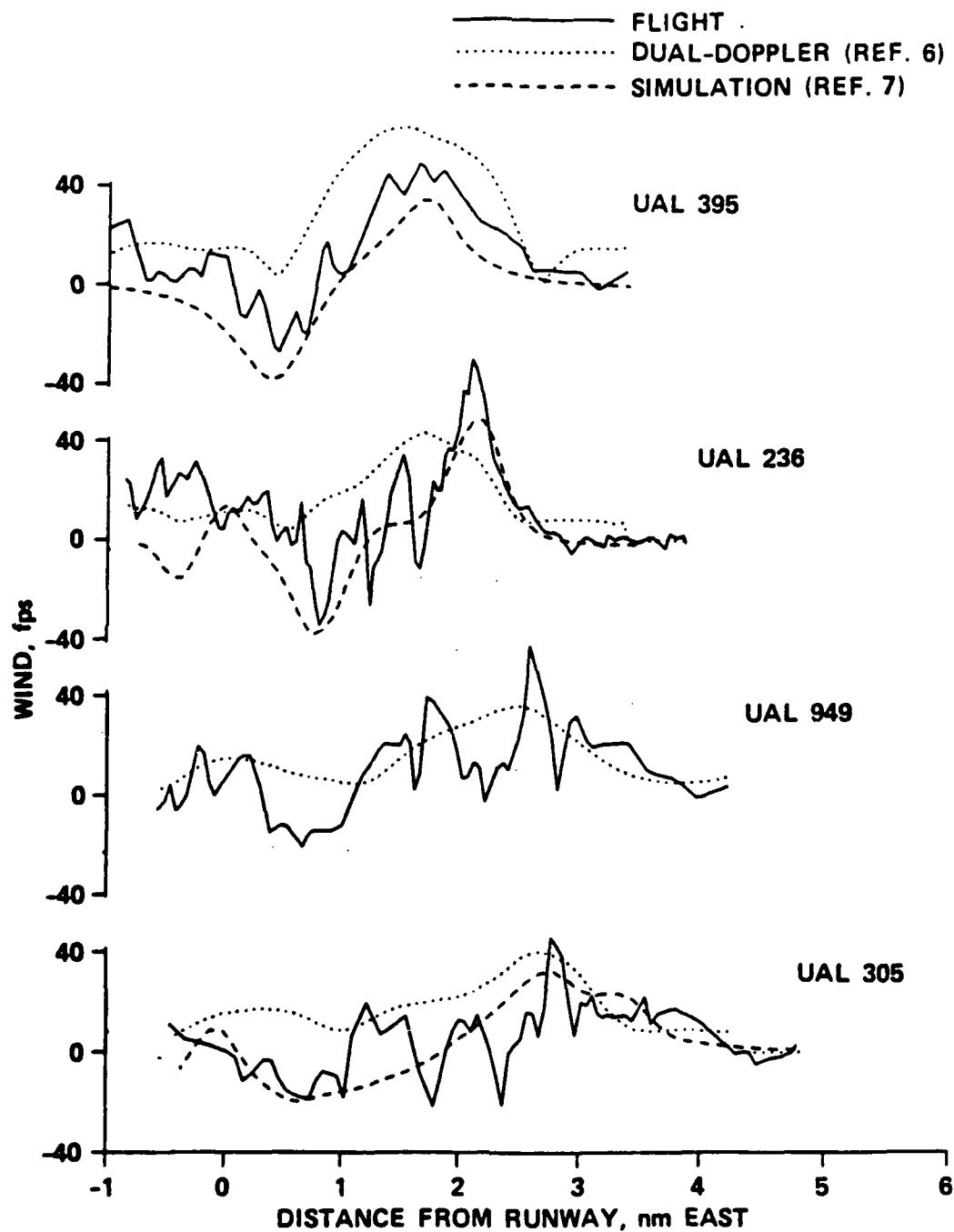


Fig. 11 Flight-path winds and winds from dual-Doppler and numerical simulation.



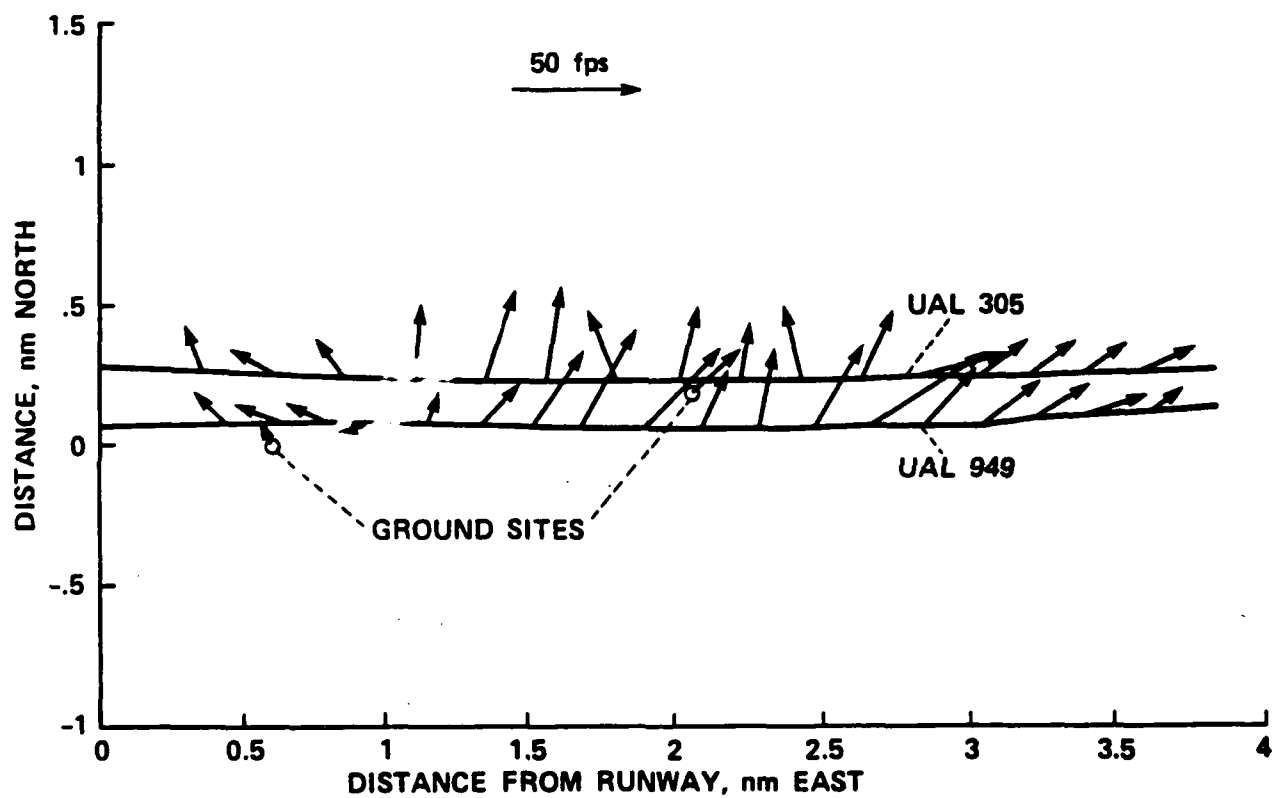


Fig. 12 Wind vectors from two airliners compared with those measured at two surface sites.

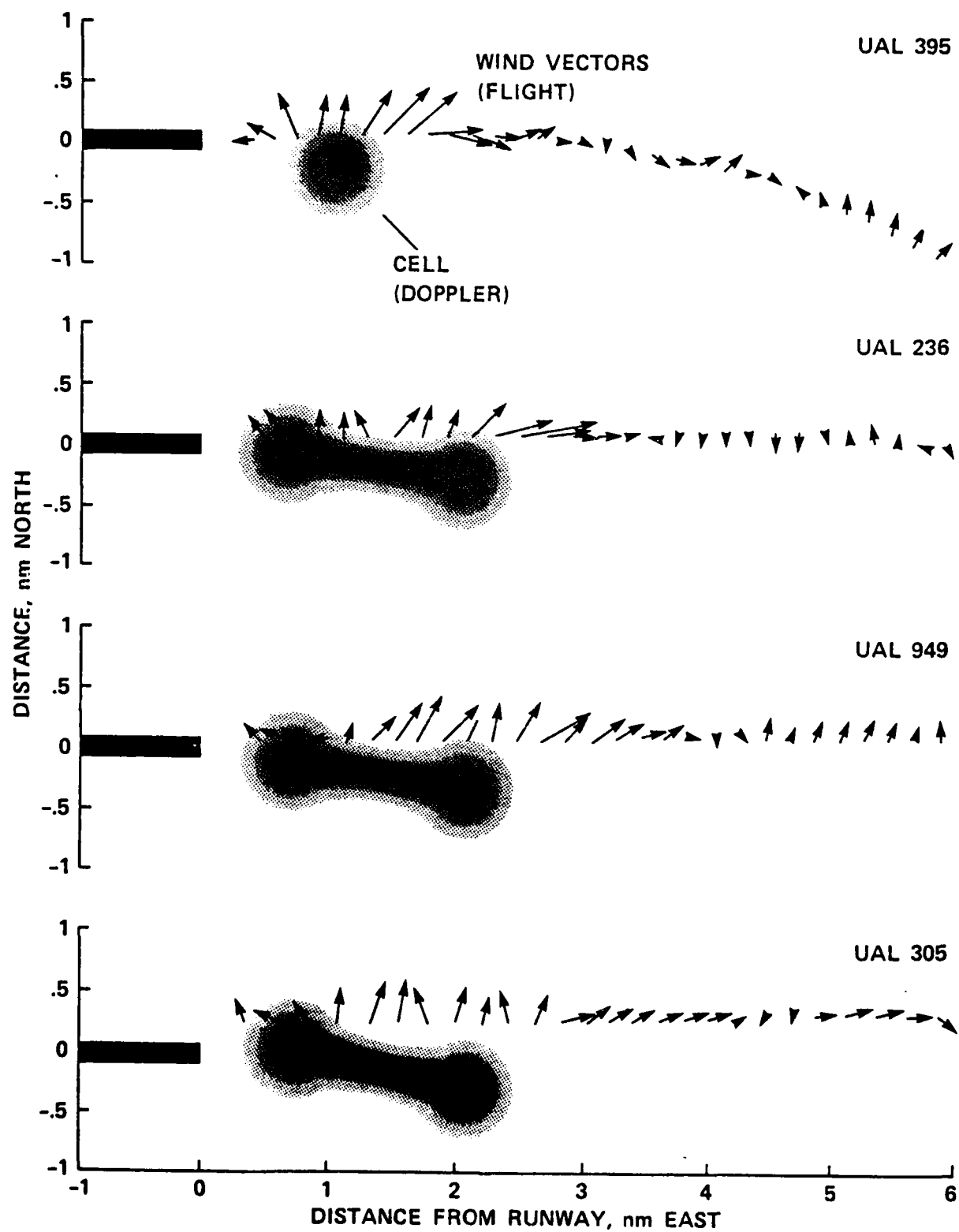


Fig. 13 Wind vectors from four airliners compared with microburst cells from dual Doppler.

Windshear Case Study: Denver, Colorado, July 11, 1988  
**SUBSTANTIATING DATA -- Appendices**

## **APPENDIX 4 -- MIT Lincoln Lab Report**

Isaminger, M. A., "WEEKLY SITE SUMMARY," FL2 Radar Site, Denver, Colorado, MIT Lincoln Laboratory.

Campbell, S., Correspondence to Roland Bowles, dated 24 March 1989, containing velocity and shear values from FLOWS for July 11, 1988, at Denver Stapleton Airport, MIT Lincoln Laboratory.

# Lincoln Lab Radar Weekly Site Summary<sup>1</sup>

Weather conditions were conducive to thunderstorms, the temperature was warm. During the 7.1 hours that the Terminal Doppler Weather Radar (TDWR) was operating, it detected 19 microbursts and three gust fronts. TDWR data were recorded on tape numbers 375 through 383, the following table is a summary.

**Table I -- Doppler Weather Radar Site Summary**

---

Event	Time UTC	Location ran/az	Deltav m/s	Reflectivity dBz
GF	2014	43/195	12	
MB	2017	32/210	12	25
MB	2020	85/337	12	45
MB	2059	20/152	20	10
MB	2059	25/168	18	
MB	2140	32/305	16	20
GF	2145	21/309	7	
GF	2149	26/280	13	
MB	2201	15/287	10	10
MB	2209	5/312	26	30
MB	2213	9/317	40	40
MB	2211	3/311	18	15
MB	2214	6/315	18	30
MB	2215	11/302	24	40
MB	2215	16/296	15	45
MB	2220	20/293	12	40
MB	2230	15/302	12	40
MB	2232	13/284	15	20
MB	2245	11/305	11	25
MB	2304	14/085	18	40
MB	2310	11/154	12	30
MB	2348	66/321	16	25

---

---

<sup>1</sup> Isaminger, M. A., "WEEKLY SITE SUMMARY," FL2 Radar Site, Denver, Colorado.

MASSACHUSETTS INSTITUTE OF TECHNOLOGY  
LINCOLN LABORATORY  
LEXINGTON, MASSACHUSETTS 02173-0073  
24 March 1989

43C-0992

Mr. Roland L. Bowles  
NASA Langley Research Center  
MS 156A  
Hampton, VA 23665

Dear Roland:

Ben Stevens and I want to thank you for the interesting visit we had with you and David Hinton on March 6th. Thanks especially to David for arranging the time on the simulator and setting up the cases. The experience of flying through events of varied location and strength was very helpful in providing insight into the microburst warning problem and motivated our subsequent discussion.

As promised, I am sending you the data on the July 11, 1988 microburst case concerning differential velocity and shear. The attached plot shows the velocity and shear values for the microburst alarm during the period 2205 MDT (first alarm) through 2220 MDT. These data were derived by examining the shear segments for each alarm to determine: 1) the segment with the largest differential velocity and 2) the segment with the largest shear. Recall that divergence (outflow) regions are made up of radial segments of generally increasing velocity which are associated together to form a two-dimensional region.

As you can see, the shear value (although somewhat underestimated by this calculation) peaks earlier than the differential velocity. Referring to Figure 6 in the paper by Elmore & Sand, it appears that the F factor is above the hazard level for the initial alarm at 2205.

Again, thanks for inviting us to Langley and we will look forward to seeing you at Lincoln. If you have any questions or comments on the data, please call me at 617/981-3386 or leave a message at 617/981-7430.

Sincerely yours,

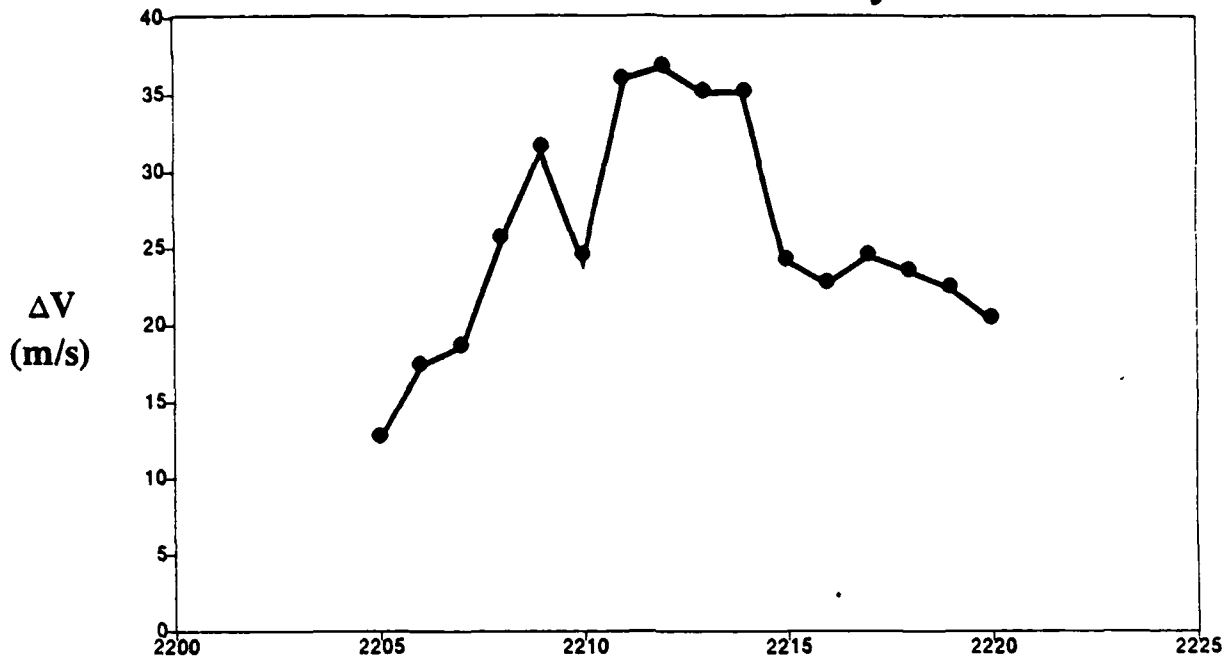
A handwritten signature in black ink that reads "Steven D. Campbell". The signature is written in a cursive style with a large, prominent "S" and "C".

Steven D. Campbell  
Staff Member, Group 43

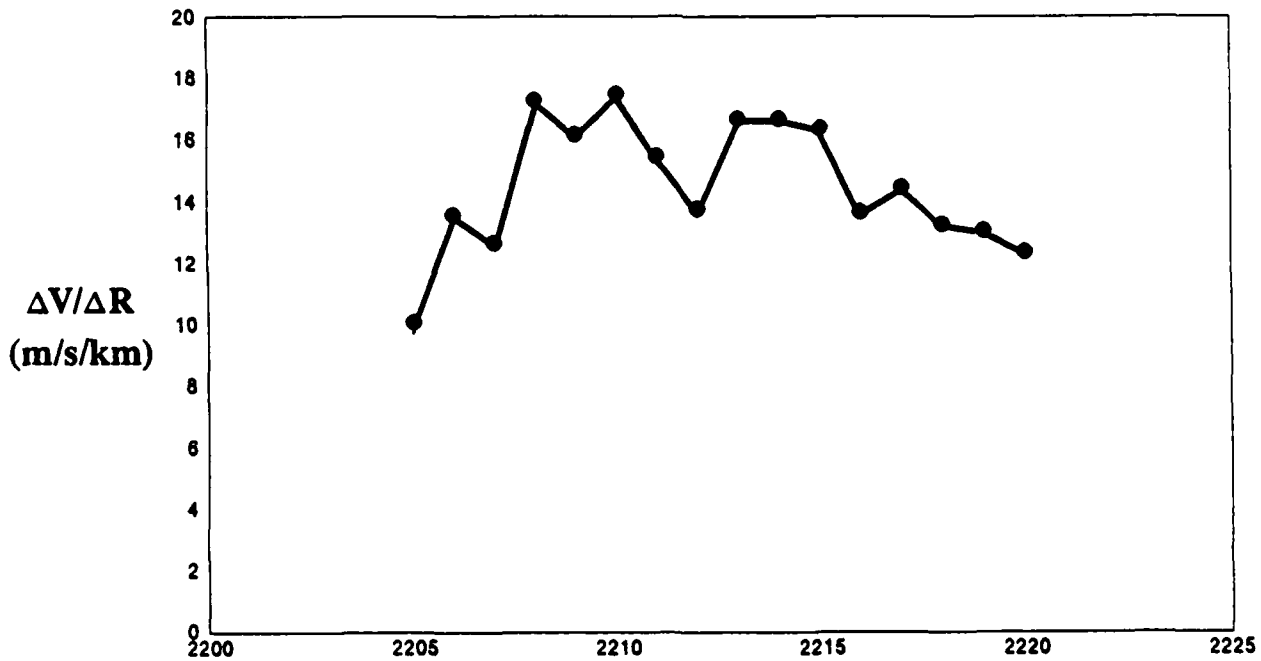
Attachments

# 11 July 88 Microburst

## Maximum Velocity



## Maximum Shear



# 11 July 88 Denver Microburst Alarm Strengths

Time (MDT)	Maximum Velocity Segment			Maximum Shear Segment			
	Velocity (m/s)	Distance (km)	Shear (m/s/km)	Velocity (m/s)	Distance (km)	Shear (m/s/km)	
2205	12.8	1.7	7.6	10.9	1.1	10.1	
2206	17.5	1.3	13.3	14.7	1.1	13.6	
2207	18.7	2.4	7.8	16.8	1.3	12.7	
2208	25.7	2.0	12.6	18.7	1.1	17.3	
2209	31.7	3.1	10.2	23.3	1.4	16.2	
2210	24.6	1.9	12.8	16.8	1.0	17.5	
2211	36.1	2.5	14.4	33.4	2.2	15.5	
2212	36.9	2.9	12.8	31.5	2.3	13.8	
2213	35.3	3.5	10.1	32.1	1.9	16.7	
2214	35.3	3.5	10.1	32.1	1.9	16.7	(coast)
2215	24.3	1.9	12.7	21.7	1.3	16.4	
2216	22.8	2.3	10.0	14.8	1.1	13.7	
2217	24.6	3.0	8.2	19.2	1.3	14.5	
2218	23.6	3.8	6.1	15.9	1.2	13.3	
2219	22.5	4.0	5.7	18.8	1.4	13.1	
2220	20.5	2.8	7.4	14.9	1.2	12.4	
2221	24.3	2.5	9.6	12.7	1.0	13.2	
2222	25.9	2.8	9.4	17.1	1.3	13.0	
2223	25.4	3.4	7.6	17.1	1.1	15.8	
2224	19.7	3.2	6.1	18.5	1.1	17.1	
2225	18.7	2.3	8.2	16.1	1.0	16.8	
2226	18.4	1.7	11.0	16.1	1.1	14.9	
2227	19.2	1.7	11.4	11.6	1.0	12.0	
2228	18.4	2.2	8.5	14.2	1.2	11.8	
2229	15.9	2.3	7.0	12.2	1.2	10.2	



Windshear Case Study: Denver, Colorado, July 11, 1988  
**SUBSTANTIATING DATA -- Appendices**

## **APPENDIX 5 -- NCAR Report**

Elmore, K.L., Politovich, M.K., Sand, W.R., "The 11 July 1988 Microburst at Stapleton International Airport, Denver, Colorado," National Center for Atmospheric Research, November 1989.

**The 11 July 1988 Microburst at  
Stapleton International Airport, Denver, Colorado**

**KIMBERLY L. ELMORE, M. K. POLITOVICH, W. R. SAND  
National Center for Atmospheric Research\*  
P. O. Box 3000  
Boulder, Colorado 80307**

November 1989

---

\* *NCAR is sponsored by the National Science Foundation*

# **The 11 July 1988 Microburst at Stapleton International Airport, Denver, Colorado**

**K. L. Elmore, M. K. Politovich, and W. R. Sand  
National Center for Atmospheric Research<sup>1</sup>  
P. O. Box 3000  
Boulder, Colorado 80307**

## **I. Introduction**

Just after 4:00 PM local time on 11 July 1988, an intense microburst developed near Stapleton International Airport in Denver, Colorado. During this time, the Terminal Doppler Weather Radar (TDWR) Operational Test and Evaluation (OT&E), sponsored by the Federal Aviation Administration (FAA), was in progress. The TDWR microburst detection algorithm provided an accurate and timely warning of the microburst to the Air Traffic Control Tower (ATCT). However, four aircraft penetrated the microburst; they fortunately traversed the microburst without serious incident.

A microburst is a strong, localized outflow from a precipitating convective cloud. Microbursts present a hazard to aviation due to abrupt changes in wind direction and strong downdrafts contained within them. The operational microburst definition during the TDWR OT&E was a 20-kt wind speed loss over 4 km or less; wind speed losses are assumed to be manifested as airspeed losses. The largest such loss observed by Doppler radar is 68 kt, which occurred during the 11 July microburst. The Doppler radar microburst algorithm running on 11 July indicated an 85-kt loss. Refinements were made to this algorithm in early August 1988 to improve its performance. The refined Algorithm reduced the 85-kt loss estimate to 70 kt, matching the dual-Doppler estimate used for ground truth.

This technical report provides a compilation of available meteorological data and some meteorological interpretations of the intense microbursts that occurred on 11 July 1988 near Stapleton Airport. These discussions include data from National Weather Service (NWS) surface and upper air measurements, Cross-chain Loran Atmospheric Sounding System (CLASS, Lauritson et al., 1987), FAA-Lincoln Laboratory Operational Weather Studies (FLOWS) mesonet (Wolfson et al., 1987), Low-Level Windshear Alert System (LLWAS) (Wilson and Flueck, 1986), and data from the FL2 10-cm and UND 5-cm radars. The 11 July weather events are presented in a descriptive narrative emphasizing the microburst occurrence. Data and data sources are given and described. Using dual-Doppler three-dimensional analyses, the microburst source region and the outflow evolution through its demise as a hazard are discussed.

---

<sup>1</sup> *NCAR is sponsored by the National Science Foundation*

Other agencies, groups, and authors providing technical reports on the 11 July microburst include: Lincoln Laboratory, TDWR algorithm; National Aviation and Space Administration (NASA), analysis of flight recorder data; MESO, Inc., numerical simulation of the event; the Federal Aviation Administration (FAA), flight recorder data analysis; and United Airlines, flight recorder data and pilot response. The information sources helped clarify the role of some of the physical mechanisms discussed in this report; in other instances, these served as a starting point for discussions presented here.

## II. Available Data

### A. Radar

FL2, a 10-cm wavelength Doppler radar operated by the Massachusetts Institute of Technology Lincoln Laboratory, was used as the test-bed instrument. Doppler radar measures only radial wind components. Using wind measurements from the low-altitude scans ( $0.3^\circ$ ,  $0.4^\circ$ , and  $0.5^\circ$  elevation), the microburst algorithm flags segments along each beam that meet microburst criteria. An NCAR-developed technique defines an all-encompassing best fit ellipse that surrounds adjacent segments and records the maximum wind speed change within the ellipse. This information is sent to the ATCT and displayed in both graphic and alphanumeric form (see Appendices A and B). The University of North Dakota (UND) 5-cm Doppler radar, located about 21 km north of FL2, gathered data during the project. Scanning patterns of the two radars were coordinated to enable dual-Doppler post-analysis (see Fig. 1).

During the TDWR OT&E, dual-Doppler radar volume scans were completed approximately every 2.5 min and included elevation angles from  $0.3^\circ$  through  $25.9^\circ$  (UND) or  $39.9^\circ$  (FL2). The CEDRIC analysis package (Mohr et al., 1986) is used for three-dimensional wind field synthesis and analysis. Two separate analyses are presented: a "high" and a "low" resolution analysis. The low-resolution analysis encompasses the greatest area and is intended to provide an overall depiction of storm morphology. It includes 14 volumes beginning around 2148 and ending at 2220<sup>2</sup>. The high-resolution analysis is useful for studying the microburst structure and for comparison between radar data and aircraft or mesonet data. There are 9 high resolution analyses, beginning at 2200 and going to 2220. All analyses are temporally spaced approximately 2.5 min apart. Raw input Doppler velocities have been corrected for a deduced storm motion of  $10 \text{ m s}^{-1}$  from  $270^\circ$ . The resulting analyses show ground-relative winds.

The low-resolution, three-dimensional analysis has 400 m horizontal grid spacing and 500 m vertical grid spacing. The lowest effective elevation angle is  $0.3^\circ$  from FL2, placing the beam center approximately 190 m above the center of the airport. Each pulse volume is a truncated cone  $1^\circ$  in width and 120 m in radial length for FL2 and 250 m for UND. Over the airport, both beams are roughly 150 m in diameter. UND scanning was synchronized with FL2 to enable three-dimensional, dual-Doppler wind analysis. For the high resolution

---

<sup>2</sup> All times are UTC unless otherwise noted.

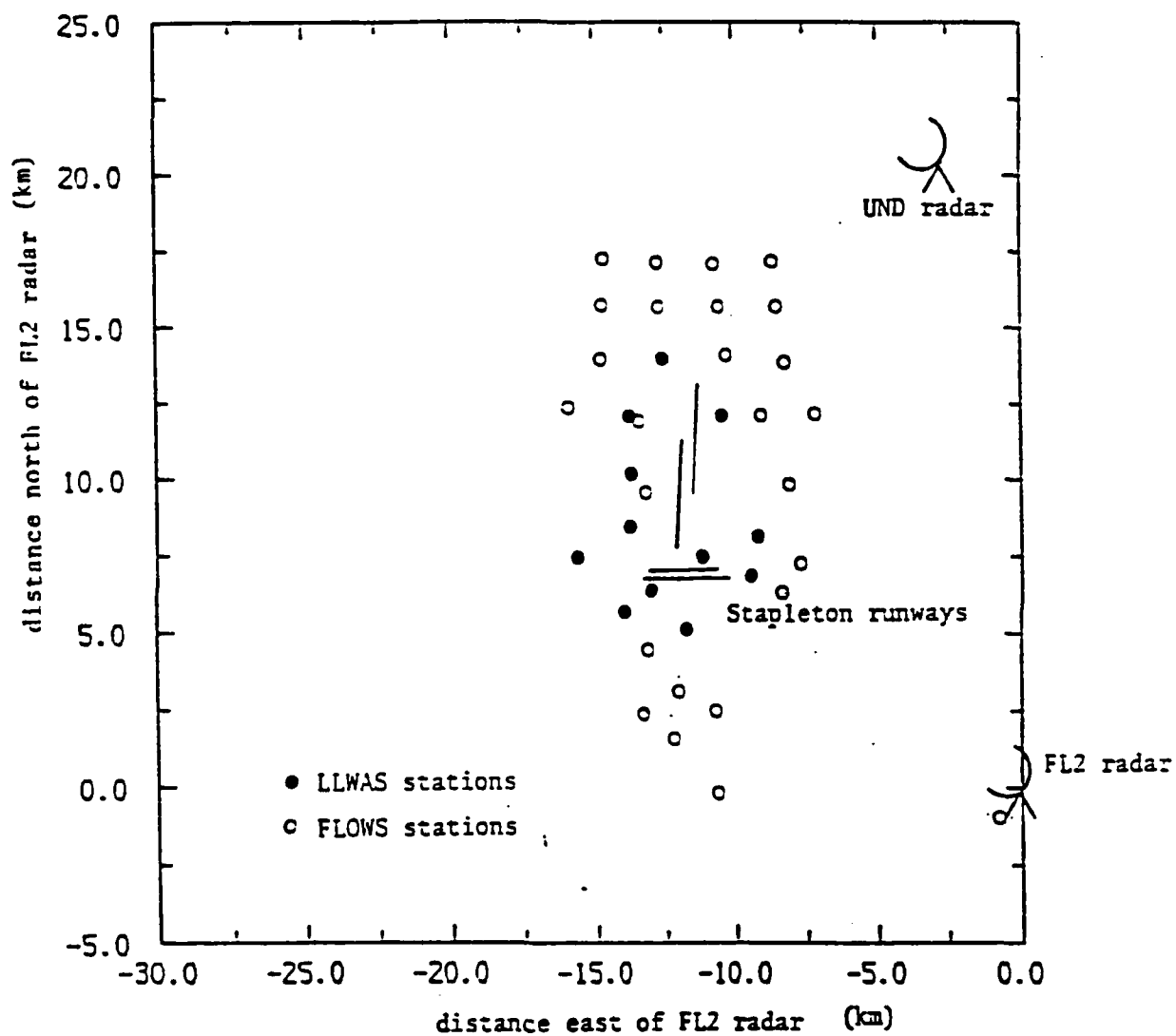


FIGURE 1. Locations of radars and surface mesonet stations during the 1988 TDWR OT&E at Stapleton International Airport, Denver, Colorado. The airport runways are also shown.

analyses, all parameters are identical except the horizontal grid spacing, which is reduced to 250 m.

Both analyses use a one-pass Cressman objective analysis scheme (Cressman, 1959) to map radar-measured radial velocity components from spherical range-azimuth-elevation space to gridded Cartesian space. In both cases, the Cressman influence radius is 1.3 times the grid spacing, which should yield a good ratio between the variance induced by the Cressman analysis and the pre-existing variance in the data (Stephens and Stitt, 1970; Stephens and Polan, 1971). Thus, the influence radius for the low-resolution analysis is 520 m horizontally and 650 m vertically. For the high-resolution analysis, the horizontal influence radius is 325 m.

The grid domain extends from 1.8 km (0.19 km AGL) to 10.8 km (9.19 km AGL) in both cases. The horizontal domain of the low-resolution analysis extends 2–30 km west and 1–23 km north of FL2. The high resolution analysis extends 2–16 km west and 1–13 km north of FL2 and is roughly one quarter of the area covered by the low resolution analysis. Stapleton Airport lies approximately 10–14 km west and 6–13 km north of FL2; the microburst impact area is on southeast edge of Stapleton Airport and well-centered in both analysis domains.

Before a consistent  $w$  component is calculated from the horizontal winds,  $u$  and  $v$  are filtered with a two-dimensional, three-point Shuman smoother (Shuman, 1955). Five passes are made through the data, yielding a  $5 \Delta s$  (where  $s$  is the grid interval) horizontal spatial resolution at the half-amplitude points, as shown in Fig. 2. The Shuman filter response is given by:

$$R_H = [(1 - \sin^2(\pi/L))(1 + \sin^2(\pi/L))]^5,$$

where  $L$  is in units of  $\Delta s$ . The low-resolution analysis resolves motions on a 2-km scale ( $5 \times 400$  m) and the high-resolution analysis resolves motions on a 1.25-km scale ( $5 \times 250$  m). Filtering is chosen to reasonably match the Cressman weighting function.

Another technique, developed by W. Wilson and K. Brislawn, uses a direct least-squares method to simultaneously map radar velocities from spherical to Cartesian space and provide  $u$  and  $v$  components; it has not yet been extended to provide full three-dimensional wind fields. This technique is used for low-altitude (190 m above ground level or AGL) analyses spaced approximately 1 min apart (Appendix D).

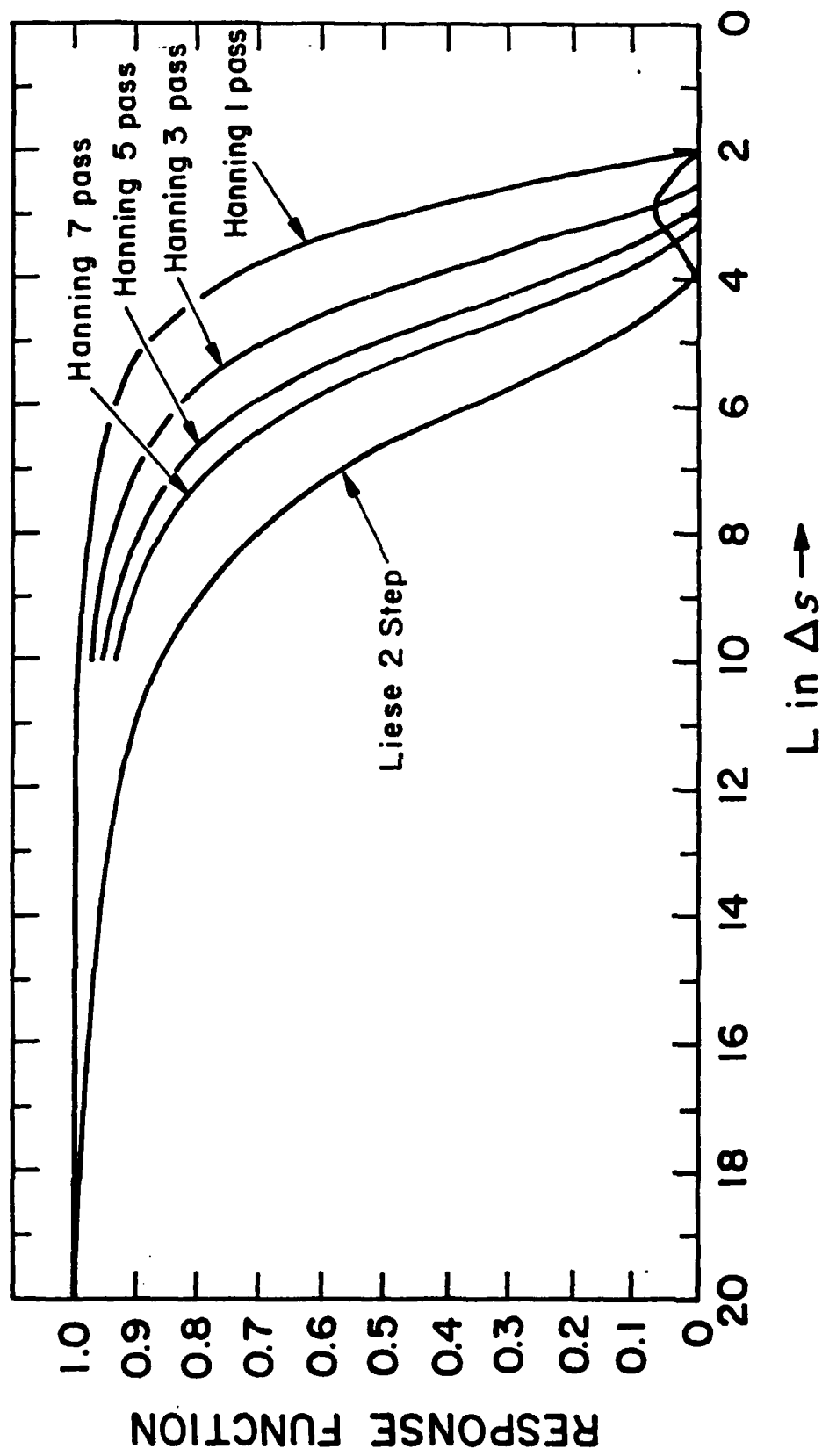


FIGURE 2. Response functions for Hanning 5 pass and Liese 2 step filters used in dual-Doppler analyses techniques. The filtering function is plotted against the length scaled as number of data grid points.

### B. F-Factor

F-factor is used as the basis for the airborne windshear detection and escape systems. F-factor calculations presented here are based upon dual-Doppler radar data and are included for comparison with F-factor derived from flight data recorders

F-factor is a nondimensional parameter derived from the horizontal and vertical winds and quantifies the effect of wind shear on aircraft performance. F is a function of aircraft total energy (kinetic plus potential) and the available total energy rate of change. Performance-decreasing F-factors are positive and performance-increasing F-factors are negative. Typically, hazardous F values are those above 0.08.

Here, F-factor is approximated by:

$$F = \frac{\frac{\partial \bar{u}}{\partial x} \times \text{TAS}}{g} - \frac{\bar{w}}{\text{TAS}},$$

where  $\partial \bar{u} / \partial x$  is the spatial derivative of  $u$  with respect to  $x$ ,  $g$  is the acceleration due to gravity,  $\bar{w}$  is the vertical wind provided by the dual-Doppler analyses, and TAS is the true airspeed of the aircraft (adapted from Bowles and Targ, 1988). F-factor is computed along east-to-west tracks using  $75 \text{ m s}^{-1}$  as the penetration airspeed (see Elmore and Sand, 1989, for a description of the calculation of F-factor from radar data). Because aircraft were approaching from the east, F-factor along tracks that extend from the runways should be representative of wind shear encountered by the approaching aircraft.

Appendix I includes diagrams of F-factor calculated from dual-Doppler analyses. These show the size, extent and intensity of expected hazard areas as well as their relation to horizontal and vertical winds. Note that F-factor generally is not dominated by the vertical or horizontal components at the level shown (190 m AGL); each component provides an approximately equal contribution to the total value.

### C. Surface Mesonet

The LLWAS and FLOWS mesonets together provide 42 stations over a  $12 \times 20 \text{ km}$  area around the airport. The LLWAS sends data to a central processing and display site every 6 sec; FLOWS data are available once per minute. The LLWAS alarm messages generated off line during the microburst are included in Appendix C (these were *not* routinely sent to the ATCT during the TDWR OT&E).

Divergence "alarms" were created during post-analysis from the combined LLWAS and FLOWS sensor network, as described by Cornman and Wilson (1989). Divergence calculations are made for 734 triangles and 336 edges defined within the networks. When divergence within a triangle or edge element exceeds a predetermined threshold, it is flagged and the probable wind shear (dots) or microburst (crosses) locations noted (see Appendix F). Appendices C and F demonstrate the ability of the surface network to sense this event.

"Robot", a software package developed by the NCAR Field Observing Facility (Corbet and Burghart, 1988) is also used to analyze the FLOWS mesonet data. This program reads



Common Mesonet Format (CMF) data and produces a number of outputs. Some of these are contained in Appendix F.

To compare LLWAS winds to radar winds, LLWAS winds are projected onto radials from each radar. These projected winds are plotted against their nearest radar gate Doppler velocities in Appendix G.

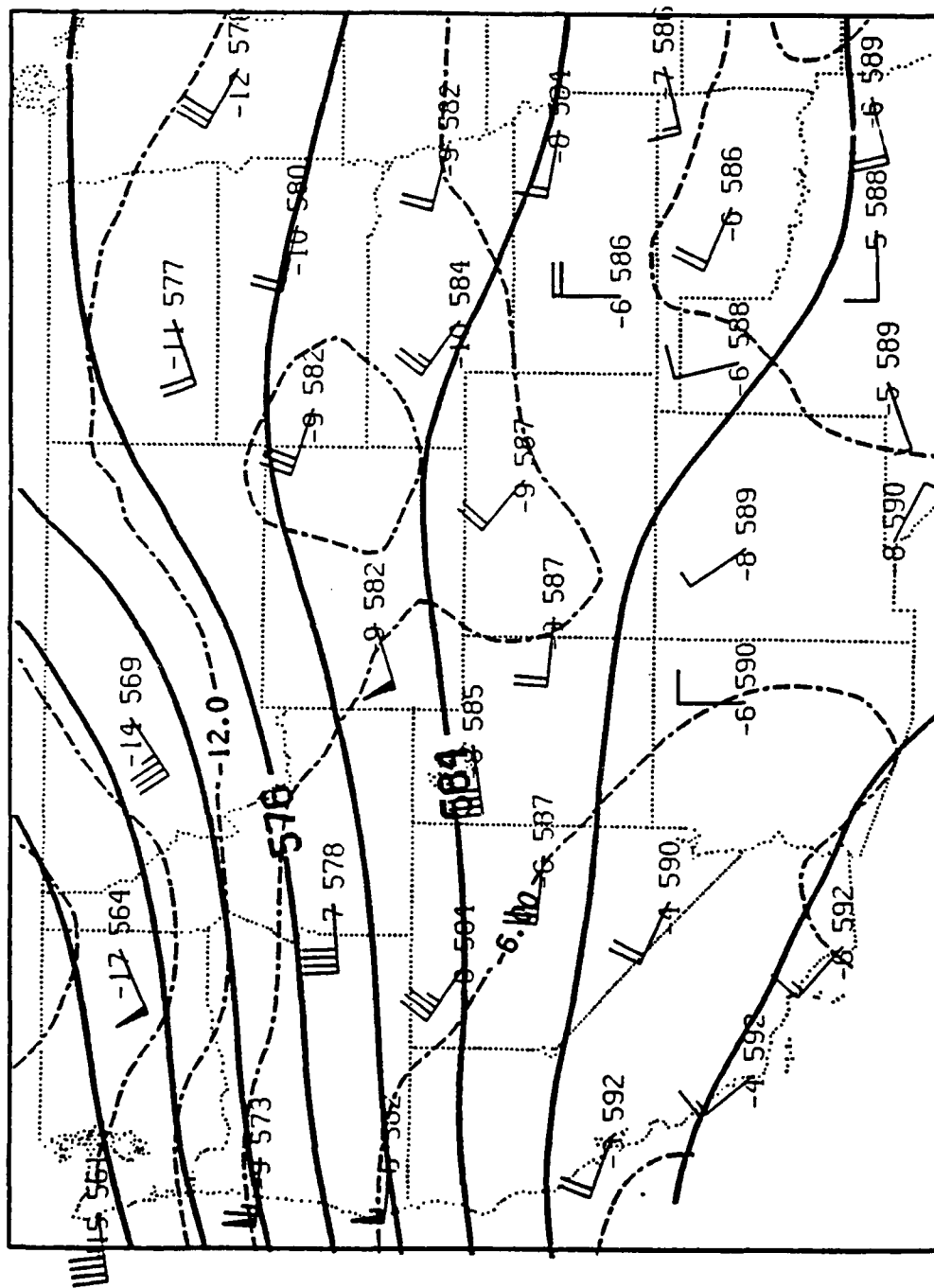
### III. Meteorological Conditions

#### A. Synoptic Setting

The major synoptic scale weather feature is a slowly-eastward-moving shallow trough over the western United States. Figures 3 and 4 show conditions at 50 kPa, 70 kPa, and 85 kPa at 12 Z and 00 Z on 11 and 12 July, respectively. At low levels (85 kPa), warm air is contained in the base of the trough. This feature is barely discernable at 70 kPa and vanishes above that level. Winds never exceed  $10 \text{ m s}^{-1}$  at any level over Colorado, Wyoming or Utah and are generally westerly.

This westerly flow advects warm, moist air over the project area throughout the day. Figure 5 shows data from the National Oceanographic and Atmospheric Administration (NOAA) thermodynamic profiler located at Stapleton Airport. Using microwave radiometry, this instrument provides vertical temperature and moisture information; equivalent potential temperature ( $\theta_e$ ) and mixing ratio contours plotted against height are also shown. Throughout the day, moisture increase in a deep layer extending from the surface to over 12 km MSL (10.4 km AGL) and reaches a maximum at 2200-2230. The maximum total precipitable water vapor content for the day is 1.05 cm.

Automatic Terminal Information Service (ATIS) weather messages are included in the ATCT voice tapes. Three messages were issued during the time of interest. ATIS-X, issued at 2145, noted a temperature-dewpoint difference of  $50^\circ\text{F}$ . Large temperature-dewpoint spreads indicate the potential for microburst activity. This difference decreased to  $40^\circ\text{F}$  for the ATIS-Y and ATIS-A messages that were broadcast at 2200 and 2203; which aircraft monitored which broadcast is unknown. A complete description of aircraft operations is included in a report by Ireland (1989).



500 mb  
1200 UTC 12-JUL-1988

FIGURE 3A-C. NWS upper level data plotted for 1200 UTC, 11 July 1988. a) 500 mb, b) 700 mb and c) 850 mb. Solid lines are constant geopotential height; dashed lines are constant temperature.

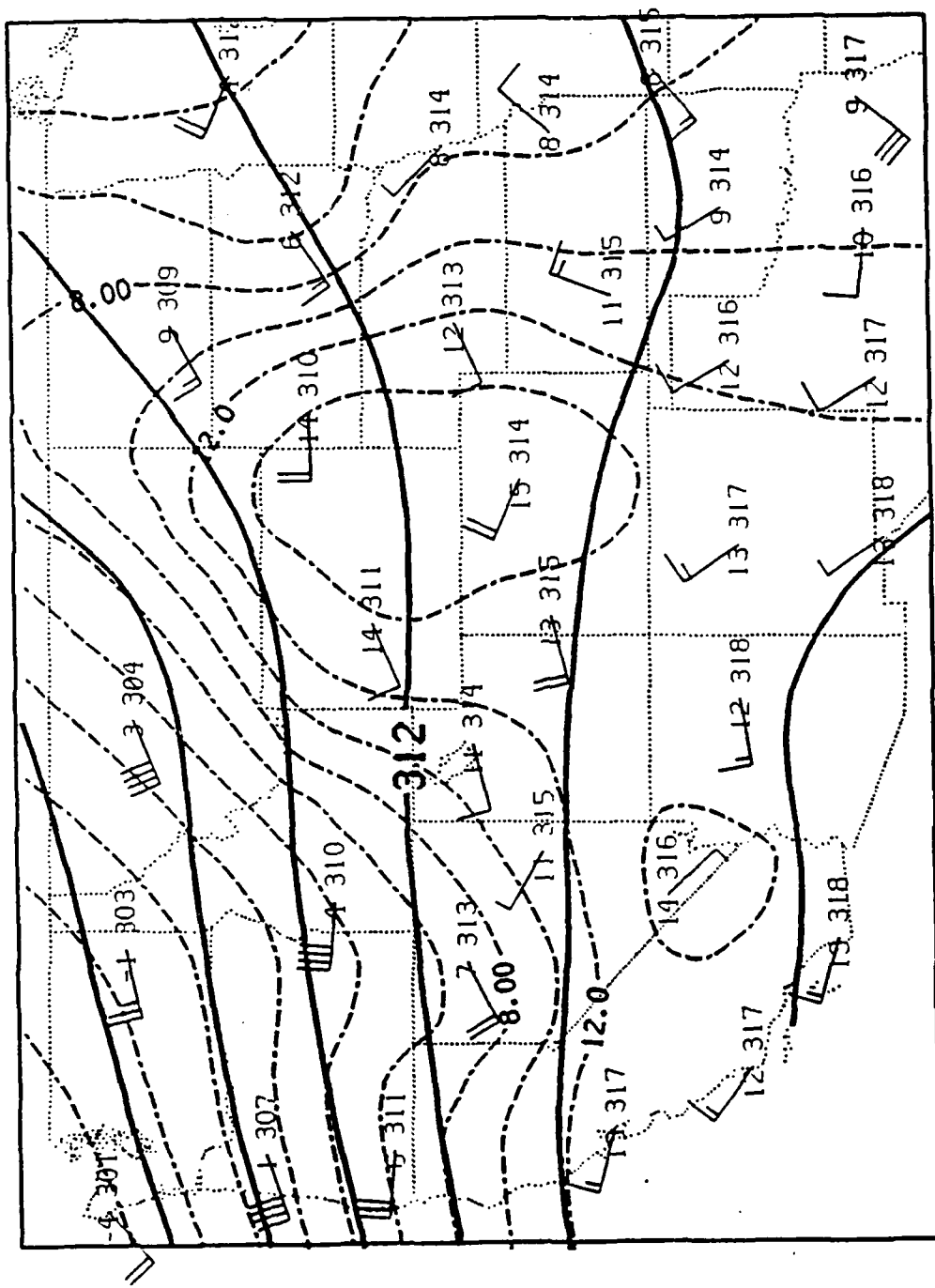
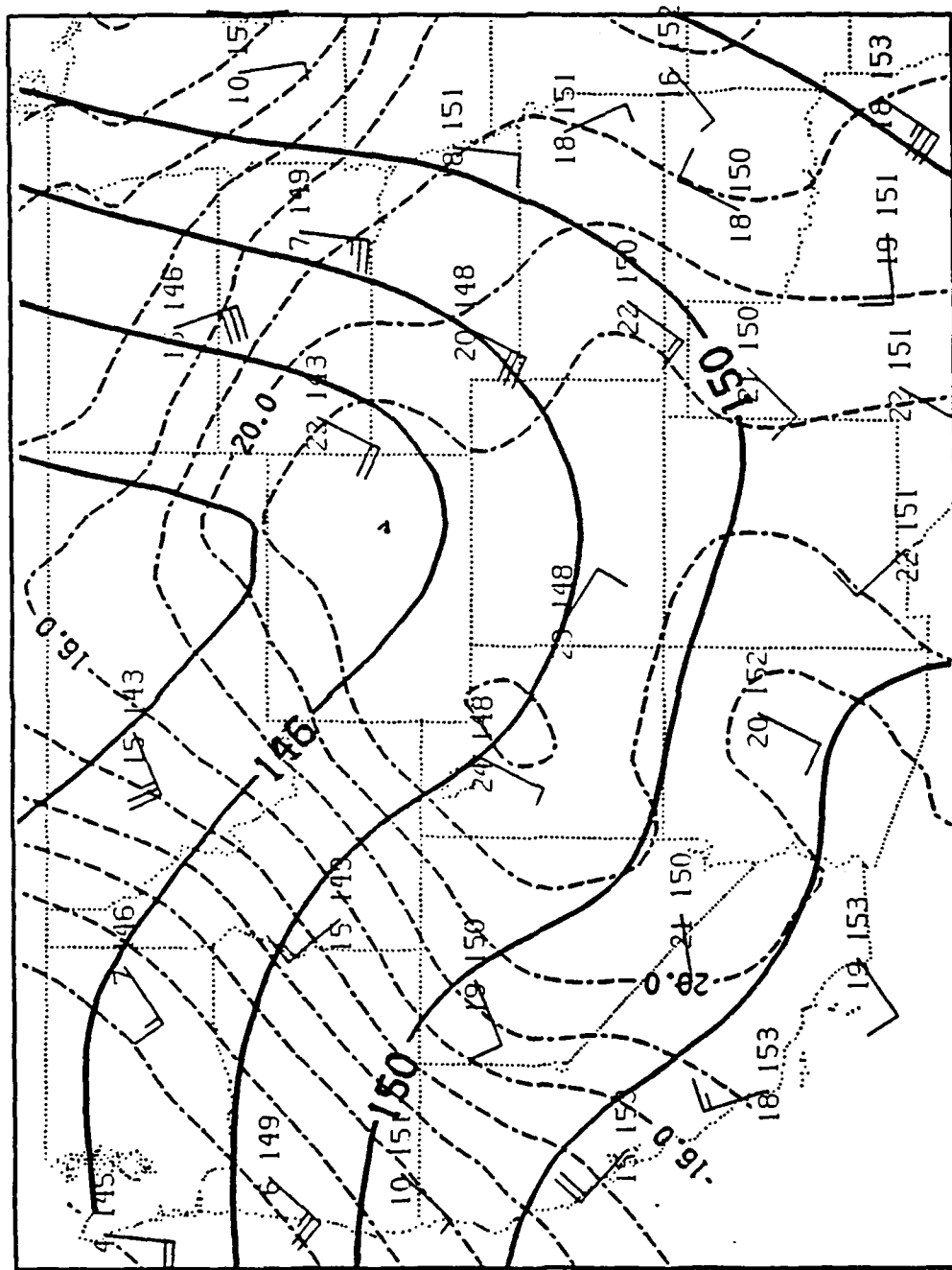


Fig. 3b



850 mb  
1200 UTC 12-JUL-1988

Fig. 3a

Borislava Stankov 12-JUL-1988 13:39:36.40

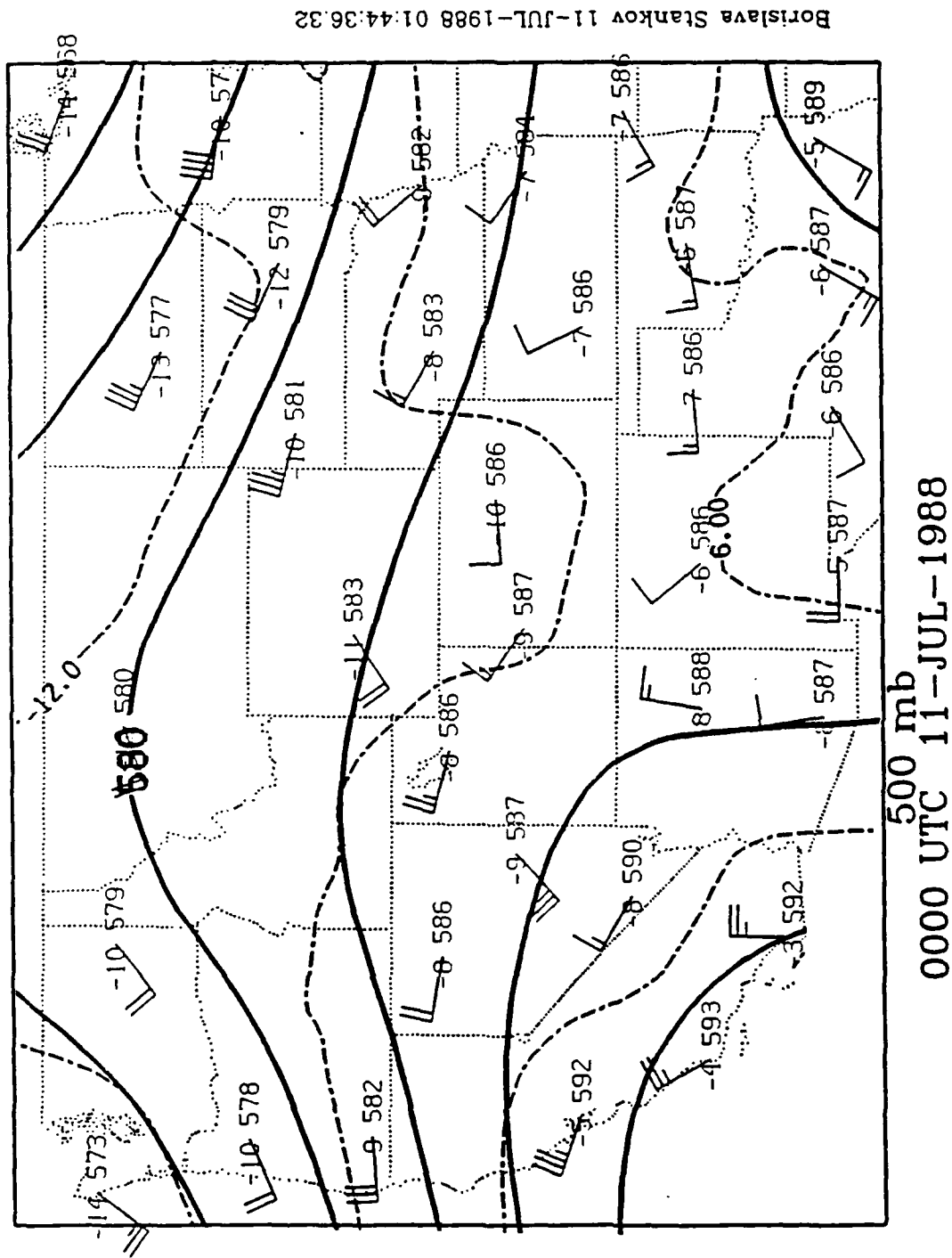


FIGURE 4A-C. As in Fig. 3 but for 0000 UTC, 12 July 1988.

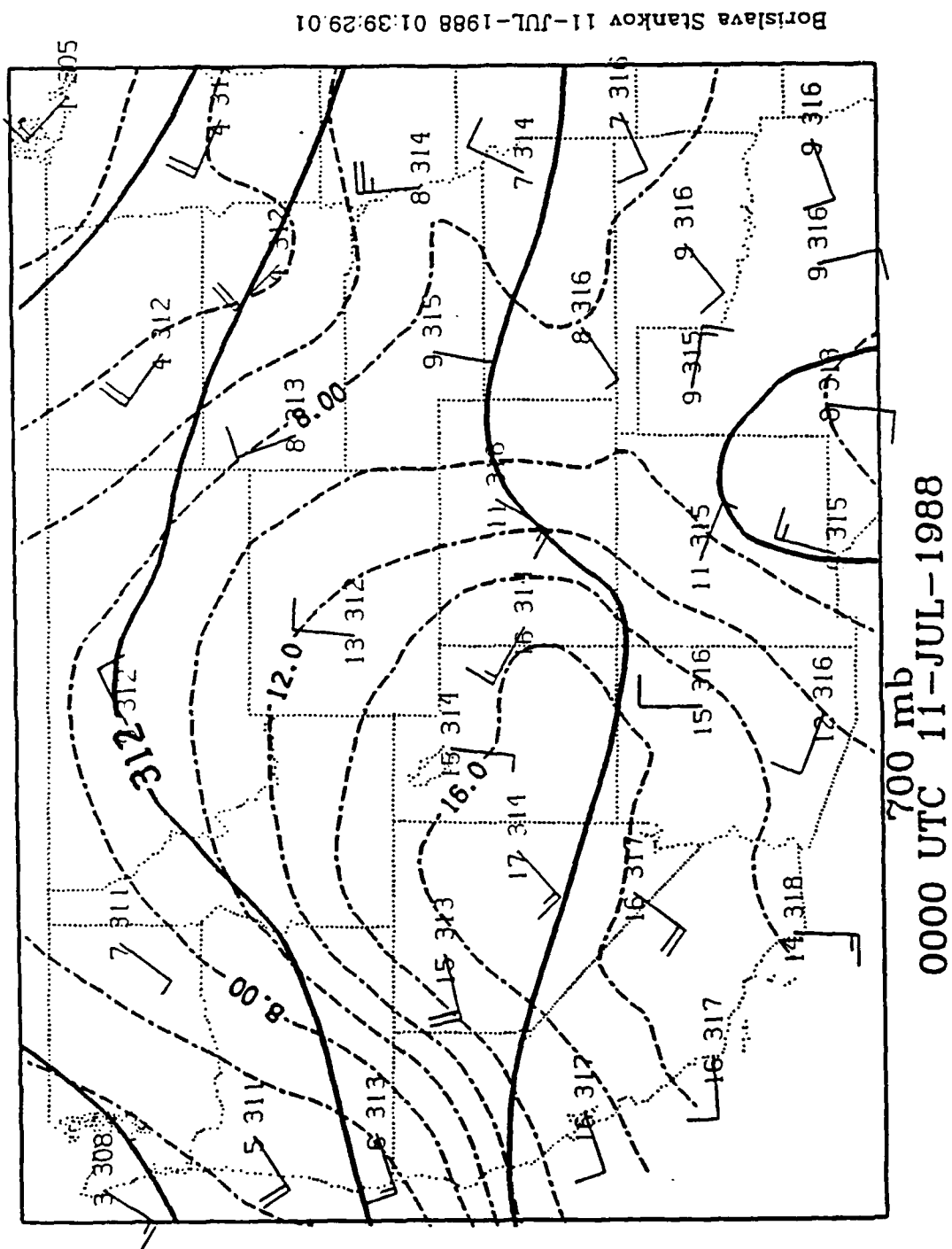
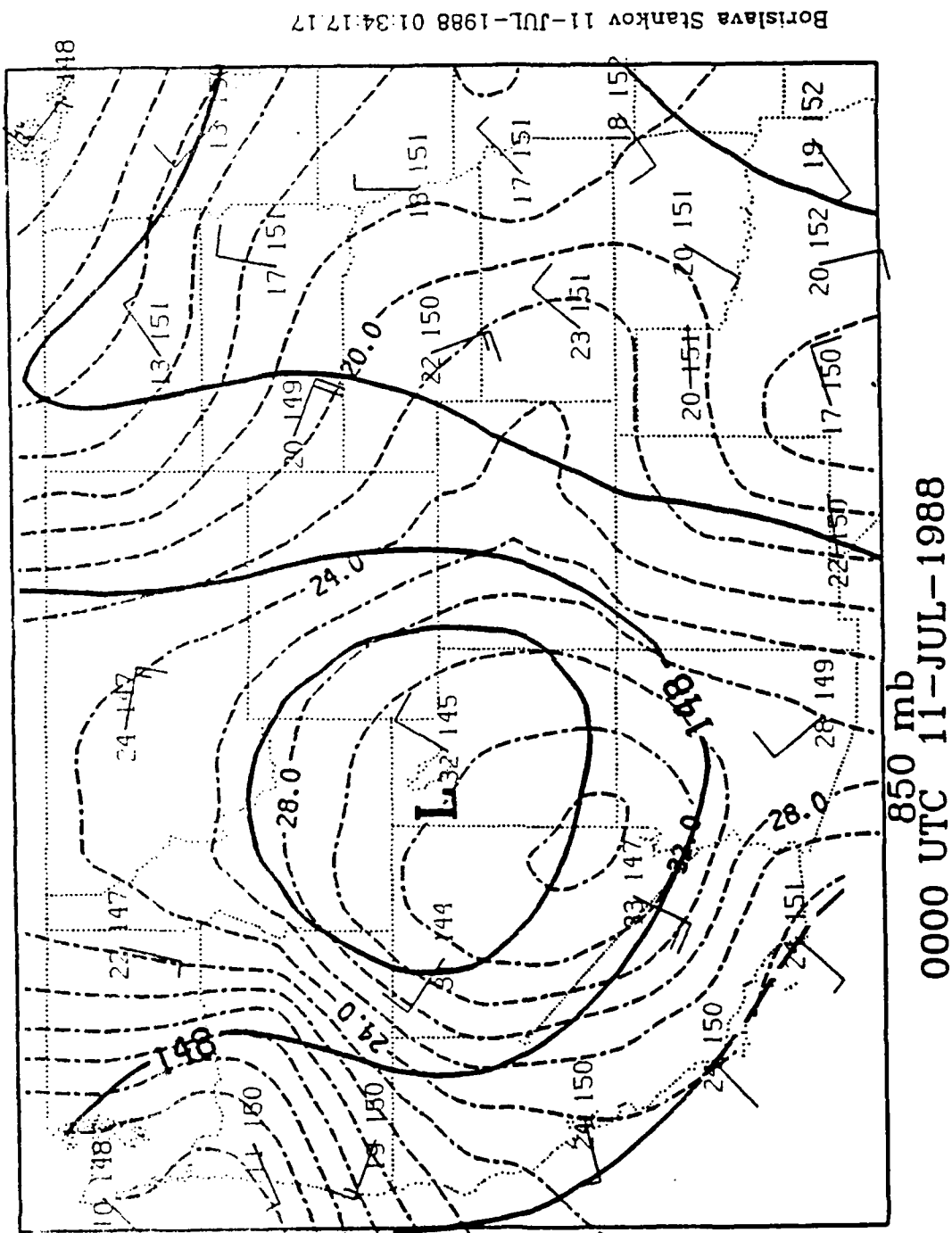


Fig. 4b



### *B. Local Sounding Analysis*

A CLASS sounding site was located at the Weather Service Forecast Office, just east of Stapleton International Airport. Two soundings were obtained prior to the microburst: at 1700 and 2004. The 1700 sounding (Fig. 6) shows a nearly dry adiabatic lapse rate from 3.4 km MSL, (1.8 km AGL, 68 kPa) to 6.0 km MSL (4.4 km AGL, 49 kPa). A moist layer (relative humidity greater than 50% ) exists between 5.4 and 6.1 km MSL (3.8 and 5.5 km AGL, 52.5 kPa to 48.5 kPa). There is marginal moist convective instability in this sounding, with a Lifted Index (LI) of -2. The equilibrium level is near 8 km (6.4 km AGL, 39 kPa). Equivalent potential temperature ( $\theta_e$ ) for both soundings is shown in Fig. 7; each trace is labelled accordingly. Above the moist layer, the atmosphere is quite dry and  $\theta_e$  decreases.

Wind structure at 1700 is also shown in Fig. 6 plotted along the right-hand side of the sounding. There are two regions of significant winds: one centered near 3.3 km MSL (1.7 km AGL, 70 kPa), with  $10 \text{ m s}^{-1}$  winds from  $295^\circ$ , and a layer of northwesterly  $10 - 15 \text{ m s}^{-1}$  winds above 6.9 km MSL (5.3 km AGL, 43.6 kPa).

Considerable changes occur by 2004, as shown in Fig. 7. Below about 7.25 km MSL (5.65 km AGL, 41.6 kPa), the entire sounding has moistened. The temperature lapse rate is dry adiabatic from the surface to 4.8 km MSL (3.2 km AGL, 57.0 kPa). Stability for moist convection remains relatively unchanged, with an LI of -2. The convective equilibrium level is poorly defined in this sounding; a lifted parcel temperature matches the environmental temperature from about 7.2 km MSL (5.6 km AGL, 41.5 kPa) to nearly 9.5 km MSL (7.9 km AGL, 31.0 kPa).

Dewpoints have increased between 5.9 and 7.0 km MSL (4.3 and 5.4 km AGL, 50.0 to 43.1 kPa), which affects the  $\theta_e$  profile by increasing  $\theta_e$  throughout the sounding (Fig. 8). A sharp, absolute minimum  $\theta_e$  of 326 K is present at 7.2 km MSL (5.6 km AGL) and a relative minimum exists between 4.8 and 5.0 km MSL (3.2 and 3.4 km AGL). Thus, saturated parcels are potentially cold and will accelerate downward if they originate at either 7.2 km MSL (5.6 km AGL) or just below 5 km MSL (3.4 km AGL).

Winds in the boundary layer are less than  $5 \text{ m s}^{-1}$  and are southeasterly from 1.6 to 2.0 km MSL (surface to 400 m AGL), becoming westerly above. Above 5.4 km MSL (3.8 km AGL, 53.0 kPa), westerly winds abruptly increase to  $10-15 \text{ m s}^{-1}$ . Above 7.0 km MSL (5.4 km AGL, 42.7 kPa), winds have a significantly stronger northerly component.

Using a surface mixing ratio of  $6.2 \text{ g kg}^{-1}$  and  $31^\circ\text{C}$  temperature, the lifted condensation level (cloud base) is 4.8 km MSL (3.2 km AGL, 57.1 kPa), and the level of free convection is 4.9 km MSL (3.3 km AGL, 56.4 kPa). Rising parcels retain their buoyancy to 8.0 km MSL (6.4 km AGL, 37.6 kPa).



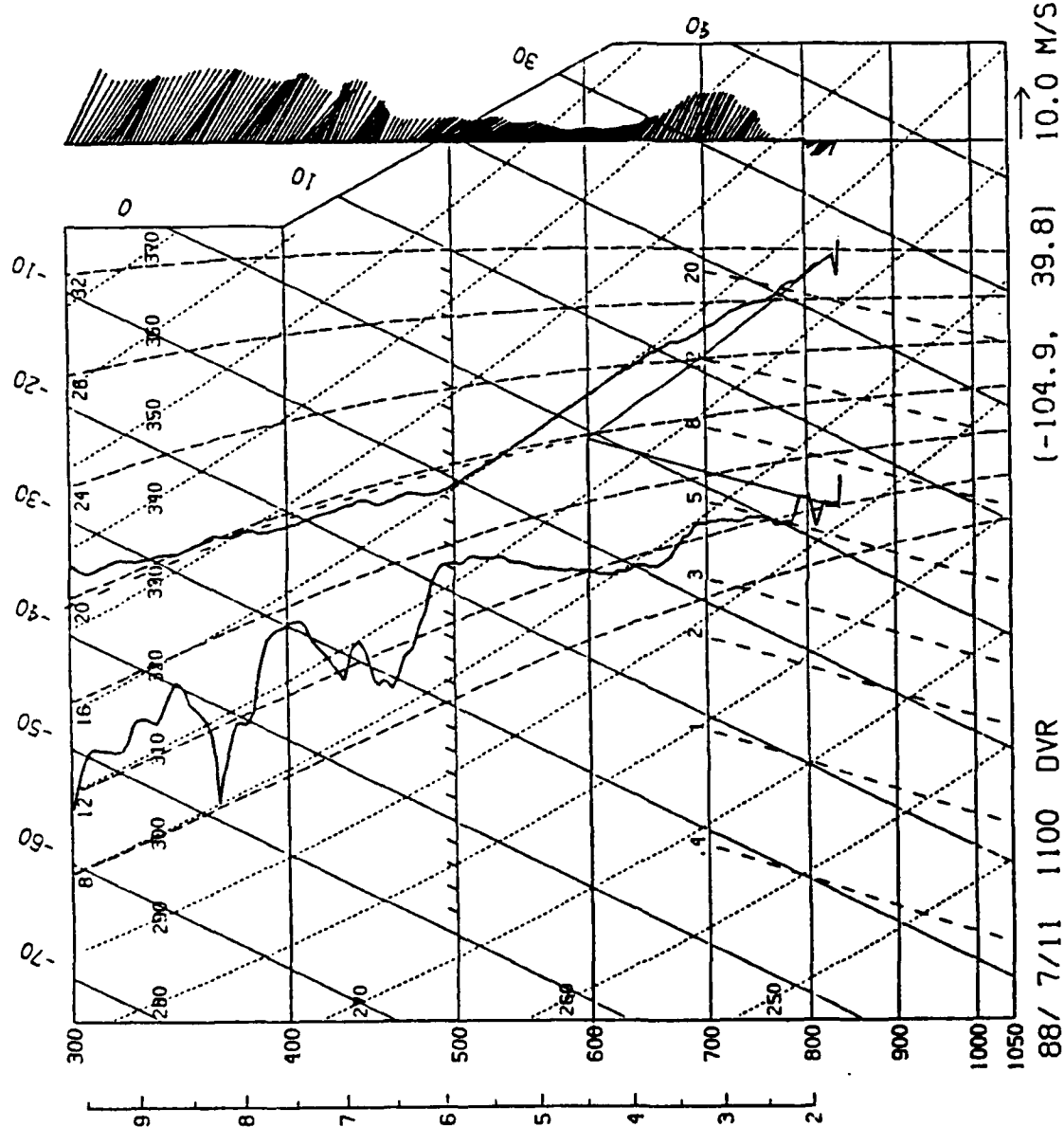


FIGURE 6. CLASS sounding from 1100 MDT (1700 UTC) 11 July 1988. Data are plotted on a skew-T diagram. Temperature and dewpoint are shown. Wind barbs on the right point in the direction the wind is blowing *toward*. Altitude in km MSL is shown on the right.

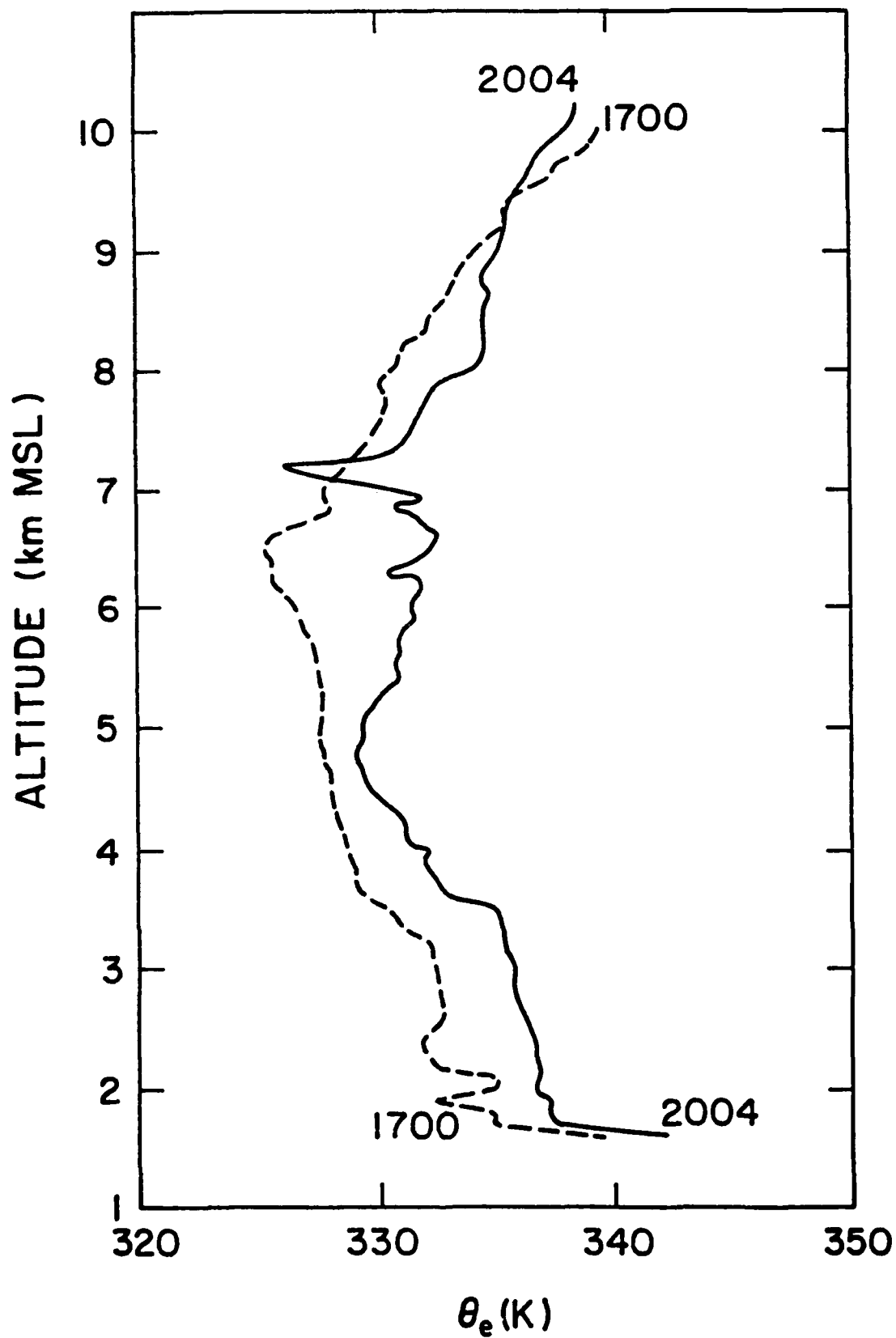
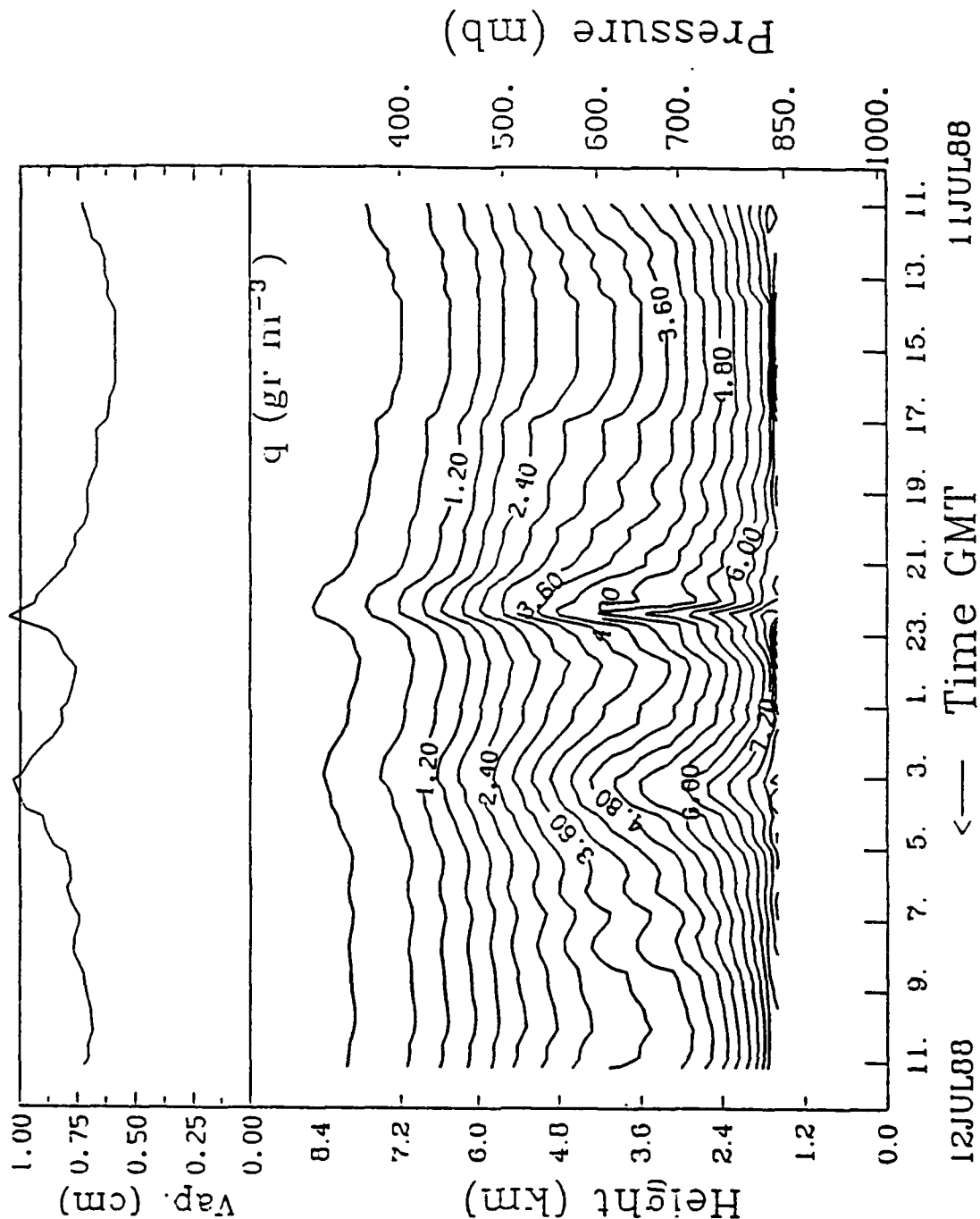


FIGURE 7. Equivalent potential temperature ( $\theta_e$ ) plotted against height from the 1700 and 2004 UTC CLASS soundings.



# STAPLETON (39.77N,104.88E),el.1611m



# STAPLETON (39.77N, 104.88E), el. 1611m

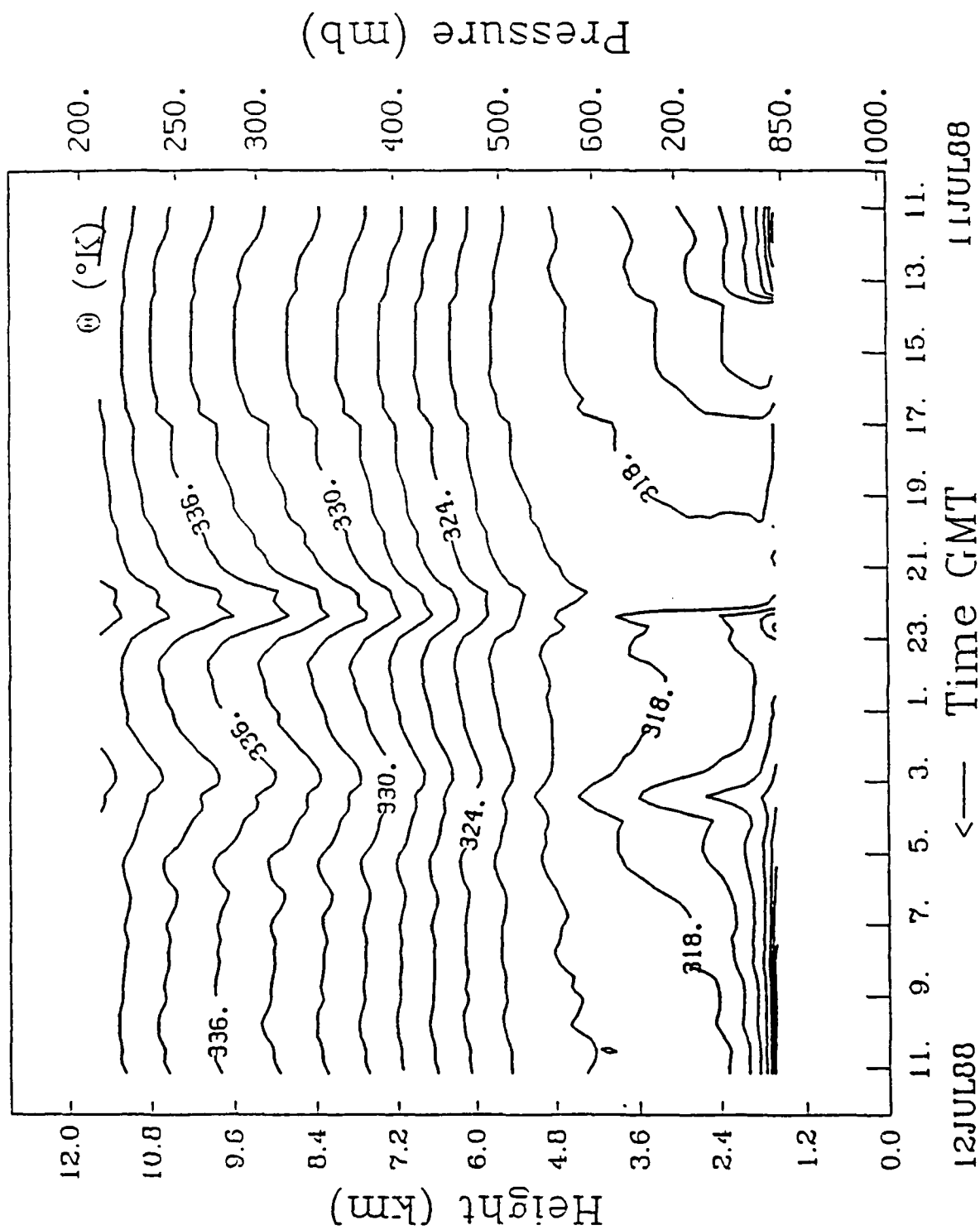


Fig. 5b

### *B. Local Sounding Analysis*

A CLASS sounding site was located at the Weather Service Forecast Office, just east of Stapleton International Airport. Two soundings were obtained prior to the microburst: at 1700 and 2004. The 1700 sounding (Fig. 6) shows a nearly dry adiabatic lapse rate from 3.4 km MSL, (1.8 km AGL, 68 kPa) to 6.0 km MSL (4.4 km AGL, 49 kPa). A moist layer (relative humidity greater than 50%) exists between 5.4 and 6.1 km MSL (3.8 and 5.5 km AGL, 52.5 kPa to 48.5 kPa). There is marginal moist convective instability in this sounding, with a Lifted Index (LI) of -2. The equilibrium level is near 8 km (6.4 km AGL, 39 kPa). Equivalent potential temperature ( $\theta_e$ ) for both soundings is shown in Fig. 7; each trace is labelled accordingly. Above the moist layer, the atmosphere is quite dry and  $\theta_e$  decreases.

Wind structure at 1700 is also shown in Fig. 6 plotted along the right-hand side of the sounding. There are two regions of significant winds: one centered near 3.3 km MSL (1.7 km AGL, 70 kPa), with 10 m s<sup>-1</sup> winds from 295°, and a layer of northwesterly 10 - 15 m s<sup>-1</sup> winds above 6.9 km MSL (5.3 km AGL, 43.6 kPa).

Considerable changes occur by 2004, as shown in Fig. 7. Below about 7.25 km MSL (5.65 km AGL, 41.6 kPa), the entire sounding has moistened. The temperature lapse rate is dry adiabatic from the surface to 4.8 km MSL (3.2 km AGL, 57.0 kPa). Stability for moist convection remains relatively unchanged, with an LI of -2. The convective equilibrium level is poorly defined in this sounding; a lifted parcel temperature matches the environmental temperature from about 7.2 km MSL (5.6 km AGL, 41.5 kPa) to nearly 9.5 km MSL (7.9 km AGL, 31.0 kPa).

Dewpoints have increased between 5.9 and 7.0 km MSL (4.3 and 5.4 km AGL, 50.0 to 43.1 kPa), which affects the  $\theta_e$  profile by increasing  $\theta_e$  throughout the sounding (Fig. 8). A sharp, absolute minimum  $\theta_e$  of 326 K is present at 7.2 km MSL (5.6 km AGL) and a relative minimum exists between 4.8 and 5.0 km MSL (3.2 and 3.4 km AGL). Thus, saturated parcels are potentially cold and will accelerate downward if they originate at either 7.2 km MSL (5.6 km AGL) or just below 5 km MSL (3.4 km AGL).

Winds in the boundary layer are less than 5 m s<sup>-1</sup> and are southeasterly from 1.6 to 2.0 km MSL (surface to 400 m AGL), becoming westerly above. Above 5.4 km MSL (3.8 km AGL, 53.0 kPa), westerly winds abruptly increase to 10-15 m s<sup>-1</sup>. Above 7.0 km MSL (5.4 km AGL, 42.7 kPa), winds have a significantly stronger northerly component.

Using a surface mixing ratio of 6.2 g kg<sup>-1</sup> and 31°C temperature, the lifted condensation level (cloud base) is 4.8 km MSL (3.2 km AGL, 57.1 kPa), and the level of free convection is 4.9 km MSL (3.3 km AGL, 56.4 kPa). Rising parcels retain their buoyancy to 8.0 km MSL (6.4 km AGL, 37.6 kPa).

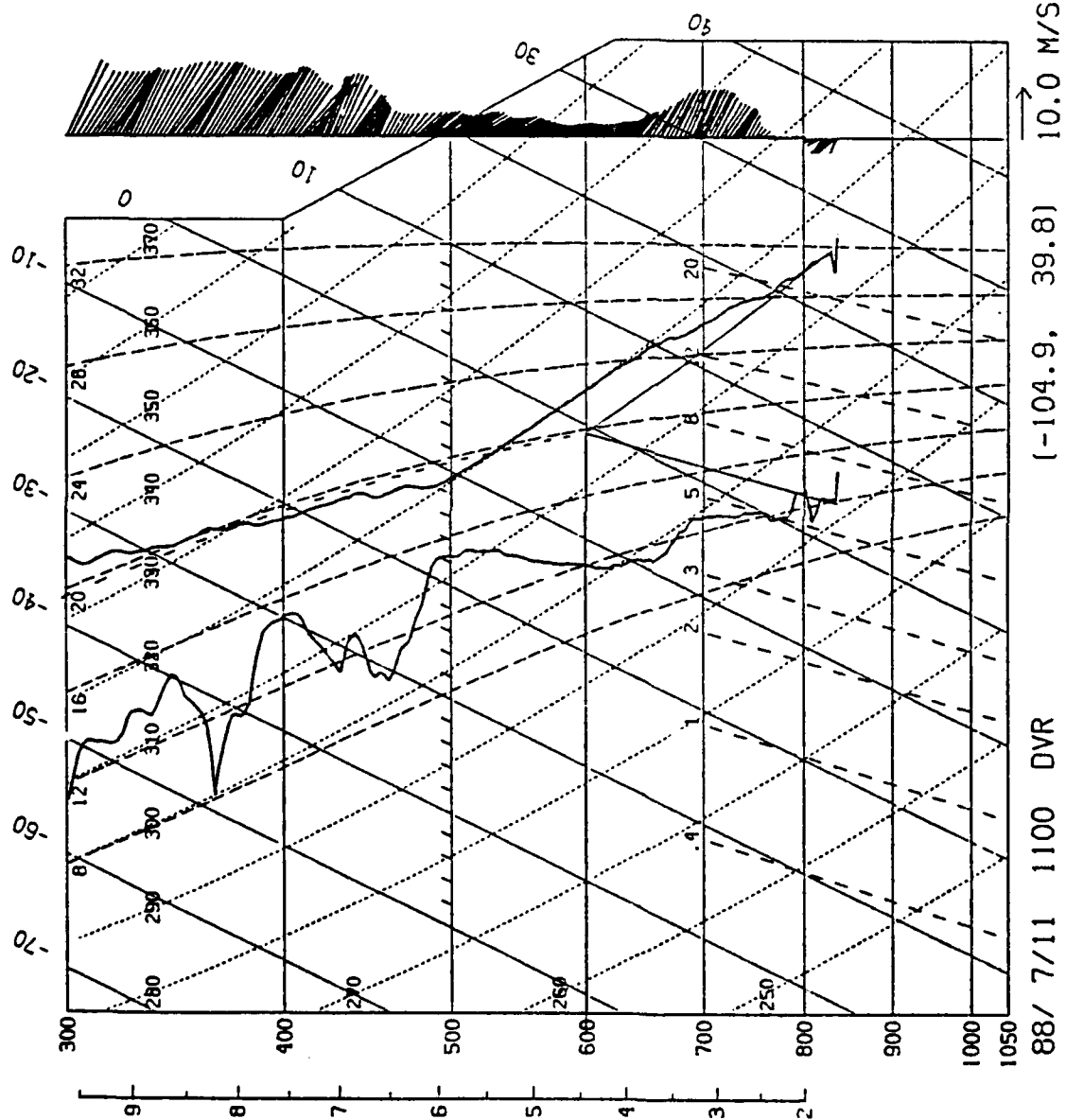


FIGURE 6. CLASS sounding from 1100 MDT (1700 UTC) 11 July 1988. Data are plotted on a skew-T diagram. Temperature and dewpoint are shown. Wind barbs on the right point in the direction the wind is blowing *toward*. Altitude in km MSL is shown on the right.

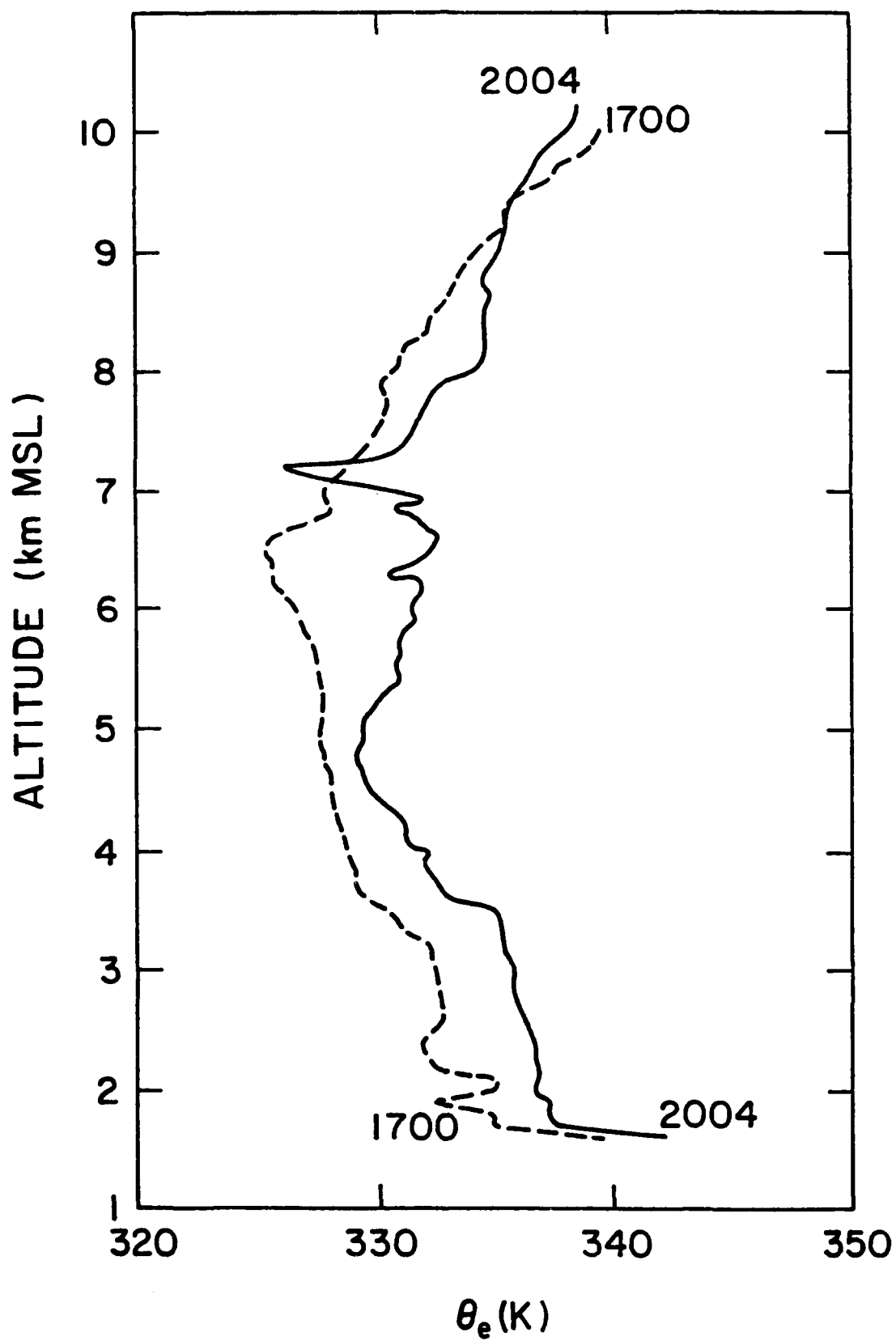


FIGURE 7. Equivalent potential temperature ( $\theta_e$ ) plotted against height from the 1700 and 2004 UTC CLASS soundings.



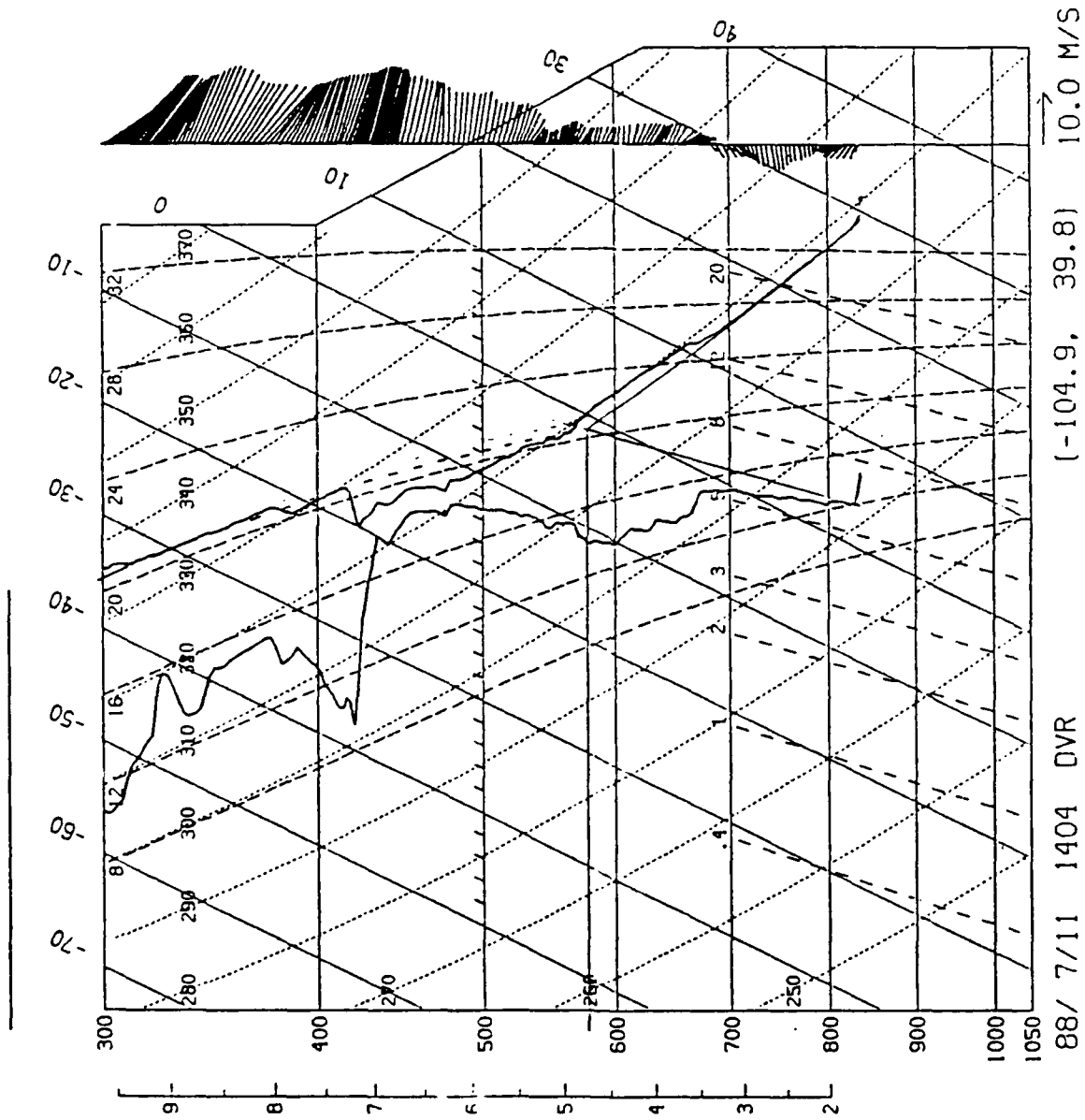


FIGURE 8. As in Fig. 6 but for 1404 MDT (2004 UTC) 11 July 1988.

## IV. Microburst Observations

### A. Overview

Figure 9 shows the expected headwind losses affecting arrivals to runway 26 (26A) derived from the TDWR algorithm operating on 11 July, the revised algorithm, the least-squares dual-Doppler post-analysis, and the LLWAS. Encounter times for the four aircraft that penetrated the microburst are noted.

Direct least-squares dual-Doppler analyses provide wind speed loss estimates above the  $10 \text{ m s}^{-1}$  (20 kt) warning threshold at 2204. These analyses will resolve a wind speed loss above threshold along a direction other than directly toward or away from FL2. The revised TDWR algorithm gives an initial warning at 2205, and the original TDWR first alarmed 1 min later at 2206. The ending alarm times also differ, as do the maximum calculated wind speed differences. The original TDWR maximum wind speed difference is 85 kt, compared to the revised TDWR value of 70 kt and the direct least-squares dual-Doppler value of 68 kt. The maximum LLWAS wind speed loss, measured at the surface rather than at 190 m aloft, is 45 kt. Reasons for the sudden increase in estimated wind speed loss near the end of the alarm period generated by the original TDWR algorithm are not known; the revised algorithm corrected this apparent error.

The first LLWAS microburst alarm occurred at 2210:42, nearly 5 min after the first TDWR alarm. There are two major reasons for this apparent discrepancy. First, the radar detected the microburst prior to its arrival at the surface. Second, the microburst was east of the 26A threshold and so not optimally located for LLWAS detection. In fact, one of the LLWAS sensors was near the center of the microburst, effectively removing it from the network; winds there are never very strong. The microburst remained east of the other LLWAS stations. Westward progress of the microburst outflow at the surface appears to have been somewhat impeded by the northwesterly outflow from the main part of the storm.

Least-squares dual-Doppler radar analyses (centered 190 m above the airport) are shown in Appendix D. Horizontal wind vectors are provided on a 0.5 km-resolution grid around the airport for 1-min intervals covering the microburst detection period. Analyses of  $\Delta V$  for the same time period are also shown. Contours indicate wind speed losses of at least  $10 \text{ m s}^{-1}$  over at most 4 km.

The first microburst begins at 2203 southeast of the airport. This event is not contained within in the airport alarm area. The TDWR algorithm detects it at 2204 (see the GSD displays in Appendix A). A larger, more intense microburst is first detected by the TDWR system at 2206. This event maintains a wind speed loss above microburst alarm levels ( $10 \text{ m s}^{-1}$  or 20 kt) until 2248. In post-analysis, the revised algorithm changed the ending alarm time to 2231. Operated off line, LLWAS did not issue a microburst warning until 2210:42. The microburst develops rapidly, reaching a maximum strength (in terms of wind speed difference across the feature) at 2213. Later, it expands in size and is joined by several other microburst cores that extend to the west-northwest. From the least-squares dual-Doppler analysis (Appendix D), a  $\Delta V$  of at least 15 kt is maintained until 2239;  $\Delta V$

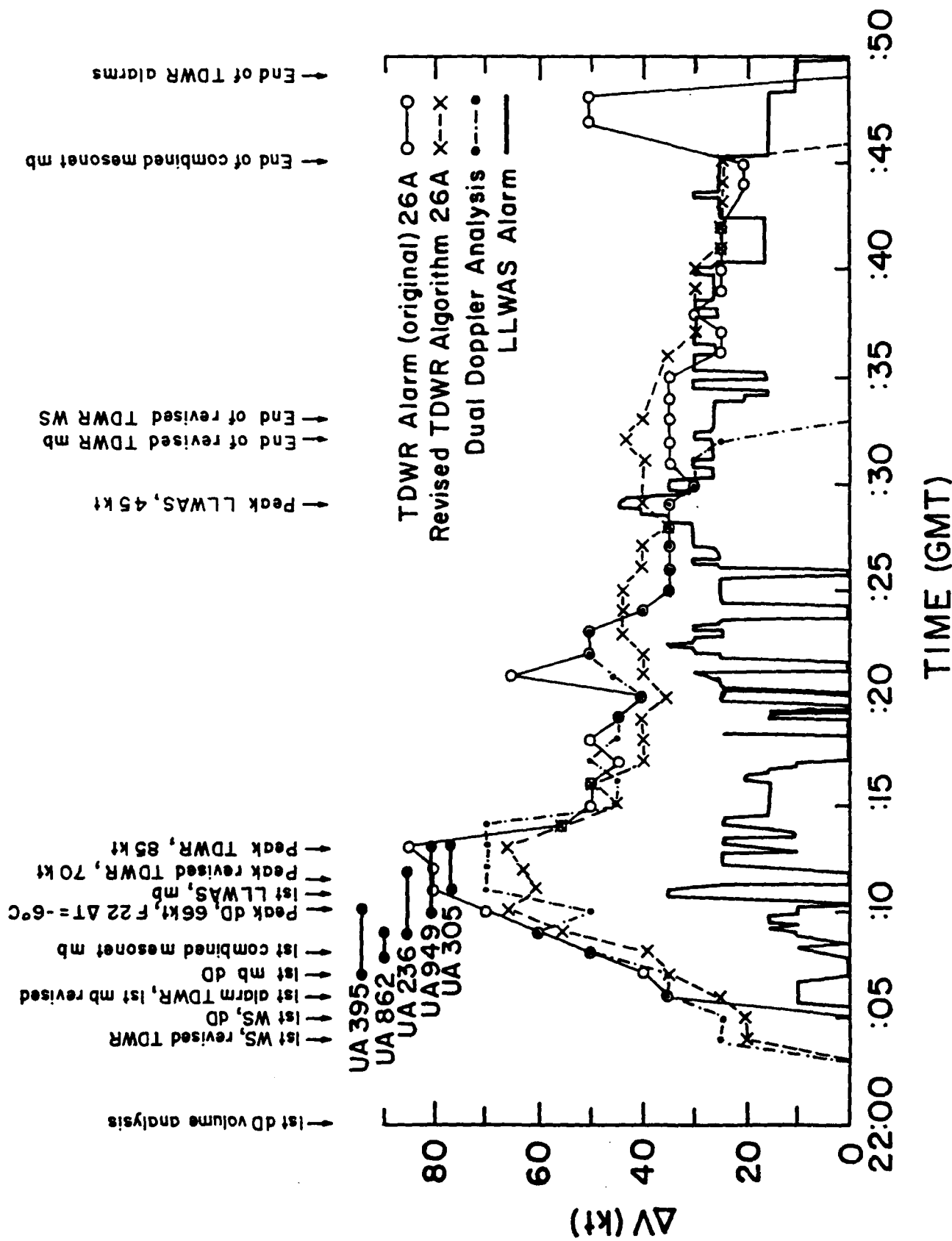


FIGURE 9. Events plotted against time for the 11 July 1988 microburst. A scale for wind shear difference in knots is indicated on the left. Data sources are indicated.

of 10 kt or greater lasts until 2248. LLWAS-generated warnings were sporadic until the final one at 2249.

The following sections present histories of the microbursts and their parent reflectivity cells using dual-Doppler and surface mesonet analyses. Three basic flow regimes exist outside the storm complex: light and variable winds from the surface up to 5 km MSL (3.4 km AGL), westerly winds between 5 and 7 km MSL (3.4 and 5.4 km AGL), and north-westerly winds above 7 km MSL (5.4 km AGL). Within the storm complex, environmental winds become relatively light. When necessary, feature locations are given as  $[x, y]$  pairs relative to FL2; the  $x$  coordinate is in km east, and the  $y$  coordinate is in km north of FL2. Stapleton airport runways are shown by heavy lines. Appendices H-J include analyses of the three-dimensional dual-Doppler radar data. The airport proper covers an area from -10 to -14 km in  $x$  and 6 to 13 km in  $y$ .

#### *B. Microburst Origins: 2130-2202*

During these discussions three reflectivity cores within the storm complex will be identified: A, B and C. The microburst affecting airport operations emanated from core C. These cores and other features are noted in the figures and in the Appendices.

The microburst-producing complex originated from two 60+ dBZ<sub>e</sub> cells which formed around 2130 over the mountains 34 km west of Stapleton. These cells grew and moved southeastward. By 2147, single Doppler radar data show a line of divergence aloft near 6.6 km MSL (5 km AGL), oriented northwest-southeast and moving to the southeast. Reflectivity at that level increases just west of Stapleton at 2155, and shortly afterwards large-scale cyclonic shear is evident at 4.6 km MSL (3 km AGL) over the airport. Surface winds are north-northeasterly across the airport (see Appendix E), temperatures are 31-32°C across the FLOWS mesonet and the air is fairly dry, with 22-25% relative humidity (RH) values (see station plots in Appendix F.)

Between 2148 and 2200, no reflectivity values in excess of 10 dBZ<sub>e</sub> are near the airport proper. Reflectivities correspond to those for clear air; there are no hydrometeors near the surface. The general storm complex is located to the west, oriented in a north-south direction. At 2148 a 30 dBZ<sub>e</sub> cell (core A in Appendices H-J) is well west of Stapleton at 190 m AGL. By 2200, core A has intensified to 38 dBZ<sub>e</sub> at 190 m AGL and remains west of Stapleton Airport. There is weak, large-scale outflow from the main storm complex; winds over the airport remain light, but have shifted from generally northerly to generally westerly. However, no significant outflow is apparent on or near the runways. As would be expected with this flow field,  $w$  and  $F$  are quiescent near the surface.

At 2200, a second core with a maximum reflectivity of 35.9 dBZ<sub>e</sub> at 6.3 km MSL (4.7 km AGL) is just southeast of the runways (core B). This core is in an area of generally westerly winds aloft, previously noted in the 2004 sounding. As is the case during this entire analysis period, horizontal flow within large regions containing reflectivities greater than roughly 25 dBZ<sub>e</sub> is relatively weak. The 37.7 dBZ<sub>e</sub> core at  $[-22.8, 14.8]$  and 6.3 km MSL (4.7 km AGL) is associated with core A (discussed above).

Maximum reflectivities in this storm are well aloft (9.3 km MSL, 7.7 km AGL) and barely exceed 40 dBZ<sub>e</sub>. The 41.0 dBZ<sub>e</sub> core at this level is not associated with core A but is a newly developing cell that soon extends to the surface. It is labelled core C and is associated with a 21 m s<sup>-1</sup> updraft at 7.8 km MSL (6.2 km AGL), the strongest updraft in the domain. Because this updraft is quite vigorous, it remains relatively erect while embedded within strong flow. Core A, the older cell, tilts appreciably with height.

Winds are northwesterly in the southern half of the grid and are generally westerly in the northern half. The northeastern and eastern parts of the analysis domain are empty because there are no scans at elevation angles high enough to include data at such close ranges.

By 2202 two small reflectivity cores (B and C) appear near the surface. Core B, located southeast of the east-west runways, contains a 22.9 dBZ<sub>e</sub> maximum. It contains a weak microburst 2.5 km across with a maximum differential just above 10 m s<sup>-1</sup>. This microburst was observed visually by one of the TDWR OT&E ATCT meteorologists from the Stapleton ATCT. The vertical velocity associated with this microburst is -3.3 m s<sup>-1</sup> at 190 m AGL, and the maximum F is 0.11.

The second reflectivity core, C, is just east of the eastern end of the east-west runway. There is no outflow associated with it yet, but it becomes the dominant microburst.

In order to examine the relationship between the reflectivity cores, three-dimensional displays of reflectivity contours were prepared. Reflectivity above 33 dBZ<sub>e</sub> is contained within the stacked horizontal contours (Figs. 10-12). the storm is viewed from the southwest; The viewer's coordinates are 40 km south, 78 km west of FL2 and at a height of 20.8 km MSL (19.2 km AGL). Figures 10a-g shows these views for the first seven analysis periods.

Core A is at the western extreme edge of the displayed domain (Fig. 10a). Core C first appears aloft (6.8 km MSL, 5.2 km AGL) at 2158 (Fig. 10e). The perspective used for these figures somewhat obscures core C, shown by a heavy dot. A plume of hydrometeors forms a "bridge" of reflectivity which extends downwind (winds near the radar-detected storm top were from the northwest) from a combination of cores A, B, and C. The updraft penetrates into to the layer of northwesterly winds noted in the previous section. These winds have spread the hydrometeors (most likely graupel) along a line oriented from northwest to southeast.

Appendix J contains selected vertical cross sections through this storm. Locations for each cross section are shown by the heavy lines in the corresponding figures from Appendix H. These cross sections are located roughly along the maximum reflectivity axis just above the surface. The horizontal axis in all these figures is labelled in km from the cross section center while the vertical axis is labelled in km AGL. Locations of features are described by their location on the horizontal axis and, where necessary, by their altitude.

Figure J1 shows core B aloft at 2148. Because this is the first analysis available, the origin of this core cannot be traced back prior to this time. The maximum updraft associated with this core is 10 m s<sup>-1</sup> at 6.8 km MSL (5.2 km AGL) just south of the cross section. There is no well defined downdraft associated with core B at this time. The

88/ 7/11 21 48 15-21 48 15 COMBIN 2148SYN DBZ ABOVE 33.00  
 (X,Y,Z) EYE POSITION (KM): ( -40.0, -78.0, 19.2)

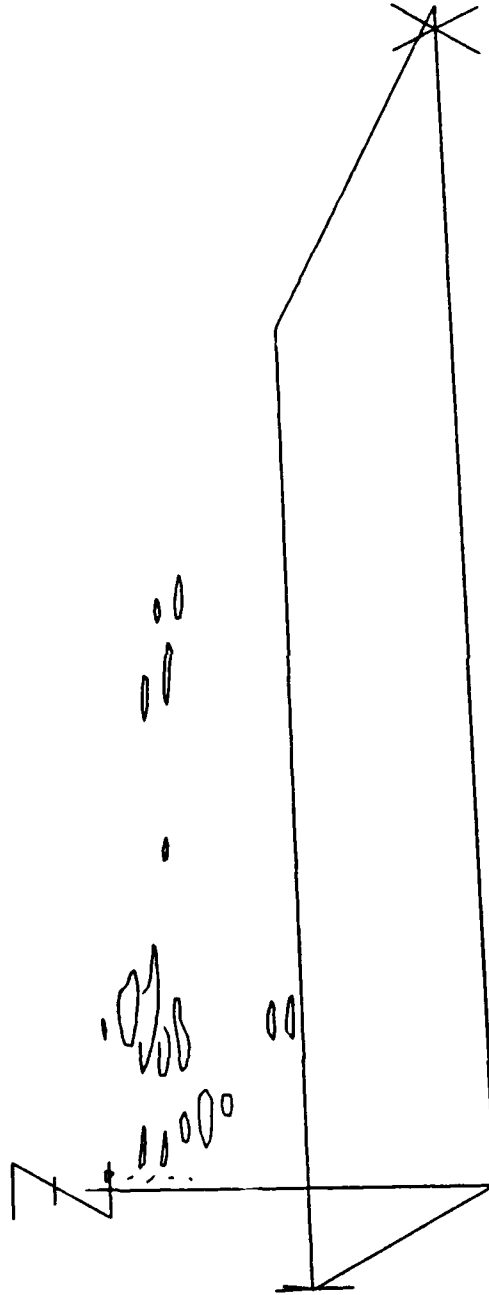


FIGURE 10A-G. Three-dimensional reflectivity perspective views of the microburst-producing storm of 11 July 1988. The viewer is looking toward the northeast and is located at 40 km west and 78 km south of FL2 and is 19.2 km MSL. The 33 dBZ<sub>e</sub> contour at discrete analysis levels (explained in the text) is contoured. Analyses for 2148, 2150, 2152, 2155, 2158, 2200, and 2202 UTC during storm development, are shown.

88/ 7/11 21 50 15-21 50 15 ABOVE 33.00  
 (X,Y,Z) EYE POSITION (KM): COMBIN 2150SYN DBZ  
 ( -40.0, -78.0, 19.2)

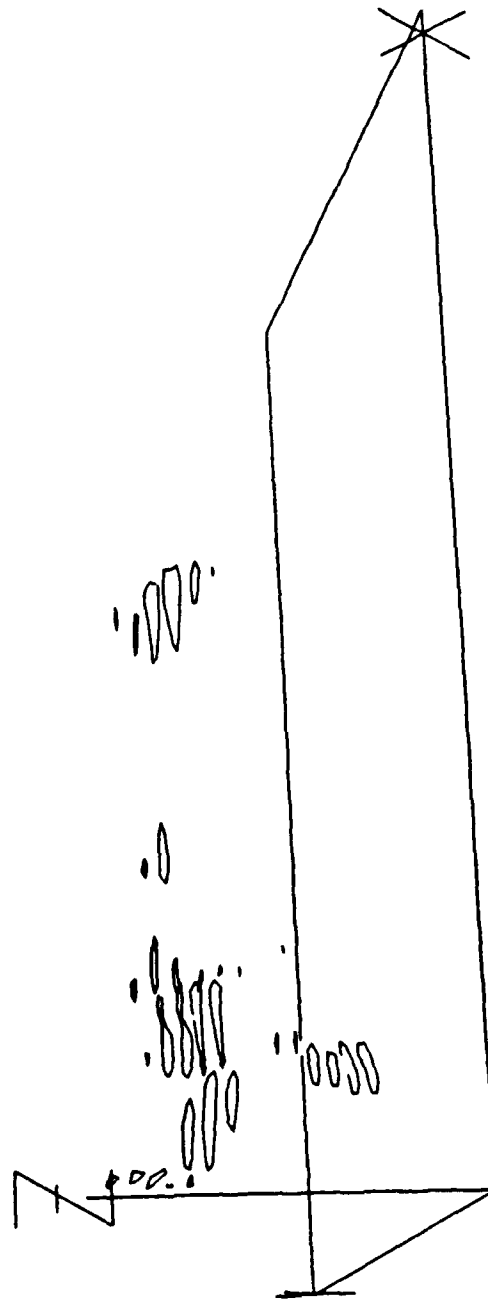


Fig. 10b

88/ 7/11 21 52 15-21 52 15 COMBIN 2152SYN DBZ ABOVE 33.00  
 (X,Y,Z) EYE POSITION (KM): ( -40.0, -78.0, 19.2)

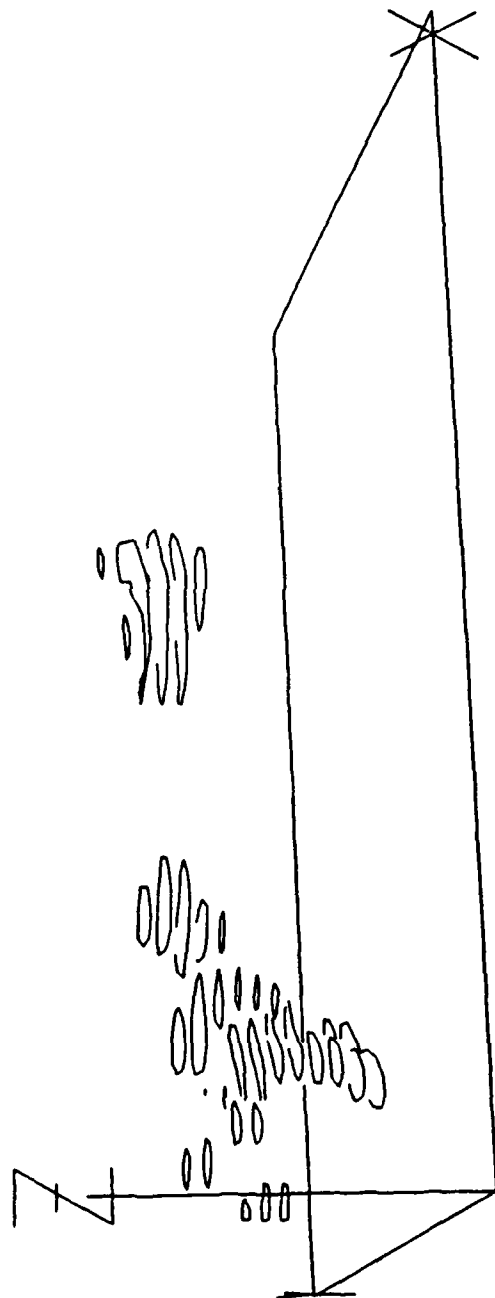


Fig. 10c



88/ 7/11    21 55 15-21 55 15    COMBIN    2155SYN    DBZ    ABOVE    33.00  
 (X,Y,Z)    EYE POSITION (KM):    ( -40.0, -78.0, 19.2)

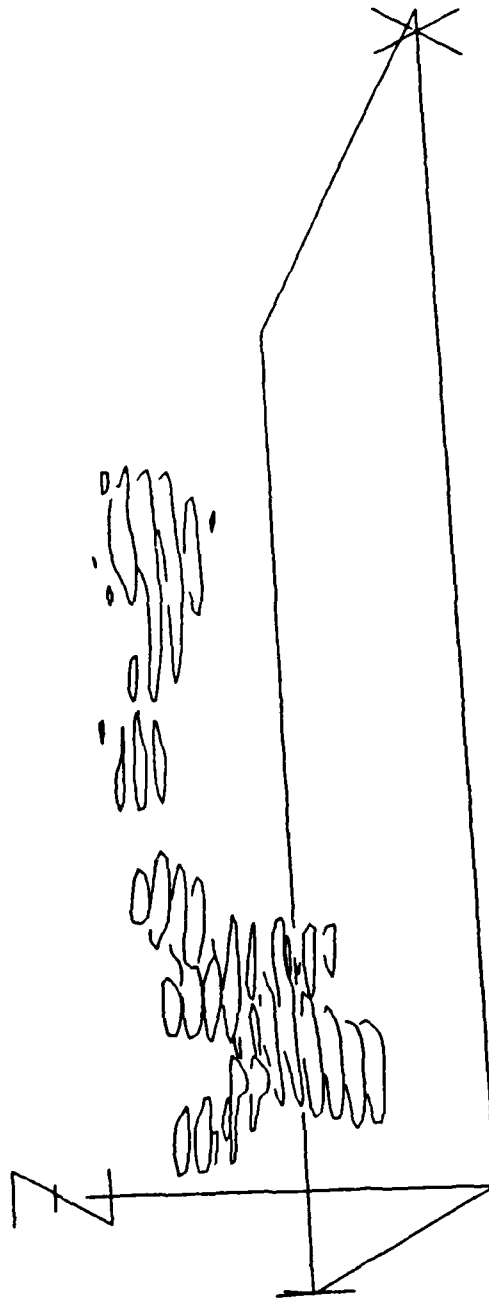


Fig. 10d

88/ 7/11 21 58 15-21 58 15 COMBIN 2158SYN DBZ ABOVE 33.00  
 (X,Y,Z) EYE POSITION (KM): { -40.0, -78.0, 19.2}

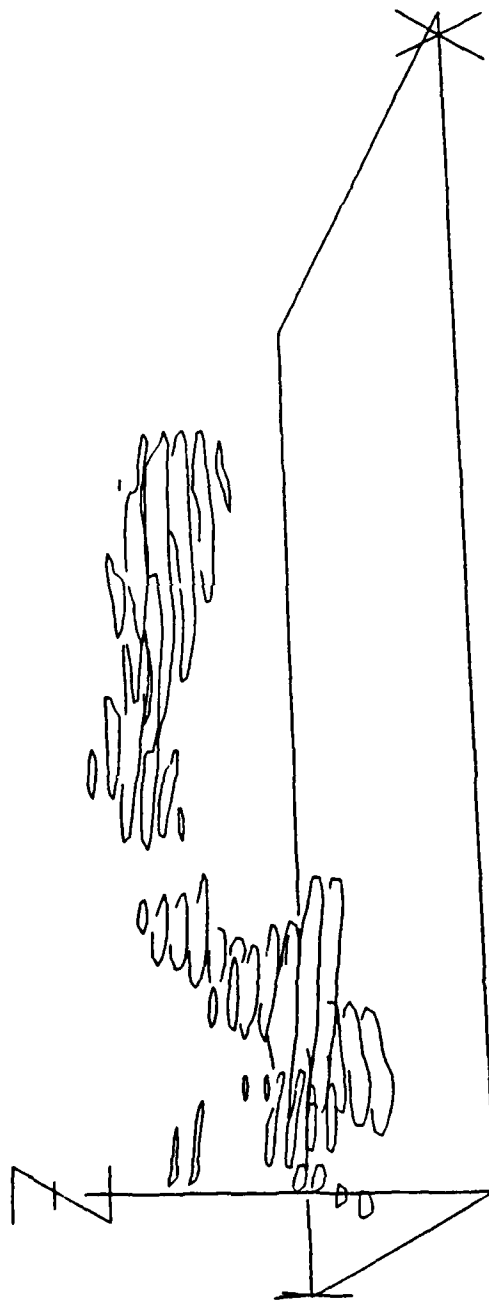


Fig. 10e

88/ 7/11 22 0 15-22 0 15 COMBIN 2200SYN DBZ ABOVE 33.00  
(X,Y,Z) EYE POSITION (KM): ( -40.0, -78.0, 19.2)

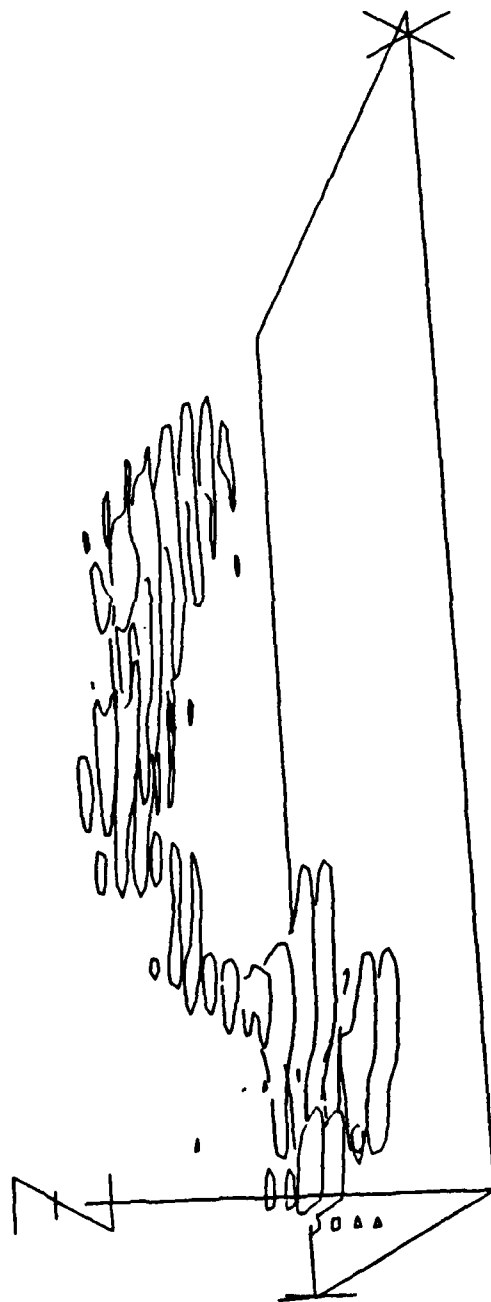


Fig. 10f

88/ 7/11    22   2 44-22   2 44    COMBIN    2202SYN    DBZ    ABOVE    33.00  
 (X,Y,Z)    EYE POSITION (KM):    ( -40.0, -78.0, 19.2)

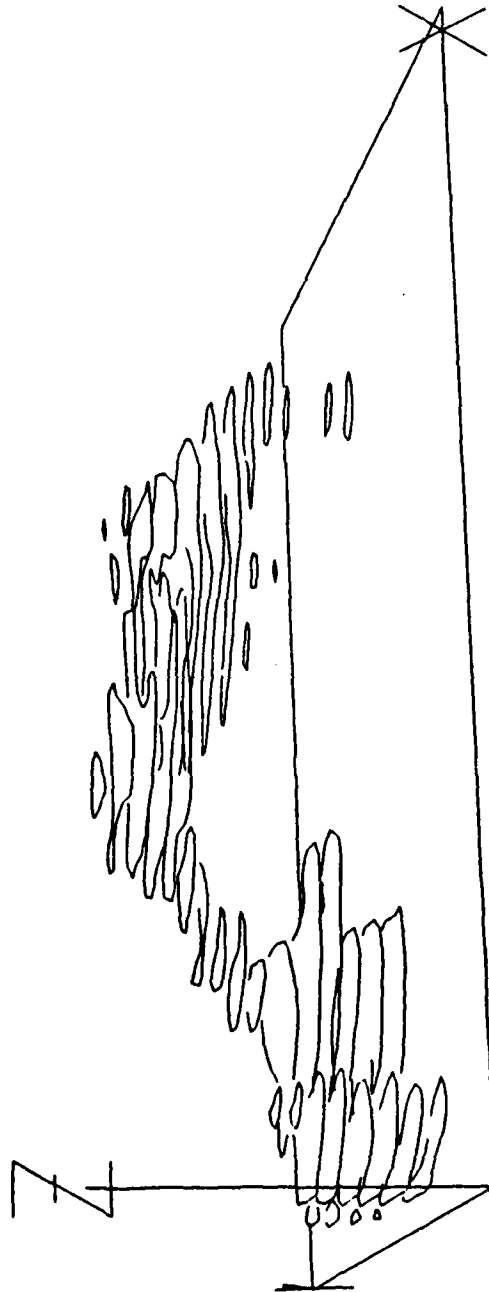


Fig. 10g

88/ 7/11 22 5 16-22 5 16 COMBIN 2205SYN DBZ ABOVE 33.00  
 (X,Y,Z) EYE POSITION (KM): ( -40.0, -78.0, 19.2)

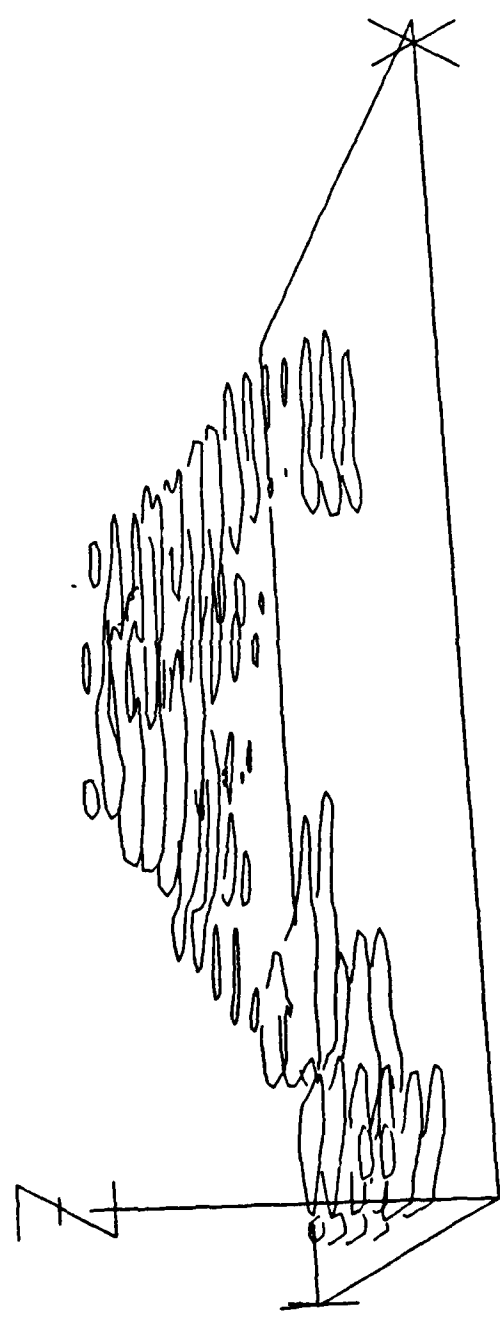


FIGURE 11A-D. As in Fig. 10 but for 2205, 2207, 2210 and 2212 UTC during the microburst alarm period.

88/ 7/11    22 7 45-22 7 45    COMBIN    2207SYN    DBZ    ABOVE    33.00  
 (X.Y.Z)    EYE POSITION (KM):    ( -40.0, -78.0, 19.2)

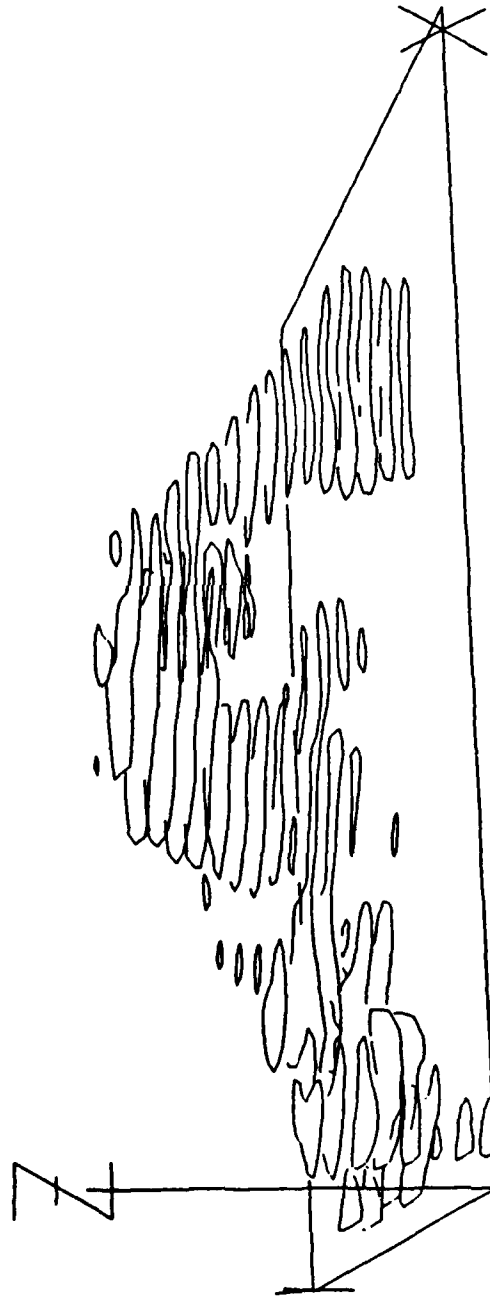


Fig. 11b

88/ 7/11    22 10 19-22 10 19    COMBIN    2210SYN    DBZ    ABOVE    33.00  
 (X,Y,Z)    EYE POSITION (KM):    ( -40.0, -78.0, 19.2)

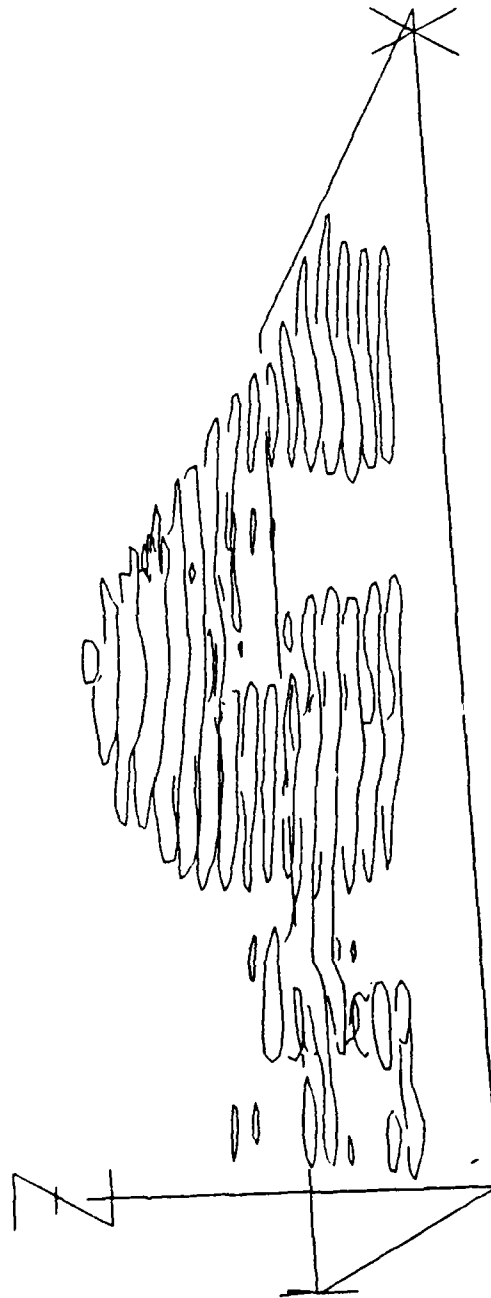


Fig. 11c

88/ 7/11      22 12 47-22 12 47      COMBIN      2212SYN      DBZ      ABOVE      33.00  
 (X,Y,Z)      EYE POSITION (KM):      ( -40.0, -78.0, 19.2)

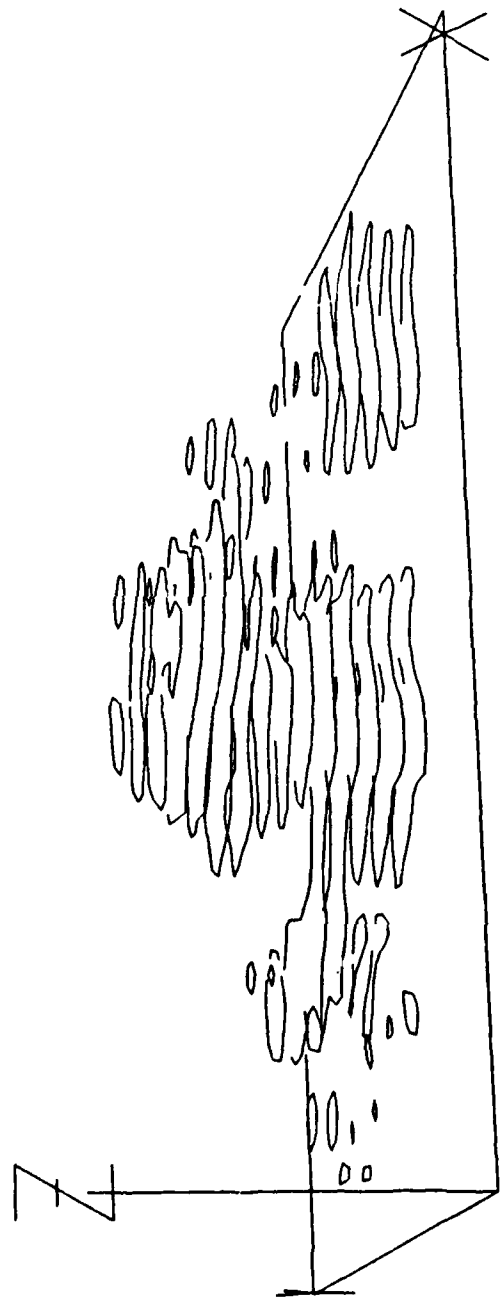


Fig. 11d



88/ 7/11    22 15 10-22 15 10    COMBIN    2215SYN    DBZ    ABOVE    33.00  
 (X,Y,Z)    EYE POSITION (KM):    [ -40.0, -78.0, 19.2]

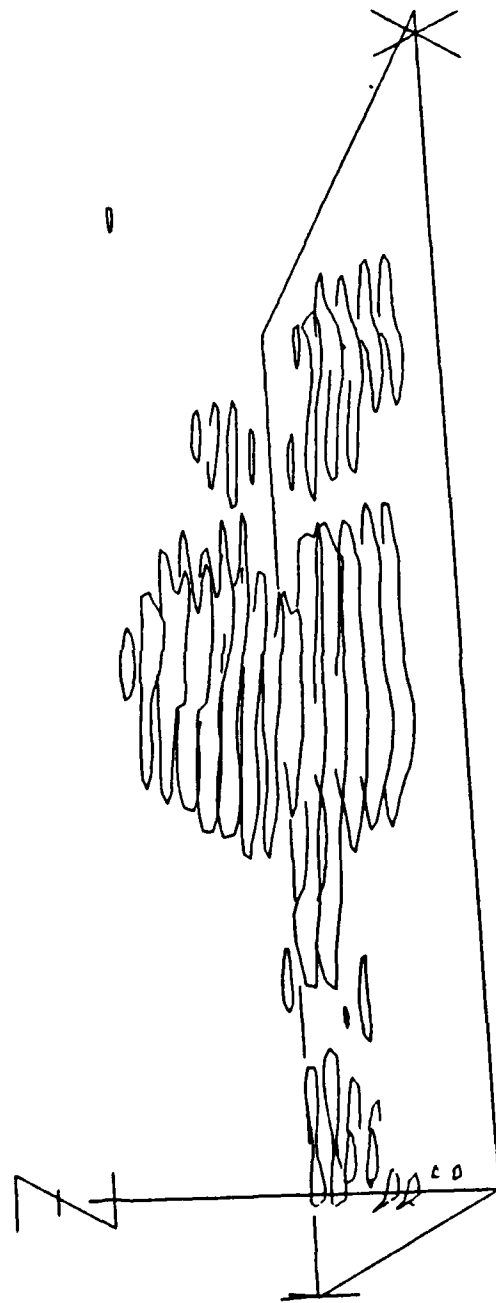


FIGURE 12A-C. As in Fig. 10 but for 2215, 2217 and 2220 UTC during storm dissipation.

88/ 7/11 22 17 47-22 17 47 COMBIN 2217SYN DBZ ABOVE 33.00  
 (X,Y,Z) EYE POSITION (KM): ( -40.0, -78.0, 19.2)

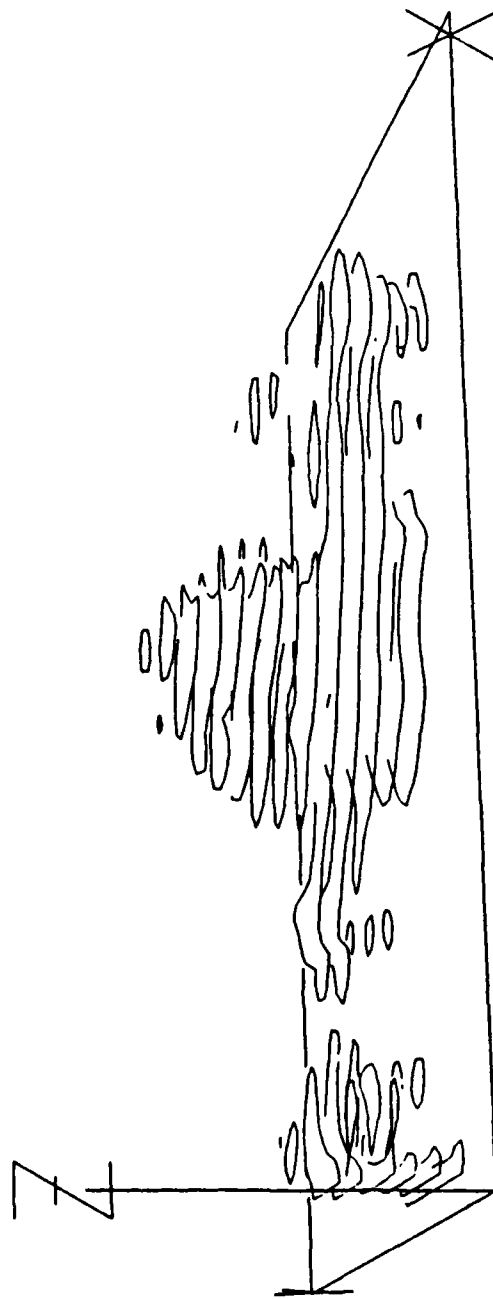


Fig. 12b

88/ 7/11 22 20 14-22 20 14 COMBIN 2220SYN DBZ ABOVE 33.00  
 (X,Y,Z) EYE POSITION (KM): { -40.0, -78.0, 19.2}

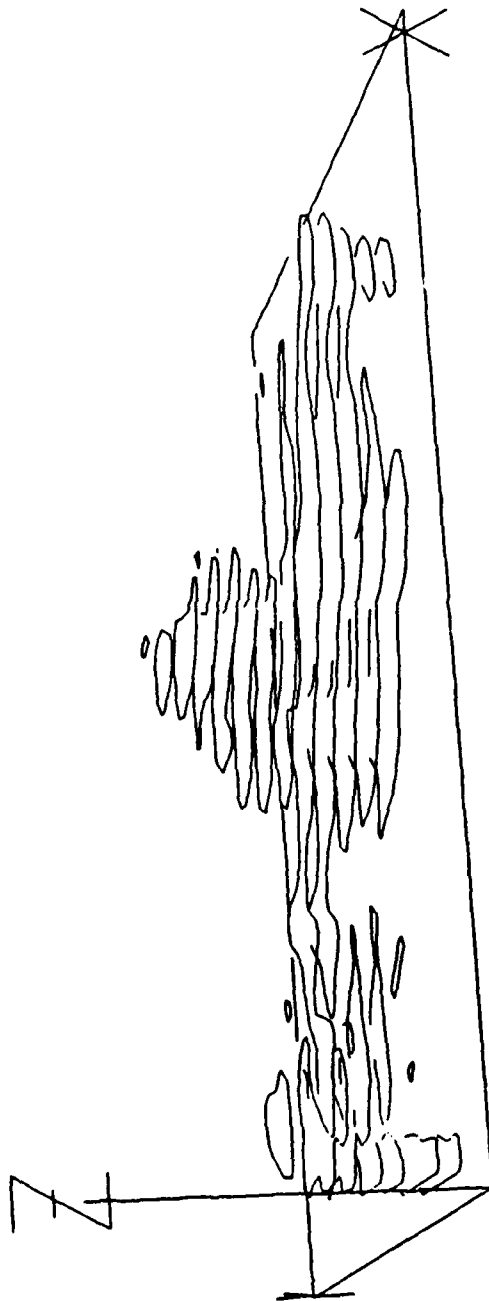


Fig. 12c

best-defined downdraft in the analysis domain is associated with core A and is also on the order of  $10 \text{ m s}^{-1}$  at midlevels.

Core C first becomes apparent at 2158 (Fig. J5), 5.2 km above the surface (6.8 km MSL). In structure it is similar to B in that the updraft supporting it is just to the south, albeit about 50% stronger with a maximum value of  $16.5 \text{ m s}^{-1}$  7.3 km MSL (5.7 km AGL). Descent of core C is clearly apparent by 2202 (Fig. J7). By this time core C is within a  $-5 \text{ m s}^{-1}$  downdraft. An  $11 \text{ m s}^{-1}$  updraft is associated with a  $35 \text{ dBZ}_e$  core at 7.8 km MSL (6.2 km AGL). Core B has descended to the surface, but there is no outflow yet associated with it.

Appendix E shows a comparison between Doppler radar winds and LLWAS winds. In these figures, LLWAS winds have been projected onto a radial from the radar; radar winds are then plotted alongside the projected LLWAS winds. Prior to the alarm period, which began at 2206, the two wind measurements show reasonable agreement, although the radar-measured wind speeds tend to be higher than those from the surface; this is expected due to surface friction.

### *C. Alarm Period: 2205-2215*

The 2205 dual-Doppler radar analyses indicate significant changes in the storm structure. The southeast microburst, B, at the 190 m AGL analysis level, has strengthened and expanded, containing  $15 \text{ m s}^{-1}$  wind speed differential over 4 km. Maximum reflectivity at its center is  $32 \text{ dBZ}_e$ , the maximum downdraft is  $-3.1 \text{ m s}^{-1}$ , and the area containing downdraft greater than  $-2.5 \text{ m s}^{-1}$  has roughly doubled from the previous analysis period. Maximum F is about 0.10.

The main microburst is associated with C. Although not yet as strong as the earlier microburst, it contains a  $12\text{--}13 \text{ m s}^{-1}$  wind speed difference over 2 km and a maximum F of 0.08. This feature is associated with a small  $-2.5 \text{ m s}^{-1}$  downdraft.

At midlevels, Core B descends to 6.3 km (7.9 km MSL) by 2205 (see Fig. J8). The updraft in the area of lower reflectivity (between the two cores, centered near 3 km AGL) increases in intensity; core B is now located on the interface between updraft and downdraft regions. The previously noted reflectivity bridge is clearly evident, emanating from core C, which remains aloft. The connection to the decaying core A extends behind this cross section to the northwest.

Significant differences between the radar and surface mesonet-measured winds become apparent by 2205. At the level of the lowest radar scan, winds in excess of  $10 \text{ m s}^{-1}$  are measured; winds remain relatively calm at the surface. For example, station 9<sup>3</sup> (see Appendix G), which is south of the airport, shows light and variable winds, but winds at the radar scan level are  $4 \text{ m s}^{-1}$  outbound from FL2 and  $10 \text{ m s}^{-1}$  outbound from UND.

By 2207, the main microburst, C, is by far the most impressive of the two. With increased east-west extent and a second, stronger reflectivity core displaced eastward from the initial core, reflectivity has increased by  $20 \text{ dBZ}_e$  in the outflow region on the eastern

---

<sup>3</sup> Appendix E shows LLWAS and FLOWS mesonet station number locations.

side of the microburst. Outflow intensity has also increased: from the eastern edge of the outflow region to its center, the wind speed difference is  $13\text{--}14\text{ m s}^{-1}$  over 2 km. Maximum downdraft velocity is  $-3.4\text{ m s}^{-1}$ ; the maximum  $F$  of 0.09 is displaced slightly eastward, centered at  $[-8.0, 6.6]$ .

The southeast microburst is decaying rapidly; the maximum downdraft is barely  $-2.5\text{ m s}^{-1}$  and reflectivity has decreased rapidly in both intensity and horizontal extent. It should be noted that this microburst was exceptionally short lived, developing from quiescence to its maximum value in only 2.5 min and then essentially disappearing only 5 min afterwards.

The core C microburst continues to intensify through 2210. The maximum downdraft is  $-4.5\text{ m s}^{-1}$  extending from the eastern outflow edge to the center. Maximum wind speed difference exceeds  $15\text{ m s}^{-1}$  over 3 km. Considerably more shear exists,  $20\text{--}25\text{ m s}^{-1}$ , across the microburst in the north-south direction. At 190 m AGL, maximum reflectivity within the outflow is  $36\text{ dBZ}_e$  (see Appendix I). A gust front from storms to the northwest is clearly evident in the northwest corner of the analysis grid.  $F$  has increased nearly 50% from 0.08 in the prior analysis to 0.11; in a span of 5 min,  $F$  within the main microburst grew from practically zero to 0.11.

The strongest downdraft observed during the microburst,  $-13\text{ m s}^{-1}$ , occurs during the analysis centered at 2210. By this time, core C has descended to the lowest radar scan level. From there, it extends almost vertically up to 7.2 km AGL, 8.8 km MSL (see Appendix J). From 7.2 km AGL (8.8 km MSL), a reflectivity plume extends downward and eastward (towards the right-hand side of the figure) and terminates at the microburst location. The cross section illustrating this also contains the  $13\text{ m s}^{-1}$  downdraft at 2.2 km AGL (3.8 km MSL). A radar bright band is centered near this level, caused by melting of frozen hydrometeors (graupel) from core C. A similar feature is associated with core B.

By this time, the FLOWS mesonet begins to show evidence of the core C microburst at the surface. Between 2209 and 2210, the temperature at station F23 (see Appendix F) drops  $6^\circ\text{C}$  from  $29^\circ$  to  $23^\circ\text{C}$ , and the wind speed increases from 7 to  $15\text{ m s}^{-1}$ . Relative humidity also increases from 24 to 43%. During the previous minute, wind speed increased from 3 to  $7\text{ m s}^{-1}$ ; these winds apparently indicate initial outflow arrival prior to any temperature or humidity signatures. Several other stations experienced wind speed increases or abrupt wind direction changes from the previous minute, especially F21 and F22 (near the eastern and western edges of the microburst). These stations did not record the accompanying thermodynamic changes at this time, however. LLWAS station L7 (Appendix G) records a sudden rise in wind speed near 2210. These wind speed fluctuations lag similar radar-measured winds by about 1 min; the first LLWAS alarm, a 35-kt loss on 26A, occurs at 2210:42.

Maximum event intensity occurs within the 2212 dual-Doppler analysis. Reflectivity near the surface peaked at  $38.4\text{ dBZ}_e$ . The microburst has expanded and intensified; maximum east-to-west differential velocity is nearly  $20\text{ m s}^{-1}$  over 3.8 km, the maximum downdraft at 190 m is  $-3.8\text{ m s}^{-1}$  and maximum  $F$  is 0.13. The  $\Delta V$  analysis (see Appendix

D) shows an expected headwind loss of  $33 \text{ m s}^{-1}$  (66 kt). This event is the strongest microburst yet analyzed using dual-Doppler techniques.

Core C reflectivity increases to almost  $39.7 \text{ dBZ}_e$ , but outflow beneath it fails to develop as rapidly or as strongly as core B. This may be due to weak pre-existing cool outflow at the surface from the storm complex; core C is further to the west than B and thus is closer to the outflow from the main storm. Core A is not clearly apparent at this time, being little more than a northwestward extension of the  $30 \text{ dBZ}_e$  contour.

At 6.3 km (7.9 km MSL), a single  $35 \text{ dBZ}_e$  reflectivity core clearly marks the mid level of core C (see Appendix H). Two cyclonic circulations are associated with this core along with significant convergence on the southeast flank. Below this level is an area of general descent and above it are mostly weak updrafts.

At 9.3 km (10.9 km MSL), maximum reflectivity within core C is  $30.7 \text{ dBZ}_e$ , 7 dB less than the value at 2207. There is still some storm-top divergence associated with core C, but the updraft beneath it has decreased to little more than  $11 \text{ m s}^{-1}$ , a decrease of  $2 \text{ m s}^{-1}$  from its previously analyzed value.

Figures 11a-d chronicle the vertical development of core C and the descent and intensification of core B. At 2205 reflectivity aloft is associated with B and is not yet reaching the lowest analysis level. The first signs of core C reaching the surface appear at 2207 and there is a clear link or "reflectivity bridge" between cores C and A. At 2210 core C is not quite as erect as at 2207; careful inspection shows that the western extreme of core C has shifted somewhat eastward above 7.3 km (8.9 km MSL). By 2212, core C has a more pronounced tilt, and reflectivity within core B continues to descend.

From 2210-2220, considerable spatial and temporal variations in wind speed are apparent in the LLWAS. This is especially evident in those stations near the edge of the microburst: L1, L2, L7, and L9. LLWAS stations report winds every 6 s and represent point values at the surface, while the 1-min radar data resolution, along with the spatial averaging that takes place within each range gate along a beam, causes temporal smoothing that tends to remove extremes in the wind measurements. Data from these stations show gustiness which is not resolved by radar measurements; LLWAS data shows higher maximum microburst wind speeds than those measured by the radars. LLWAS alarms during this time are sporadic and do not maintain a constant strength ( $\Delta V = 10 \text{ m s}^{-1}$  or 20 kt) as shown in Fig. 9. Cornman et al. (1989) discuss the significance of small-scale fluctuations in microburst winds.

#### D. Dissipation: 2215-2300

Although this event maintains the defined microburst strength through 2228 (using the revised Lincoln Laboratory algorithm), the parent storm begins weakening well before this time. The storm collapses and downdrafts continue to "feed" the surface outflow.

By 2215, the microburst outflow expands further, extending past the analysis domain eastern edge. Core C has decreased in areal coverage somewhat while essentially maintaining peak reflectivity (37 dBZ<sub>e</sub>). Outflow from C, constituting the main microburst, has become distorted by outflow from the main storm complex and is now quite complex. Maximum east-to-west velocity differential is down to 15-20 m s<sup>-1</sup> over 6-7 km; the *microburst* has expanded into a *macroburst*. Its presence is slowing the advance of a gust front from the main storm complex: towards both the northeast and southwest the gust front has advanced farther than in the immediate microburst/macroburst vicinity.

Two distinct downdraft maxima are apparent in the 2215 high-resolution horizontal cross section (Appendix I): near [-9.4, 5.2] and [-5.0, 7.0], with velocities of -3.2 and -3.0 m s<sup>-1</sup>, respectively. Because several downdrafts exist in close proximity, this may be thought of as a multiple microburst event. The maximum F, 0.11 at this time, is located almost coincident with the downdraft centered [-5.0, 7.0]. A second maximum, 0.09, is coincident with the downdraft at [-9.4, 5.2].

Approaching from the northwest, the gust front occupies the northwest third of the analysis grid. Associated with it is a performance-enhancing region, with peak F values of -0.07 to -0.09. The strongest updraft associated with the gust front has decreased to little more than 11 m s<sup>-1</sup> from the prior 13 m s<sup>-1</sup> maximum.

Aloft, a single reflectivity core is again observed at the 6.3 km AGL level (7.9 km MSL), as shown in Appendix H. The convergence region southeast of the core remains accompanied by a weak downdraft, and in the northern part of the analysis grid flow remains generally northwesterly. Westerly winds, part of weak outflow from convection to the west, have returned to the southern 4 km of the domain. The boundary of these westerlies is moving slowly eastward.

The 30 dBZ<sub>e</sub> contour has descended from 7.2 km to 6.7 km (8.8 km to 7.3 km MSL). A well-defined updraft no longer supports core C; none are visible in the vertical cross section (Appendix J) nor present within a km to either side of it. A general area of 6-7 m s<sup>-1</sup> updraft remains aloft, no longer extending to the surface.

Flow throughout the region is generally northwesterly at 9.3 km (10.9 km MSL) and core C, decreases rapidly in area and intensity (see Appendix H). Core C has also begun to accelerate southeastward. Its maximum reflectivity has decreased to 25.7 dBZ<sub>e</sub>, almost 5 dBZ<sub>e</sub> down from the previous scan.

The flow field at 2217, shown in Appendix I, has become quite complicated as the microburst continues to expand. Reflectivities are decreasing with maxima of only 35 to 36 dBZ<sub>e</sub>. Associated with the outflow region is a bow-echo pattern with minimum reflectivity near [-9.2, 7.4], indicating dry air entrainment aloft and hydrometeor extinction through evaporation or sublimation.

A meaningful differential velocity estimate is difficult because much of the event is beyond the eastern edge of the analysis domain. There are, however, two distinct hazard regions associated with this microburst: between  $[-2.0, 6.8]$  and  $[-5.8, 6.8]$  lies a wind speed loss of  $20\text{--}22\text{ m s}^{-1}$  over  $3.8\text{ km}$ , while between  $[-7.0, 5.0]$  and  $[-10.2, 5.0]$  a  $10\text{--}12\text{ m s}^{-1}$  loss over  $3.2\text{ km}$  exists. The strongest downdraft is  $-3.3\text{ m s}^{-1}$  at  $[-5.6, 6.8]$ .

Along with these two hazardous shear areas are two regions of significant  $F$  (see Appendix I). The easternmost area contains  $F = 0.11$  and the westernmost contains  $F = 0.09$ ; there is a third maximum at  $[8.2, 6.8]$  where  $F$  is just below  $0.09$ . None of these values are significantly different from the 2215 analysis.

The southeastward moving gust front is impinging upon the microburst outflow, resulting in a better defined (sharper) leading edge. A broad, northeast-southwest area of negative  $F$  values marks this region, with a  $-0.10$  peak at  $[-11.0, 8.8]$ .

Most reflectivity in descending core B is close to the surface; core C remains suspended aloft. A  $-10\text{ m s}^{-1}$  downdraft, the strongest in this cross section, is  $1.7\text{ km AGL}$  ( $3.3\text{ km MSL}$ ) at  $9\text{ km}$ .

The reflectivity pattern clearly shows that this storm complex has entered the dissipation stage. The  $30\text{ dBZ}_e$  contour has descended another  $0.5\text{ km}$ . A reflectivity bright band is vertically centered at  $1.7\text{ km}$  ( $3.3\text{ km MSL}$ ), evidence that most hydrometeors in this area are melting as they descend. There is general descent below  $3.7\text{ km AGL}$  ( $5.3\text{ km MSL}$ ) from  $-3\text{ km}$  to the right-hand edge of the cross section. Maximum downdraft intensity is  $-8.3\text{ m s}^{-1}$  near  $3\text{ km}$ , vertically centered at  $2\text{ km}$  ( $3.6\text{ km MSL}$ ).

The last vertical cross section shown in Appendix J covers the analysis time centered at 2220; it contains no significant updrafts, and there are none within  $1\text{ km}$  of either side of it. The storm is clearly collapsing: there is downdraft almost everywhere below  $5\text{ km AGL}$  ( $6.6\text{ km MSL}$ ). Maximum reflectivity is located between  $1.7$  and  $2\text{ km AGL}$  ( $3.3$  and  $3.6\text{ km MSL}$ ), centered around the melting level.

Near the surface, the reflectivity pattern continues to evolve rapidly and is generally decreasing, with a maximum value of  $35.9\text{ dBZ}_e$ . Surface outflow has expanded considerably and become quite complex, rendering any single velocity differential estimate inadequate for hazard characterization. At  $190\text{ m AGL}$ , most air is generally descending and this analysis time contains the strongest downdrafts. The two strongest are at  $[-6.4, 7.5]$  and  $[-4.0, 6.6]$ , which are both descending at  $-4.6\text{ m s}^{-1}$ .

Due to these downdrafts, this analysis also contains the largest  $F$  values:  $0.17$  at  $[-4.0, 7.0]$ ,  $0.14$  at  $[-6.6, 8.0]$ , and  $0.12$  at  $[-7.8, 6.4]$ . Patterns of  $F$  near the surface are becoming more complicated, further evidence that this is not a single event but a closely spaced (temporally and spatially) collection of events.

Temperatures across the FLOWS mesonet slowly decline during this period. The main microburst affected only a few stations, F23, F22 and possibly F21. The rest of the mesonet is affected by multiple outflow centers, which do not produce intense winds or temperature falls equivalent to the main microburst. Temperatures decrease  $5\text{--}8^\circ\text{C}$  while relative humidity increases by  $8\text{--}21\%$  over the mesonet. Southwesterly flow over the



northern and central stations and northwesterly flow over the extreme southern stations (Appendix F) reflect the general southeast-northwest outflow orientation.

The largest temperature drop is from 29°C to 21°C at FLOWS station F23, occurring between 2209 and 2211. Proctor (1989) discusses a possible relation between the microburst-induced surface temperature drop and the outflow wind speed. Using his technique, an 8°C drop roughly corresponds to a  $20 \text{ m s}^{-1}$  outflow, which is in fair agreement with these observations. An earlier Fawbush and Miller (1954) formula yields a  $25 \text{ m s}^{-1}$  estimate.

Storm dissipation is illustrated in Figs. 12a–c. By 2215, the area around core B containing reflectivity greater than 33 dBZ<sub>e</sub> has decreased substantially as have reflectivity values aloft in core C. A radar bright band develops by 2217, with an upper limit of 3.3 km MSL (1.7 km AGL) in the radar analysis; the 0°C level from the 2004 sounding (Fig. 6) is 3.75 km (2.05 km AGL). Core C is tilting eastward at a steeper angle, and by 2220 the radar bright band increases more in area while core C rapidly decays.

After 2220, the microburst parent cell dissipates and leaves only weak, low-level divergence. The storm complex develops into a line and moves southeastward. Additional outflow from new cells, which are weaker than earlier cells, triggers convection on the southeast end of the line. As it moves away from the airport, the line becomes indistinct, and precipitation develops over a wide area.

#### *E. Air Parcel Trajectory Analysis*

Recall the 2004 sounding (Fig. 6) and the general minimum  $\theta_e$  area at 7 km MSL (5.4 km AGL). Also recall the presence of two distinct wind regimes at 7 and 10 km MSL (5.4 and 8.4 km AGL): westerly winds at 7 km MSL (5.4 km AGL) in the northern and southern thirds of the analysis grid, strong northwesterly winds above 10 km MSL (8.4 km AGL), and weak flow within the active convection. The reflectivity plume most likely develops as the updraft penetrates the strong northwesterly winds above 10 km (8.4 km AGL). As the updraft weakens above the equilibrium level, it is sheared downwind and the hydrometeors carried up to that level (probably graupel) begin to descend.

Figures 13–15 show air parcel trajectories computed using dual-Doppler-derived winds. The process of retrieving dual-Doppler winds removes hydrometeor motions using an assumed reflectivity-terminal fallspeed relationship. Thus, the trajectories shown are air parcel trajectories and should not be confused with hydrometeor trajectories. Starting at 2212 and computing trajectories back in time, air parcel locations at 2148 are determined. Parcels are initiated at 2.2 km MSL (400 m AGL). If initiated at heights much below this, many parcels exit the bottom of the grid (because  $w \neq 0.0$  at 190 m), terminating their respective trajectories. Many more trajectories than those displayed were examined, but these are representative trajectories for most parcels within the microburst at 400 m AGL by 2212.

Three-dimensional perspective views of trajectory ribbons are shown in Fig. 13. Distances along the  $z$  axis are stretched by a factor of 1.5 for these figures. Each axis is labelled with 25 tick marks. Thus, each tick mark represents 1.12 km in the  $x$  direction

11 JULY 1988  
 XNN= -30.0 XNY= -2.0  
 YNN= 1.0 YNY= 23.0  
 ZNN= 1.6 ZNY= 10.8  
 ZSTRETCH FACTOR= 1.5  
 EYE= -40. -78. 19.

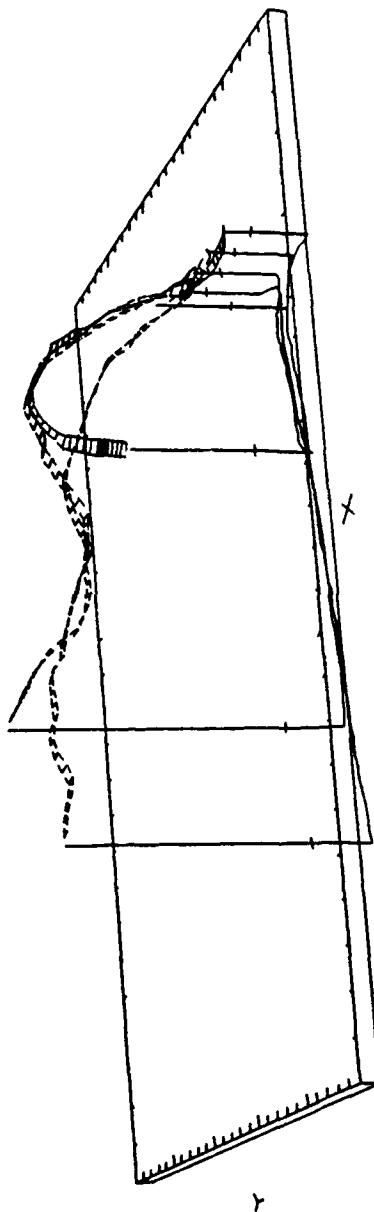


FIGURE 13. Air parcel trajectories obtained from dual-Doppler analysis. The trajectories are shown in three dimensions with projections on a horizontal plane indicated. Each tick mark along a trajectory ribbon indicates 30 s of travel.

FRAME= 10  
 DATE= 10-25-89  
 TIME= 11:55:39

and 0.88 km in the  $y$  direction. Each trajectory terminus is labelled with a vertical bar, and a short dash indicates where each of those bars intersects the surface. The bars then continue downward until they reach 0 km MSL. Trajectory ribbons are illustrated such that rotation along the path is indicated by twisting of the ribbon. Along these four trajectories there is little rotation until the parcels approach the ground where flow begins to diverge.

Figure 14a shows the same trajectories plotted with projections onto each of the three orthogonal ( $x, y, z$ ) surfaces. Vertical bars along these trajectories are plotted every 30 s. Air within the microburst at 2212 clearly originates well aloft and to the west of the surface outflow.

Figure 14b shows the projection of each trajectory onto the  $y$ - $z$  plane. On this figure, north is to the right so that the viewer is looking toward the west. Three of the parcels originated at heights between 4.5 and 5.1 km (2.9 and 3.5 km AGL). The fourth, which appears to have originated at 2.6 km (1.0 km AGL), in actuality did not; the trajectory prematurely ended due to some missing data in one of the analysis volumes. Two of the parcels are clearly in updraft at 2200, the earliest analysis time available. None of the parcels are displaced appreciably north or south until they began to diverge at the surface.

Figure 14c shows parcel trajectories projected onto the  $x$ - $z$  plane. East is to the right in this figure; the viewer is looking north through the trajectory paths. All trajectories originate between 4.5 and 9 km west of their 2212 position. This places these parcel origins west and slightly south of core B, as previously shown in Fig. 14b. This makes sense because within the 2200 vertical cross section the maximum updraft is displaced somewhat south of the cross section location.

In Fig. 14d, the track of each trajectory is projected onto the  $x$ - $y$  plane, and horizontal displacements of each parcel can be clearly observed. Throughout the analysis time, until diverging near the ground, these parcels were generally moving toward the east-northeast.

Figures 15a-k show the same air parcel trajectories broken into segments and overlaid on three-dimensional reflectivity perspective plots. Using the information from earlier figures, the general location of each trajectory can be deduced on these two-dimensional projections. Each trajectory segment is computed over a 2.5-min time interval and projected onto the reflectivity perspective plot that corresponds to the analyzed volume centered on that 2.5 min span. For example, the trajectory segments shown in Fig. 15c indicate the paths taken by the displayed air parcels during the time between roughly 2151:00 and 2153:45, a 2.5-min span centered on 2152:15, the center time of the 2152 analysis.

Previous figures showed that all air parcel trajectories remained relatively well confined to a narrow east-west corridor between about 5 and 7 km MSL (3.4 and 5.4 km AGL). Thus, these trajectories are south or, from this perspective, in front of, regions of reflectivity greater than 33 dBZ.

Early in the analysis period, there are two groups of trajectories: those at midlevels and those that are slowly ascending from 1-2 km AGL (2.6-3.6 km MSL). These two groups merge between 2158 and 2200 at a height of 3.4-5.4 km AGL (5-7 km MSL). At this time, they intersect the developing reflectivity region. By 2202, the air parcel

11 JULY 1988  
 XMM= -30.0 KMX= -2.0  
 YMM= 1.0 YMX= 23.0  
 ZMM= 1.6 ZMX= 10.8  
 ZSTRETCH FACTOR= 1.5  
 EYE= -40. -78. 19.

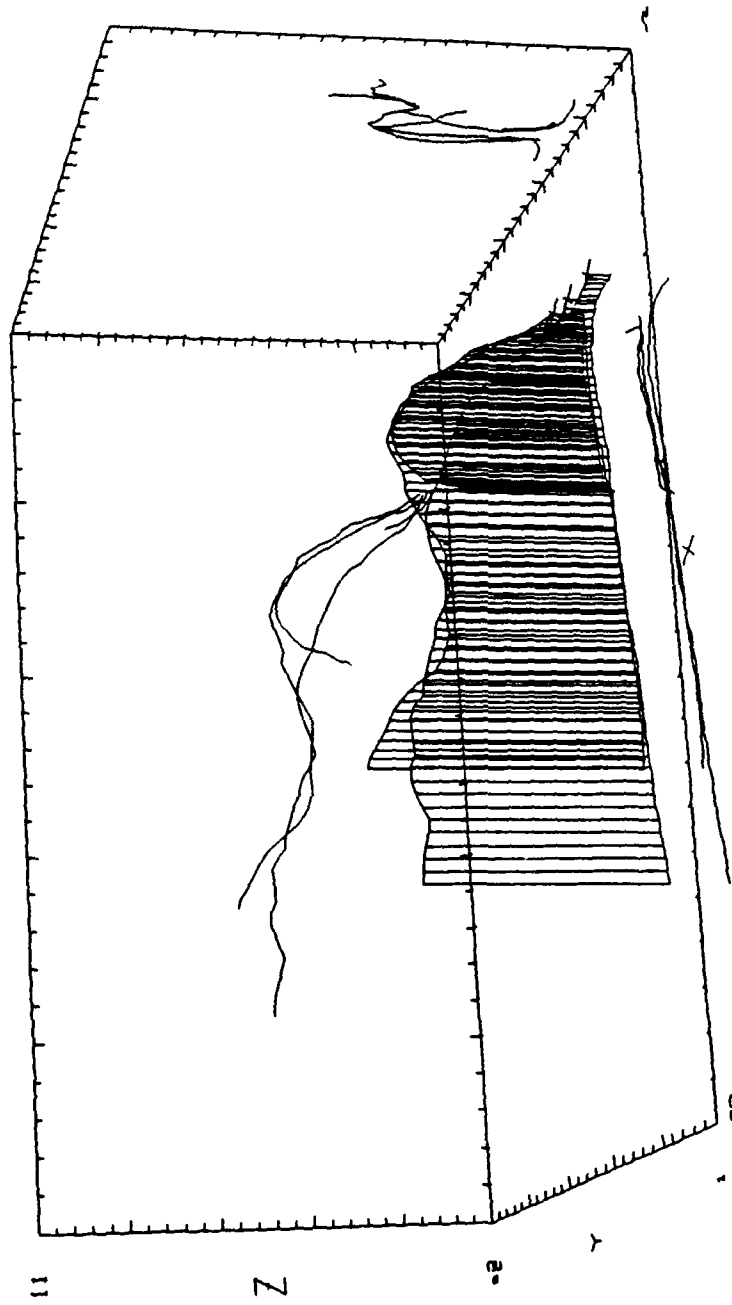
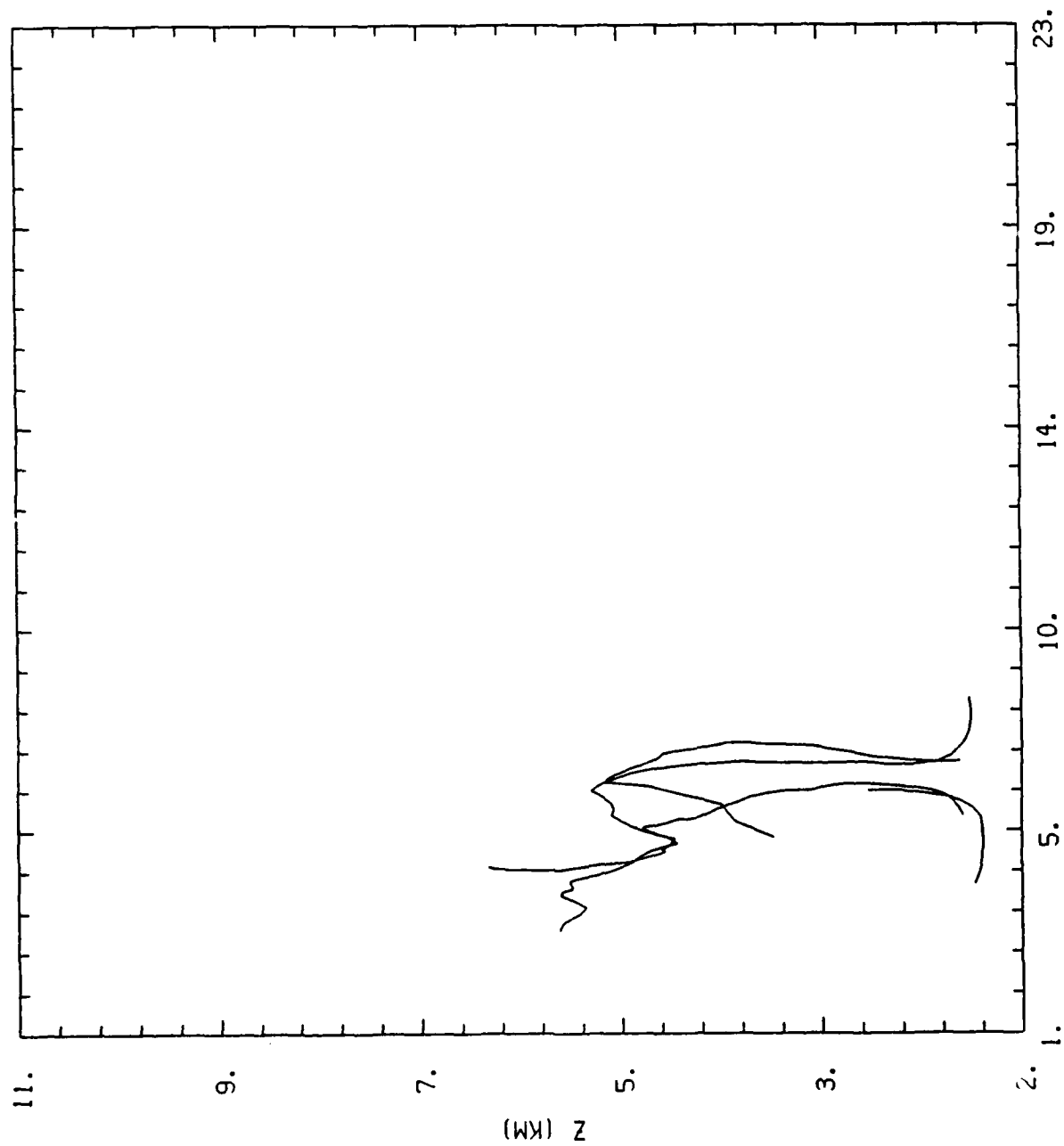


FIGURE 14A-C. As in Fig. 13 but projections on the  $[x, y, z]$  surfaces are shown. Trajectory projections are shown on a) all three surfaces, b) the  $y - z$  surface, c) the  $x - z$  surface and d) the  $x - y$  surface.

FRAME= 19  
 DATE= 10-25-89  
 TIME= 12:02:19

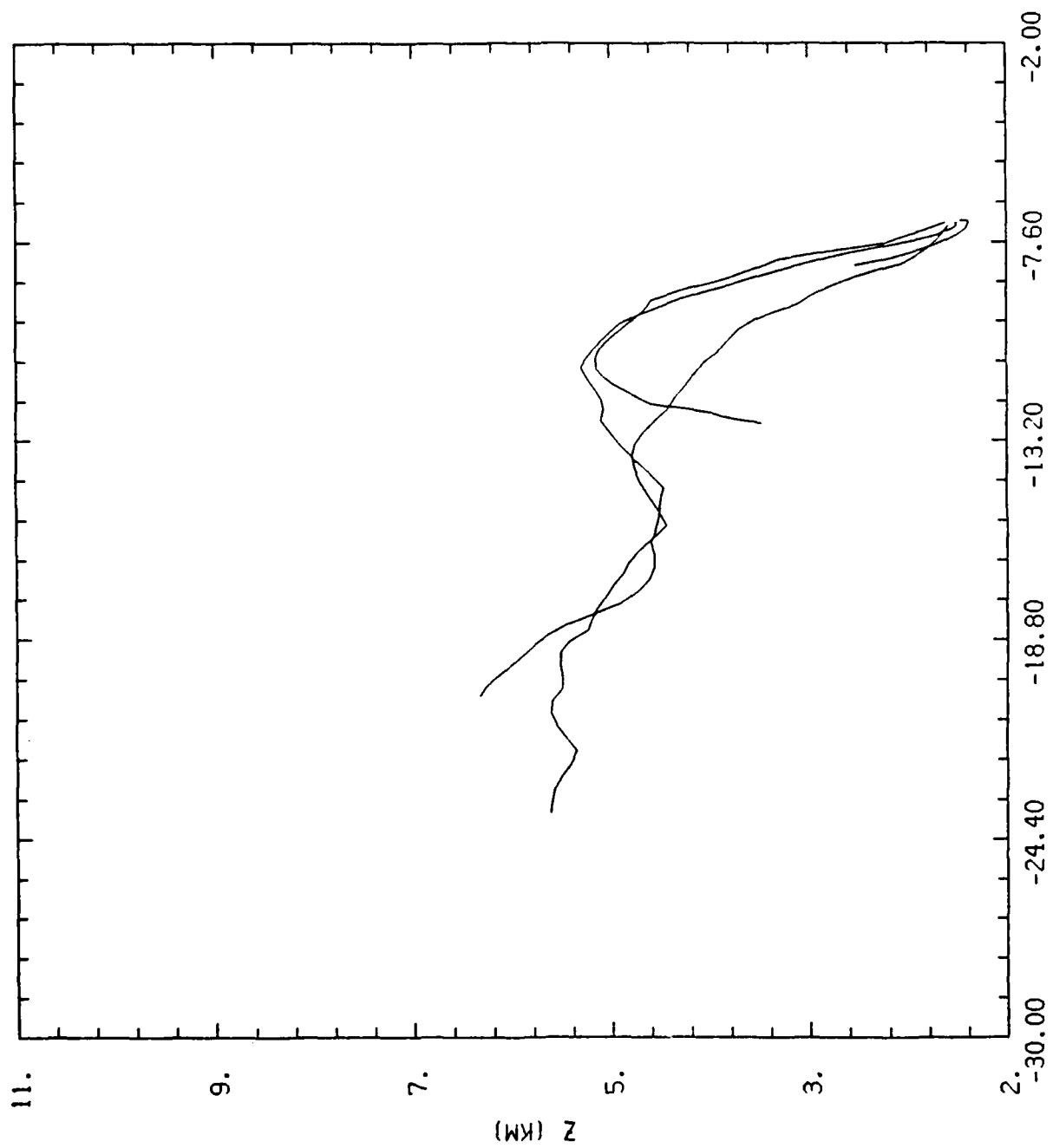
11 JULY 1988



FRAME= 11  
DATE= 10-25-89  
TIME= 11:55:56

Y (KM)  
Fig. 14b

11 JULY 1988

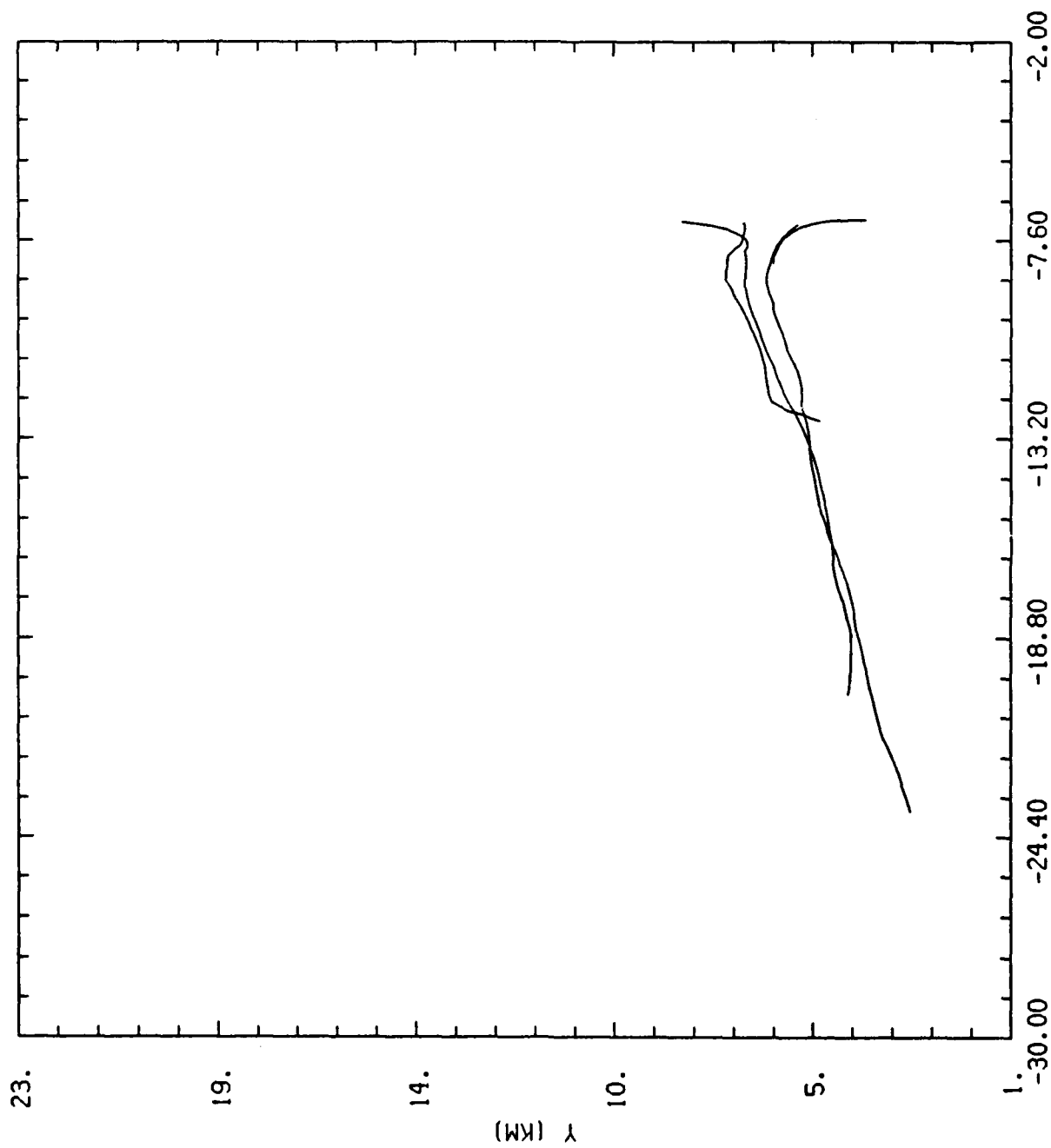


FRAME = 12  
DATE = 10-25-89  
TIME = 11:56:11

X (KM)

Fig. 14c

11 JULY 1988



FROM: 13  
DATE: 10-25-89  
TIME: 11:56:26

X (KM)  
Fig. 14d

88/ 7/11 21 48 15-21 48 15 COMBIN 21485YN DBZ ABOVE 33.00  
 (X,Y,Z) EYE POSITION (KM): (-40.0, -78.0, 19.2)

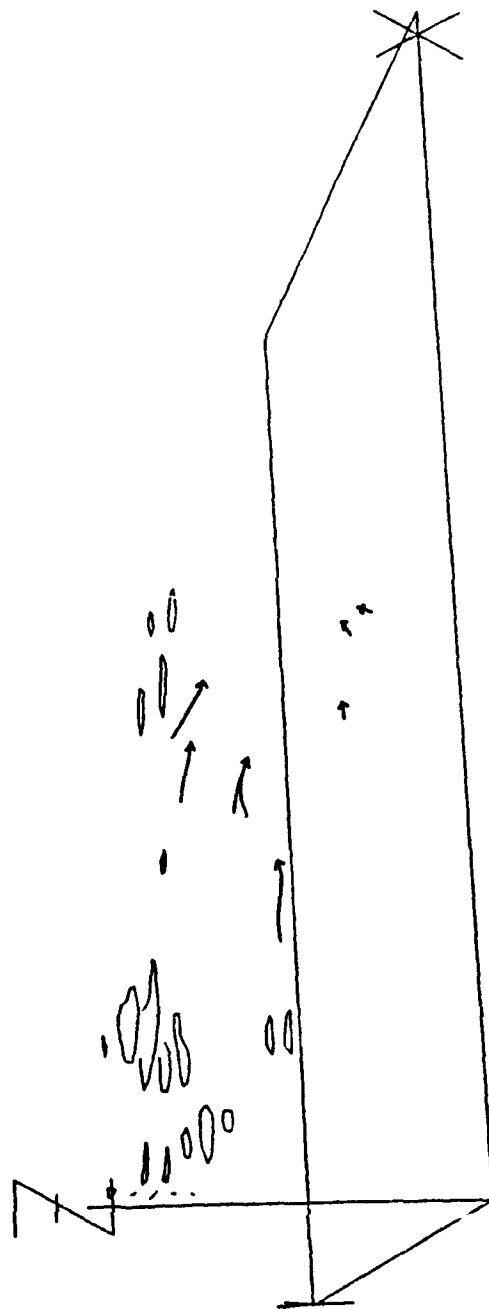


FIGURE 15A-K. Air parcel trajectory segments projected onto three-dimensional reflectivity perspective views for air parcels within the microburst at 2212. Each segment traces an air parcel for a 2.5 min period centered on the analysis time indicated.



88/ 7/11 21 50 15-21 50 15  
 (X,Y,Z) EYE POSITION (KM):  
 LUMINANCE (-40.0, -78.0, 19.2)  
 TOTAL 00.00

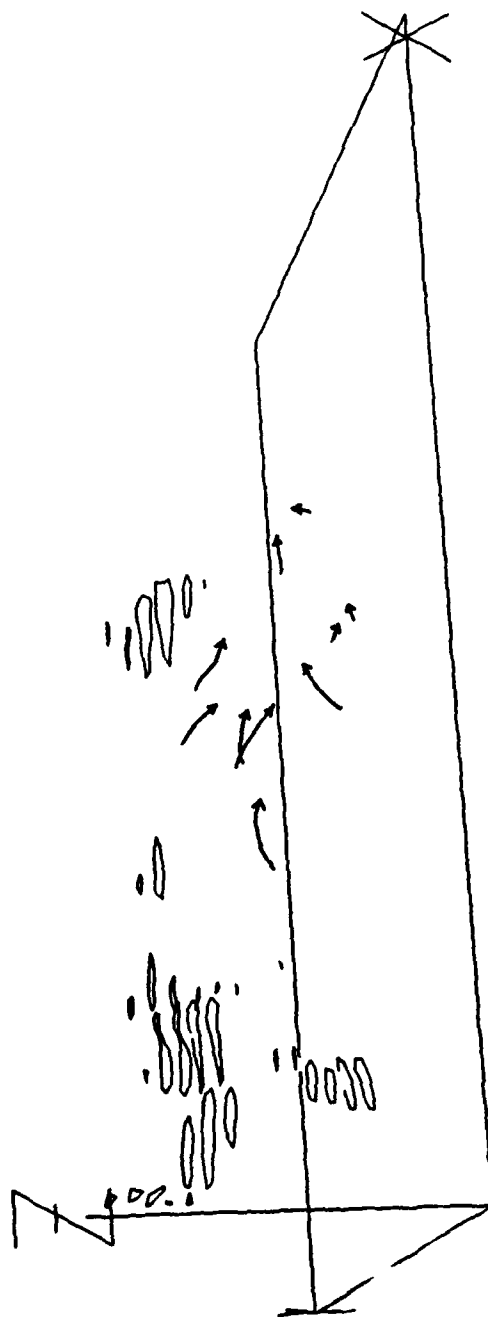


Fig. 15b

88/ 7/11    21 52 15-21 52 15    LUMBIN    215231N    102    55.50  
 (X,Y,Z)    EYE POSITION (KM):    ( -40.0, -78.0, 19.2)

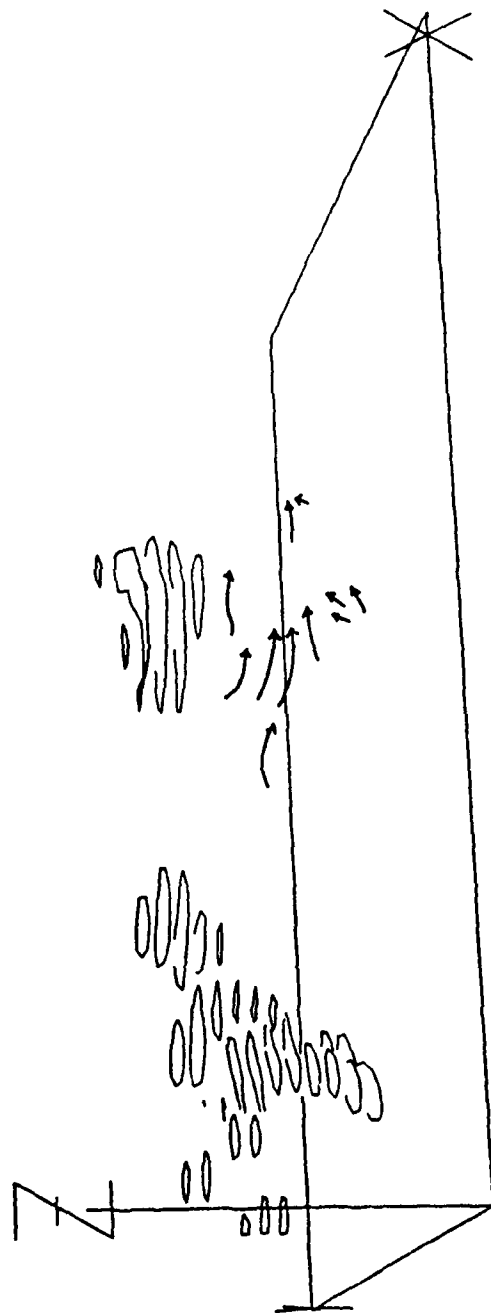


Fig. 15c

88/ 7/11    21 58 15-21 58 15    COMBIN    2158SYN    UBZ    HDUVE    33.00  
 (X,Y,Z)    EYE POSITION (KM):    ( -40.0, -78.0, 19.2)

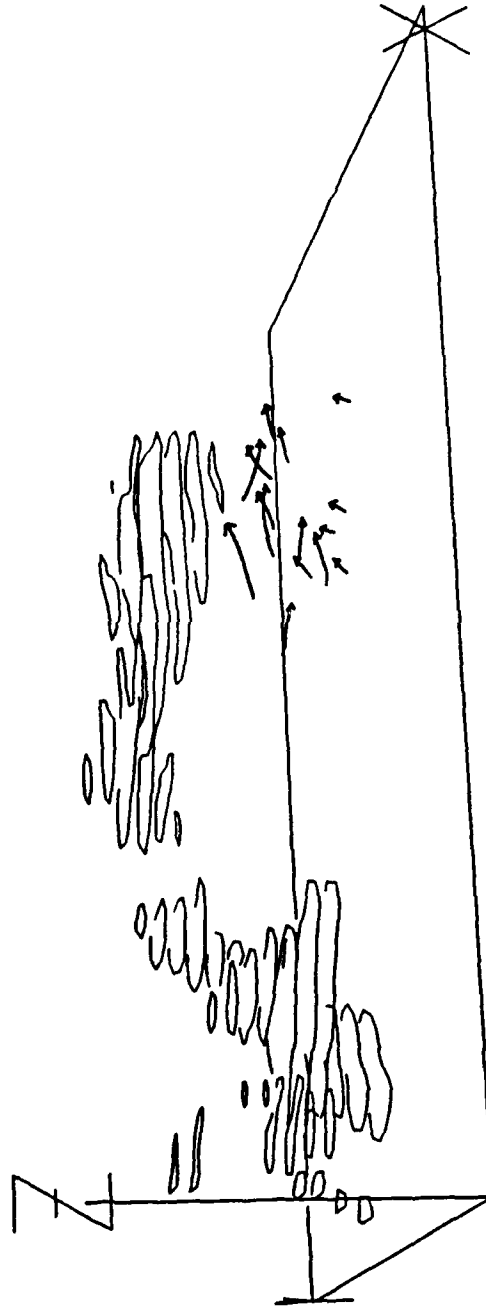


Fig. 15e

88/ 7/11 21 55 15-21 55 15  
 (X,Y,Z) EYE POSITION (KM): ( -40.0, -78.0, 19.2)

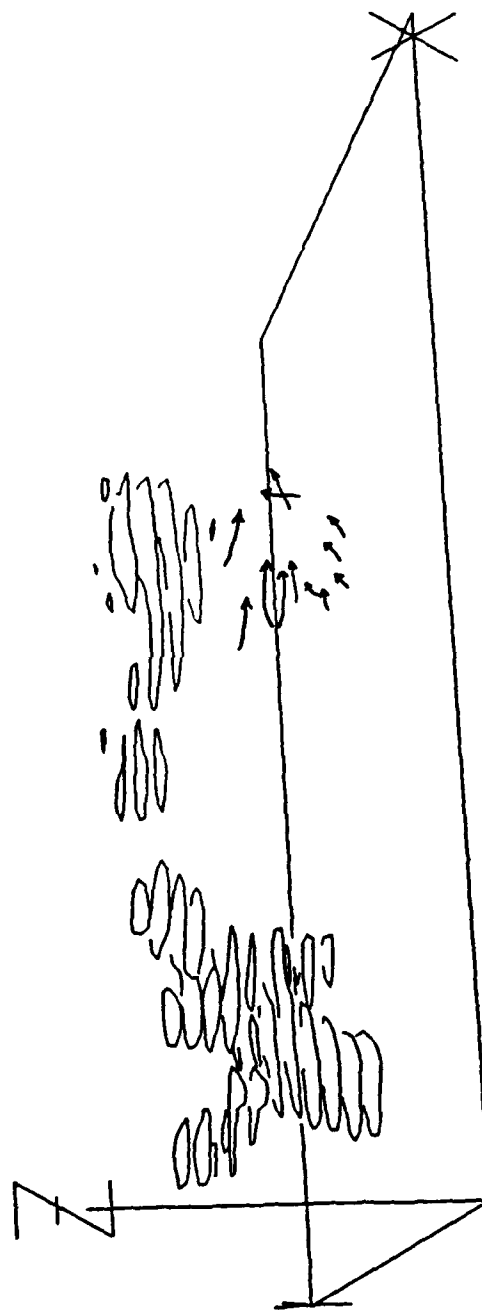


Fig. 15d

88/ 7/11    22 0 15-22 0 15    COMBIN    2200SYN    DBZ    ABOVE    33.00  
 (X,Y,Z)    EYE POSITION (KM):    ( -40.0, -78.0, 19.2)

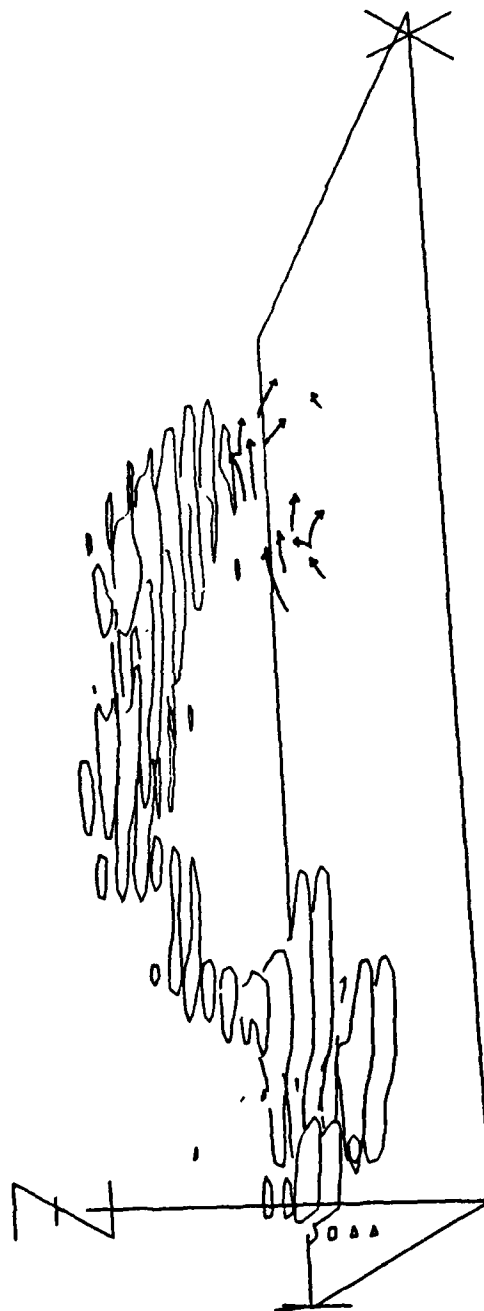


Fig. 15f

88/ 7/11    22   2 44-22   2 44    COMBIN   2202SYN   UBZ    HDOVE   JJ.00  
 (X,Y,Z)    EYE POSITION (KM):    ( -40.0, -78.0, 19.2)

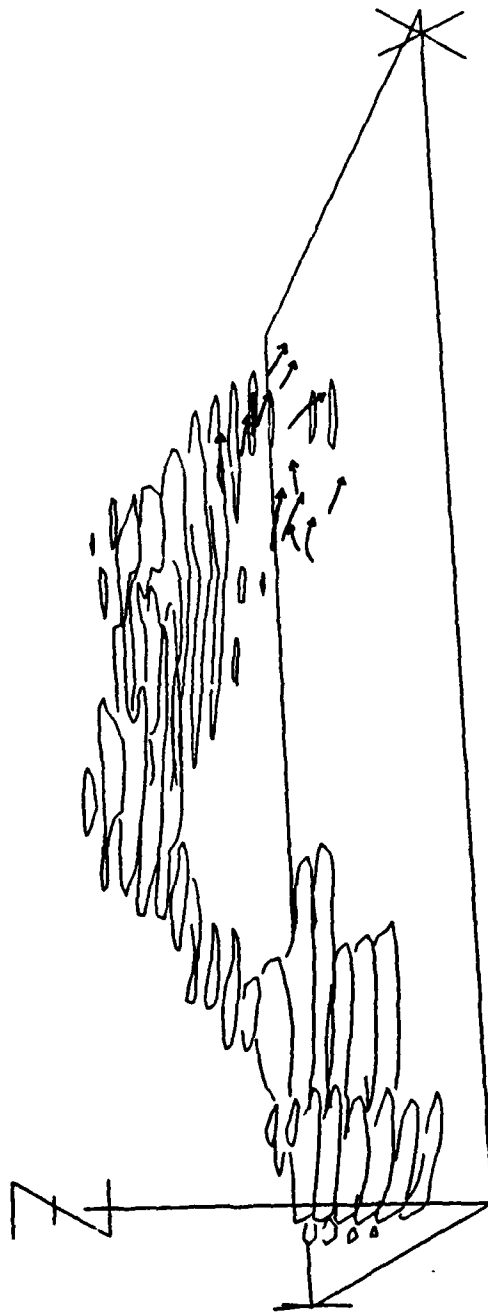


Fig. 15g

88/ 7/11    22 5 16-22 5 16    COMBIN    2205SYN    UBZ    HBUVE    33.00  
 (X,Y,Z)    EYE POSITION (KM):    ( -40.0, -78.0, 19.2)

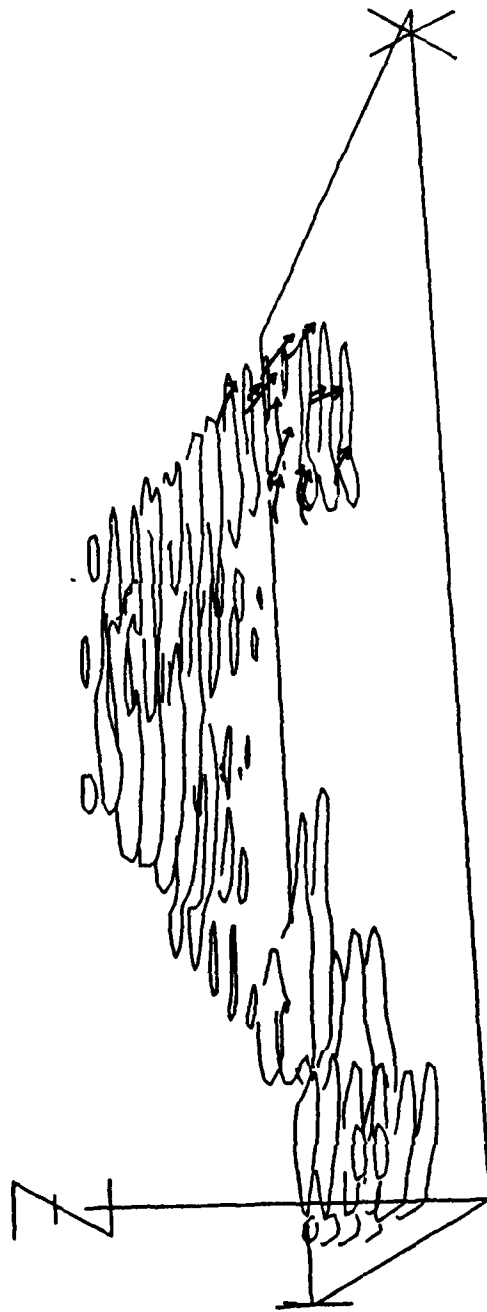


Fig. 15h

88/ 7/11 22 7 45-22 7 45 COMBIN 2207SYN DBZ ABOVE 33.00  
 (X,Y,Z) EYE POSITION (KM): ( -40.0, -78.0, 19.2)

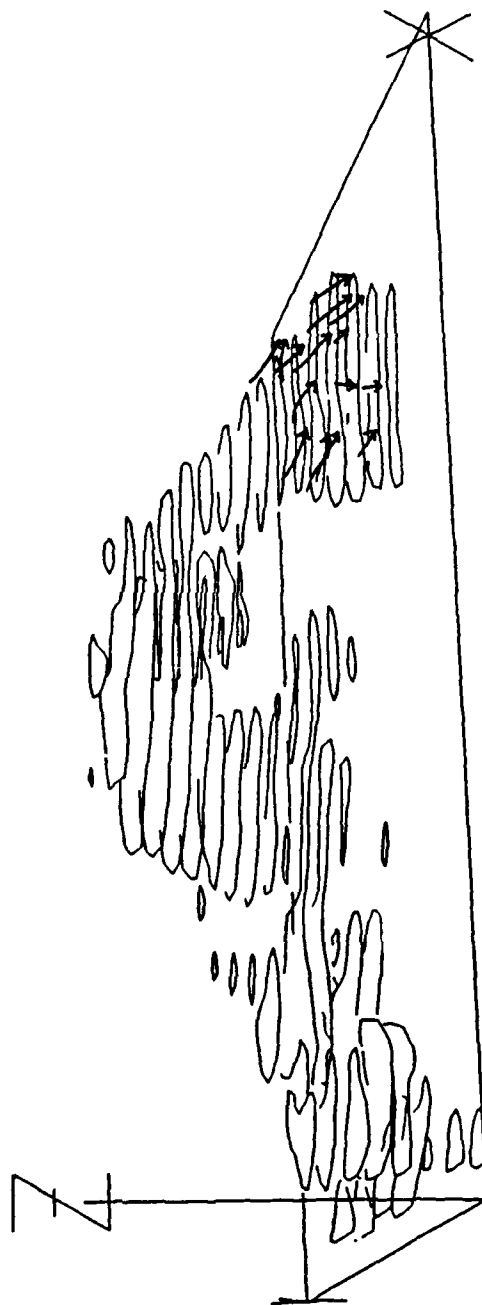


Fig. 15i



88/ 7/11    22 10 19-22 10 19    COMBIN    2210SYN    DBZ    ABOVE    33.00  
 (X,Y,Z)    EYE POSITION (KM):    ( -40.0, -78.0, 19.2)

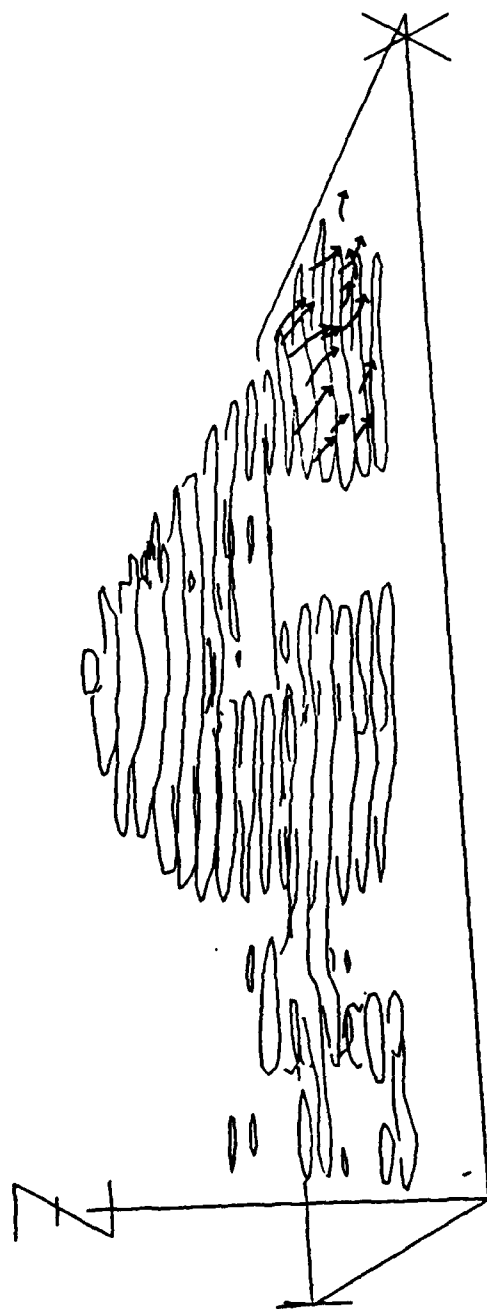


Fig. 15j

00/ 1/11 22 12 17-22 12-11  
 (X,Y,Z) EYE POSITION (KM): (-40.0, -78.0, 19.2)

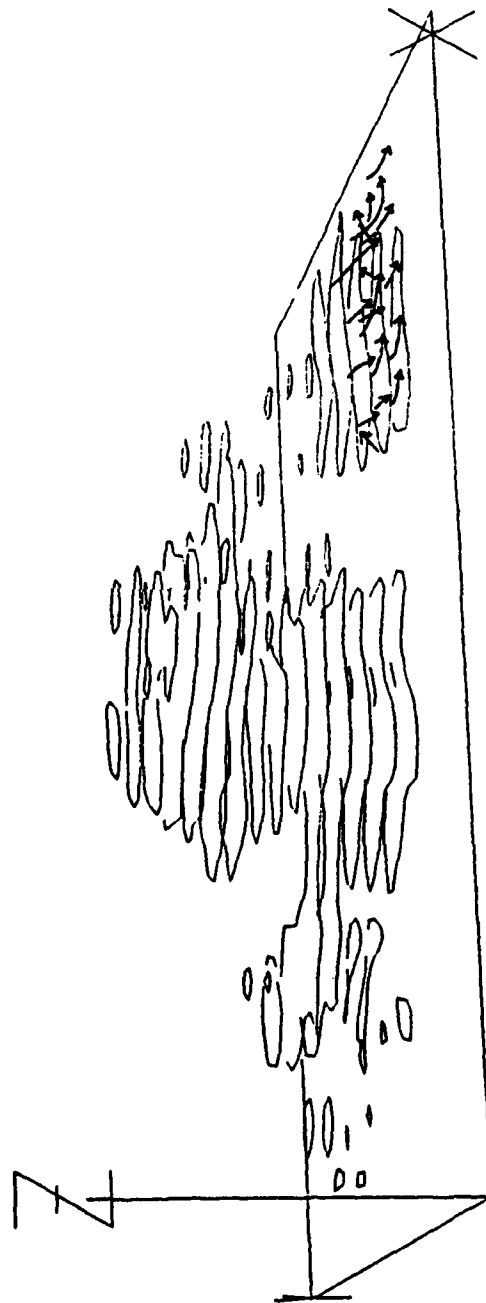


Fig..15k

trajectories are clearly within the region of reflectivity greater than 33 dBZ<sub>e</sub> and have begun to descend. After this time, the region of high reflectivity rapidly descends and the downdraft accelerates until it impinges upon the surface between 2210 and 2212, creating the microburst.

Figure 16 shows a set of 20 trajectories that are all initiated on a regular  $0.75 \times 0.75$  km grid centered on the microburst at 2212. This figure shows that no parcel originated from a height above 6.25 km (4.65 km AGL); none of the origins were above the minimum  $\theta_e$  level.

To examine this further, trajectories progressing forward with time are initiated within the general area that reverse trajectories indicate 2212 surface parcels originate at. However, these air parcels were initiated at heights above 7.2 km (5.6 km AGL). The trajectories began at 2148. Of the 32 parcel locations chosen for this analysis, only a few descended a significant distance. All parcels showed significant displacement to the south and east and most ascended to near echo top. In general, it is likely that no air parcels originating above the minimum  $\theta_e$  level descended to the surface during this microburst. Yet, it is quite clear that the hydrometeors did come from above 7.2 km. The region responsible for most of the cooling and downdraft acceleration is the broad area of low  $\theta_e$  located between 5 and 7 km MSL (3.4 and 5.4 km AGL).

Figure 17 presents a simplified, schematic evolution of this microburst prior to its arrival at the surface. This figure depicts hydrometeor trajectories, not air parcel trajectories. Hydrometeors form and are carried upward in several strong convective updrafts that exist in a region where environmental winds are generally light due to effects of preexisting convection. As air parcels reach the equilibrium level, hydrometeors continue to grow until they become too heavy to be supported by the updrafts and begin slowly falling. However, the strong convective updrafts reach a level of strong northwesterly winds aloft. These winds then carry the hydrometeor plume east, but more importantly, south of the preexisting convective area. Thus, as they descend these hydrometeors reach a level of low  $\theta_e$  air that does not exist within the environment contaminated by convection. As any liquid water evaporates and the frozen hydrometeors sublimate, air containing them becomes very negatively buoyant and begins to accelerate rapidly downward, ultimately reaching the surface as a microburst.

## V. Concluding Remarks

On 11 July 1988, atmospheric conditions were conducive to initiation and maintenance of deep convection. The temperature lapse rate was nearly dry adiabatic to 5.2 km (4.6 km AGL). Warm, moist air aloft advected into the area from the west throughout the day and winds near the surface were generally easterly, which may have provided extra lifting at the edge of the mountains to aid in storm development. In the sounding analysis, three features were evident which contributed significantly to the development of the intense microburst: a region of strong westerly winds with a maximum at 6.8–7.2 km (5.2–5.6 km AGL), a sharp minimum in  $\theta_e$  at 7.2 km (5.6 km AGL) with a secondary minimum near

11 JULY 1988

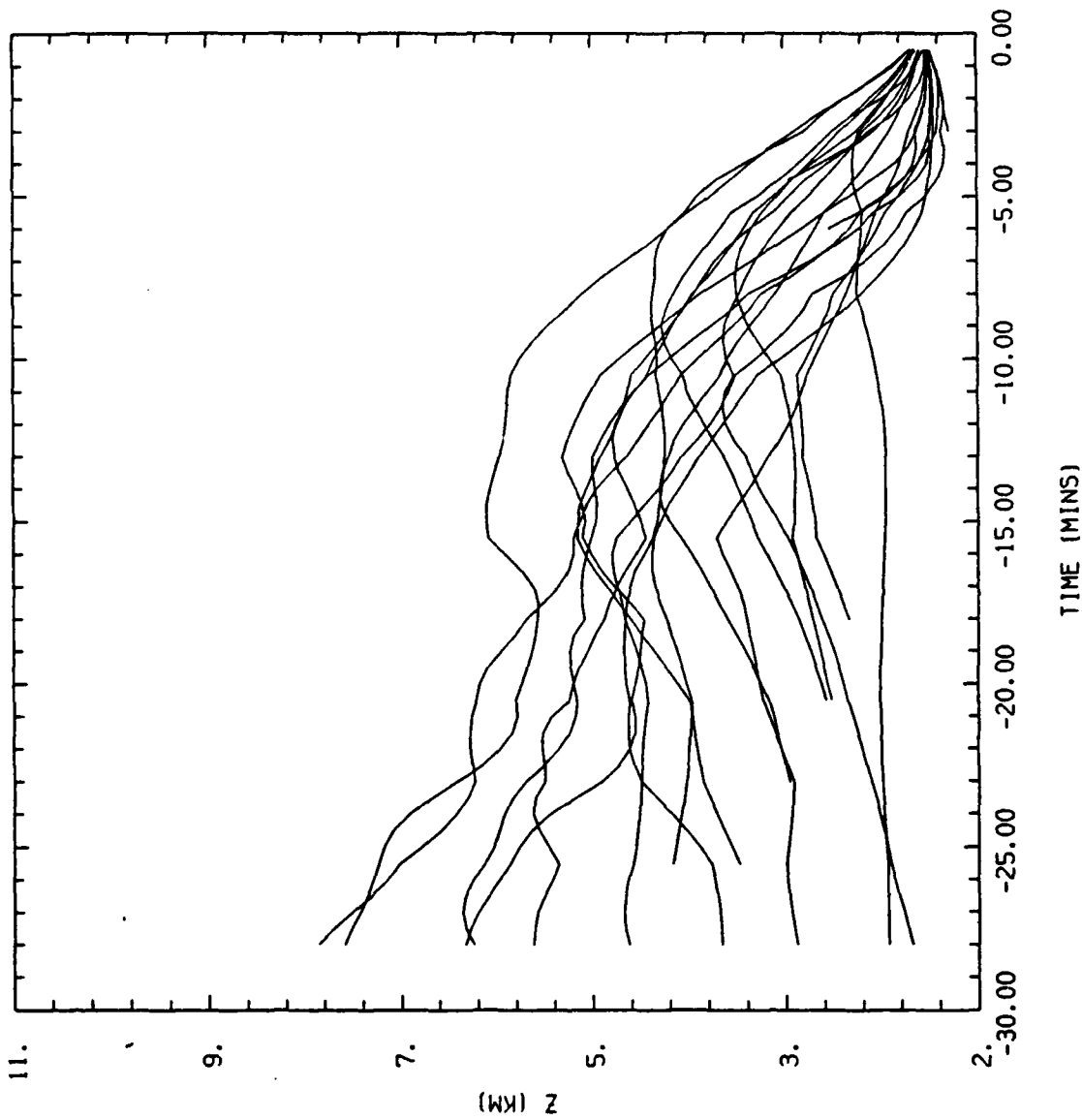
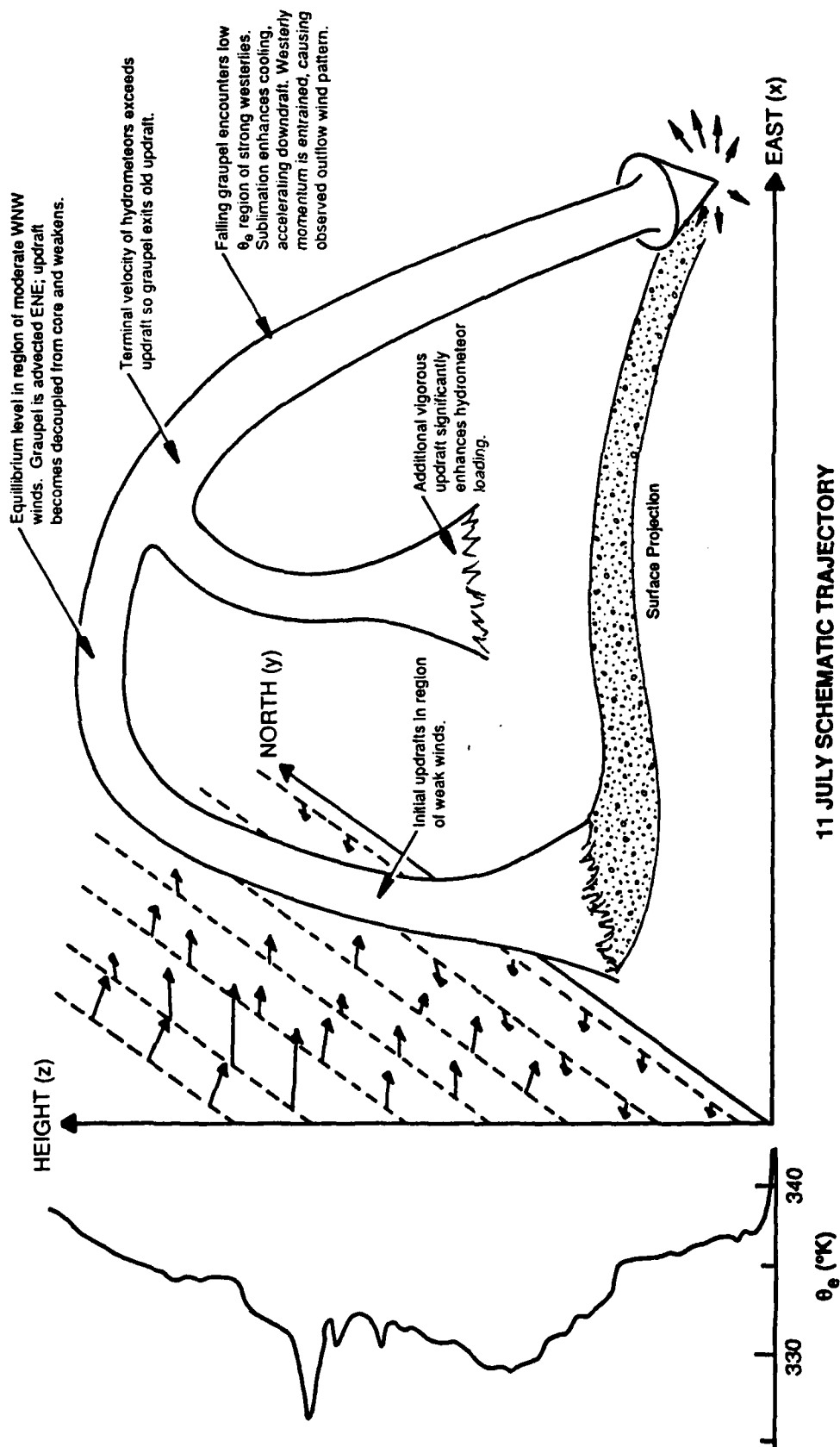


FIGURE 16. A set of 20 trajectories all initiated a 400 m AGL on a rectangular  $4 \times 5$  grid with  $0.75 \times 0.75$  km spacing. All trajectories are initiated at 2212 and proceed backwards in time. Time is along the horizontal axis while height is along the vertical axis.



#### 11 JULY SCHEMATIC TRAJECTORY

FIGURE 17. A schematic diagram depicting the evolution of particle trajectories responsible for the 11 July microburst. The sounding to the left indicates  $\theta_e$  with height near the time of the microburst. Three-dimensional wind structure aloft may be deduced by the wind vectors on the left-hand side of the figure immediately left of the  $\theta_e$  sounding.

5 km (3.4 km AGL), and a high amount of mid-level (around 5–7.2 km, 3.4–5.6 km AGL) moisture.

The parent storm was initiated over the mountains and then moved east-southeast. Updrafts within this complex carried hydrometeors well aloft into a region of strong northwesterlies. Slightly west-northwest of the airport a new cell developed that also contained strong updrafts lifting precipitation particles, presumably graupel, high into the storm complex. These new hydrometeors were carried to the southeast as they reached the level of strong northwesterly winds and merged with similar material from earlier convection to the northwest. As they moved away from the main storm updraft, they fell through fairly moist air, which retarded their sublimation rate. Near 7.2 km (5.6 km AGL), they reached a drier layer containing strong westerly winds where they began sublimating rapidly creating a region of cool air which began to accelerate downward.

Two descending reflectivity cores were created in this manner. One was carried farther to the east and eventually descended to the surface ahead of low-level outflow produced by the main storm cell. Since it descended onto a relatively undisturbed boundary layer, this outflow became quite intense, and created the strong microburst on 26A. The second core descended into a boundary layer heavily modified by storm outflow, which resulted both in spreading it in a northwest-southeasterly elongation and diminishing its intensity. This was the larger and weaker microburst core south and west of the airport.

These microbursts lasted less than a half hour; outflow from the subsequent line of cells lasted over an hour. The microbursts clearly originated from a core aloft whose development is observed in the dual-Doppler radar analyses. Furthermore, the main microburst clearly originated when a reflectivity core exited a region that had been heavily modified by pre-existing convection and entered a region retaining a region of low  $\theta_e$  air at mid levels as described in the sounding analyses above. Because temperatures were below freezing in this region, the phase changes that occurred were sublimation and evaporation of supercooled liquid water. Sublimation will more effectively cool air than evaporation alone. This sublimation appears to have created a very cold pool of air aloft much denser than its environment, possibly explaining the rapid onset and unusual strength of this event.

This report describes the microburst development almost 25 minutes prior to its most intense period over Stapleton International Airport and nearly 20 min before there was any evidence of it at the surface. Core C appears after about 7 to 10 min of sustained 7–10  $\text{m s}^{-1}$  updraft in a region roughly between cores A and B. The forcing required to initiate the parent updraft could have come from a convergence line that existed over the airport for some time prior to this. It is not yet clear whether or not this updraft is surface-based or whether it originated well above the surface aided by some forcing mechanism aloft. Further work is continuing on the the origins of this microburst.

### Acknowledgements

The TDWR project has benefited from the participation of many people. In particular, we would like to recognize contributions by Steve Campbell (Lincoln Laboratory), Fred Proctor (MESO, Inc.), Roland Bowles (NASA) and Rod Wingrove (NASA). Bob Ireland of United Airlines provided a thorough analysis of flight recorder data. Cleon Biter, as Operations Director for the 1988 TDWR OT&E, and John McCarthy, as the Director of the RAP, contributed a great deal toward the success of the program. Dr. Borislava Stankov of NOAA provided the weather maps and profiler data. The help of Patrice Kucera and Terry Trieu in radar data analysis is also acknowledged.

This work was is funded by NCAR, the National Science Foundation, and the FAA (through Interagency Agreement DTFA01-82-Y-10513).

### References

- R. Bowles, and R. Targ, 1988: Windshear detection and avoidance: Airborne systems perspective. 16<sup>th</sup> Congress of the International Council of the Aeronautical Sciences, Jerusalem, Israel.
- Corbet, J. and C. Burghart, 1988: A User's Manual for Robot. NCAR Field Observing Facility internal publication, 52 pp. (available from NCAR/FOF, P.O. Box 3000, Boulder, CO 80307)
- Cornman, L.B., P.C. Kucera, M.R. Hjelmfelt and K.L. Elmore, 1989: Short time-scale fluctuations in microburst outflows as observed by Doppler radar and anemometers. *Preprints, 24<sup>th</sup> Conference on Radar Meteorology*, Tallahassee, Fla., 27-31 March 1989, Amer. Meteor. Soc., Boston, Mass., pp 150-153.
- Cornman, L.B. and F.W. Wilson, 1989: Microburst detection from mesonet data. *Preprints, Third International Conference on the Aviation Weather System*, January 30-February 3, Anaheim, Calif., Amer. Meteor. Soc., Boston, Mass., 35-40.
- Cressman, G.P., 1959: An operational objective analysis system. *Mon. Wea. Rev.*, **87**, 367-374.
- Elmore, K.E., and W. R. Sand, 1989: A cursory study of F-factor applied to Doppler radar. *Preprints, Third International Conference on the Aviation Weather System*, January 30-February 3, Anaheim, Calif., Amer. Meteor. Soc., Boston, Mass., 130-134.
- Fawbush, E.J. and R.C. Miller, 1954: A basis for forecasting peak wind gusts in non-frontal thunderstorms. *Bull. Amer. Meteor. Soc.*, **35**, 13-19.
- Ireland, B., 1989: Flight Safety Incident Investigation 88-46. United Airlines Report.
- Lauritson, D, Z. Malekmadani, C. Moreland, R. McBeth, 1987: The Cross Chain Loran Atmospheric Sounding System (CLASS). Extended abstracts, Sixth Symposium Meteor. Obs. and Instruments., New Orleans, Amer. Meteor. Soc., Boston, Mass., 340-343.
- Mohr, C.G., L.J. Miller, R.L. Vaughan and H.W. Frank, 1986: Merger of mesoscale data sets into a common Cartesian format for efficient and systematic analyses. *J. Atmos. and Oceanic Tech.*, **3**, 143-161.

- Proctor, F.H., 1989: A relationship between peak temperature drop and velocity differential in a microburst. *Preprints, Third International Conference on the Aviation Weather System*, January 30-February 3, Anaheim, Calif., Amer. Meteor. Soc., 5-8.
- Shuman, F. G., 1955: A method of designing finite-different smoothing operators to meet specification. *Joint Numerical Weather Prediction Unit Tech. Memo.*, no. 7.
- Stephens, J.J. and A.L. Polan, 1971: Spectral modification by objective analysis. *Mon. - Wea. Rev.*, **99**, 374-378.
- Stephens, J.J. and J.M. Stitt, 1970: Optimum influence radii for interpolation with the method of successive corrections. *Mon. Wea. Rev.*, **98**, 680-687.
- Wilson, F.W., Jr. and J. A. Flueck, 1986: A study of the methodology of low-altitude wind shear detection with special emphasis on the Low Level Wind Shear concept. Report No. DOT/FAA/PM-86/4. U.S. Dept. of Transportation, Federal Aviation Administration, Washington, D.C.
- Wolfson, M. M., J.T. DiStefano and B. E. Forman, 1987: The FLOWS (FAA-Lincoln Laboratory Operational Weather Studies) automatic weather station network in operation. Project Report ATC-134, MIT Lincoln Laboratory, Report NO. DOT/FAA/PM-85-27. U.S. Dept. of Transportation Federal Aviation Administration, Washington, D.C.



### Figure Captions

- FIGURE 1. Locations of radars and surface mesonet stations during the 1988 TDWR OT&E at Stapleton International Airport, Denver, Colorado. The airport runways are also shown.
- FIGURE 2. Response functions for Hanning 5 pass and Liese 2 step filters used in dual-Doppler analyses techniques. The filtering function is plotted against the length scaled as number of data grid points.
- FIGURE 3A-C. NWS upper level data plotted for 1200 UTC, 11 July 1988. a) 500 mb, b) 700 mb and c) 850 mb. Solid lines are constant geopotential height; dashed lines are constant temperature.
- FIGURE 4A-C. As in Fig. 3 but for 0000 UTC, 12 July 1988.
- FIGURE 5. Data from the NOAA 6 channel microwave radiometer from 1100 UTC 11 July 1988 through 1100 UTC 12 July 1988. Time runs from right to left. Potential temperature ( $\theta$ ) and total water vapor mixing ratio ( $q$ ) are shown from the surface to nearly 12 km MSL.
- FIGURE 6. CLASS sounding from 1100 MDT (1700 UTC) 11 July 1988. Data are plotted on a skew-T diagram. Temperature and dewpoint are shown. Wind barbs on the right point in the direction the wind is blowing *toward*. Altitude in km MSL is shown on the right.
- FIGURE 7. Equivalent potential temperature ( $\theta_e$ ) plotted against height from the 1700 and 2004 UTC CLASS soundings.
- FIGURE 8. As in Fig. 6 but for 1404 MDT (2004 UTC) 11 July 1988.
- FIGURE 9. Events plotted against time for the 11 July 1988 microburst. A scale for wind shear difference in knots is indicated on the left. Data sources are indicated.
- FIGURE 10A-G. Three-dimensional reflectivity perspective views of the microburst-producing storm of 11 July 1988. The viewer is looking toward the northeast and is located at 40 km west and 78 km south of FL2 and is 19.2 km MSL. The 33 dBZ<sub>e</sub> contour at discrete analysis levels (explained in the text) is contoured. Analyses for 2148, 2150, 2152, 2155, 2158, 2200, and 2202 UTC during storm development, are shown.
- FIGURE 11A-D. As in Fig. 10 but for 2205, 2207, 2210 and 2212 UTC during the microburst alarm period.
- FIGURE 12A-C. As in Fig. 10 but for 2215, 2217 and 2220 UTC during storm dissipation.
- FIGURE 13. Air parcel trajectories obtained from dual-Doppler analysis. The trajectories are shown in three dimensions with projections on a horizontal plane indicated. Each tick mark along a trajectory ribbon indicates 30 s of travel.
- FIGURE 14A-C. As in Fig. 13 but projections on the  $[x, y, z]$  surfaces are shown. Trajectory projections are shown on a) all three surfaces, b) the  $y - z$  surface, c) the  $x - z$  surface and d) the  $x - y$  surface.

FIGURE 15A-K. Air parcel trajectory segments projected onto three-dimensional reflectivity perspective views for air parcels within the microburst at 2212. Each segment traces an air parcel for a 2.5 min period centered on the analysis time indicated.

FIGURE 16. A set of 20 trajectories all initiated a 400 m AGL on a rectangular  $4 \times 5$  grid with  $0.75 \times 0.75$  km spacing. All trajectories are initiated at 2212 and proceed backwards in time. Time is along the horizontal axis while height is along the vertical axis.

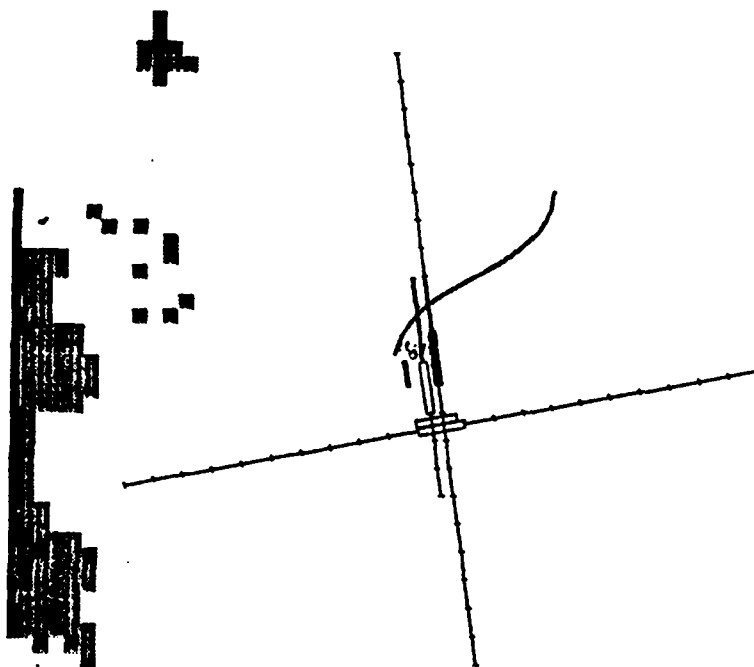
FIGURE 17. A schematic diagram depicting the evolution of particle trajectories responsible for the 11 July microburst. The sounding to the left indicates  $\theta_e$  with height near the time of the microburst. Three-dimensional wind structure aloft may be deduced by the wind vectors on the left-hand side of the figure immediately left of the  $\theta_e$  sounding.

## **Appendix A: Geographical Situation Display (GSD)**

These diagrams are printed directly from the display screen at the TDWR verifier's station and are the displays sent to the airport control tower. These cover the time period pertinent to the intense microbursts.

The runways are shown as elongated rectangles; when darkened they indicate an alarmed state. Approaches to each runway, marked in 1 nm divisions, are also shown and are highlighted when alarmed. Gust fronts are indicated by long curving lines, wind shear alerts by open ellipses and microbursts by darkened ellipses. The numerical values enclosed by the alarms indicate the maximum expected airspeed loss in kt. Precipitation is shown by shaded areas which correspond to the six Weather Service radar intensity levels. Range rings are in nm.

The correct date and time are given by PDATE and MTIME near the bottom right of each display. The GSD microbursts are updated every minute; the gust fronts are updated every 5 min and the last update time is indicated by GTIME.



NCAR GSD

RANGE

☐ 5m ☒ 10m ☐ 30m ☐ 50m

SCREEN

☒ 1 ☒ 2 ☒ 3 ☒ 4  
☒ 5 ☒ 6 ☒ 7 ☒ 8

MAPS

☐ Vortec & lines  
☐ ASR rings  
☐ Airports  
☐ Interstates

PRECIPITATION LEVELS

☒ OFF ☒ MIN ☐ 3-6 ☐ 8-9

WIND SHIFT:

☒ OFF ☒ ON

DATE: 09/09/88

TIME: 17:59:55

PDATE: 07/11/88

MTIME: 21:36:01

OTIME: 21:34:00

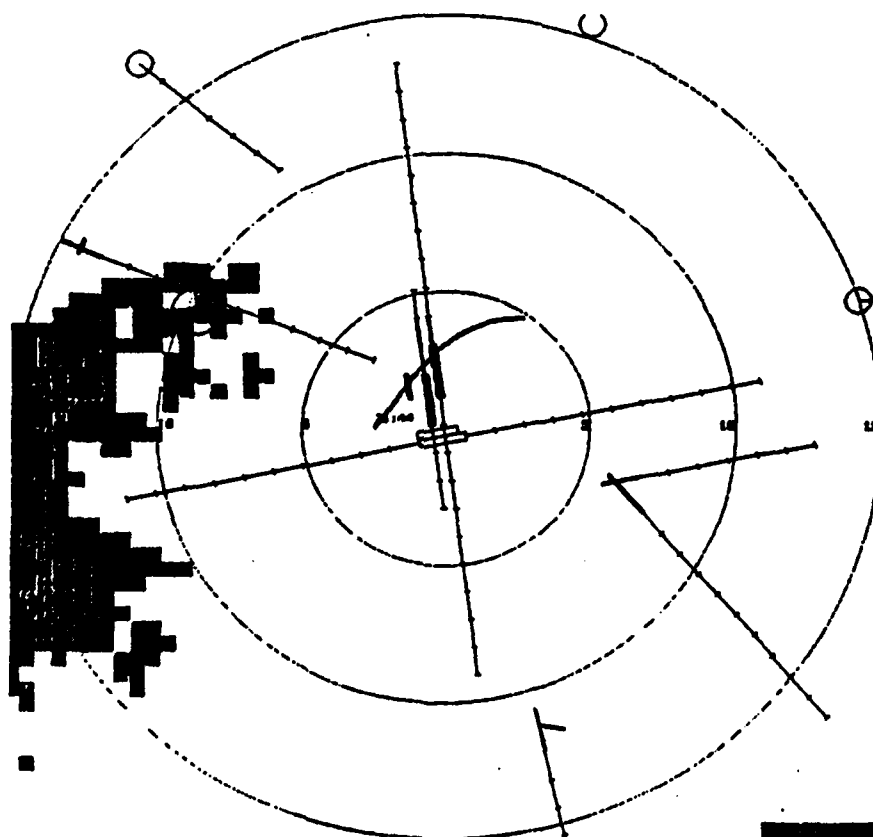
MB: UP

JF: UP

PRECIP: UP

LLMAS: DOWN

[Print Screen](#)



NCAR GSD

RANGE

☐ 5m ☒ 10m ☐ 30m ☐ 50m

SCREEN

☒ 1 ☒ 2 ☒ 3 ☒ 4  
☒ 5 ☒ 6 ☒ 7 ☒ 8

MAPS

☐ Vortec & lines  
☐ ASR rings  
☐ Airports  
☐ Interstates

PRECIPITATION LEVELS

☒ OFF ☒ MIN ☐ 3-6 ☐ 8-9

WIND SHIFT:

☒ OFF ☒ ON

DATE: 09/09/88

TIME: 18:10:47

PDATE: 07/11/88

MTIME: 21:48:04

OTIME: 21:46:02

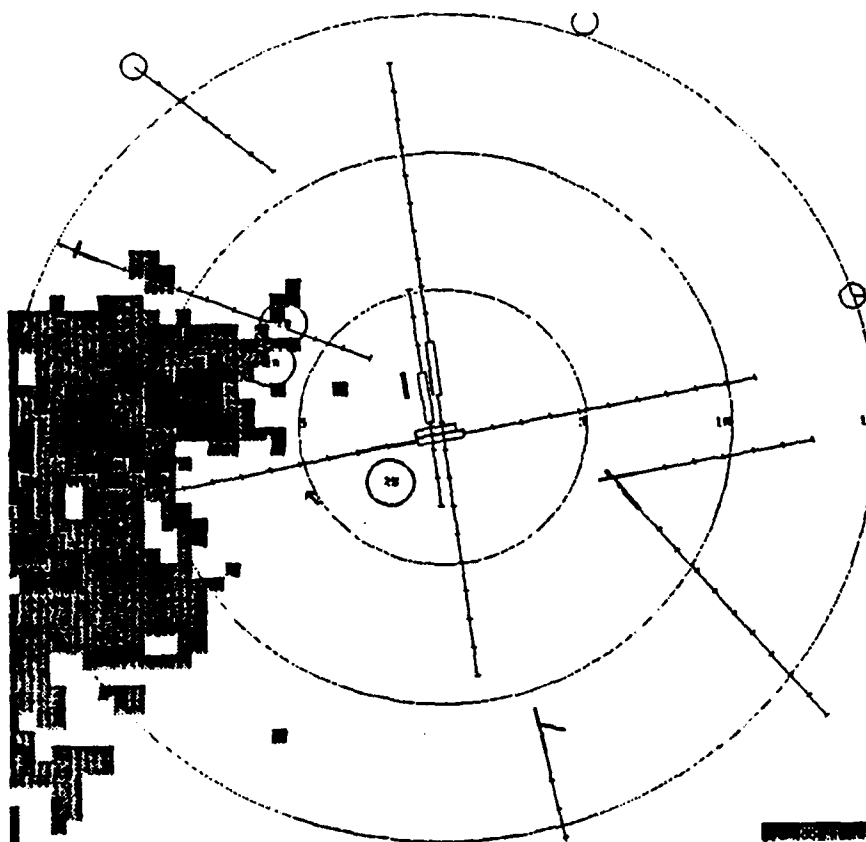
MB: UP

JF: UP

PRECIP: UP

LLMAS: DOWN

[Print Screen](#)



NCAR GSD

RANGE

☒ 3m ☒ 15m ☒ 30m ☒ 50m

SCREEN

☒ 1 ☒ 2 ☒ 3 ☒ 4  
☒ 5 ☒ 6 ☒ 7 ☒ 8

MAPS

☐ Vortec & fines  
☒ ASR rings  
☒ Airports  
☐ Interstates

PRECIPITATION LEVELS

☒ OFF ☒ 1-2 ☒ 3-4 ☒ 5-6

WIND SHIFT:

☒ OFF ☒ ON

DATE: 09/09/88

TIME: 18:23:19

PDATE: 07/11/88

MTIME: 21:56:39

OTIME: 21:54:01

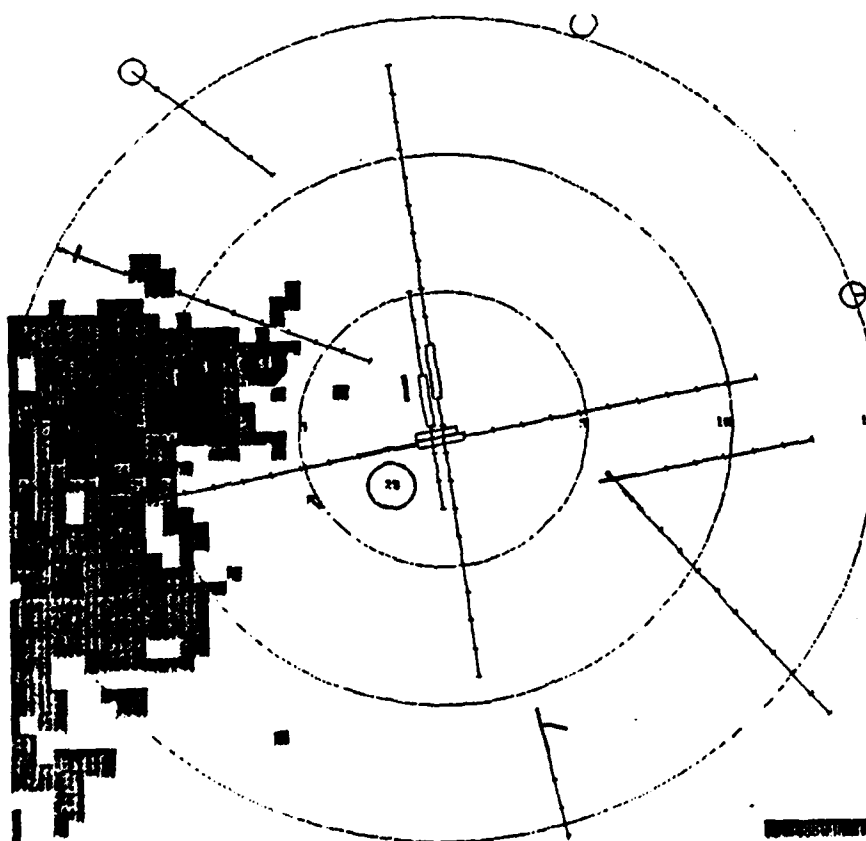
MB: UP

GF: UP

PRECIP: UP

LLWS: DOWN

☒ Print Screen



NCAR GSD

RANGE

☒ 3m ☒ 15m ☒ 30m ☒ 50m

SCREEN

☒ 1 ☒ 2 ☒ 3 ☒ 4  
☒ 5 ☒ 6 ☒ 7 ☒ 8

MAPS

☐ Vortec & fines  
☒ ASR rings  
☒ Airports  
☐ Interstates

PRECIPITATION LEVELS

☒ OFF ☒ 1-2 ☒ 3-4 ☒ 5-6

WIND SHIFT:

☒ OFF ☒ ON

DATE: 09/09/88

TIME: 18:24:59

PDATE: 07/11/88

MTIME: 21:58:03

OTIME: 21:54:01

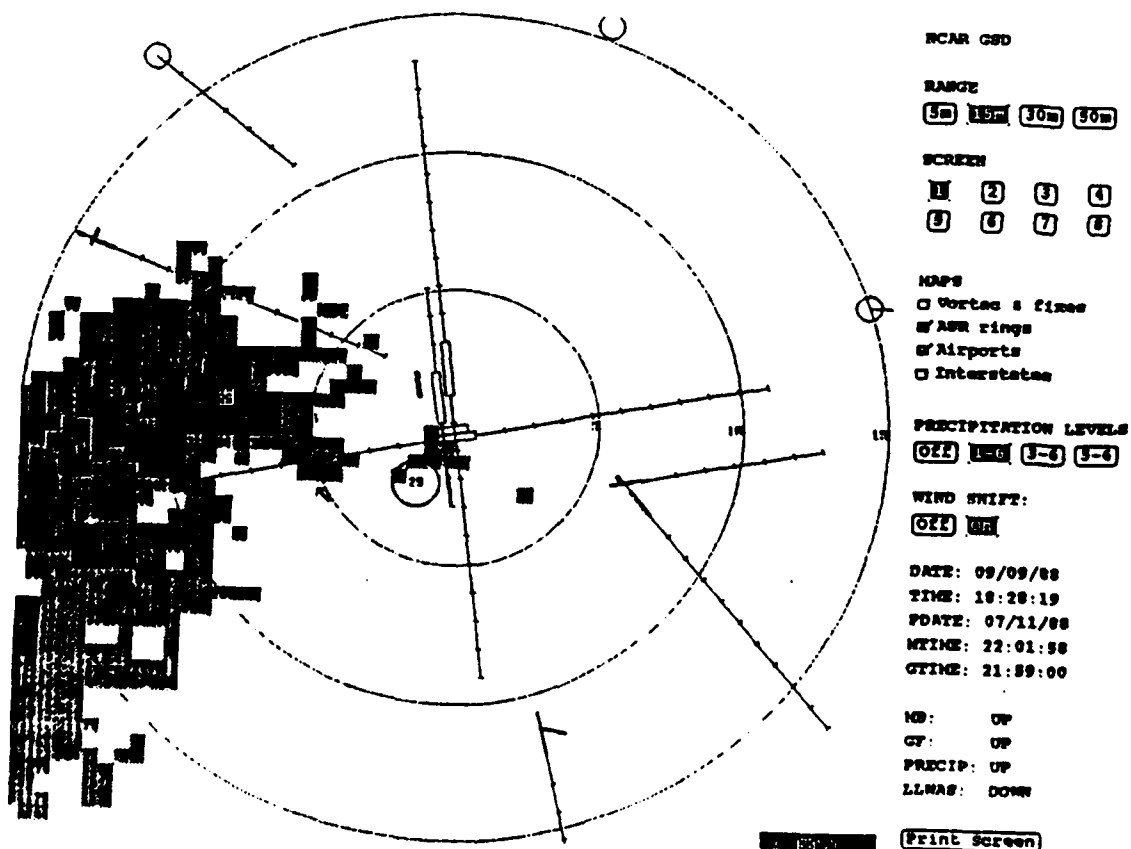
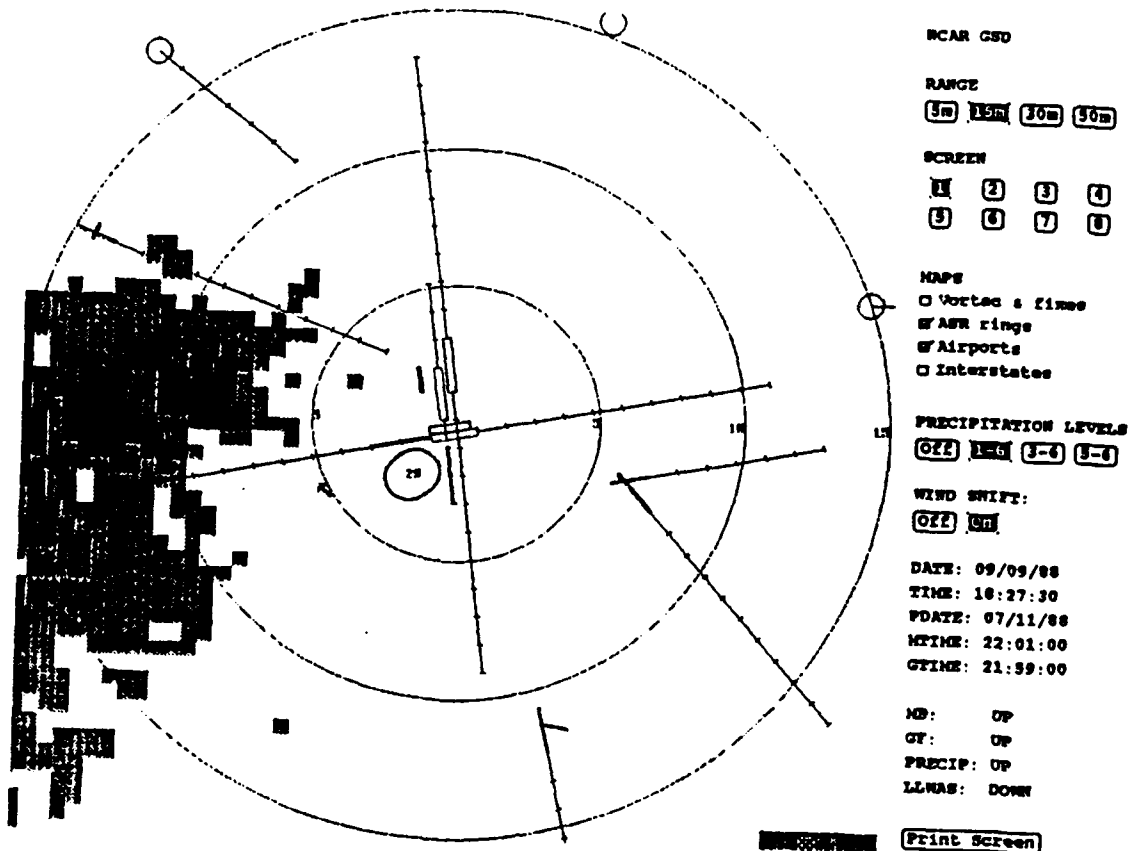
MB: UP

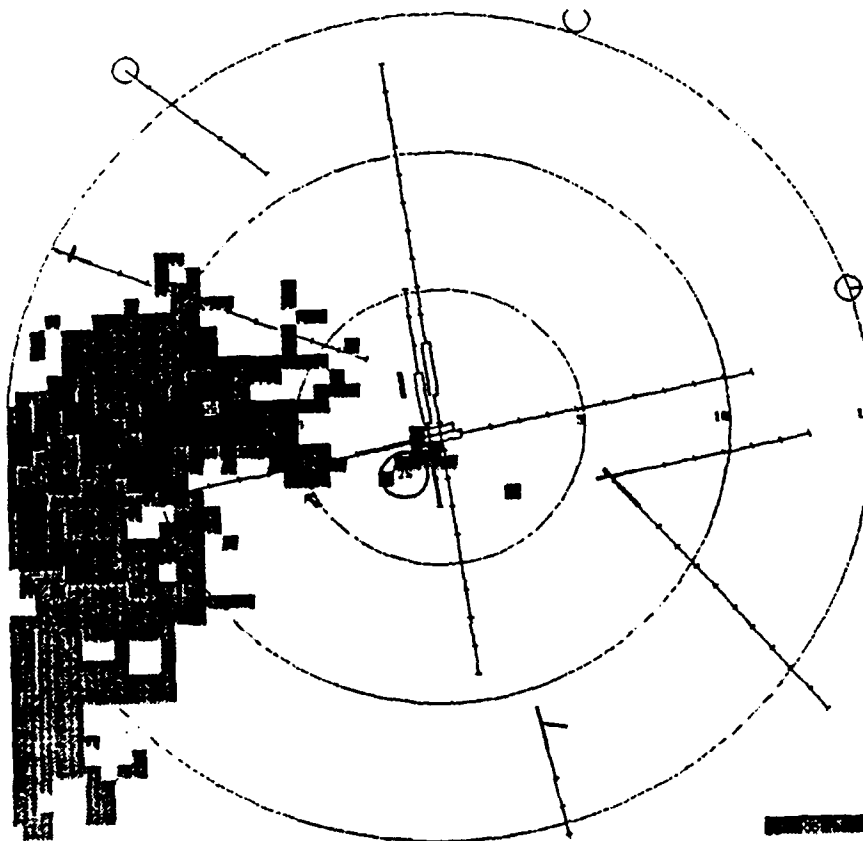
GF: UP

PRECIP: UP

LLWS: DOWN

☒ Print Screen





NCAR GSD

RANGE

☐ 5m ☐ 15m ☐ 30m ☐ 50m

SCREEN

☐ 1 ☐ 2 ☐ 3 ☐ 4  
☐ 5 ☐ 6 ☐ 7 ☐ 8

MAPS

☐ Vortec & lines  
☐ ASR rings  
☐ Airports  
☐ Interstates

PRECIPITATION LEVELS

☐ OFF ☐ 1-6 ☐ 3-8 ☐ 5-8

WIND SHIFT:

☐ OFF ☐ ON

DATE: 09/09/88

TIME: 18:29:12

FOATE: 07/11/88

MTIME: 22:02:57

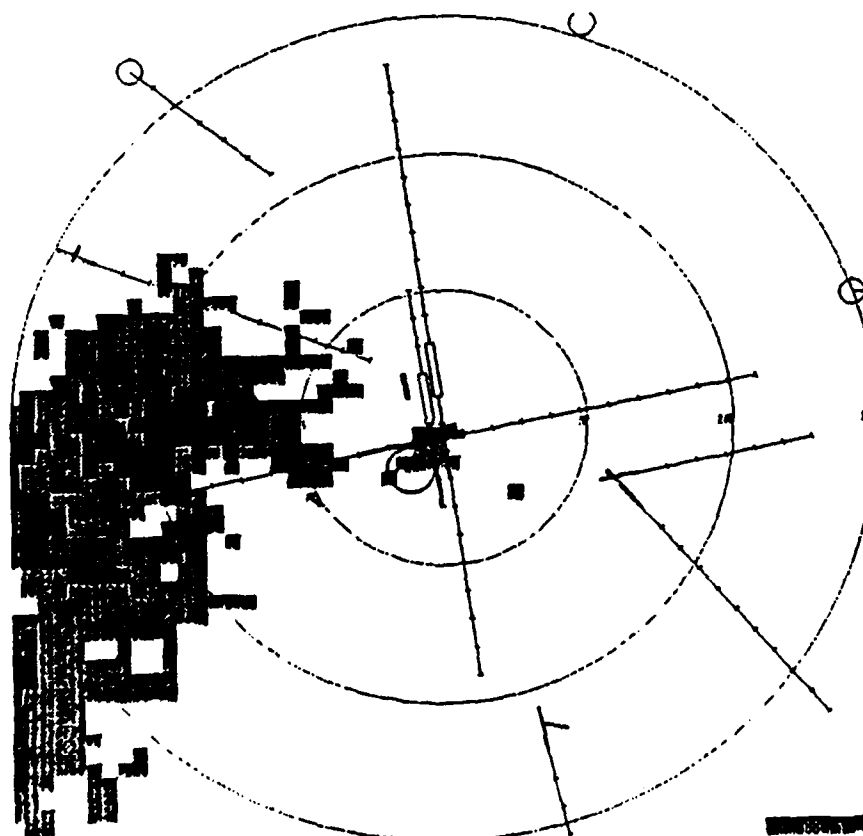
OTIME: 21:59:00

MB: UP

CT: UP

PRECIP: UP

LLWS: DOWN



NCAR GSD

RANGE

☐ 5m ☐ 15m ☐ 30m ☐ 50m

SCREEN

☐ 1 ☐ 2 ☐ 3 ☐ 4  
☐ 5 ☐ 6 ☐ 7 ☐ 8

MAPS

☐ Vortec & lines  
☐ ASR rings  
☐ Airports  
☐ Interstates

PRECIPITATION LEVELS

☐ OFF ☐ 1-6 ☐ 3-8 ☐ 5-8

WIND SHIFT:

☐ OFF ☐ ON

DATE: 09/09/88

TIME: 18:30:49

FOATE: 07/11/88

MTIME: 22:04:01

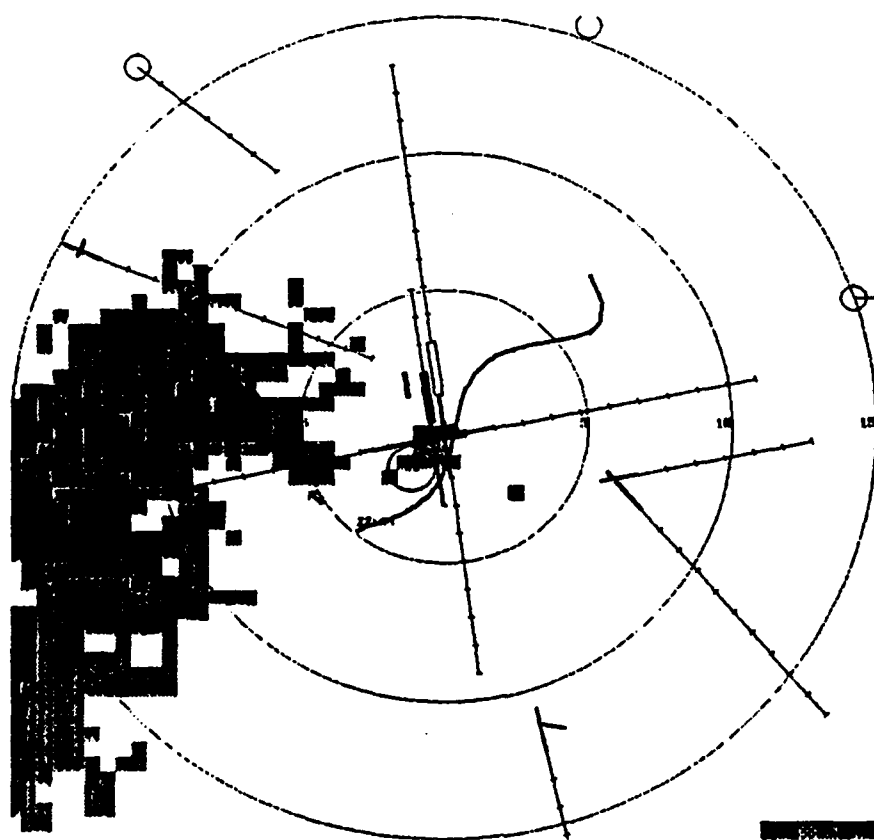
OTIME: 21:59:00

MB: UP

CT: UP

PRECIP: UP

LLWS: DOWN



NCAR GSD

RANGE

☒ 5m ☒ 15m ☒ 30m ☒ 50m

SCREEN

☒ 1 ☒ 2 ☒ 3 ☒ 4  
☒ 5 ☒ 6 ☒ 7 ☒ 8

MAPS

☒ Vortices & lines  
☒ ASR rings  
☒ Airports  
☒ Interstates

PRECIPITATION LEVELS

☒ 0.2 ☒ 1.0 ☒ 3-6 ☒ 8-1

WIND SHIFT:

☒ OFF ☒ ON

DATE: 09/09/88

TIME: 18:31:40

PDATE: 07/11/88

WTIME: 22:04:01

GTIME: 22:04:01

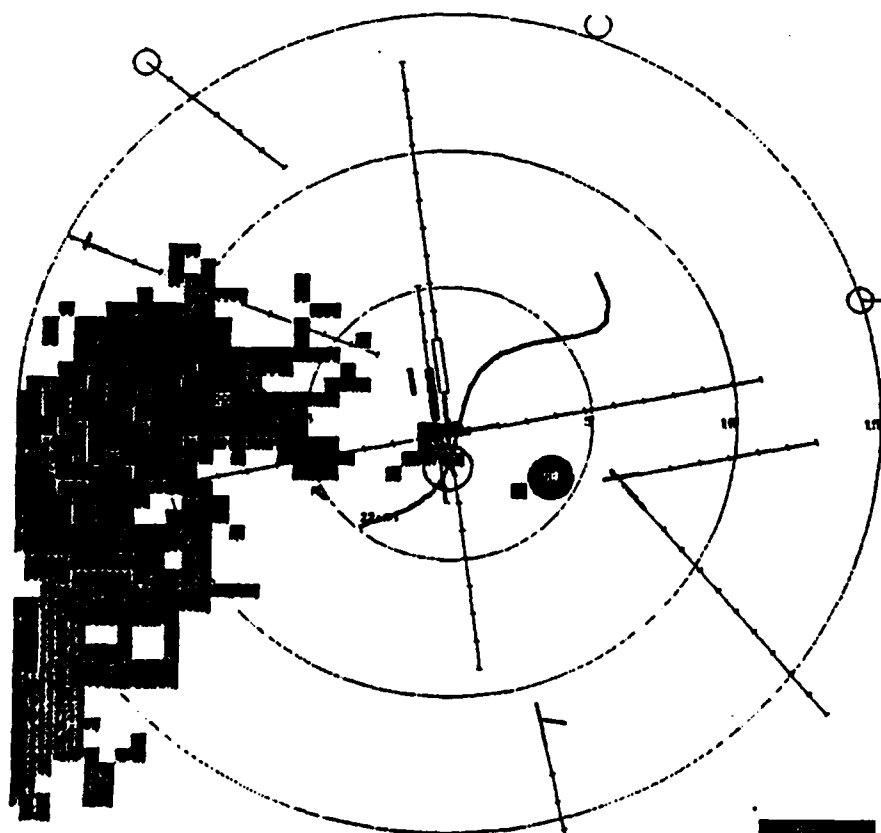
MB: UP

GT: UP

PRECIP: UP

LLWS: DOWN

☒ Print Screen



NCAR GSD

RANGE

☒ 5m ☒ 15m ☒ 30m ☒ 50m

SCREEN

☒ 1 ☒ 2 ☒ 3 ☒ 4  
☒ 5 ☒ 6 ☒ 7 ☒ 8

MAPS

☒ Vortices & lines  
☒ ASR rings  
☒ Airports  
☒ Interstates

PRECIPITATION LEVELS

☒ 0.2 ☒ 1.0 ☒ 3-6 ☒ 8-1

WIND SHIFT:

☒ OFF ☒ ON

DATE: 09/09/88

TIME: 18:31:40

PDATE: 07/11/88

WTIME: 22:05:04

GTIME: 22:04:01

MB: UP

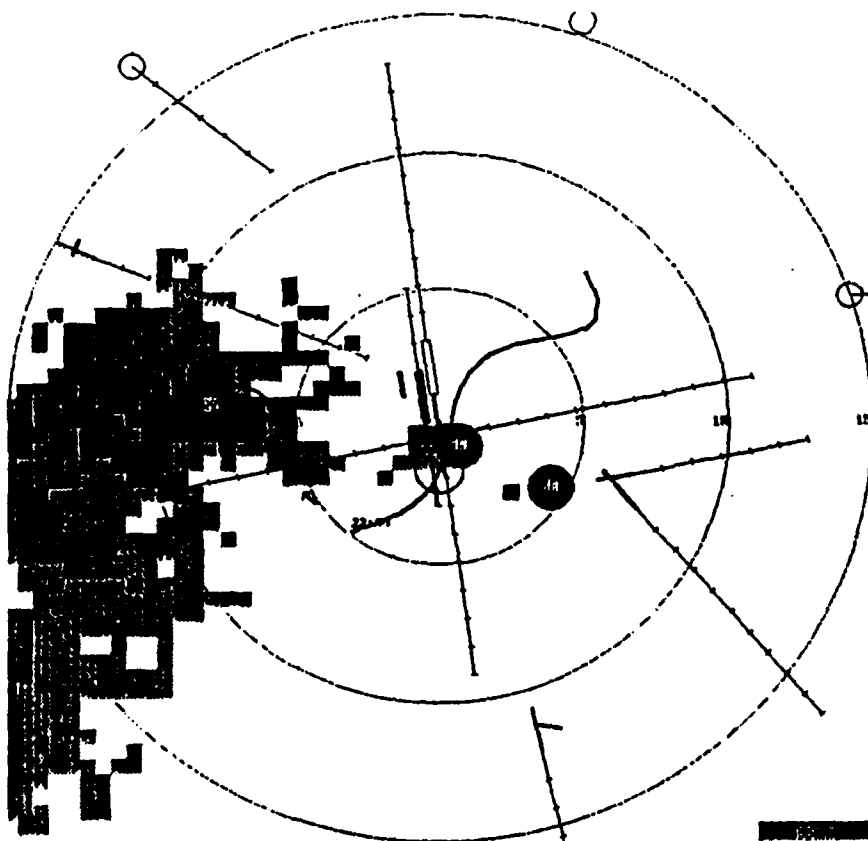
GT: UP

PRECIP: UP

LLWS: DOWN

☒ Print Screen





NCAR GSD

RANGE

☐ 5m ☐ 10m ☐ 30m ☐ 50m

SCREEN

☐ 1 ☐ 2 ☐ 3 ☐ 4  
☐ 5 ☐ 6 ☐ 7 ☐ 8

MAPS

☐ Vortec & lines  
☐ WASH rings  
☐ Airports  
☐ Interstates

PRECIPITATION LEVELS

☐ 0.2 ☐ 1.0 ☐ 3-4 ☐ 5-6

WIND SHIFT:

☐ 0.2 ☐ 1.0

DATE: 09/09/88

TIME: 18:32:33

PDATE: 07/11/88

MYTIME: 22:06:01

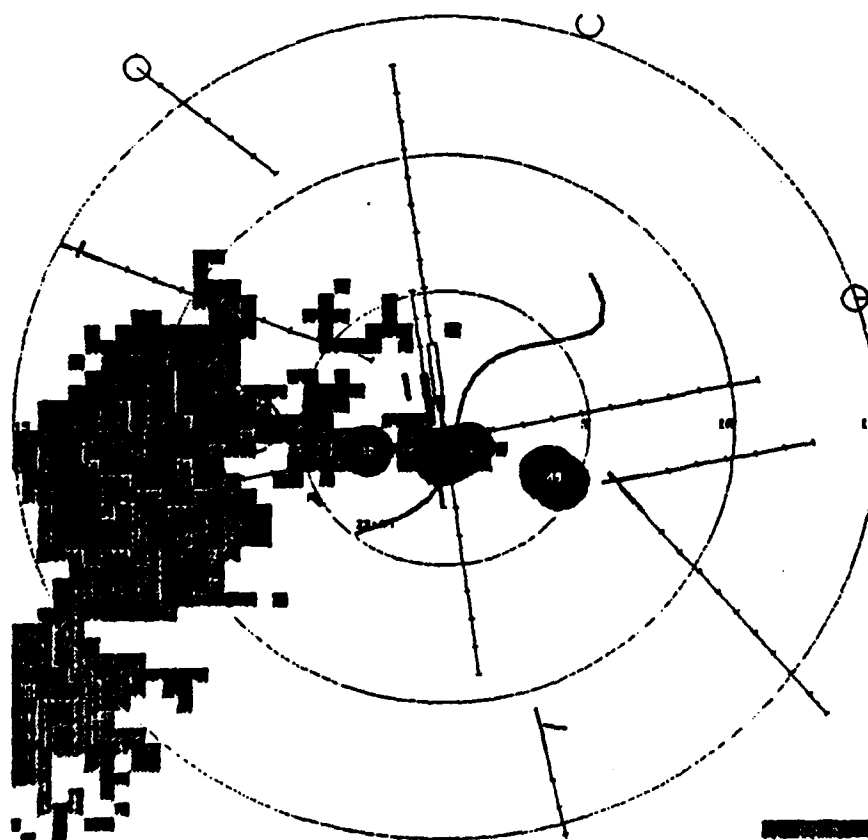
OTIME: 22:04:01

MO: UP

GT: UP

PRECIP: UP

LLWAS: DOWN



NCAR GSD

RANGE

☐ 5m ☐ 10m ☐ 30m ☐ 50m

SCREEN

☐ 1 ☐ 2 ☐ 3 ☐ 4  
☐ 5 ☐ 6 ☐ 7 ☐ 8

MAPS

☐ Vortec & lines  
☐ WASH rings  
☐ Airports  
☐ Interstates

PRECIPITATION LEVELS

☐ 0.2 ☐ 1.0 ☐ 3-4 ☐ 5-6

WIND SHIFT:

☐ 0.2 ☐ 1.0

DATE: 09/09/88

TIME: 18:34:12

PDATE: 07/11/88

MYTIME: 22:06:58

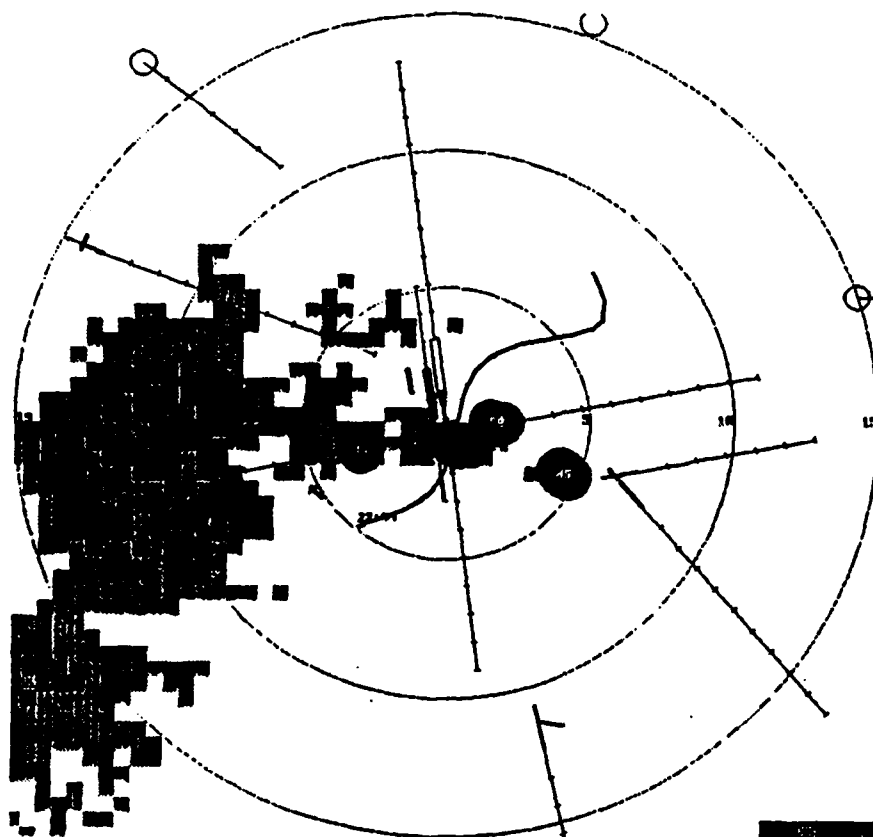
OTIME: 22:04:01

MO: UP

GT: UP

PRECIP: UP

LLWAS: DOWN



BCAR GSD

RANGE

5m 15m 30m 50m

SCREEN

1 2 3 4  
5 6 7 8

MAPS

☐ Vortec & lines  
☐ ASR rings  
☐ Airports  
☐ Interstates

PRECIPITATION LEVELS

0-2 3-4 5-6 7-8

WIND SHIFT:

0-2 3-4

DATE: 09/09/88

TIME: 18:38:02

PDATE: 07/11/88

WTIME: 22:08:03

OTIME: 22:04:01

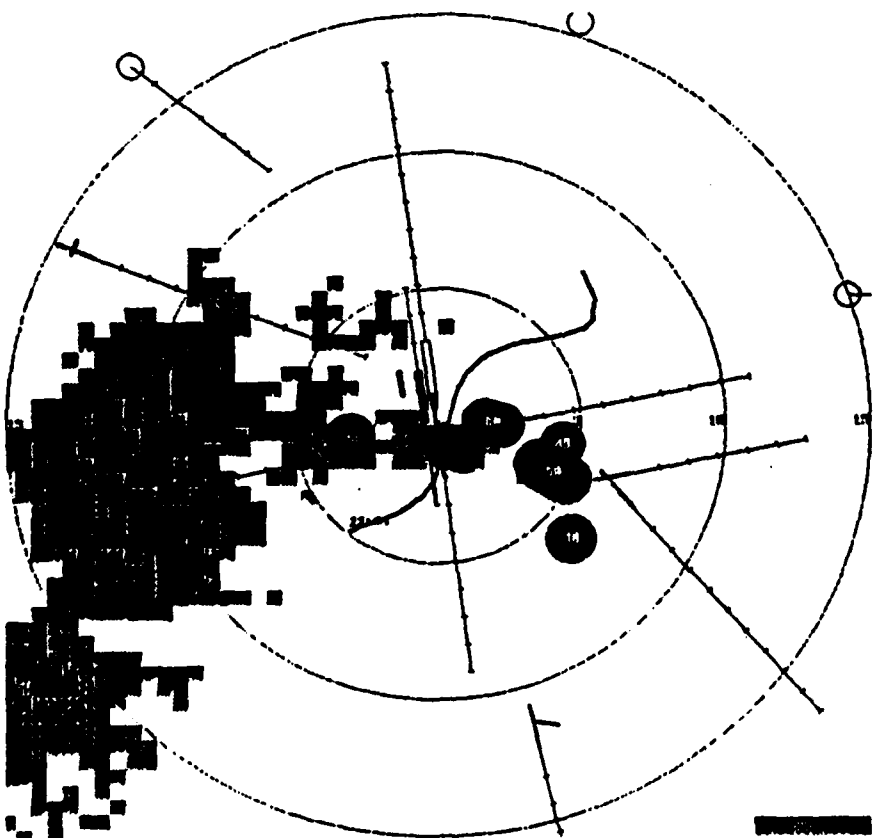
MD: UP

GF: UP

PRECIP: UP

LLWS: DOWN

Print Screen



BCAR GSD

RANGE

5m 15m 30m 50m

SCREEN

1 2 3 4  
5 6 7 8

MAPS

☐ Vortec & lines  
☐ ASR rings  
☐ Airports  
☐ Interstates

PRECIPITATION LEVELS

0-2 3-4 5-6 7-8

WIND SHIFT:

0-2 3-4

DATE: 09/09/88

TIME: 18:38:44

PDATE: 07/11/88

WTIME: 22:09:00

OTIME: 22:04:01

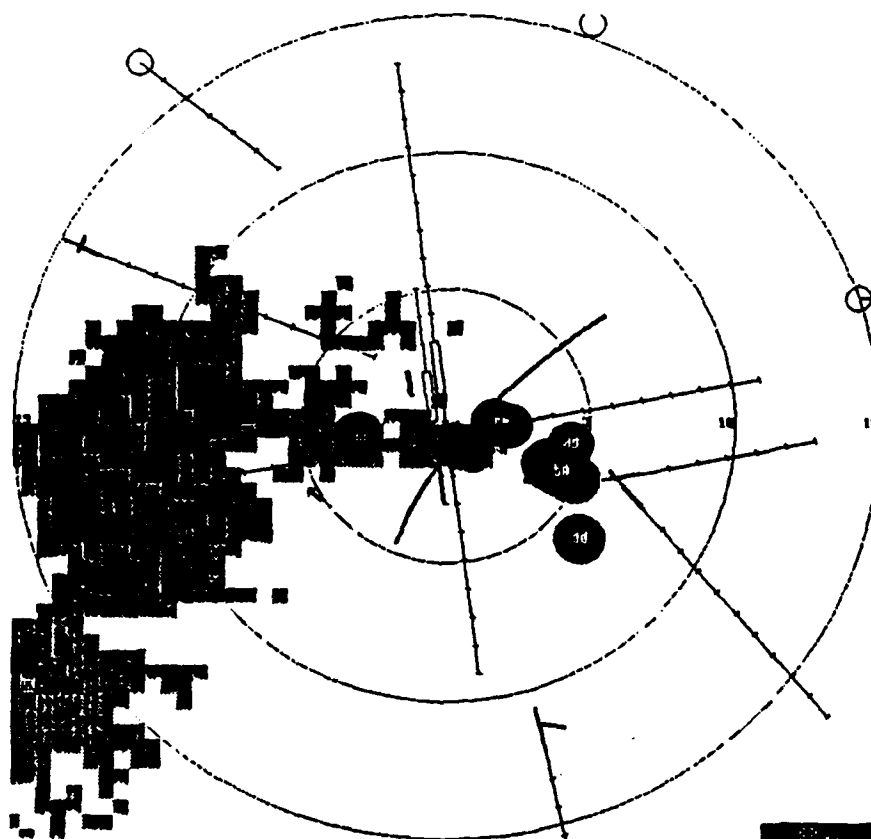
MD: UP

GF: UP

PRECIP: UP

LLWS: DOWN

Print Screen



NCAR GSD

RANGE

☐ 5m ☐ 10m ☐ 30m ☐ 50m

SCREEN

☐ 1 ☐ 2 ☐ 3 ☐ 4  
☐ 5 ☐ 6 ☐ 7 ☐ 8

MAPS

☐ Vortec & lines  
☐ ASR rings  
☐ Airports  
☐ Interstates

PRECIPITATION LEVELS

☐ OFF ☐ 1mm ☐ 2-5 ☐ 5-8

WIND SHIFT:

☐ OFF ☐ ON

DATE: 09/09/88

TIME: 18:37:30

PDAT: 07/11/88

WTIME: 22:09:00

OTIME: 22:09:00

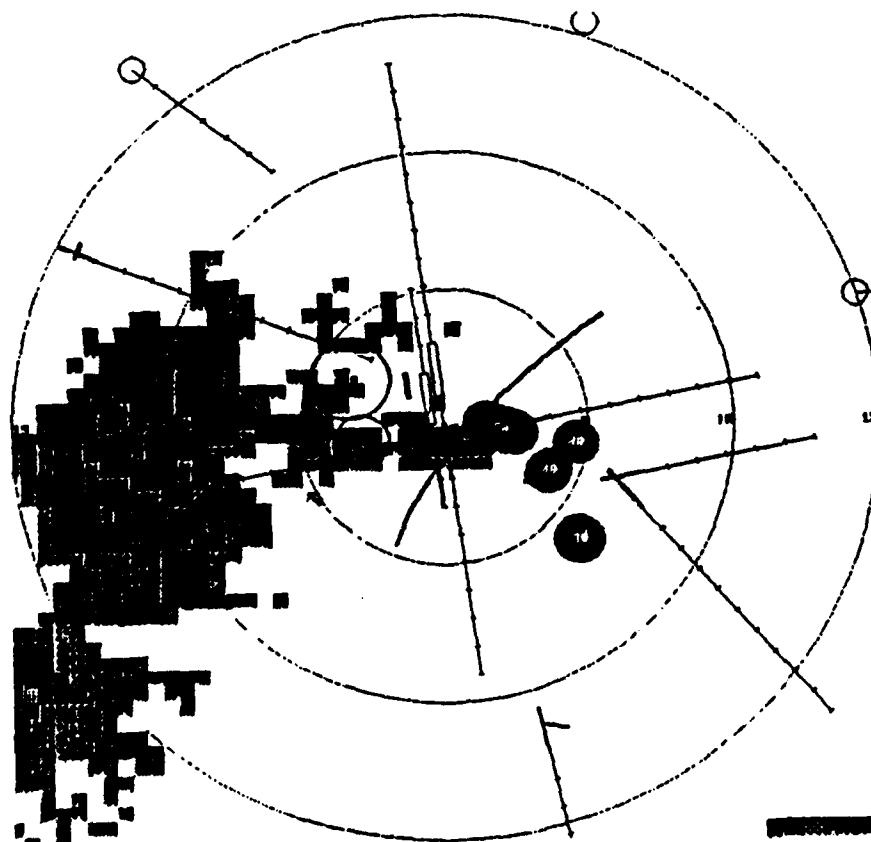
MD: UP

OT: UP

PRECIP: UP

LLWS: DOWN

[Print Screen](#)



NCAR GSD

RANGE

☐ 5m ☐ 10m ☐ 30m ☐ 50m

SCREEN

☐ 1 ☐ 2 ☐ 3 ☐ 4  
☐ 5 ☐ 6 ☐ 7 ☐ 8

MAPS

☐ Vortec & lines  
☐ ASR rings  
☐ Airports  
☐ Interstates

PRECIPITATION LEVELS

☐ OFF ☐ 1mm ☐ 2-5 ☐ 5-8

WIND SHIFT:

☐ OFF ☐ ON

DATE: 09/09/88

TIME: 18:37:37

PDAT: 07/11/88

WTIME: 22:10:03

OTIME: 22:09:00

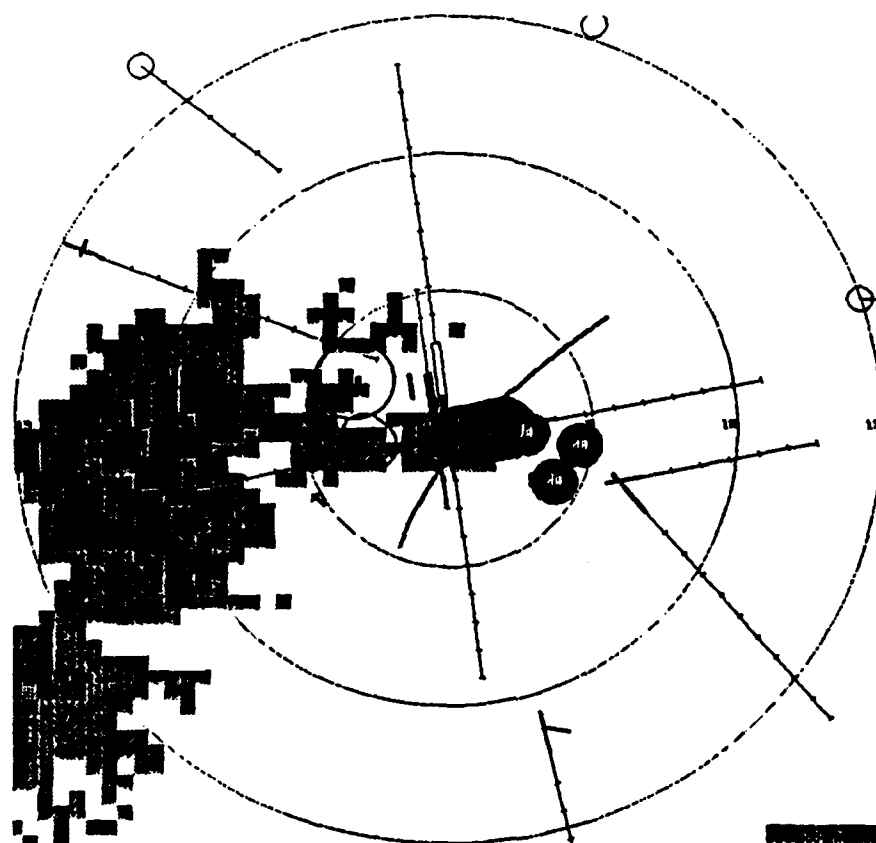
MD: UP

OT: UP

PRECIP: UP

LLWS: DOWN

[Print Screen](#)



NCAR GSD

RANGE

5m 10m 30m 50m

SCREEN

1 2 3 4  
5 6 7 8

MAPS

☐ Vortec & fines  
☐ AWR rings  
☐ Airports  
☐ Interstates

PRECIPITATION LEVELS

022 100 3-4 5-6

WIND SHIFT:

022 00

DATE: 09/09/88

TIME: 18:38:23

PDATE: 07/11/88

MTIME: 22:11:00

OTIME: 22:09:00

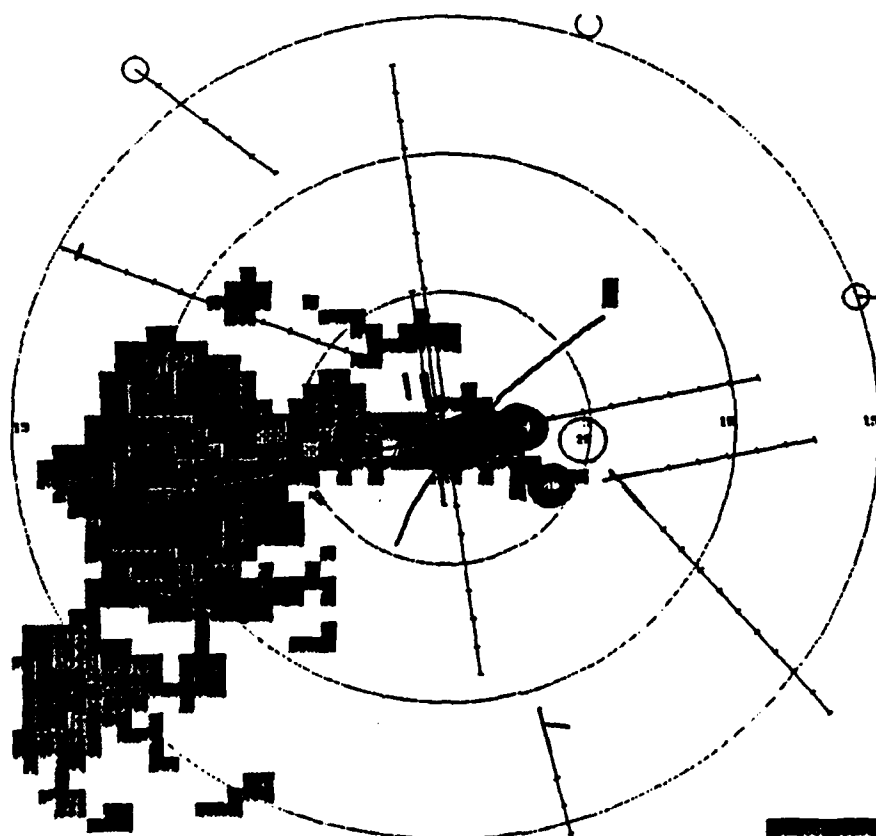
MD: UP

GF: UP

PRECIP: UP

LLWAS: DOWN

Print Screen



NCAR GSD

RANGE

5m 10m 30m 50m

SCREEN

1 2 3 4  
5 6 7 8

MAPS

☐ Vortec & fines  
☐ AWR rings  
☐ Airports  
☐ Interstates

PRECIPITATION LEVELS

022 100 3-4 5-6

WIND SHIFT:

022 00

DATE: 09/09/88

TIME: 18:40:02

PDATE: 07/11/88

MTIME: 22:11:50

OTIME: 22:09:00

MD: UP

GF: UP

PRECIP: UP

LLWAS: DOWN

Print Screen



NCAR GSD

RANGE

☐ 5m ☐ 15m ☐ 30m ☐ 50m

SCREEN

☐ 1 ☐ 2 ☐ 3 ☐ 4  
☐ 5 ☐ 6 ☐ 7 ☐ 8

MAPS

☐ Vortec & fixes  
☐ ASR rings  
☐ Airports  
☐ Interstates

PRECIPITATION LEVELS

☐ OFF ☐ 1-5 ☐ 3-6 ☐ 5-6

WIND SHIFT:

☐ OFF ☐ On

DATE: 09/09/88

TIME: 18:40:33

PDATE: 07/11/88

WTIME: 22:12:56

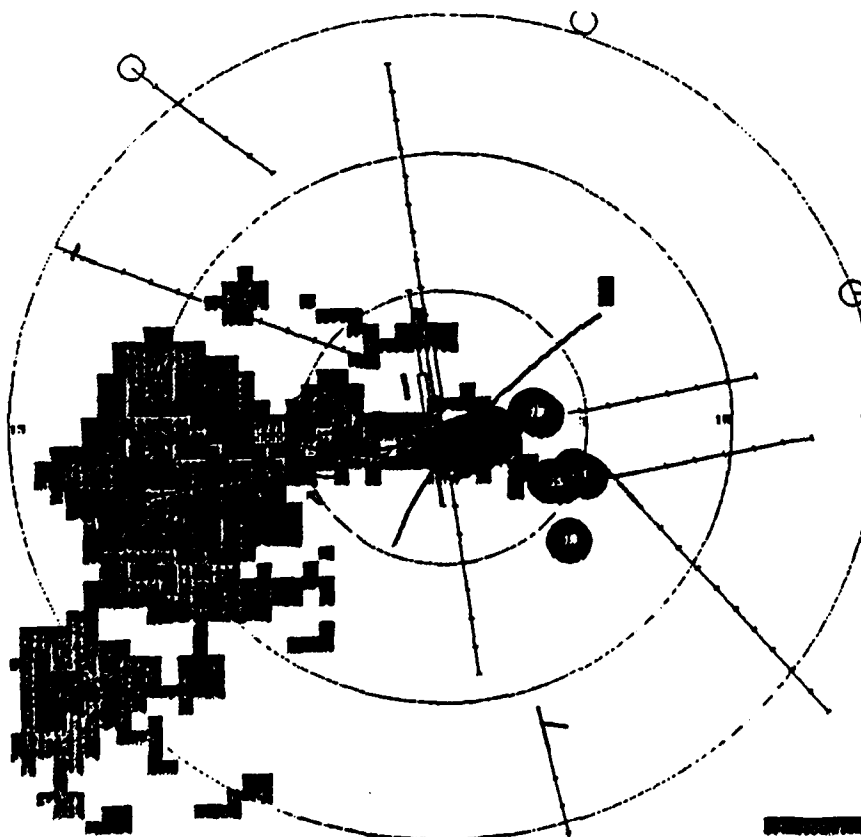
GTIME: 22:09:00

MB: UP

GT: UP

PRECIP: UP

LLWAS: DOWN



NCAR GSD

RANGE

☐ 5m ☐ 15m ☐ 30m ☐ 50m

SCREEN

☐ 1 ☐ 2 ☐ 3 ☐ 4  
☐ 5 ☐ 6 ☐ 7 ☐ 8

MAPS

☐ Vortec & fixes  
☐ ASR rings  
☐ Airports  
☐ Interstates

PRECIPITATION LEVELS

☐ OFF ☐ 1-5 ☐ 3-6 ☐ 5-6

WIND SHIFT:

☐ OFF ☐ On

DATE: 09/09/88

TIME: 18:41:44

PDATE: 07/11/88

WTIME: 22:14:00

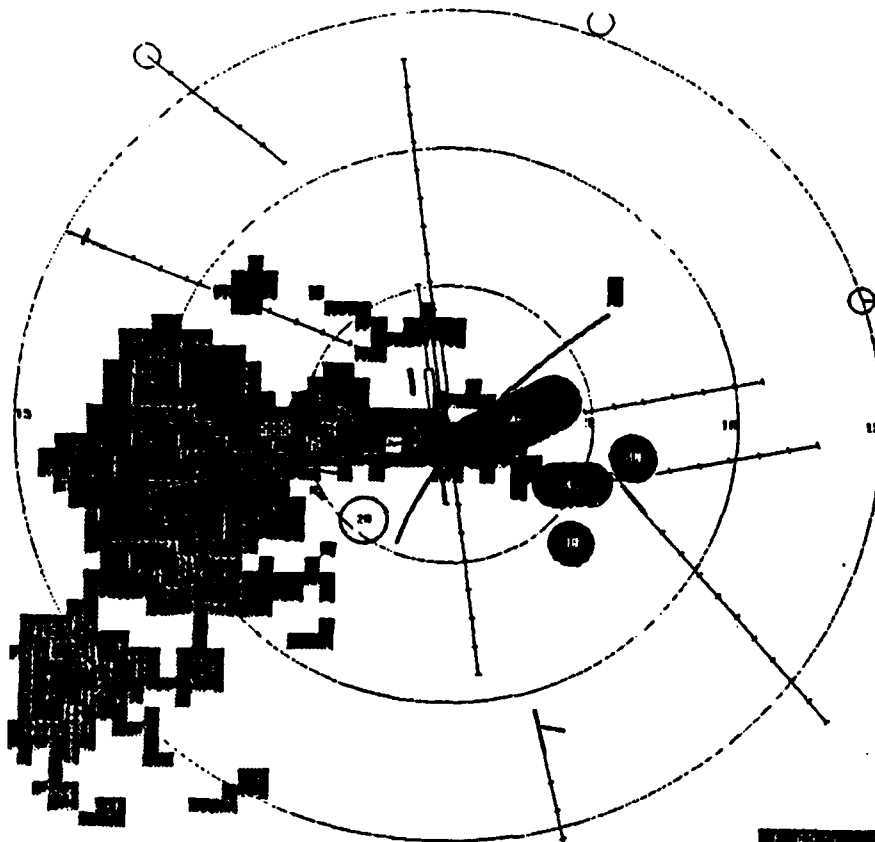
GTIME: 22:09:00

MB: UP

GT: UP

PRECIP: UP

LLWAS: DOWN



NCAR GSD

RANGE

☒ 5m ☒ 15m ☒ 30m ☒ 50m

SCREEN

☒ 1 ☒ 2 ☒ 3 ☒ 4  
☒ 5 ☒ 6 ☒ 7 ☒ 8

MAPS

☒ Vortec & fines  
☒ ASR rings  
☒ Airports  
☒ Interstates

PRECIPITATION LEVELS

☒ OFF ☒ 1-5 ☒ 3-6 ☒ 5-8

WIND SHIFT:

☒ OFF ☒ ON

DATE: 09/09/88

TIME: 18:42:35

PDATE: 07/11/88

MTIME: 22:15:02

GTIME: 22:09:00

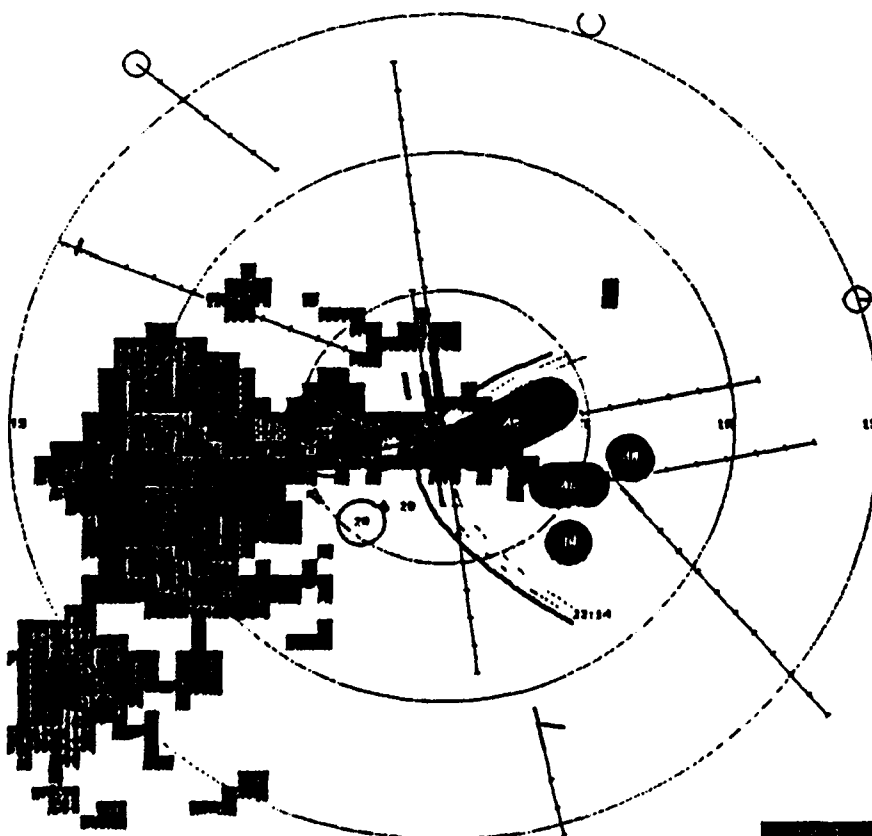
MB: UP

GT: UP

PRECIP: UP

LLWAS: DOWN

☒ Print Screen



NCAR GSD

RANGE

☒ 5m ☒ 15m ☒ 30m ☒ 50m

SCREEN

☒ 1 ☒ 2 ☒ 3 ☒ 4  
☒ 5 ☒ 6 ☒ 7 ☒ 8

MAPS

☒ Vortec & fines  
☒ ASR rings  
☒ Airports  
☒ Interstates

PRECIPITATION LEVELS

☒ OFF ☒ 1-5 ☒ 3-6 ☒ 5-8

WIND SHIFT:

☒ OFF ☒ ON

DATE: 09/09/88

TIME: 18:42:23

PDATE: 07/11/88

MTIME: 22:15:02

GTIME: 22:14:00

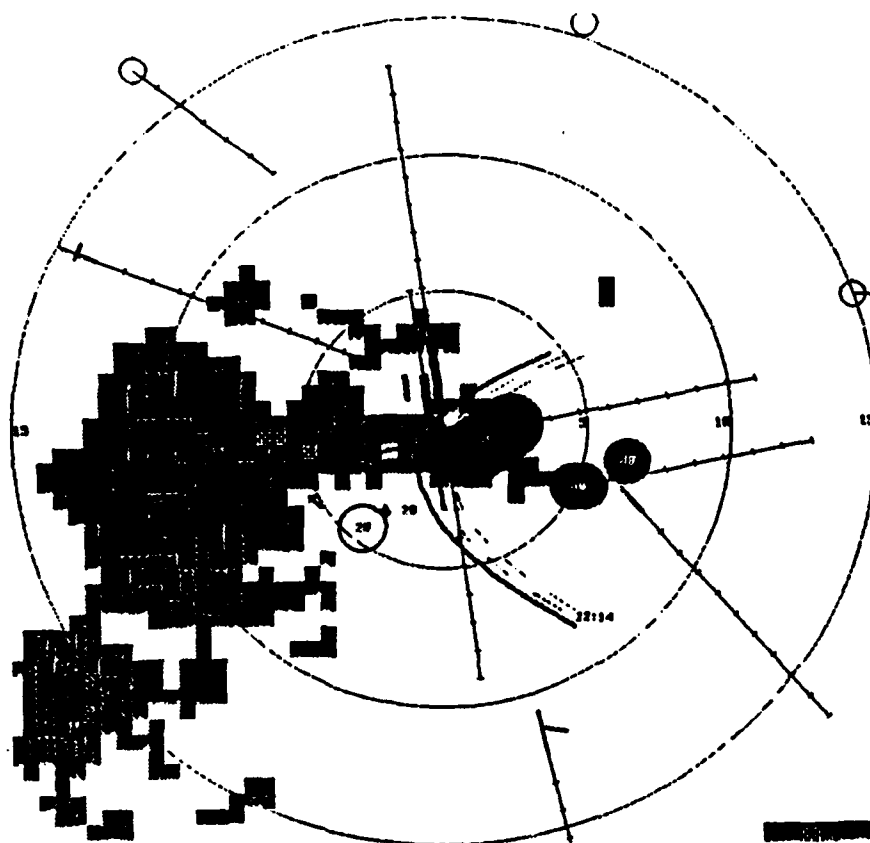
MB: UP

GT: UP

PRECIP: UP

LLWAS: DOWN

☒ Print Screen



NCAR GSD

RANGE

5m 10m 30m 50m

SCREEN

1 2 3 4  
5 6 7 8

MAPS

☐ Vortec & lines  
☐ W/ASR rings  
☐ Airports  
☐ Interstates

PRECIPITATION LEVELS

OFF LOW 3-4 5-6

WIND SHIFT:

OFF ON

DATE: 09/09/88

TIME: 18:44:12

PDATE: 07/11/88

MTIME: 22:16:01

OTIME: 22:14:00

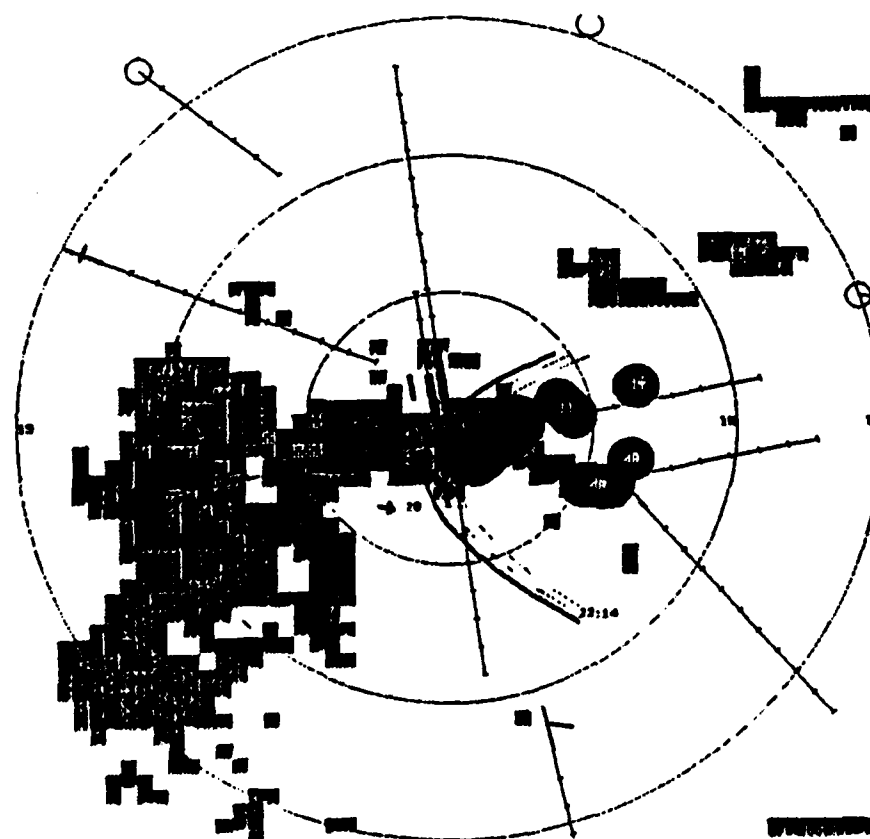
MD: UP

GT: UP

PRECIP: UP

LLWS: DOWN

Print Screen



NCAR GSD

RANGE

5m 10m 30m 50m

SCREEN

1 2 3 4  
5 6 7 8

MAPS

☐ Vortec & lines  
☐ W/ASR rings  
☐ Airports  
☐ Interstates

PRECIPITATION LEVELS

OFF LOW 3-4 5-6

WIND SHIFT:

OFF ON

DATE: 09/09/88

TIME: 18:48:06

PDATE: 07/11/88

MTIME: 22:16:58

OTIME: 22:14:00

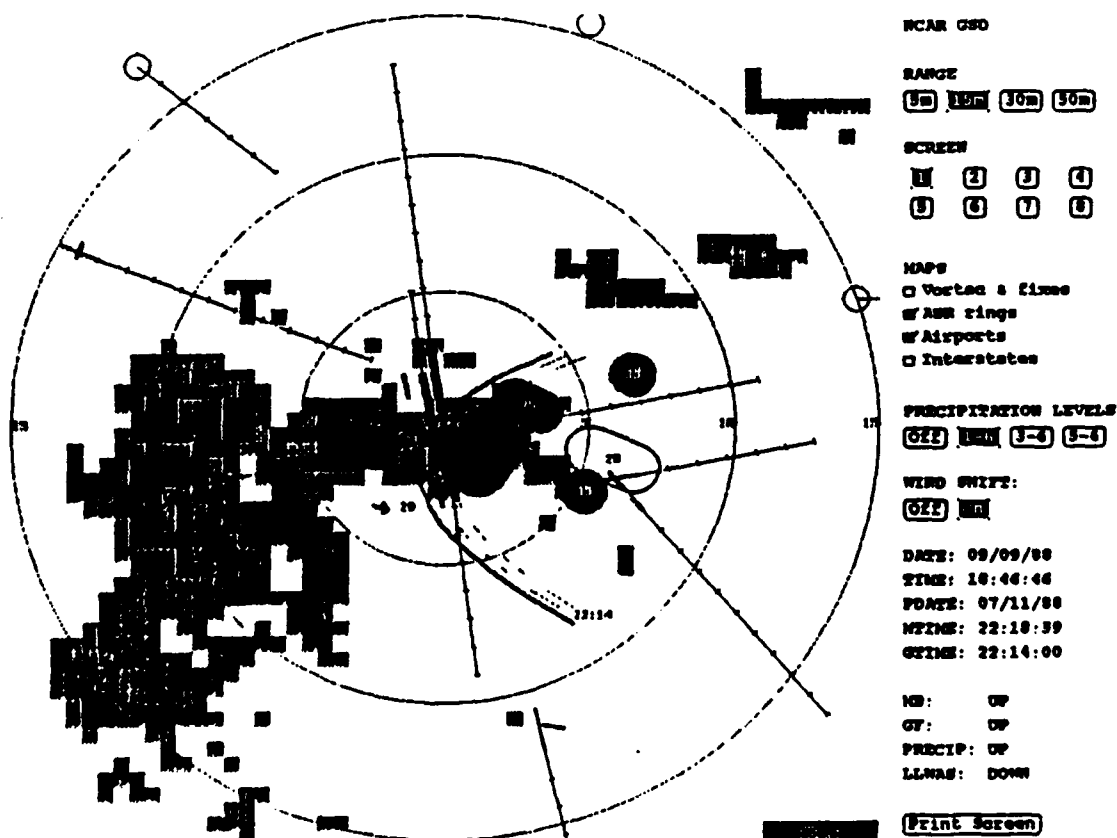
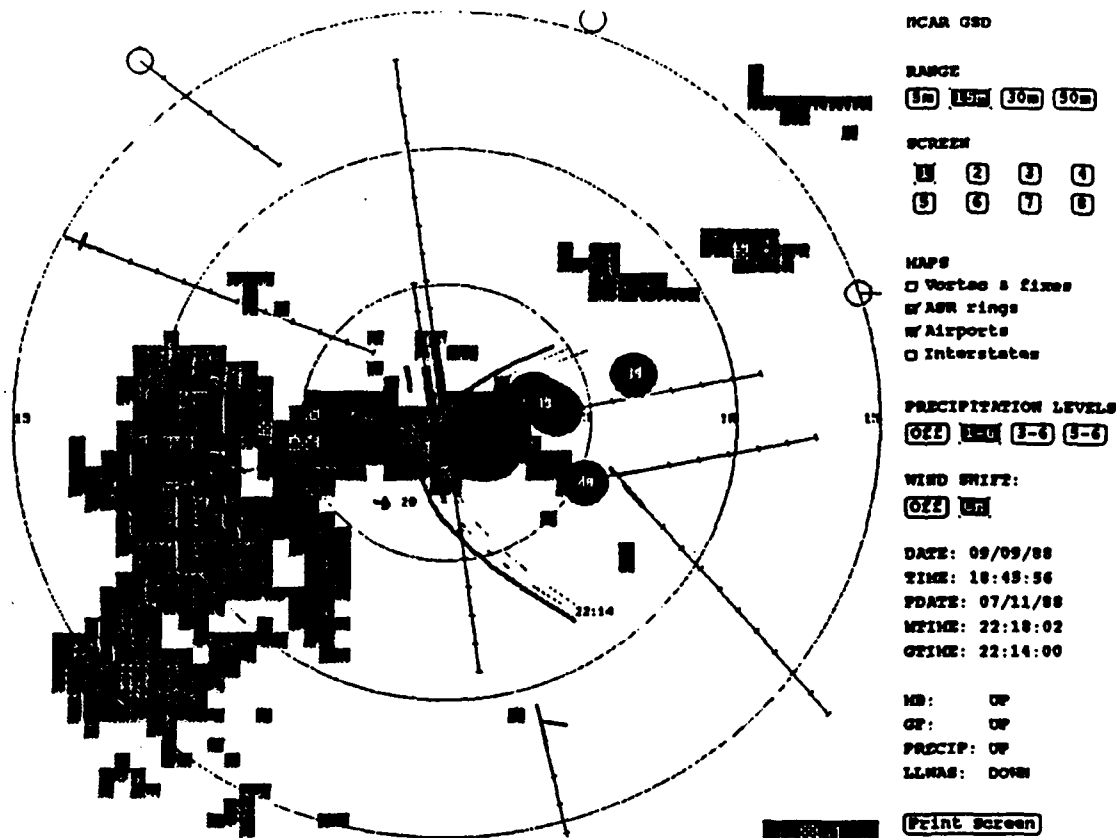
MD: UP

GT: UP

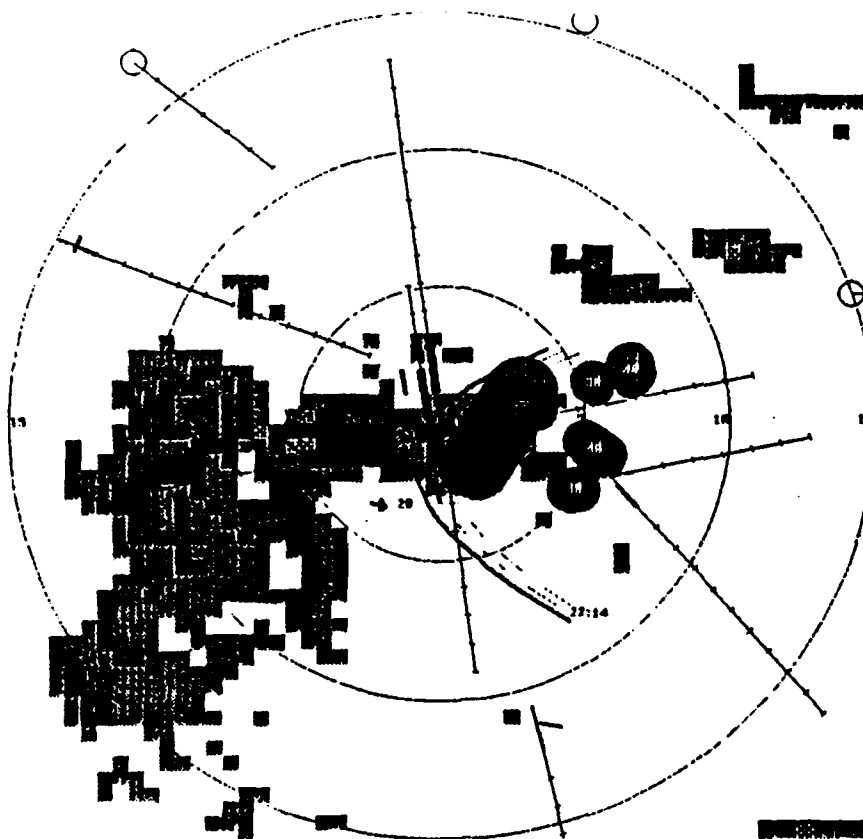
PRECIP: UP

LLWS: DOWN

Print Screen







NCAR GSD

RANGE

☐ 5m ☐ 15m ☐ 30m ☐ 50m

SCREEN

☐ 1 ☐ 2 ☐ 3 ☐ 4  
☐ 5 ☐ 6 ☐ 7 ☐ 8

MAPS

☐ Vortec & fixes  
☐ W/ASR rings  
☐ W/Airports  
☐ Interstates

PRECIPITATION LEVELS

☐ OFF ☐ 1-5 ☐ 3-6 ☐ 5-6

WIND SHIFT:

☐ OFF ☐ ON

DATE: 09/09/88

TIME: 18:48:29

PDATE: 07/11/88

MTIME: 22:20:03

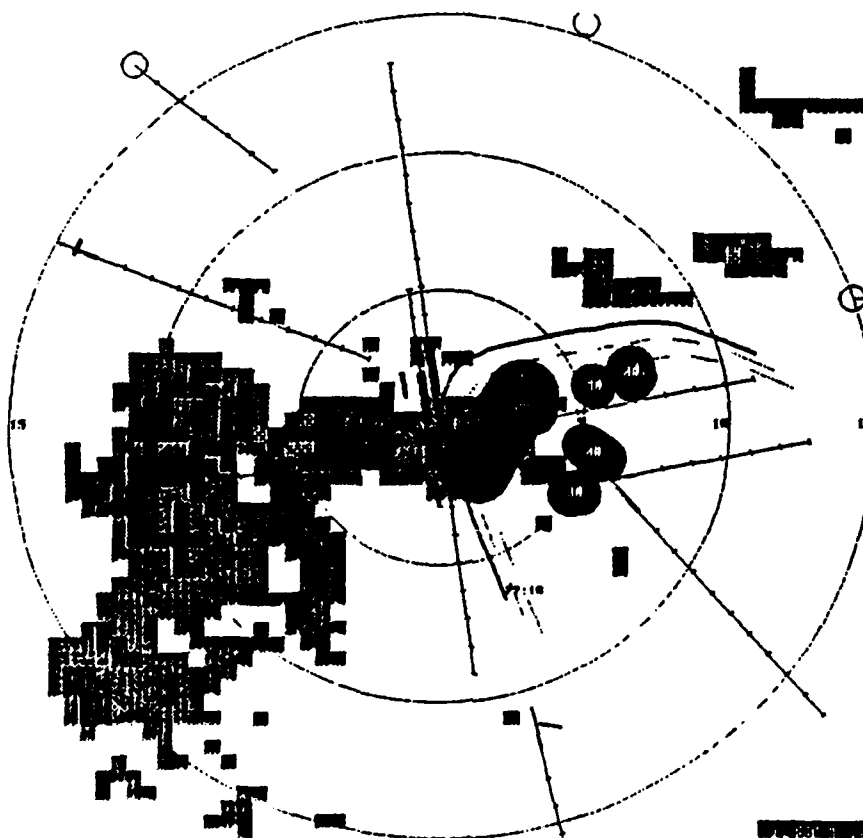
OTIME: 22:14:00

MB: UP

GT: UP

PRECIP: UP

LLWAS: DOWN



NCAR GSD

RANGE

☐ 5m ☐ 15m ☐ 30m ☐ 50m

SCREEN

☐ 1 ☐ 2 ☐ 3 ☐ 4  
☐ 5 ☐ 6 ☐ 7 ☐ 8

MAPS

☐ Vortec & fixes  
☐ W/ASR rings  
☐ W/Airports  
☐ Interstates

PRECIPITATION LEVELS

☐ OFF ☐ 1-5 ☐ 3-6 ☐ 5-6

WIND SHIFT:

☐ OFF ☐ ON

DATE: 09/09/88

TIME: 18:48:29

PDATE: 07/11/88

MTIME: 22:20:03

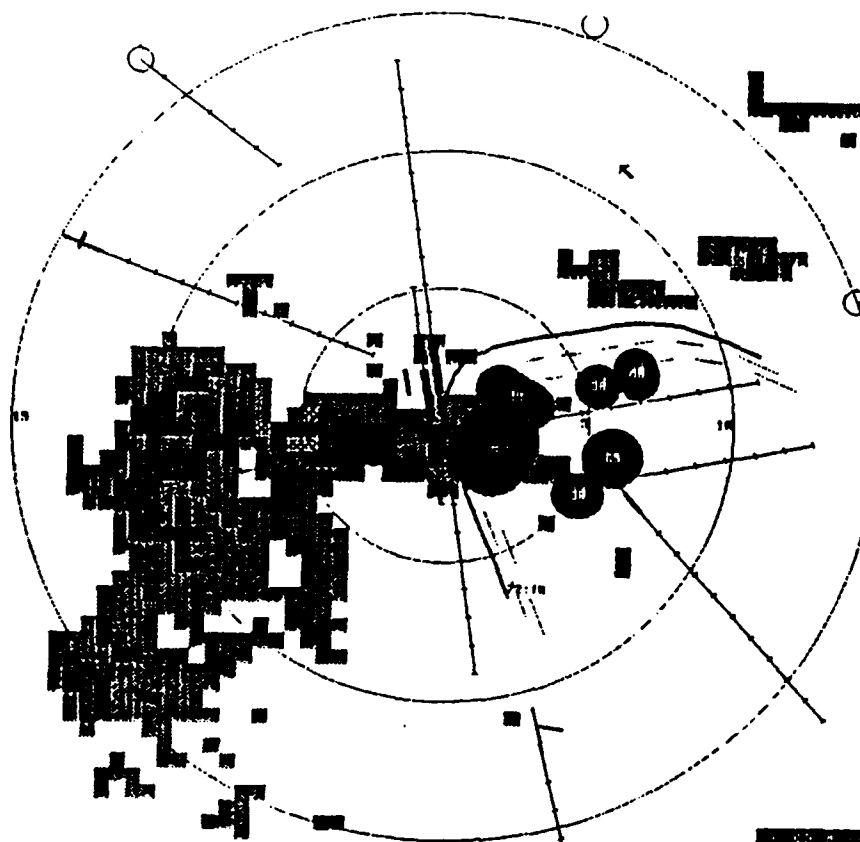
OTIME: 22:18:59

MB: UP

GT: UP

PRECIP: UP

LLWAS: DOWN



NCAR GSD

RANGE

☒ 5m ☒ 15m ☐ 30m ☐ 50m

SCREEN

☒ 1 ☐ 2 ☐ 3 ☐ 4  
☐ 5 ☐ 6 ☐ 7 ☐ 8

MAPS

☐ Vortec & fixes  
☐ ASR rings  
☐ Airports  
☐ Interstates

PRECIPITATION LEVELS

☒ 0-2 ☐ 3-6 ☐ 3-6 ☐ 3-6

WIND SHIFT:

☒ Off ☐ On

DATE: 09/09/88

TIME: 18:49:18

PDATE: 07/11/88

MTIME: 22:20:59

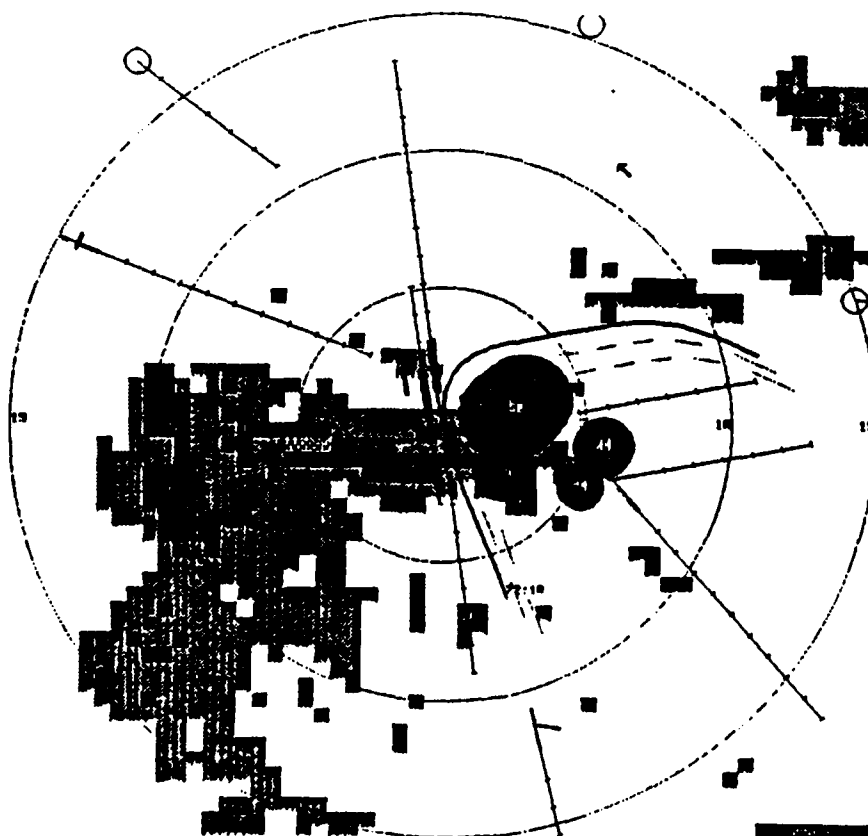
OTIME: 22:18:59

MD: UP

GF: UP

PRECIP: UP

LLWAS: DOWN



NCAR GSD

RANGE

☒ 5m ☒ 15m ☐ 30m ☐ 50m

SCREEN

☒ 1 ☐ 2 ☐ 3 ☐ 4  
☐ 5 ☐ 6 ☐ 7 ☐ 8

MAPS

☐ Vortec & fixes  
☐ ASR rings  
☐ Airports  
☐ Interstates

PRECIPITATION LEVELS

☒ 0-2 ☐ 3-6 ☐ 3-6 ☐ 3-6

WIND SHIFT:

☒ Off ☐ On

DATE: 09/09/88

TIME: 18:50:08

PDATE: 07/11/88

MTIME: 22:21:57

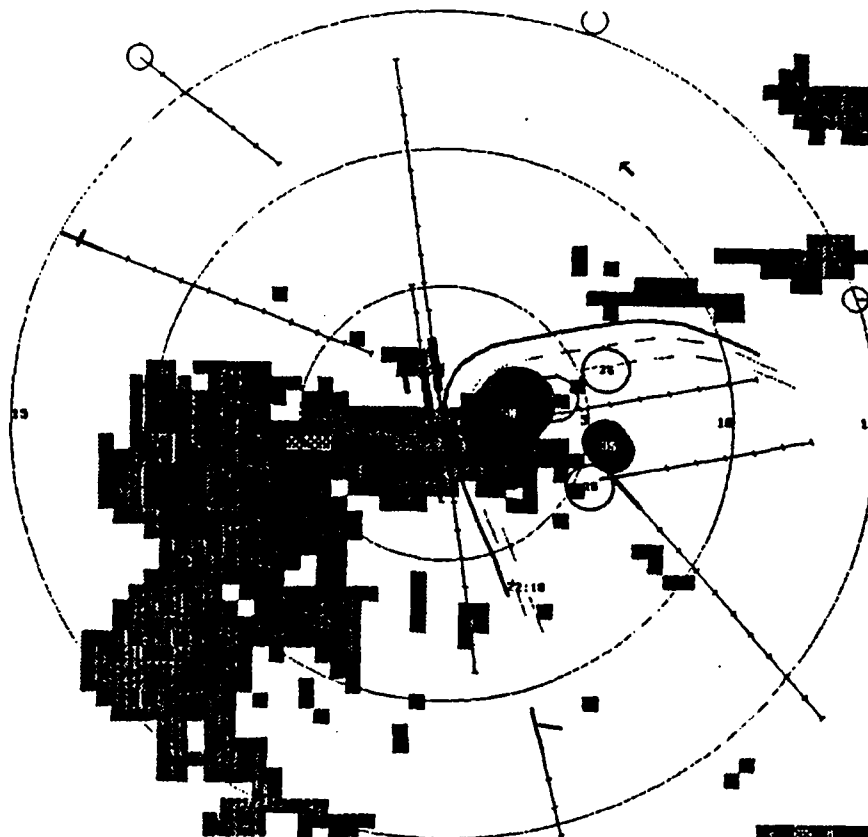
OTIME: 22:18:59

MD: UP

GF: UP

PRECIP: UP

LLWAS: DOWN



NCAR GSD

RANGE

☒ 5m ☒ 15m ☐ 30m ☐ 45m

SCREEN

☒ 1 ☒ 2 ☒ 3 ☒ 4  
☒ 5 ☒ 6 ☒ 7 ☒ 8

MAPS

☐ Vortec & lines  
☐ ASH rings  
☐ Airports  
☐ Interstates

PRECIPITATION LEVELS

☒ OFF ☒ 100 ☐ 3-4 ☐ 5-6

WIND SHIFT:

☒ OFF ☐ ON

DATE: 09/09/88

TIME: 18:50:58

PODATE: 07/11/88

MTIME: 22:22:55

GTIME: 22:18:59

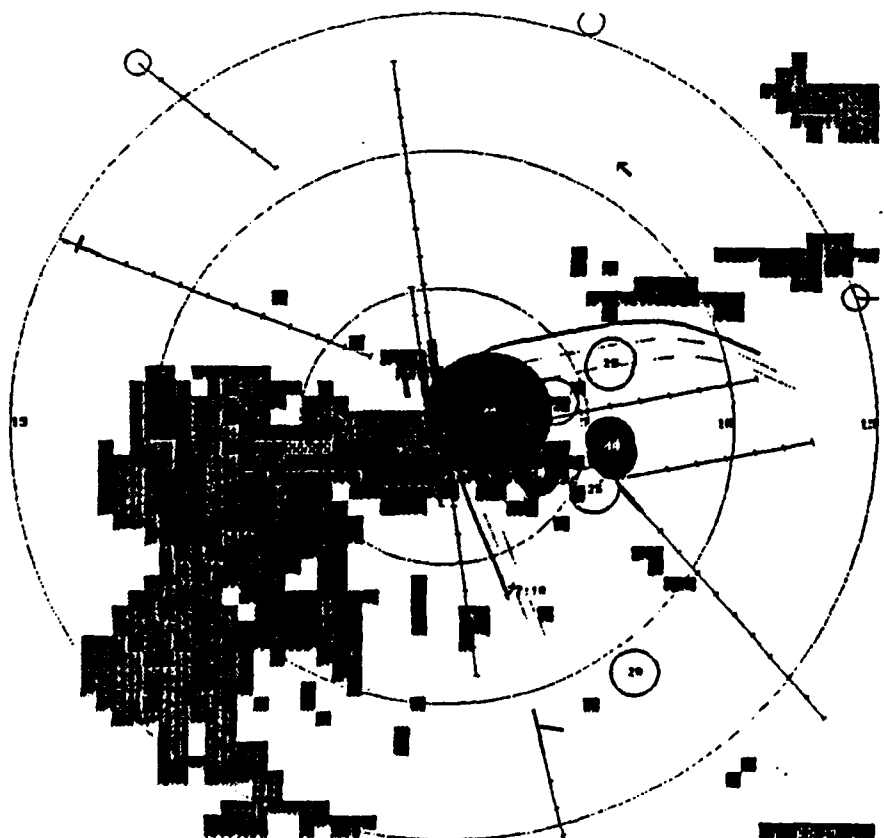
MB: UP

CF: UP

PRECIP: UP

LLWAS: DOWN

[Print Screen](#)



NCAR GSD

RANGE

☒ 5m ☒ 15m ☐ 30m ☐ 45m

SCREEN

☒ 1 ☒ 2 ☒ 3 ☒ 4  
☒ 5 ☒ 6 ☒ 7 ☒ 8

MAPS

☐ Vortec & lines  
☐ ASH rings  
☐ Airports  
☐ Interstates

PRECIPITATION LEVELS

☒ OFF ☒ 100 ☐ 3-4 ☐ 5-6

WIND SHIFT:

☒ OFF ☐ ON

DATE: 09/09/88

TIME: 18:52:59

PODATE: 07/11/88

MTIME: 22:23:59

GTIME: 22:18:59

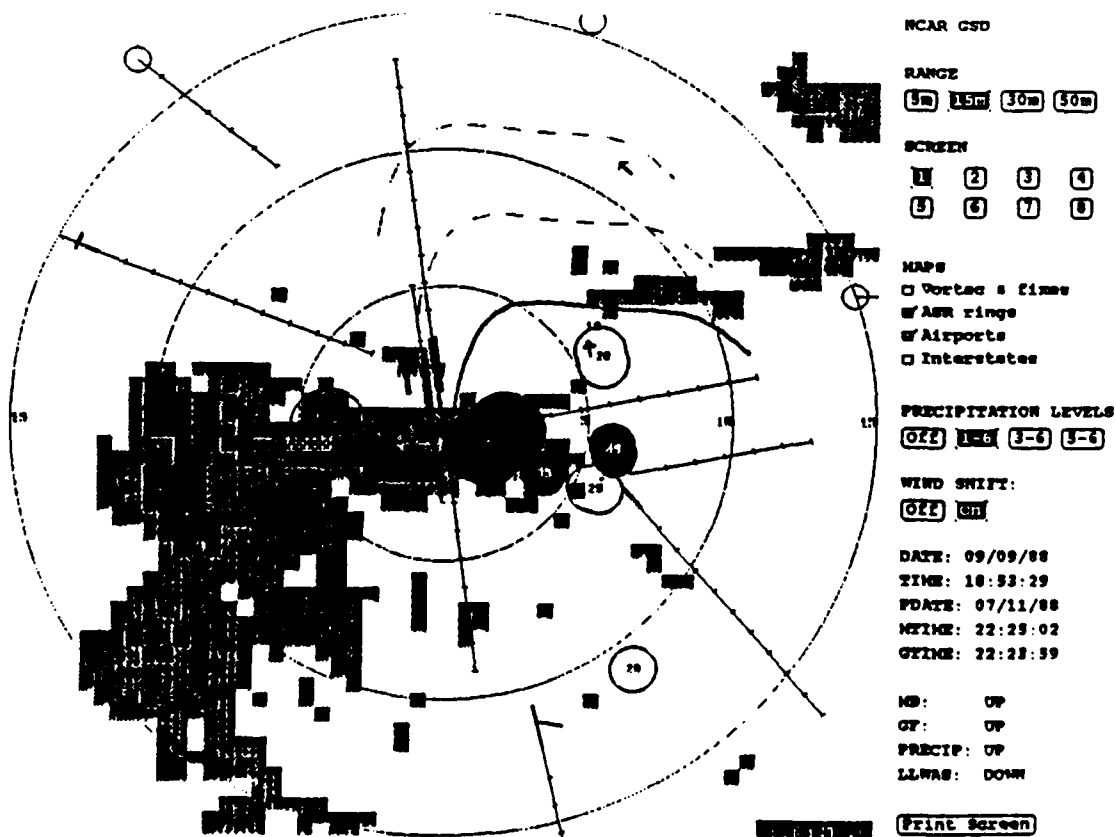
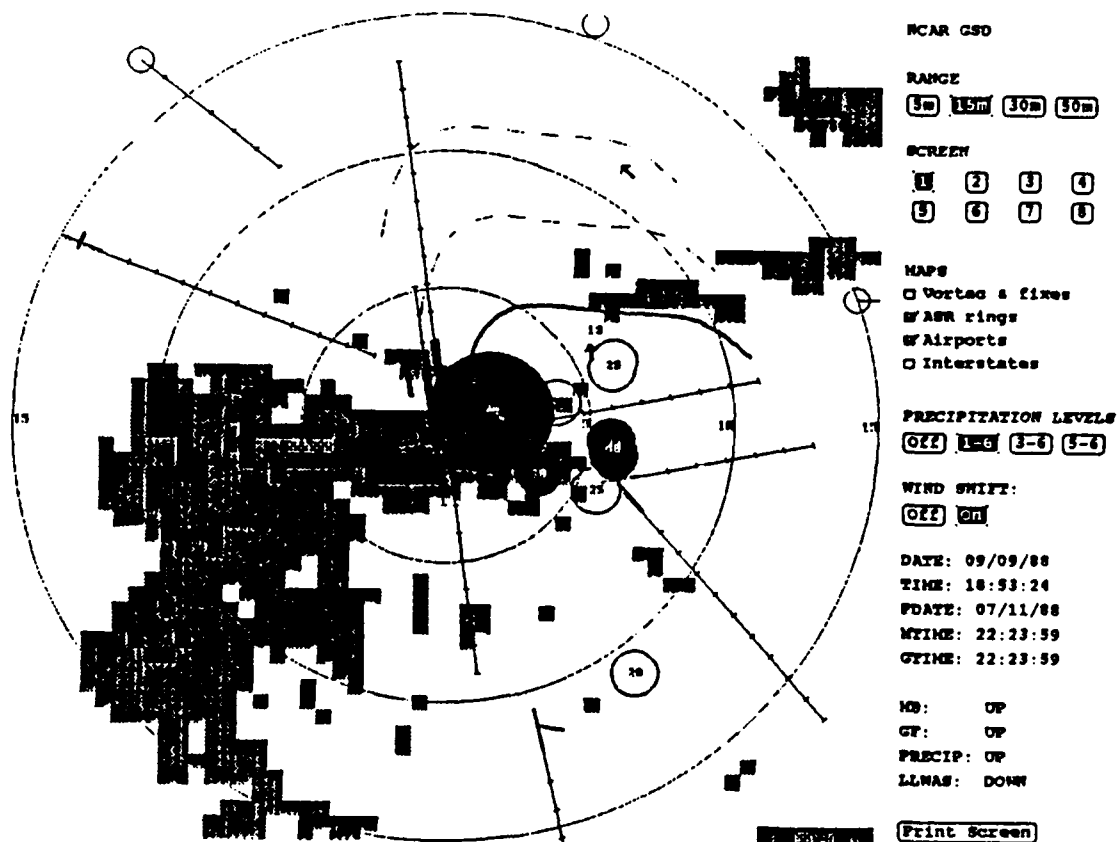
MB: UP

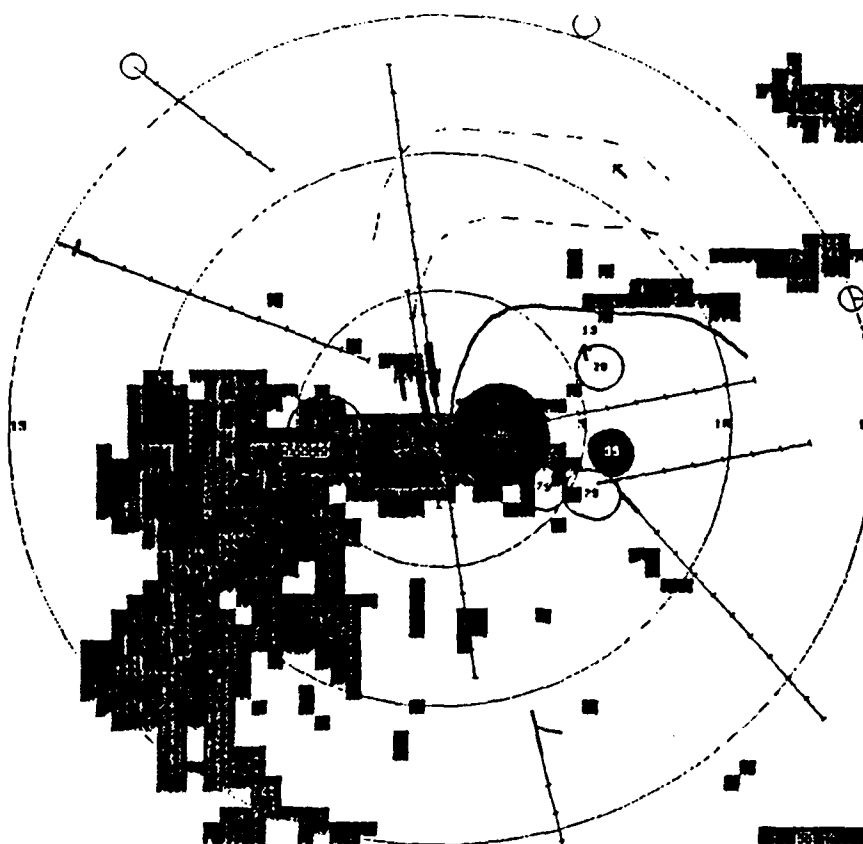
CF: UP

PRECIP: UP

LLWAS: DOWN

[Print Screen](#)





NCAR GSD

RANGE

5m 15m 30m 50m

SCREEN

1 2 3 4  
5 6 7 8

MAPS

☐ Vortec & lines  
☐ ASR rings  
☐ Airports  
☐ Interstates

PRECIPITATION LEVELS

OFF LOW 3-6 5-8

WIND SHIFT:

OFF ON

DATE: 09/09/88

TIME: 18:54:18

FOATE: 07/11/88

NTIME: 22:26:00

OTIME: 22:23:59

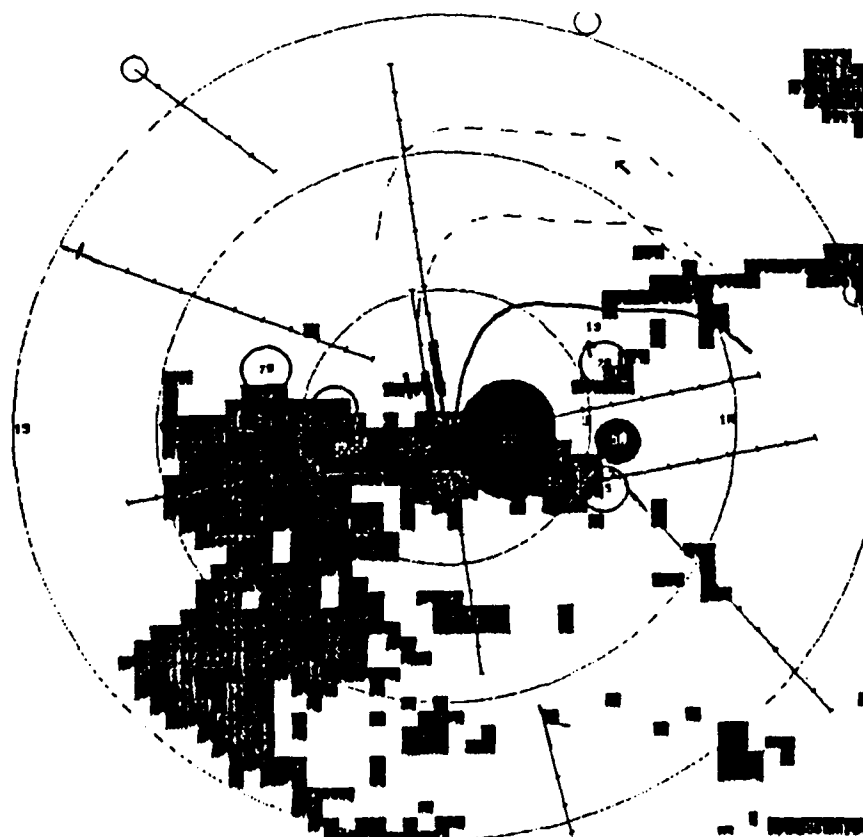
MO: UP

GY: UP

PRECIP: UP

LLWAS: DOWN

Print Screen



NCAR GSD

RANGE

5m 15m 30m 50m

SCREEN

1 2 3 4  
5 6 7 8

MAPS

☐ Vortec & lines  
☐ ASR rings  
☐ Airports  
☐ Interstates

PRECIPITATION LEVELS

OFF LOW 3-4 5-6

WIND SHIFT:

OFF ON

DATE: 09/09/88

TIME: 18:55:55

FOATE: 07/11/88

NTIME: 22:26:57

OTIME: 22:23:59

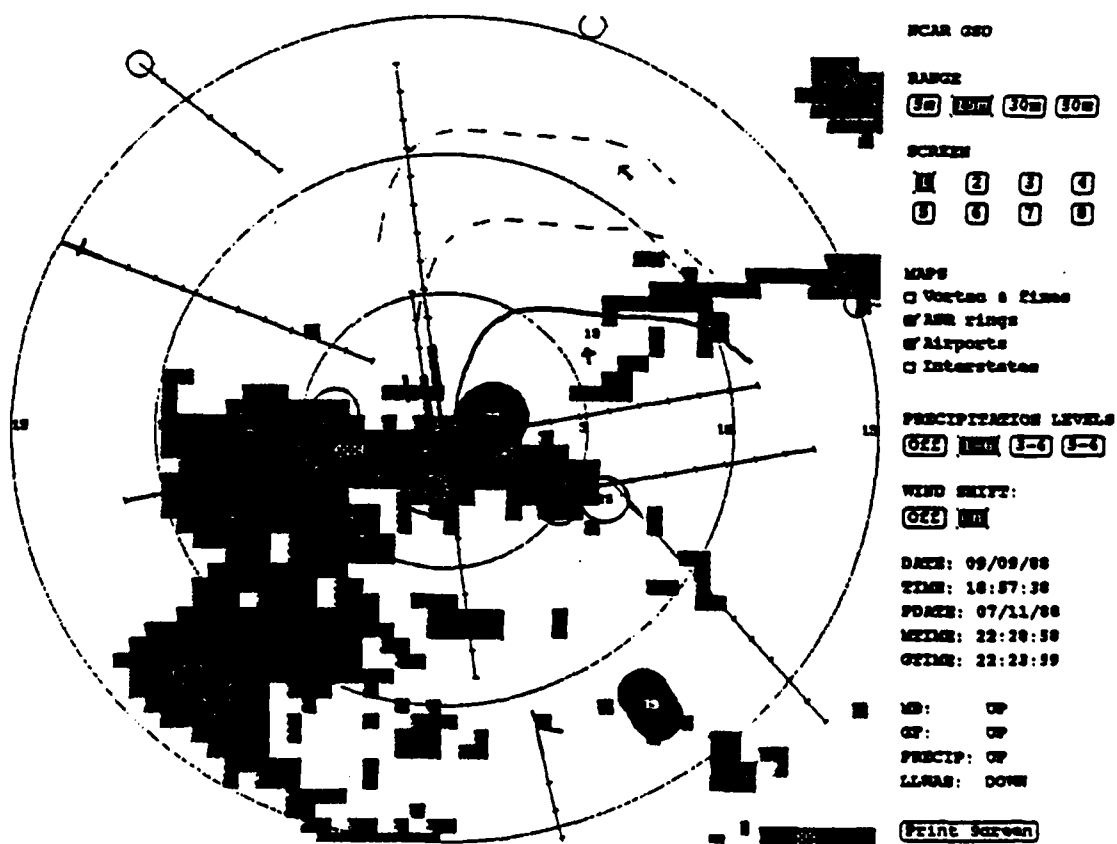
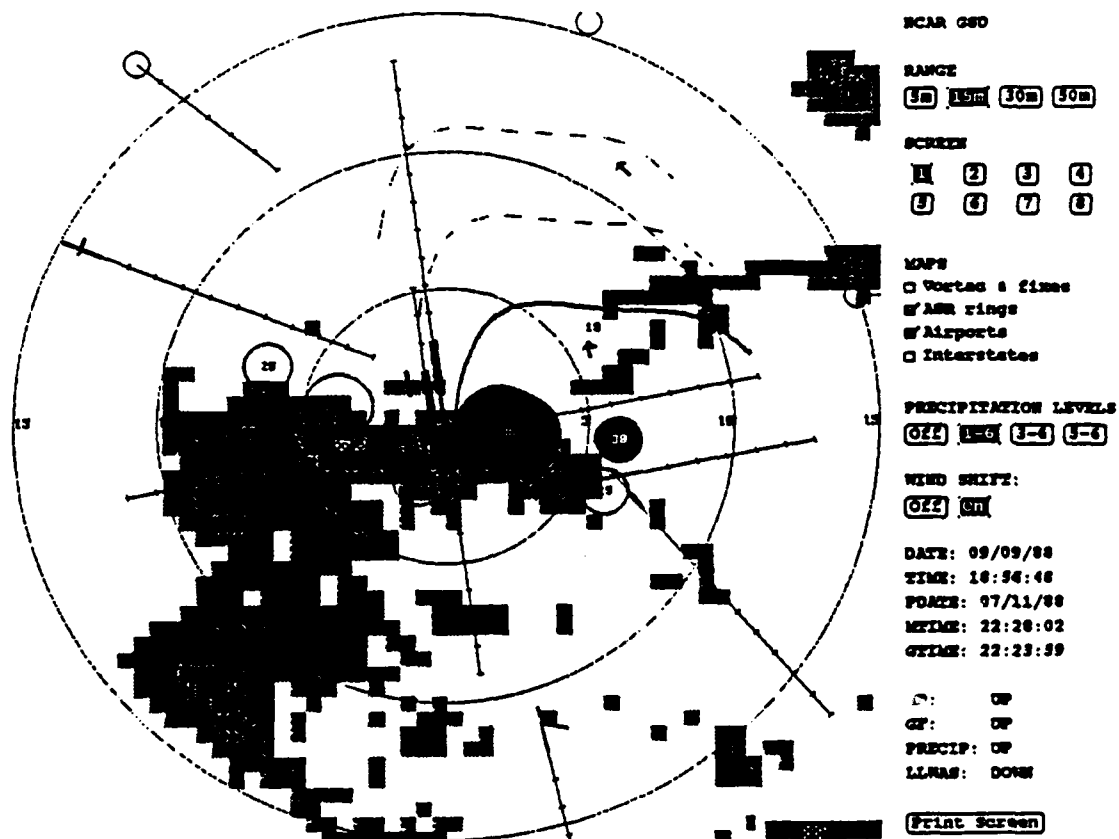
MO: UP

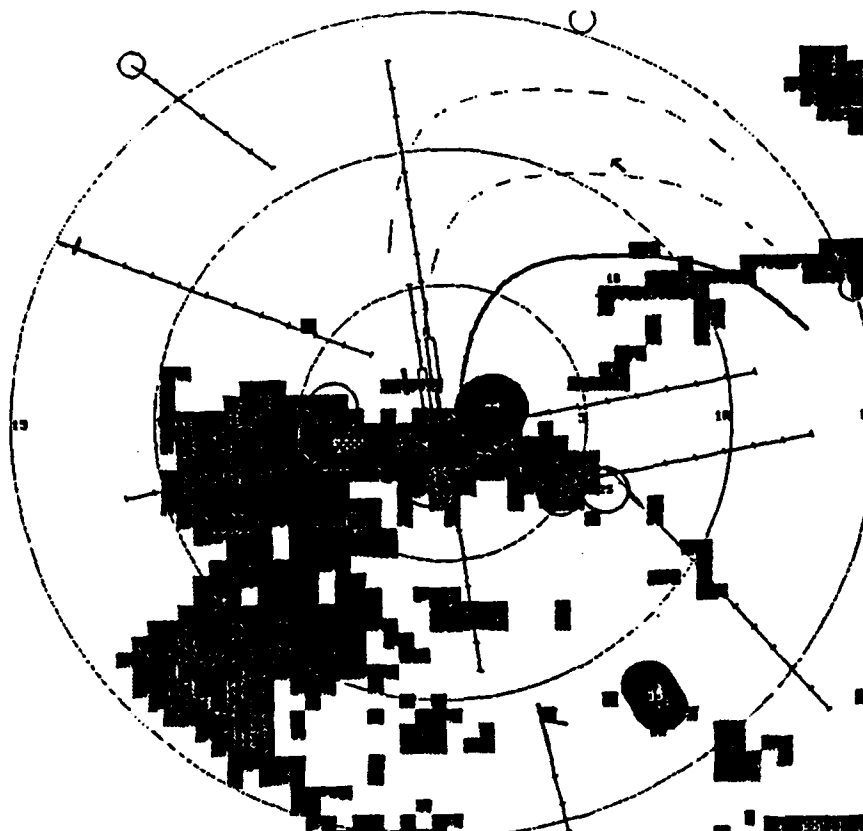
GY: UP

PRECIP: UP

LLWAS: DOWN

Print Screen





NCAR GSD

RANGE  
☒ 5m ☒ 10m ☒ 30m ☒ 50m

SCREEN  
☒ 1 ☒ 2 ☒ 3 ☒ 4  
☒ 5 ☒ 6 ☒ 7 ☒ 8

MAPS  
☒ Vortec & lines  
☒ AM rings  
☒ Airports  
☒ Interstates

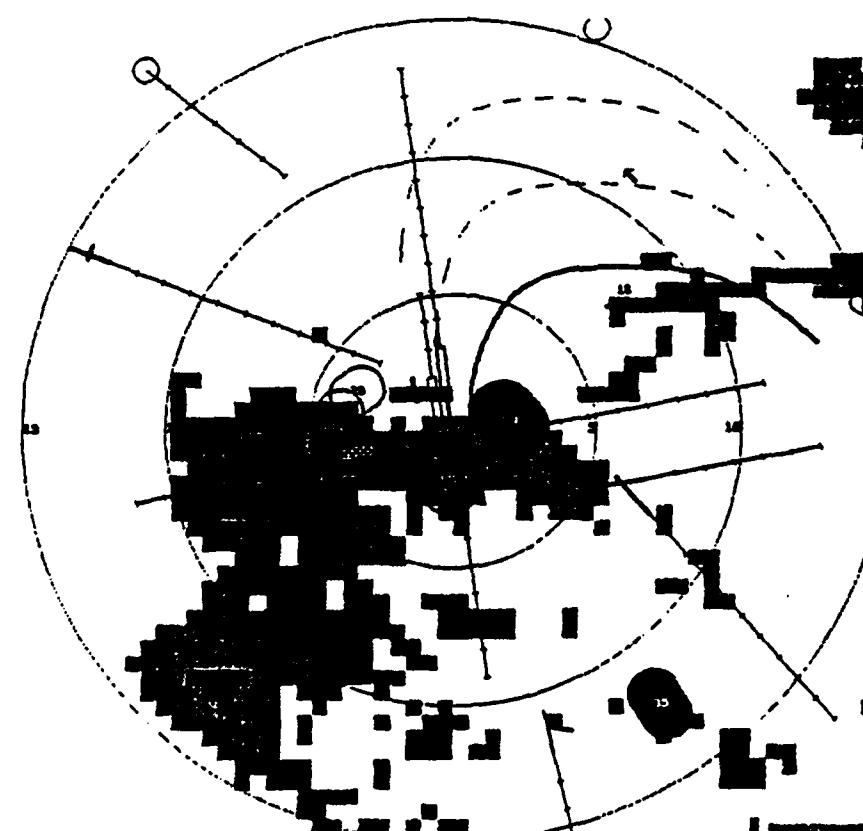
PRECIPITATION LEVELS  
☒ 0-2 ☒ 3-4 ☒ 5-6 ☒ 7-8

WIND SHIFT:  
☒ 0-2 ☒ 3-4

DATE: 09/09/88  
 TIME: 18:58:24  
 POWER: 07/11/88  
 MTIME: 22:28:58  
 GTIME: 22:28:58

MO: UP  
 GF: UP  
 PRECIP: UP  
 LLWS: DOWN

[Print Screen](#)



NCAR GSD

RANGE  
☒ 5m ☒ 10m ☒ 30m ☒ 50m

SCREEN  
☒ 1 ☒ 2 ☒ 3 ☒ 4  
☒ 5 ☒ 6 ☒ 7 ☒ 8

MAPS  
☒ Vortec & lines  
☒ AM rings  
☒ Airports  
☒ Interstates

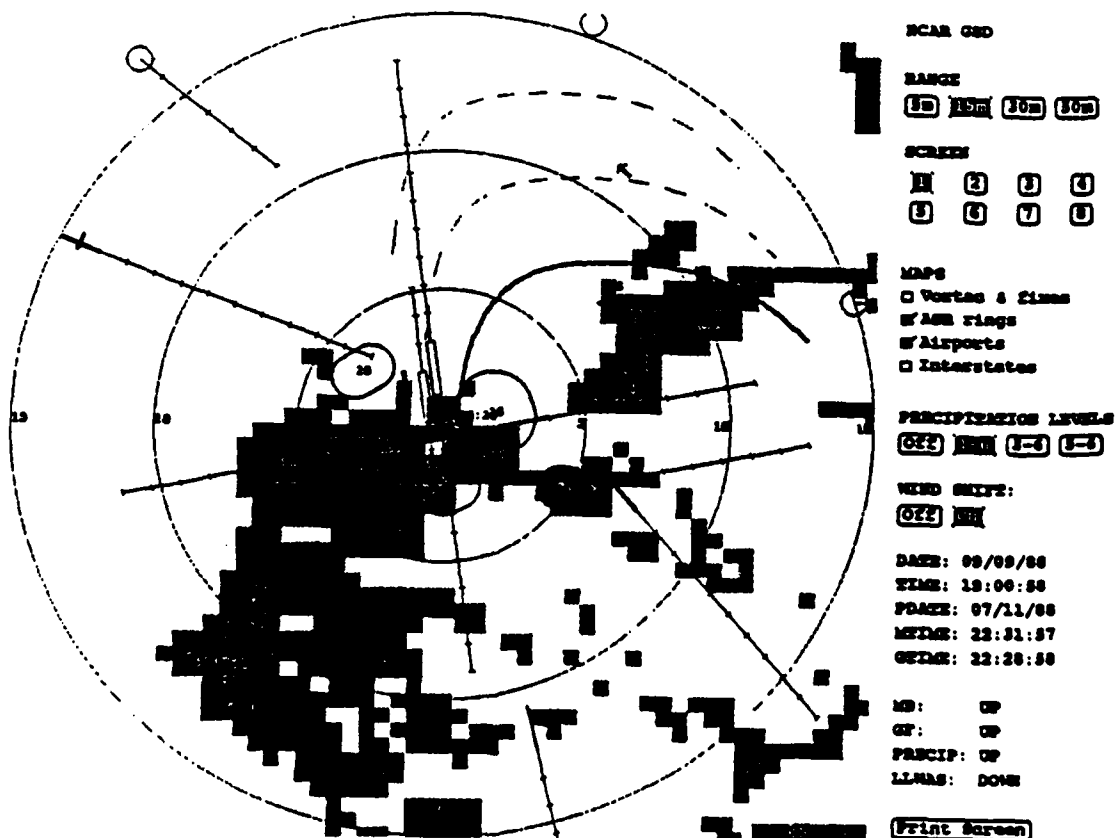
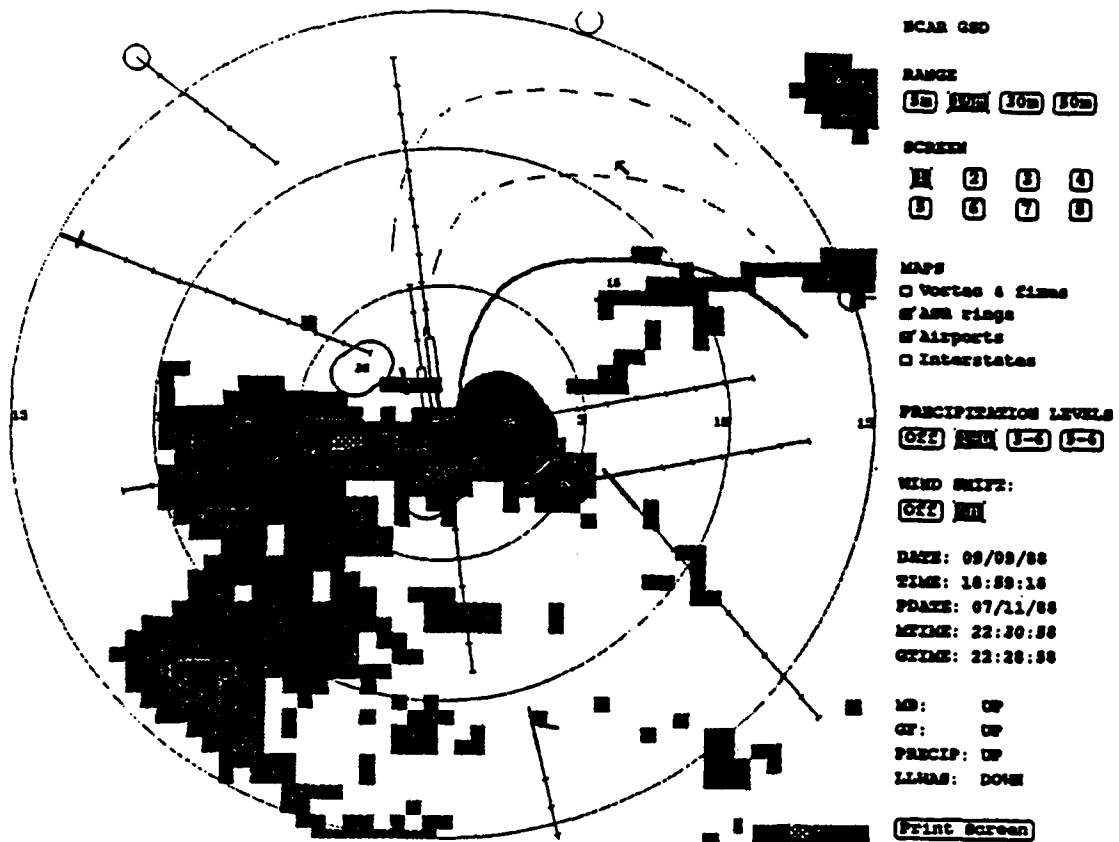
PRECIPITATION LEVELS  
☒ 0-2 ☒ 3-4 ☒ 5-6 ☒ 7-8

WIND SHIFT:  
☒ 0-2 ☒ 3-4

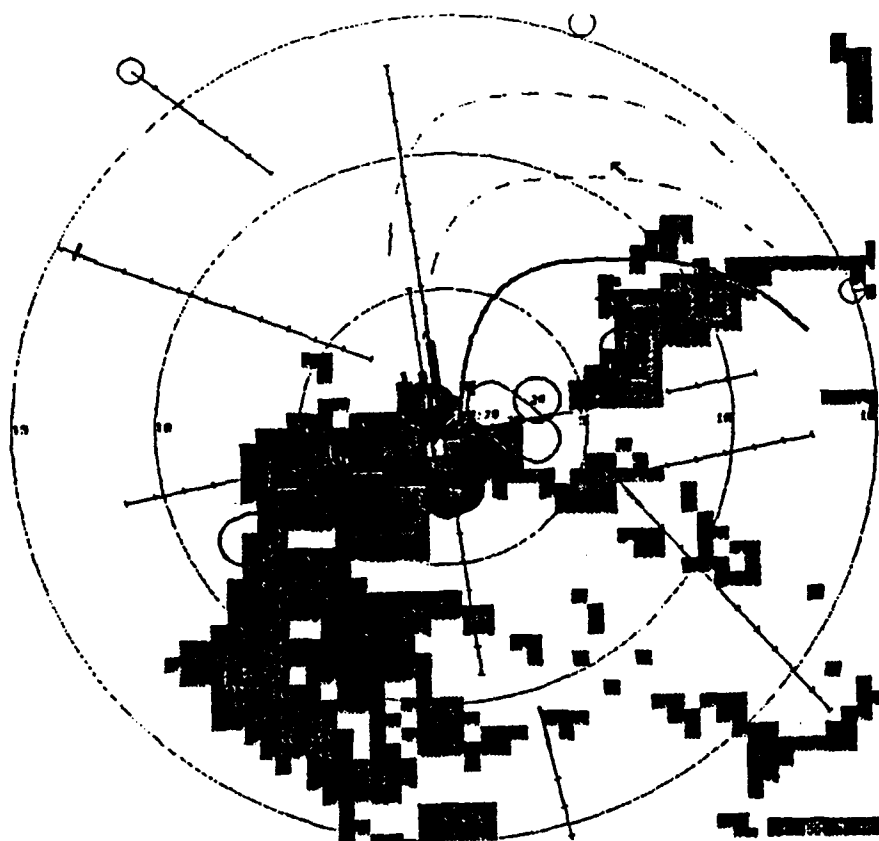
DATE: 09/09/88  
 TIME: 18:58:30  
 POWER: 07/11/88  
 MTIME: 22:30:02  
 GTIME: 22:28:58

MO: UP  
 GF: UP  
 PRECIP: UP  
 LLWS: DOWN

[Print Screen](#)







NCAR GSD

RANGE

☐ 5m ☐ 10m ☐ 30m ☐ 50m

SCREEN

☐ 1 ☐ 2 ☐ 3 ☐ 4  
☐ 5 ☐ 6 ☐ 7 ☐ 8

MAPS

☐ Vortex & lines  
☐ ASM rings  
☐ Airports  
☐ Interstates

PRECIPITATION LEVELS

☐ OFF ☐ MIN ☐ 3-4 ☐ 5-6

WIND SHIFT:

☐ OFF ☐ ON

DATE: 09/09/88

TIME: 19:01:48

PDATE: 07/11/88

MTIME: 22:32:55

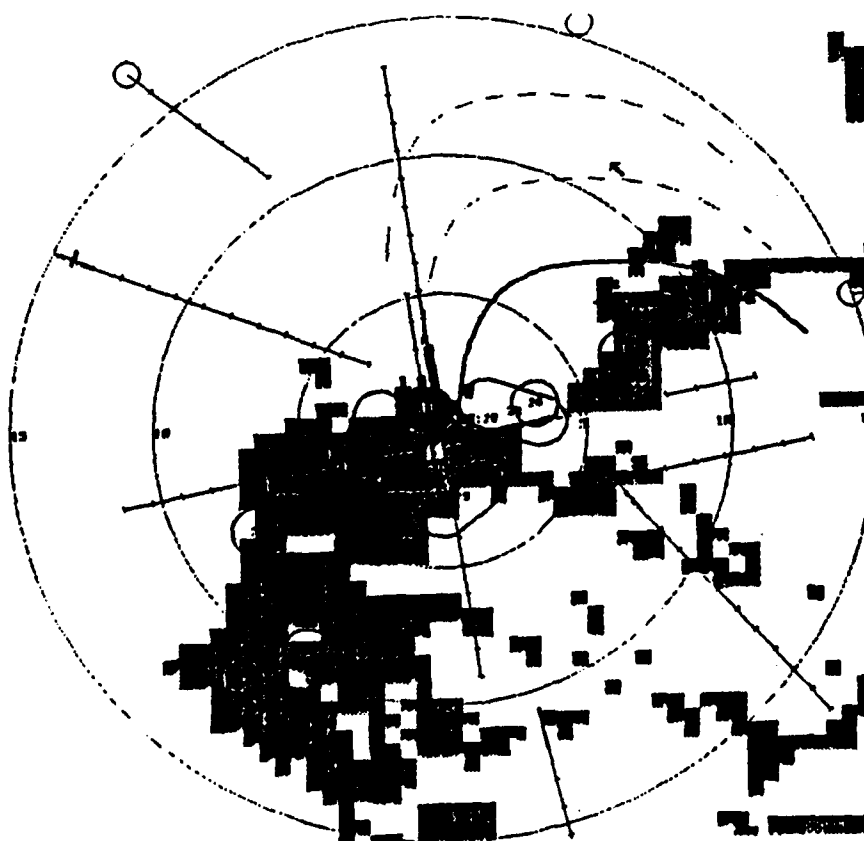
OTIME: 22:28:58

MD: UP

GT: UP

PRECIP: UP

LLWS: DOWN



NCAR GSD

RANGE

☐ 5m ☐ 10m ☐ 30m ☐ 50m

SCREEN

☐ 1 ☐ 2 ☐ 3 ☐ 4  
☐ 5 ☐ 6 ☐ 7 ☐ 8

MAPS

☐ Vortex & lines  
☐ ASM rings  
☐ Airports  
☐ Interstates

PRECIPITATION LEVELS

☐ OFF ☐ MIN ☐ 3-4 ☐ 5-6

WIND SHIFT:

☐ OFF ☐ ON

DATE: 09/09/88

TIME: 19:02:29

PDATE: 07/11/88

MTIME: 22:33:59

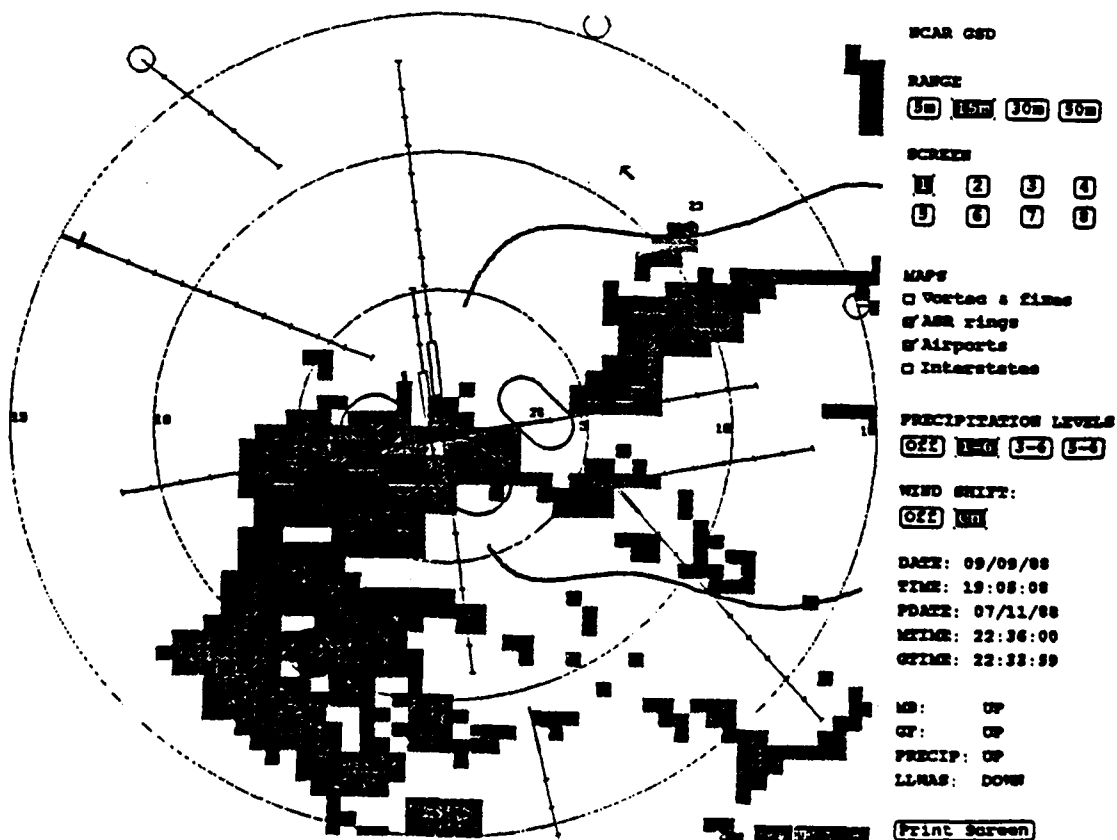
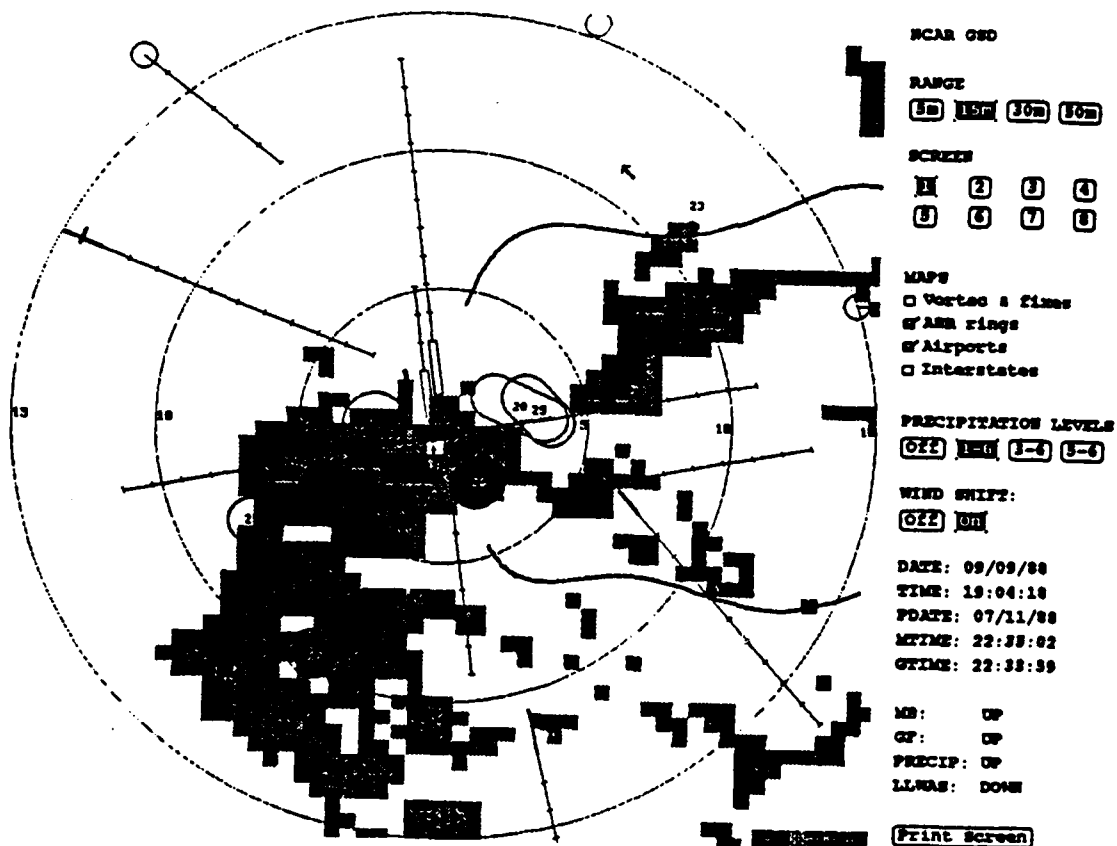
OTIME: 22:28:58

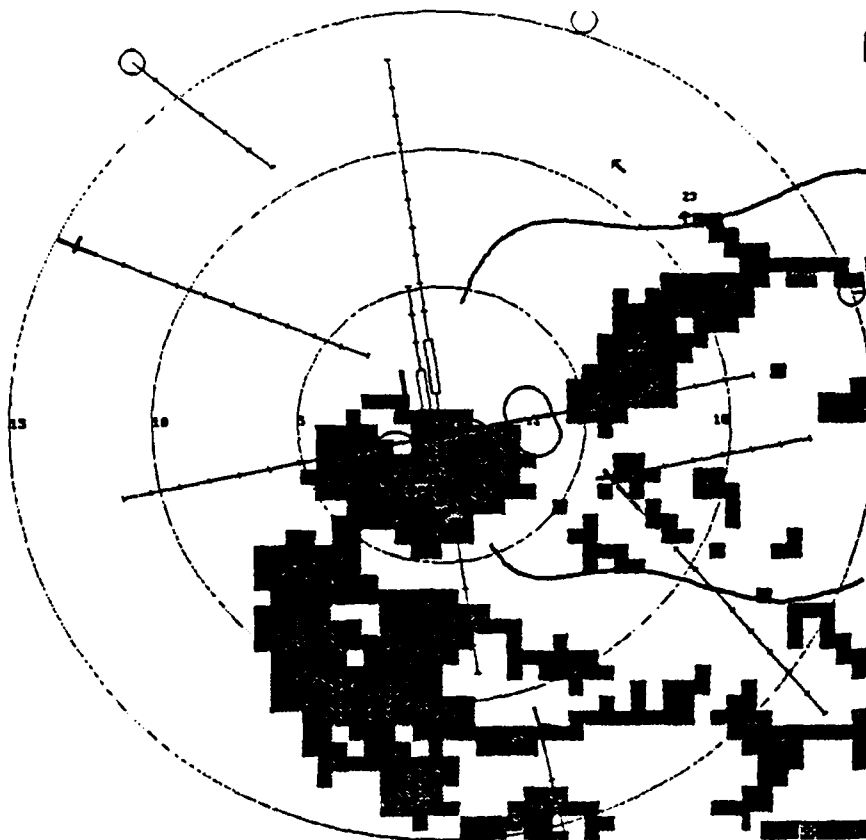
MD: UP

GT: UP

PRECIP: UP

LLWS: DOWN





NCAR GSD

RANGE

☐ 5m ☐ 10m ☐ 30m ☐ 50m

SCREEN

☐ 1 ☐ 2 ☐ 3 ☐ 4  
☐ 5 ☐ 6 ☐ 7 ☐ 8

MAPS

☐ Vortec & Lines  
☐ ASH rings  
☐ Airports  
☐ Interstates

PRECIPITATION LEVELS

☐ OFF ☐ MIN ☐ 3-6 ☐ 8-6

WIND SHIFT:

☐ OFF ☐ MIN

DATE: 09/09/88

TIME: 19:08:30

PDAT: 07/11/88

MTIME: 22:36:57

OTIME: 22:33:39

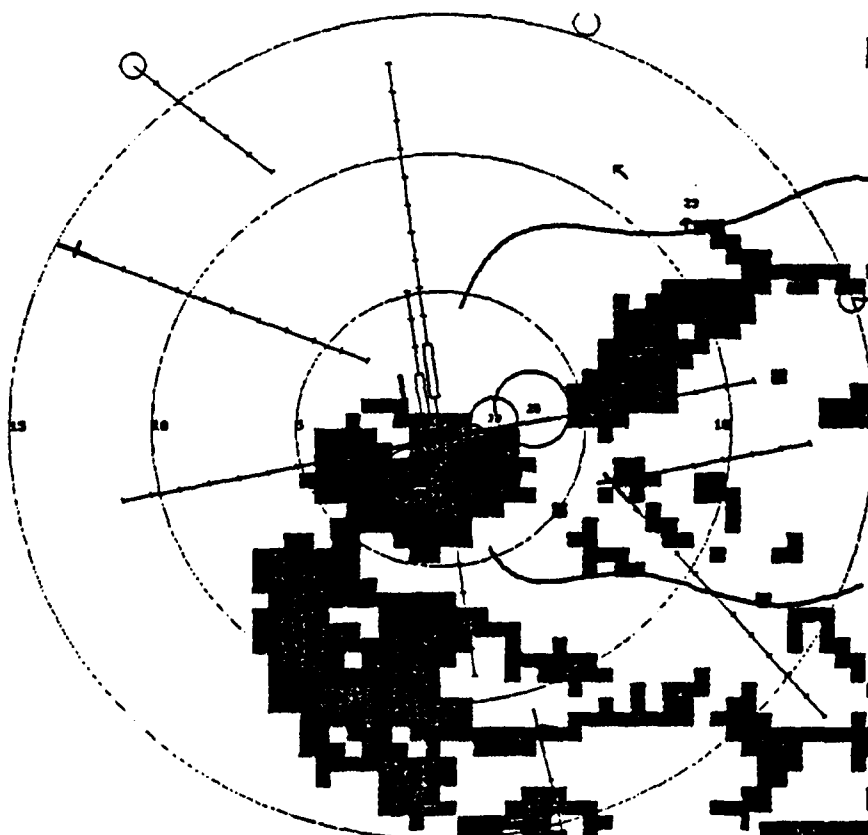
MB: UP

OT: UP

PRECIP: UP

LLWS: DOWN

[Print Screen](#)



NCAR GSD

RANGE

☐ 5m ☐ 10m ☐ 30m ☐ 50m

SCREEN

☐ 1 ☐ 2 ☐ 3 ☐ 4  
☐ 5 ☐ 6 ☐ 7 ☐ 8

MAPS

☐ Vortec & Lines  
☐ ASH rings  
☐ Airports  
☐ Interstates

PRECIPITATION LEVELS

☐ OFF ☐ MIN ☐ 3-6 ☐ 8-6

WIND SHIFT:

☐ OFF ☐ MIN

DATE: 09/09/88

TIME: 19:06:48

PDAT: 07/11/88

MTIME: 22:38:02

OTIME: 22:33:39

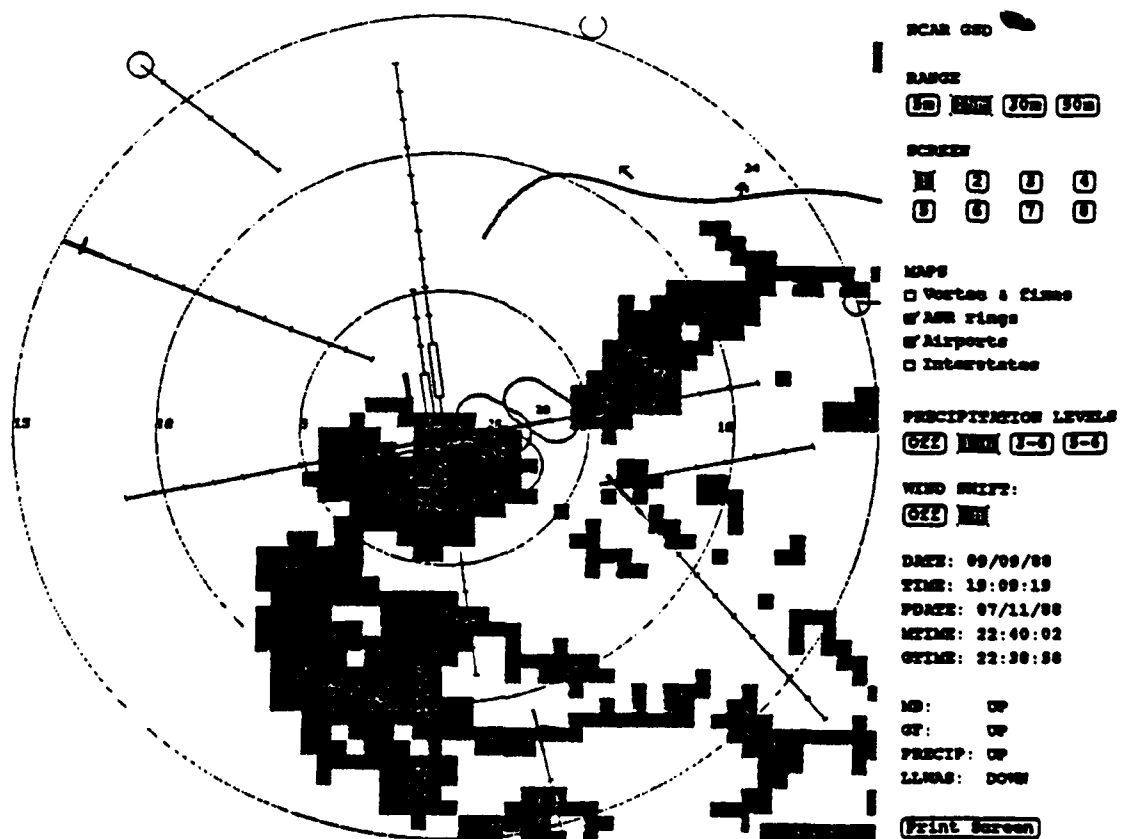
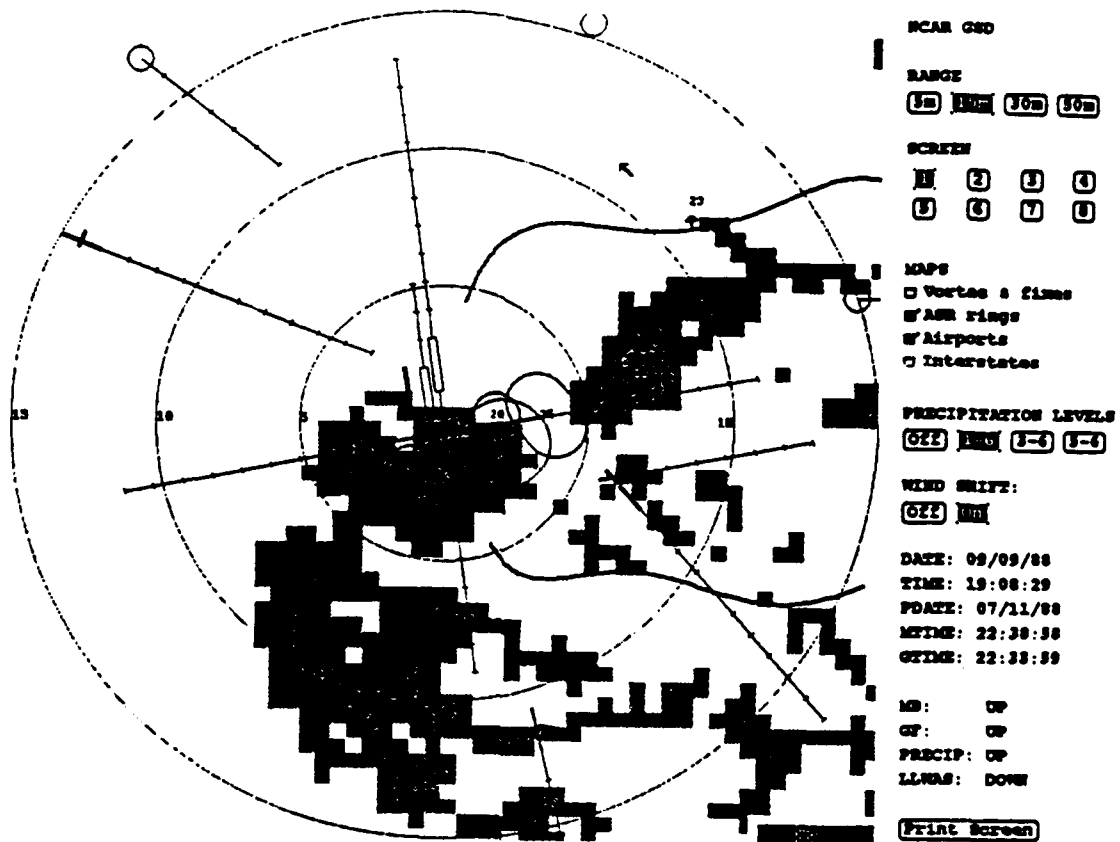
MB: UP

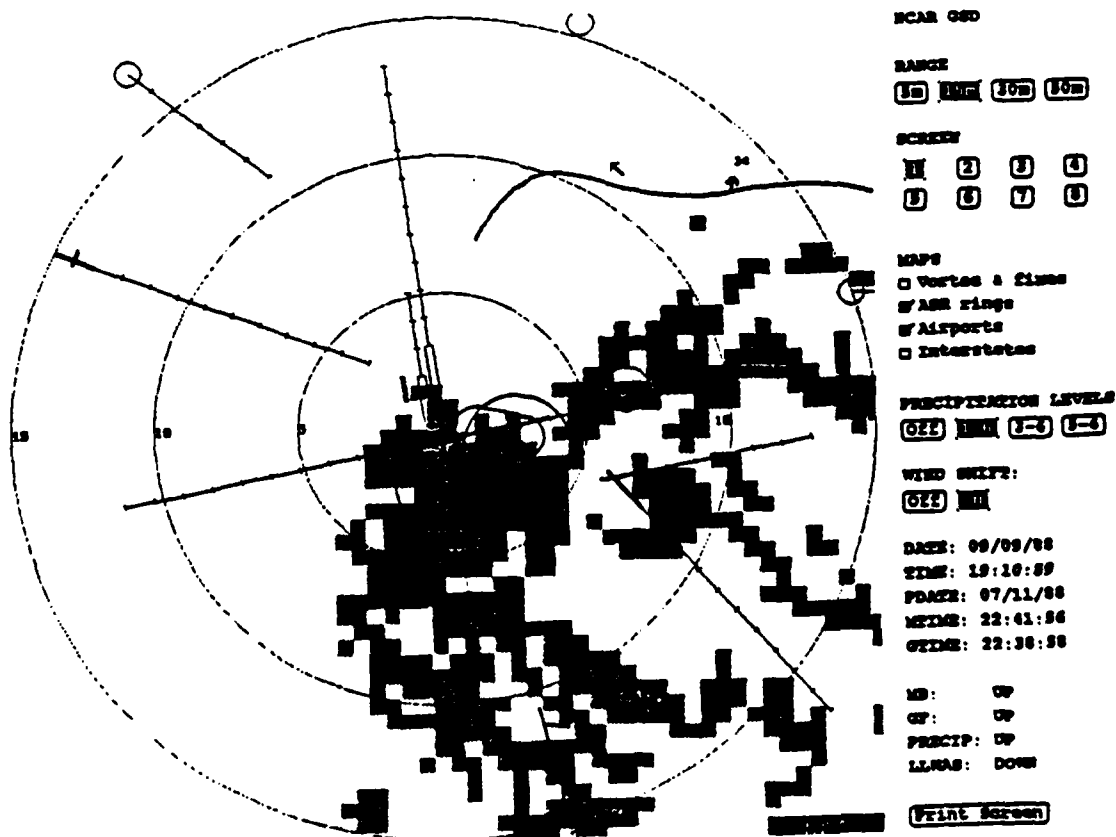
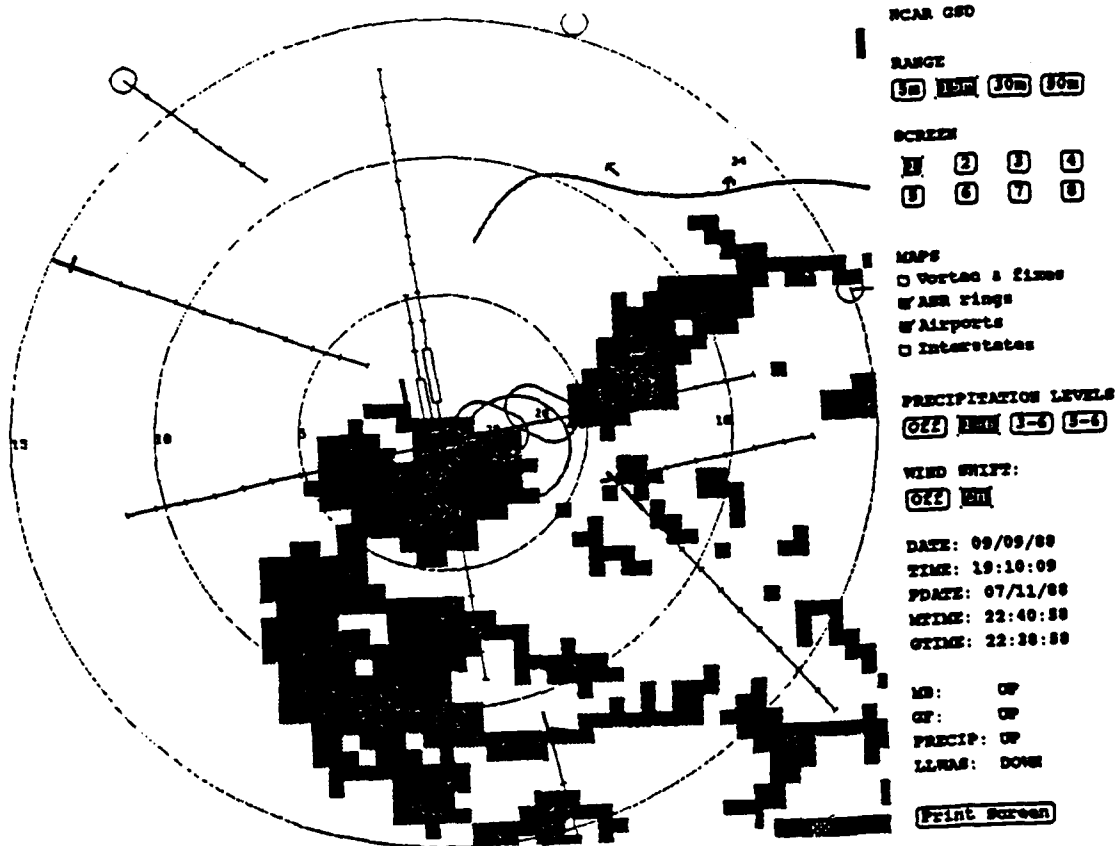
OT: UP

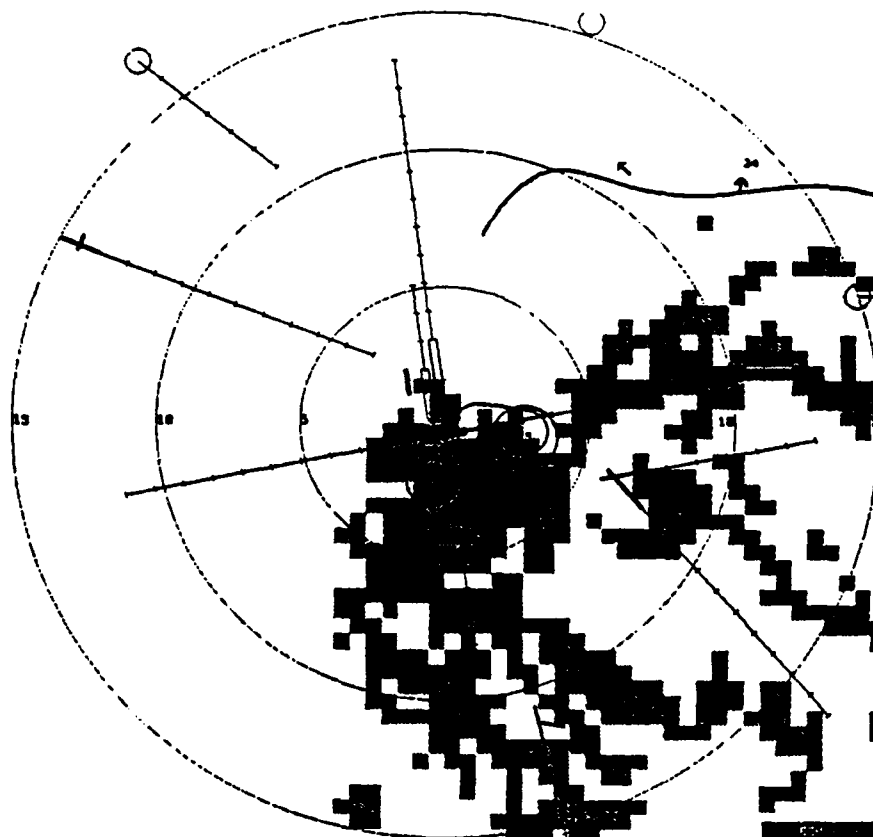
PRECIP: UP

LLWS: DOWN

[Print Screen](#)







NCAR GSD

RANGE

☐ 30 ☐ 60 ☐ 90 ☐ 120

SCREEN

☐ 1 ☐ 2 ☐ 3 ☐ 4  
☐ 5 ☐ 6 ☐ 7 ☐ 8

MAPS

☐ Vortices & lines  
☐ ASR rings  
☐ Airports  
☐ Interstates

PRECIPITATION LEVELS

☐ 0.2 ☐ 0.5 ☐ 1-2 ☐ 3-6

WIND SHIFT:

☐ 0.2 ☐ 0.5

DATE: 09/09/88

TIME: 19:11:47

PDATE: 07/11/88

MTIME: 22:42:54

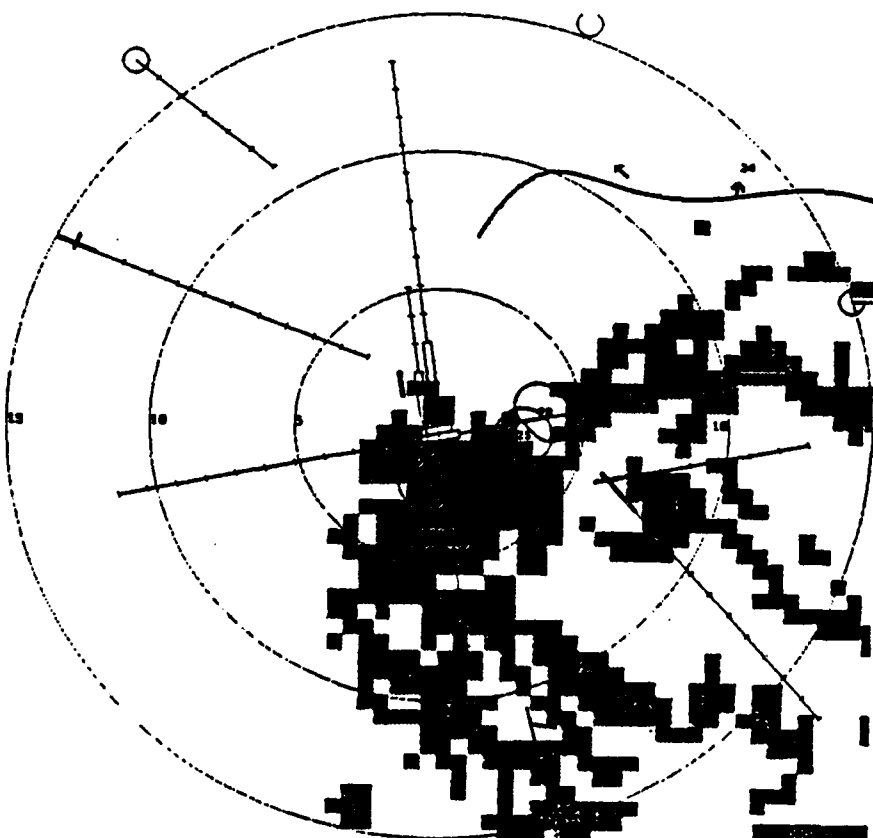
OTIME: 22:38:58

MD: UP

CF: UP

PRCIP: UP

LLWS: DOWN



NCAR GSD

RANGE

☐ 30 ☐ 60 ☐ 90 ☐ 120

SCREEN

☐ 1 ☐ 2 ☐ 3 ☐ 4  
☐ 5 ☐ 6 ☐ 7 ☐ 8

MAPS

☐ Vortices & lines  
☐ ASR rings  
☐ Airports  
☐ Interstates

PRECIPITATION LEVELS

☐ 0.2 ☐ 0.5 ☐ 1-2 ☐ 3-6

WIND SHIFT:

☐ 0.2 ☐ 0.5

DATE: 09/09/88

TIME: 19:13:27

PDATE: 07/11/88

MTIME: 22:43:58

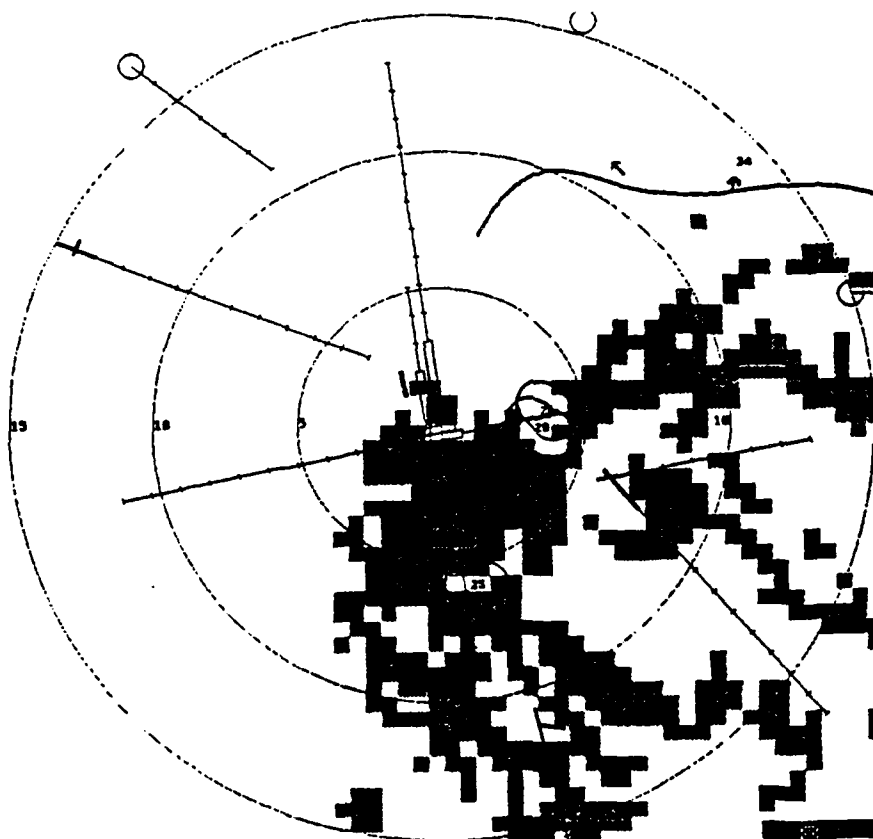
OTIME: 22:38:58

MD: UP

CF: UP

PRCIP: UP

LLWS: DOWN



NCAR GSD

RANGE

☒ 5m ☒ 15m ☒ 30m ☒ 60m

SCREEN

☒ 1 ☒ 2 ☒ 3 ☒ 4  
☒ 5 ☒ 6 ☒ 7 ☒ 8

MAPS

☐ Vortex & lines  
☐ WAA rings  
☐ Airports  
☐ Interstates

PRECIPITATION LEVELS

☒ 0-2 ☒ 3-6 ☒ 7-9 ☒ 10-15

WIND SHIFT:

☒ 0-2 ☒ 3-6

DATE: 09/09/88

TIME: 19:14:18

PDAT: 07/11/88

MTIME: 22:48:00

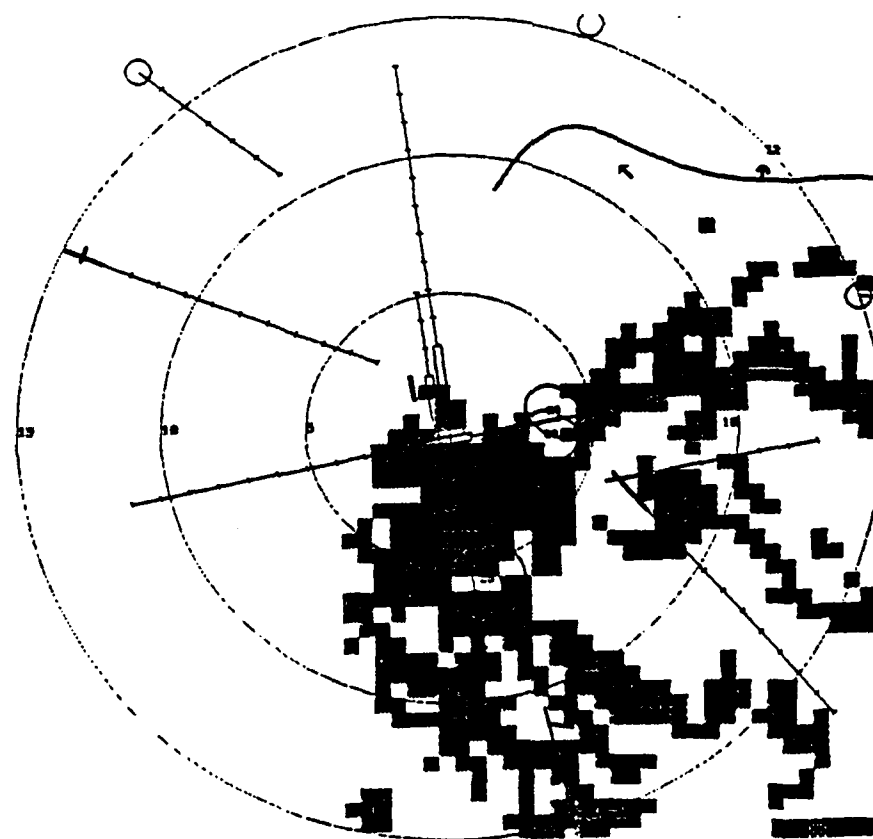
OTIME: 22:38:58

MD: UP

GT: UP

PRECIP: UP

LLWS: DOWN



NCAR GSD

RANGE

☒ 5m ☒ 15m ☒ 30m ☒ 60m

SCREEN

☒ 1 ☒ 2 ☒ 3 ☒ 4  
☒ 5 ☒ 6 ☒ 7 ☒ 8

MAPS

☐ Vortex & lines  
☐ WAA rings  
☐ Airports  
☐ Interstates

PRECIPITATION LEVELS

☒ 0-2 ☒ 3-6 ☒ 7-9 ☒ 10-15

WIND SHIFT:

☒ 0-2 ☒ 3-6

DATE: 09/09/88

TIME: 19:18:09

PDAT: 07/11/88

MTIME: 22:48:58

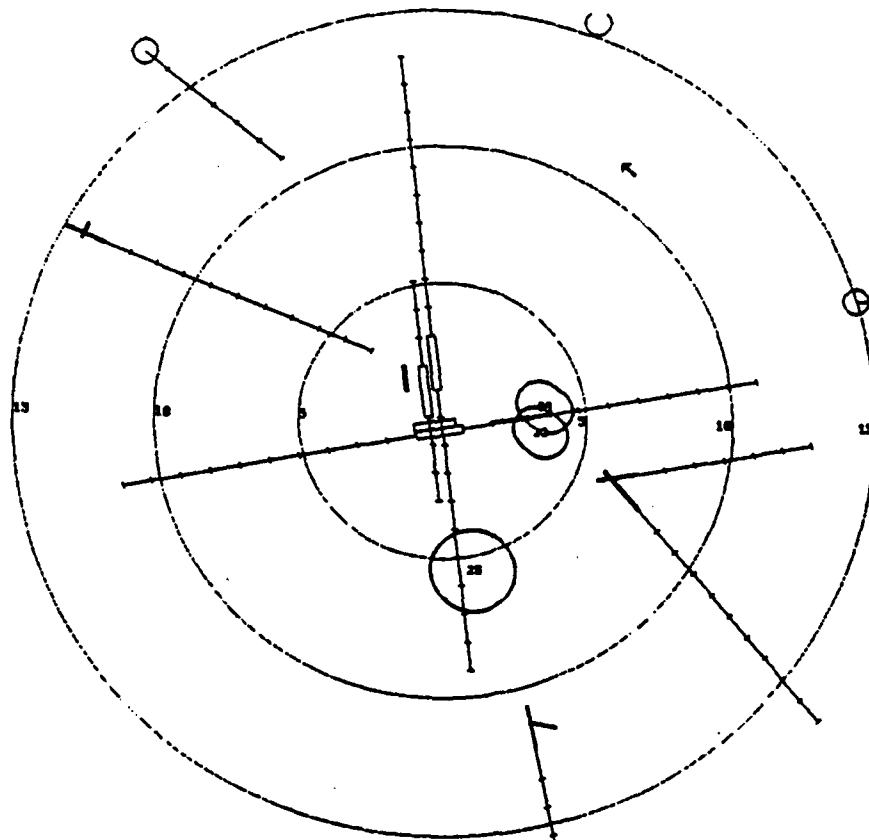
OTIME: 22:48:58

MD: UP

GT: UP

PRECIP: UP

LLWS: DOWN



NCAR QSD

RANGE

15m 30m 45m 60m

SCREEN

1 2 3 4  
5 6 7 8

MAPS

☐ Vertec & Time  
☐ ASR rings  
☐ Airports  
☐ Interstates

PRECIPITATION LEVELS

0-2 3-4 5-6 7-8

WIND SHIFT:

0-2 3-4

DATE: 09/09/88

TIME: 20:20:31

FOATE: 07/11/88

MTIME: 22:46:58

OTIME: 22:43:58

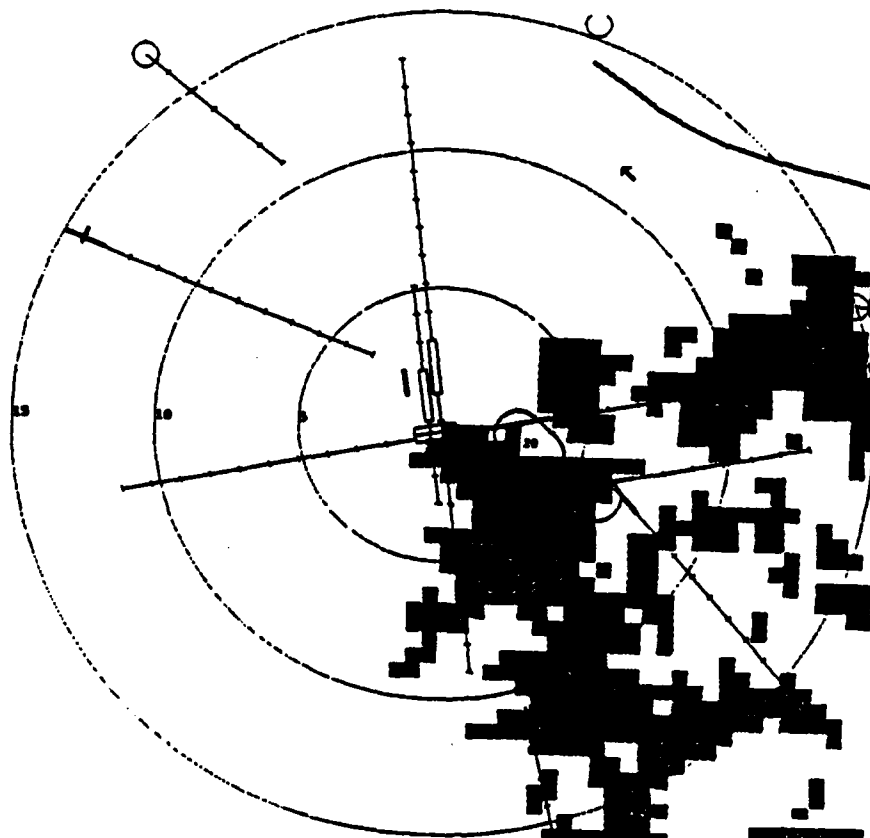
MB: UP

GF: DOWN

PRECIP: DOWN

LLWS: DOWN

[Print Screen](#)



NCAR QSD

RANGE

15m 30m 45m 60m

SCREEN

1 2 3 4  
5 6 7 8

MAPS

☐ Vertec & Time  
☐ ASR rings  
☐ Airports  
☐ Interstates

PRECIPITATION LEVELS

0-2 3-4 5-6 7-8

WIND SHIFT:

0-2 3-4

DATE: 09/09/88

TIME: 20:32:40

FOATE: 07/11/88

MTIME: 22:50:57

OTIME: 22:48:57

MB: UP

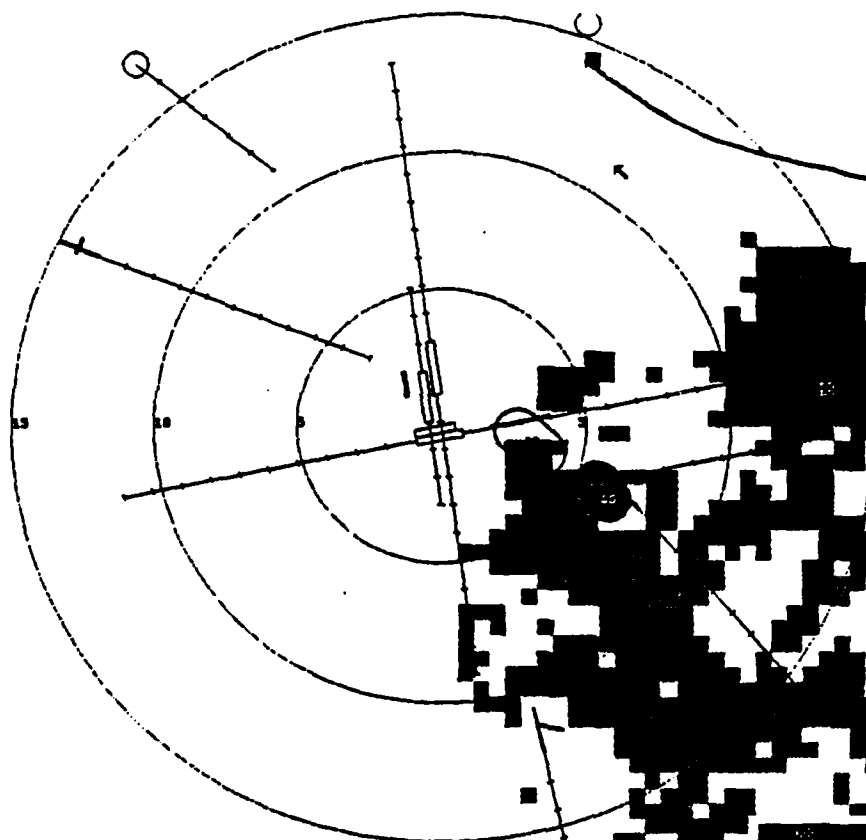
GF: UP

PRECIP: UP

LLWS: DOWN

[Print Screen](#)





SCAR OSD

RANGE

☐ 5m ☐ 15m ☐ 30m ☐ 50m

SCREEN

☐ 1 ☐ 2 ☐ 3 ☐ 4  
☐ 5 ☐ 6 ☐ 7 ☐ 8

MAPS

☐ Vortex & lines  
☐ of AWE rings  
☐ of Airports  
☐ of Interstates

PRECIPITATION LEVELS

☐ 0.25 ☐ 0.50 ☐ 1.00 ☐ 2.00

WIND SHIFT:

☐ 0.25 ☐ 0.50

DATE: 09/09/88

TIME: 20:33:31

PDATE: 07/11/88

MTIME: 22:51:58

OTIME: 22:48:57

MD: UP

CV: UP

PRECIP: UP

LLWS: DOWN

[Print Screen](#)

## Appendix B: TDWR Alphanumeric Alarms

Alphanumeric alarms from the TDWR algorithm are listed; all alarms for 11 July 1988 are included.

For the TDWR alarms, the date and time at the top of the first column are indicate when these were re-analyzed in playback mode. The date and time at the top of the second column are the real date and the microburst alarm update time, from the third column, the real date and the gust front alarm update time (only every 5 min).

The TDWR data are interpreted as:

WSA 35RA 200 8 10K+ RWY: Wind shear alert, runway 350 right approach, threshold winds from 200 ° at 8 kt, expect airspeed gain of 10 kt on the runway

MBA 35LA 230 6 35k- 3MF: Microburst alert, runway 350 left approach, threshold winds from 230 ° at 6 kt, expect airspeed loss of 35 kt on 3 mile final

TDWR ALARMS for 30-AUG-88, hour 15

11was_t:30-AUG-88 15:30:47	mb_t: NONE	gf_t: NONE
35RA 200 9	35LA 200 9	8A 180 7
35RD 200 8	35LD 190 5	8D 200 6
17LA 200 8	17RA 190 5	26A 200 6
17LD 200 9	17RD 200 9	26D 180 7

11was_t:30-AUG-88 15:44:18	mb_t:11-JUL-88 21:35:02	gf_t:11-JUL-88 21:34:00
WSA 35RA 200 8 10k+ RWY	35LA 200 7	8A 200 5
WSA 35RD 210 8 10k+ RWY	WSA 35LD 220 6 10k+ JMD	8D 190 7
WSA 17LA 210 8 10k+ 2MF	WSA 17RA 220 6 10k+ 3MF	26A 190 7
WSA 17LD 200 8 10k+ RWY	17RD 200 7	26D 200 5

11was_t:30-AUG-88 15:49:26	mb_t:11-JUL-88 21:40:03	gf_t:11-JUL-88 21:38:59
35RA 200 7	35LA 200 7	8A 200 4
35RD 200 9	35LD 200 7	8D 220 4
17LA 200 9	17RA 200 7	26A 220 4
17LD 200 7	17RD 200 7	26D 200 4

11was_t:30-AUG-88 15:55:34	mb_t:11-JUL-88 21:45:04	gf_t:11-JUL-88 21:44:02
WSA 35RA 200 8 10k+ RWY	WSA 35LA 190 6 10k+ RWY	8A 190 8
WSA 35RD 200 6 10k+ RWY	WSA 35LD 190 7 10k+ RWY	8D 190 6
WSA 17LA 200 6 10k+ 1MF	WSA 17RA 190 7 10k+ 2MF	26A 190 6
WSA 17LD 200 8 10k+ RWY	WSA 17RD 190 6 10k+ RWY	26D 190 8

TDWR ALARMS for 30-AUG-88, hour 16

11was_t:30-AUG-88 16:01:32	mb_t:11-JUL-88 21:50:04	gf_t:11-JUL-88 21:49:00
35RA 200 7	35LA 200 5	8A 160 5
35RD 190 3	35LD 200 5	8D 190 6
17LA 190 3	17RA 200 5	26A 190 6
17LD 200 7	17RD 200 5	26D 160 5

11was_t:30-AUG-88 16:08:33	mb_t:11-JUL-88 21:56:59	gf_t:11-JUL-88 21:54:01
35RA 200 7	35LA 220 7	WSA 8A 180 5 25k- 2MF
35RD 190 4	35LD 200 5	8D 200 5
17LA 190 4	17RA 200 5	26A 200 5
17LD 200 7	17RD 220 7	WSA 26D 180 5 25k- 1MD

11was_t:30-AUG-88 16:10:57	mb_t:11-JUL-88 21:59:00	gf_t:11-JUL-88 21:54:01
35RA 180 4	35LA 220 6	8A 180 3
35RD 190 5	35LD 200 5	8D 200 6
17LA 190 5	17RA 200 5	26A 200 6
17LD 180 4	17RD 220 6	26D 180 3

11was_t:30-AUG-88 16:13:04	mb_t:11-JUL-88 22:01:00	gf_t:11-JUL-88 21:59:00
35RA 200 5	WSA 35LA 190 6 25k- 3MF	WSA 8A 170 4 25k- 2MF
35RD 210 8	35LD 180 1	8D 200 5
17LA 210 8	17RA 180 3	26A 200 5
17LD 200 5	WSA 17RD 190 6 25k- 2MD	WSA 26D 170 4 25k- 1MD

11was_t:30-AUG-88 16:14:00	mb_t:11-JUL-88 22:01:58	gf_t:11-JUL-88 21:59:00
35RA 220 6	WSA 35LA 200 4 25k- 3MF	8A 170 3
35RD 200 5	35LD 190 6	8D 220 6
17LA 200 5	17RA 190 6	26A 220 6
17LD 220 6	WSA 17RD 200 4 25k- 2MD	26D 170 3

11was_t:30-AUG-88 16:15:00	mb_t:11-JUL-88 22:02:57	gf_t:11-JUL-88 21:59:00
35RA 190 5	WSA 35LA 170 3 25k- 3MF	WSA 8A 180 4 25k- 2MF
35RD 200 4	35LD 170 5	8D 200 5
17LA 200 4	17RA 170 5	26A 200 5
17LD 190 5	WSA 17RD 170 3 25k- 2MD	WSA 26D 180 4 25k- 1MD

llwas t:30-AUG-88 16:16:08 WSA 35RA 190 6 25k- 3MF 35ND 210 5 17LA 210 5 WSA 17LD 190 6 25k- 3MD	mb_t:11-JUL-88 22:04:01 WSA 35LA 210 5 25k- 3MF 35LD 190 4 17NA 180 4 WSA 17RD 210 5 25k- 1MD	gf_t:11-JUL-88 21:59:00 WSA 8A 180 4 25k- 2MF 8D 220 6 25k- HWY 26A 220 6 25k- HWY 26D 180 4 25k- HWY
llwas t:30-AUG-88 16:17:09 WSA 35RA 180 7 25k- 3MF 35ND 210 6 17LA 210 6 WSA 17LD 180 7 25k- 2MD	mb_t:11-JUL-88 22:05:04 WSA 35LA 210 4 25k- 3MF 35LD 210 5 17NA 210 5 WSA 17RD 210 4 25k- 1MD	gf_t:11-JUL-88 21:59:00 WSA 8A 190 4 25k- HWY 8D 200 5 25k- HWY 26A 200 5 25k- HWY 26D 190 4 25k- HWY
llwas t:30-AUG-88 16:17:29 WSA 35RA 170 7 25k- 3MF 35ND 200 8 17LA 200 8 WSA 17LD 170 7 25k- 2MD	mb_t:11-JUL-88 22:05:04 5 WSA 35LA 200 6 25k- 3MF 35LD 210 5 10k+ HWY 17NA 210 5 10k+ HWY WSA 17RD 200 6 25k- 1MD	gf_t:11-JUL-88 22:04:01 WSA 8A 180 5 25k- HWY 8D 200 5 25k- HWY 26A 200 5 25k- HWY 26D 180 5 25k- HWY
llwas t:30-AUG-88 16:18:23 MBA 35RA 180 5 35k- 3MF 35RD 200 8 17LA 200 8 MBA 17LD 180 5 35k- 2MD	mb_t:11-JUL-88 22:06:01 6 MBA 35LA 200 6 35k- 3MF 35LD 200 5 10k+ HWY 17RA 200 5 10k+ HWY MBA 17RD 200 6 35k- 1MD	gf_t:11-JUL-88 22:04:01 MBA 8A 170 5 35k- HWY 8D 190 3 35k- HWY 26A 190 3 35k- 1MF 26D 170 5 35k- HWY
llwas t:30-AUG-88 16:19:31 MBA 35RA 190 5 35k- 3MF 35RD 200 6 17LA 200 6 MBA 17LD 190 5 35k- 2MD	mb_t:11-JUL-88 22:06:58 7 MBA 35LA 220 5 35k- 3MF 35LD 200 4 10k+ HWY 17NA 200 4 10k+ HWY MBA 17RD 220 5 35k- 1MD	gf_t:11-JUL-88 22:04:01 MBA 8A 150 4 35k- 3MF 8D 200 7 35k- HWY 26A 200 7 35k- 1MF 26D 150 4 35k- HWY
llwas t:30-AUG-88 16:20:39 MBA 35RA 180 5 35k- 3MF 35RD 210 4 17LA 210 4 MBA 17LD 180 5 35k- 2MD	mb_t:11-JUL-88 22:08:03 8 MBA 35LA 230 6 35k- 2MF 35LD 210 6 10k+ HWY 17NA 210 6 10k+ HWY MBA 17RD 230 6 35k- 1MD	gf_t:11-JUL-88 22:04:01 MBA 8A 150 3 35k- 3MF 8D 220 7 50k- HWY 26A 220 7 50k- 2MF 26D 150 3 35k- HWY
llwas t:30-AUG-88 16:21:53 MBA 35RA 210 7 35k- 3MF 35ND Calm 17LA 180 3 MBA 17LD 210 8 35k- 2MD	mb_t:11-JUL-88 22:09:00 MBA 35LA 210 5 35k- 2MF 35LD 190 3 10k+ HWY 17NA 200 4 10k+ HWY MBA 17RD 230 4 35k- 1MD	gf_t:11-JUL-88 22:04:01 MBA 8A Calm 35k- 3MF 8D 200 5 60k- HWY 26A 200 5 60k- 3MF 26D Calm 35k- HWY
llwas t:30-AUG-88 16:23:08 WSA 35RA 210 5 10k+ 3MF 35ND 190 3 17LA 190 3 WSA 17LD 210 5 10k+ 1MD	mb_t:11-JUL-88 22:10:03 WSA 35LA 200 4 10k+ 3MF 35LD 210 7 10k+ HWY 17RA 210 7 10k+ HWY WSA 17RD 200 4 10k+ HWY	gf_t:11-JUL-88 22:04:01 MBA 8A 200 4 50k- 3MF 8D 200 7 50k- HWY 26A 200 7 50k- 3MF 26D 200 4 50k- HWY
llwas t:30-AUG-88 16:23:28 WSA 35RA 210 5 20k+ 3MF 35ND 190 8 17LA 190 8 WSA 17LD 210 5 20k+ 2MD	mb_t:11-JUL-88 22:10:03 WSA 35LA 200 4 20k+ 3MF 35LD 220 6 17RA 220 6 WSA 17RD 200 4 20k+ 1MD	gf_t:11-JUL-88 22:09:00 MBA 8A 200 5 50k- 3MF 8D 200 6 50k- HWY 26A 200 6 50k- 3MF 26D 200 5 50k- HWY
llwas t:30-AUG-88 16:24:09 MBA 35RA 210 3 35k- 3MF 35RD 190 7 17LA 190 7 MBA 17LD 210 3 35k- 1MD	mb_t:11-JUL-88 22:11:00 MBA 35LA 200 5 35k- 2MF 35LD 230 5 35k- HWY 17NA 230 5 35k- HWY MBA 17RD 200 5 35k- HWY	gf_t:11-JUL-88 22:09:00 MBA 8A 190 4 35k- 3MF 8D 200 5 70k- HWY 26A 200 5 70k- 3MF 26D 190 4 35k- HWY
llwas t:30-AUG-88 16:25:23 MBA 35RA 200 7 45k- 3MF 35RD 190 6 17LA 190 6 MBA 17LD 200 7 45k- 1MD	mb_t:11-JUL-88 22:11:58 MBA 35LA 200 6 45k- 2MF 35LD 220 5 45k- HWY 17NA 220 5 45k- HWY MBA 17RD 200 6 45k- HWY	gf_t:11-JUL-88 22:09:00 MBA 8A 180 4 45k- 3MF 8D 200 5 70k- HWY 26A 200 5 70k- 3MF 26D 180 4 45k- HWY
llwas t:30-AUG-88 16:26:18 MBA 35RA 210 5 35k- 3MF 35RD Calm 17LA Calm MBA 17LD 210 5 35k- 1MD	mb_t:11-JUL-88 22:12:56 MBA 35LA 180 5 35k- 2MF 35LD 220 7 35k- HWY 17NA 220 7 35k- HWY MBA 17RD 180 5 35k- HWY	gf_t:11-JUL-88 22:09:00 MBA 8A 180 5 35k- 3MF 8D 200 5 70k- HWY 26A 200 5 70k- 3MF 26D 180 5 35k- HWY

11was t:30-AUG-88 16:27:26	mb_t:11-JUL-88 22:14:00	gf_t:11-JUL-88 22:09:00
MBA 35RA 190 6 45k- 3MF	MBA 35LA 180 3 45k- 3MF	MHA 8A 170 3 45k- 3MF
35HD 210 5	35LD 220 5	MHA 8D 210 5 70k- HWY
17LA 210 5	17HA 220 5	MHA 26A 210 5 70k- 3MF
MBA 17LD 190 6 45k- 1MD	MBA 17RD 180 3 45k- 1MD	MHA 26D 170 3 45k- HWY
11was t:30-AUG-88 16:28:40	mb_t:11-JUL-88 22:15:02	gf_t:11-JUL-88 22:09:00
MBA 35RA 190 6 45k- 3MF	MBA 35LA 170 3 45k- 2MF	MHA 8A 170 3 45k- 3MF
35HD 200 7	35LD 200 6	MHA 8D 230 5 45k- HWY
17LA 200 7	17HA 200 6	MHA 26A 230 5 45k- 3MF
MBA 17LD 190 6 45k- 1MD	MBA 17RD 170 3 45k- 1MD	MHA 26D 170 3 45k- HWY
11was t:30-AUG-88 16:29:00	mb_t:11-JUL-88 22:15:02	gf_t:11-JUL-88 22:14:00
MBA 35RA 180 5 45k- 3MF	MHA 35LA Calm 45k- 2MF	MBA 8A 170 3 45k- 3MF
WSA 35HD 210 6 20k- HWY	WSA 35LD 190 6 20k- HWY	MHA 8D 220 4 45k- HWY
WSA 17LA 210 6 20k- HWY	WSA 17HA 190 6 20k- HWY	MHA 26A 220 4 45k- 3MF
MBA 17LD 180 5 45k- 1MD	MBA 17RD Calm 45k- 1MD	MHA 26D 170 3 45k- HWY
11was t:30-AUG-88 16:29:42	mb_t:11-JUL-88 22:16:01	gf_t:11-JUL-88 22:14:00
MHA 35HA 190 5 45k- 3MF	MBA 35LA 190 5 45k- 3MF	MHA 8A 170 5 45k- 3MF
WSA 35HD 230 7 20k- HWY	WSA 35LD 180 3 20k- HWY	MHA 8D 210 5 45k- HWY
WSA 17LA 230 7 20k- HWY	WSA 17RA 180 3 20k- HWY	MHA 26A 210 5 45k- 3MF
MBA 17LD 190 5 45k- 2MD	MBA 17RD 190 5 45k- 1MD	MHA 26D 170 5 45k- HWY
11was t:30-AUG-88 16:30:45	mb_t:11-JUL-88 22:16:58	gf_t:11-JUL-88 22:14:00
MBA 35HA 190 7 50k- 3MF	MHA 35LA 240 5 50k- 3MF	MBA 8A 170 5 50k- HWY
WSA 35HD 240 3 20k- HWY	WSA 35LD 180 4 20k- HWY	MHA 8D 220 5 50k- HWY
WSA 17LA 240 3 20k- HWY	WSA 17RA 180 4 20k- HWY	MHA 26A 220 5 50k- 3MF
MHA 17LD 190 7 50k- 2MD	MHA 17RD 240 5 50k- 1MD	MHA 26D 170 5 50k- HWY
11was t:30-AUG-88 16:31:52	mb_t:11-JUL-88 22:18:02	gf_t:11-JUL-88 22:14:00
MHA 35HA Calm 45k- 3MF	MBA 35LA 230 3 45k- 3MF	MHA 8A 160 4 45k- 3MF
WSA 35HD 200 7 20k- HWY	MBA 35LD 220 6 45k- HWY	MHA 8D 210 3 45k- HWY
WSA 17LA 200 7 20k- HWY	MHA 17HA 220 6 45k- HWY	MHA 26A 210 3 45k- 3MF
MBA 17LD Calm 45k- 1MD	MBA 17RD 230 3 45k- HWY	MHA 26D 160 4 45k- HWY
11was t:30-AUG-88 16:33:00	mb_t:11-JUL-88 22:18:59	gf_t:11-JUL-88 22:14:00
MHA 35HA 190 5 45k- 3MF	MHA 35LA 210 5 45k- 3MF	MHA 8A 170 4 45k- 3MF
WSA 35HD 190 6 20k- HWY	WSA 35LD 210 5 20k- HWY	MHA 8D 180 8 45k- HWY
WSA 17LA 190 6 20k- HWY	WSA 17RA 210 5 20k- HWY	MHA 26A 180 8 45k- 3MF
MBA 17LD 190 5 45k- 2MD	MHA 17RD 210 5 45k- 1MD	MHA 26D 170 4 45k- HWY
11was t:30-AUG-88 16:33:54	mb_t:11-JUL-88 22:20:03	gf_t:11-JUL-88 22:14:00
MBA 35HA 190 4 40k- 3MF	MBA 35LA 210 6 40k- 3MF	MHA 8A 160 5 40k- 3MF
MHA 35HD 180 3 20k- HWY	WSA 35LD 190 6 20k- HWY	MHA 8D 190 7 40k- HWY
WSA 17LA 180 3 20k- HWY	WSA 17HA 190 6 20k- HWY	MHA 26A 190 7 40k- 3MF
MHA 17LD 190 4 40k- 2MD	MHA 17RD 210 6 40k- 1MD	MHA 26D 160 5 40k- HWY
11was t:30-AUG-88 16:35:02	mb_t:11-JUL-88 22:20:59	gf_t:11-JUL-88 22:18:59
MHA 35HA 190 5 45k- 3MF	MHA 35LA 200 5 45k- 3MF	MHA 8A 150 5 45k- 3MF
WSA 35HD 210 6 20k- HWY	WSA 35LD 230 5 20k- HWY	MHA 8D 200 6 45k- HWY
MHA 17LA 210 6 20k- HWY	WSA 17RA 210 5 20k- HWY	MHA 26A 200 6 45k- 3MF
MBA 17LD 190 5 45k- 2MD	MHA 17RD 200 5 45k- 1MD	MHA 26D 150 5 45k- HWY
11was t:30-AUG-88 16:36:10	mb_t:11-JUL-88 22:21:57	gf_t:11-JUL-88 22:18:59
MHA 35HA 190 5 20k- 3MF	WSA 35LA 220 3 20k- 3MF	MHA 8A 150 5 50k- 3MF
WSA 35HD 170 4 20k- HWY	WSA 35LD 220 4 20k- HWY	MHA 8D 170 3 50k- HWY
MHA 17LA 170 4 20k- HWY	WSA 17HA 220 4 20k- HWY	MHA 26A 170 3 50k- 3MF
MBA 17LD 190 5 20k- HWY	WSA 17RD 220 3 20k- HWY	MHA 26D 150 5 50k- HWY
11was t:30-AUG-88 16:36:44	mb_t:11-JUL-88 22:21:57 25?	gf_t:11-JUL-88 22:18:59
MHA 35HA 190 6 20k- 3MF	WSA 35LA 230 5 20k- 2MF	MHA 8A 160 5 50k- 3MF
WSA 35HD 180 5 20k- HWY	WSA 35LD 210 4 20k- HWY	MHA 8D 180 4 50k- HWY
MHA 17LA 180 5 20k- HWY	WSA 17HA 210 4 20k- HWY	MHA 26A 180 4 50k- 3MF
MBA 17LD 190 6 20k- HWY	WSA 17RD 230 5 20k- HWY	MHA 26D 160 5 50k- HWY
11was t:30-AUG-88 16:38:38	mb_t:11-JUL-88 22:23:59	gf_t:11-JUL-88 22:18:59
MHA 35HA 210 4 40k- 3MF	MHA 35LA 220 5 40k- 2MF	MHA 8A 180 3 40k- 3MF
MHA 35HD 200 7 40k- HWY	MHA 35LD Calm 40k- HWY	MHA 8D 200 4 40k- HWY
MHA 17LA 200 7 40k- HWY	MHA 17HA Calm 40k- HWY	MHA 26A 200 4 40k- 3MF
MBA 17LD 210 4 40k- HWY	MHA 17RD 220 5 40k- HWY	MHA 26D 180 3 40k- HWY

llwas_t:30-AUG-88 16:39:26	mb_t:11-JUL-88 22:25:02	gf_t:11-JUL-88 22:18:59
MHA 35HA 210 4 35k- 3MF	MBA 35LA 220 5 35k- 3MF	MHA 8A 170 3 35k- 3MF
WSA 35ND 210 6 20k+ HWY	WSA 35LD Calm 20k+ HWY	MHA 8D 180 5 35k- HWY
WSA 17LA 210 6 20k+ HWY	WSA 17HA Calm 20k+ HWY	MHA 26A 180 5 35k- 3MF
MHA 17LD 210 4 35k- 1MD	MBA 17ND 220 5 35k- 1MD	MHA 26D 170 3 35k- HWY
llwas_t:30-AUG-88 16:40:28	mb_t:11-JUL-88 22:26:00	gf_t:11-JUL-88 22:21:59
MHA 35HA 210 3 35k- 3MF	WSA 35LA 210 4 20k+ 2MF	MHA 8A 180 3 35k- 3MF
WSA 35ND 220 6 20k+ HWY	WSA 35LD 170 3 20k+ HWY	MBA 8D 210 6 35k- HWY
MHA 17LA 220 6 20k+ HWY	WSA 17HA 170 3 20k+ HWY	MHA 26A 210 6 35k- 3MF
MHA 17LD 210 3 35k- 1MD	WSA 17ND 210 4 20k+ HWY	MHA 26D 180 3 35k- HWY
llwas_t:30-AUG-88 16:41:21	mb_t:11-JUL-88 22:26:00	gf_t:11-JUL-88 22:23:59
MHA 35HA 220 3 35k- 3MF	WSA 35LA 210 3 20k+ 2MF	MHA 8A Calm 35k- 3MF
WSA 35ND 230 4 20k+ HWY	WSA 35LD 200 4 20k+ HWY	MBA 8D 220 6 35k- HWY
WSA 17LA 230 4 20k+ HWY	WSA 17HA 200 4 20k+ 1MF	MHA 26A 220 6 35k- 3MF
MHA 17LD 220 3 35k- 1MD	WSA 17ND 210 3 20k+ HWY	MHA 26D Calm 35k- HWY
llwas_t:30-AUG-88 16:41:48	mb_t:11-JUL-88 22:26:57	gf_t:11-JUL-88 22:23:59
MHA 35HA 200 4 35k- 3MF	WSA 35LA Calm 25k- 3MF	MHA 8A Calm 35k- 3MF
WSA 35ND 230 3 20k+ HWY	WSA 35LD Calm 20k+ HWY	MBA 8D 210 5 35k- HWY
WSA 17LA 230 3 20k+ HWY	WSA 17HA Calm 20k+ 1MF	MHA 26A 210 5 35k- 3MF
MHA 17LD 200 4 35k- 2MD	WSA 17ND Calm 25k- 2MD	MBA 26D Calm 35k- HWY
llwas_t:30-AUG-88 16:42:22	mb_t:11-JUL-88 22:26:57	gf_t:11-JUL-88 22:23:59
MHA 35HA 190 6 35k- 3MF	WSA 35LA 210 5 25k- 3MF	MHA 8A Calm 35k- 3MF
WSA 35ND Calm 20k+ HWY	WSA 35LD Calm 20k+ HWY	MBA 8D 210 7 35k- HWY
WSA 17LA Calm 20k+ 1MF	WSA 17HA Calm 20k+ 1MF	MHA 26A 210 7 35k- 3MF
MHA 17LD 190 6 35k- 2MD	WSA 17ND 210 5 25k- 2MD	MBA 26D Calm 35k- HWY
llwas_t:30-AUG-88 16:42:43	mb_t:11-JUL-88 22:28:02	gf_t:11-JUL-88 22:21:59
MHA 35HA 190 4 35k- 3MF	WSA 35LA 180 3 25k- 3MF	MHA 8A Calm 35k- 3MF
WSA 35ND Calm 20k+ HWY	WSA 35LD 220 3 20k+ HWY	MBA 8D 200 6 35k- HWY
WSA 17LA Calm 20k+ 1MF	WSA 17HA 220 3 20k+ 1MF	MHA 26A 200 6 35k- 3MF
MHA 17LD 190 4 35k- 1MD	WSA 17ND 180 3 25k- 2MD	MHA 26D Calm 35k- HWY
MHA 35HA 190 5 35k- 3MF	WSA 35LA 200 5 25k- 3MF	MHA 8A 170 3 35k- 3MF
WSA 35ND Calm 20k+ HWY	WSA 35LD 230 5 20k+ HWY	MHA 8D 220 7 35k- HWY
WSA 17LA Calm 20k+ 1MF	WSA 17HA 210 5 20k+ 2MF	MHA 26A 220 7 35k- 3MF
MHA 17LD 190 5 35k- 1MD	WSA 17ND 200 5 25k- 2MD	MHA 26D 170 3 35k- HWY
llwas_t:30-AUG-88 16:43:50	mb_t:11-JUL-88 22:28:58	gf_t:11-JUL-88 22:23:59
WSA 35HA 200 5 20k- 3MF	WSA 35LA 200 4 20k- 3MF	MHA 8A 180 5 30k- 3MF
WSA 35ND Calm 20k+ HWY	WSA 35LD Calm 20k+ HWY	MBA 8D 230 7 30k- HWY
WSA 17LA Calm 20k+ 1MF	WSA 17HA Calm 20k+ 2MF	MHA 26A 230 7 30k- 3MF
WSA 17LD 200 5 20k- 3MD	WSA 17ND 200 4 20k- 2MD	MBA 26D 180 5 30k- HWY
llwas_t:30-AUG-88 16:44:37	mb_t:11-JUL-88 22:30:02	gf_t:11-JUL-88 22:23:59
WSA 35HA Calm 25k- 3MF	WSA 35LA 180 3 25k- 3MF	MHA 8A 200 4 30k- 3MF
WSA 35ND 180 5 20k+ HWY	WSA 35LD 220 6 20k+ HWY	MBA 8D 230 6 30k- HWY
WSA 17LA 180 5 20k+ 1MF	WSA 17HA 220 6 20k+ 2MF	MHA 26A 230 6 30k- 3MF
WSA 17LD Calm 25k- 3MD	WSA 17ND 180 3 25k- 2MD	MBA 26D 200 4 30k- HWY
llwas_t:30-AUG-88 16:45:04	mb_t:11-JUL-88 22:30:02	gf_t:11-JUL-88 22:28:58
WSA 35HA 190 5 25k- 3MF	WSA 35LA 220 6 25k- 3MF	MHA 8A 190 4 30k- 3MF
35ND 190 6	35LD 220 6	MBA 8D 230 6 30k- HWY
17LA 190 6	17HA 220 6	MHA 26A 230 6 30k- 3MF
WSA 17LD 190 5 25k- 3MD	WSA 17ND 220 6 25k- 2MD	MHA 26D 190 4 30k- HWY
llwas_t:30-AUG-88 16:45:39	mb_t:11-JUL-88 22:30:02	gf_t:11-JUL-88 22:28:58
WSA 35HA 180 3 25k- 3MF	WSA 35LA 210 5 25k- 3MF	MHA 8A 180 4 30k- 3MF
WSA 35ND 190 7 15k+ HWY	WSA 35LD 230 6 15k+ HWY	MBA 8D 230 6 30k- HWY
WSA 17LA 190 7 15k+ HWY	WSA 17HA 230 6 15k+ HWY	MHA 26A 230 6 30k- 3MF
WSA 17LD 180 3 25k- 3MD	WSA 17ND 210 5 25k- 2MD	MBA 26D 180 4 30k- HWY
llwas_t:30-AUG-88 16:45:59	mb_t:11-JUL-88 22:30:58	gf_t:11-JUL-88 22:28:58
WSA 35HA 180 4 25k- 3MF	WSA 35LA 210 5 25k- 3MF	MHA 8A 180 5 30k- HWY
WSA 35ND 200 6 15k+ HWY	WSA 35LD 230 4 15k+ HWY	MBA 8D 230 6 30k- HWY
WSA 17LA 200 6 15k+ HWY	WSA 17HA 230 4 15k+ HWY	MHA 26A 230 6 30k- 3MF
WSA 17LD 180 4 25k- 3MD	WSA 17ND 210 5 25k- 2MD	MBA 26D 180 5 30k- HWY

llwas_t:30-AUG-88 16:46:40	mb_t:11-JUL-88 22:30:58	gf_t:11-JUL-88 22:28:58
WSA 35HA 210 7 25k- 3MP :	WSA 35LA 230 7 25k- 3MP :	MMA 8A 180 3 30k- HWY
WSA 35ND 200 5 15k+ HWY :	WSA 35LD Calm 15k+ HWY :	MMA 8D 230 6 30k- HWY
WSA 17LA 200 5 15k+ HWY :	WSA 17HA Calm 15k+ 1MP :	MMA 26A 230 6 30k- 3MP
WSA 17LD 210 7 25k- 3MD :	WSA 17HD 230 7 25k- 2MD :	MMA 26D 180 3 30k- HWY
llwas_t:30-AUG-88 16:47:07	mb_t:11-JUL-88 22:31:57	gf_t:11-JUL-88 22:28:58
WSA 35HA 210 4 25k- 3MP :	WSA 35LA 230 5 25k- 3MP :	WSA 8A 180 3 25k- HWY
WSA 35ND 190 4 15k+ HWY :	WSA 35LD Calm 15k+ HWY :	WSA 8D 230 5 25k- HWY
WSA 17LA 190 4 15k+ HWY :	WSA 17HA Calm 15k+ 1MP :	WSA 26A 230 5 25k- 3MP
WSA 17LD 210 4 25k- 3MD :	WSA 17HD 230 5 25k- 2MD :	WSA 26D 180 3 25k- HWY
llwas_t:30-AUG-88 16:47:40	mb_t:11-JUL-88 22:31:57	gf_t:11-JUL-88 22:28:58
WSA 35HA Calm 25k- 3MP :	WSA 35LA 240 5 25k- 3MP :	WSA 8A 150 3 25k- HWY
WSA 35ND 190 5 15k+ HWY :	WSA 35LD Calm 15k+ HWY :	WSA 8D 230 3 25k- HWY
WSA 17LA 190 5 15k+ 1MP :	WSA 17HA Calm 15k+ 1MP :	WSA 26A 230 3 25k- 3MP
WSA 17LD Calm 25k- 3MD :	WSA 17HD 240 5 25k- 2MD :	WSA 26D 150 3 25k- HWY
llwas_t:30-AUG-88 16:48:35	mb_t:11-JUL-88 22:31:57	gf_t:11-JUL-88 22:28:58
WSA 35HA 190 6 25k- 3MP :	WSA 35LA 240 4 25k- 3MP :	WSA 8A 170 5 25k- HWY
WSA 35ND 190 3 15k+ HWY :	WSA 35LD 190 3 15k+ HWY :	WSA 8D 270 3 25k- HWY
WSA 17LA 190 3 15k+ 1MP :	WSA 17HA 190 3 15k+ 2MP :	WSA 26A 270 3 25k- 3MP
WSA 17LD 190 6 25k- 3MD :	WSA 17HD 240 4 25k- 2MD :	WSA 26D 170 5 25k- HWY
llwas_t:30-AUG-88 16:51:10	mb_t:11-JUL-88 22:31:57	gf_t:11-JUL-88 22:28:58
WSA 35HA Calm 25k- 3MP :	WSA 35LA 230 5 25k- 3MP :	WSA 8A 190 3 25k- HWY
35ND 170 5 :	35LD Calm :	WSA 8D 230 4 25k- HWY
17LA 170 5 :	17HA Calm :	WSA 26A 230 4 25k- 3MP
WSA 17LD Calm 25k- 3MD :	WSA 17HD 230 5 25k- 2MD :	WSA 26D 190 3 25k- HWY

## **Appendix C: Low Level Windshear Alarm System (LLWAS) Alarms**

Alarms from the LLWAS at Stapleton are listed; all alarms for 11 July 1988 are included.

These are coded in the same manner as for the TDWR alphanumeric alarm messages.



LLWAS ALARMS for 11-JUL-88, hour 21

11-JUL-88 21:21:01

35RA		35LA		8A
35RD		35LD		8D
17LA		17RA		26A
17LD		17RD		26D

11-JUL-88 21:23:17

WSA 35RA 10k- 2MF		WSA 35LA 10k- 1MF		8A
WSA 35RD 10k- RWT		WSA 35LD 10k- RWT		8D
WSA 17LA 10k- RWT		WSA 17RA 10k- RWT		26A
WSA 17LD 10k- RWT		WSA 17RD 10k- RWT		26D

11-JUL-88 21:23:44

35RA		35LA		8A
35RD		35LD		8D
17LA		17RA		26A
17LD		17RD		26D

LLWAS ALARMS for 11-JUL-88, hour 22

11-JUL-88 22:04:41

WSA 35RA 10k- 2MF		WSA 35LA 10k- 1MF		8A
WSA 35RD 10k- RWT		WSA 35LD 10k- RWT		8D
WSA 17LA 10k- RWT		WSA 17RA 10k- 1MF		26A
WSA 17LD 10k- RWT		WSA 17RD 10k- RWT		26D

11-JUL-88 22:05:22

WSA 35RA 10k- 2MF		WSA 35LA 10k- 1MF		8A
WSA 35RD 10k- RWT		WSA 35LD 10k- RWT		8D
WSA 17LA 10k- RWT		WSA 17RA 10k- RWT		26A
WSA 17LD 10k- RWT		WSA 17RD 10k- RWT		26D

11-JUL-88 22:05:56

WSA 35RA 10k- 2MF		WSA 35LA 10k- 1MF		8A
WSA 35RD 10k- RWT		WSA 35LD 10k- RWT		8D
WSA 17LA 10k- RWT		WSA 17RA 10k- RWT		WSA 26A 10k- RWT
WSA 17LD 10k- RWT		WSA 17RD 10k- RWT		WSA 26D 10k- RWT

11-JUL-88 22:06:02

WSA 35RA 10k- 2MF		WSA 35LA 10k- 1MF		WSA 8A 10k- 2MF
WSA 35RD 10k- RWT		WSA 35LD 10k- RWT		WSA 8D 10k- RWT
WSA 17LA 10k- RWT		WSA 17RA 10k- RWT		WSA 26A 10k- RWT
WSA 17LD 10k- RWT		WSA 17RD 10k- RWT		WSA 26D 10k- RWT

11-JUL-88 22:06:23

WSA 35RA 10k- 2MF		WSA 35LA 10k- 1MF		8A
WSA 35RD 10k- RWT		WSA 35LD 10k- RWT		8D
WSA 17LA 10k- RWT		WSA 17RA 10k- RWT		WSA 26A 10k- RWT
WSA 17LD 10k- RWT		WSA 17RD 10k- RWT		WSA 26D 10k- RWT

11-JUL-88 22:06:43

35RA		35LA		8A
35RD		35LD		8D
17LA		17RA		WSA 26A 10k- RWT
17LD		17RD		WSA 26D 10k- RWT

11-JUL-88 22:06:58

35RA		35LA		8A
35RD		35LD		8D
17LA		17RA		26A
17LD		17RD		26D

11-JUL-88 22:07:51

WSA 35RA 10k- 1MF		WSA 35LA 10k- RWT		8A
WSA 35RD 10k- RWT		WSA 35LD 10k- RWT		8D
WSA 17LA 10k- RWT		WSA 17RA 10k- 1MF		26A
WSA 17LD 10k- RWT		WSA 17RD 10k- RWT		26D

11-JUL-88 22:08:12	35RA 35RD 17LA 17LD	35LA 35LD 17RA 17RD	WSA 8A 10k- RWT WSA 8D 10k- RWT WSA 26A 10k- 2MF 26D
11-JUL-88 22:08:19	35RA 35RD 17LA 17LD	35LA 35LD 17RA 17RD	8A 8D 26A 26D
11-JUL-88 22:08:46	WSA 35RA 15k- 3MF pab 35RD 17LA WSA 17LD 15k- 1MD pab	WSA 35LA 15k- 3MF pab 35LD 17RA WSA 17RD 15k- RWT pab	WSA 8A 15k- 1MF WSA 8D 15k- RWT WSA 26A 15k- 1MF WSA 26D 10k- RWT
11-JUL-88 22:08:53	WSA 35RA 15k- 3MF 35RD 17LA WSA 17LD 15k- 1MD	WSA 35LA 15k- 3MF 35LD 17RA WSA 17RD 15k- RWT	WSA 8A 10k- 1MF WSA 8D 10k- RWT WSA 26A 10k- 2MF WSA 26D 10k- RWT
11-JUL-88 22:09:00	WSA 35RA 15k- 3MF pab 35RD 17LA WSA 17LD 15k- 1MD pab	WSA 35LA 15k- 3MF pab 35LD 10k- RWT WSA 17RA 10k- RWT WSA 17RD 15k- RWT pab	WSA 8A 10k- 1MF WSA 8D 10k- RWT WSA 26A 10k- 2MF WSA 26D 10k- RWT
11-JUL-88 22:09:07	WSA 35RA 15k- 3MF pab 35RD 17LA WSA 17LD 15k- 1MD pab	WSA 35LA 15k- 3MF pab 35LD 17RA WSA 17RD 15k- RWT pab	WSA 8A 10k- 1MF WSA 8D 10k- RWT WSA 26A 15k- 2MF WSA 26D 15k- RWT
11-JUL-88 22:09:13	WSA 35RA 15k- 3MF 35RD 17LA WSA 17LD 15k- 1MD	WSA 35LA 15k- 3MF 35LD 17RA WSA 17RD 15k- RWT	WSA 8A 10k- 1MF WSA 8D 10k- RWT WSA 26A 10k- 2MF WSA 26D 10k- RWT
11-JUL-88 22:09:34	WSA 35RA 15k- 3MF 35RD 17LA WSA 17LD 15k- 1MD	WSA 35LA 15k- 3MF 35LD 17RA WSA 17RD 15k- RWT	WSA 8A 10k- 1MF WSA 8D 10k- RWT pab WSA 26A 15k- 2MF pab WSA 26D 15k- RWT
11-JUL-88 22:09:41	WSA 35RA 15k- 3MF 35RD 17LA WSA 17LD 15k- 1MD	WSA 35LA 15k- 3MF 35LD 17RA WSA 17RD 15k- RWT	WSA 8A 10k- 1MF WSA 8D 10k- RWT WSA 26A 15k- 2MF WSA 26D 15k- RWT
11-JUL-88 22:09:47	WSA 35RA 15k- 3MF 35RD 17LA WSA 17LD 15k- 1MD	WSA 35LA 15k- 3MF 35LD 17RA WSA 17RD 15k- RWT	WSA 8A 10k- 1MF WSA 8D 10k- RWT pab WSA 26A 15k- 2MF pab WSA 26D 15k- RWT
11-JUL-88 22:09:54	WSA 35RA 10k- 3MF 35RD 17LA WSA 17LD 10k- 1MD	WSA 35LA 10k- 3MF 35LD 17RA WSA 17RD 10k- RWT	WSA 8A 10k- 1MF WSA 8D 10k- RWT WSA 26A 10k- 2MF WSA 26D 10k- RWT
11-JUL-88 22:10:08	WSA 35RA 10k- 3MF 35RD 17LA WSA 17LD 10k- 2MD	WSA 35LA 10k- 3MF 35LD 17RA WSA 17RD 10k- 1MD	WSA 8A 10k- 1MF pab WSA 8D 10k- RWT WSA 26A 10k- 1MF WSA 26D 10k- RWT pab
11-JUL-88 22:10:14	WSA 35RA 10k- 3MF 35RD 17LA WSA 17LD 10k- 1MD	WSA 35LA 10k- 3MF 35LD 17RA WSA 17RD 10k- RWT	8A 8D 26A WSA 26D 10k- RWT
11-JUL-88 22:10:21	WSA 35RA 15k- 3MF 35RD 17LA WSA 17LD 15k- 1MD	WSA 35LA 15k- 3MF 35LD 17RA WSA 17RD 15k- RWT	8A 8D 26A WSA 26D 10k- RWT
11-JUL-88 22:10:35	WSA 35RA 10k- 3MF 35RD 17LA WSA 17LD 10k- 1MD	WSA 35LA 10k- 3MF 35LD 17RA WSA 17RD 10k- RWT	8A 8D 26A WSA 26D 10k- RWT
11-JUL-88 22:10:42	WSA 35RA 10k- 3MF 35RD 17LA WSA 17LD 10k- 1MD	WSA 35LA 10k- 3MF 35LD 17RA WSA 17RD 10k- RWT	WSA 8A 35k- RWT WSA 8D 35k- RWT WSA 26A 35k- 3MF WSA 26D 35k- RWT

11-JUL-88 22:10:55	WSA 35RA 10k- 3MF 35RD 17LA WSA 17LD 10k- RWT	WSA 35LA 10k- 3MF 35LD 17RA WSA 17RD 10k- RWT	NBA 8A 35k- RWT NBA 8D 35k- RWT NBA 26A 35k- 3MF NBA 26D 35k- RWT
11-JUL-88 22:11:02	WSA 35RA 10k- 3MF 35RD 17LA WSA 17LD 10k- 1MD	WSA 35LA 10k- 3MF 35LD 17RA WSA 17RD 10k- RWT	NBA 8A 30k- RWT NBA 8D 30k- RWT NBA 26A 30k- 3MF NBA 26D 30k- RWT
11-JUL-88 22:11:09	WSA 35RA 10k- 3MF 35RD 17LA WSA 17LD 10k- 1MD	WSA 35LA 10k- 3MF 35LD 17RA WSA 17RD 10k- RWT	NBA 8A 25k- RWT NBA 8D 25k- RWT NBA 26A 25k- 3MF NBA 26D 25k- RWT
11-JUL-88 22:11:23	35RA 35RD 17LA 17LD	35LA 35LD 17RA 17RD	WSA 8A 20k+ 1MF pub WSA 8D 20k+ RWT pub WSA 26A 20k+ 2MF WSA 26D 20k+ RWT pub
11-JUL-88 22:11:30	35RA 35RD 17LA 17LD	35LA 35LD 17RA 17RD	WSA 8A 20k+ 1MF pub WSA 8D 20k+ RWT WSA 26A 20k+ 2MF WSA 26D 20k+ RWT pub
11-JUL-88 22:11:43	35RA 35RD 17LA 17LD	35LA 35LD 17RA 17RD	WSA 8A 20k+ RWT WSA 8D 20k+ RWT WSA 26A 20k+ 2MF WSA 26D 20k+ RWT
11-JUL-88 22:11:57	35RA 35RD 17LA 17LD	35LA 35LD 17RA 17RD	WSA 8A 10k- 2MF WSA 8D 10k- RWT WSA 26A 10k- 3MF WSA 26D 10k- RWT
11-JUL-88 22:12:04	35RA 35RD 17LA 17LD	35LA 35LD 17RA 17RD	NBA 8A 25k- 2MF NBA 8D 25k- RWT NBA 26A 25k- 3MF NBA 26D 25k- RWT
11-JUL-88 22:12:17	WSA 35RA 15k- 3MF WSA 35RD 10k- RWT WSA 17LA 10k- RWT WSA 17LD 15k- RWT	WSA 35LA 15k- 3MF WSA 35LD 10k- RWT WSA 17RA 10k- RWT WSA 17RD 15k- RWT	NBA 8A 25k- 2MF NBA 8D 25k- RWT NBA 26A 25k- 3MF NBA 26D 25k- RWT
11-JUL-88 22:12:31	WSA 35RA 10k- 3MF WSA 35RD 10k- RWT WSA 17LA 10k- RWT WSA 17LD 10k- RWT	WSA 35LA 10k- 3MF WSA 35LD 10k- RWT WSA 17RA 10k- RWT WSA 17RD 10k- RWT	NBA 8A 25k- 2MF NBA 8D 25k- RWT NBA 26A 25k- 3MF NBA 26D 25k- RWT
11-JUL-88 22:12:44	WSA 35RA 10k- 3MF WSA 35RD 10k- RWT WSA 17LA 10k- RWT WSA 17LD 10k- RWT	WSA 35LA 10k- 2MF WSA 35LD 10k- RWT WSA 17RA 10k- RWT WSA 17RD 10k- RWT	NBA 8A 25k- 2MF NBA 8D 25k- RWT NBA 26A 25k- 3MF NBA 26D 25k- RWT
11-JUL-88 22:12:51	WSA 35RA 10k- 3MF 35RD 17LA WSA 17LD 10k- 1MD	WSA 35LA 10k- 2MF WSA 35LD 10k- RWT WSA 17RA 10k- RWT WSA 17RD 10k- RWT	WSA 8A 10k- RWT WSA 8D 10k- RWT WSA 26A 10k- 3MF WSA 26D 10k- RWT
11-JUL-88 22:13:05	WSA 35RA 10k- 3MF 35RD 17LA WSA 17LD 10k- 1MD	WSA 35LA 10k- 2MF WSA 35LD 10k- RWT WSA 17RA 10k- RWT WSA 17RD 10k- RWT	NBA 8A 25k- RWT NBA 8D 25k- RWT NBA 26A 25k- 3MF NBA 26D 25k- RWT
11-JUL-88 22:13:18	WSA 35RA 10k- 3MF 35RD 17LA WSA 17LD 10k- 1MD	WSA 35LA 10k- 2MF 35LD 17RA WSA 17RD 10k- RWT	NBA 8A 25k- RWT NBA 8D 25k- RWT NBA 26A 25k- 3MF NBA 26D 25k- RWT
11-JUL-88 22:13:25	WSA 35RA 10k- 3MF 35RD 17LA WSA 17LD 10k- 1MD	WSA 35LA 10k- 2MF 35LD 17RA WSA 17RD 10k- RWT	WSA 8A 10k- 1MF pub WSA 8D 10k- RWT WSA 26A 10k- 3MF WSA 26D 10k- RWT pub
11-JUL-88 22:13:32	WSA 35RA 10k- 3MF 35RD 17LA WSA 17LD 10k- 1MD	WSA 35LA 10k- 2MF 35LD 17RA WSA 17RD 10k- RWT	WSA 8A 25k+ 1MF pub WSA 8D 25k+ RWT WSA 26A 25k+ 3MF WSA 26D 10k- RWT pub

11-JUL-88 22:13:38	WSA 35RA 10k- 3MF	WSA 35LA 10k- 2MF	WSA 8A 25k+ RWT
	35RD	35LD	WSA 8D 25k+ RWT
	17LA	17RA	WSA 26A 25k+ 2MF
WSA 17LD 10k- 1MD	WSA 17RD 10k- RWT	WSA 26D 10k- RWT	
11-JUL-88 22:13:45	WSA 35RA 10k- 3MF	WSA 35LA 10k- 2MF	WSA 8A 25k+ RWT
	35RD	35LD	WSA 8D 25k+ RWT
	17LA	17RA	WSA 26A 15k- 3MF
WSA 17LD 10k- 1MD	WSA 17RD 10k- RWT	WSA 26D 15k- RWT	
11-JUL-88 22:13:52	WSA 35RA 15k- 3MF	WSA 35LA 15k- 2MF	WSA 8A 25k+ 1MF
	35RD	35LD	WSA 8D 25k+ RWT
	17LA	17RA	WSA 26A 20k- 3MF
WSA 17LD 15k- RWT	WSA 17RD 15k- RWT	WSA 26D 20k- RWT	
11-JUL-88 22:13:59	NBA 35RA 25k- 3MF	NBA 35LA 25k- 2MF	NBA 8A 25k- 2MF
	35RD	35LD	NBA 8D 25k- RWT
	17LA	17RA	NBA 26A 25k- 3MF
NBA 17LD 25k- RWT	NBA 17RD 25k- RWT	NBA 26D 25k- RWT	
11-JUL-88 22:14:06	NBA 35RA 25k- 3MF	NBA 35LA 25k- 2MF	NBA 8A 25k- 2MF
	35RD	NBA 35LD 25k- RWT	NBA 8D 25k- RWT
	17LA	NBA 17RA 25k- RWT	NBA 26A 25k- 3MF
NBA 17LD 25k- RWT	NBA 17RD 25k- RWT	NBA 26D 25k- RWT	
11-JUL-88 22:14:12	WSA 35RA 20k- 3MF	WSA 35LA 20k- 2MF	WSA 8A 10k- 2MF
	35RD	WSA 35LD 15k- RWT	WSA 8D 10k- RWT
	17LA	WSA 17RA 15k- 2MF	WSA 26A 20k- 2MF
WSA 17LD 20k- RWT	WSA 17RD 20k- RWT	WSA 26D 20k- RWT	
11-JUL-88 22:14:19	WSA 35RA 20k- 3MF	WSA 35LA 20k- 2MF	WSA 8A 10k- 1MF
	35RD	WSA 35LD 15k- RWT	WSA 8D 10k- RWT
	17LA	WSA 17RA 15k- RWT	WSA 26A 15k- 2MF
WSA 17LD 20k- 1MD	WSA 17RD 20k- RWT	WSA 26D 15k- RWT	
11-JUL-88 22:14:26	WSA 35RA 20k- 3MF	WSA 35LA 20k- 2MF	WSA 8A 10k- 1MF
	35RD	WSA 35LD 15k- RWT	WSA 8D 10k- RWT
	17LA	WSA 17RA 15k- RWT	WSA 26A 15k- 2MF
WSA 17LD 20k- RWT	WSA 17RD 20k- RWT	WSA 26D 15k- RWT	
11-JUL-88 22:14:33	WSA 35RA 20k- 3MF	WSA 35LA 20k- 2MF	WSA 8A 10k- 1MF
	35RD	WSA 35LD 15k- RWT	WSA 8D 10k- RWT
	17LA	WSA 17RA 15k- 2MF	WSA 26A 15k- 3MF
WSA 17LD 20k- RWT	WSA 17RD 20k- RWT	WSA 26D 15k- RWT	
11-JUL-88 22:14:40	WSA 35RA 20k- 3MF	WSA 35LA 20k- 2MF	WSA 8A 10k- 2MF
	35RD	WSA 35LD 15k- RWT	WSA 8D 10k- RWT
	17LA	WSA 17RA 15k- 2MF	WSA 26A 15k- 3MF
WSA 17LD 20k- RWT	WSA 17RD 20k- RWT	WSA 26D 15k- RWT	
11-JUL-88 22:14:47	WSA 35RA 20k- 3MF	WSA 35LA 20k- 2MF	WSA 8A 15k- 2MF
	35RD	WSA 35LD 20k- RWT	WSA 8D 15k- RWT
	17LA	WSA 17RA 20k- 2MF	WSA 26A 15k- 3MF
WSA 17LD 20k- RWT	WSA 17RD 20k- RWT	WSA 26D 15k- RWT	
11-JUL-88 22:14:53	WSA 35RA 20k- 3MF	WSA 35LA 20k- 2MF	WSA 8A 10k- 2MF
	35RD	WSA 35LD 20k- RWT	WSA 8D 10k- RWT
	17LA	WSA 17RA 20k- 3MF	WSA 26A 15k- 3MF
WSA 17LD 20k- RWT	WSA 17RD 20k- RWT	WSA 26D 15k- RWT	
11-JUL-88 22:15:07	WSA 35RA 20k- 3MF	WSA 35LA 20k- 2MF	WSA 8A 15k- 2MF
	35RD	WSA 35LD 15k- RWT	WSA 8D 15k- RWT
	17LA	WSA 17RA 15k- 2MF	WSA 26A 15k- 3MF
WSA 17LD 20k- RWT	WSA 17RD 20k- RWT	WSA 26D 15k- RWT	
11-JUL-88 22:15:14	WSA 35RA 15k- 3MF	WSA 35LA 15k- 2MF	WSA 8A 15k- 2MF
	35RD	WSA 35LD 15k- RWT	WSA 8D 15k- RWT pub
	17LA	WSA 17RA 15k- 2MF	WSA 26A 15k- 3MF
WSA 17LD 15k- RWT	WSA 17RD 15k- RWT	WSA 26D 15k- RWT	
11-JUL-88 22:15:21	WSA 35RA 15k- 3MF	WSA 35LA 15k- 2MF	WSA 8A 15k- 2MF
	35RD	WSA 35LD 15k- RWT	WSA 8D 15k- RWT pub
	17LA	WSA 17RA 15k- 2MF	WSA 26A 15k- 3MF pub
WSA 17LD 15k- RWT	WSA 17RD 15k- RWT	WSA 26D 15k- RWT	
11-JUL-88 22:15:28	WSA 35RA 15k- 3MF	WSA 35LA 15k- 2MF	WSA 8A 15k- 2MF
	35RD	WSA 35LD 15k- RWT	WSA 8D 15k- RWT pub
	17LA	WSA 17RA 15k- 2MF	WSA 26A 15k- 2MF pub
WSA 17LD 15k- RWT	WSA 17RD 15k- RWT	WSA 26D 15k- RWT	

C-6

11-JUL-88 22:18:46 WSA 35RA 10k- 3MF 35RD 17LA WSA 17LD 10k- 2MD	WSA 35LA 10k- 3MF 35LD 17RA WSA 17RD 10k- 1MD	WSA 8A 30k+ RWT WSA 8D 30k+ RWT pab WSA 26A 30k+ 2MF pab WSA 26D 30k+ RWT
11-JUL-88 22:18:53 WSA 35RA 10k- 3MF 35RD 17LA WSA 17LD 10k- 2MD	WSA 35LA 10k- 3MF 35LD 17RA WSA 17RD 10k- 1MD	WSA 8A 30k+ RWT WSA 8D 30k+ RWT pab WSA 26A 30k+ 2MF pab WSA 26D 15k- RWT
11-JUL-88 22:19:00 WSA 35RA 10k- 3MF 35RD 17LA WSA 17LD 10k- 1MD	WSA 35LA 10k- 3MF 35LD 17RA WSA 17RD 10k- RWT	WSA 8A 25k+ RWT WSA 8D 25k+ RWT pab WSA 26A 25k+ 2MF pab WSA 26D 25k+ RWT
11-JUL-88 22:19:07 WSA 35RA 10k- 3MF 35RD 17LA WSA 17LD 10k- 1MD	WSA 35LA 10k- 3MF 35LD 17RA WSA 17RD 10k- RWT	WSA 8A 15k- 2MF WSA 8D 15k- RWT pab WSA 26A 15k- 3MF pab WSA 26D 15k- RWT
11-JUL-88 22:19:14 WSA 35RA 15k- 3MF 35RD 17LA WSA 17LD 15k- 1MD	WSA 35LA 15k- 3MF 35LD 17RA WSA 17RD 15k- RWT	WSA 8A 30k+ RWT WSA 8D 30k+ RWT pab WSA 26A 15k- 3MF pab WSA 26D 15k- RWT
11-JUL-88 22:19:20 WSA 35RA 15k- 3MF 35RD 17LA WSA 17LD 15k- 1MD	WSA 35LA 15k- 3MF 35LD 17RA WSA 17RD 15k- RWT	WSA 8A 30k+ RWT WSA 8D 30k+ RWT pab WSA 26A 30k+ 2MF pab WSA 26D 30k+ RWT
11-JUL-88 22:19:27 WSA 35RA 15k- 3MF 35RD 17LA WSA 17LD 15k- 1MD	WSA 35LA 15k- 3MF 35LD 17RA WSA 17RD 15k- RWT	WSA 8A 30k+ RWT WSA 8D 30k+ RWT pab WSA 26A 30k+ 2MF pab WSA 26D 15k- RWT
11-JUL-88 22:19:34 WSA 35RA 15k- 3MF pab 35RD 17LA WSA 17LD 15k- 1MD pab	WSA 35LA 15k- 3MF pab 35LD 17RA WSA 17RD 15k- RWT pab	WSA 8A 15k- 2MF WSA 8D 15k- RWT pab WSA 26A 15k- 2MF pab WSA 26D 15k- RWT
11-JUL-88 22:19:41 WSA 35RA 20k- 3MF pab 35RD 17LA WSA 17LD 20k- RWT pab	WSA 35LA 20k- 3MF pab 35LD 17RA WSA 17RD 20k- RWT pab	WSA 8A 25k+ RWT WSA 8D 25k+ RWT pab WSA 26A 25k+ 2MF pab WSA 26D 25k+ RWT
11-JUL-88 22:19:55 WSA 35RA 20k- 3MF pab 35RD 17LA WSA 17LD 20k- RWT pab	WSA 35LA 20k- 3MF pab 35LD 17RA WSA 17RD 20k- RWT pab	NBA 8A 25k- 2MF NBA 8D 25k- RWT NBA 26A 25k- 3MF NBA 26D 25k- RWT
11-JUL-88 22:20:01 WSA 35RA 15k- 3MF 35RD 17LA WSA 17LD 15k- RWT	WSA 35LA 15k- 3MF 35LD 17RA WSA 17RD 15k- RWT	NBA 8A 25k- 2MF NBA 8D 25k- RWT NBA 26A 25k- 3MF NBA 26D 25k- RWT
11-JUL-88 22:20:08 WSA 35RA 15k- 3MF 35RD 17LA WSA 17LD 15k- 1MD	WSA 35LA 15k- 3MF 35LD 17RA WSA 17RD 15k- RWT	NBA 8A 25k- 2MF NBA 8D 25k- RWT NBA 26A 25k- 3MF NBA 26D 25k- RWT
11-JUL-88 22:20:15 WSA 35RA 20k- 3MF 35RD 17LA WSA 17LD 20k- 1MD	WSA 35LA 20k- 3MF 35LD 17RA WSA 17RD 20k- RWT	NBA 8A 25k- 2MF NBA 8D 25k- RWT NBA 26A 25k- 3MF NBA 26D 25k- RWT
11-JUL-88 22:20:29 WSA 35RA 25k- 3MF 35RD 17LA WSA 17LD 25k- RWT	WSA 35LA 25k- 3MF 35LD 17RA WSA 17RD 25k- RWT	WSA 8A 35k+ RWT WSA 8D 35k+ RWT pab WSA 26A 35k+ 2MF pab WSA 26D 35k+ RWT
11-JUL-88 22:20:35 NBA 35RA 25k- 3MF 35RD 17LA NBA 17LD 25k- RWT	NBA 35LA 25k- 3MF 35LD 17RA NBA 17RD 25k- RWT	NBA 8A 25k- 2MF NBA 8D 25k- RWT NBA 26A 25k- 3MF NBA 26D 25k- RWT
11-JUL-88 22:20:42 NBA 35RA 25k- 3MF 35RD 17LA NBA 17LD 25k- RWT	NBA 35LA 25k- 3MF 35LD 17RA NBA 17RD 25k- RWT	NBA 8A 25k- 2MF NBA 8D 25k- RWT NBA 26A 25k- 3MF NBA 26D 25k- RWT

11-JUL-88 22:22:04	NBA 35RA 30k- 3MF	NBA 35LA 30k- 3MF	NBA 8A 30k- 2MF
WSA 35RD 15k- RWT	NBA 35LD 25k- RWT	NBA 8D 30k- RWT	
WSA 17LA 15k- RWT	NBA 17RA 25k- RWT	NBA 26A 30k- 3MF	
NBA 17LD 30k- RWT	NBA 17RD 30k- RWT	NBA 26D 30k- RWT	
11-JUL-88 22:22:24	NBA 35RA 30k- 3MF	NBA 35LA 30k- 3MF	NBA 8A 30k- 2MF
WSA 35RD 15k- RWT	NBA 35LD 25k- RWT	NBA 8D 30k- RWT	
WSA 17LA 15k- RWT	NBA 17RA 25k- RWT	NBA 26A 30k- 1MF	
NBA 17LD 30k- RWT	NBA 17RD 30k- RWT	NBA 26D 30k- RWT	
11-JUL-88 22:22:31	NBA 35RA 35k- 3MF	NBA 35LA 35k- 3MF	NBA 8A 35k- 2MF
WSA 35RD 15k- RWT	NBA 35LD 25k- RWT	NBA 8D 35k- RWT	
WSA 17LA 15k- RWT	NBA 17RA 25k- RWT	NBA 26A 35k- 1MF	
NBA 17LD 35k- RWT	NBA 17RD 35k- RWT	NBA 26D 35k- RWT	
11-JUL-88 22:22:44	NBA 35RA 30k- 3MF	NBA 35LA 30k- 3MF	NBA 8A 30k- 2MF
WSA 35RD 15k- RWT	NBA 35LD 25k- RWT	NBA 8D 30k- RWT	
WSA 17LA 15k- RWT	NBA 17RA 25k- RWT	NBA 26A 30k- 1MF	
NBA 17LD 30k- RWT	NBA 17RD 30k- RWT	NBA 26D 30k- RWT	
11-JUL-88 22:22:51	NBA 35RA 30k- 3MF	NBA 35LA 30k- 3MF	NBA 8A 30k- 2MF
WSA 35RD 10k- RWT	NBA 35LD 25k- RWT	NBA 8D 30k- RWT	
WSA 17LA 10k- RWT	NBA 17RA 25k- RWT	NBA 26A 30k- RWT	
NBA 17LD 30k- RWT	NBA 17RD 30k- RWT	NBA 26D 30k- RWT	
11-JUL-88 22:22:58	NBA 35RA 25k- 3MF	NBA 35LA 25k- 3MF	NBA 8A 25k- 2MF
WSA 35RD 10k- RWT	NBA 35LD 25k- RWT	NBA 8D 25k- RWT	
WSA 17LA 10k- RWT	NBA 17RA 25k- RWT	NBA 26A 25k- RWT	
NBA 17LD 25k- RWT	NBA 17RD 25k- RWT	NBA 26D 25k- RWT	
11-JUL-88 22:23:05	NBA 35RA 25k- 3MF	NBA 35LA 25k- 3MF	NBA 8A 25k- 2MF
WSA 35RD 10k- RWT	NBA 35LD 10k- RWT	NBA 8D 25k- RWT	
WSA 17LA 10k- RWT	NBA 17RA 10k- RWT	NBA 26A 25k- RWT	
NBA 17LD 25k- RWT	NBA 17RD 25k- RWT	NBA 26D 25k- RWT	
11-JUL-88 22:23:11	NBA 35RA 30k- 3MF	NBA 35LA 30k- 3MF	NBA 8A 30k- 2MF
WSA 35RD 10k- RWT	NBA 35LD 25k- RWT	NBA 8D 30k- RWT	
WSA 17LA 10k- RWT	NBA 17RA 25k- RWT	NBA 26A 30k- 1MF	
NBA 17LD 30k- RWT	NBA 17RD 30k- RWT	NBA 26D 30k- RWT	
11-JUL-88 22:23:32	NBA 35RA 30k- 3MF	NBA 35LA 30k- 3MF	NBA 8A 30k- 2MF
35RD	NBA 35LD 25k- RWT	NBA 8D 30k- RWT	
17LA	NBA 17RA 25k- RWT	NBA 26A 30k- RWT	
NBA 17LD 30k- 1MD	NBA 17RD 30k- RWT	NBA 26D 30k- RWT	
11-JUL-88 22:23:39	NBA 35RA 25k- 3MF	NBA 35LA 25k- 3MF	NBA 8A 25k- 2MF
35RD	35LD	NBA 8D 25k- RWT	
17LA	17RA	NBA 26A 25k- RWT	
NBA 17LD 25k- 1MD	NBA 17RD 25k- RWT	NBA 26D 25k- RWT	
11-JUL-88 22:23:45	WSA 35RA 15k- 3MF	WSA 35LA 15k- 3MF	WSA 8A 35k+ RWT
35RD	35LD	WSA 8D 35k+ RWT pub	
17LA	17RA	WSA 26A 30k+ 2MF pub	
WSA 17LD 15k- 1MD	WSA 17RD 15k- RWT	WSA 26D 30k+ RWT	
11-JUL-88 22:23:52	WSA 35RA 15k- 3MF	WSA 35LA 15k- 3MF	WSA 8A 30k+ RWT
35RD	35LD	WSA 8D 30k+ RWT pub	
17LA	17RA	WSA 26A 30k+ 2MF pub	
WSA 17LD 15k- 1MD	WSA 17RD 15k- RWT	WSA 26D 30k+ RWT	
11-JUL-88 22:23:59	WSA 35RA 15k- 3MF	WSA 35LA 15k- 3MF	WSA 8A 25k+ RWT
35RD	35LD	WSA 8D 25k+ RWT pub	
17LA	17RA	WSA 26A 25k+ 2MF pub	
WSA 17LD 15k- 1MD	WSA 17RD 15k- RWT	WSA 26D 25k+ RWT	
11-JUL-88 22:24:13	WSA 35RA 15k- 3MF	WSA 35LA 15k- 3MF	WSA 8A 25k+ RWT
35RD	35LD	WSA 8D 25k+ RWT pub	
17LA	17RA	WSA 26A 25k+ 2MF pub	
WSA 17LD 15k- RWT	WSA 17RD 15k- RWT	WSA 26D 25k+ RWT	
11-JUL-88 22:24:19	WSA 35RA 10k- 3MF	WSA 35LA 10k- 3MF	WSA 8A 30k+ RWT
35RD	35LD	WSA 8D 30k+ RWT pub	
17LA	17RA	WSA 26A 30k+ 2MF pub	
WSA 17LD 10k- 1MD	WSA 17RD 10k- RWT	WSA 26D 30k+ RWT	
11-JUL-88 22:24:26	WSA 35RA 15k- 3MF	WSA 35LA 15k- 3MF	WSA 8A 30k+ 1MF
35RD	35LD	WSA 8D 30k+ RWT pub	
17LA	17RA	WSA 26A 30k+ 2MF pub	
WSA 17LD 15k- RWT	WSA 17RD 15k- RWT	WSA 26D 30k+ RWT	

11-JUL-88 22:24:33	WSA 35RA 20k- 3MF	WSA 35LA 20k- 3MF	NBA 8A 25k- 2MF
35RD	35LD	NBA 8D 25k- RWT	
17LA	17RA	NBA 26A 25k- 2MF	
WSA 17LD 20k- RWT	WSA 17RD 20k- RWT	NBA 26D 25k- RWT	
11-JUL-88 22:24:40	WSA 35RA 25k- 3MF	WSA 35LA 25k- 3MF	NBA 8A 25k- 2MF
35RD	35LD	NBA 8D 25k- RWT	
17LA	17RA	NBA 26A 25k- 2MF	
WSA 17LD 25k- RWT	WSA 17RD 25k- RWT	NBA 26D 25k- RWT	
11-JUL-88 22:24:47	WSA 35RA 25k- 3MF	WSA 35LA 25k- 3MF	NBA 8A 25k- 2MF
WSA 35RD 10k- RWT	WSA 35LD 10k- RWT	NBA 8D 25k- RWT	
WSA 17LA 10k- RWT	WSA 17RA 10k- RWT	NBA 26A 25k- 2MF	
WSA 17LD 25k- RWT	WSA 17RD 25k- RWT	NBA 26D 25k- RWT	
11-JUL-88 22:24:53	WSA 35RA 20k- 3MF	WSA 35LA 20k- 3MF	NBA 8A 25k- 2MF
WSA 35RD 10k- RWT	WSA 35LD 10k- RWT	NBA 8D 25k- RWT	
WSA 17LA 10k- RWT	WSA 17RA 10k- RWT	NBA 26A 25k- 2MF	
WSA 17LD 20k- RWT	WSA 17RD 20k- RWT	NBA 26D 25k- RWT	
11-JUL-88 22:25:07	WSA 35RA 20k- 3MF	WSA 35LA 20k- 3MF	NBA 8A 25k- 2MF
35RD	35LD	NBA 8D 25k- RWT	
17LA	17RA	NBA 26A 25k- RWT	
WSA 17LD 20k- 1MD	WSA 17RD 20k- RWT	NBA 26D 25k- RWT	
11-JUL-88 22:25:14	NBA 35RA 25k- 3MF	NBA 35LA 25k- 3MF	NBA 8A 25k- 2MF
35RD	NBA 35LD 25k- RWT	NBA 8D 25k- RWT	
17LA	NBA 17RA 25k- RWT	NBA 26A 25k- RWT	
NBA 17LD 25k- 1MD	NBA 17RD 25k- RWT	NBA 26D 25k- RWT	
11-JUL-88 22:25:27	NBA 35RA 25k- 3MF	NBA 35LA 25k- 3MF	NBA 8A 25k- 2MF
35RD	NBA 35LD 25k- RWT	NBA 8D 25k- RWT	
17LA	NBA 17RA 25k- 2MF	NBA 26A 25k- 1MF	
NBA 17LD 25k- RWT	NBA 17RD 25k- RWT	NBA 26D 25k- RWT	
11-JUL-88 22:25:42	WSA 35RA 25k- 3MF	WSA 35LA 25k- 3MF	NBA 8A 25k- 2MF
WSA 35RD 15k- RWT	WSA 35LD 15k- RWT	NBA 8D 25k- RWT	
WSA 17LA 15k- 1MF	WSA 17RA 15k- 2MF	NBA 26A 25k- 2MF	
WSA 17LD 25k- RWT	WSA 17RD 25k- RWT	NBA 26D 25k- RWT	
11-JUL-88 22:25:48	WSA 35RA 25k- 3MF	WSA 35LA 25k- 3MF	WSA 8A 15k- 2MF
WSA 35RD 15k- RWT	WSA 35LD 15k- RWT	WSA 8D 15k- RWT	
WSA 17LA 15k- 1MF	WSA 17RA 15k- 2MF	WSA 26A 15k- 2MF	
WSA 17LD 25k- RWT	WSA 17RD 25k- RWT	WSA 26D 15k- RWT	
11-JUL-88 22:25:55	WSA 35RA 25k- 3MF	WSA 35LA 25k- 3MF	WSA 8A 25k+ RWT
WSA 35RD 10k- RWT	WSA 35LD 10k- RWT	WSA 8D 25k+ RWT	
WSA 17LA 10k- 1MF	WSA 17RA 10k- 2MF	WSA 26A 25k+ 2MF	
WSA 17LD 25k- RWT	WSA 17RD 25k- RWT	WSA 26D 10k- RWT	
11-JUL-88 22:26:02	WSA 35RA 25k- 3MF	WSA 35LA 25k- 3MF	WSA 8A 25k+ 1MF
WSA 35RD 10k- RWT	WSA 35LD 10k- RWT	WSA 8D 25k+ RWT	
WSA 17LA 10k- 1MF	WSA 17RA 10k- 2MF	WSA 26A 25k+ 2MF	
WSA 17LD 25k- RWT	WSA 17RD 25k- RWT	WSA 26D 10k- RWT	
11-JUL-88 22:26:09	WSA 35RA 25k- 3MF	WSA 35LA 25k- 3MF	NBA 8A 25k- 2MF
WSA 35RD 15k- RWT	WSA 35LD 15k- RWT	NBA 8D 25k- RWT	
WSA 17LA 15k- 1MF	WSA 17RA 15k- 2MF	NBA 26A 25k- RWT	
WSA 17LD 25k- RWT	WSA 17RD 25k- RWT	NBA 26D 25k- RWT	
11-JUL-88 22:26:16	NBA 35RA 25k- 3MF	NBA 35LA 25k- 3MF	NBA 8A 30k- 2MF
WSA 35RD 15k- RWT	NBA 35LD 25k- RWT	NBA 8D 30k- RWT	
WSA 17LA 15k- 1MF	NBA 17RA 25k- 2MF	NBA 26A 30k- 1MF	
NBA 17LD 25k- RWT	NBA 17RD 25k- RWT	NBA 26D 30k- RWT	
11-JUL-88 22:26:22	NBA 35RA 25k- 3MF	NBA 35LA 25k- 3MF	NBA 8A 30k- 2MF
WSA 35RD 15k- RWT	NBA 35LD 25k- RWT	NBA 8D 30k- RWT	
WSA 17LA 15k- 1MF	NBA 17RA 25k- 2MF	NBA 26A 30k- 2MF	
NBA 17LD 25k- RWT	NBA 17RD 25k- RWT	NBA 26D 30k- RWT	
11-JUL-88 22:26:29	NBA 35RA 25k- 3MF	NBA 35LA 25k- 3MF	NBA 8A 25k- 2MF
WSA 35RD 15k- RWT	NBA 35LD 25k- RWT	NBA 8D 25k- RWT	
WSA 17LA 15k- 1MF	NBA 17RA 25k- 2MF	NBA 26A 25k- 2MF	
NBA 17LD 25k- RWT	NBA 17RD 25k- RWT	NBA 26D 25k- RWT	
11-JUL-88 22:26:36	NBA 35RA 25k- 3MF	NBA 35LA 25k- 3MF	NBA 8A 25k- 2MF
WSA 35RD 10k- RWT	NBA 35LD 25k- RWT	NBA 8D 25k- RWT	
WSA 17LA 10k- 1MF	NBA 17RA 25k- 2MF	NBA 26A 25k- 2MF	
NBA 17LD 25k- RWT	NBA 17RD 25k- RWT	NBA 26D 25k- RWT	



C-10

C-11

C-12

NBA	8A	30k-	4m.
NBA	8D	30k-	RWT
NBA	26A	30k-	3MF
NBA	26D	30k-	RWT

NBA 8A 25k- 2MF  
NBA 8D 25k- RWT  
NBA 26A 25k- 2MF  
NBA 26D 25k- RWT

NBA	8A	25k-	2MF
NBA	8D	25k-	RWT
NBA	26A	25k-	2MF
NBA	26D	25k-	RWT

NBA 8A 25k- 2MF  
NBA 8D 25k- 2WY  
NBA 26A 25k- 2MF  
NBA 26D 25k- 2WY

RBA 8A 30k- 2MF  
RBA 8D 30k- 2WT  
RBA 26A 30k- 2MF  
RBA 26D 30k- 2WT

NBA 8A 30k- 2MF  
NBA 8D 30k- RWT  
NBA 26A 30k- 2MF  
NBA 26D 30k- RWT

MBA	8A	30k-	2MF
MBA	8D	30k-	RWY
MBA	26A	30k-	2MF
MBA	26D	30k-	RWY

NBA	8A	30k-	2MP
NBA	8D	30k-	RWT
NBA	26A	30k-	2MP
NBA	26D	30k-	RWT

MBA	8A	30k-	2MF
MBA	8D	30k-	RWY
MBA	26A	30k-	2MF
MBA	26D	30k-	RWY

MBA	8A	30k-	2MF
MBA	8D	30k-	RWY
MBA	26A	30k-	2MF
MBA	26D	30k-	RWY

MBA	8A	30k-	2MF
MBA	8D	30k-	2WY
MBA	26A	30k-	2MF
MBA	26D	30k-	2WY

1 MHA 8A 30k- 2MF  
1 MHA 8D 30k- 2WY  
1 MHA 26A 30k- 2MF  
1 MHA 26D 30k- 2WY

1	NBA	8A	25k-	2MF
1	NBA	8D	25k-	2WY
1	NBA	26A	25k-	2MF
1	NBA	26D	25k-	2WY

NBA	8A	25k-	2MF
NBA	8D	25k-	RWT
NBA	26A	25k-	2MF
NBA	26D	25k-	RWT

NBA	8A	25k-	2MF
NBA	8D	25k-	RWT
NBA	26A	25k-	2MF
NBA	26D	25k-	RWT

1	NBA	8A	30k-	2MF
1	NBA	8D	30k-	RWY
1	NBA	26A	30k-	2MF
1	NBA	26D	30k-	RWY

C-14

WSA 35RA 20k- 3MF  
WSA 35RD 15k- RWT  
WSA 17LA 15k- RWT  
WSA 17LD 20k- RWT

WSA 35LA 20k- 2MF  
WSA 35LB 15k- RWT  
WSA 17RA 15k- RWT  
WSA 17RD 20k- RWT

WSA 8A 15k- 2MF  
WSA 8D 15k- RWT  
WSA 26A 15k- 3MF  
WSA 26D 15k- RWT

WSA 35RA 25k- JMF  
WSA 35RD 15k- RWT  
WSA 17LA 15k- RWT  
WSA 17LD 25k- RWT

WSA 35LA 25k- 2MF  
WSA 35LD 15k- RWT  
WSA 17RA 15k- RWT  
WSA 17RD 25k- RWT

WSA 8A 15k- 2NP  
WSA 8D 15k- 2WT  
WSA 26A 15k- 3NP  
WSA 26D 15k- 2WT

WSA 15RA 25k- 3MF  
WSA 15RD 15k- RWY  
WSA 17LA 15k- RWY  
WSA 17LD 25k- RWY

WSA 35LA 25k- 3MF  
WSA 35LD 15k- RWT  
WSA 17RA 15k- RWT  
WSA 17RD 25k- RWT

WSA 8A 15k- 2M7  
WSA 8D 15k- RWT  
WSA 26A 15k- 3M7  
WSA 26D 15k- RWT

NBA 35RA 25k- 3MF  
WSA 35RD 10k- 2WY  
WSA 17LA 10k- 2WY  
NBA 17LD 25k- 2WY

NBA 35LA 25k- JMF  
NBA 35LD 25k- RWT  
NBA 17RA 25k- RWT  
NBA 17RD 25k- RWT

NBA 8A 25k- 2M7  
NBA 8D 25k- 2WY  
NBA 26A 25k- 3M1  
NBA 26D 25k- 2WY

MBA 35RA 25k- JNY  
WSA 35RD 10k- RWT  
WSA 17LA 10k- RWT  
MBA 17LD 25k- RWT

NBA 35LA 25k- 3MF  
 NBA 35LD 25k- 2WT  
 NBA 17RA 25k- 2WT  
 NBA 17RD 25k- 2WT

NBA 8A 25k- 2MI  
NBA 8D 25k- 2WY  
NBA 16A 25k- 2MI  
NBA 16D 25k- 2WY

NBA 15RA 13k- JMF  
WSA 15RD 13k- RWT  
WSA 17LA 13k- RWT  
NBA 17LD 25k- RWT

NBA 35LA 25k- 3MI  
NBA 35LD 25k- 2WY  
NBA 172A 25k- RWY  
NBA 172D 25k- RWY

月入	8A	25k-	2M
月入	8D	25k-	2W
月入	26A	25k-	2M
月入	16D	25k-	2W

MBA	35RA	150	3NF
WSA	35RD	150	RWY
WSA	17LA	150	RWY
MBA	17LD	250	RWY

NBA 35LA 25k- 3M  
NBA 35LD 25k- 2W  
NBA 17RA 25k- 1M  
NBA 17RD 25k- 2W

NSA 8A 25k- 2M  
NSA 8D 25k- 2W  
NSA 26A 25k- 1M  
NSA 26D 25k- 2W

MDA 35RA 25k- JHF  
 WSA 35RD 15k- RWT  
 WSA 17LA 15k- RWT  
 MDA 17LD 25k- RWT

MBA 35LA 25k- 3M  
MBA 35LD 25k- BW  
MBA 17RA 25k- 1M  
MBA 17RD 25k- BW

NBA 8A 25k- 2M  
NBA 8D 25k- 2W  
NBA 26A 25k- 2M  
NBA 26D 25k- 2W

11-506-88 22:45:2  
MBA 35RA 30k- 3MR  
WSA 35RD 15k- RWT  
WSA 17LA 15k- RWT  
MBA 17LD 30k- RWT

MBA 35LA 30k- 3M  
MBA 35LD 30k- 2V  
MBA 17RA 30k- 1M  
MBA 17RD 30k- 2V

NBA	8A	30k-	21
NBA	8D	30k-	21
NBA	26A	30k-	21
NBA	26D	30k-	21

11-30E-86 221437Z  
HBA 35BA 30k- 3MA  
WSA 35BD 15k- 2WY  
WSA 17LA 15k- 2WY  
HBA 17LD 30k- 2WY

MBA 35LA 30k- 31  
MBA 35LD 30k- R  
MBA 17RA 30k- R  
MBA 17RD 30k- R

NBA	8A	30k-	21
NBA	8D	30k-	21
NBA	26A	30k-	21
NBA	26D	30k-	21

11-JUL-88 221431  
MBA 35RA 25k- 3M  
WSA 35RD 10k- RW  
WSA 17LA 10k- RW  
MBA 17LD 25k- RW

NBA 35LA 25k- 3  
NBA 35LD 25k- 2  
NBA 17RA 25k- 2  
NBA 17RD 25k- 2

NBA	8A	25k-	2
NBA	8D	25k-	R
NBA	26A	25k-	2
NBA	26D	25k-	R

11-JUL-88 22:44  
MBA 35RA 25k- 3M  
35RD  
17LA  
MBA 17LD 25k- 1M

NBA 35LA 25k- 3  
NBA 35LD 25k- 2  
NBA 17RA 25k- 2  
NBA 17RD 25k- 1

NBA	8A	25k-	2
NBA	8D	25k-	2
NBA	26A	25k-	2
NBA	26D	25k-	2

11-JUL-88 22:44  
HBA 35RA 25k- 3M  
15RD  
17LA  
HBA 17LD 25k- RM

NBA 35LA 25k- 3  
NBA 35LD 25k- 2  
NBA 17RA 25k- 2  
NBA 17RD 25k- 2

WBA	8A	25k-	2
WBA	8D	25k-	W
WBA	26A	25k-	2
WBA	26D	25k-	2

MDA 35RA 25k- 3M  
 WSA 35RD 17k- RW  
 WSA 17LA 10k- RW  
 MDA 17LD 25k- RW

NBA 35LA 25k-  
NBA 35LD 25k-  
NBA 17RA 25k-  
NBA 17RD 25k-

NBA	8A	252-	2
NBA	8D	252-	2
NBA	26A	252-	2
NBA	26D	252-	2

11-306-33 11-437  
MBA 35RA 29k- 38  
35RD  
17LA  
MBA 17LD 29k- 11

NBA 35LA 29k-  
NBA 35LD 29k-  
NBA 17RA 29k-  
NBA 17RD 29k-

1	NBA	8A	29k-
1	NBA	8D	29k-
2	NBA	26A	29k-
1	NBA	26B	29k-

NSA 17LA 29k- 1

1  
1  
1  
1

NBA	33LA	25k-
NBA	33LD	25k-
NBA	17RA	25k-
NBA	17RD	25k-

1	NDA	8A	25k-
1	NDA	8D	25k-
1	NDA	26A	25k-
1	NDA	26D	25k-

C-16

11-JUL-88 22:49:20							
WSA 35LA 20k- 3MF		WSA 35LA 20k- 3MF		WSA 8A 10k- 1MF			
35ND		WSA 35LD 10k- RWT		WSA 8D 10k- RWT			
17LA		WSA 17RA 10k- RWT		WSA 26A 10k- 3MF			
WSA 17LD 20k- 1MD		WSA 17RD 20k- RWT		WSA 26D 10k- RWT			

11-JUL-88 22:49:27					
WSA 35RA 20k- 3MF		WSA 35LA 20k- 3MF		WSA 8A 10k- RWT	
35RD		WSA 35LD 10k- RWT		WSA 8D 10k- RWT	
17LA		WSA 17RA 10k- RWT		WSA 26A 10k- 3MF	
WSA 17LD 20k- 1MD		WSA 17RD 20k- RWT		WSA 26D 10k- RWT	

```

11-JUL-88 22:49:34
35BA 35LA WSA 8A 10k- RWT
35RD 35LD WSA 8D 10k- RWT
17LA 17RA WSA 26A 10k- 1MF
17LD 17RD WSA 26D 10k- RWT

```

11-JUL-88 22:49:54				
35RA		35LA		8A
35RD		35LD		8D
17LA		17RA		26A
17LD		17RD		26D



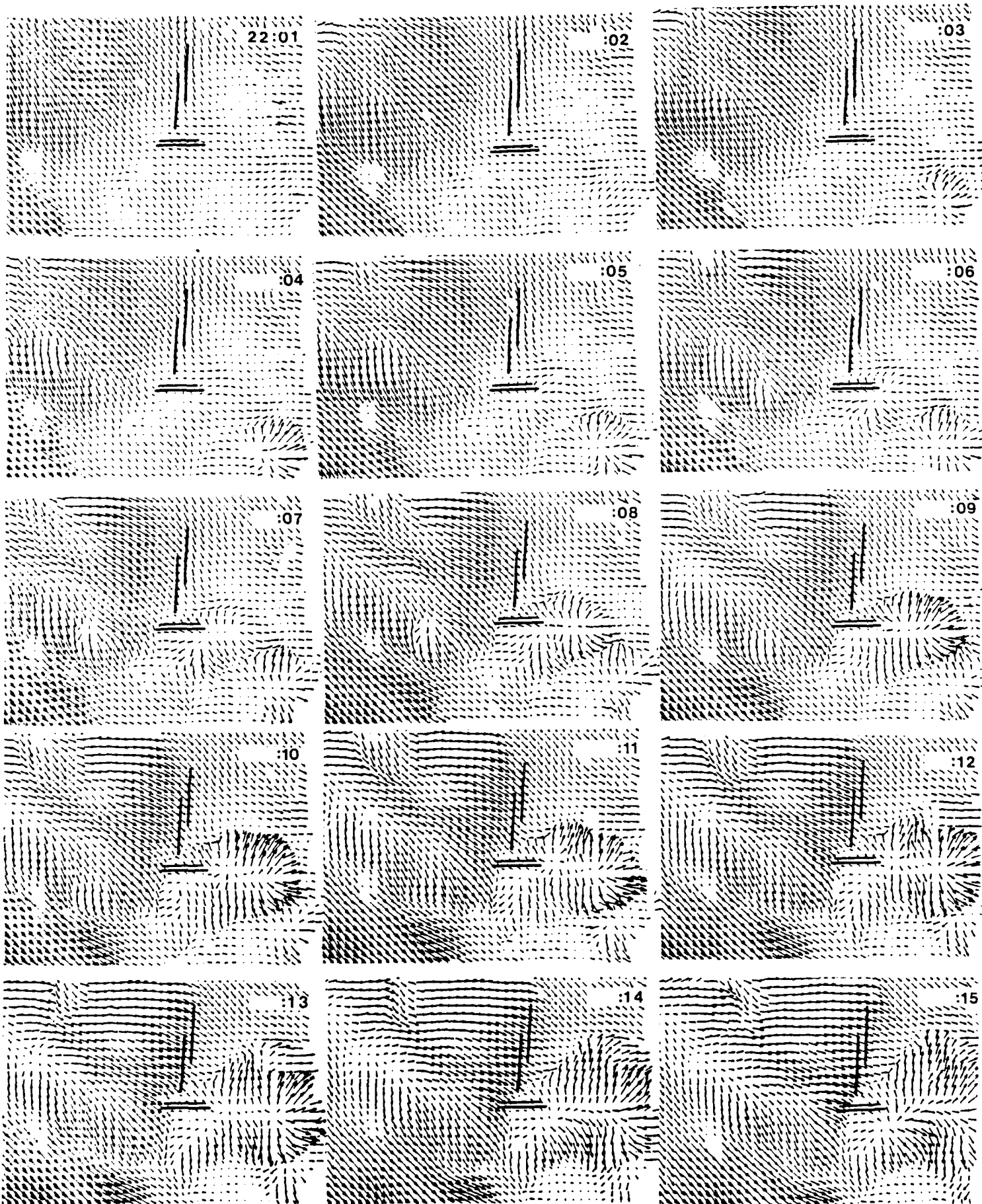
## **Appendix D: Low Level dual Doppler Analyses: Wind vectors and $\Delta V$**

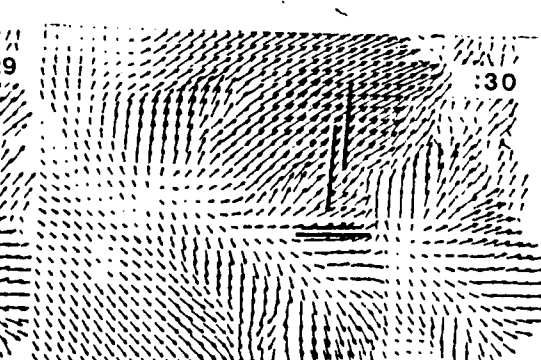
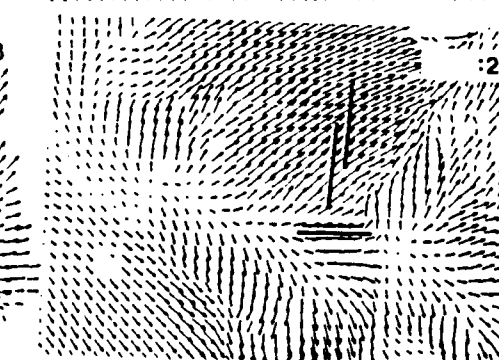
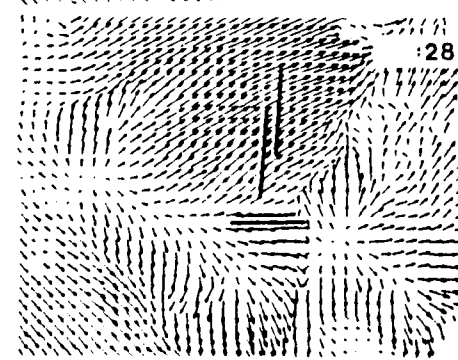
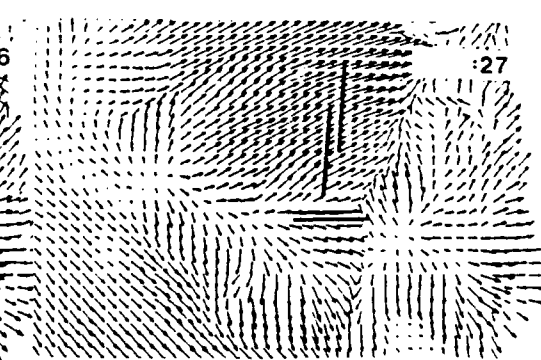
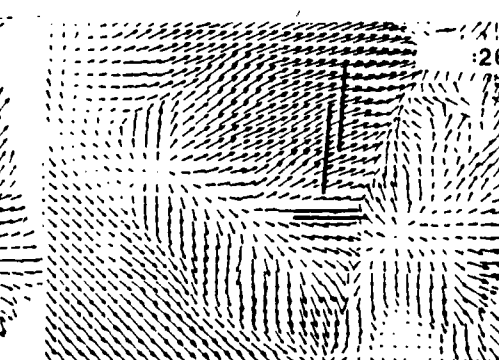
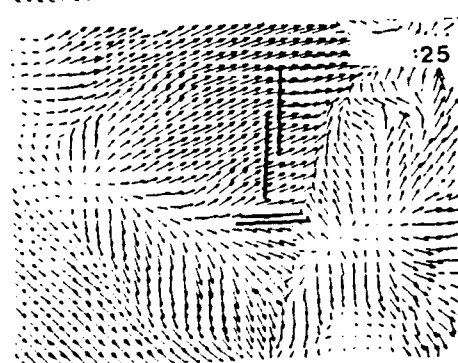
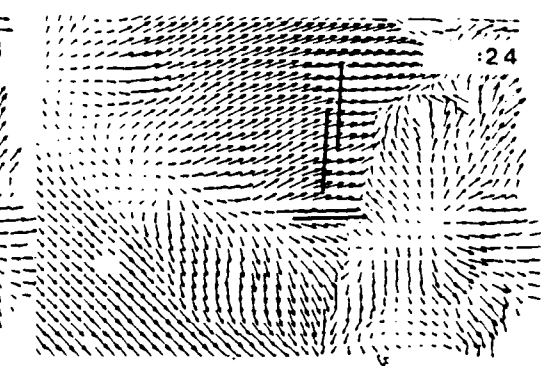
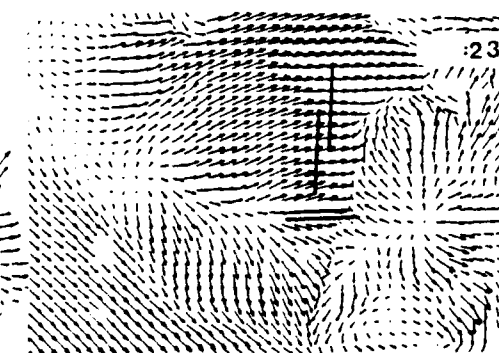
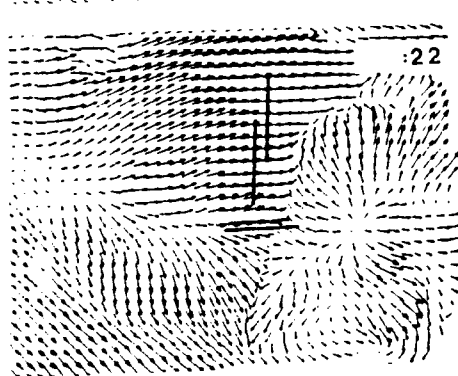
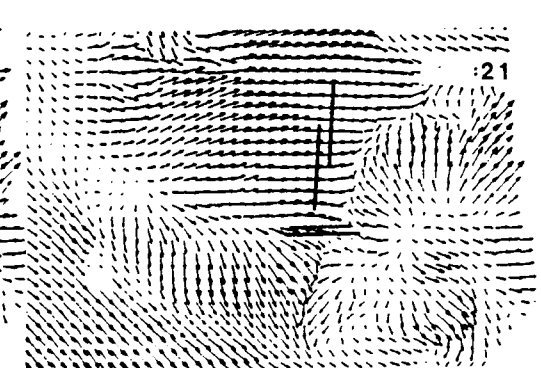
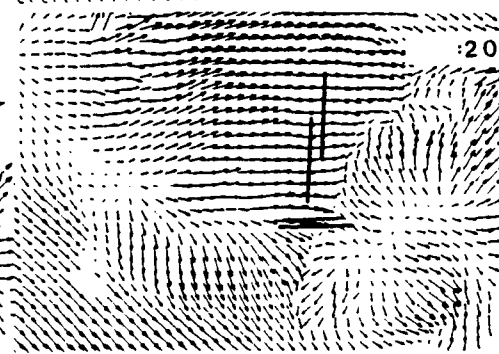
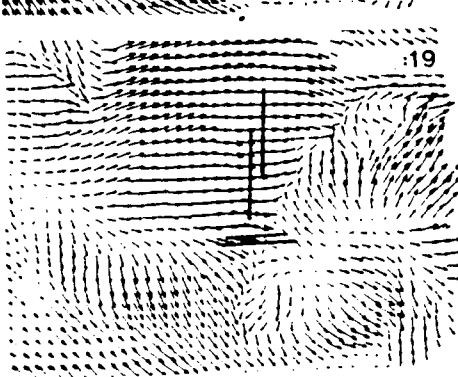
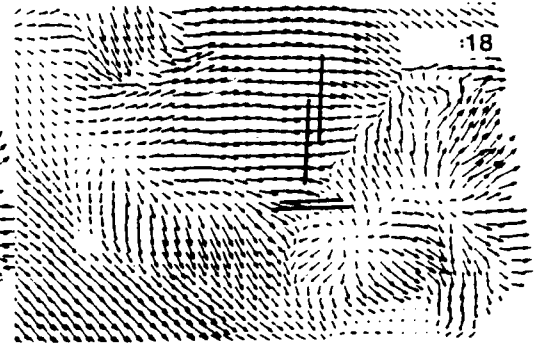
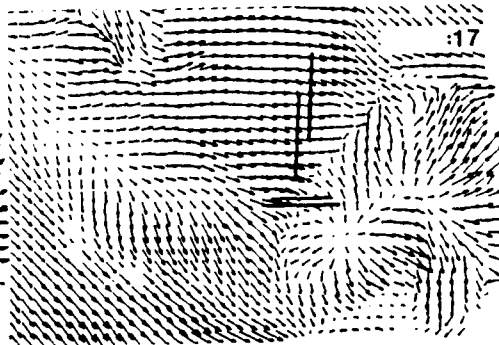
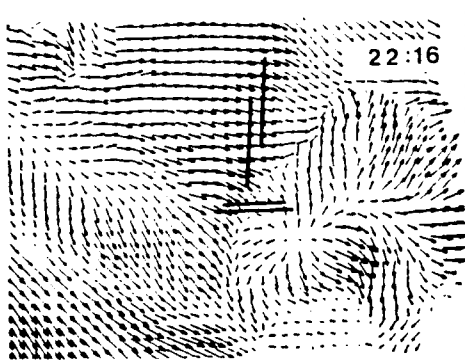
These are 1 min resolution low level (approximately 190 m AGL) dual Doppler analyses on a 0.5 km-spaced Cartesian grid during the time of the microbursts. Minutes after 2200 UTC are shown in each diagram's upper left hand column. Stapleton runways are indicated.

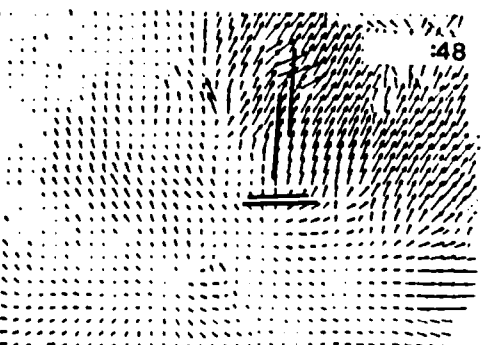
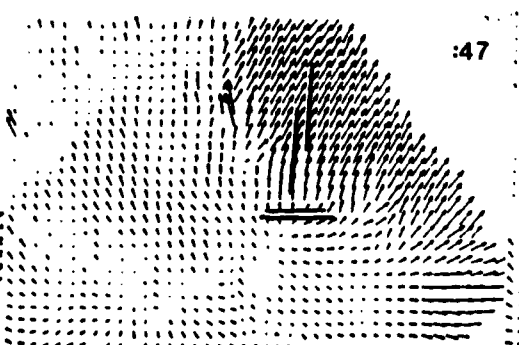
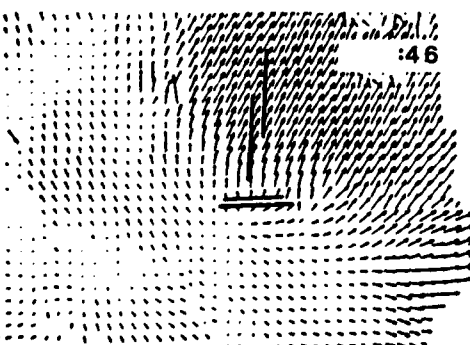
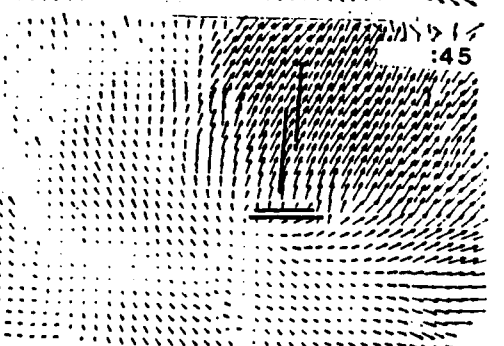
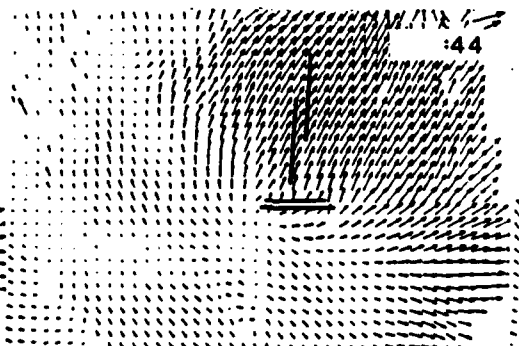
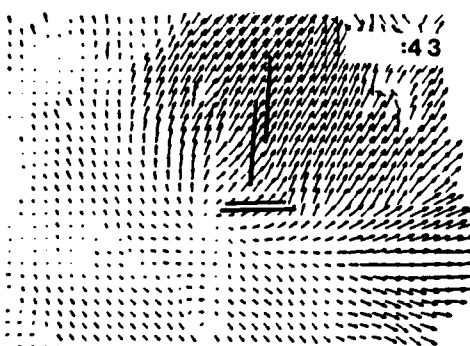
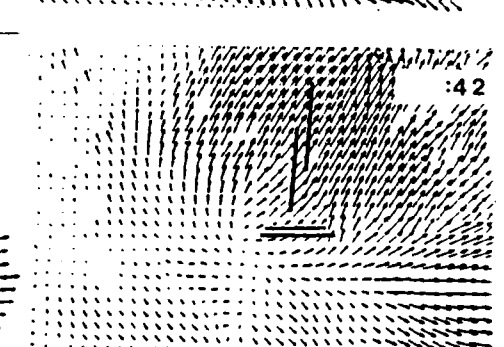
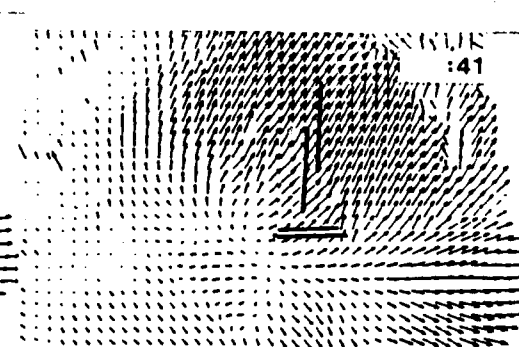
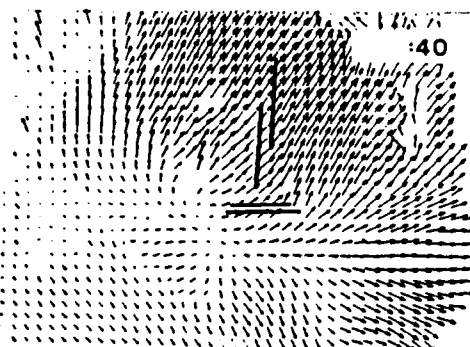
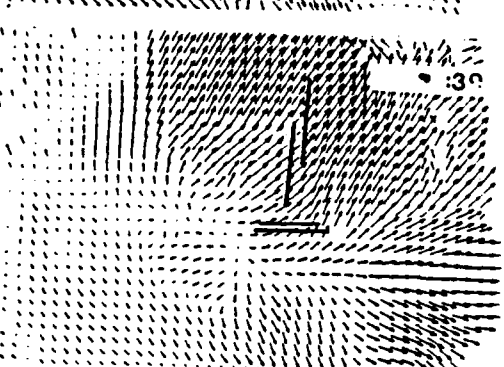
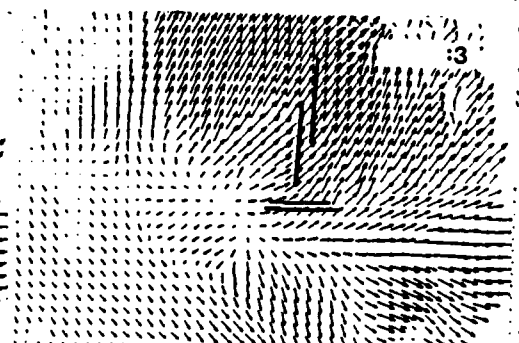
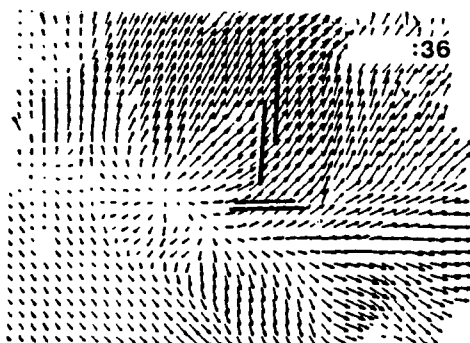
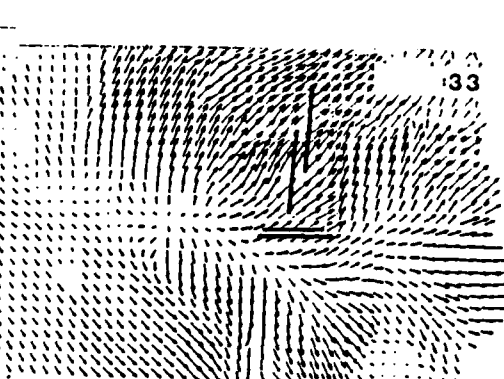
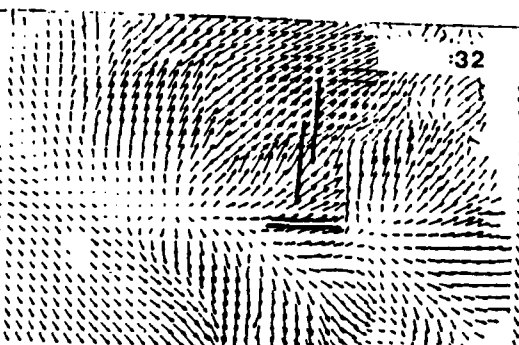
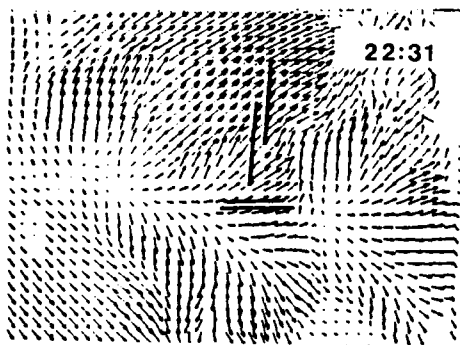
These diagrams show horizontal wind vectors and contoured  $\Delta V$  values for the 11 July microbursts. A routine was implemented which searched for the maximum wind velocity loss across a 2 km radius circle centered at each grid point. This maximum  $\Delta V$  was assigned to the point, then those values were contoured to obtain the diagrams shown here.

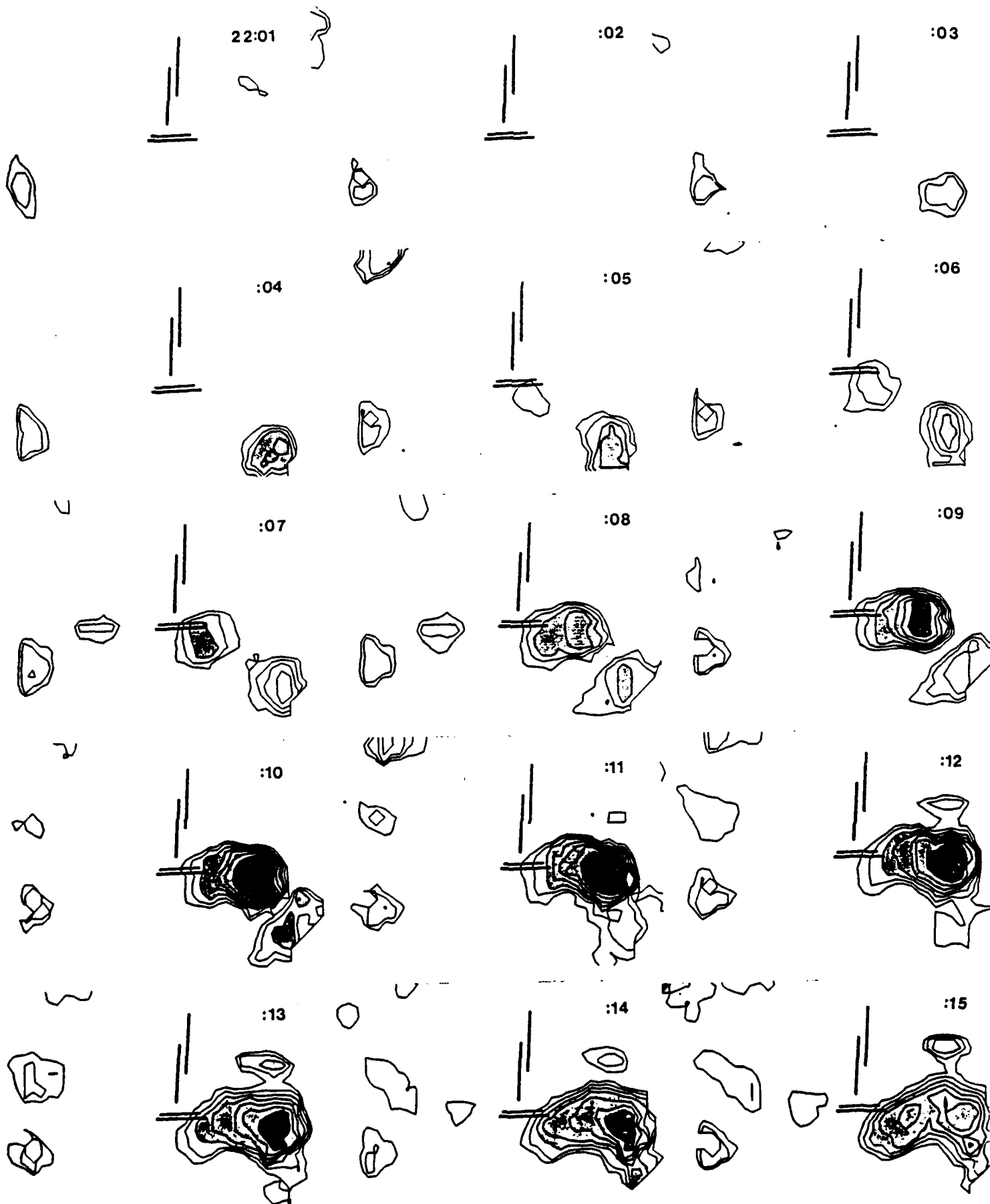
The lowest contoured level is a  $\Delta V$  of  $10 \text{ m s}^{-1}$  (20 kt), and the contour interval is  $2.5 \text{ m s}^{-1}$  (5 kt). The first contour corresponds to the original TDWR microburst alarm level and revised TDWR "wind shear" alarm level. Light shading denotes  $\Delta V$  of  $15 \text{ m s}^{-1}$  which corresponds to the revised TDWR "microburst" alarm. The darker shading indicates  $\Delta V$  of  $25 \text{ m s}^{-1}$ , the solid area is at  $\Delta V$   $35 \text{ m s}^{-1}$ .

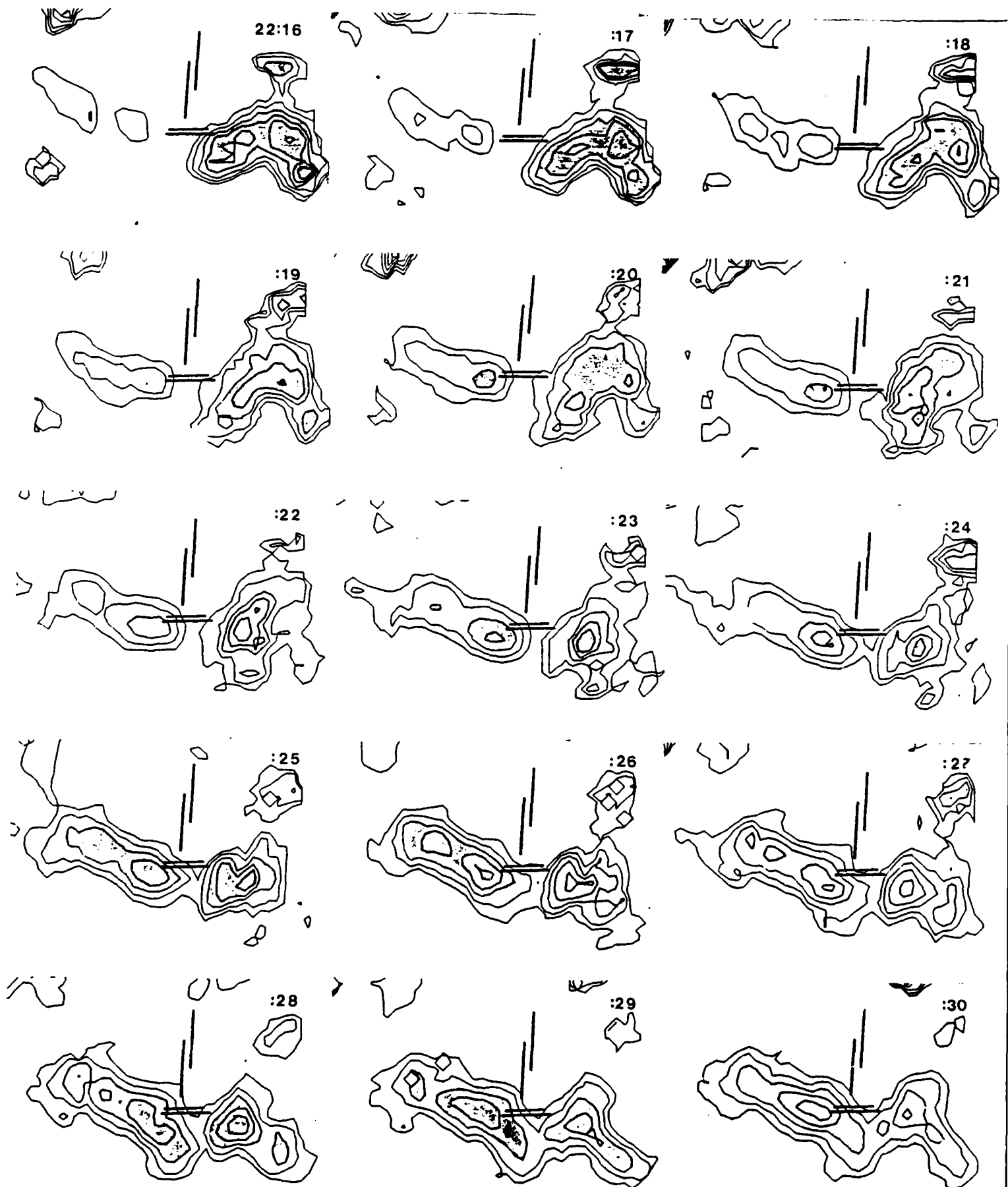
This analysis was performed using the NCAR CEDRIC radar analysis package. Missing data from each individual radar were first filled using a median filling technique, then unfolded, then smoothed. The smoothing technique averaged 1 adjacent gate on each side of the beam, and 2 along the beam for FL2, and 1X1 for UND. The smoothed data were then remapped onto a Cartesian grid with 0.5 km resolution, then the velocity components from each radar used to find the true horizontal wind velocity. This routine was a streamlined version of the processing package described in the text and was used for the summer's ground-truthing exercise.

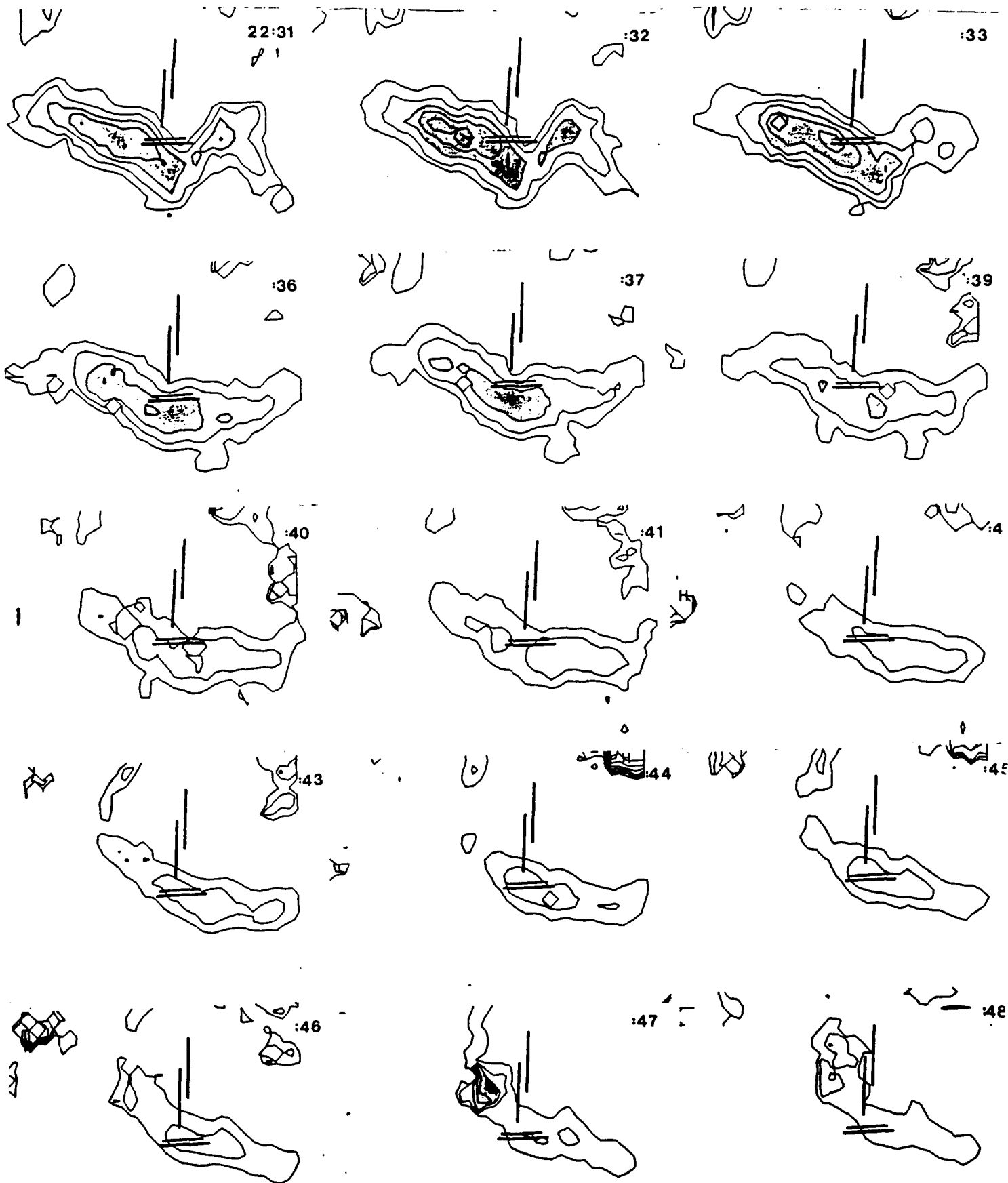












## **Appendix E: Combined LLWAS/FLOWS Surface Mesonet Winds**

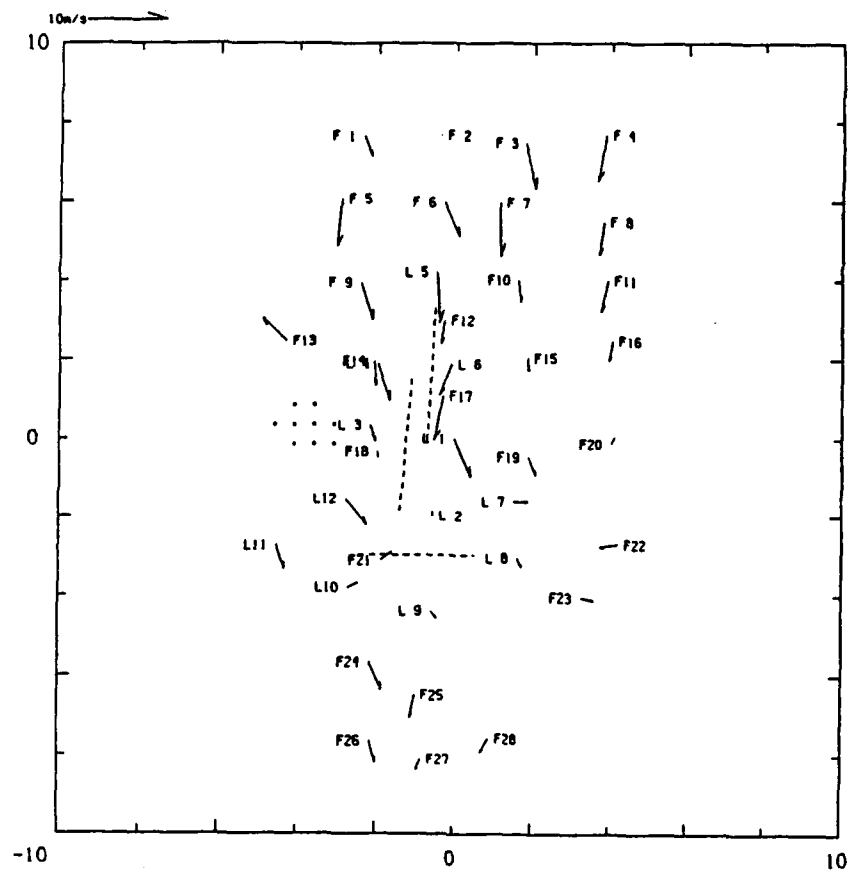
Wind vectors (pointing in the direction the wind is blowing *toward*) are shown in these plots for the times pertaining to the microburst. "L" numbers are LLWAS stations and "F" numbers are FLOWS stations. A scale wind vector is shown on each plot. The Stapleton runways are shown. The plots are centered at the centerpoint (L1) of the runways and the axes are labelled in km away from that center. Dots indicate approximate areas for microbursts causing divergence levels above threshold value (approximately the TDWR "wind shear" alarm level) and crosses indicate those areas for stronger divergence (approximately TDWR "microburst" alarm level). Station F13 was not operating correctly throughout the time period.



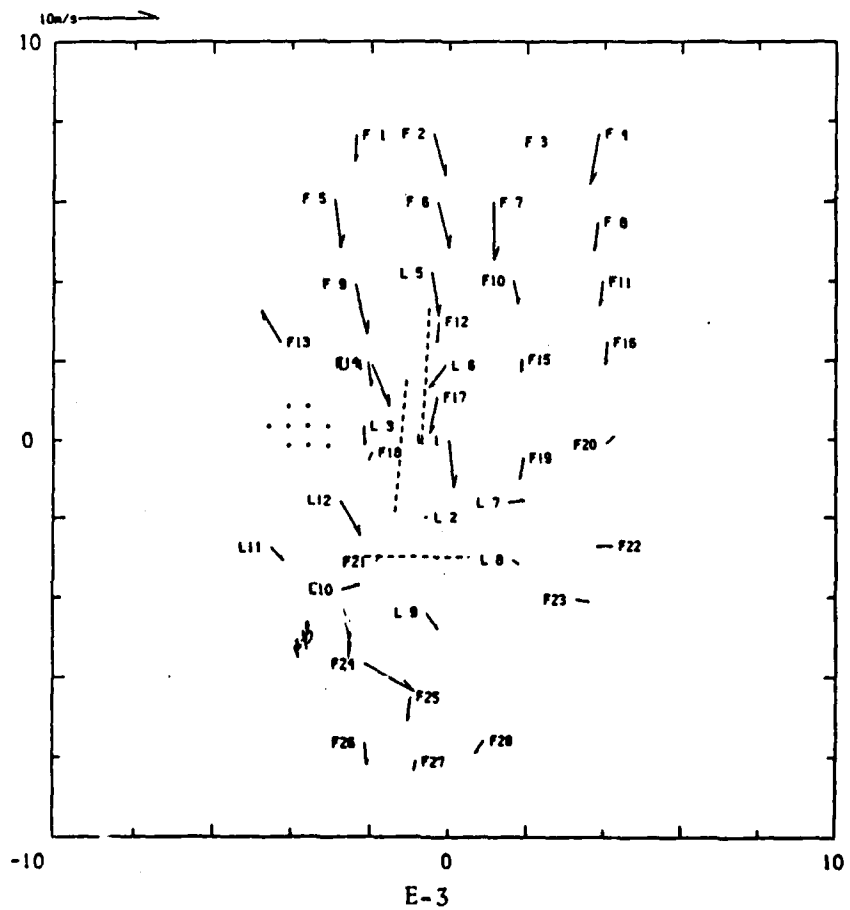
~~LF~~ 5/10/02  
**Appendix J: Combined LLWAS-FLOWS Mesonet Data**

Wind vectors (pointing in the direction the wind is blowing *toward*) are shown in these plots for the times pertaining to the microburst. "L" numbers are LLWAS stations and "F" numbers are FLOWS stations. A scale wind vector is shown on each plot. The Stapleton runways are shown. The plots are centered at the centerpoint (L1) of the runways and the axes are labelled in km away from that center. Dots indicate approximate areas for microbursts causing divergence levels above threshold value (approximately the TDWR "wind shear" alarm level) and crosses indicate those areas for stronger divergence (approximately TDWR "microburst" alarm level). Station F13 was not operating correctly throughout the time period.

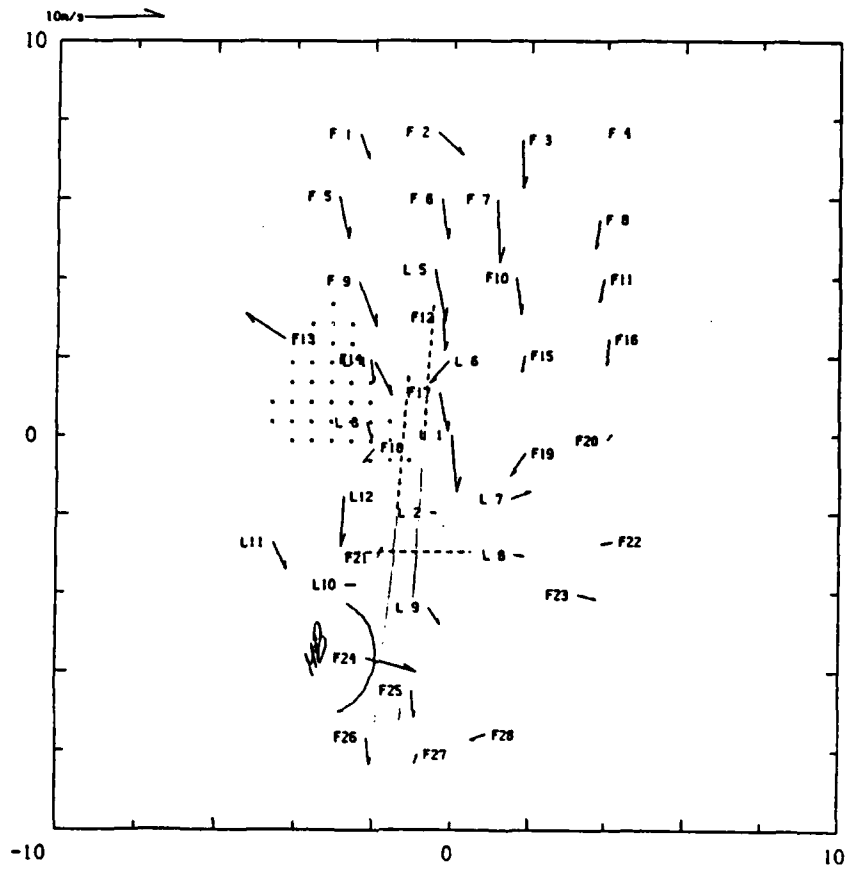
88/07/11-22:03:00 LLWAS-FLOWS MESONET (km x km)



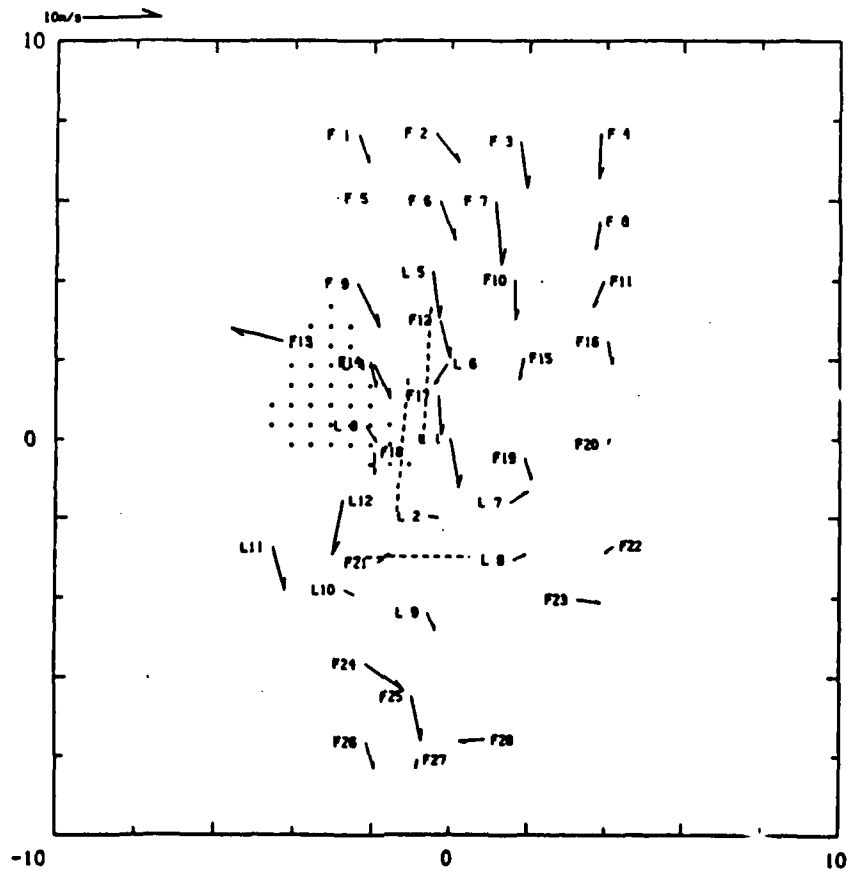
88/07/11-22:04:00 LLWAS-FLOWS MESONET (km x km)



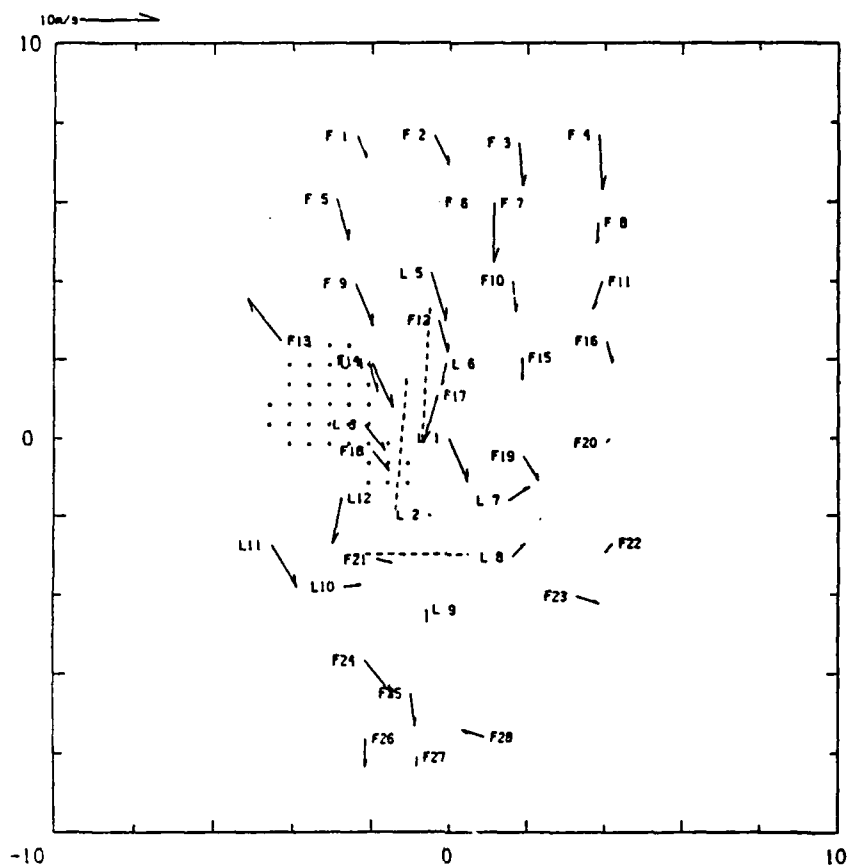
88/07/11-22:05:00 LLWAS-FLOWS MESONET (km x km)



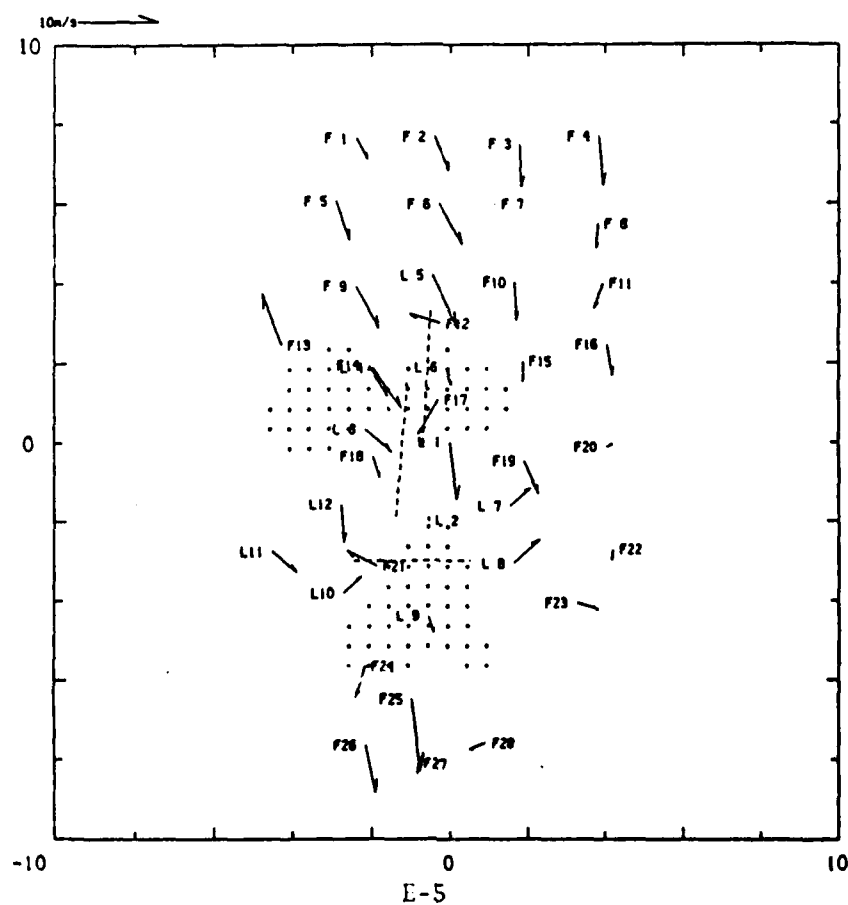
88/07/11-22:06:00 LLWAS-FLOWS MESONET (km x km)



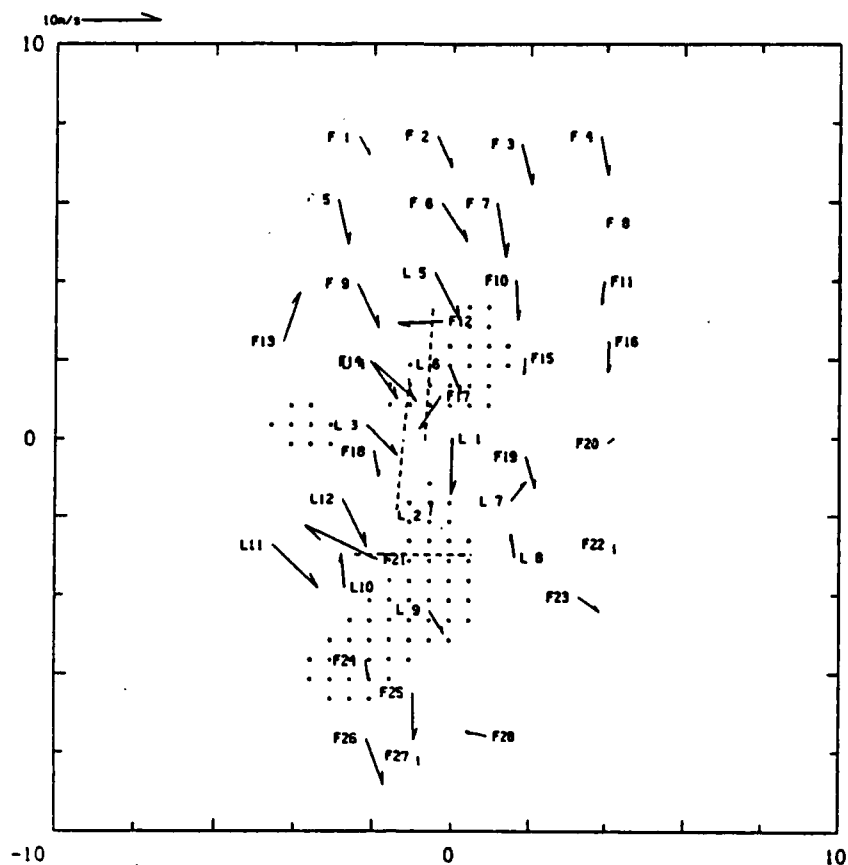
88/07/11-22:07:00 LLWAS-FLOWS MESONET (km x km)



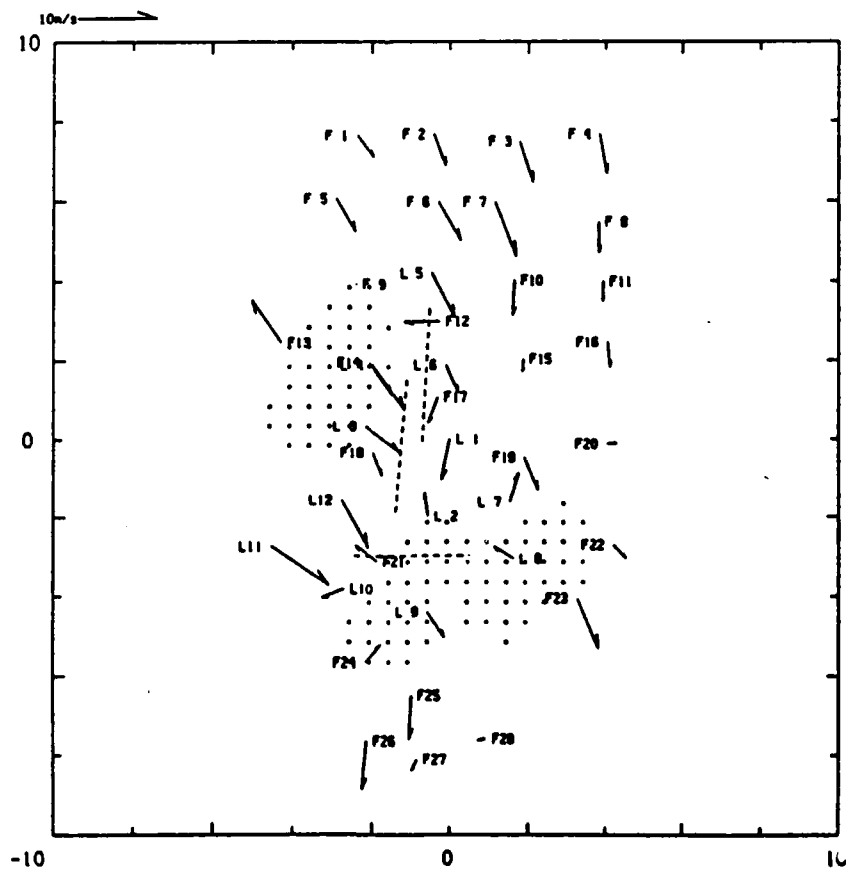
88/07/11-22:08:00 LLWAS-FLOWS MESONET (km x km)



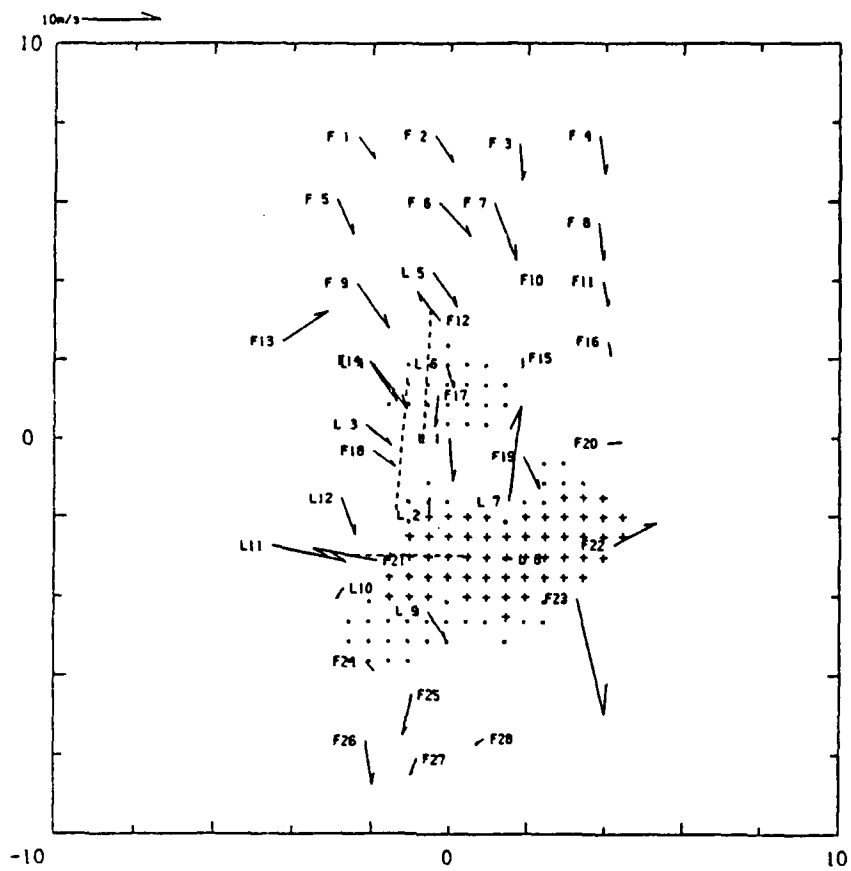
88/07/11-22:09:00 LLWAS-FLOWS MESONET (km x km)



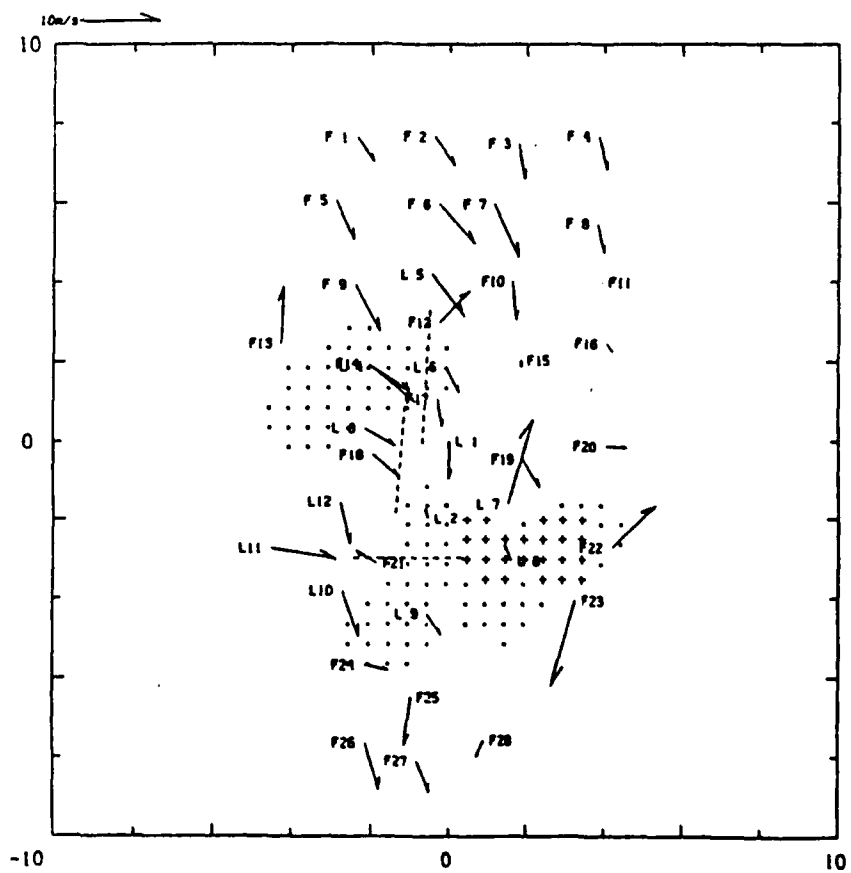
88/07/11-22:10:00 LLWAS-FLOWS MESONET (km x km)



88/07/11-22:11:00 LLWAS-FLOWS MESONET (km x km)



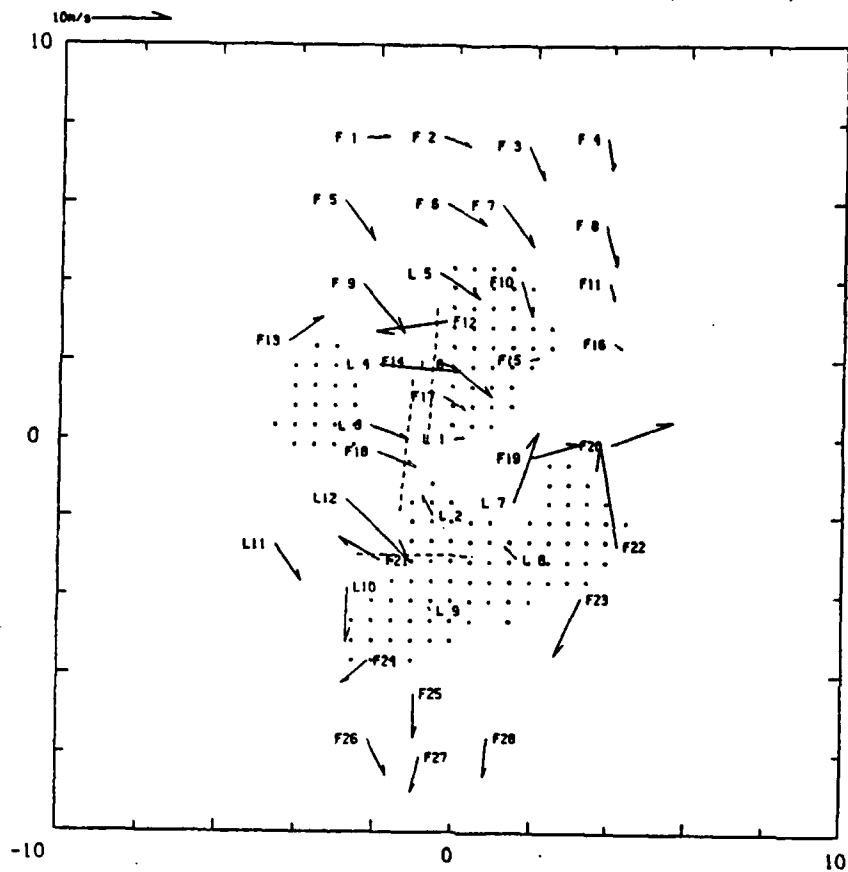
88/07/11-22:12:00 LLWAS-FLOWS MESONET (km x km)



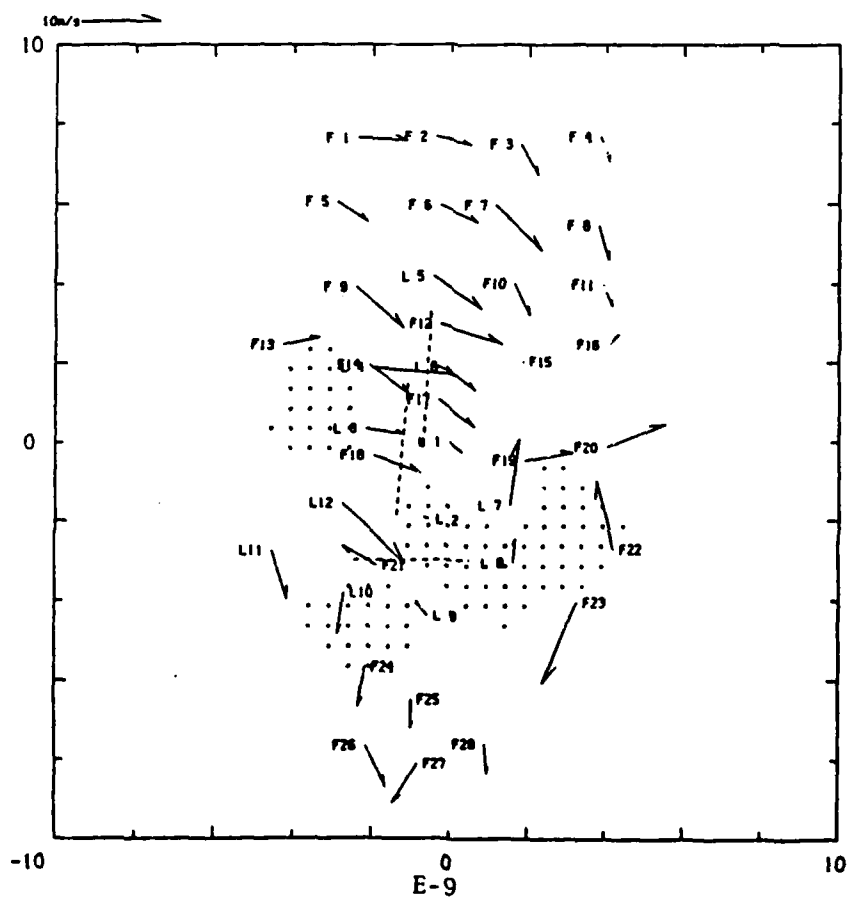
Arrows show axis of the flow field at 10 cm/sec

Labels: F1, F2, F3, F4, F5, F6, F7, F8, F9, F10, F11, F12, F13, F14, F15, F16, F17, F18, F19, F20, F21, F22, F23, F24, F25, F26, F27, F28, L1, L2, L3, L4, L5, L6, L7, L8, L9, L10, L11, L12.

88/07/11-22:15:00 LLWAS-FLOWS MESONET (km x km)

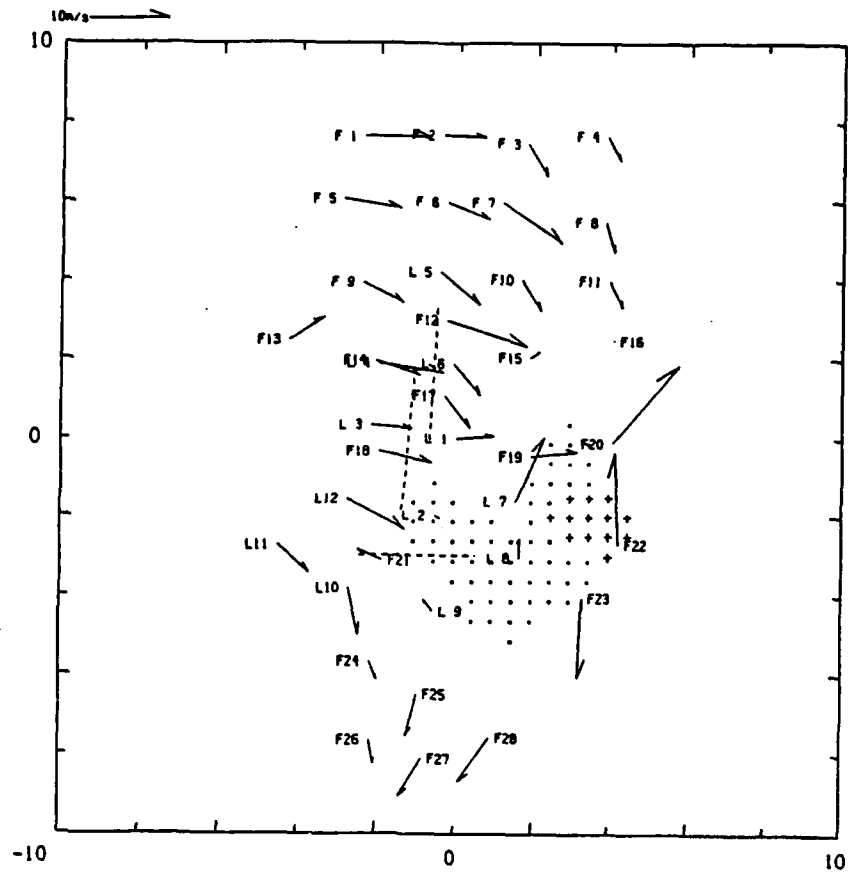


88/07/11-22:16:00 LLWAS-FLOWS MESONET (km x km)

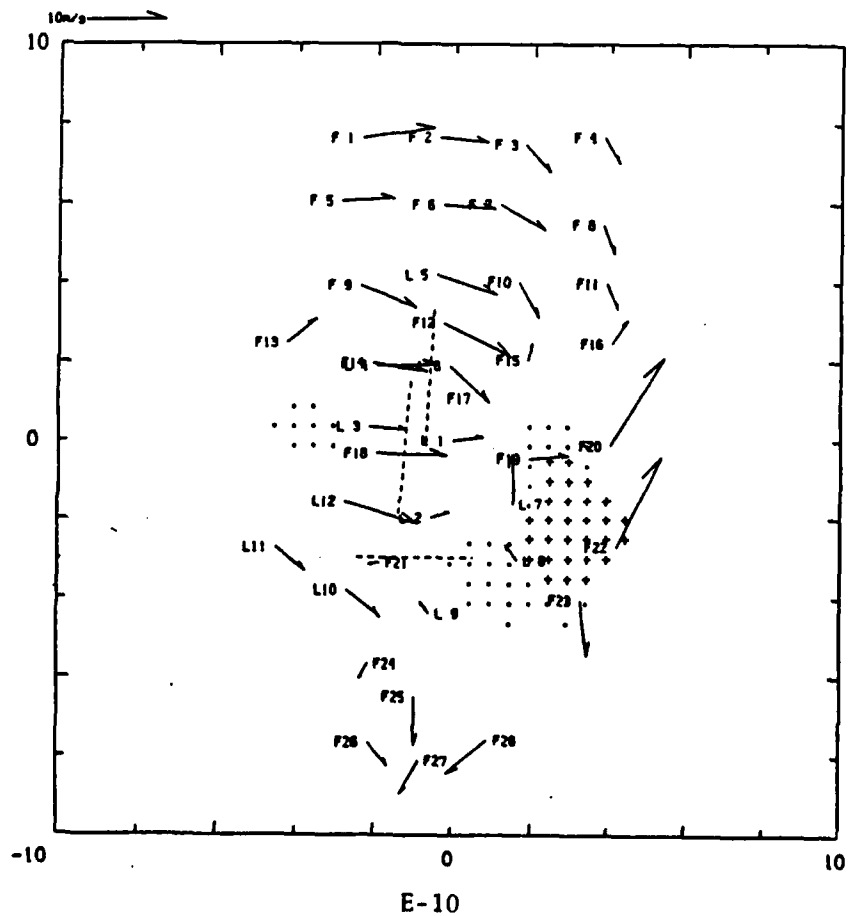




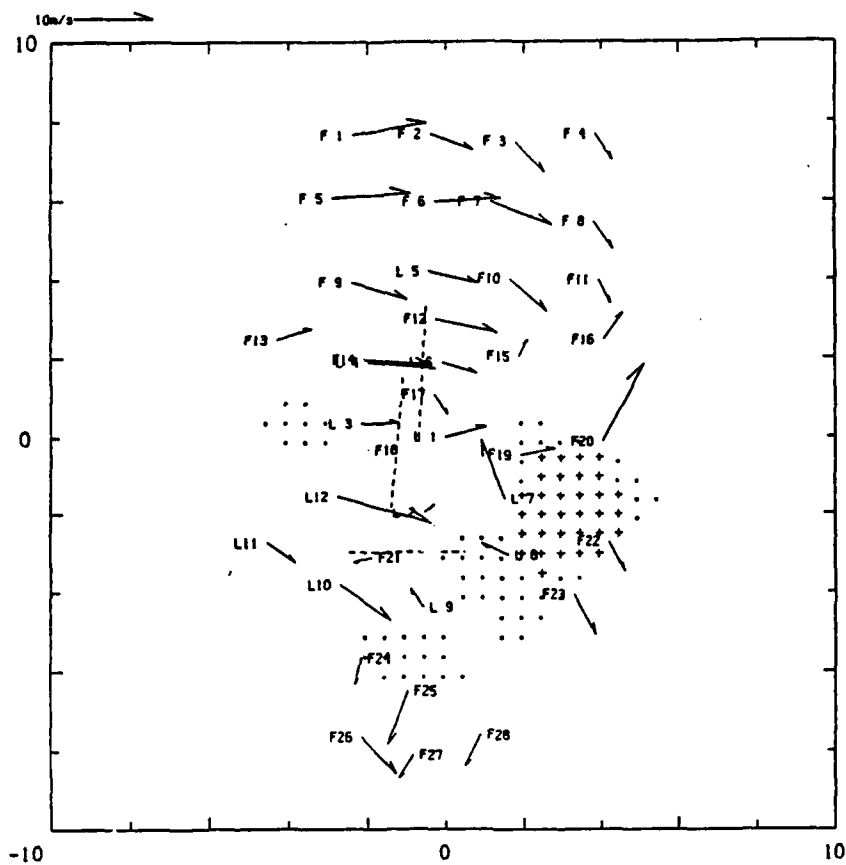
88/07/11-22:17:00 LLWAS-FLOWS MESONET (km x km)



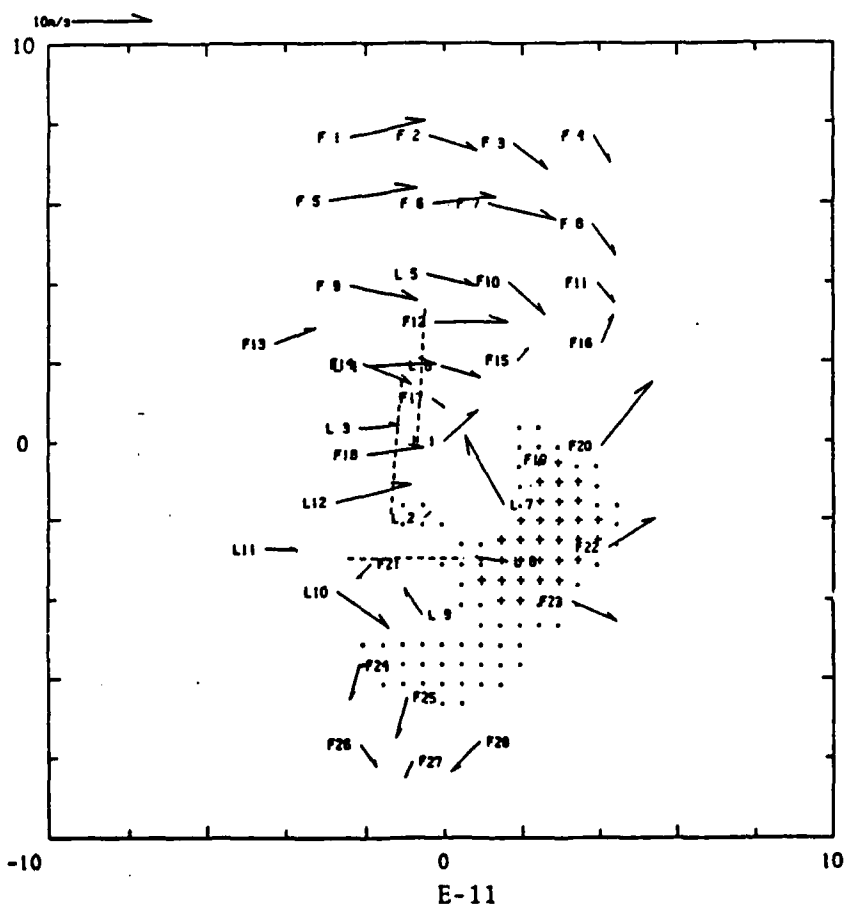
88/07/11-22:18:00 LLWAS-FLOWS MESONET (km x km)



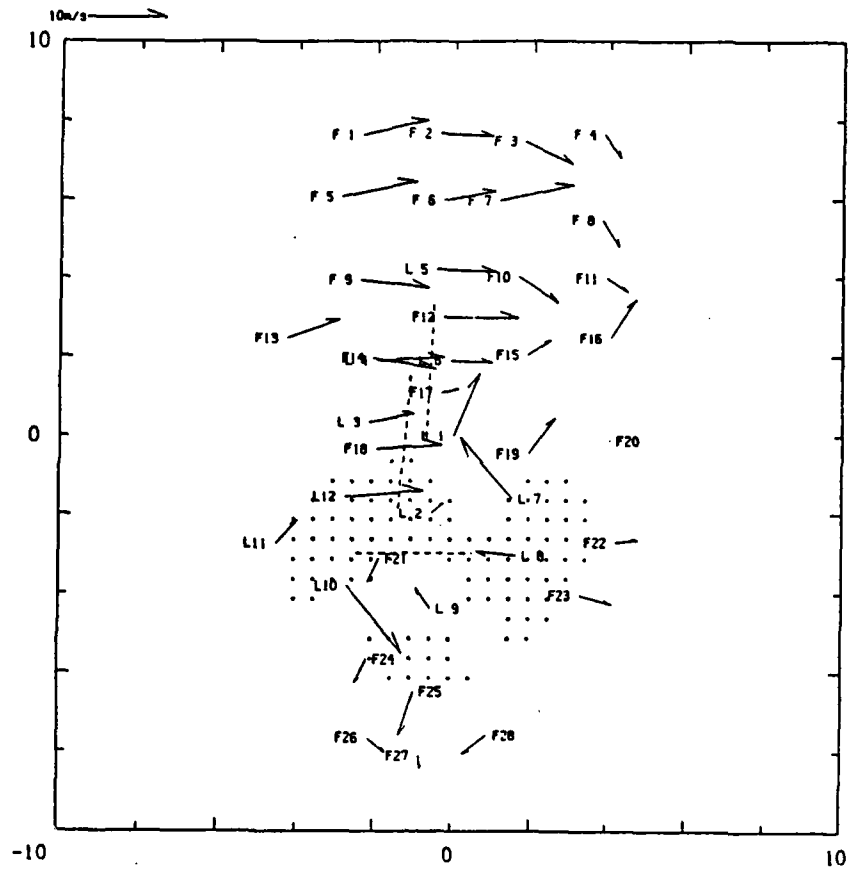
88/07/11-22:19:00 LLWS-FLOWS MESONET (km x km)



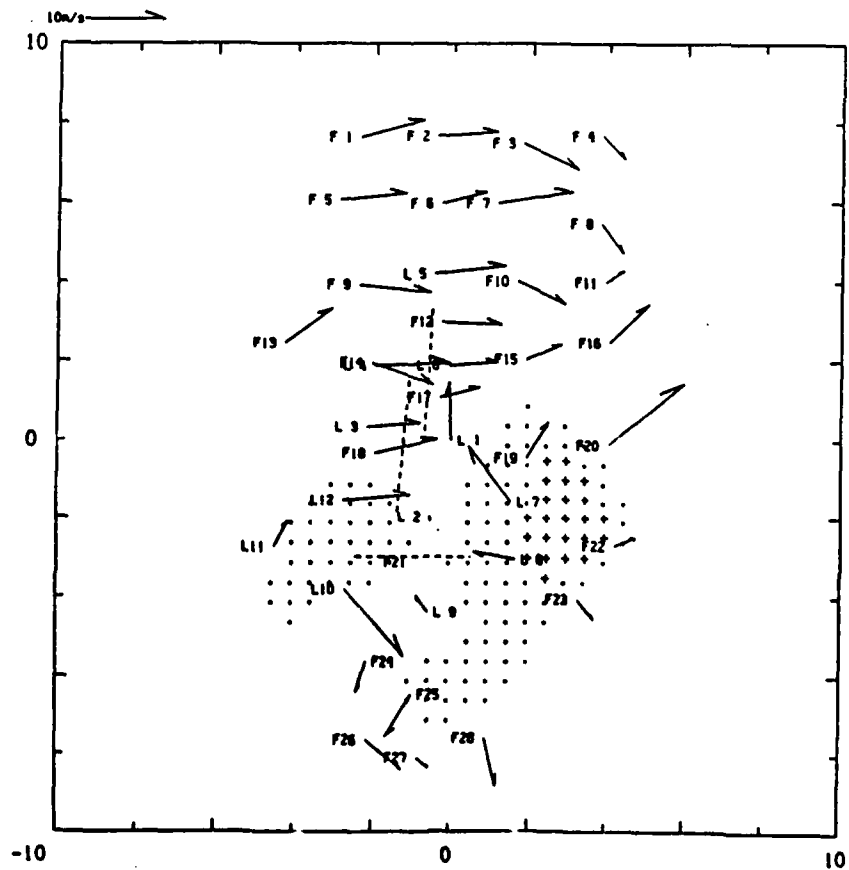
88/07/11-22:20:00 LLWS-FLOWS MESONET (km x km)



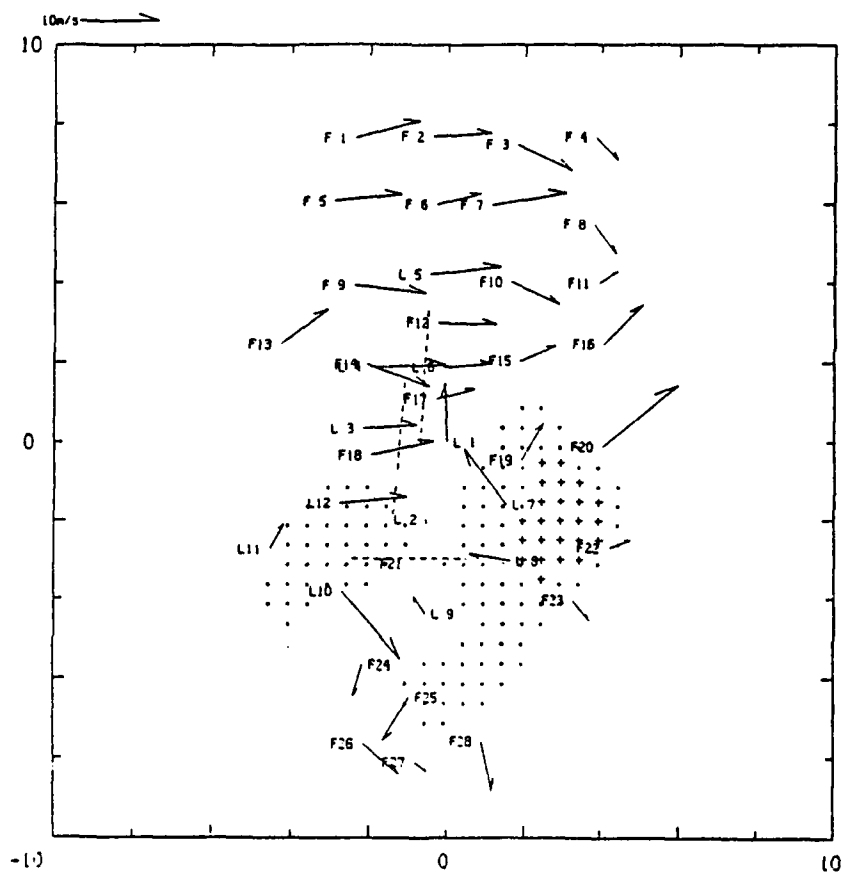
88/07/11-22:21:00 LLWAS-FLOWS MESONET (km x km)



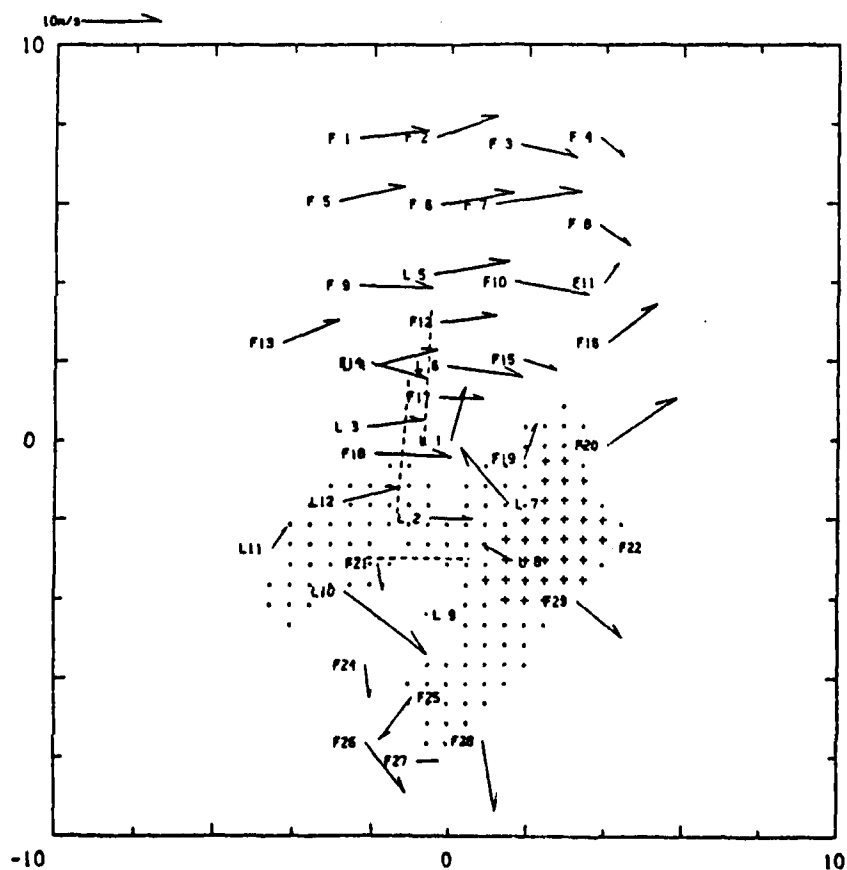
88/07/11-22:22:00 LLWAS-FLOWS MESONET (km x km)



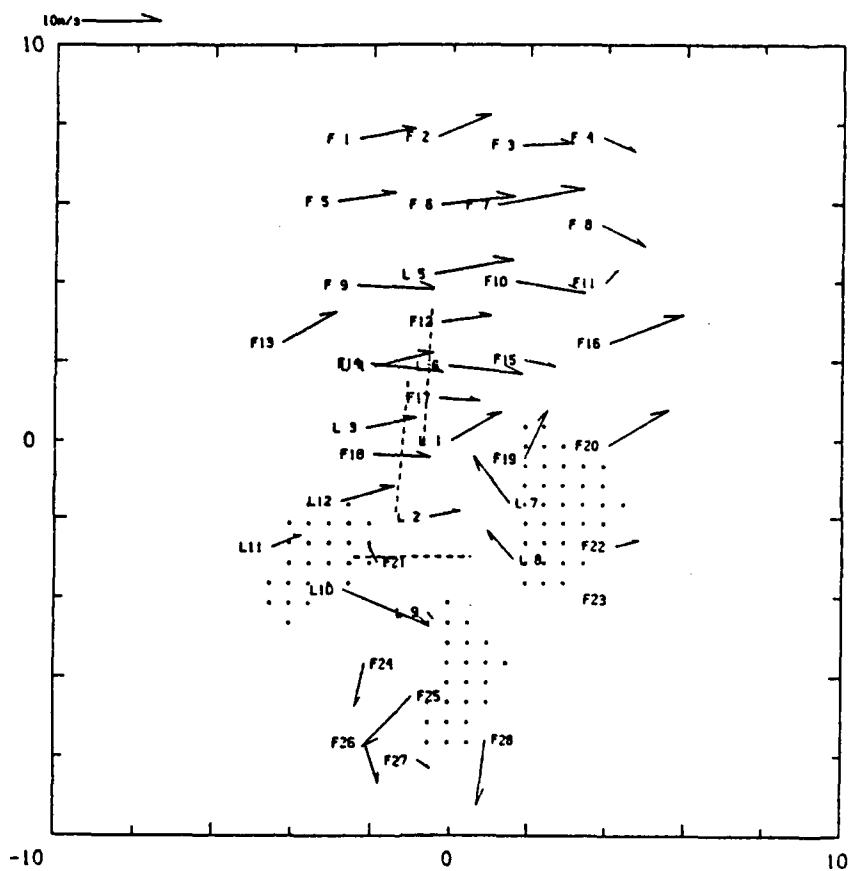
88/07/11-22:22:00 LLWAS-FLOWS MESONET (km x km)



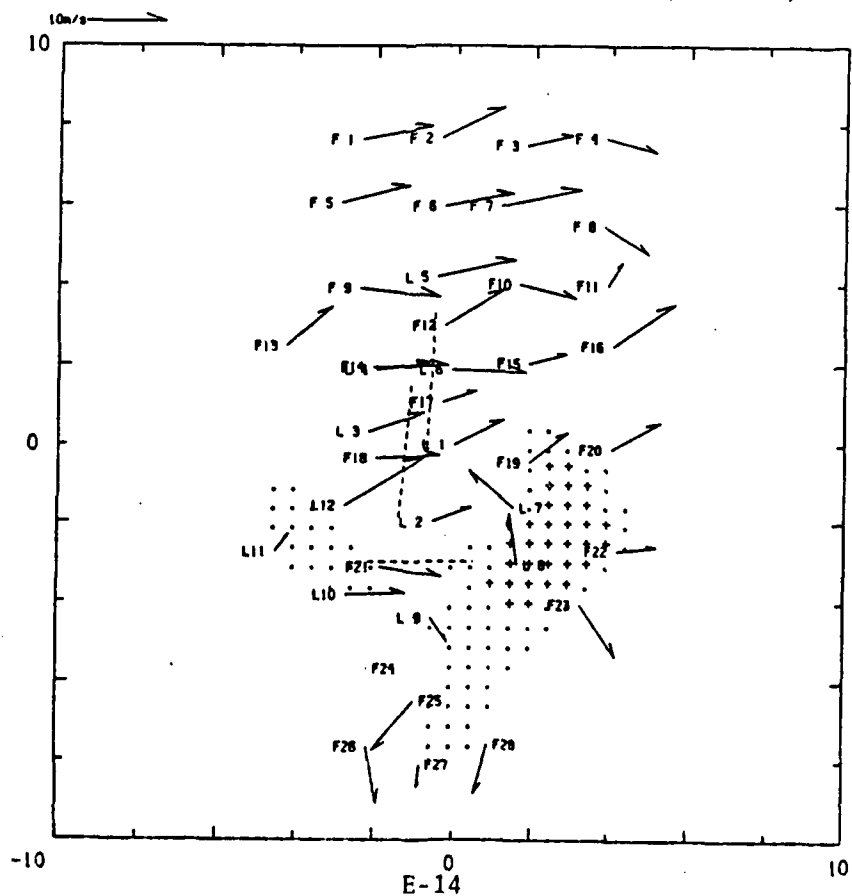
88/07/11-22:23:00 LLWAS-FLOWS MESONET (km x km)



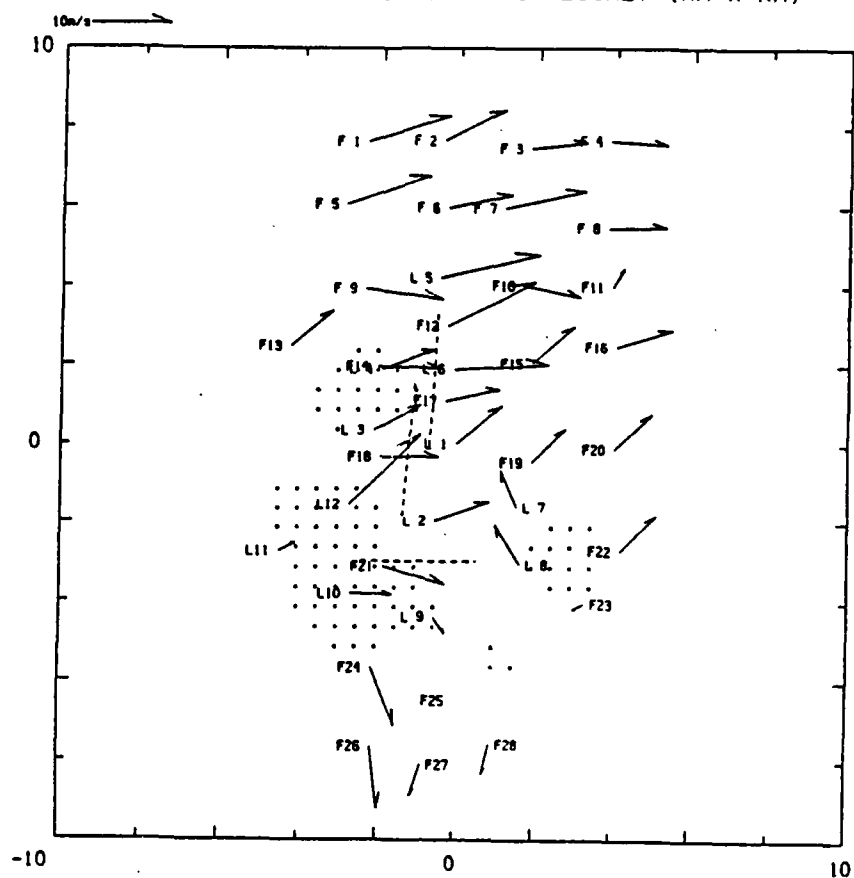
88/07/11-22:24:00 LLWAS-FLOWS MESONET (km x km)



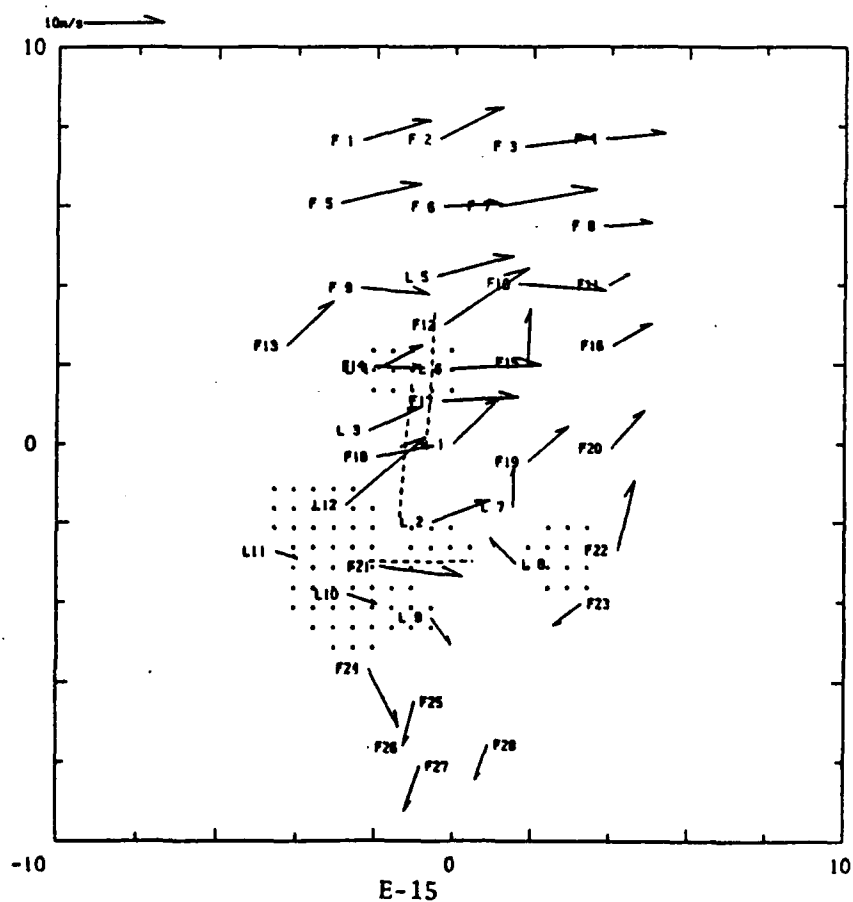
88/07/11-22:25:00 LLWAS-FLOWS MESONET (km x km)



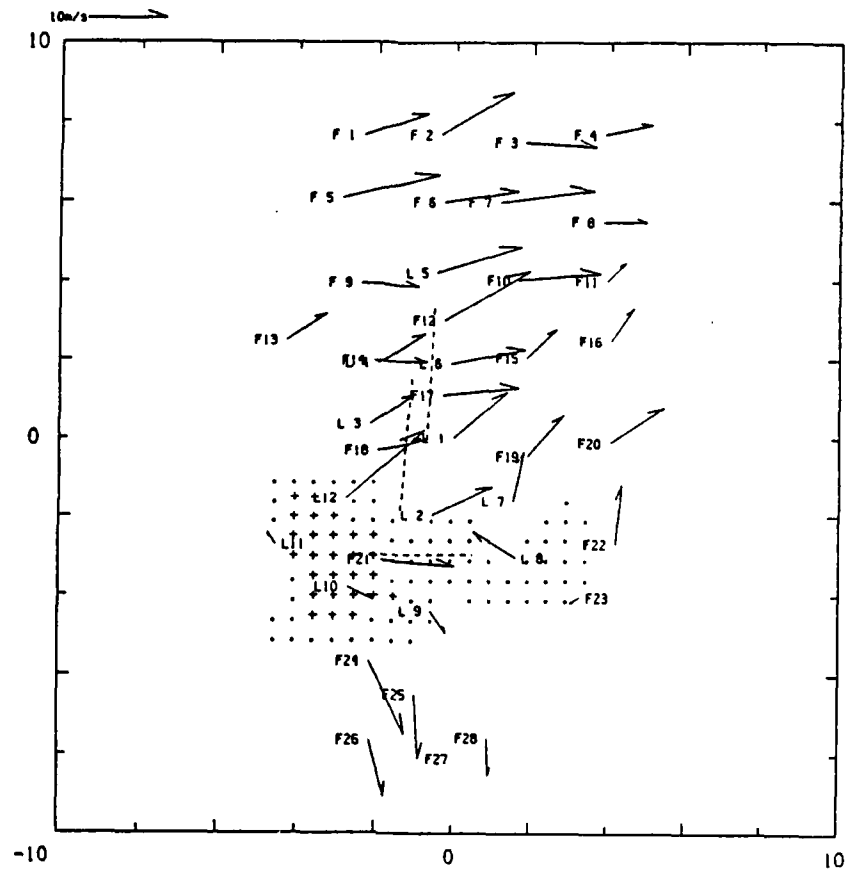
88/07/11-22:26:00 LLWAS-FLOWS MESONET (km x km)



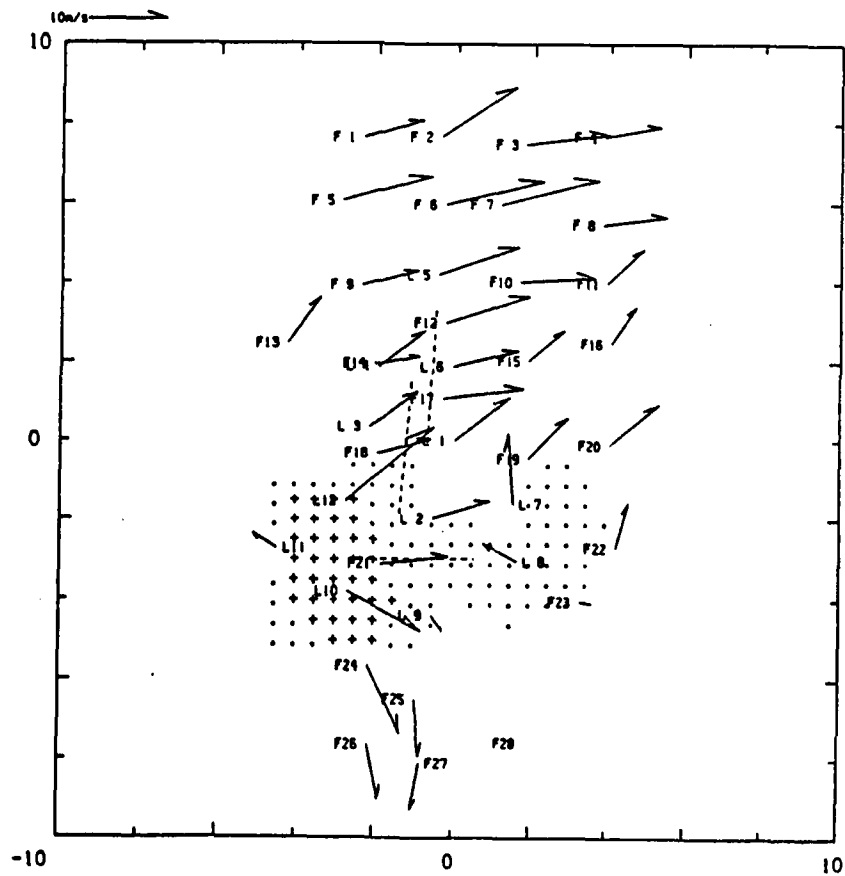
88/07/11-22:27:00 LLWAS-FLOWS MESONET (km x km)



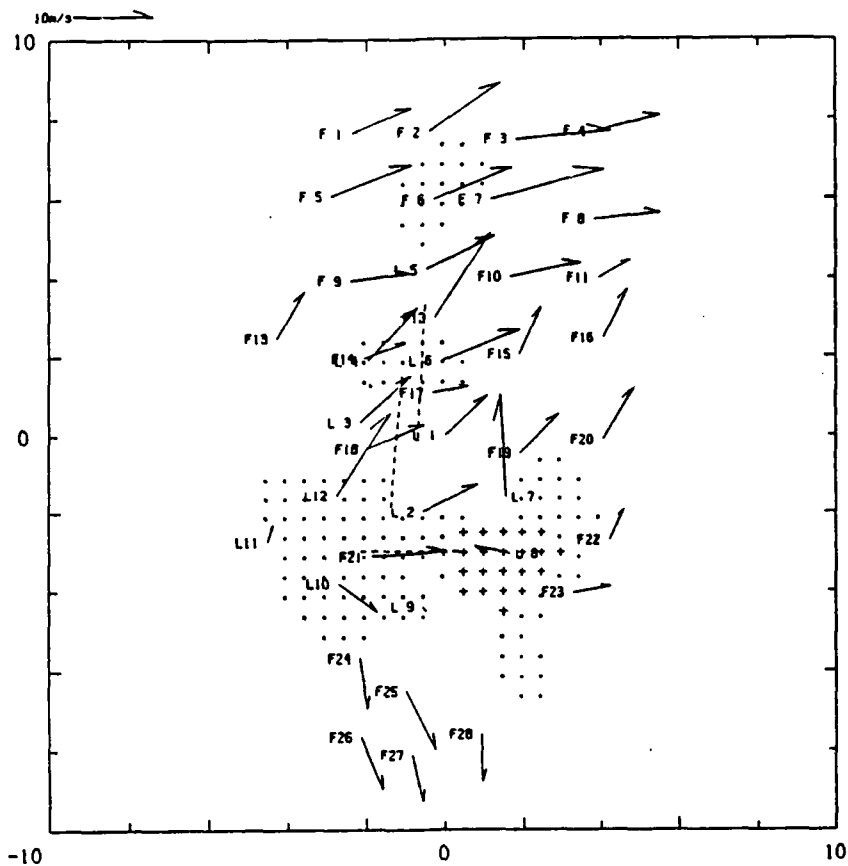
88/07/11-22:28:00 LLWAS-FLOWS MESONET (km x km)



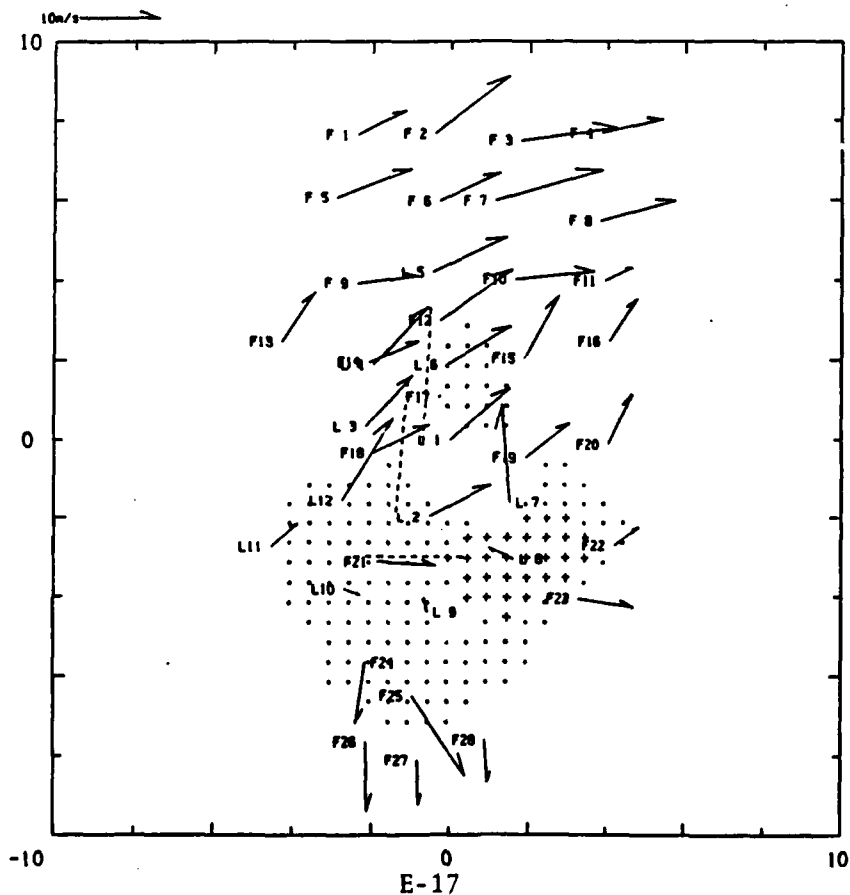
88/07/11-22:29:00 LLWAS-FLOWS MESONET (km x km)



88/07/11-22:30:00 LLWAS-FLOWS MESONET (km x km)

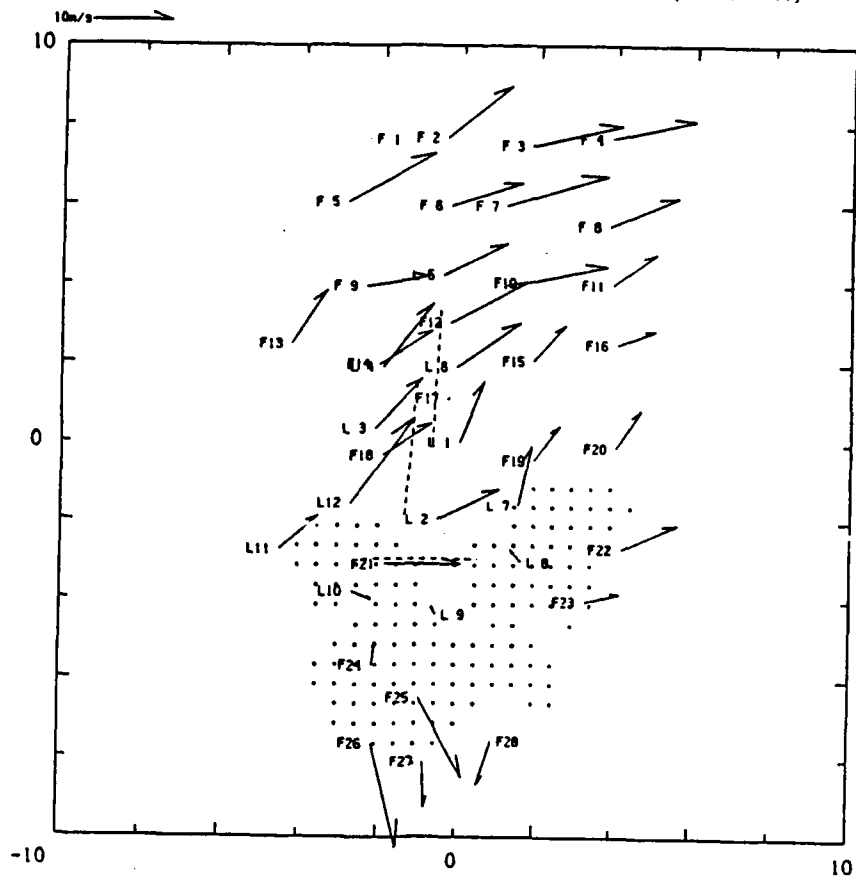


88/07/11-22:31:00 LLWAS-FLOWS MESONET (km x km)

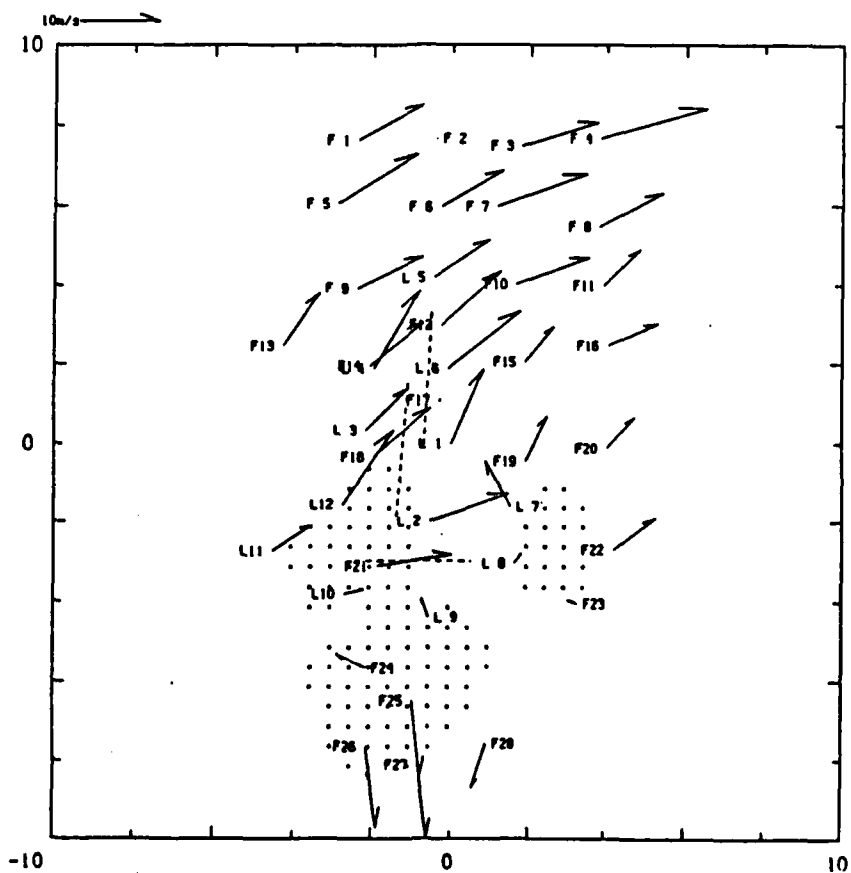




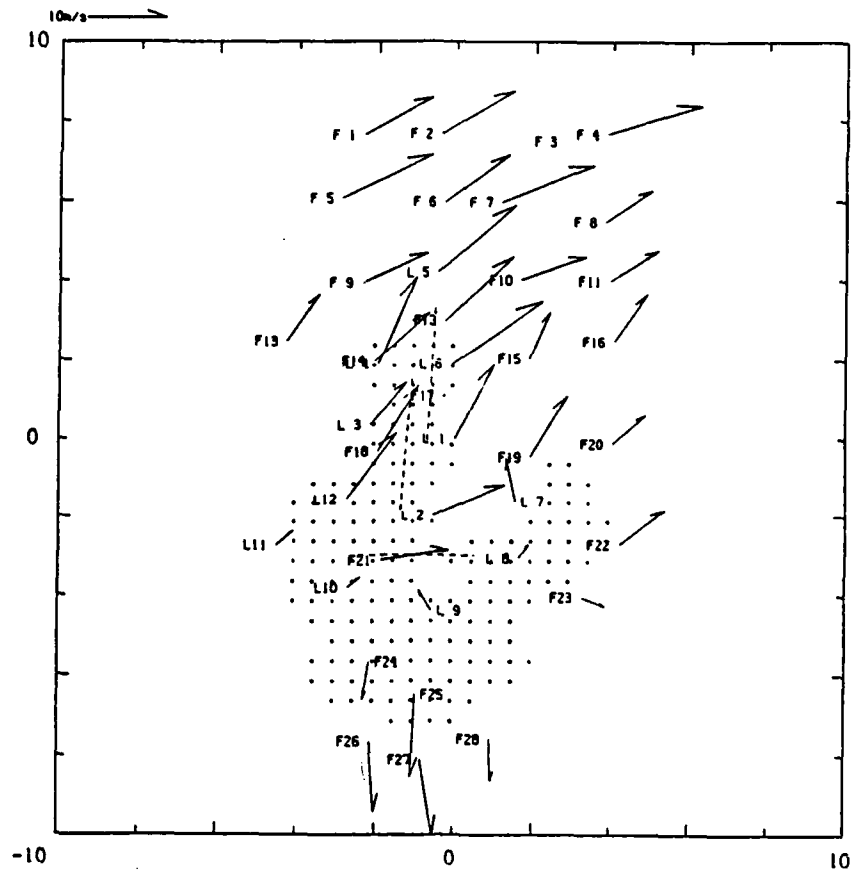
88/07/11-22:32:00 LLWAS-FLOWS MESONET (km x km)



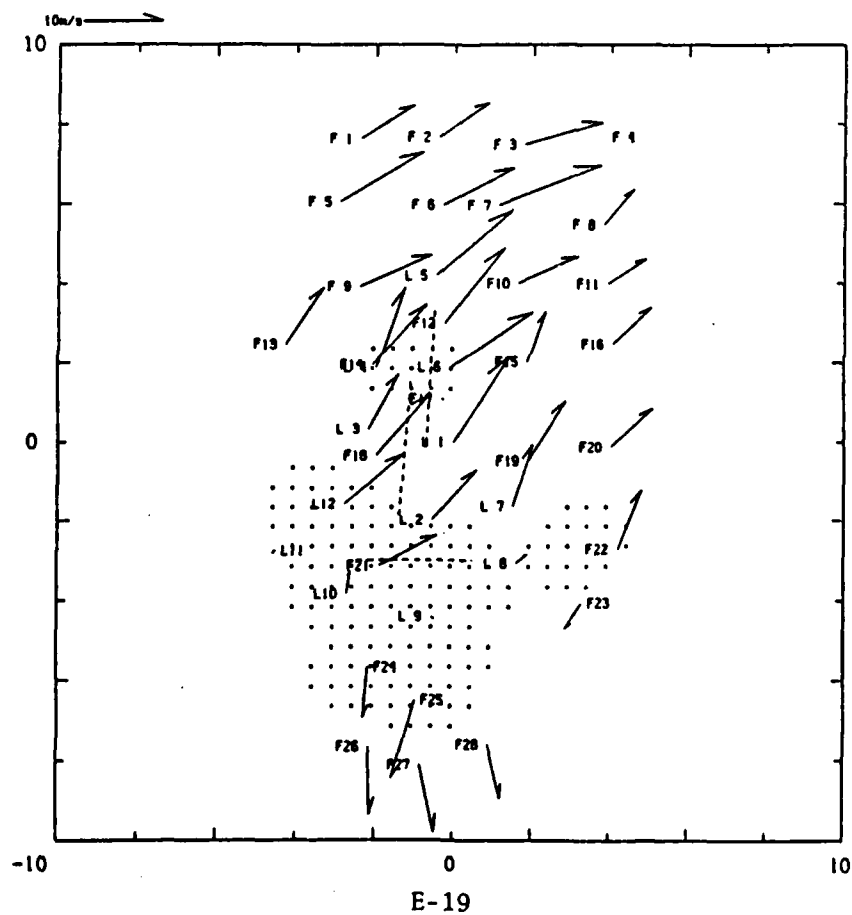
88/07/11-22:33:00 LLWAS-FLOWS MESONET (km x km)



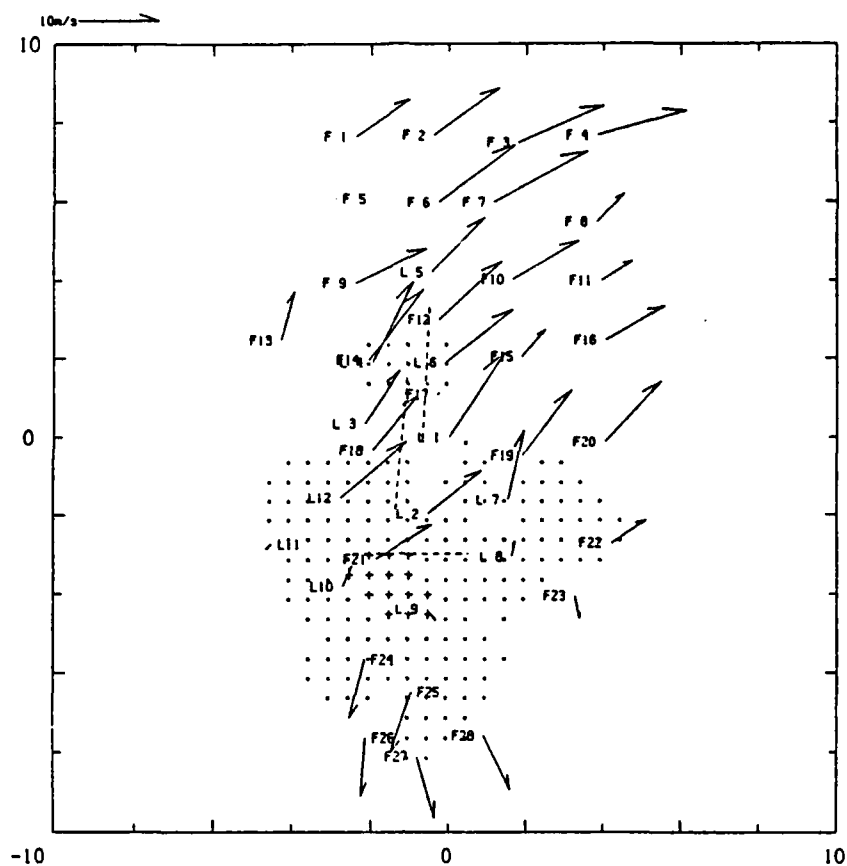
88/07/11-22:34:00 LLWAS-FLOWS MESONET (km x km)



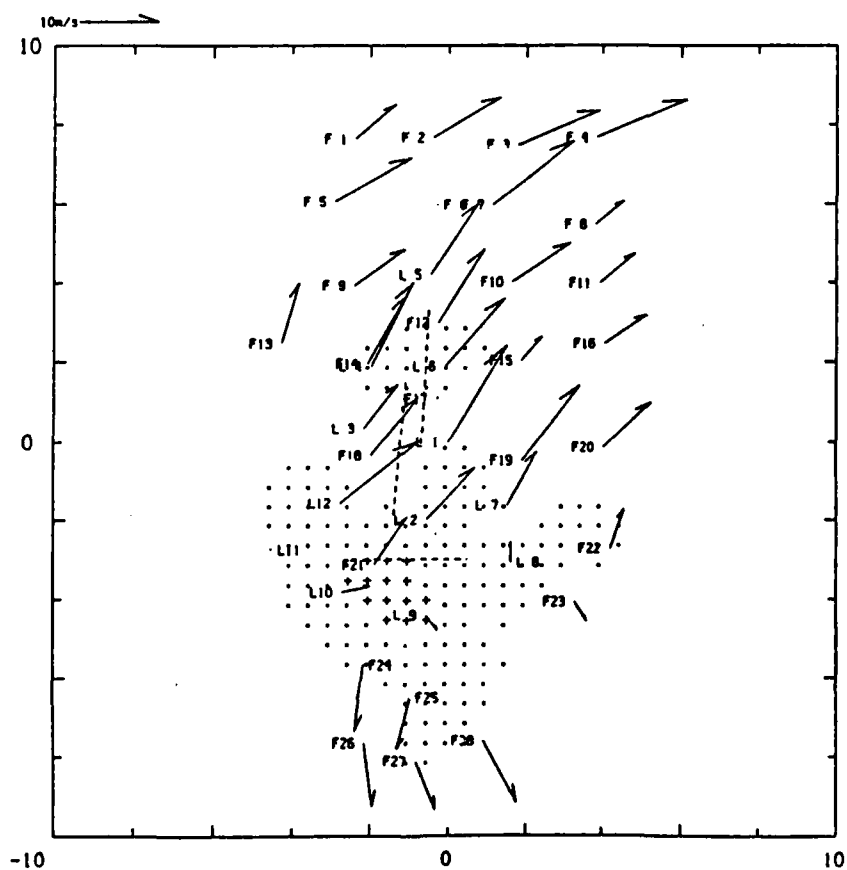
88/07/11-22:35:00 LLWAS-FLOWS MESONET (km x km)



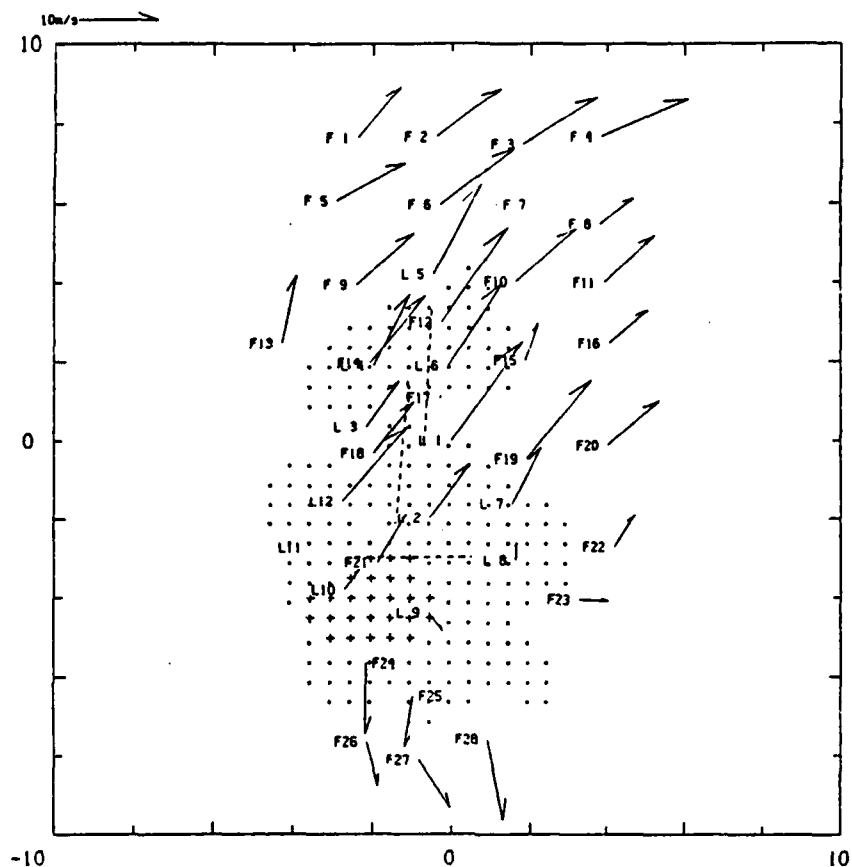
88/07/11-22:36:00 LLWAS-FLOWS MESONET (km x km)



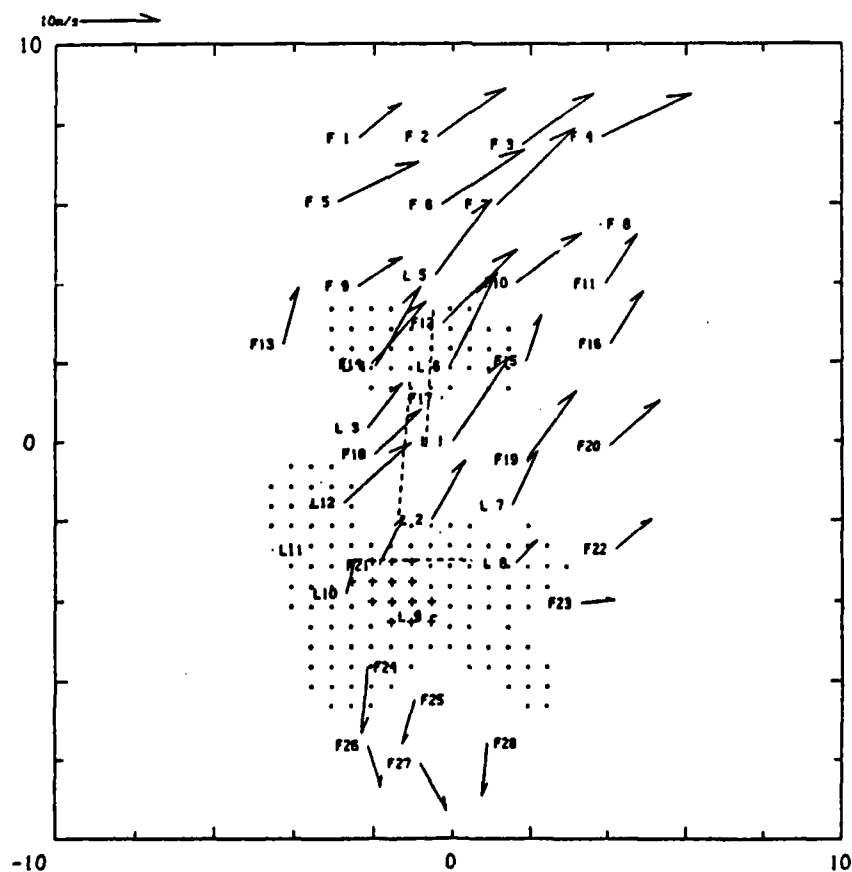
88/07/11-22:37:00 LLWAS-FLOWS MESONET (km x km)



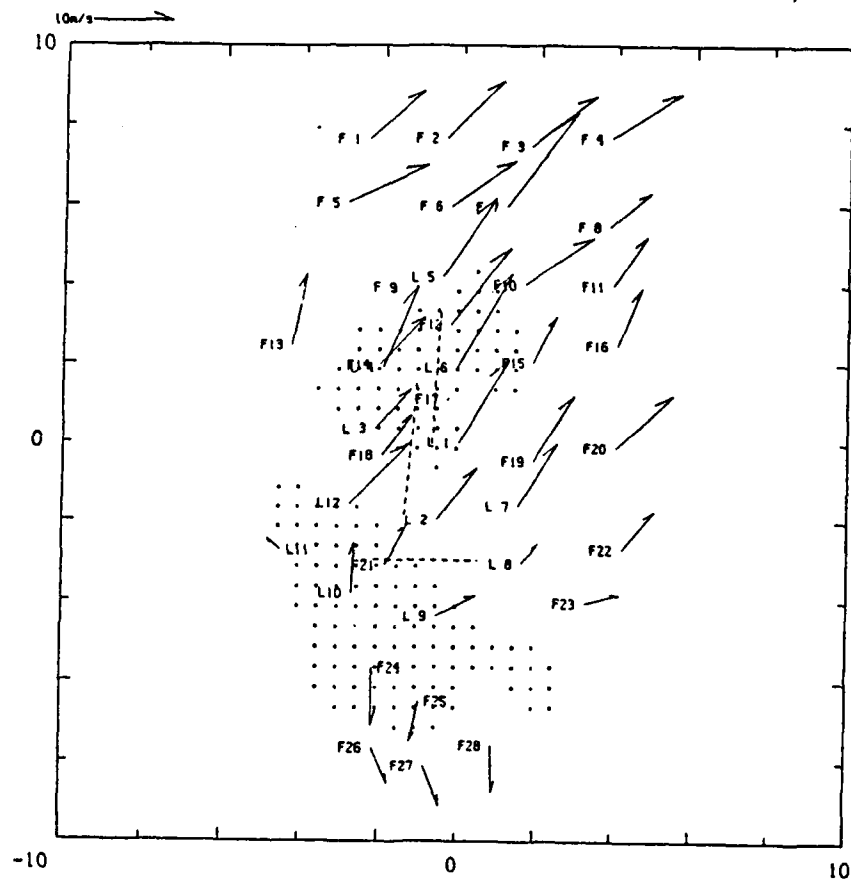
88/07/11-22:38:00 LLWAS-FLOWS MESONET (km x km)



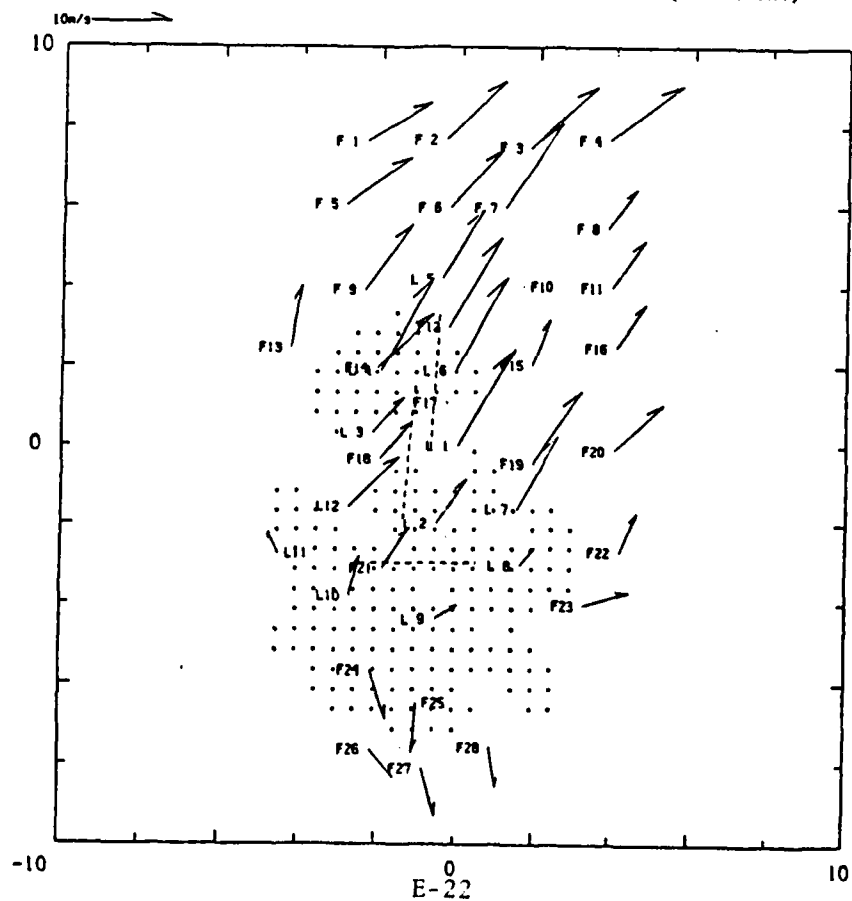
88/07/11-22:39:00 LLWAS-FLOWS MESONET (km x km)



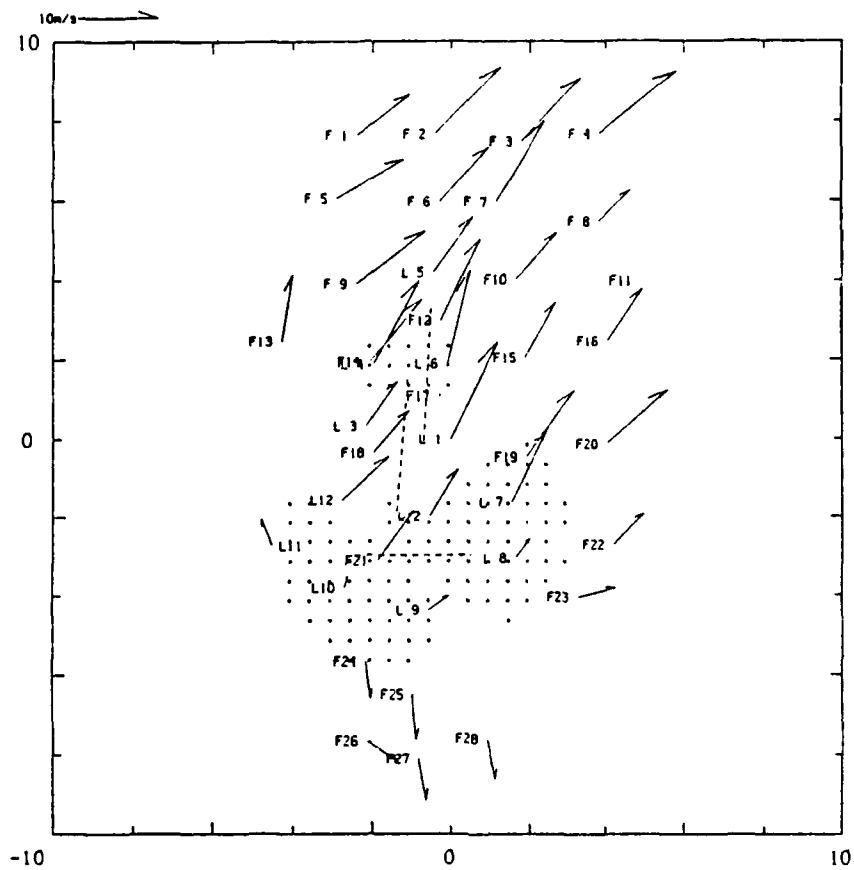
88/07/11-22:40:00 LLWAS-FLOWS MESONET (km x km)



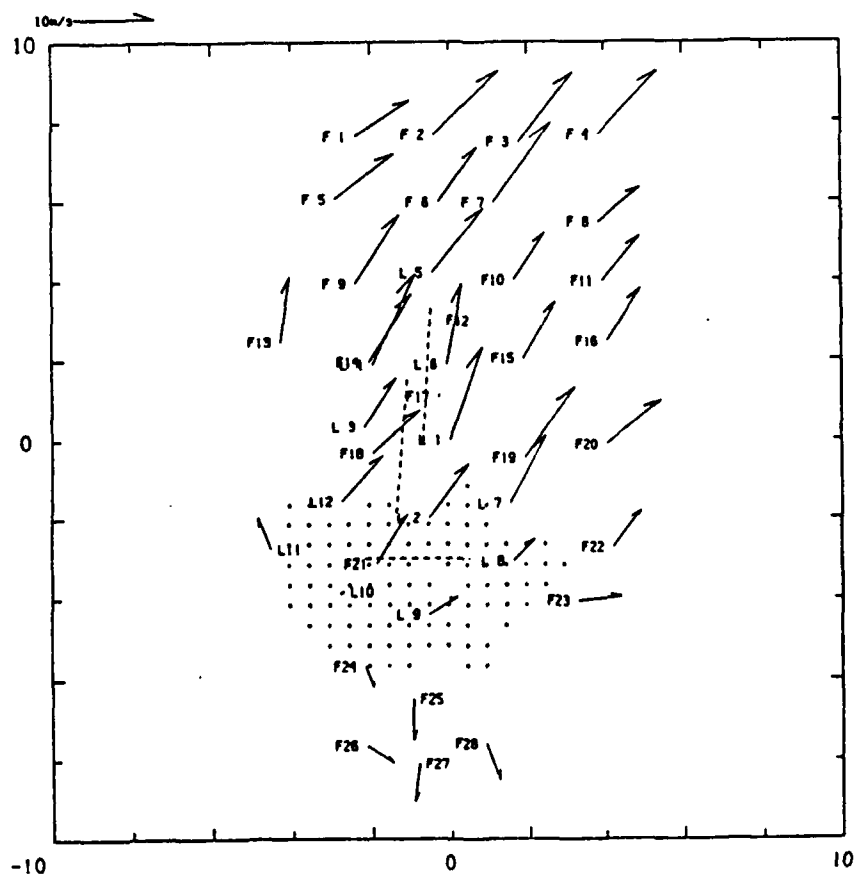
88/07/11-22:41:00 LLWAS-FLOWS MESONET (km x km)



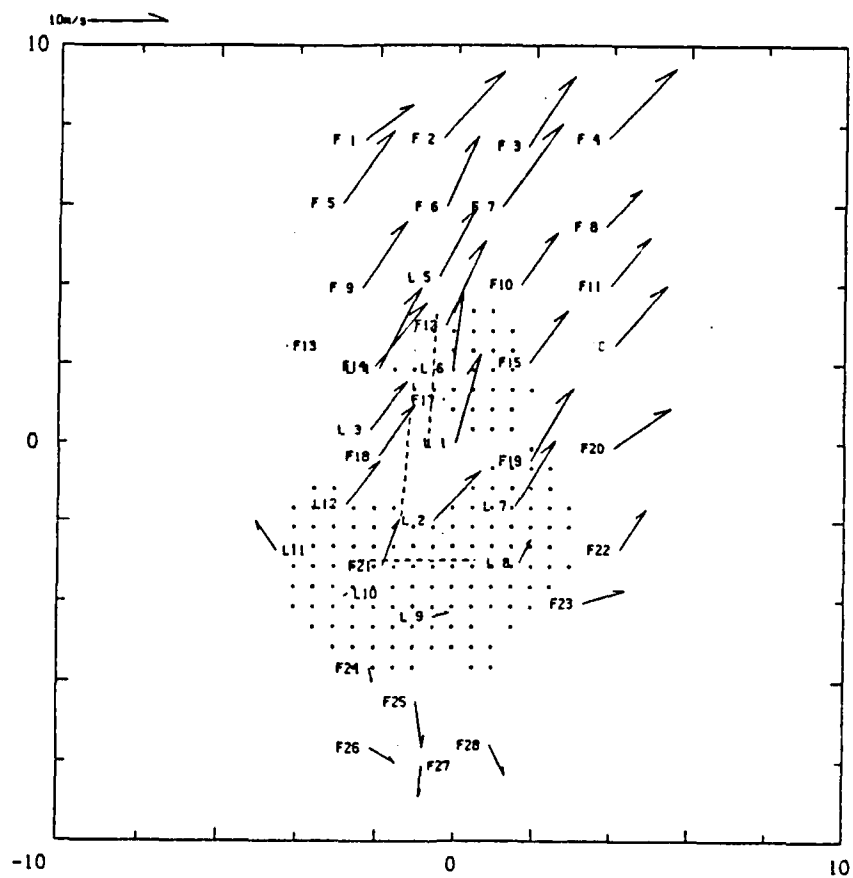
88/07/11-22:42:00 LLWAS-FLOWS MESONET (km x km)



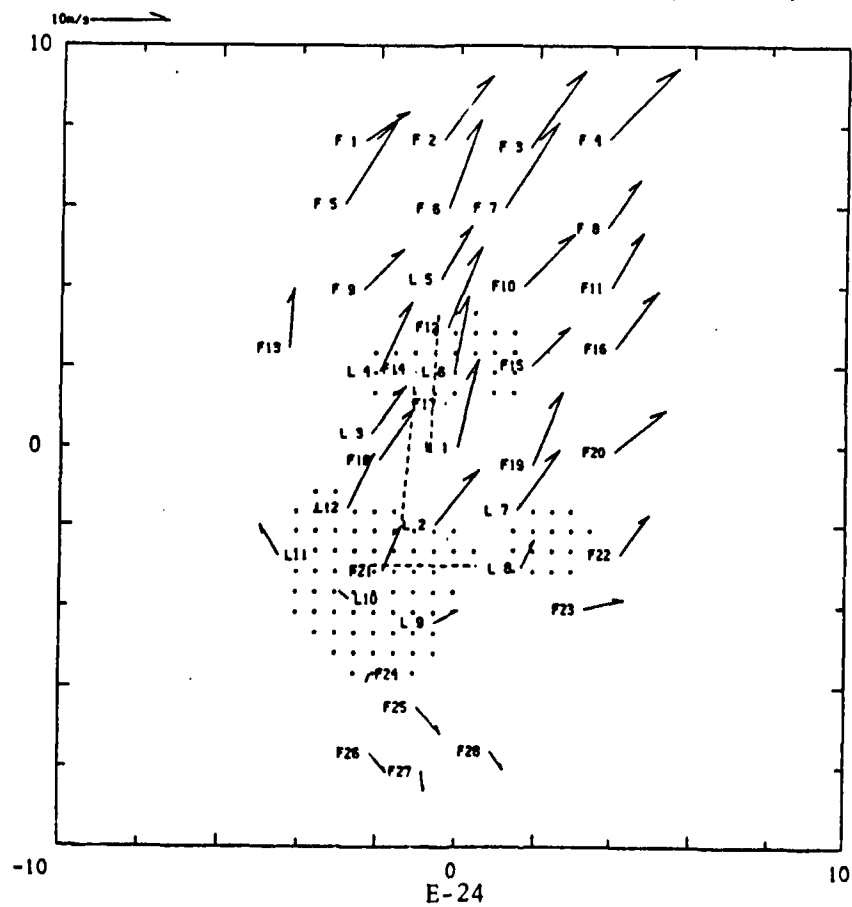
88/07/11-22:43:00 LLWAS-FLOWS MESONET (km x km)



88/07/11-22:44:00 LLWAS-FLOWS MESONET (km x km)



88/07/11-22:45:00 LLWAS-FLOWS MESONET (km x km)

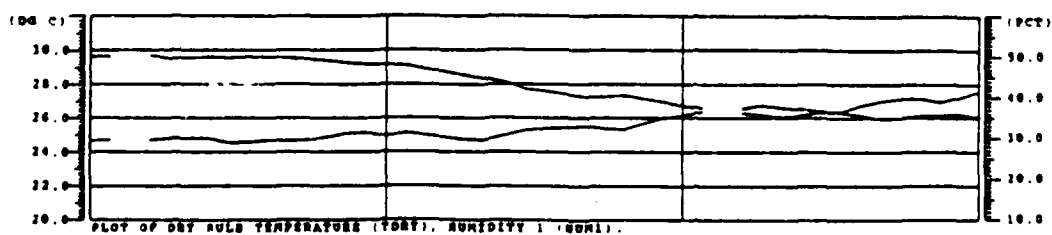
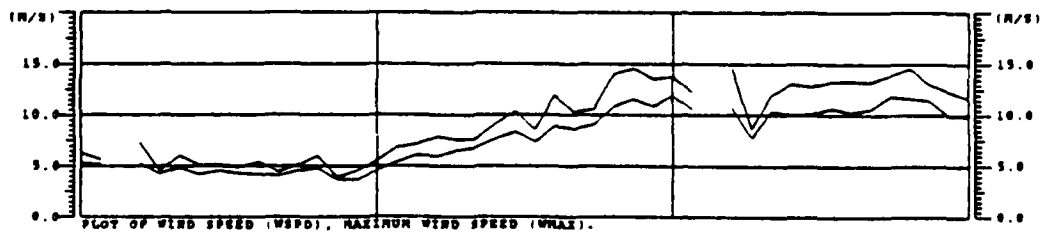
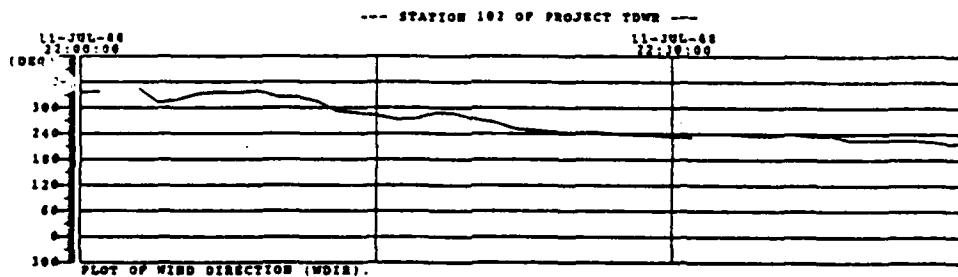
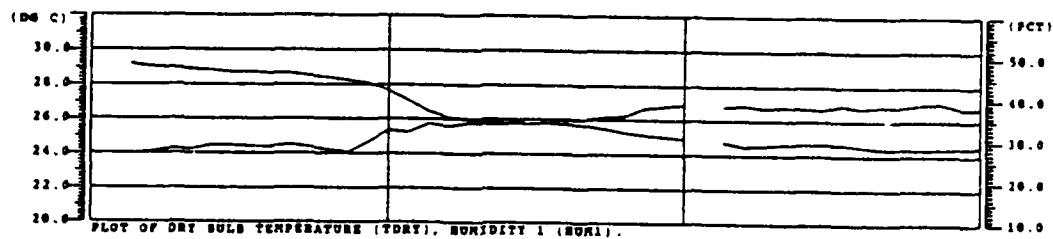
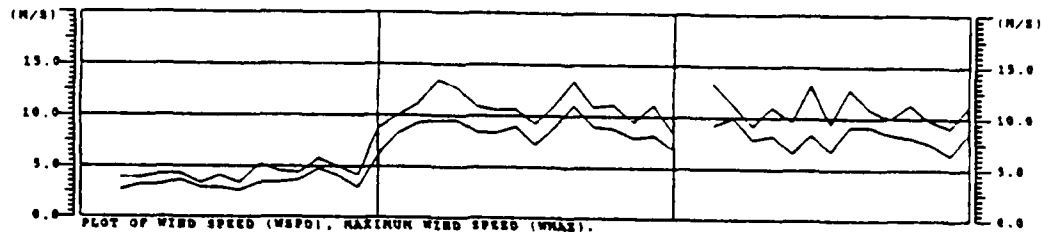
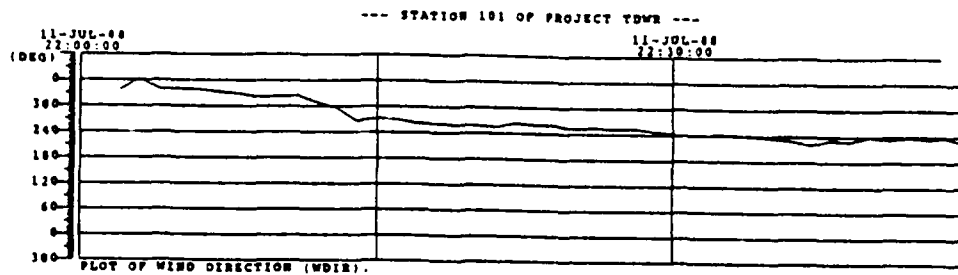


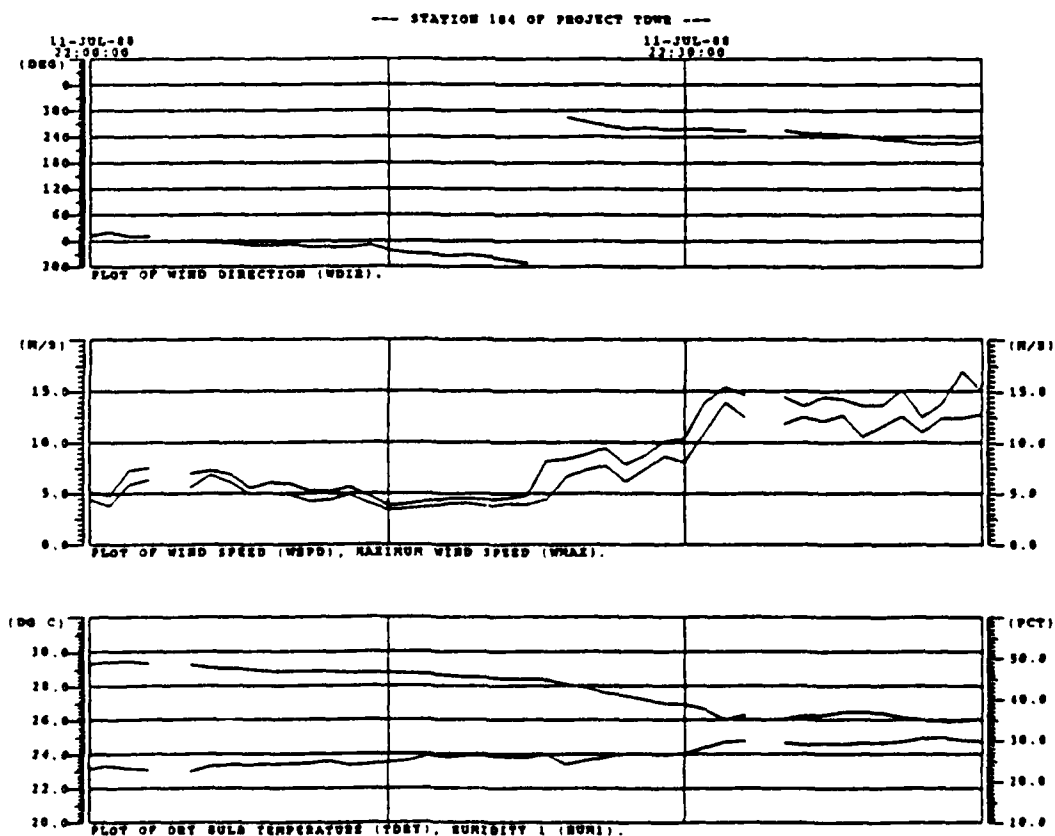
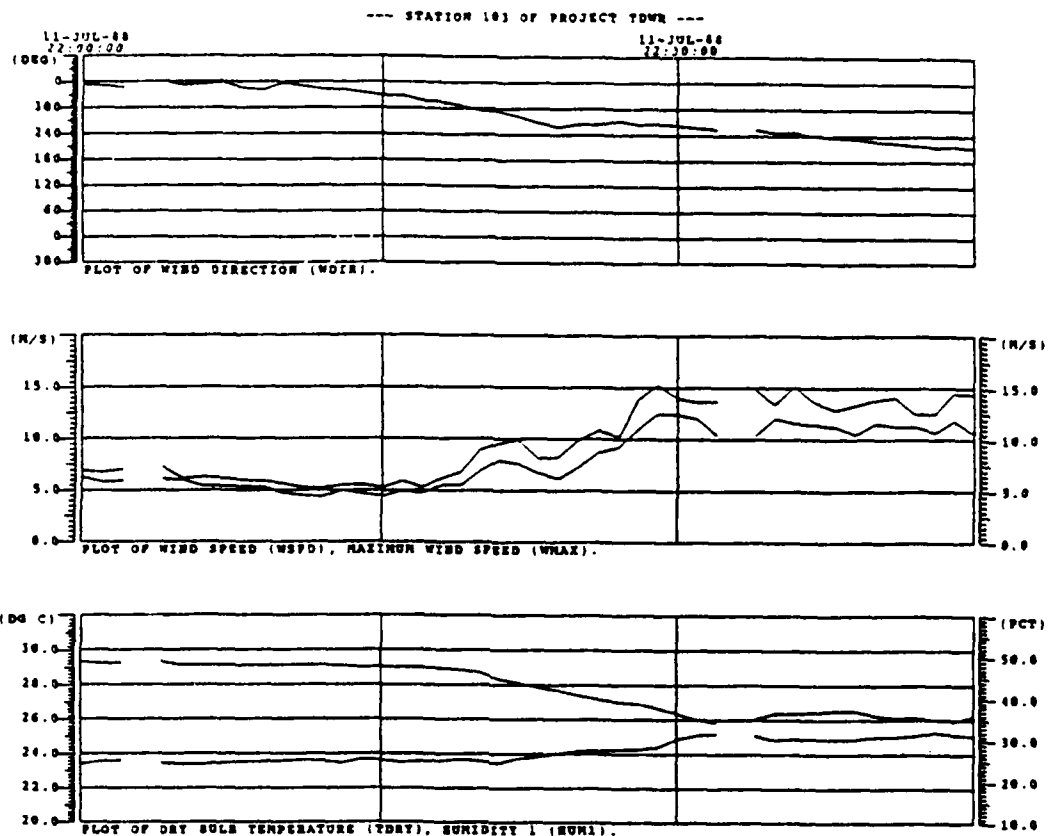
## **Appendix F: Surface sensor measurements from FLOWS**

These plots show time series of temperature, relative humidity, average and maximum wind speed and wind direction (from true north) for the FLOWS mesonet stations. Axes are marked in the appropriate units.

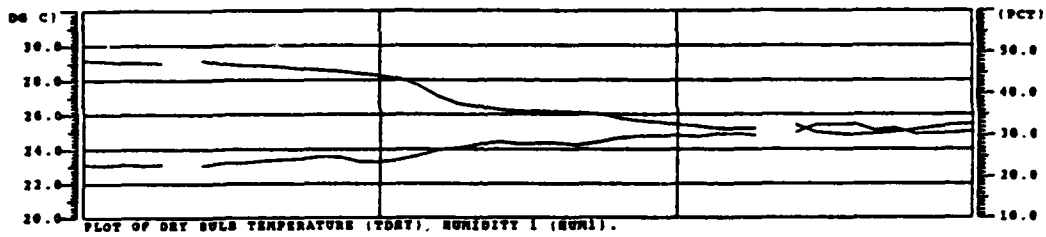
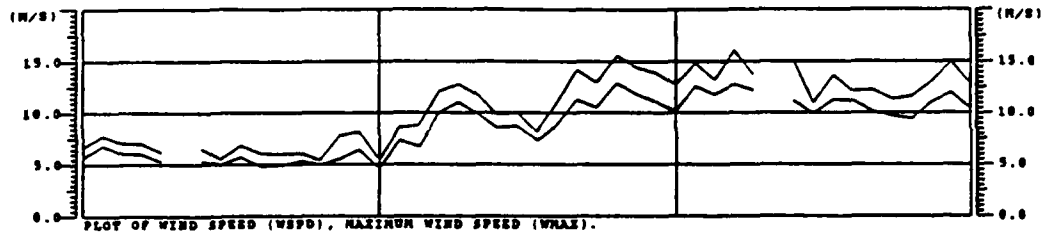
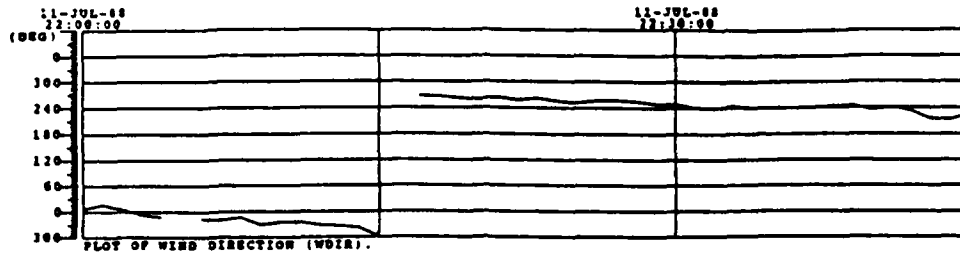
The station locations are shown in Appendix J. Station F30 was located at the FL2 radar.



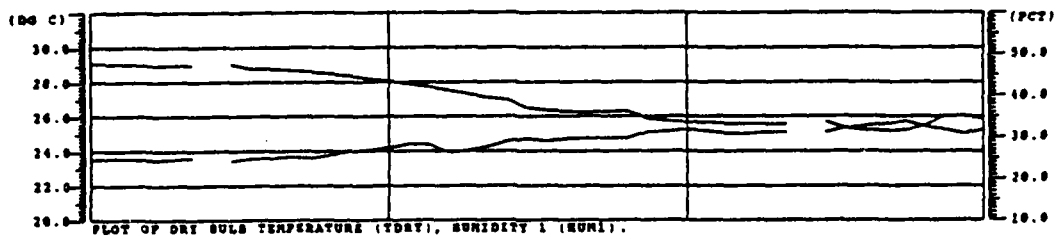
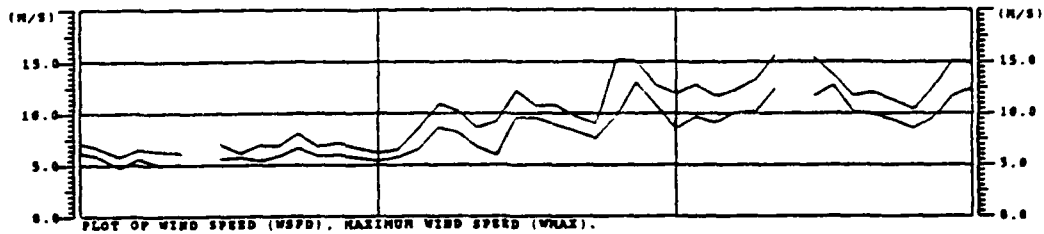
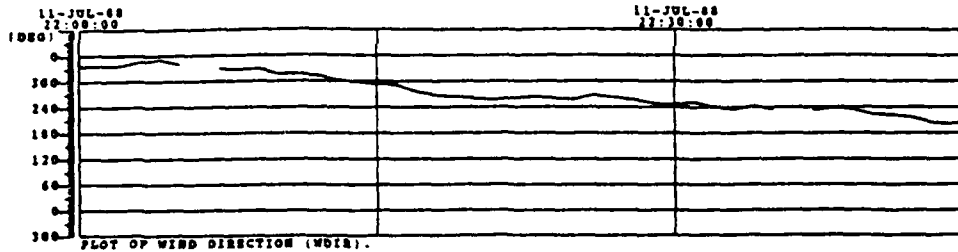




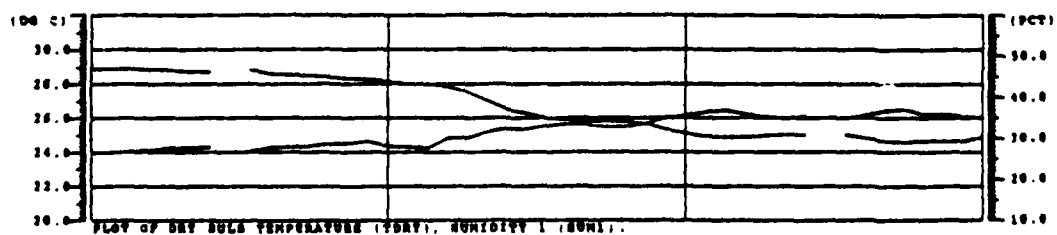
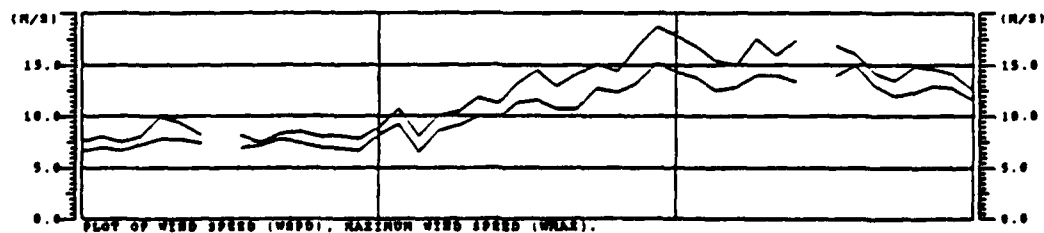
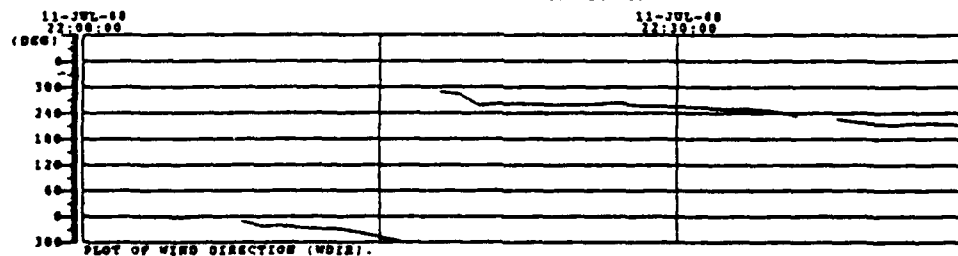
--- STATION 105 OF PROJECT TOWER ---



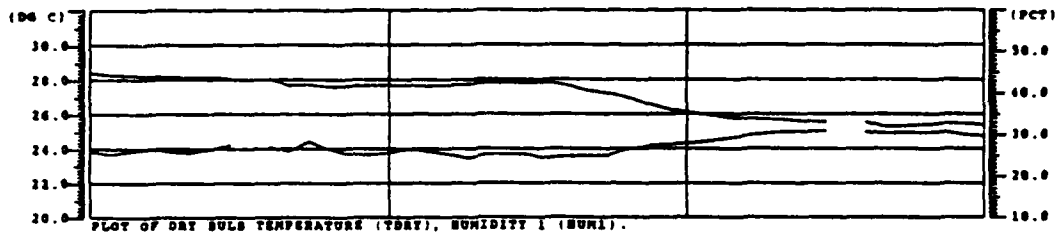
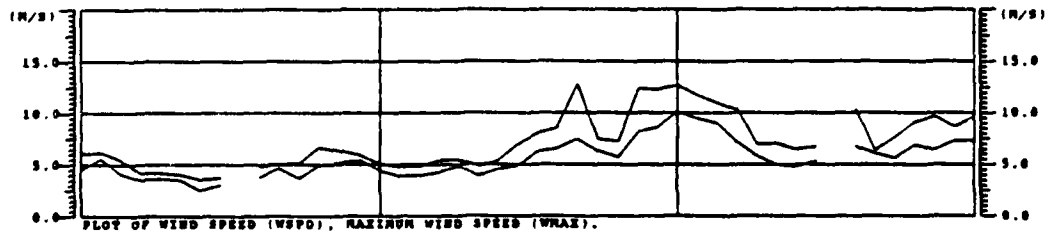
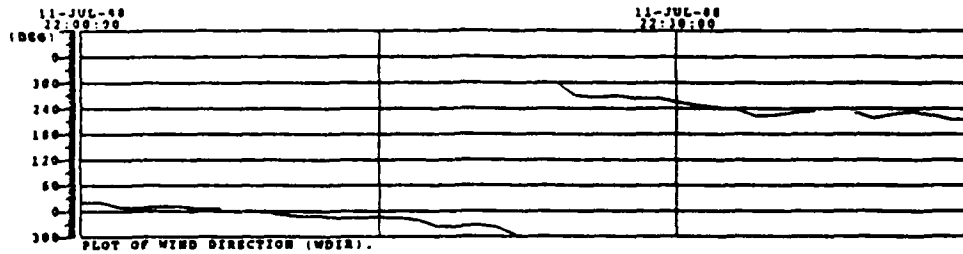
--- STATION 106 OF PROJECT TOWER ---



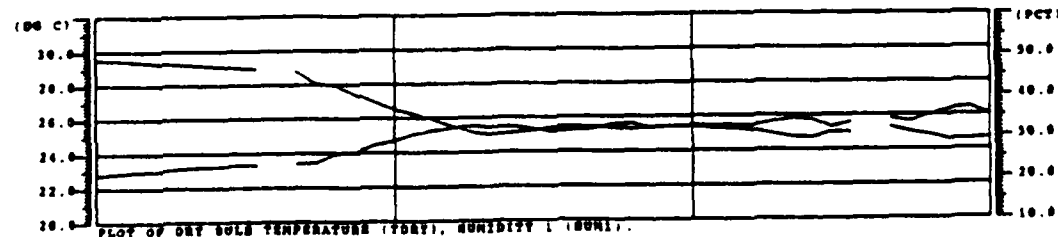
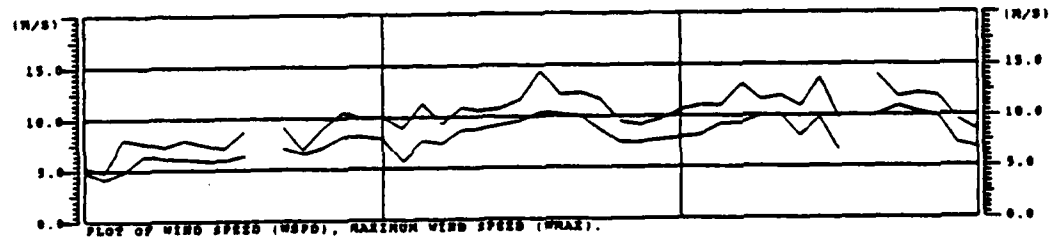
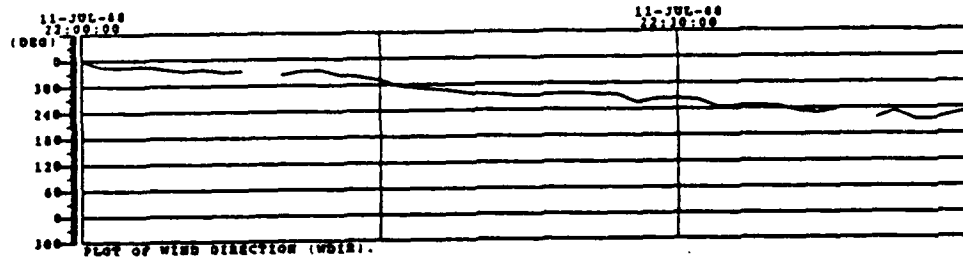
--- STATION 107 OF PROJECT TOWER ---



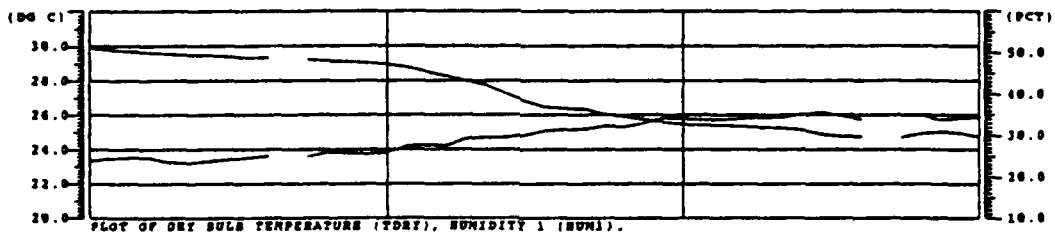
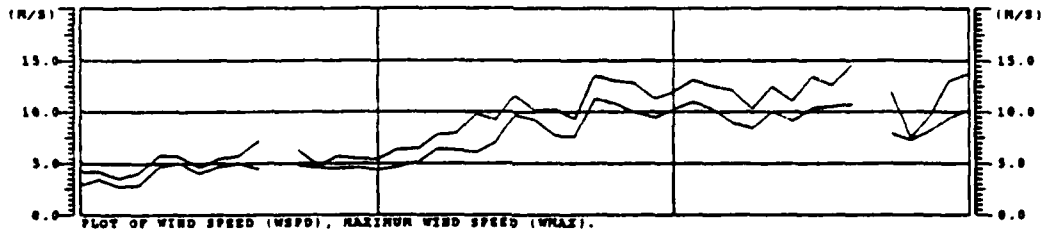
--- STATION 108 OF PROJECT TOWER ---



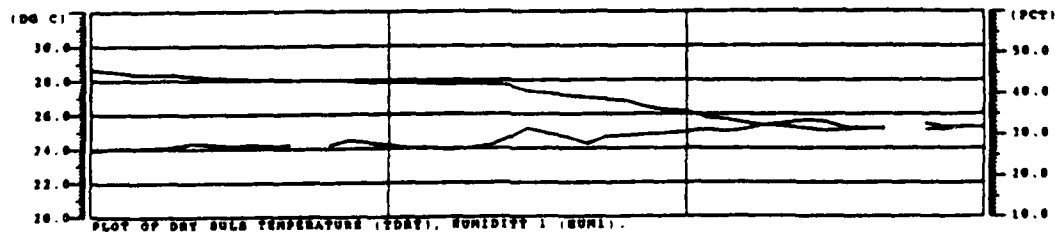
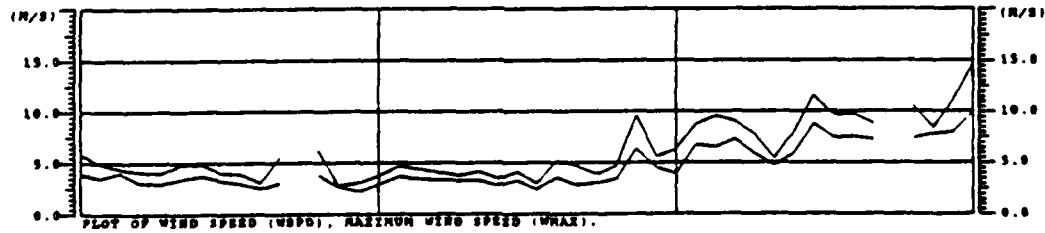
--- STATION 109 OF PROJECT TOWER ---

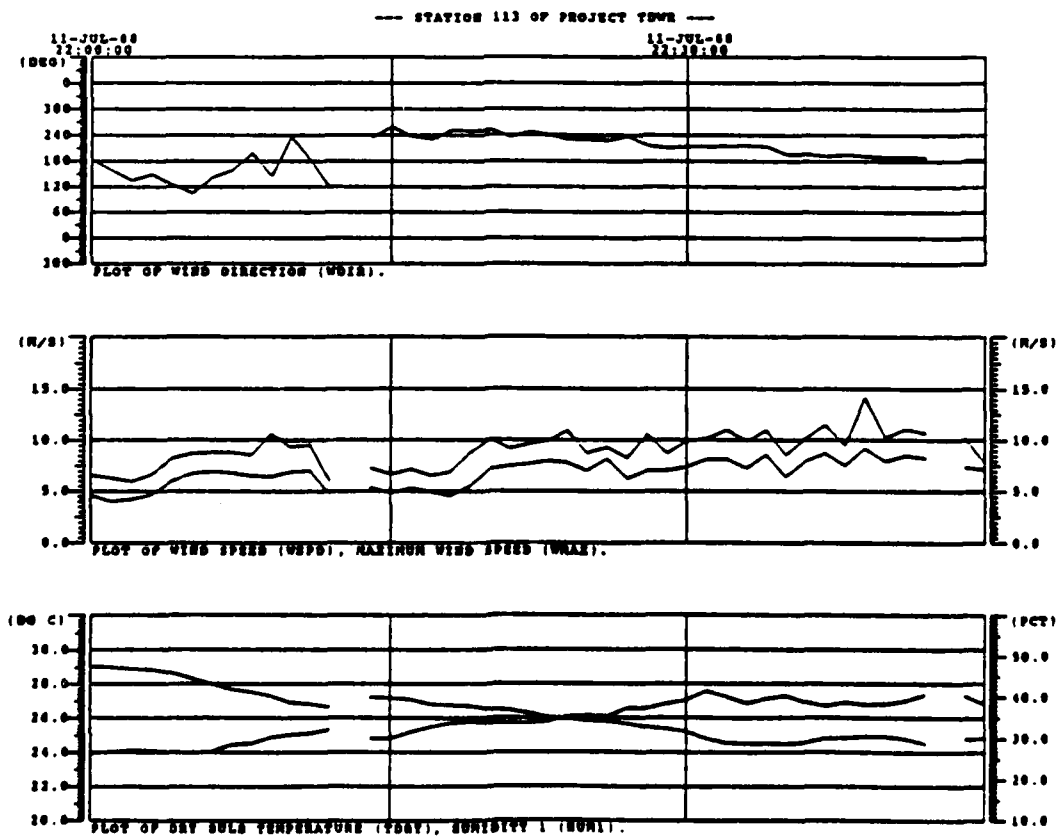
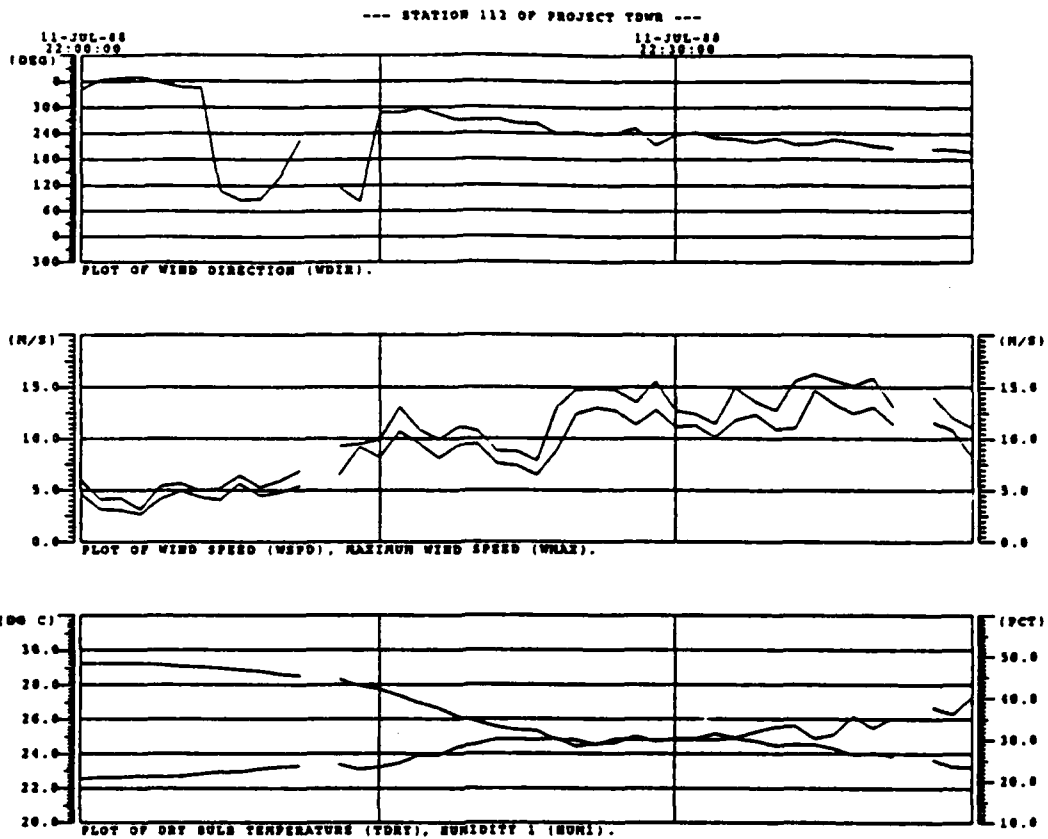


--- STATION 110 OF PROJECT TOWER ---

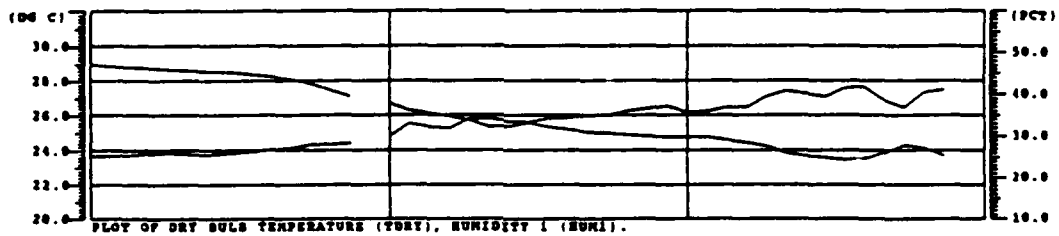
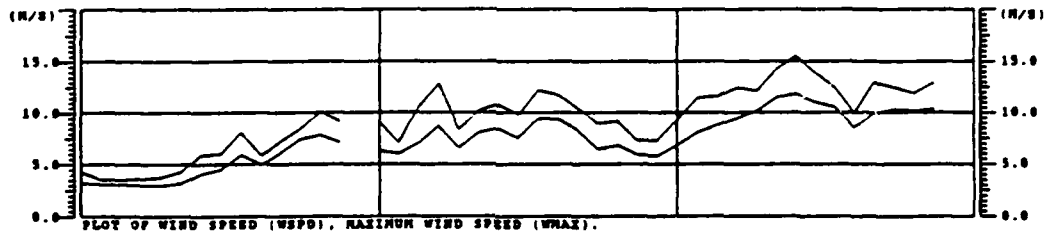
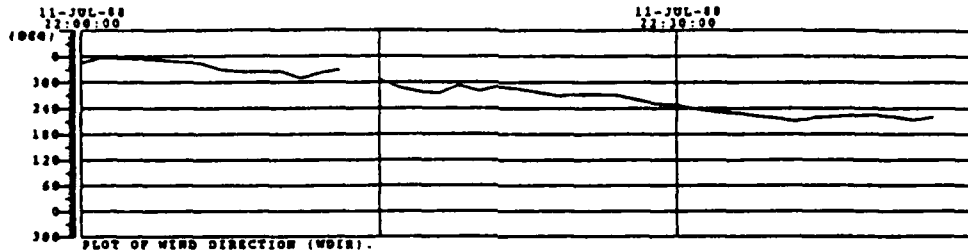


--- STATION 111 OF PROJECT TOWER ---

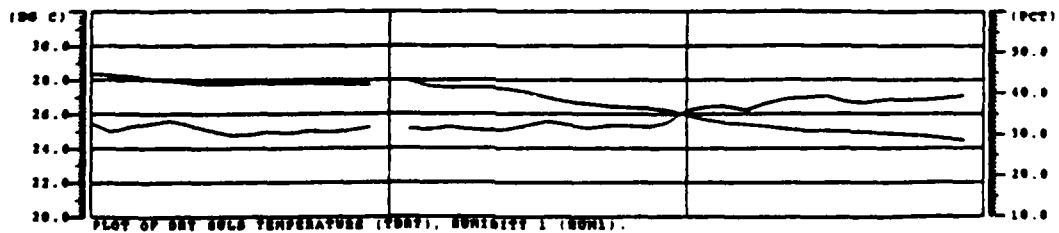
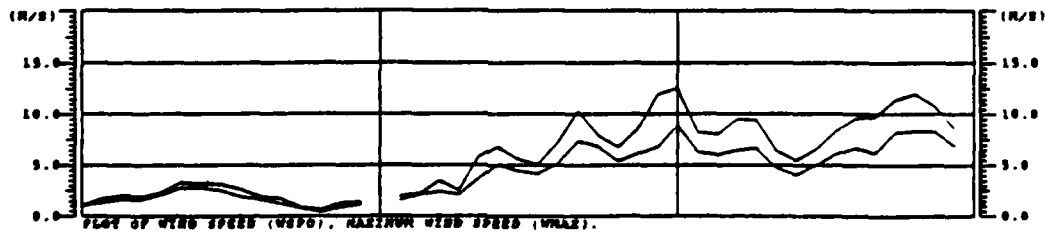




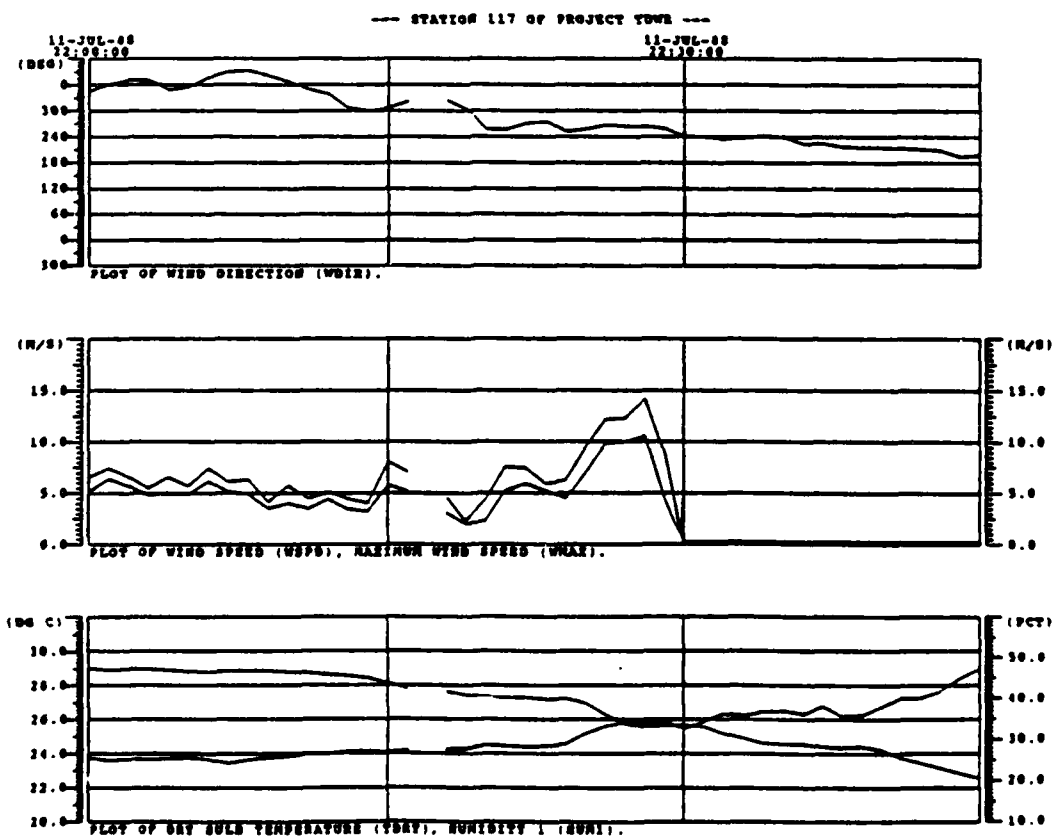
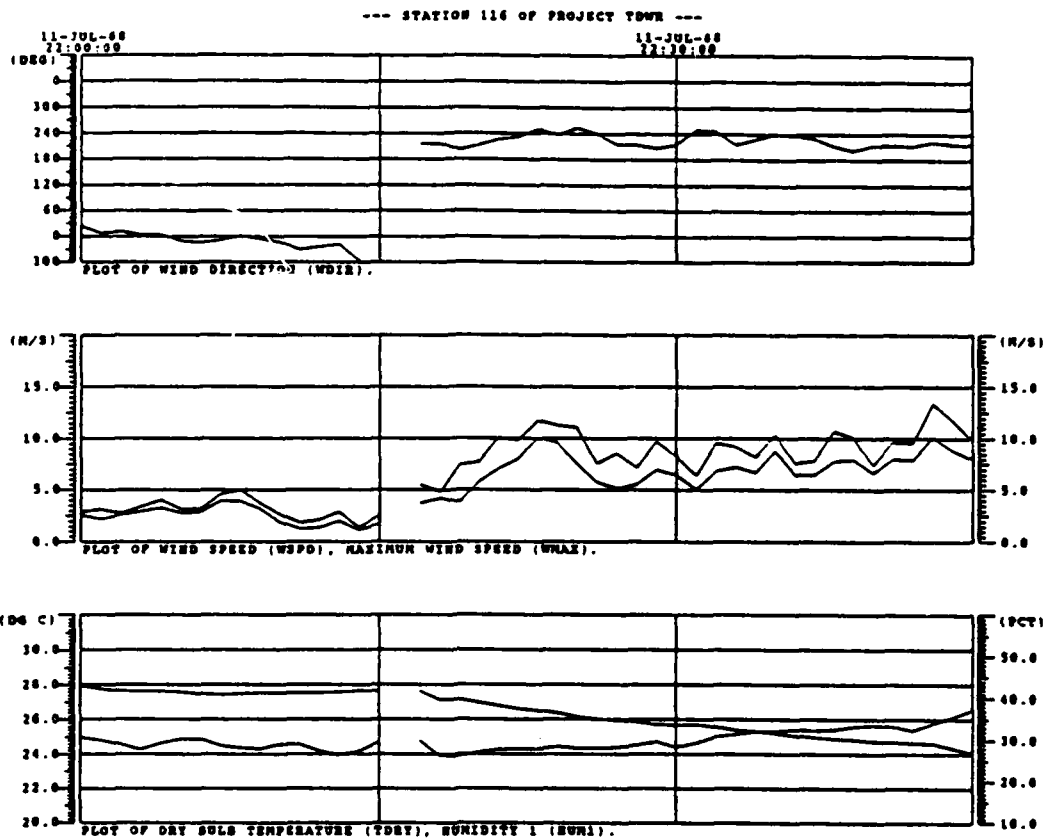
--- STATION 114 OF PROJECT TOWN ---

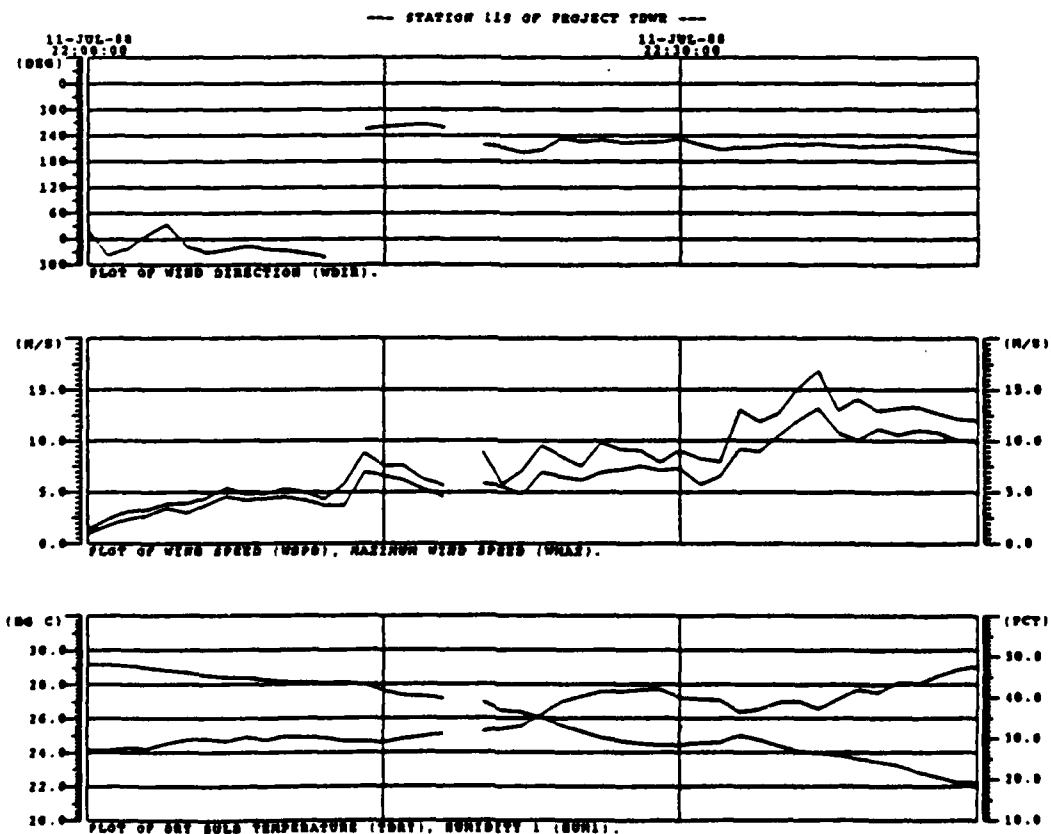
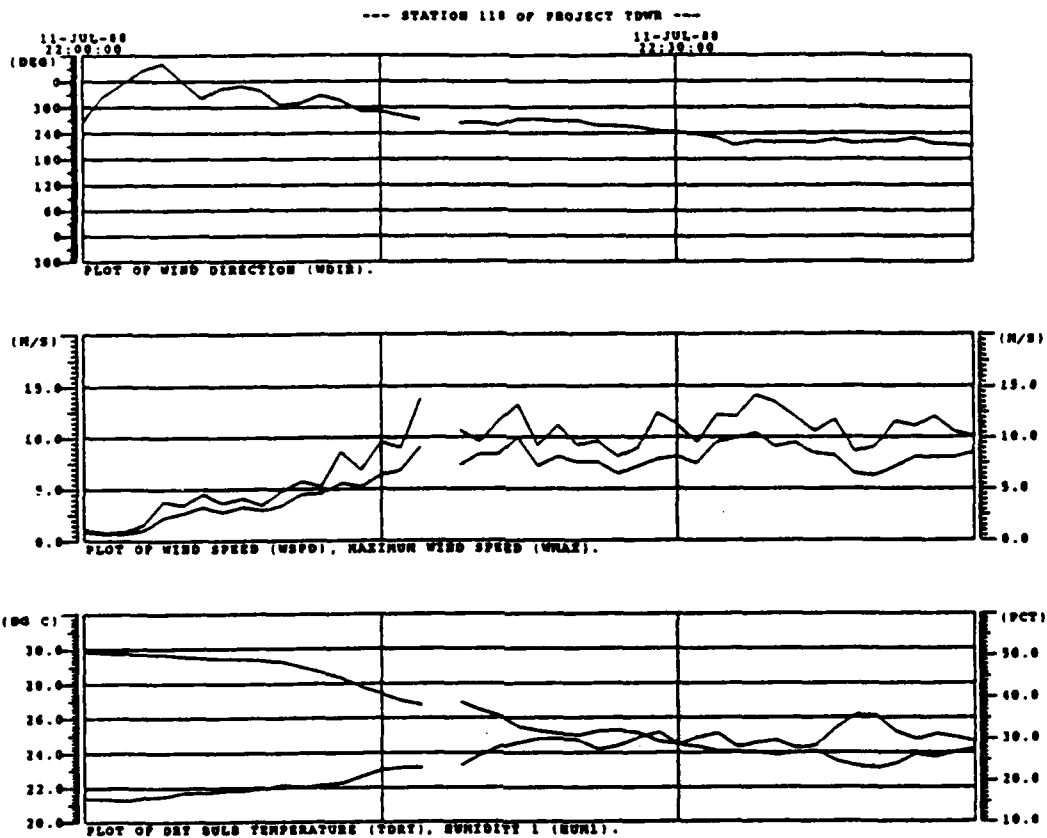


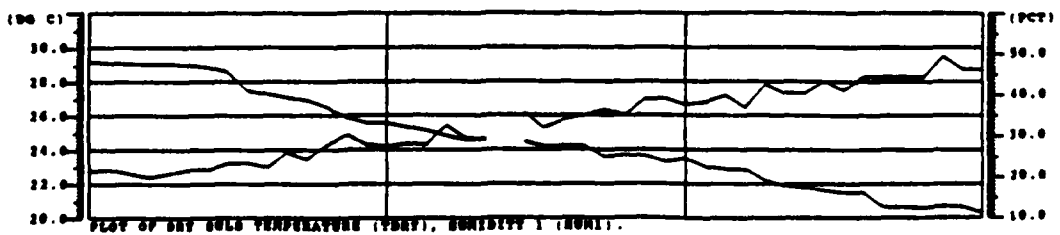
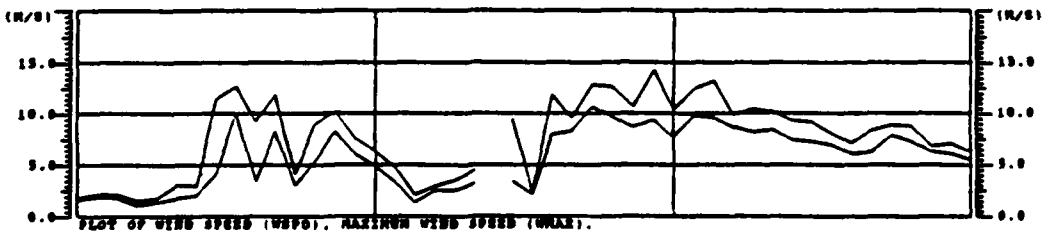
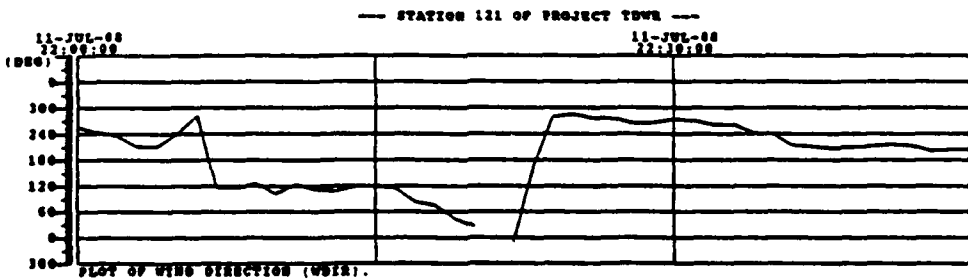
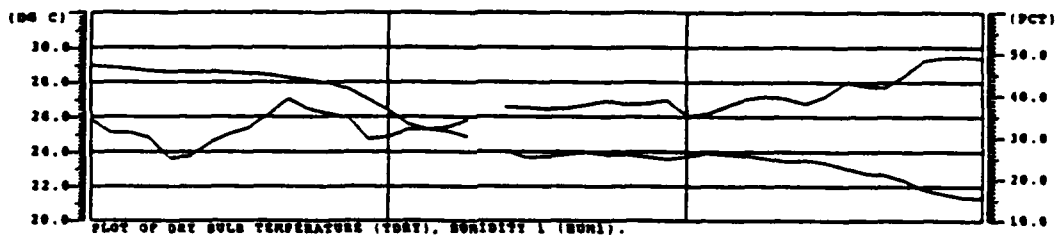
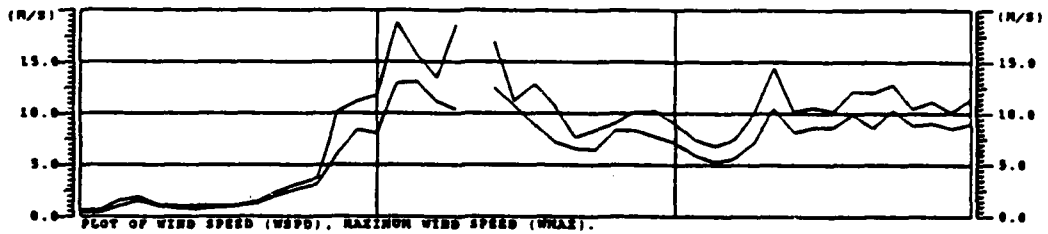
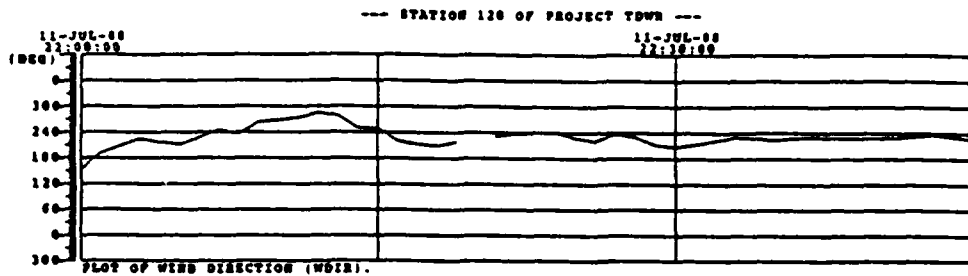
--- STATION 115 OF PROJECT TOWN ---

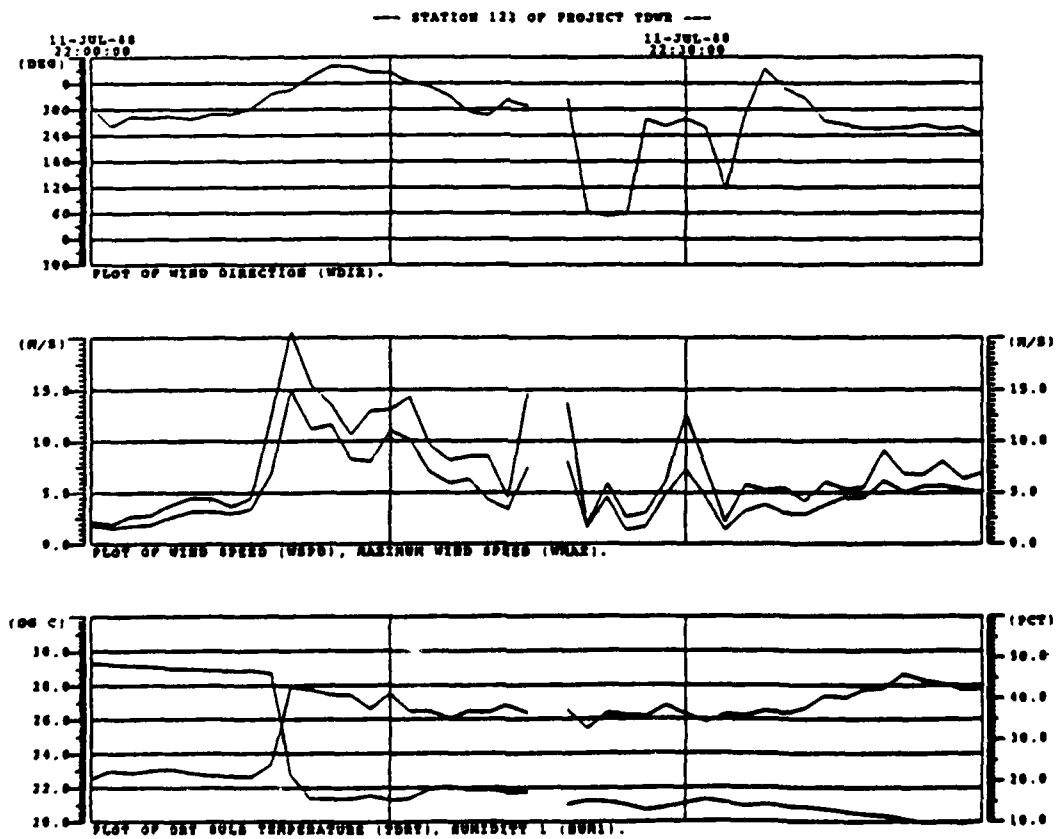
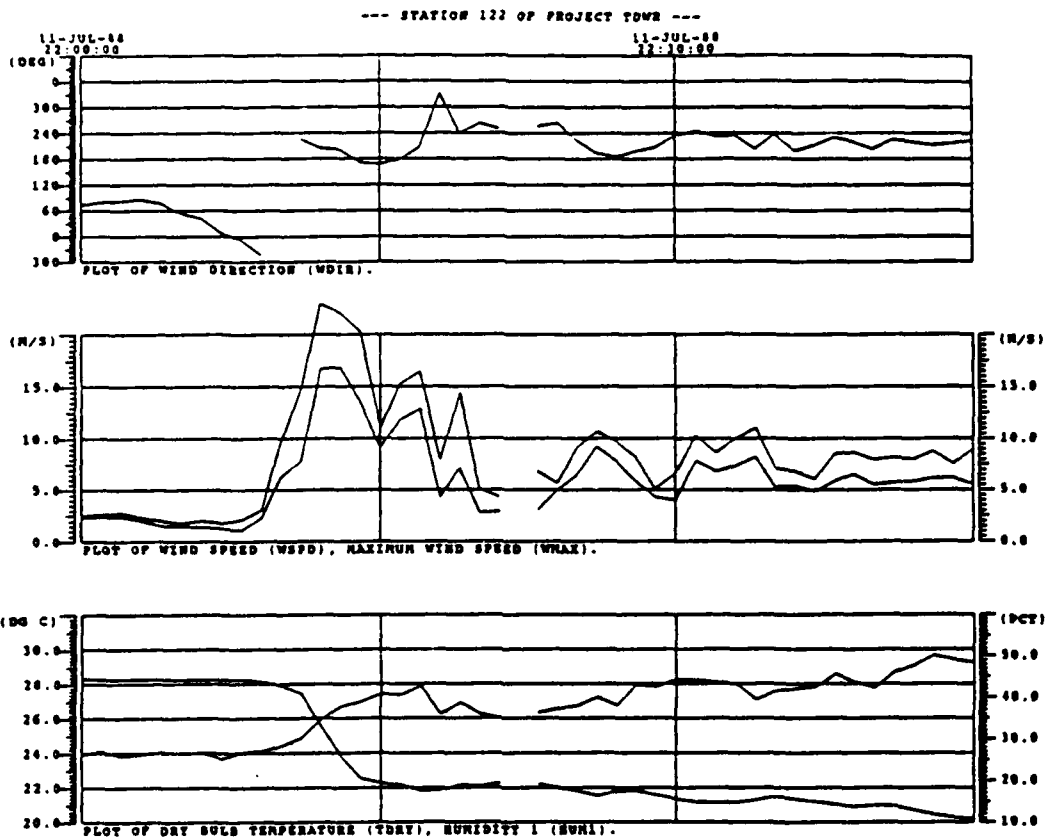










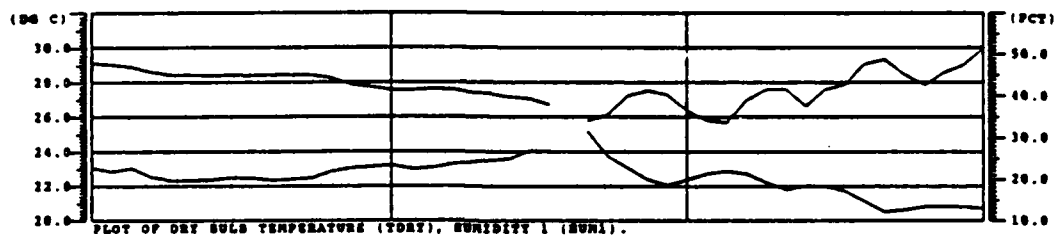
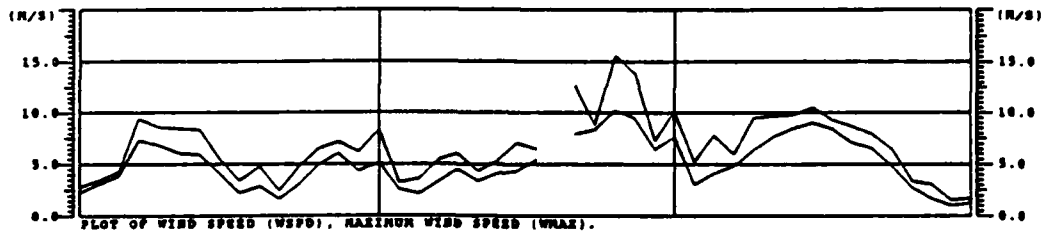


11-JUL-88 22:00:00 11-JUL-88 22:10:00

(DEG)

360  
300  
240  
180  
120  
60  
0  
300

PLOT OF WIND DIRECTION (WDIR).



11-JUL-68 22:00:00

11-JUL-68 22:10:00

11-JUL-68 22:20:00

(DEG)

360

300

240

180

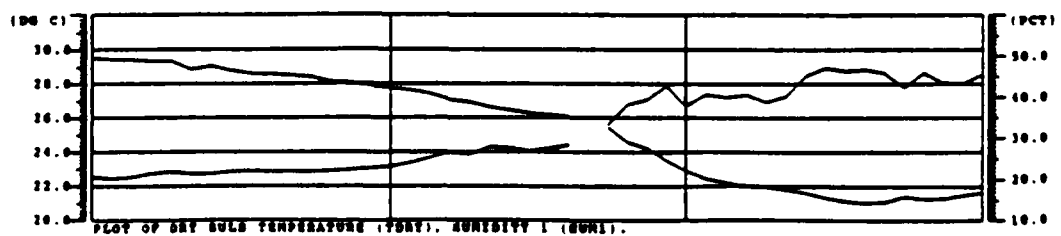
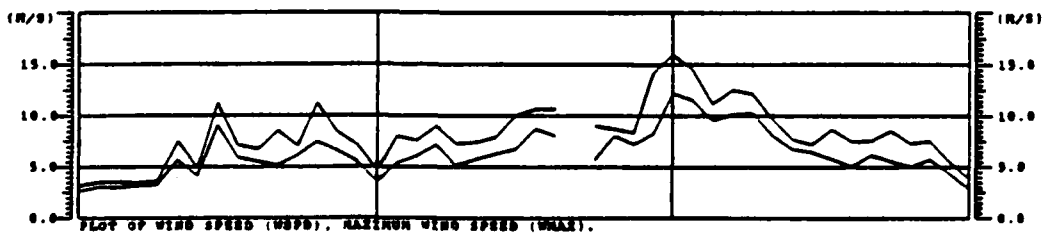
120

60

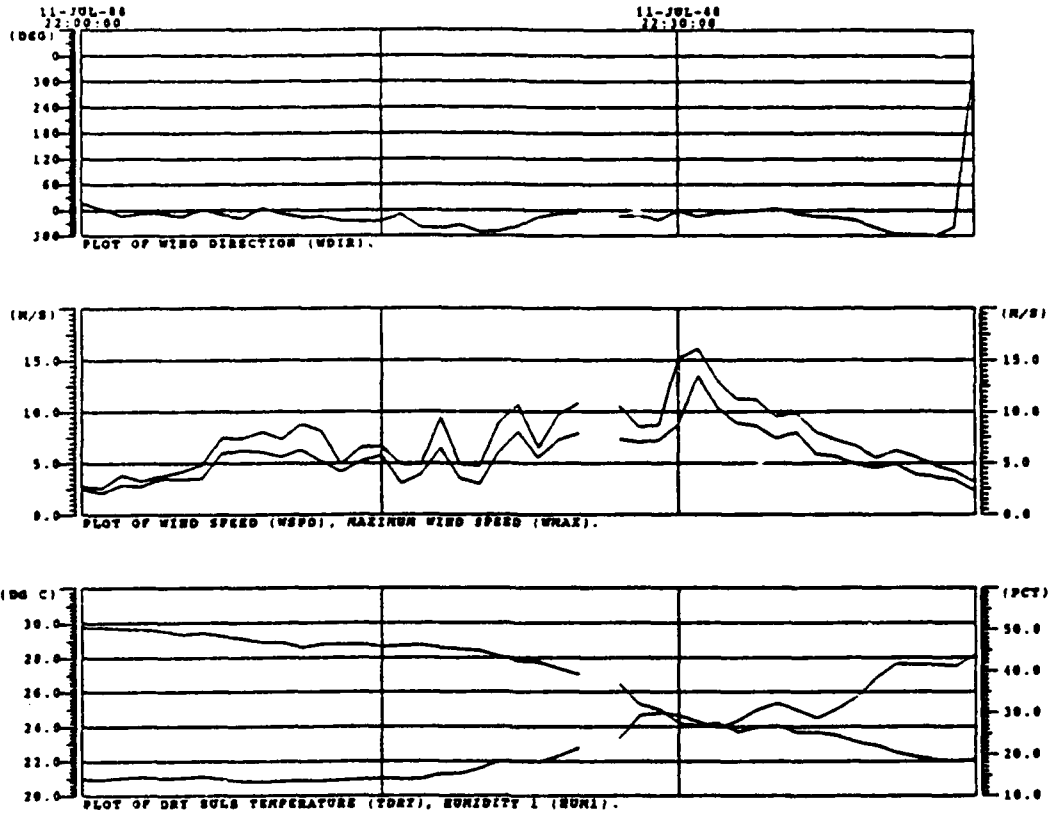
0

360

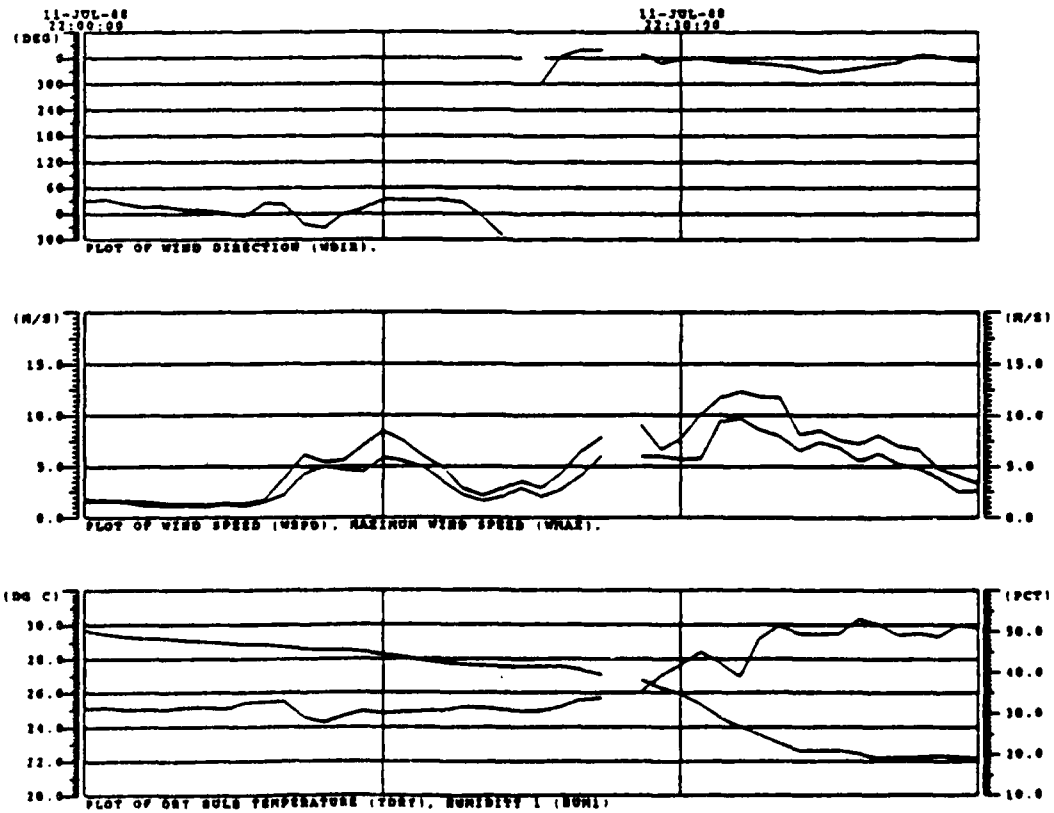
PLOT OF WIND DIRECTION (WDIR).

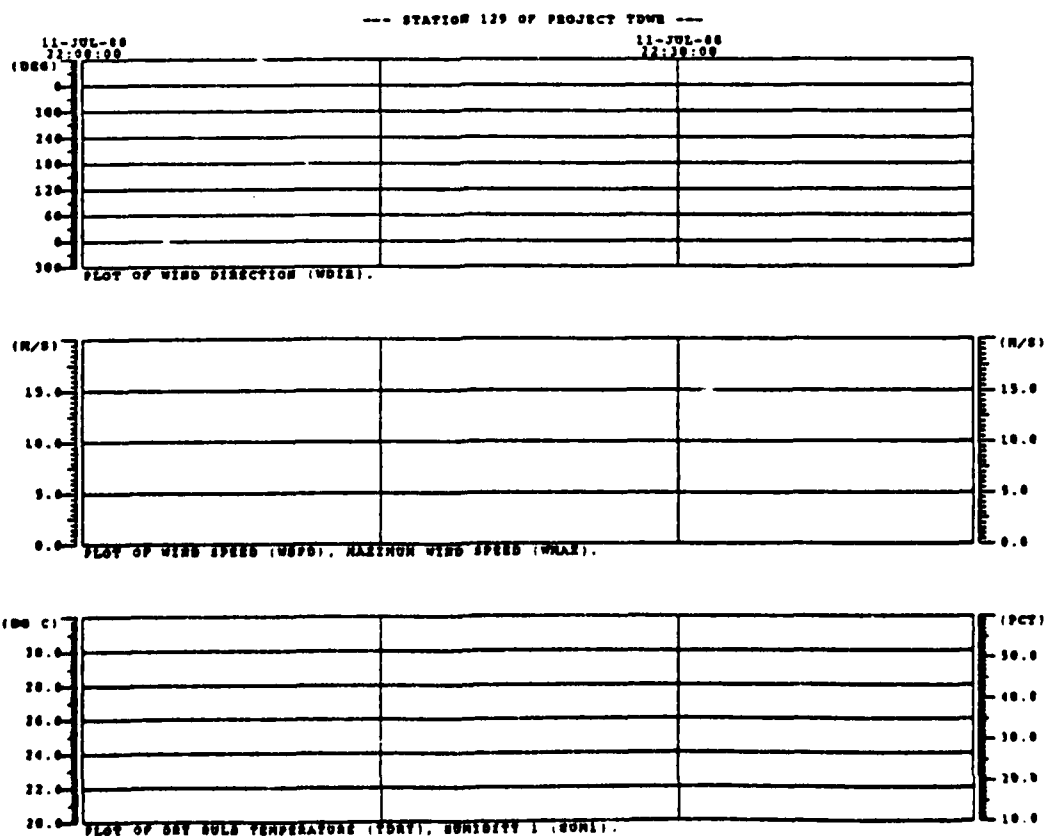
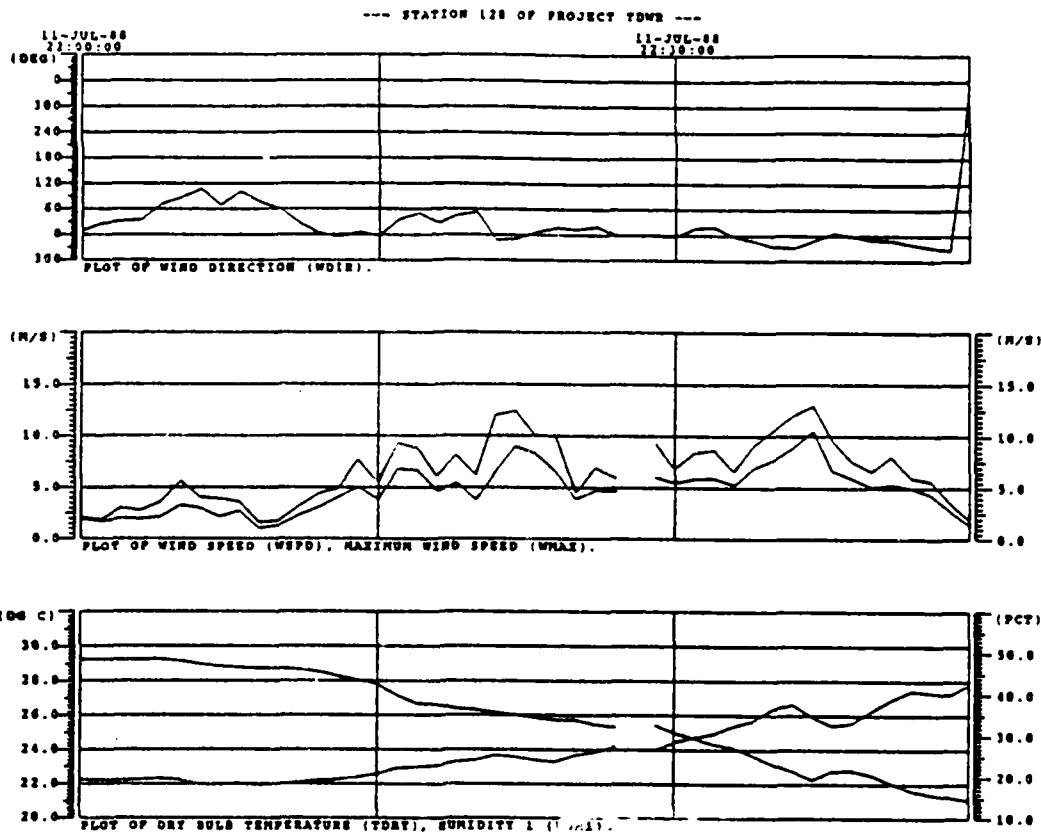


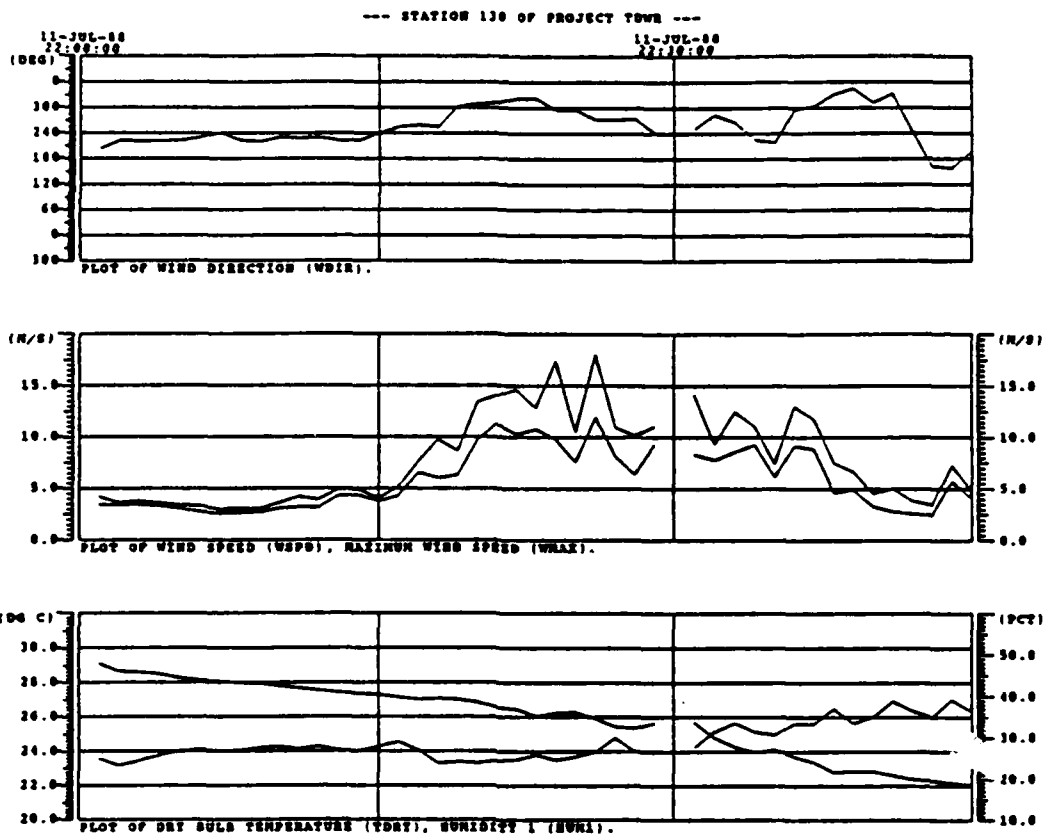
--- STATION 126 OF PROJECT TOWN ---



--- STATION 127 OF PROJECT TOWN ---





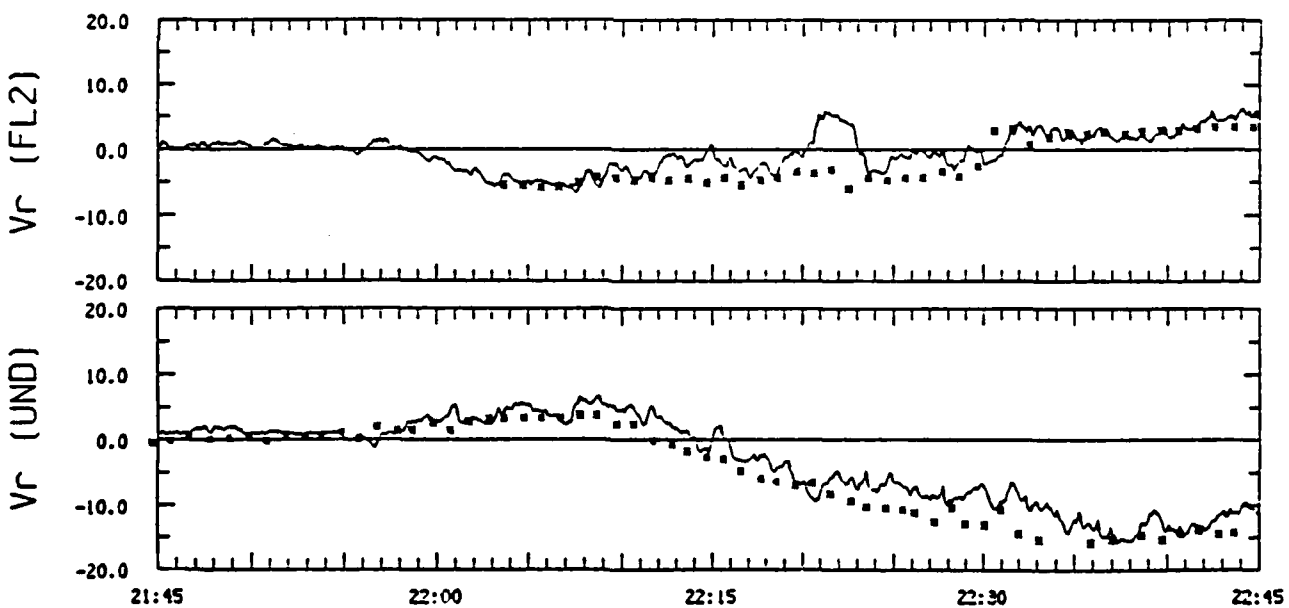
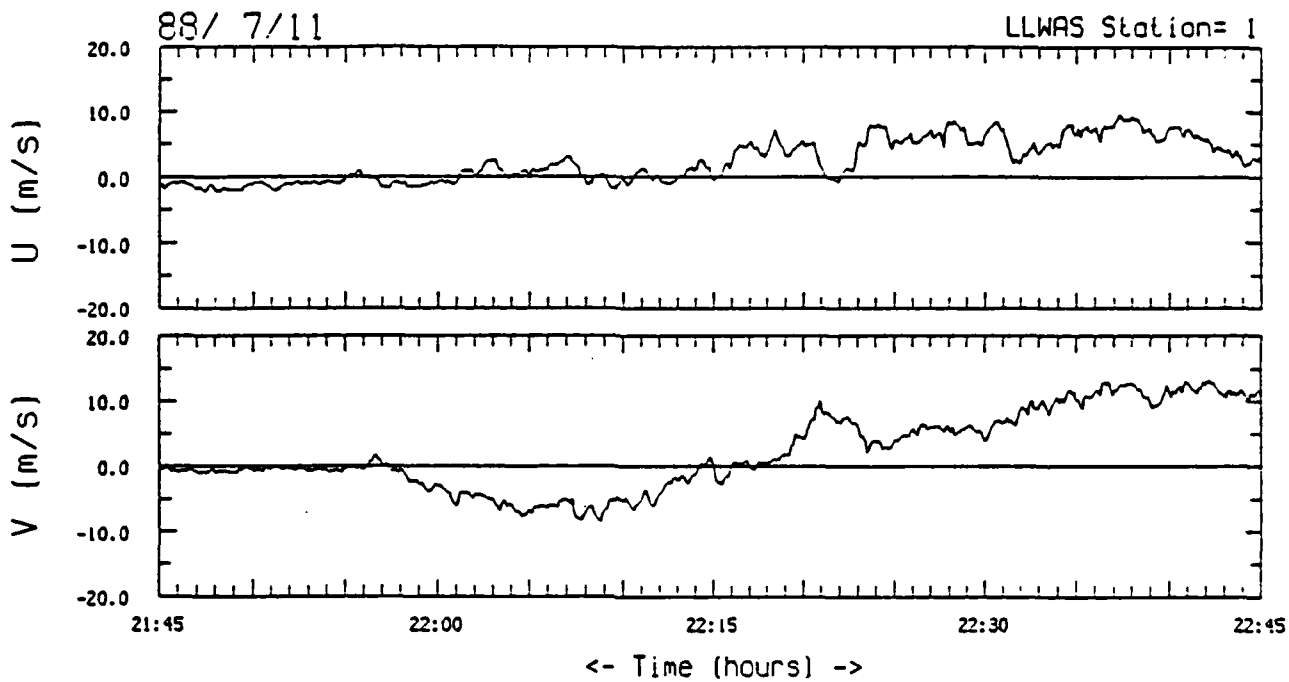


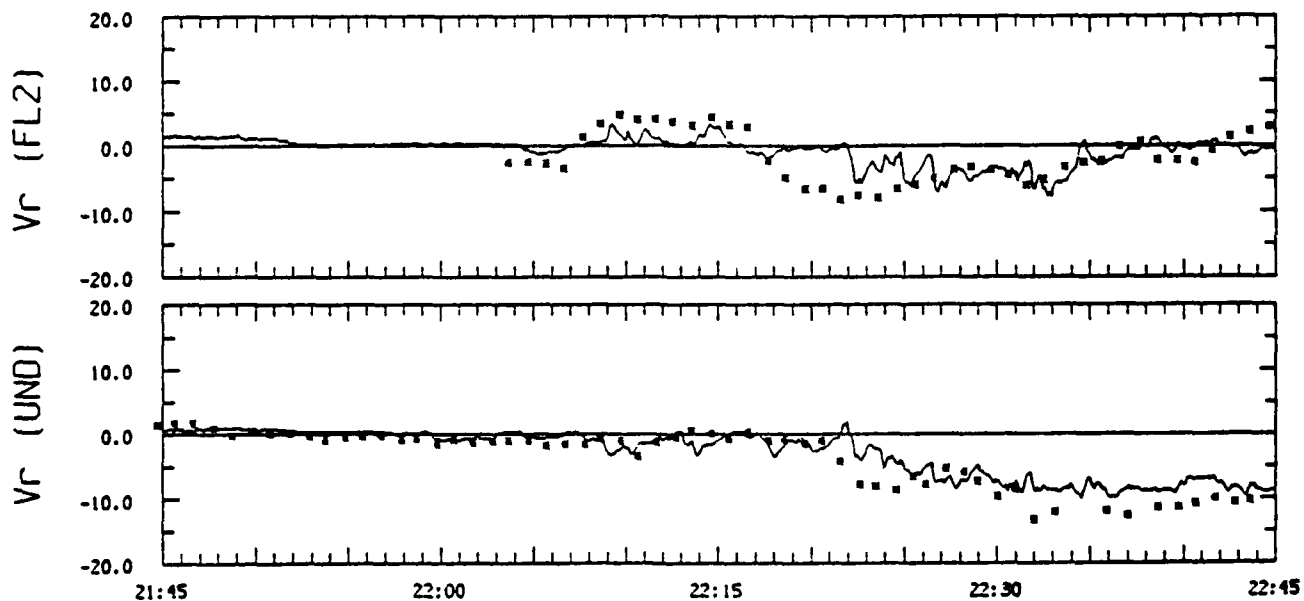
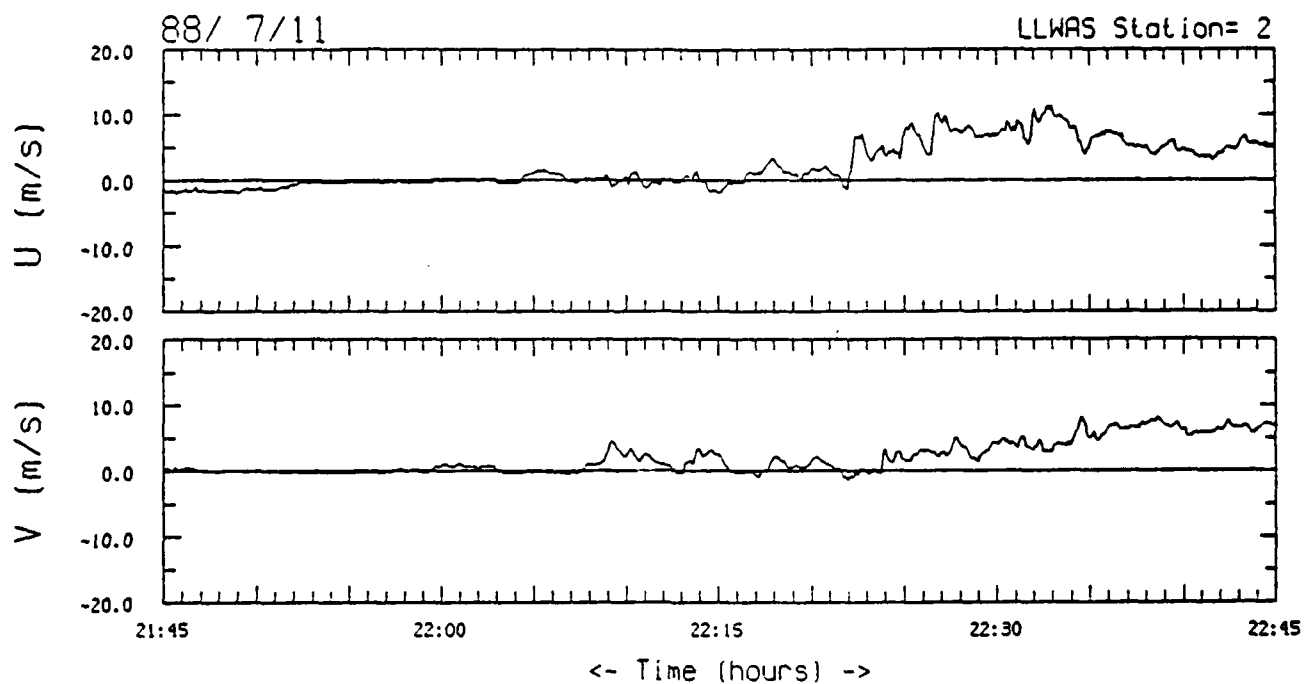


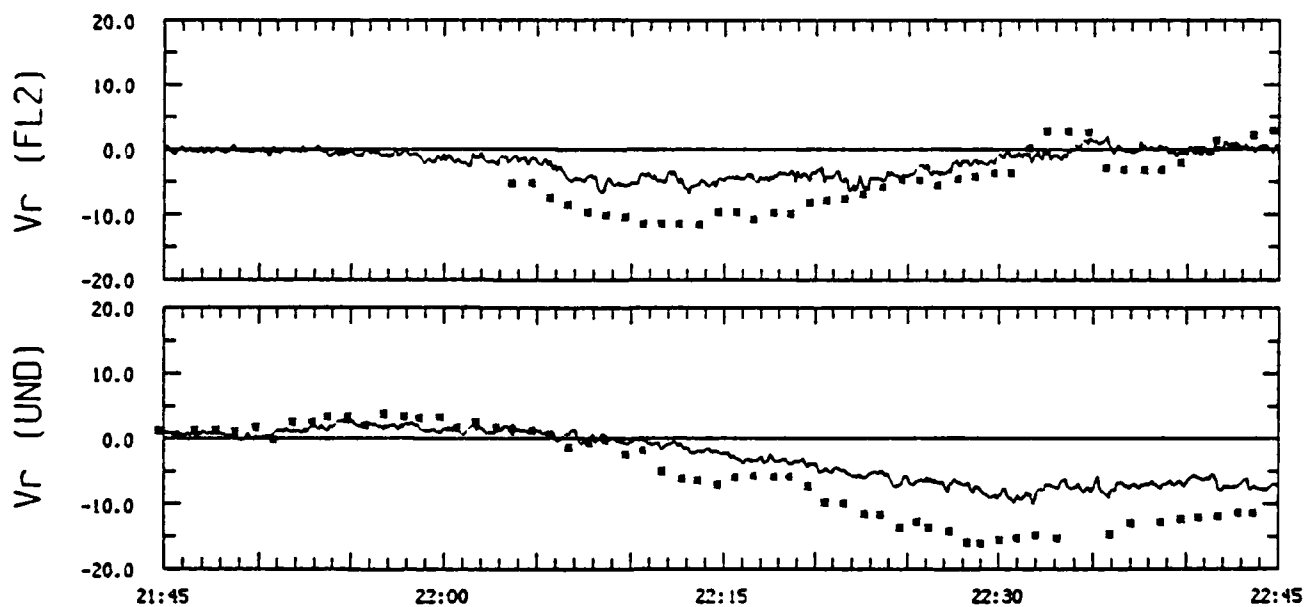
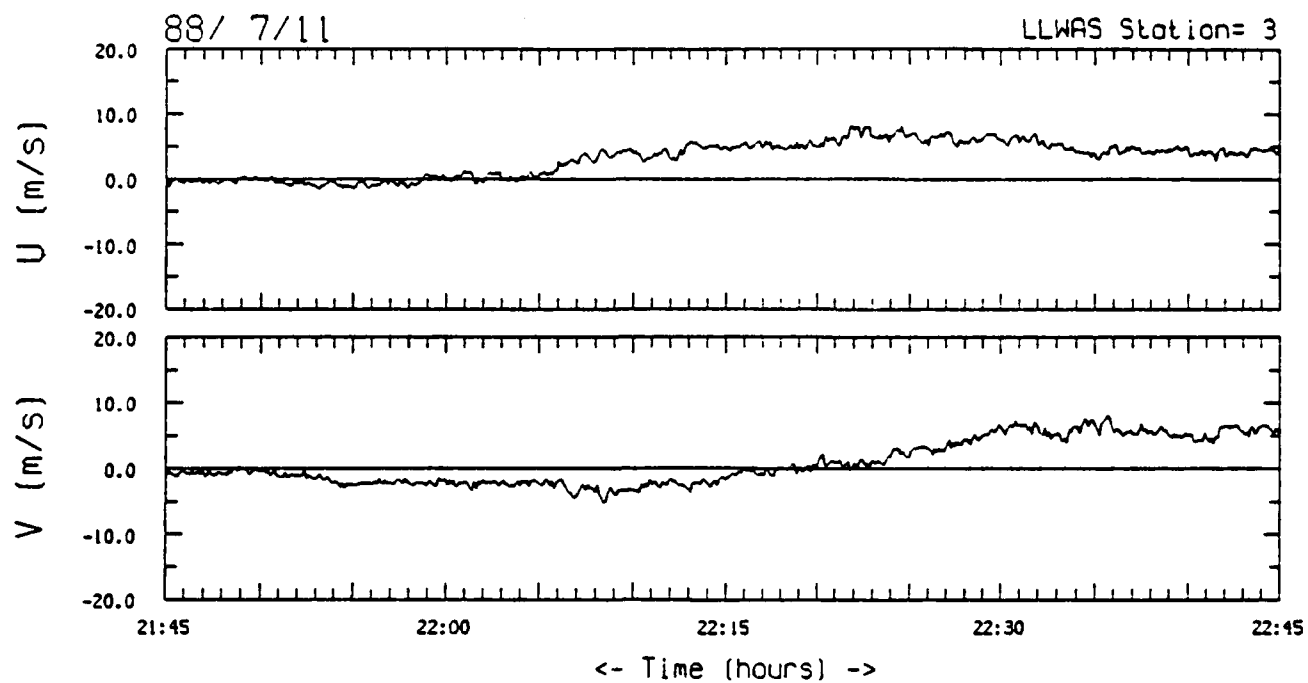
### **Appendix G: LLWAS/Doppler Radar Winds**

These plots show wind speeds from the twelve LLWAS stations and from the FL2 and UND radars. U (easterly) and V (northerly) components are shown for the 6 sec LLWAS data in the upper panels. The lower panels show the wind components in the radial direction from each of the two project radars, with the 1 min radar data, from the gate nearest each LLWAS station, superimposed as asterisks.

LLWAS station locations are shown in Appendix E..

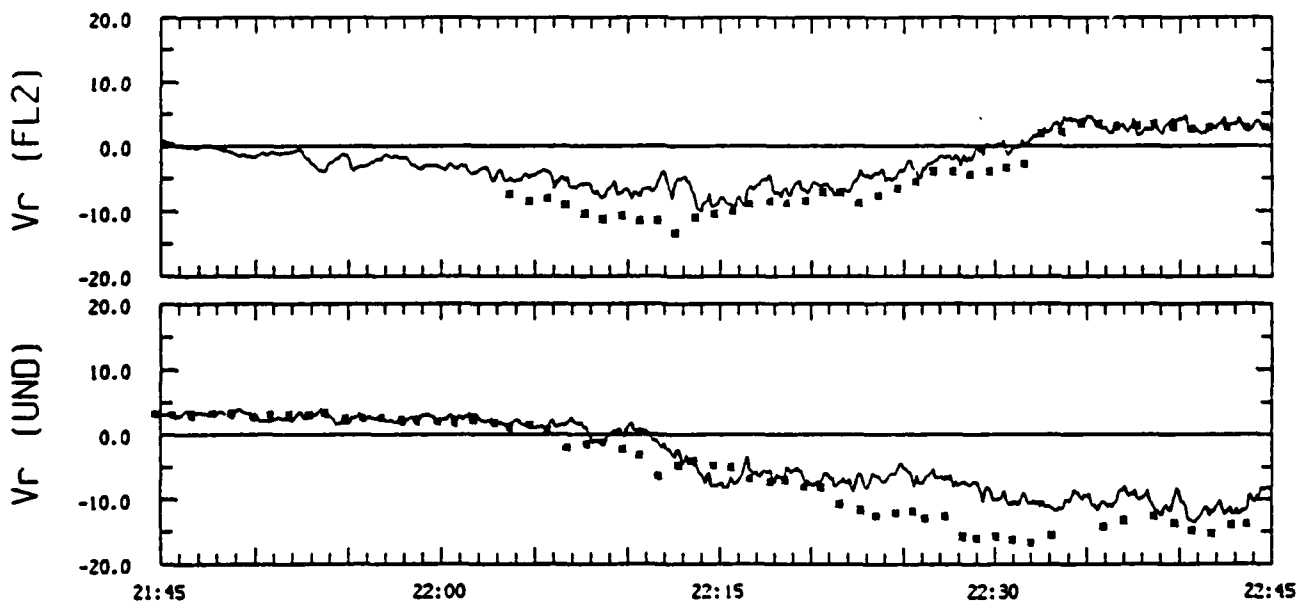
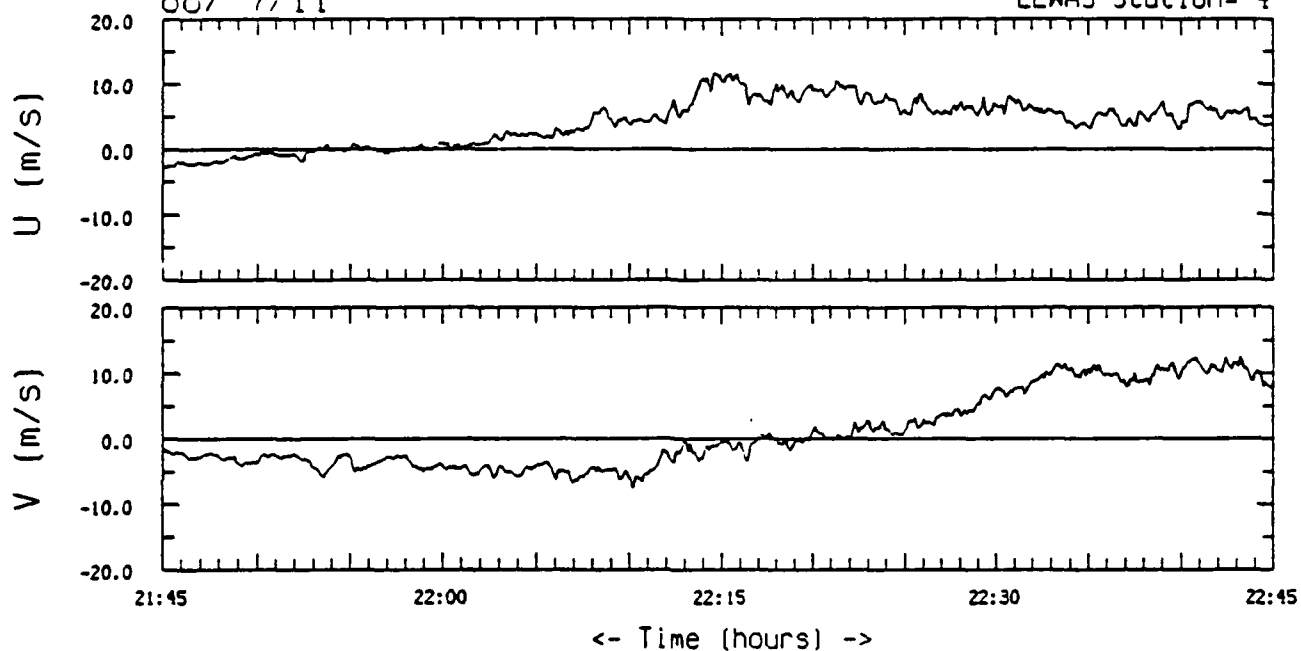


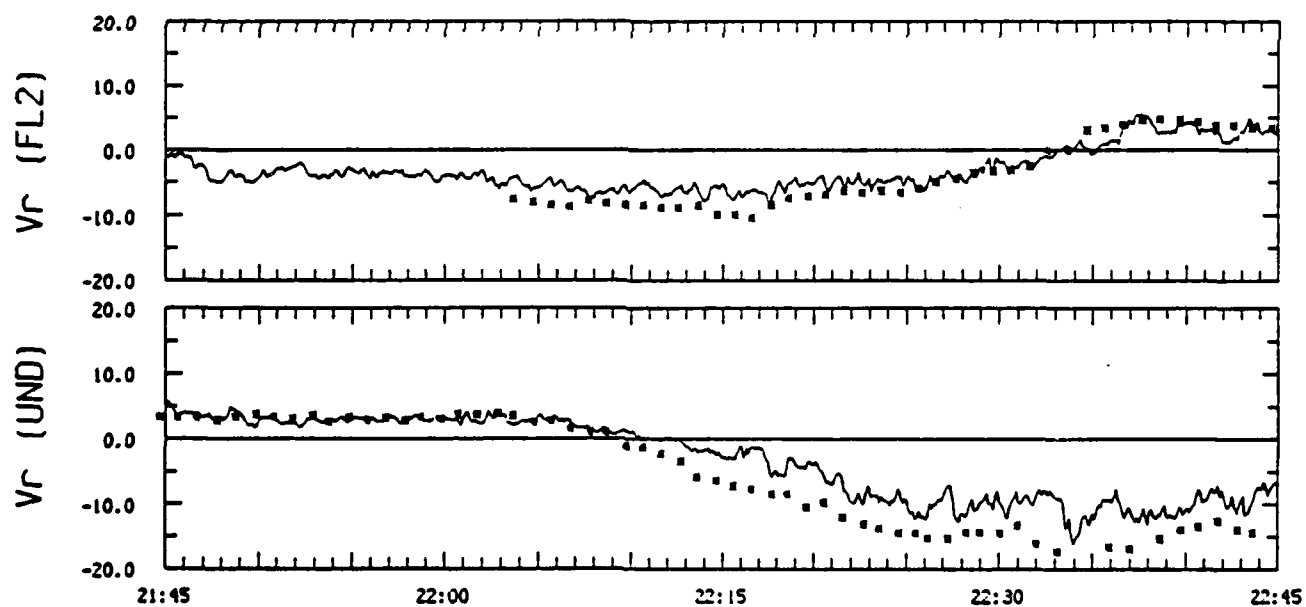
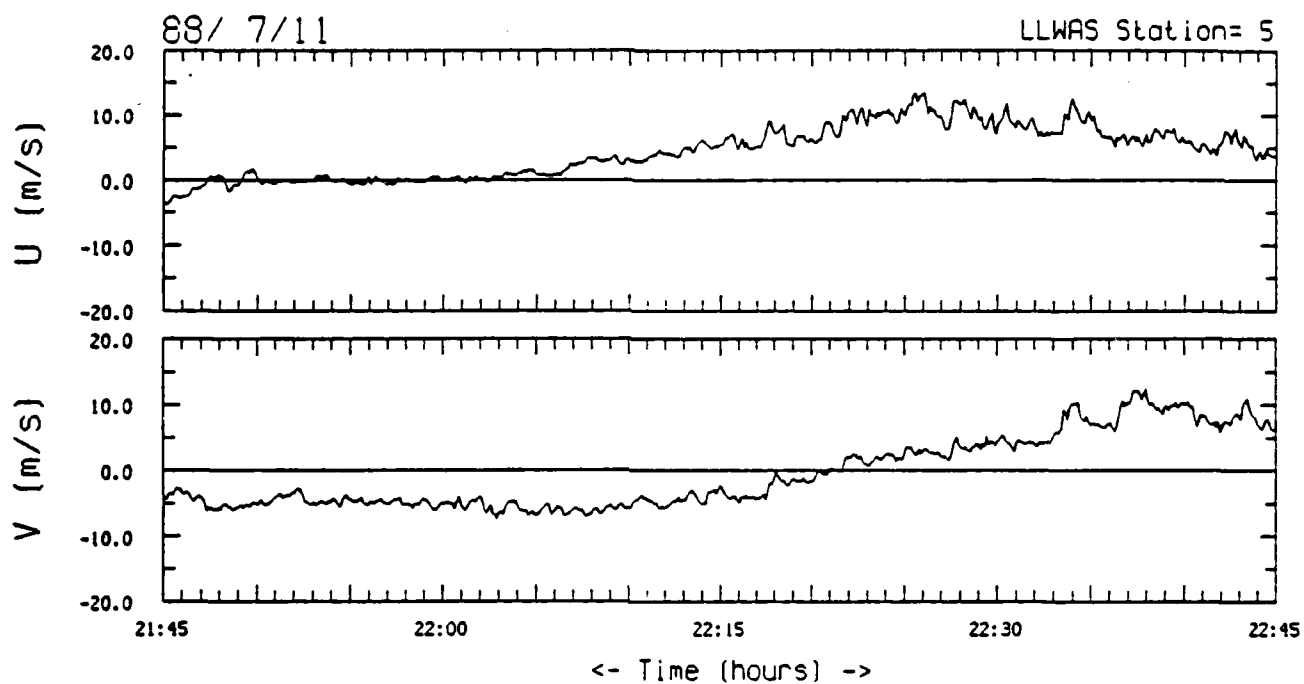




68/ 7/11

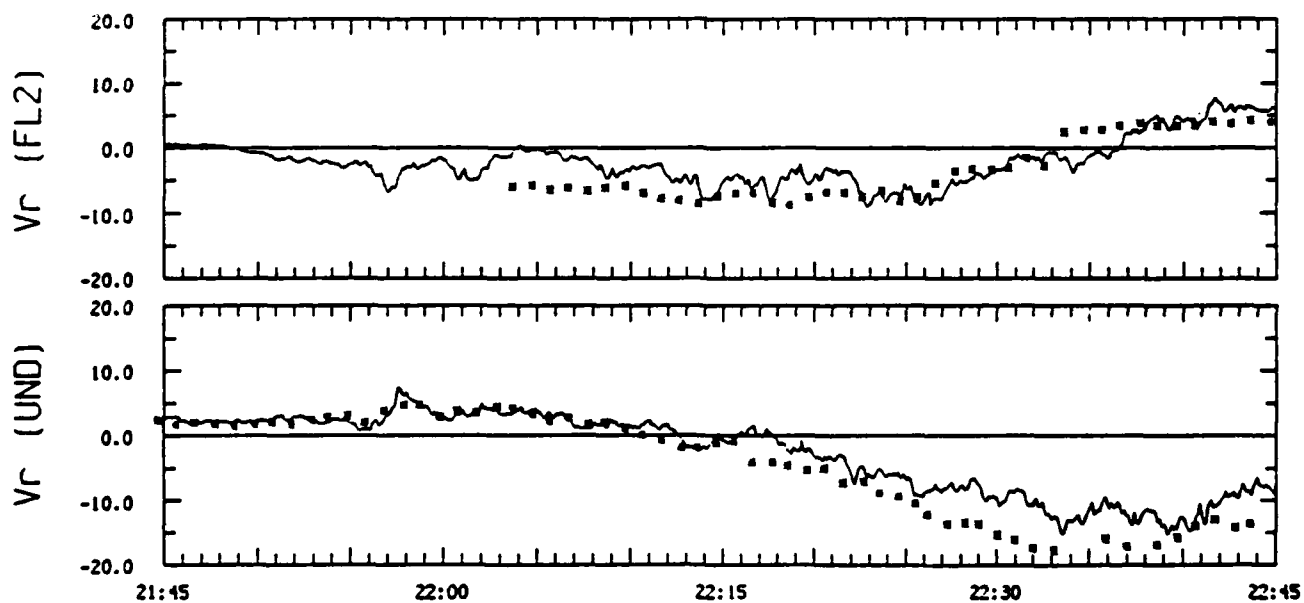
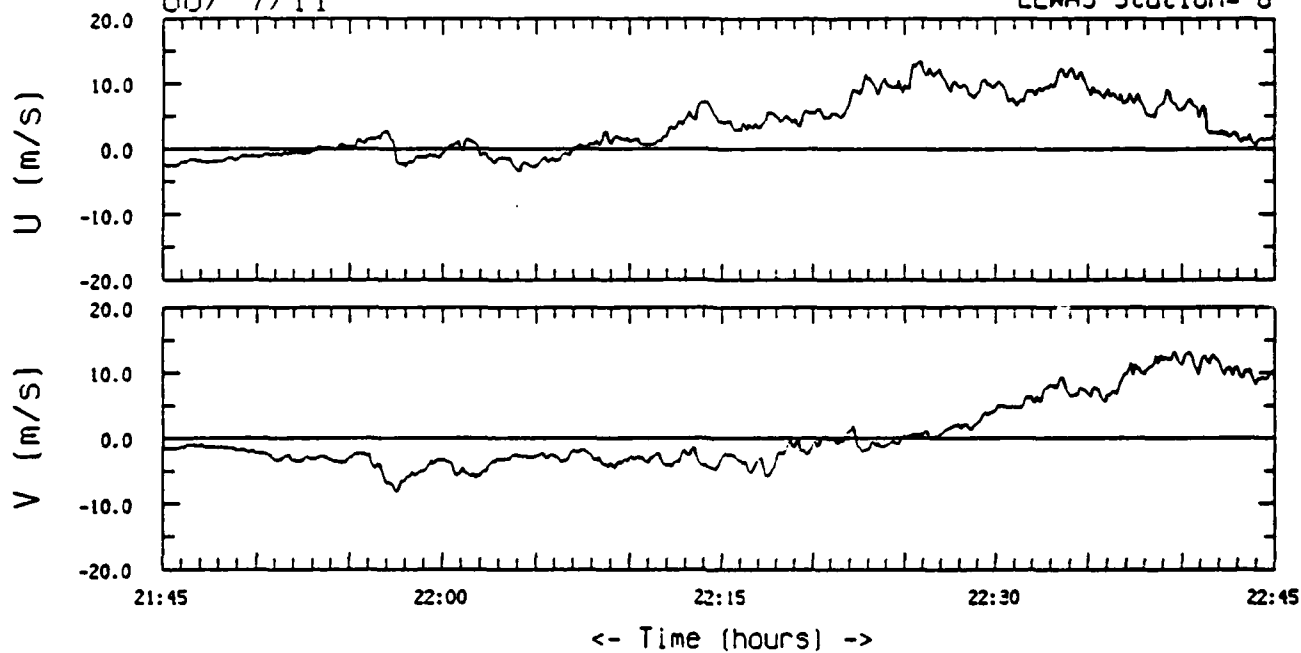
LLWAS Station= 4

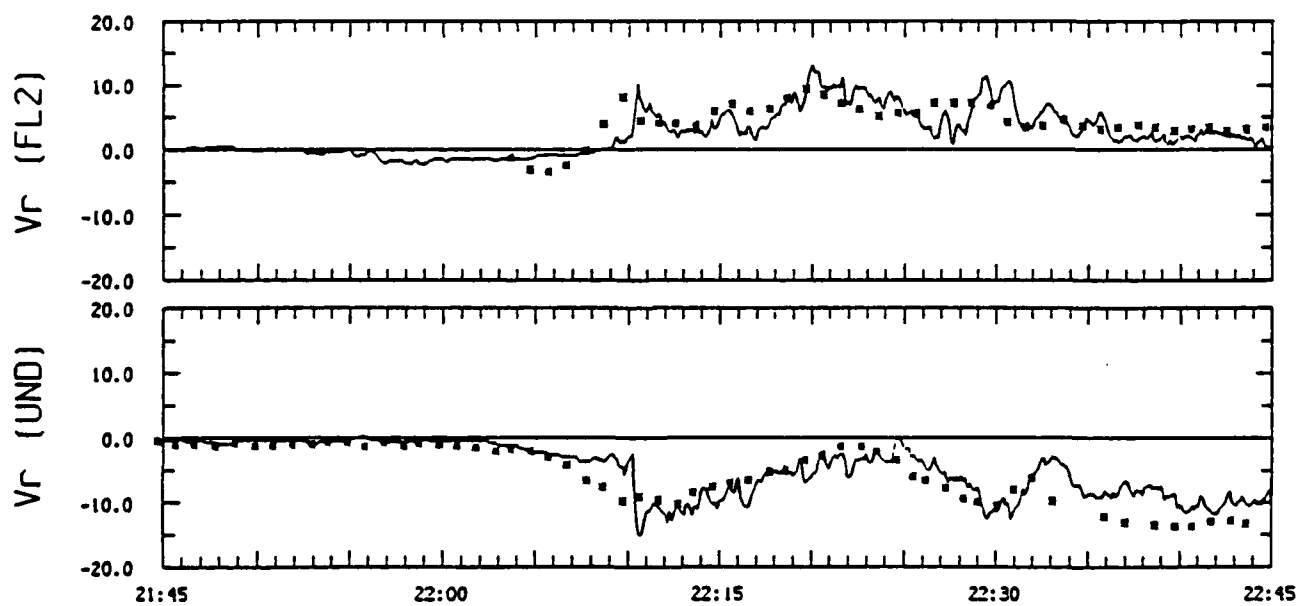
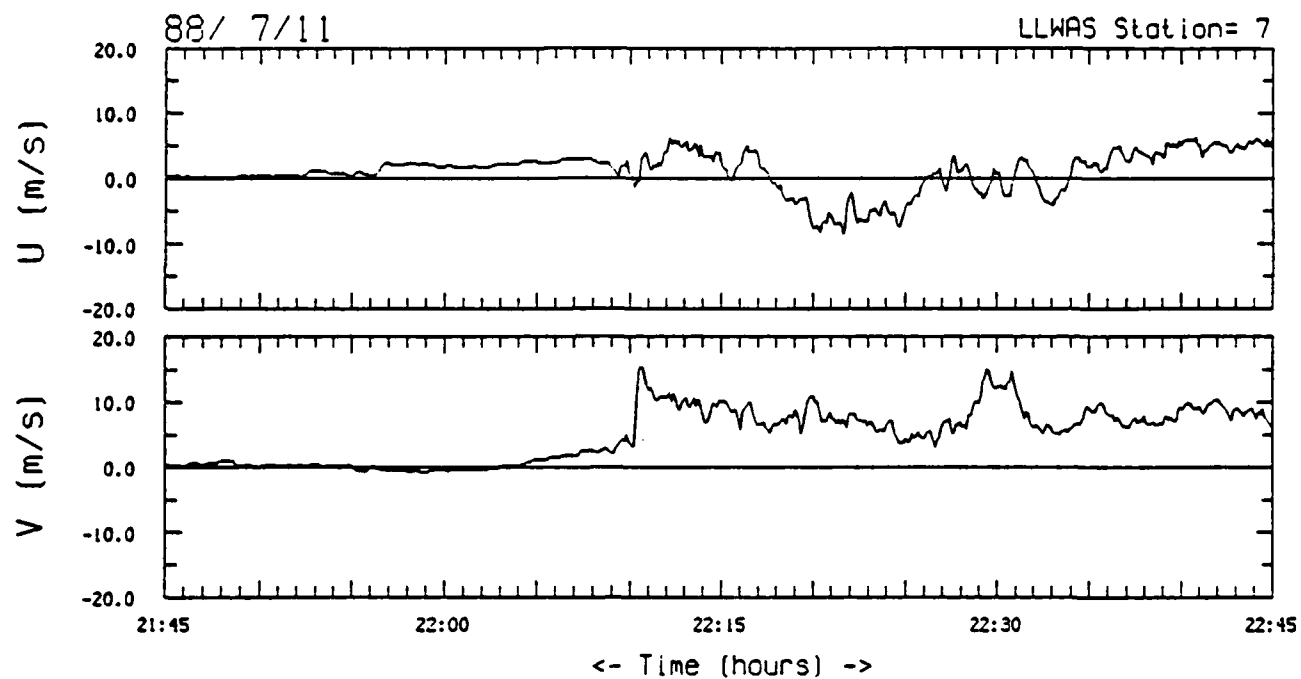




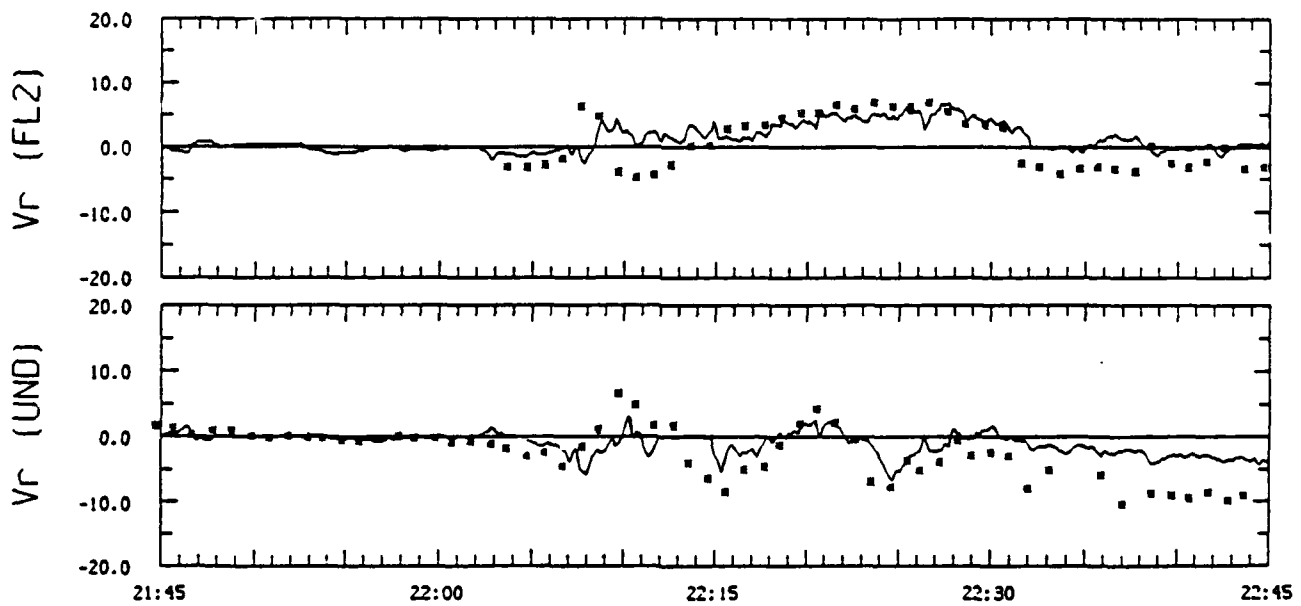
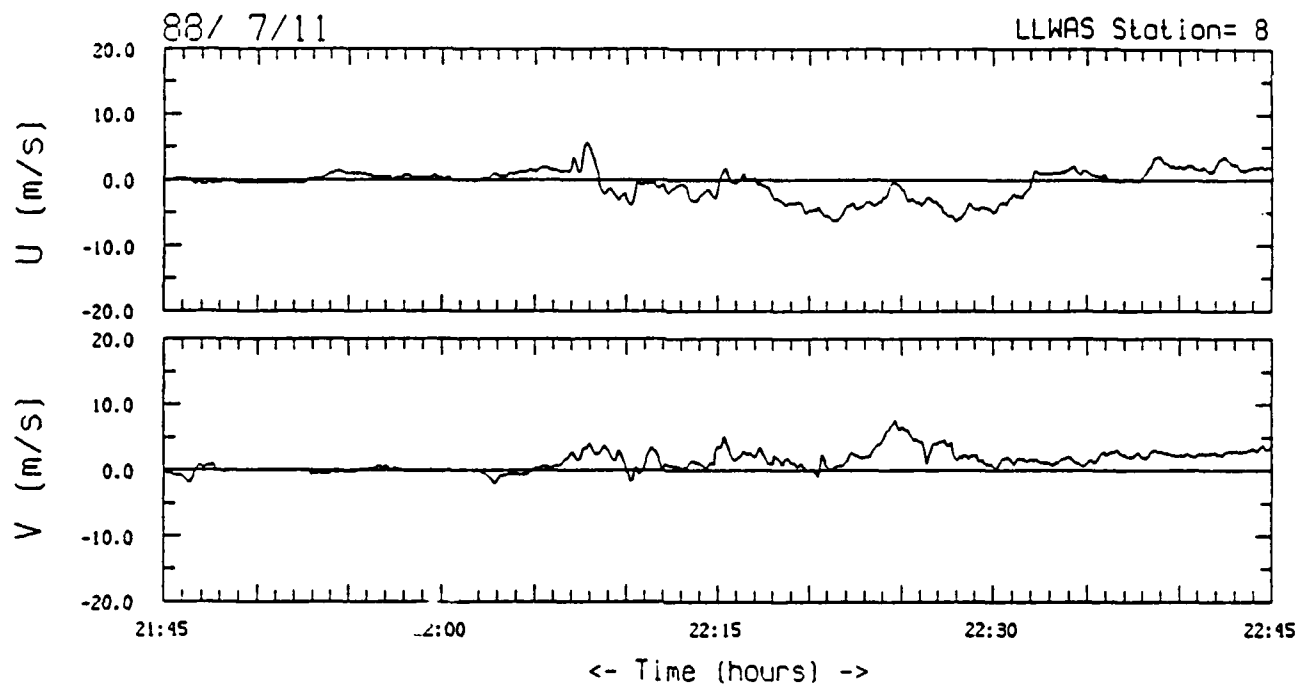
88/ 7/11

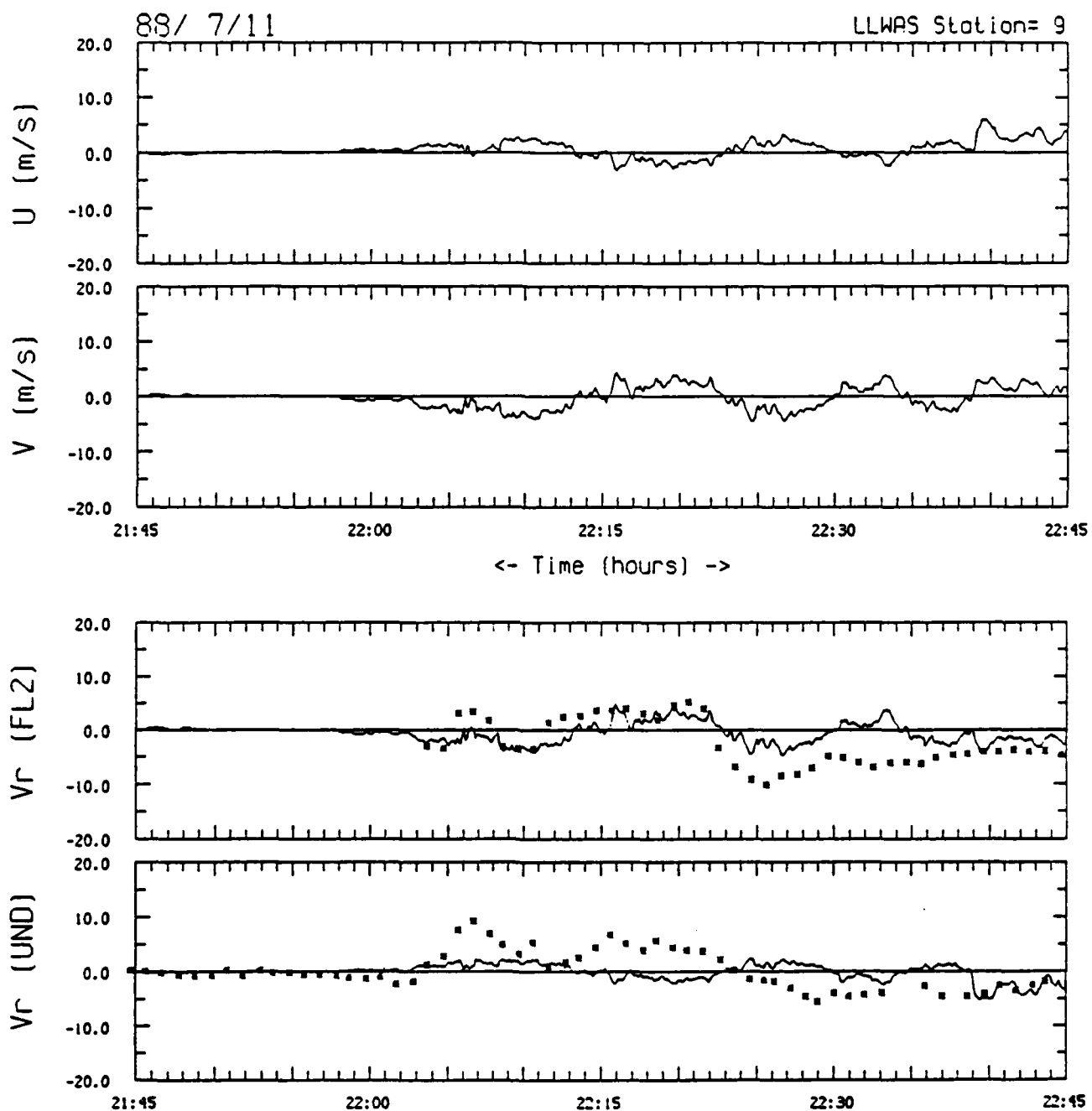
LLWAS Station= 6

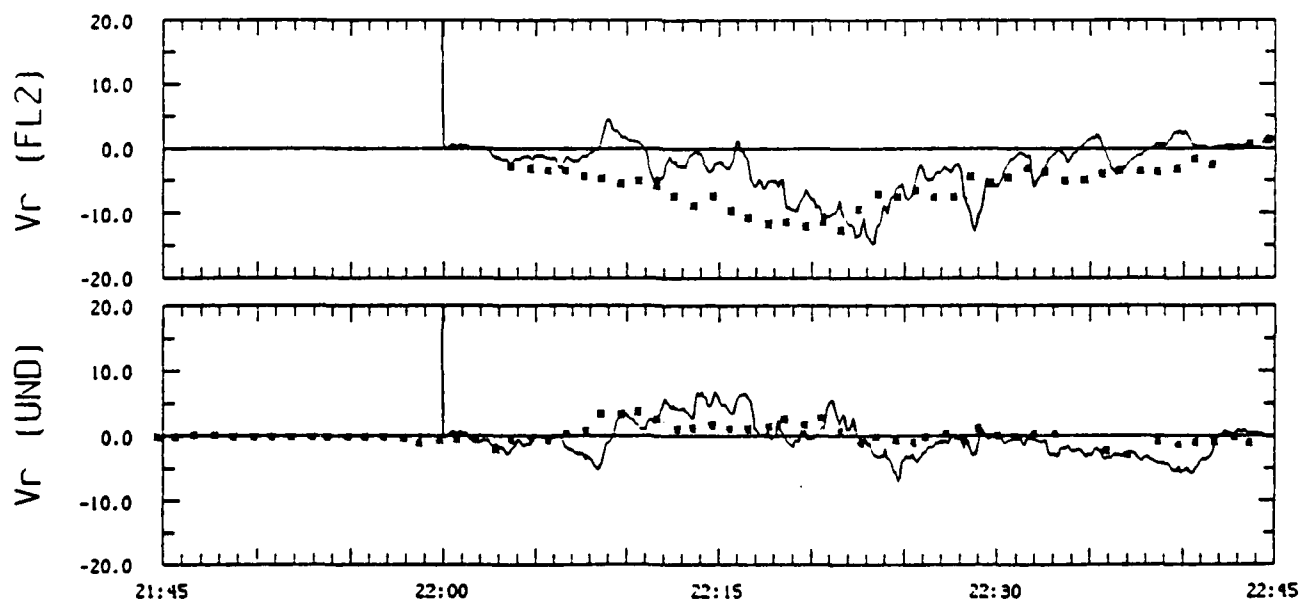
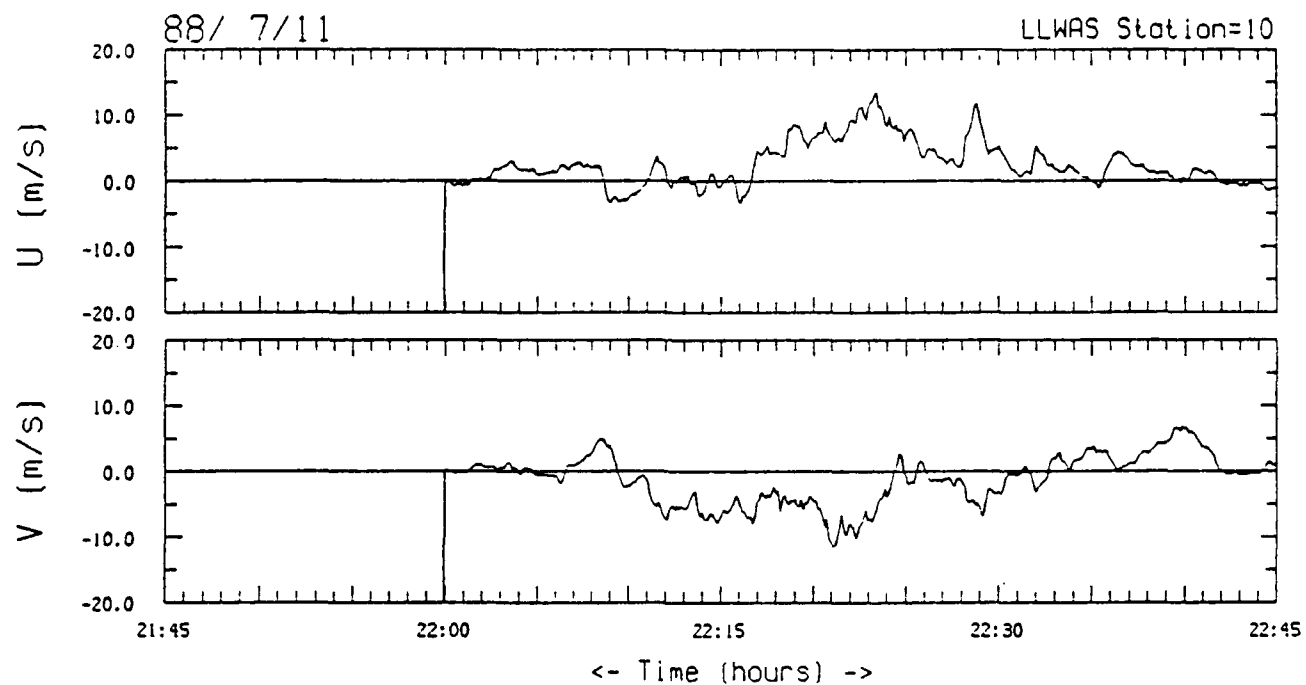


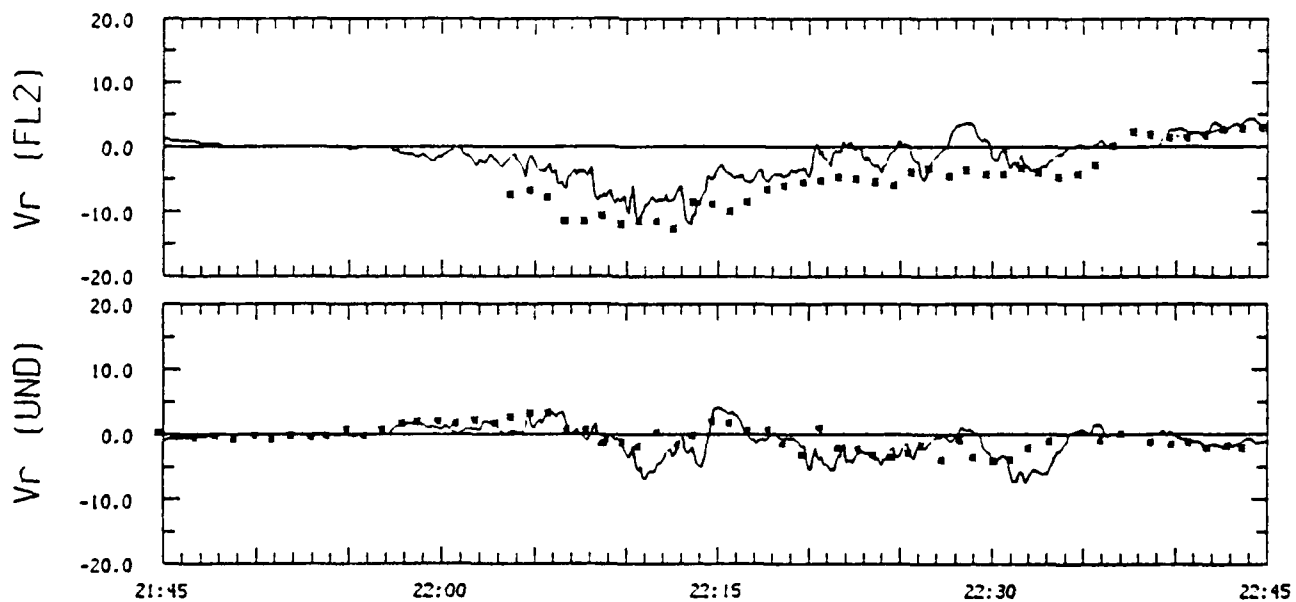
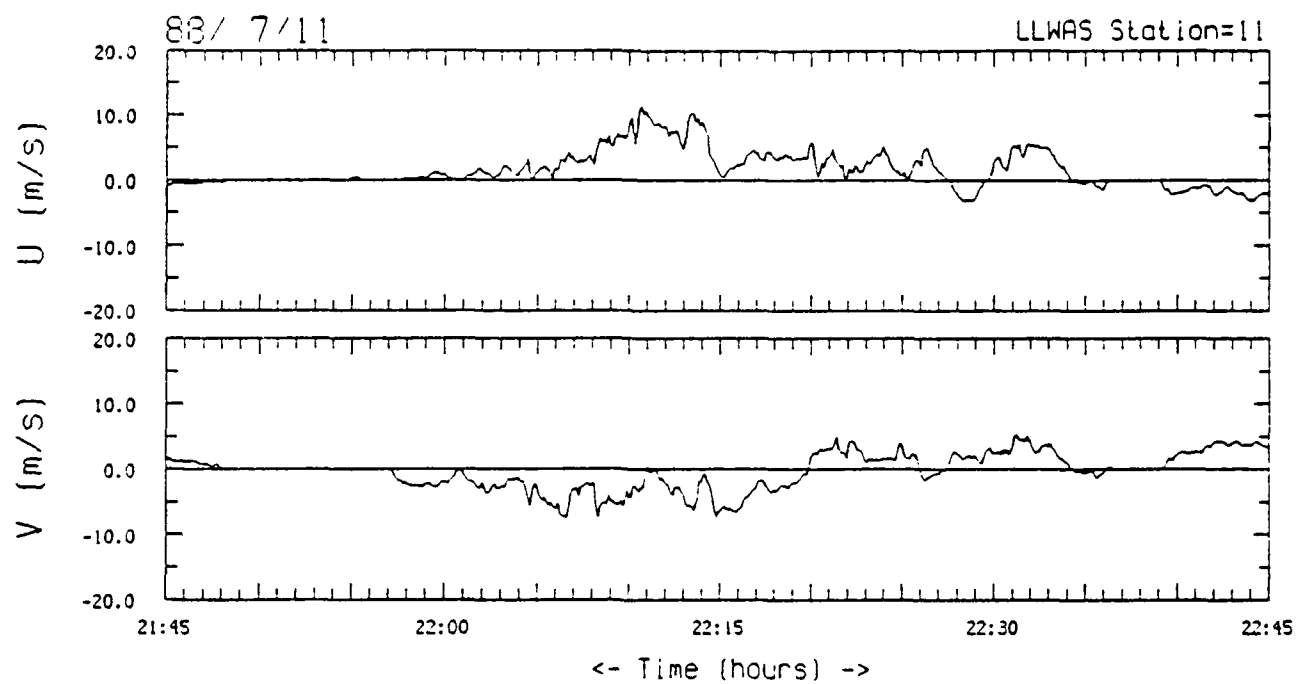


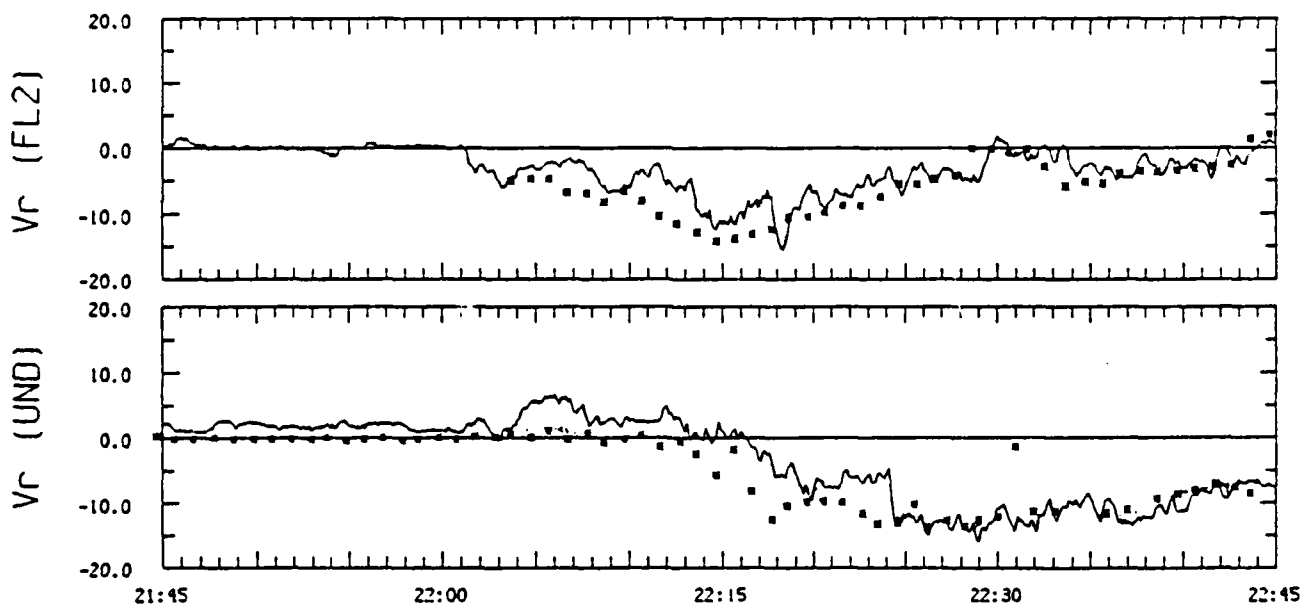
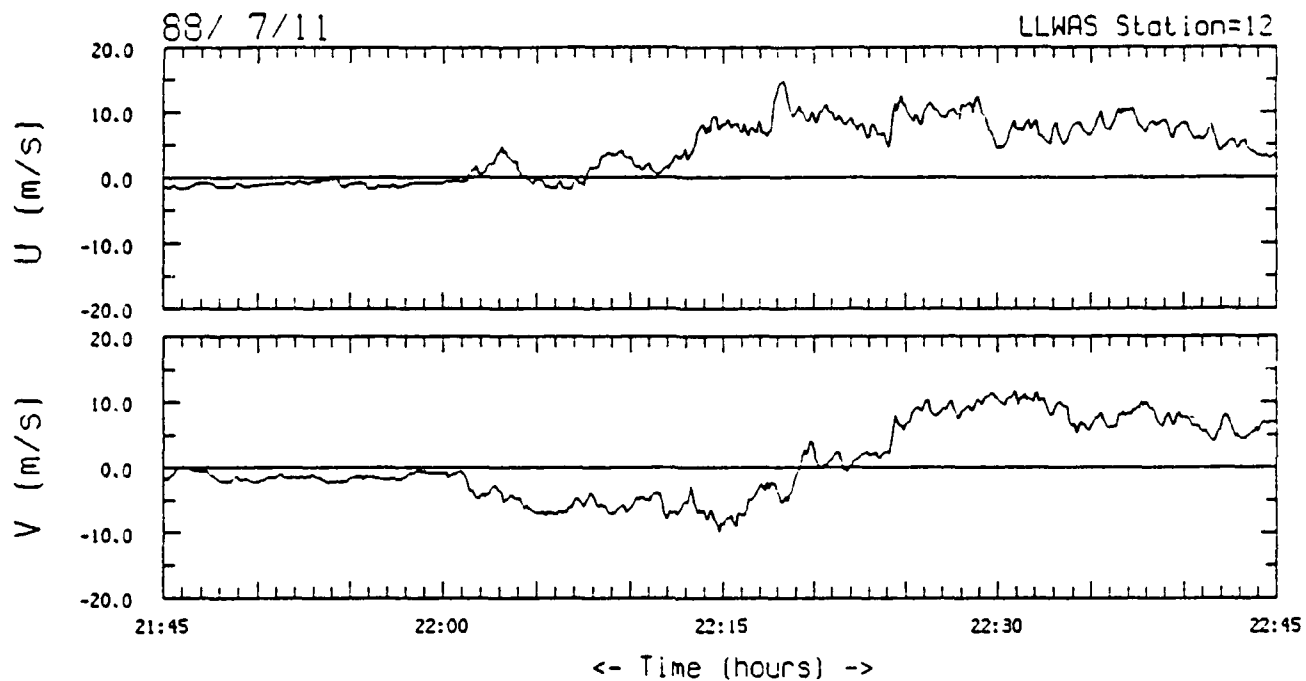












## **Appendix H: Dual Doppler Radar Low Resolution Analyses**

These plots show horizontal wind vectors with radar reflectivity contours overlaid for 0.19, 4.69 and 7.69 km AGL (1.8, 6.3 and 9.3 km MSL). X and Y axis labels are in km east and north of the FL2 radar, respectively. The top line above each plot gives the date, time, altitude AGL and overlay field. On the right are the contour levels (values followed by 's') and maximum field value (value followed by 'x'). A scale wind vector is provided in the lower right hand corner. Relative minima ('L') and maxima ('H') of the contoured field are indicated on the diagrams.

The analysis techniques used to produce these plots are described in the text.

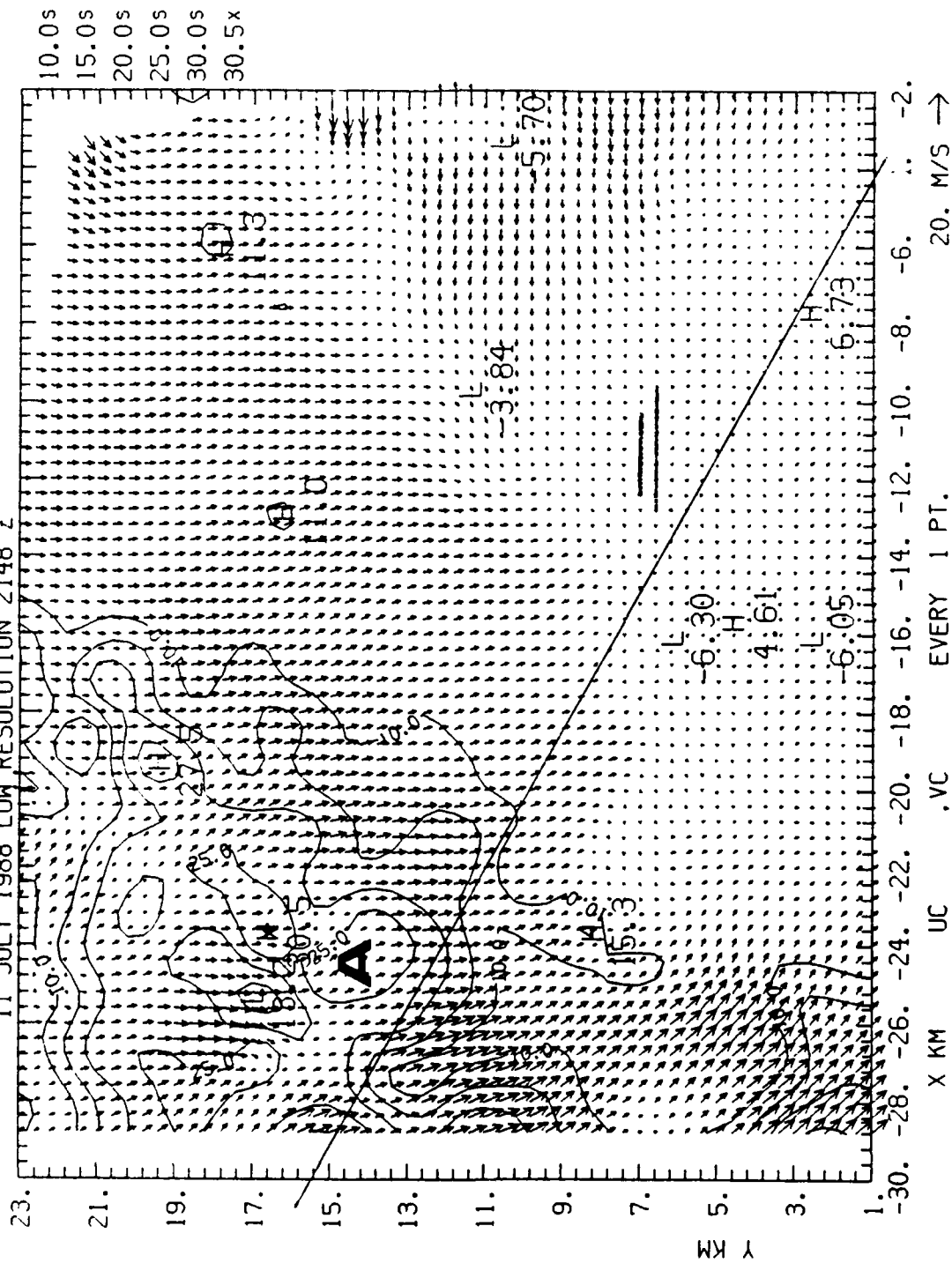
DBZ  
0 DEG

```
COMBIN
ORIGIN={ 0.0
```

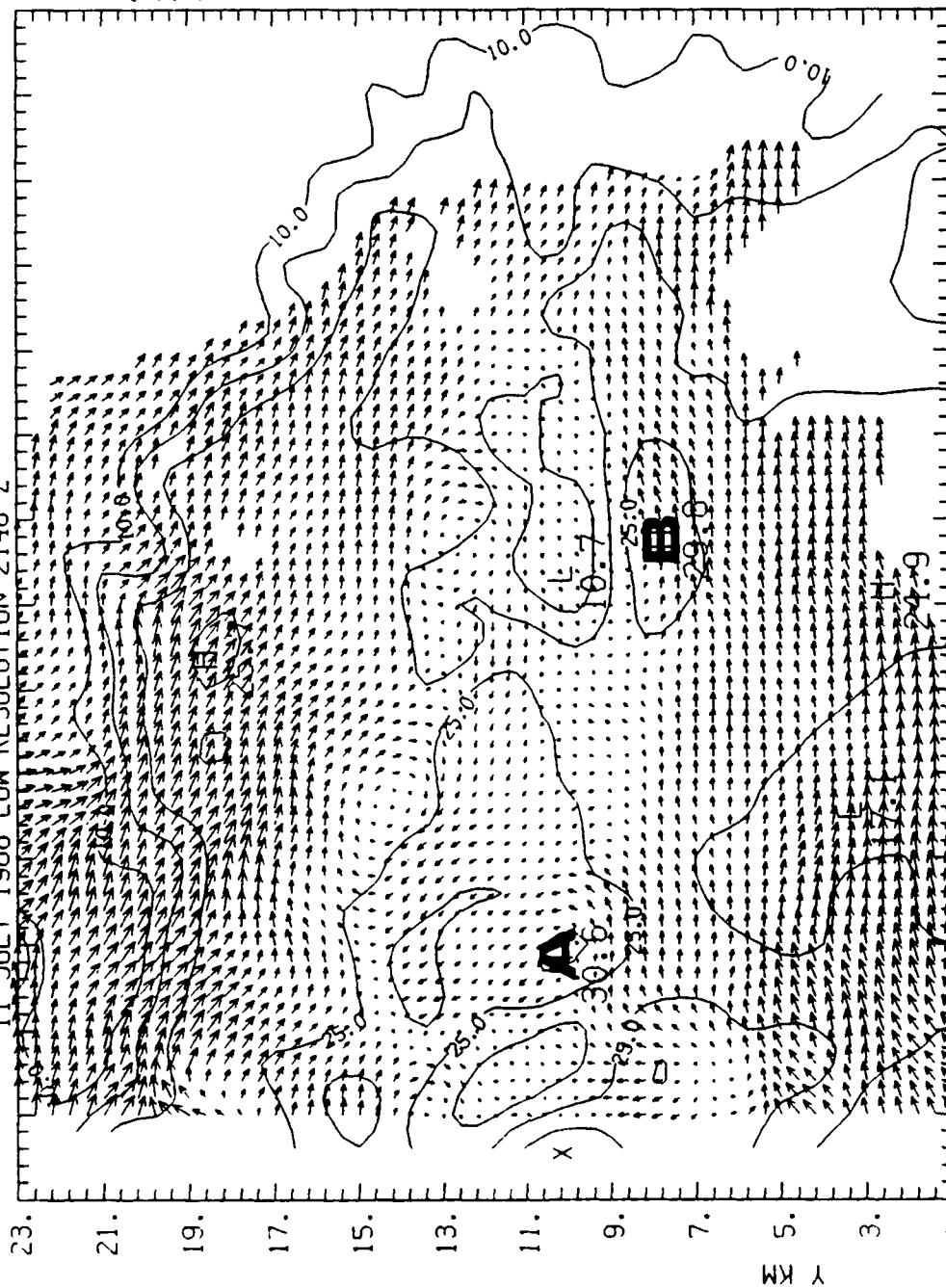
21 48 15-21 48 15

(AS OF 10/04/89)

11 JULY 1988 LOW RESOLUTION 2148 Z



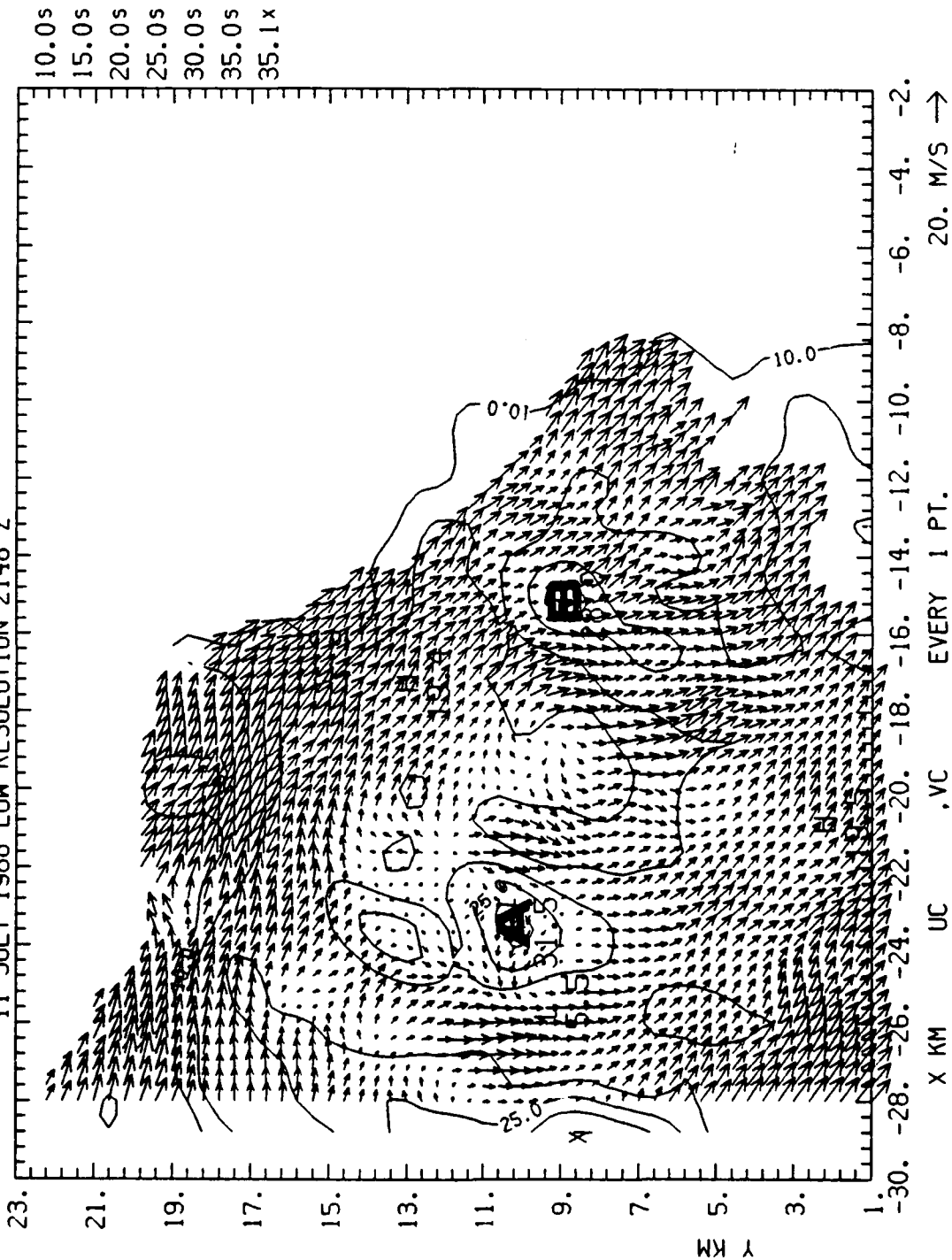
10.0s  
15.0s  
20.0s  
25.0s  
30.0s  
32.8x



X KM	UC	.VC	EVERY 1 PT.	20. M/S	→



88/ 7/11 21 48 15-21 48 15 COMBIN Z = 7.69 KM DBZ  
 (AS OF 10/04/89) ORIGIN=( 0.00, 0.00) KM X-AXIS= 90.0 DEG  
 11 JULY 1988 LOW RESOLUTION 2148 Z



```

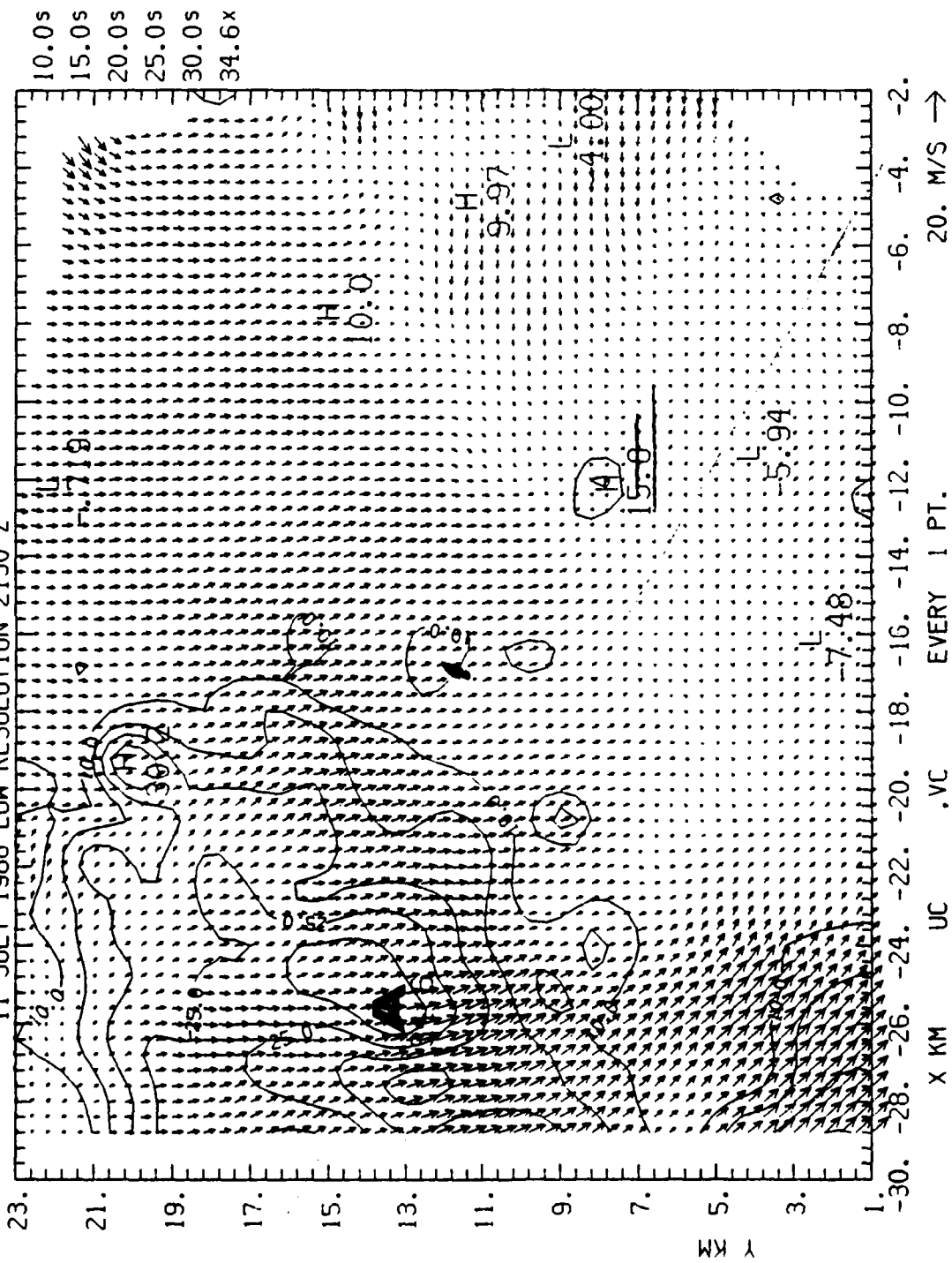
88/ 7/11      21 50 15-21 50 15      COMBIN      Z =      0.19 KM      DBZ
(AS OF 10/04/89)      ORIGIN=(      0.00,      0.00) KM      X-AXIS= 90.0 DEG

```

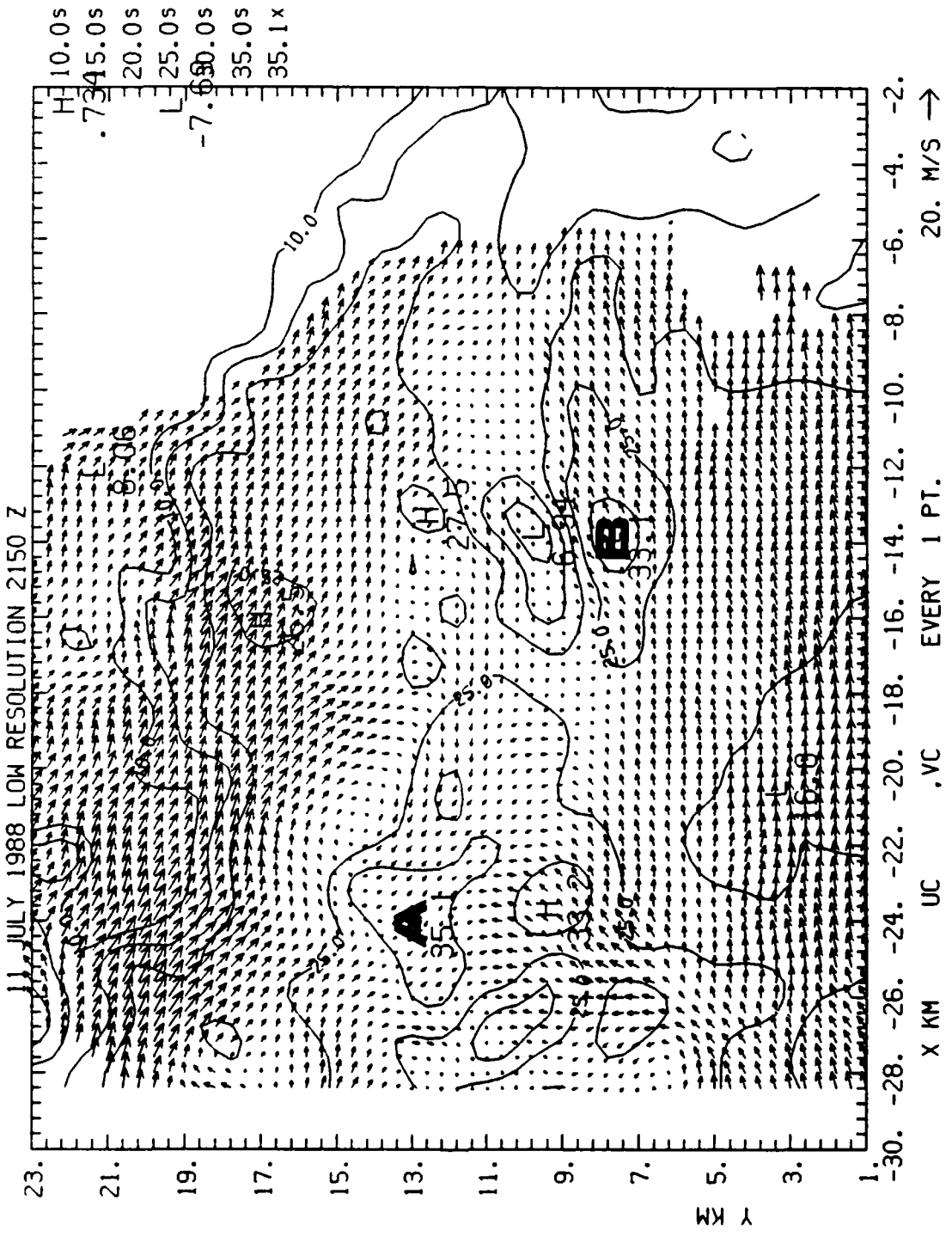
88/ 7/11	21 50 15-21 50 15	COMBIN	Z =	0.19 KM	DBZ
----------	-------------------	--------	-----	---------	-----

ORIGIN=( 0.00, 0.00) KM X-AXIS= 90.0 DEG

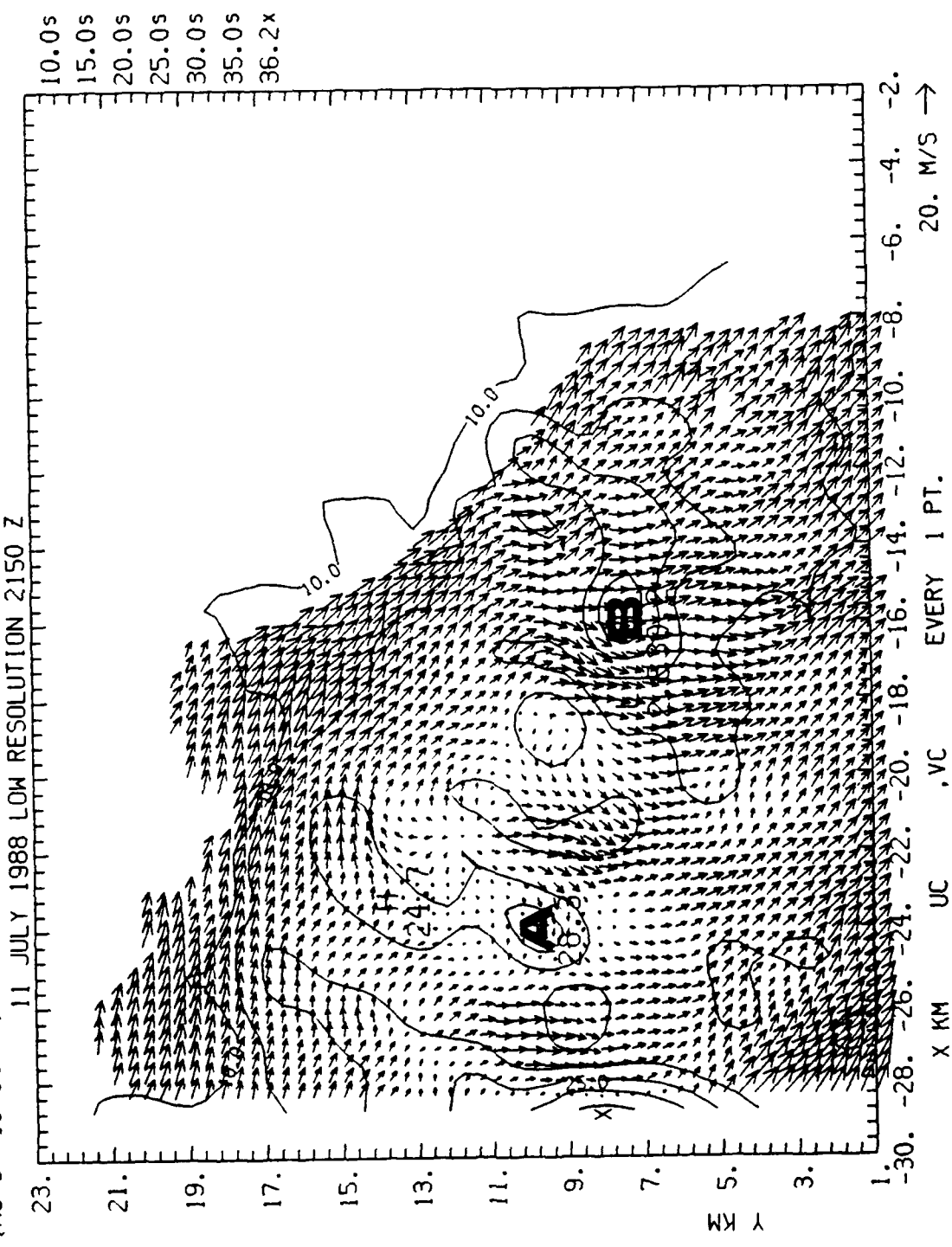
11 JULY 1988 LOW RESOLUTION 2150 Z



88/ 7/11 21 50 15-21 50 15 COMBIN Z = 4.69 KM ' DBZ  
 (AS OF 10/04/89) ORIGIN=( 0.00, 0.00) KM X-AXIS= 90.0 DEG



88/ 7/11 21 50 15-21 50 15 COMBIN Z = 7.69 KM ' DBZ  
 (AS OF 10/04/89) ORIGIN=( 0.00, 0.00) KM X-AXIS= 90.0 DEG



```

88/ 7/11      21 52 15-21 52 15      COMBIN      Z =      0.19 KM      1 DBZ
(RS OF 10/04/89)      ORIGIN=( 0.00,      0.00) KM      X-AXIS= 90.0 DEG

```

Z = 0.19 KM DBZ

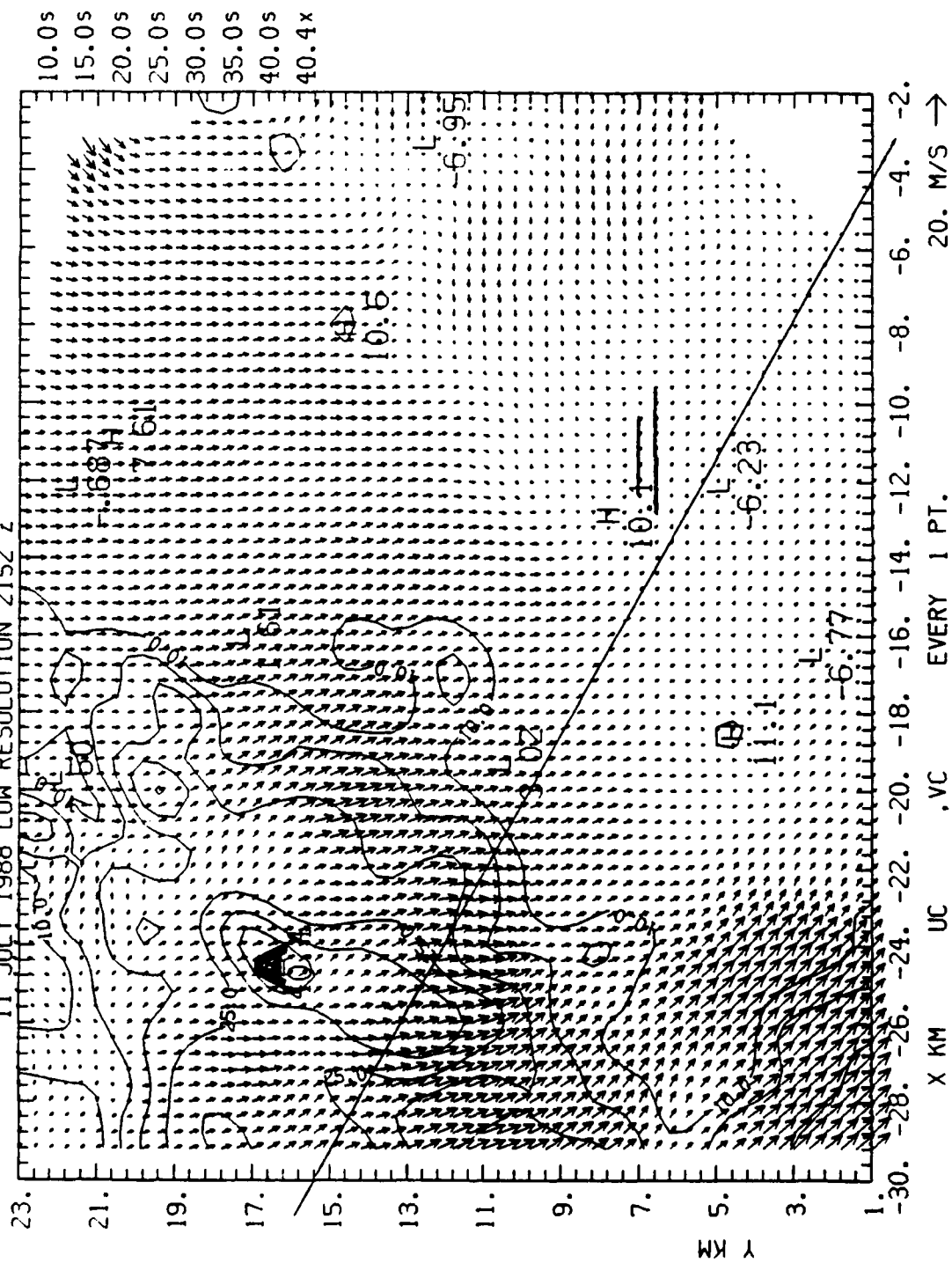
COMBIN

21 52 15-21 52 15

88/ 7/11

(AS OF 10/04/89) ORIGIN=( 0.00, 0.00) KM X-AXIS= 90.0 DEG

11 JUL Y 1988 LOW RESOLUTION 2152 Z

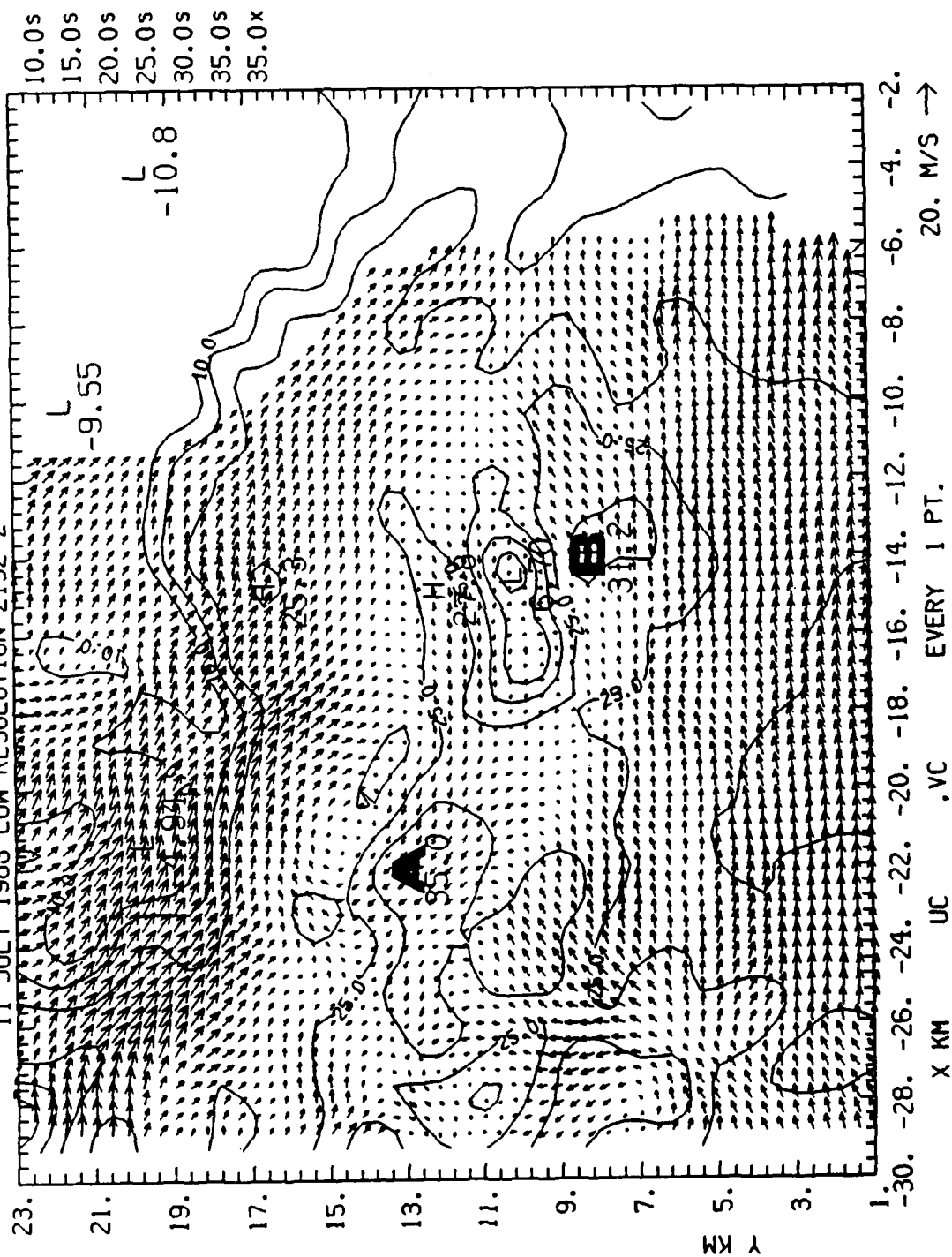


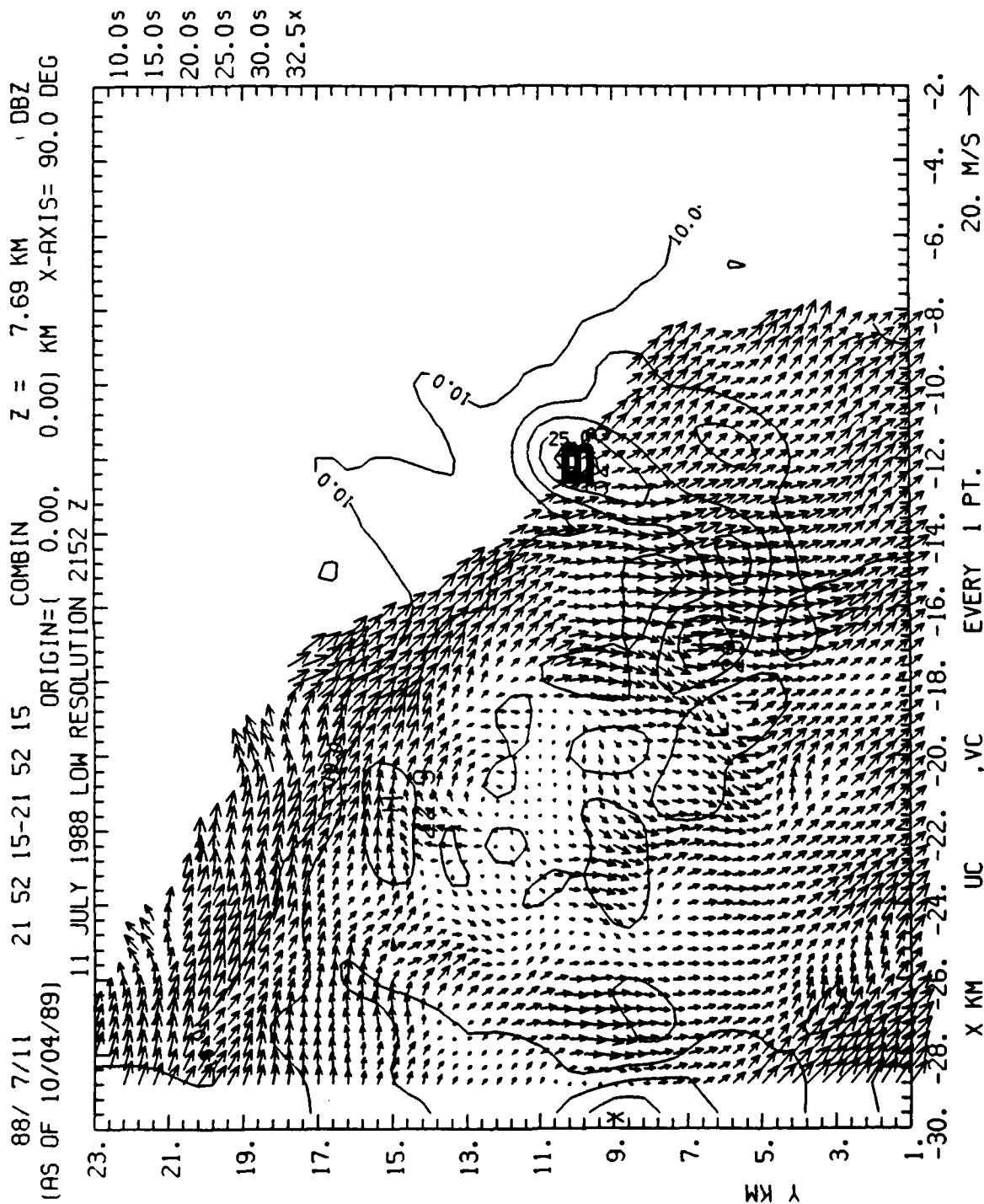
```

88/ 7/11      21 52 15-21 52 15      COMBIN      Z =      4.69 KM      ' DBZ
(IAS OF 10/04/89)      ORIGIN=(      0.00,      0.00) KM      X-AXIS= 90.0 DEG

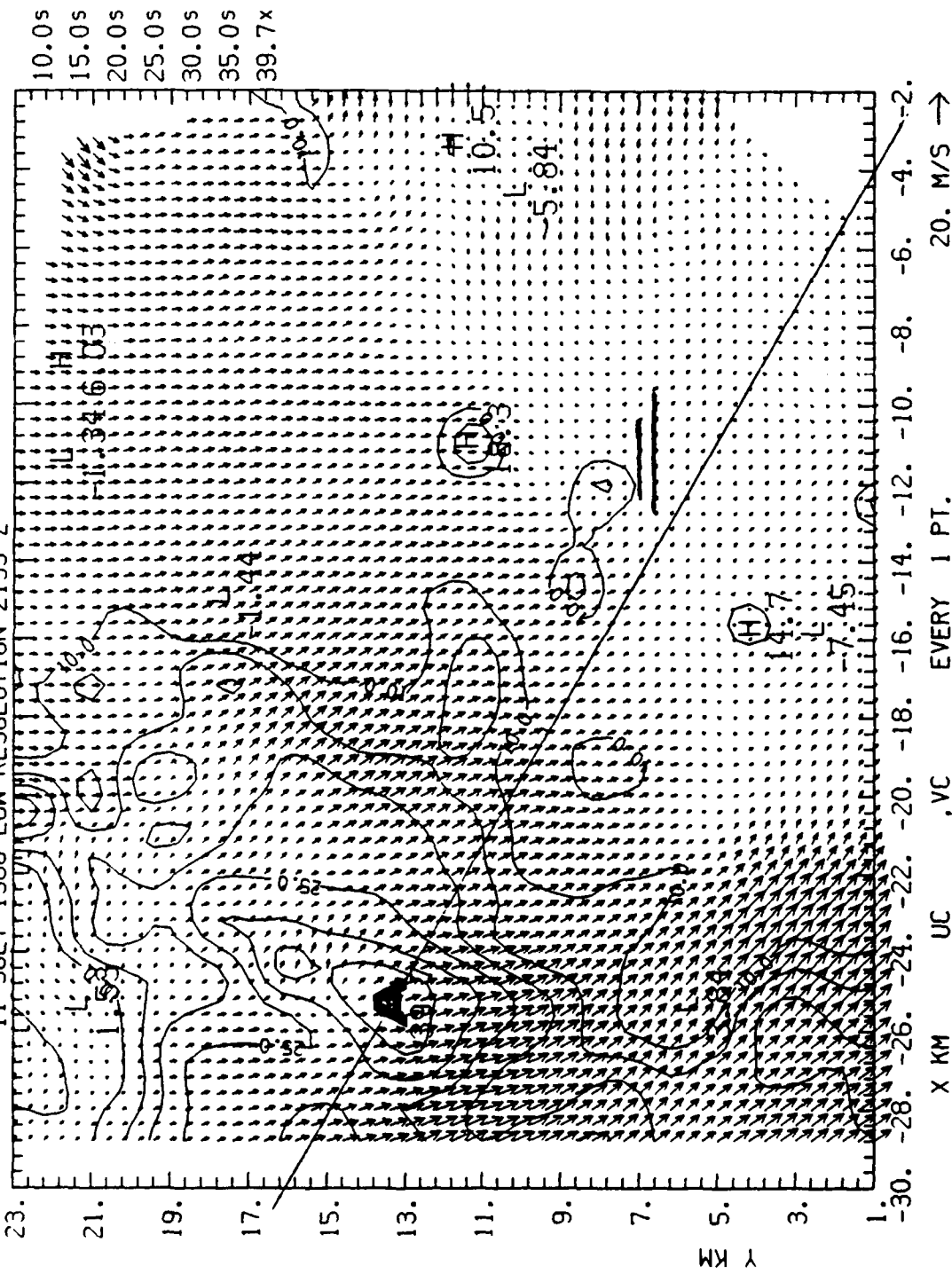
```

11 JULY 1988 LOW RESOLUTION 2152 Z

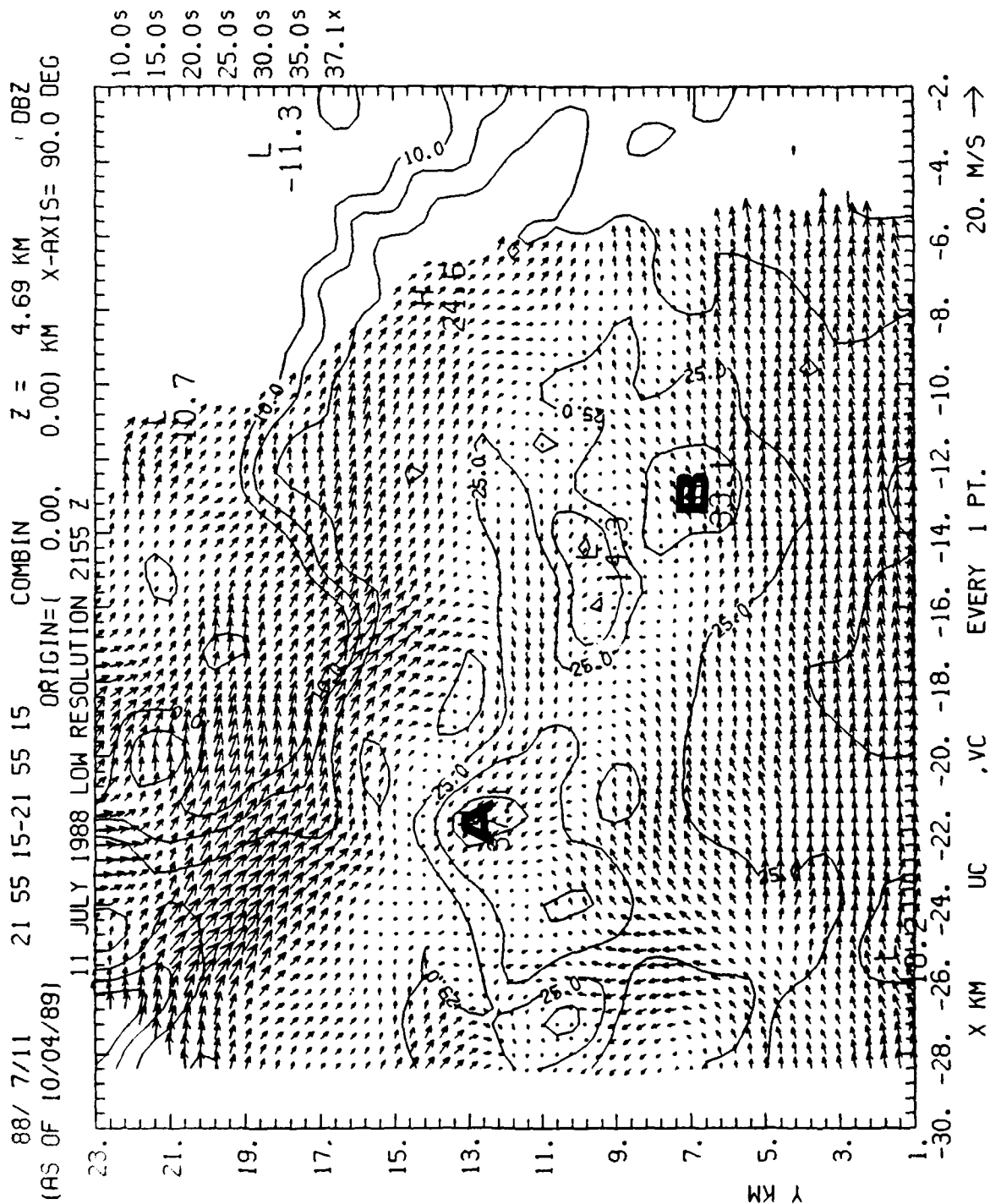




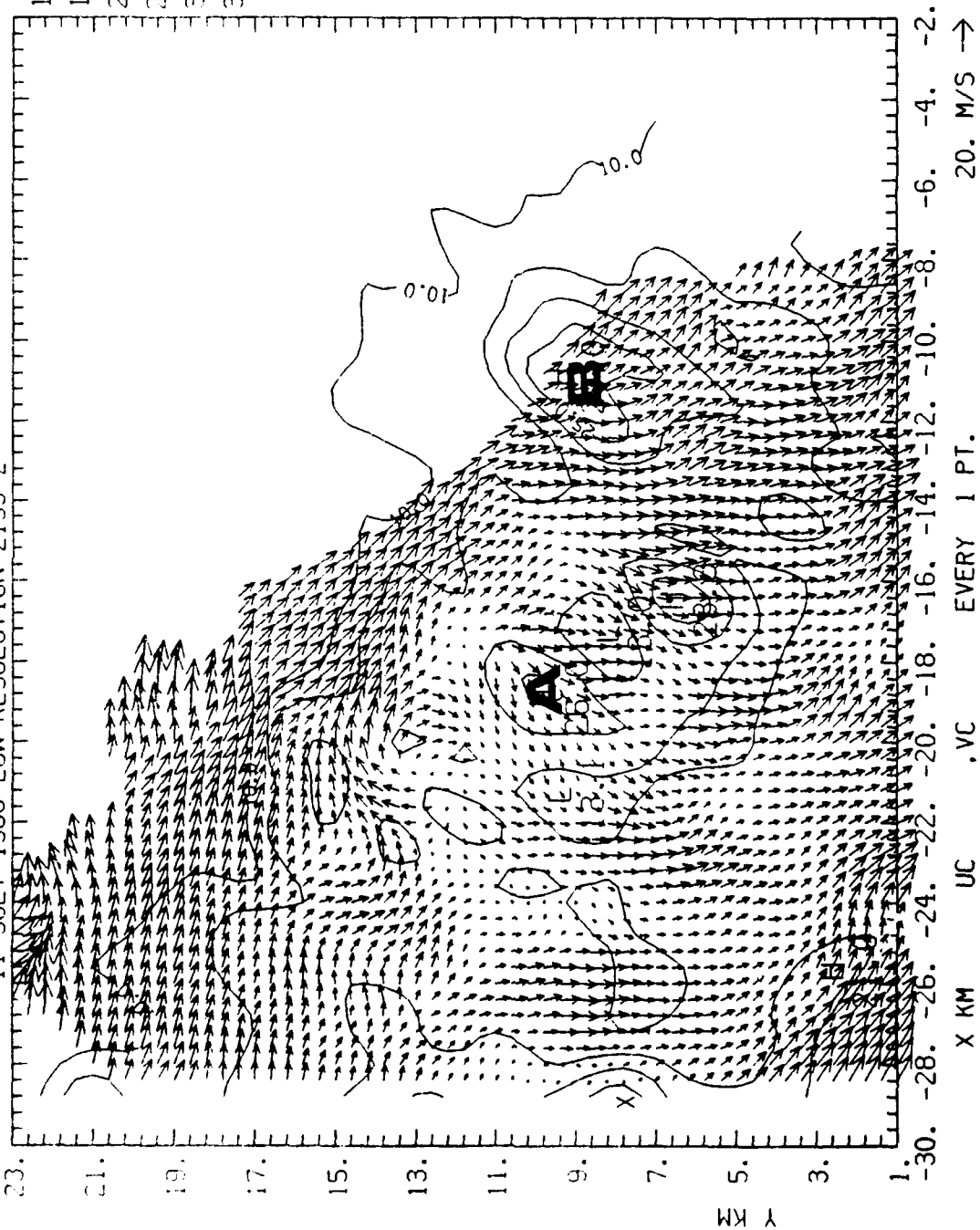
11 JULY 1988 LOW RESOLUTION 2155 Z



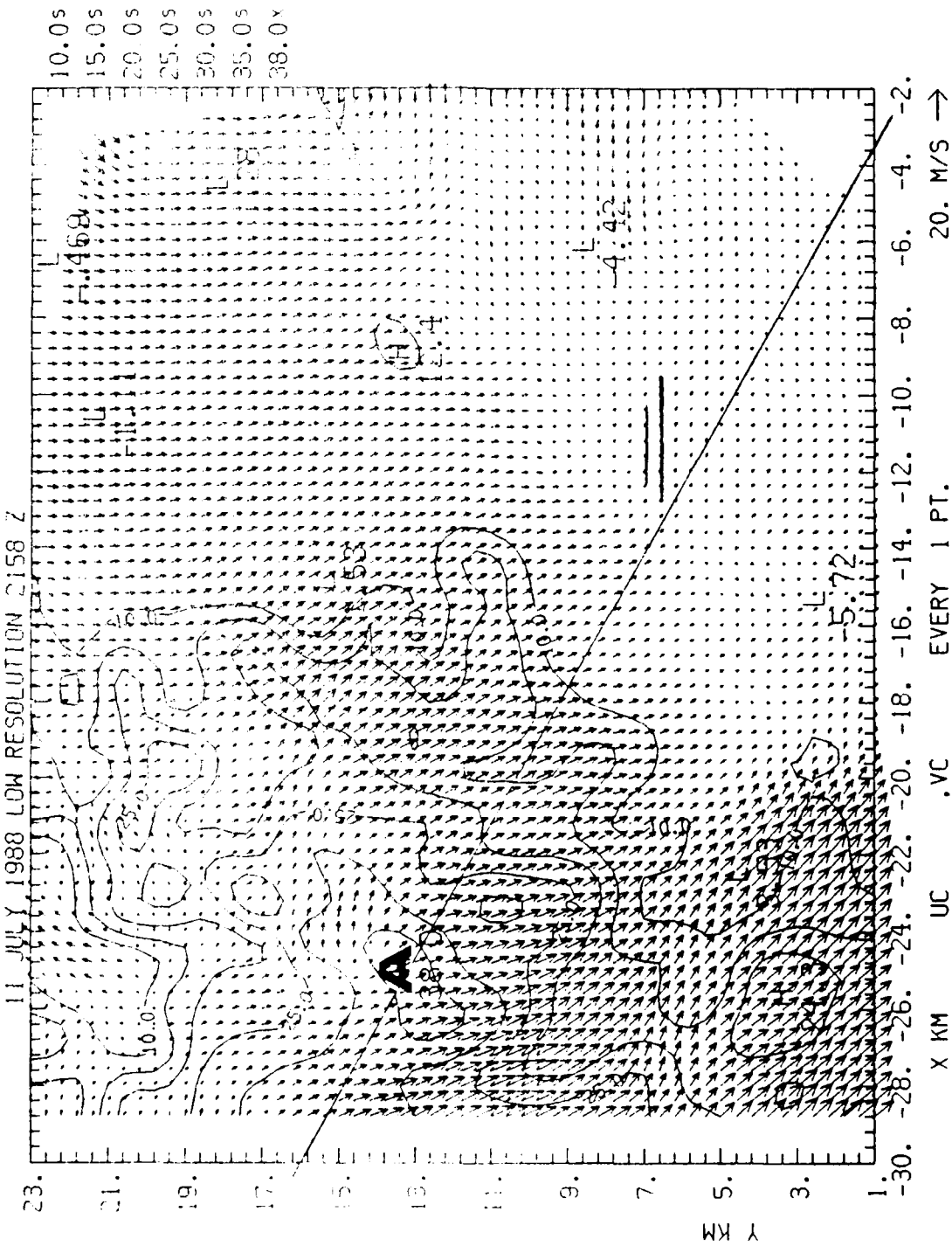




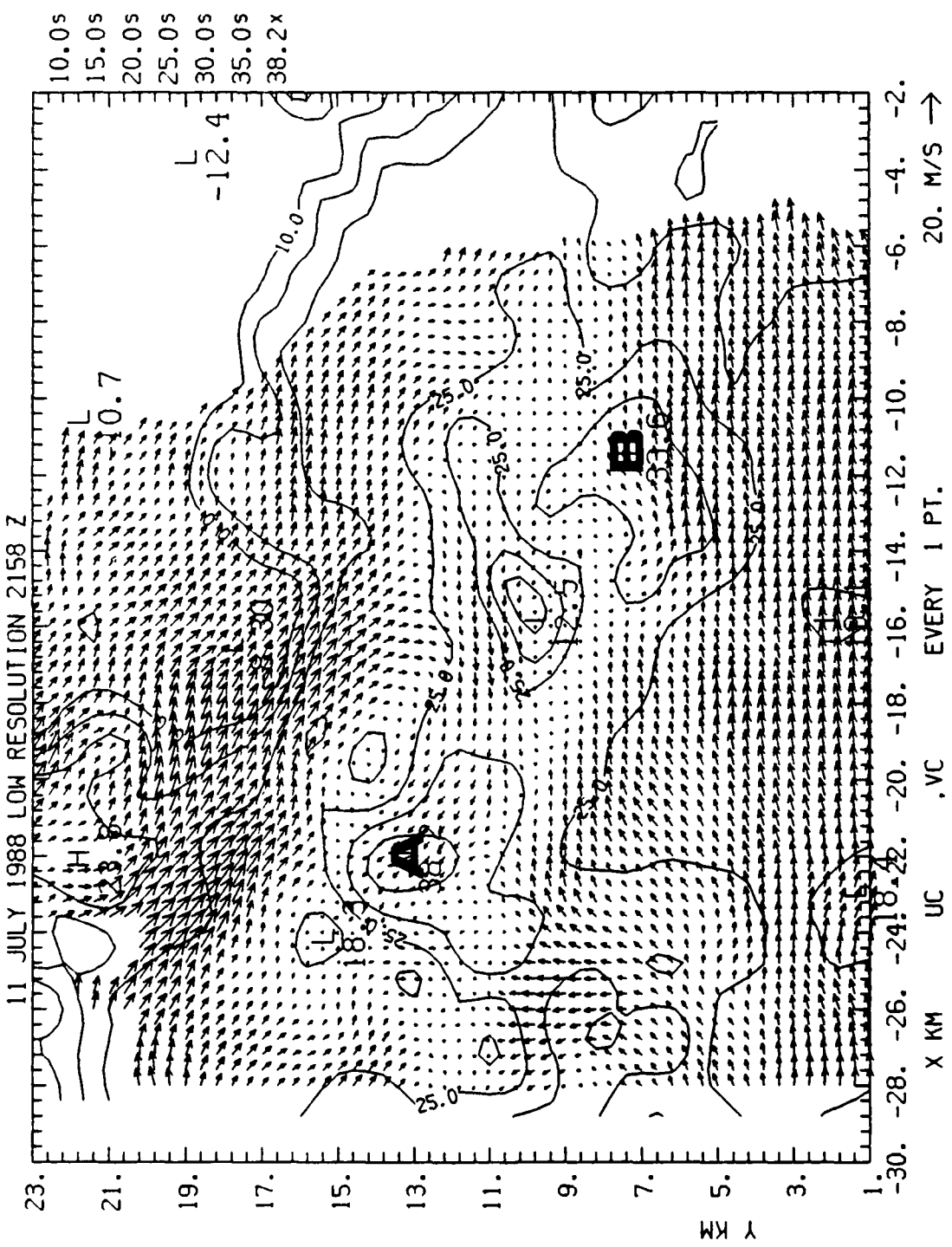
10.0s  
15.0s  
20.0s  
25.0s  
30.0s  
32.3x



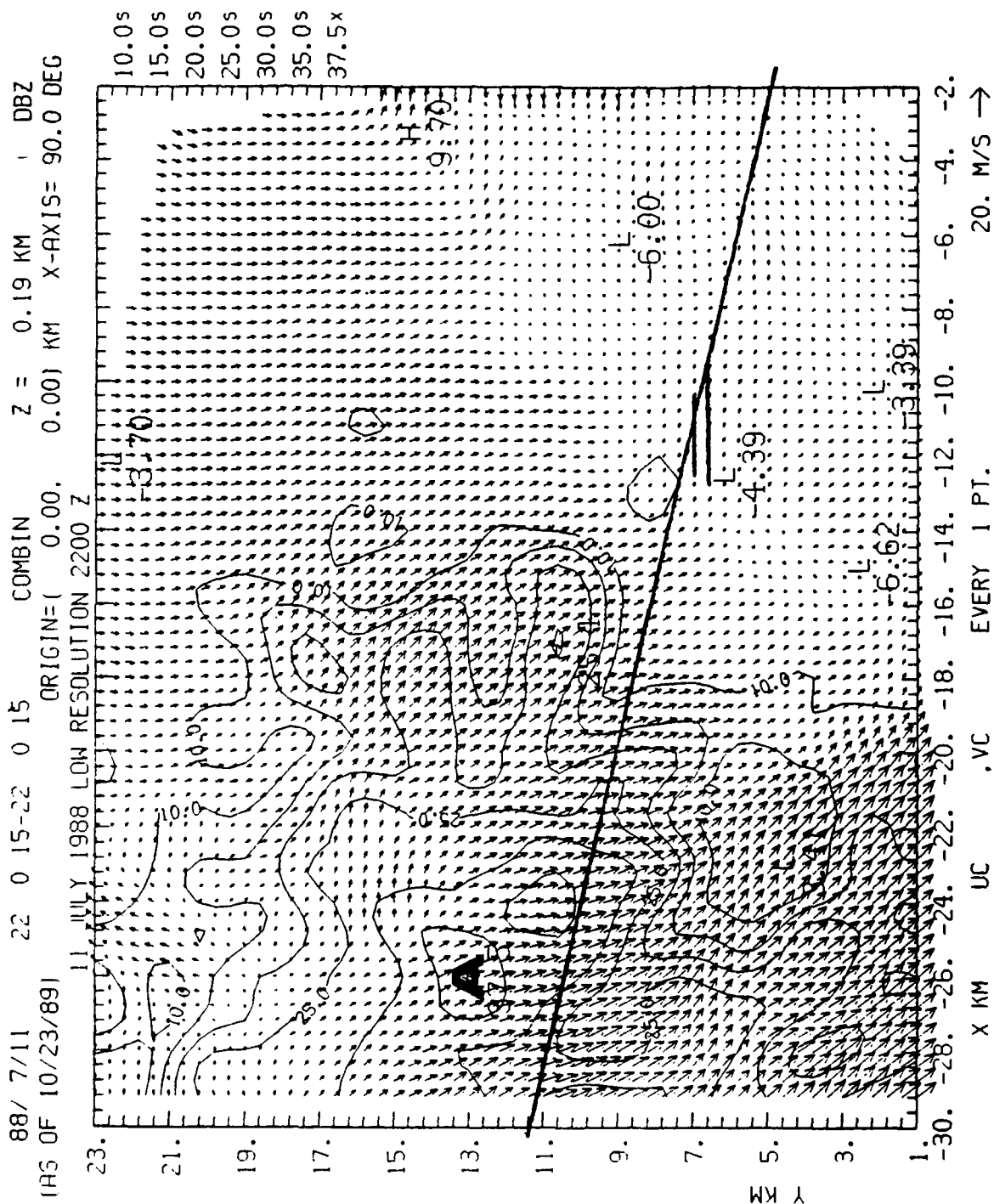
88/ 7/11 21 58 15-21 58 15 COMBIN Z = 0.19 KM CBZ  
 (AS OF 10/04/89) ORIGIN=( 0.00, 0.00) KM X-AXIS= 90.0 DEG



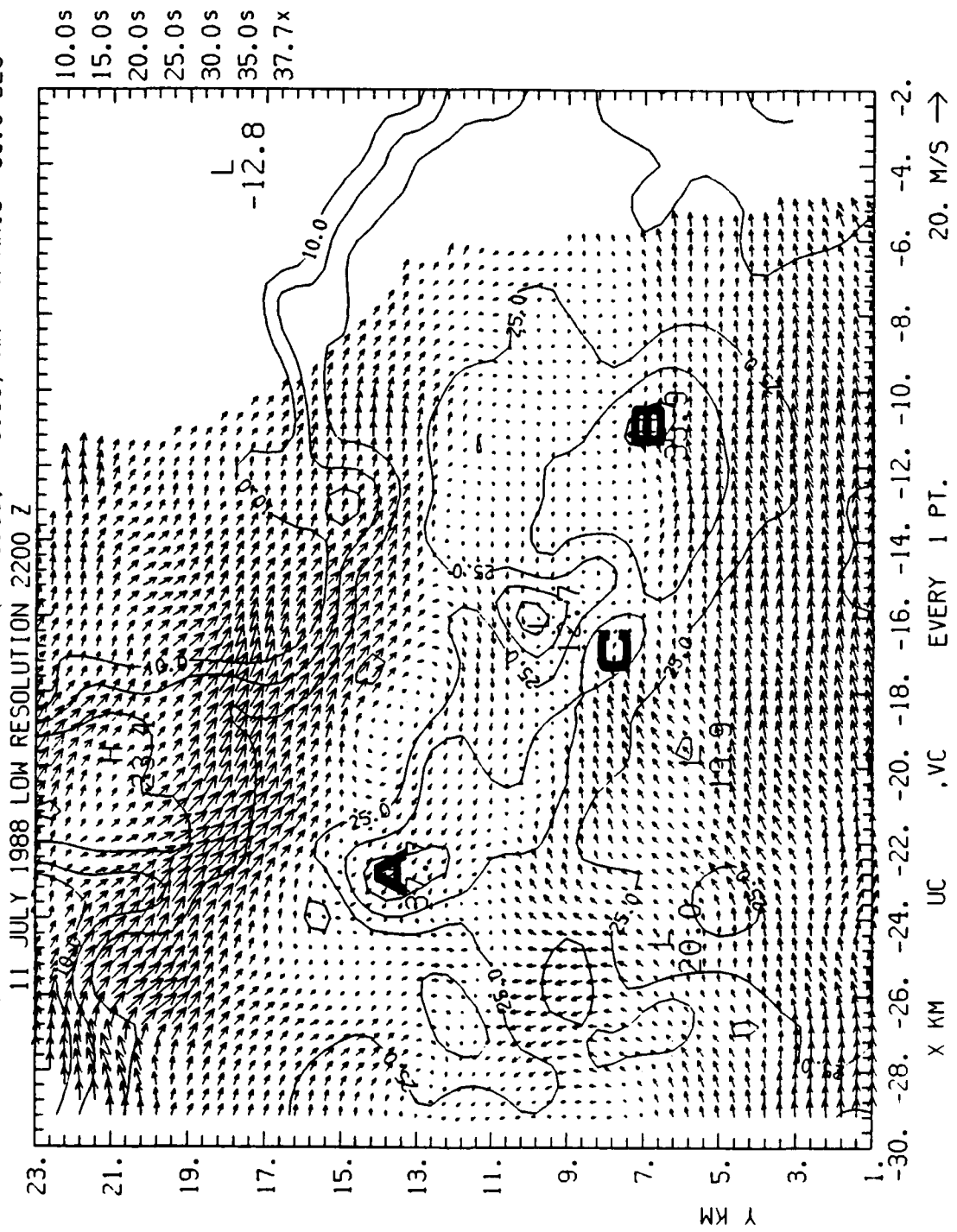
88/ 7/11 21 58 15-21 58 15 COMBIN Z = 4.69 KM ' DBZ  
 (AS OF 10/04/89) ORIGIN={ 0.00, 0.00} KM X-AXIS= 90.0 DEG



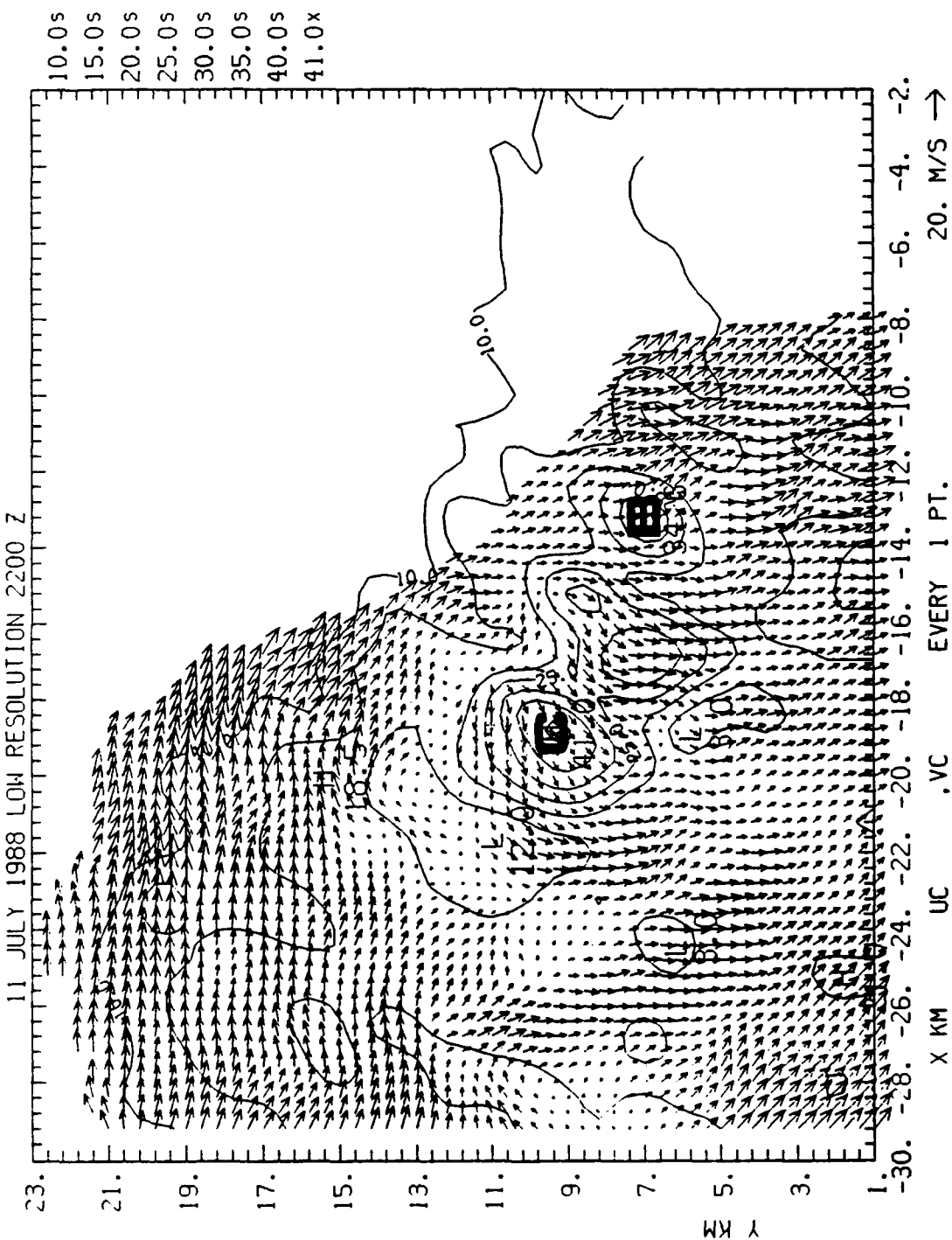




88/ 7/11 22 0 15-22 0 15 COMBIN Z = 4.69 KM ' DBZ  
 (AS OF 10/23/89) ORIGIN=( 0.00, 0.00) KM X-AXIS= 90.0 DEG



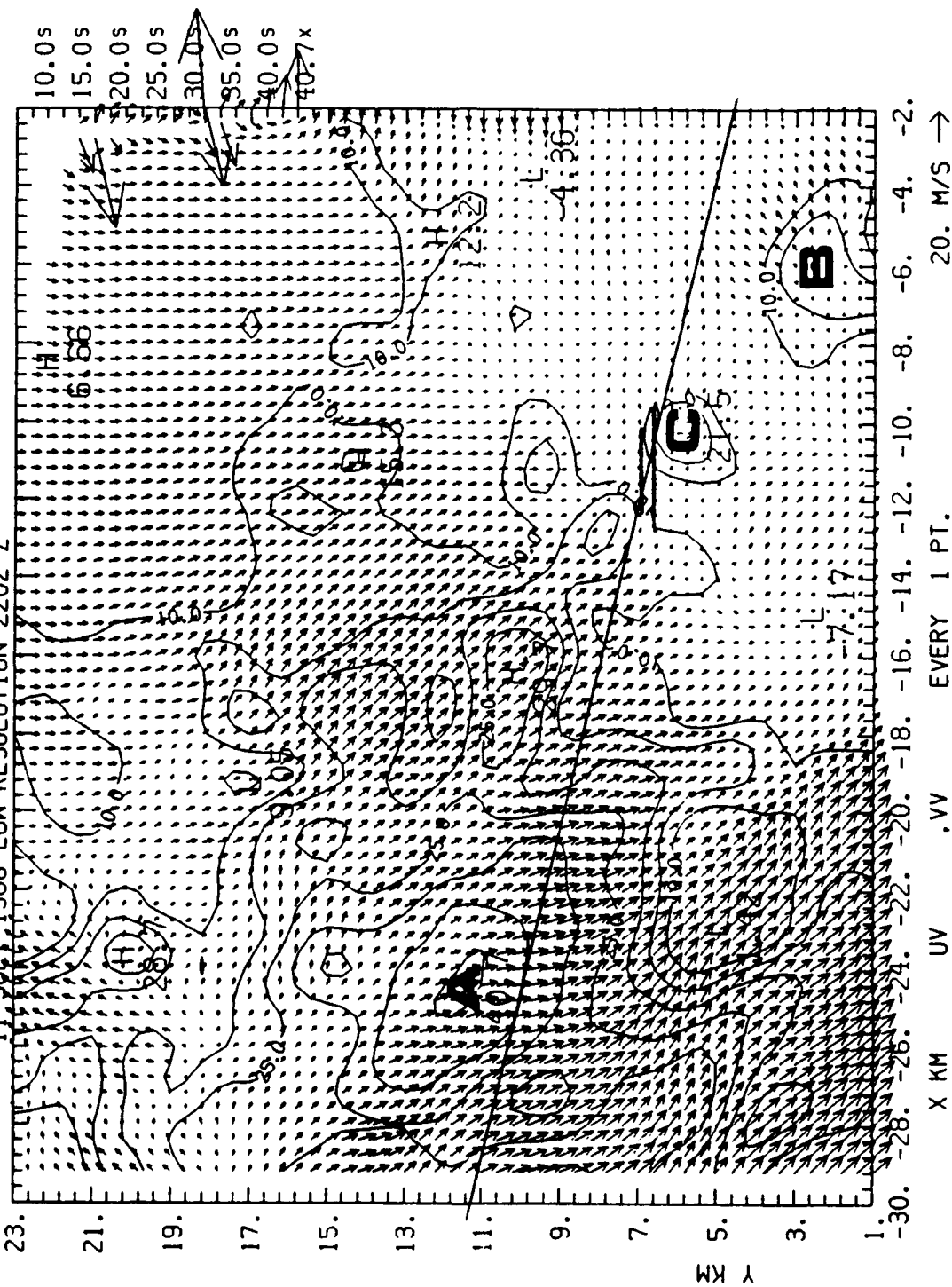
88/ 7/11 22 0 15-22 0 15 COMBIN Z = 7.69 KM DBZ  
 IAS OF 10/23/89) ORIGIN=1 0.00, 0.00) KM X-AXIS= 90.0 DEG



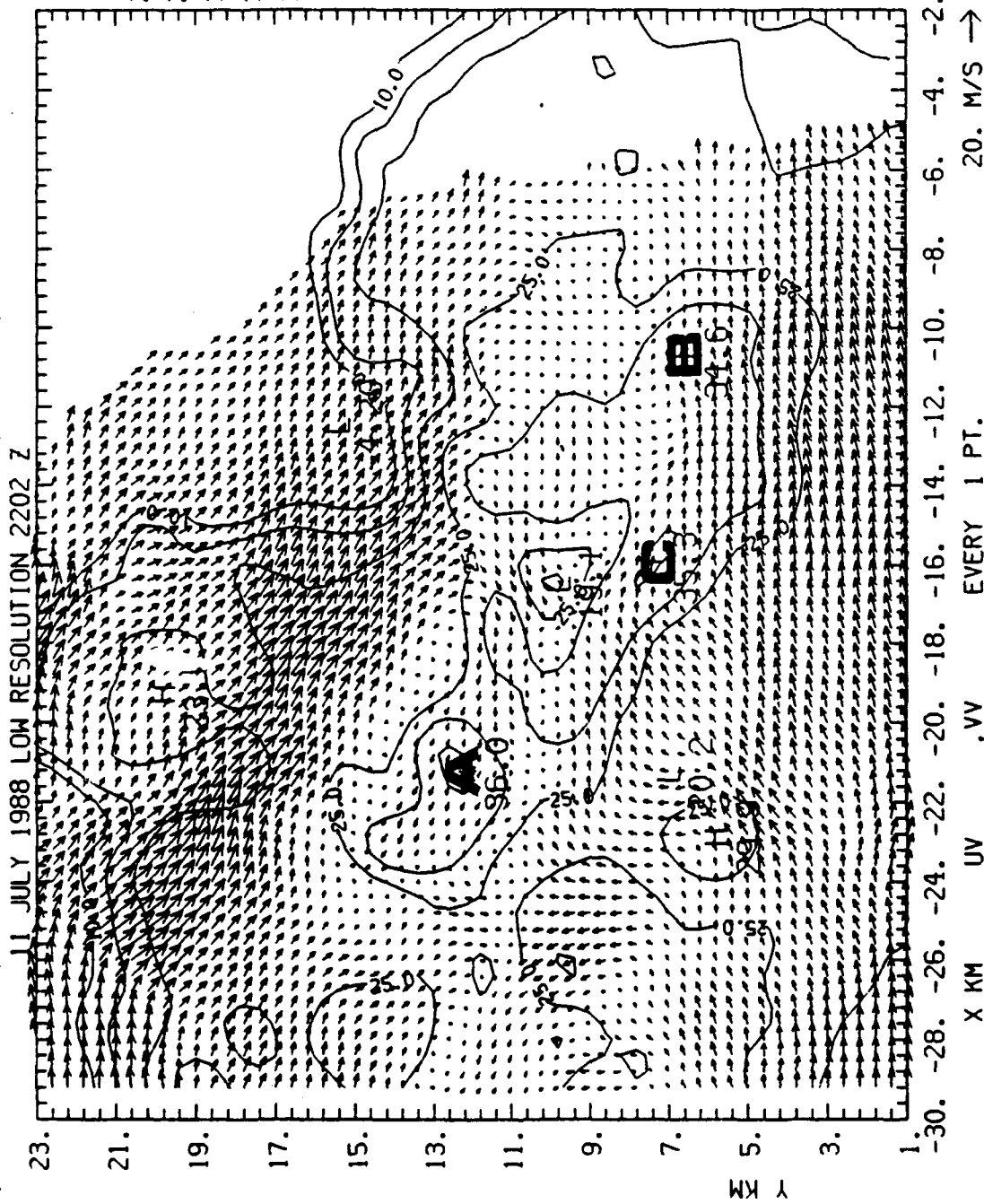


0 DE

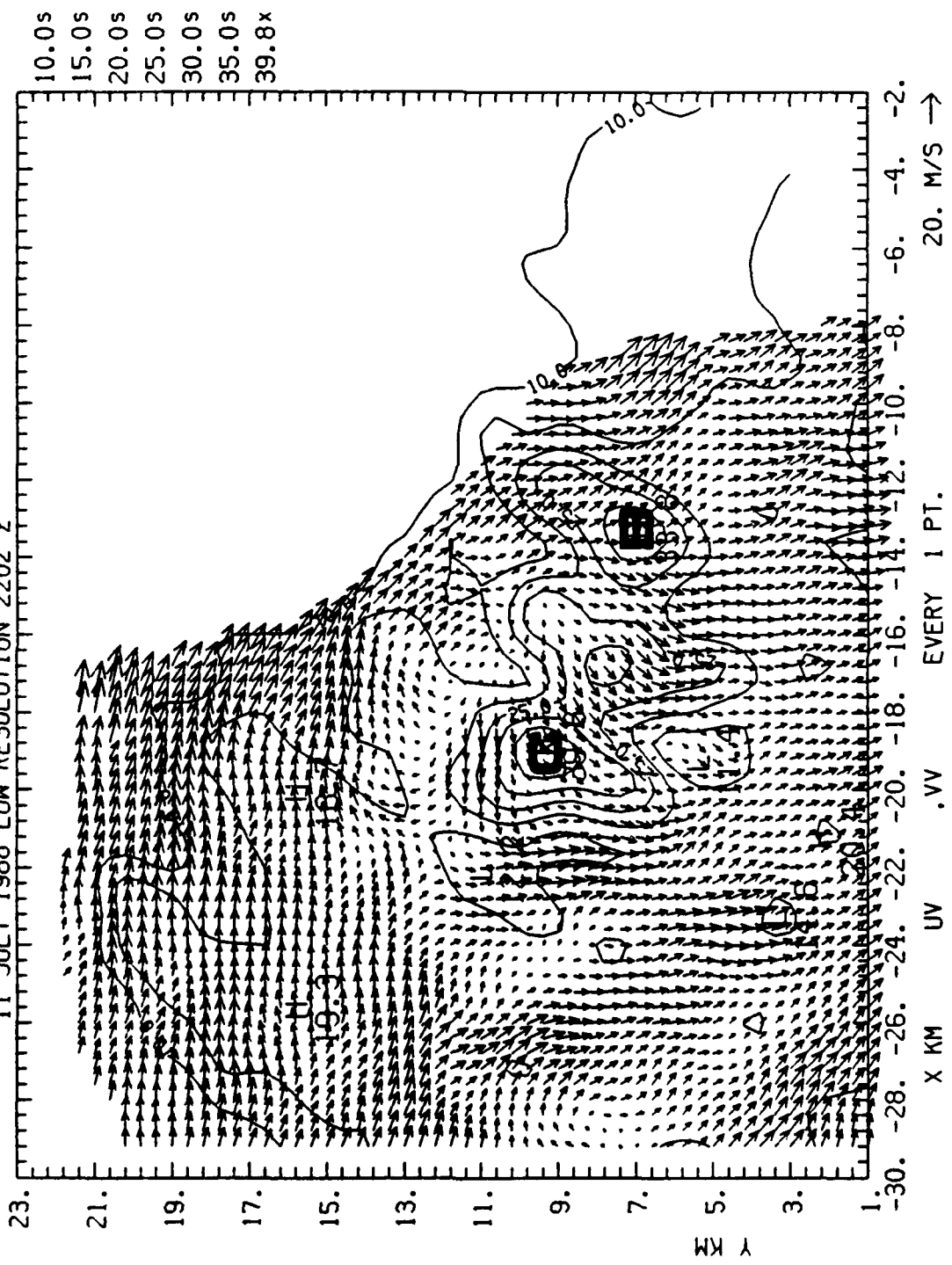
3



10.0s  
15.0s  
20.0s  
25.0s  
30.0s  
35.0s  
36.0x



88/ 7/11 22 2 47-22 2 47 COMBIN Z = 7.69 KM DBZ  
 (RS OF 06/23/89) ORIGIN=( 0.00, 0.00) KM X-AXIS= 90.0 DEG  
 11 JULY 1988 LOW RESOLUTION 2202 Z

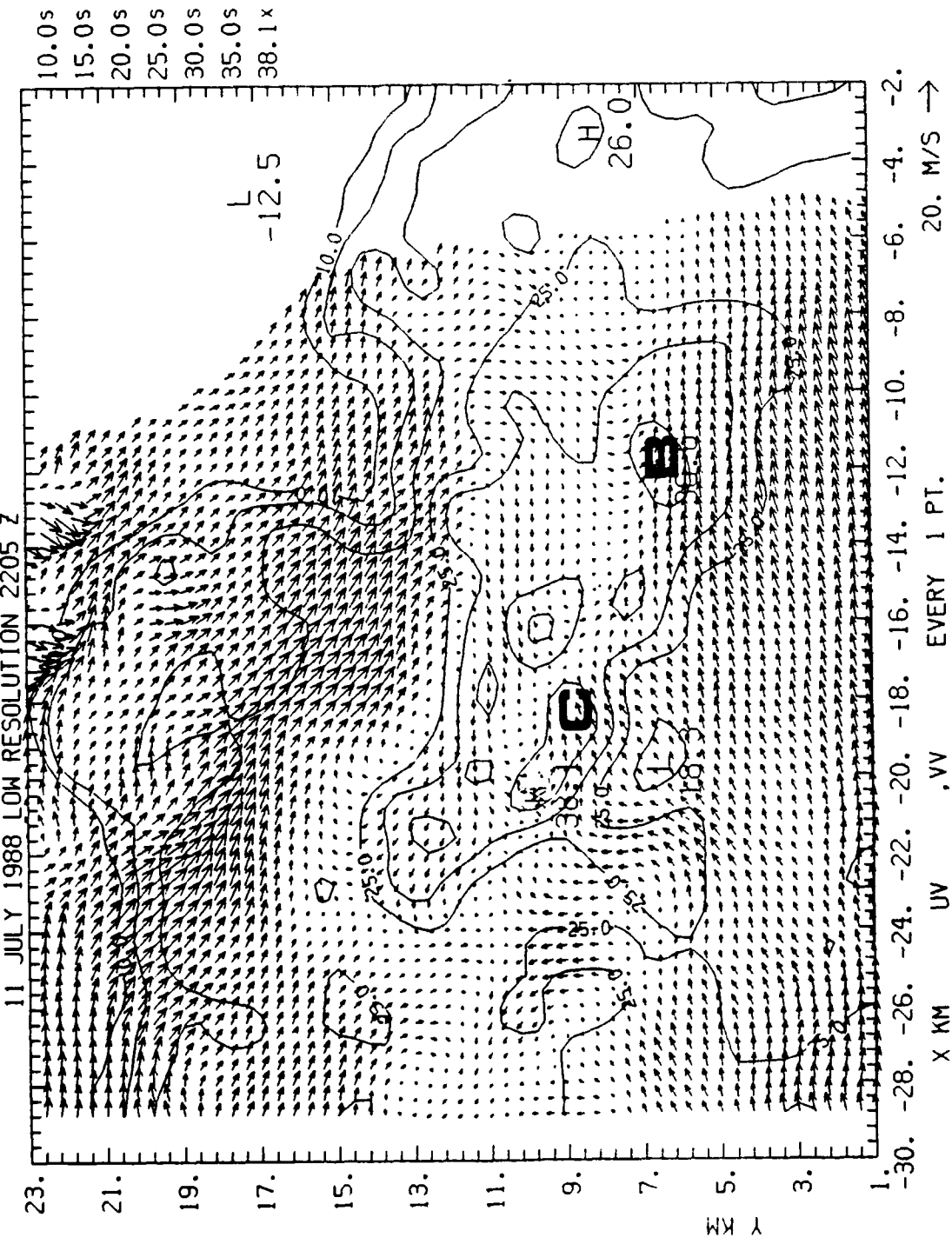


```
(AS OF 06/23/89)
ORIGIN=( 0.00, 0.00) KM X-AXIS= 90.0 DEG
```

111 JULY 1988 LOW RESOLUTION 2205 Z



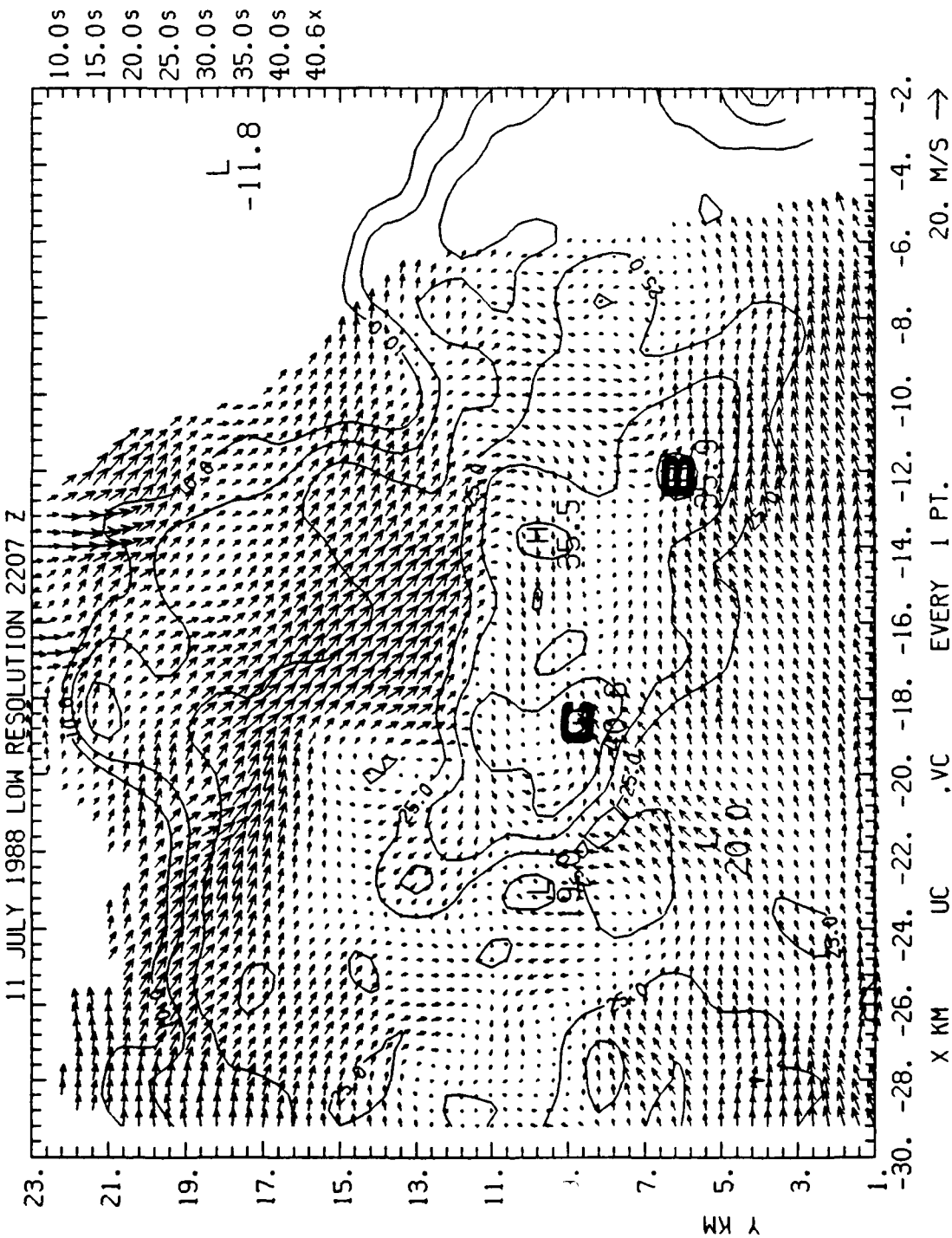
88/ 7/11 22 5 47-22 5 47 COMBIN Z = 4.69 KM ' DBZ  
 (AS OF 06/23/89) ORIGIN=( 0.00, 0.00) KM X-AXIS= 90.0 DEG





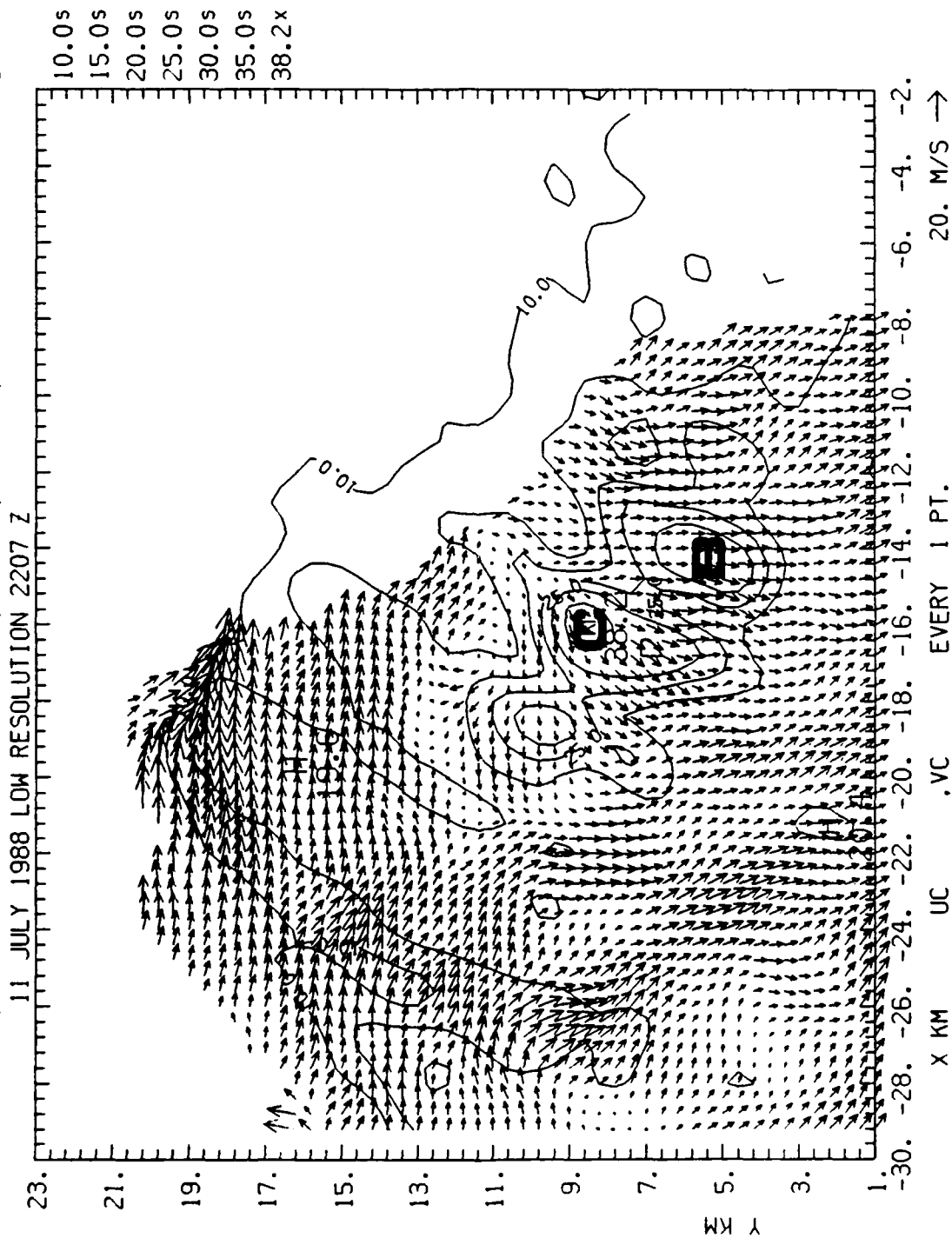


88/ 7/11 22 7 45-22 7 45 COMBIN Z = 4.69 KM DBZ  
 (AS OF 10/04/89) ORIGIN=( 0.00, 0.00) KM X-AXIS= 90.0 DEG

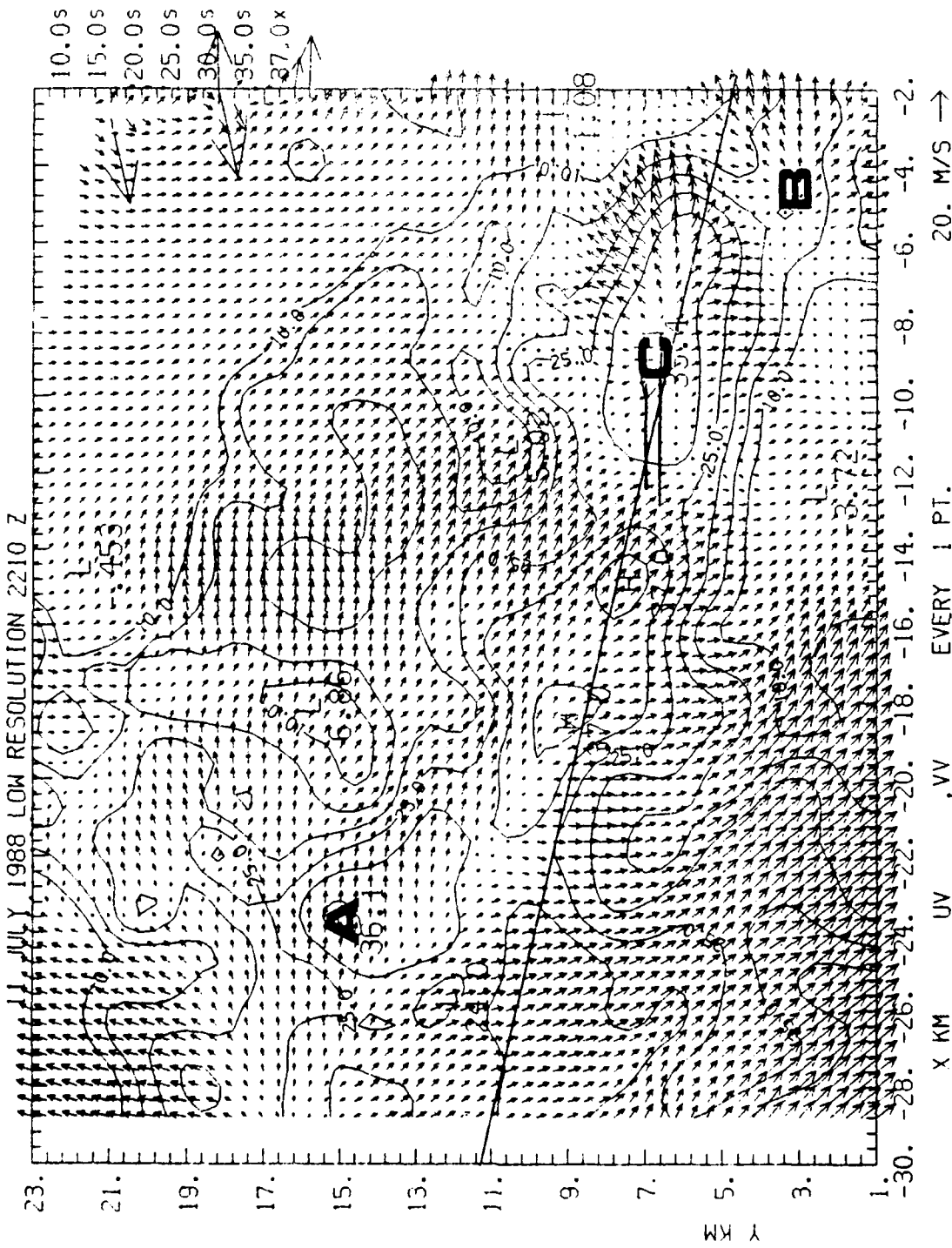




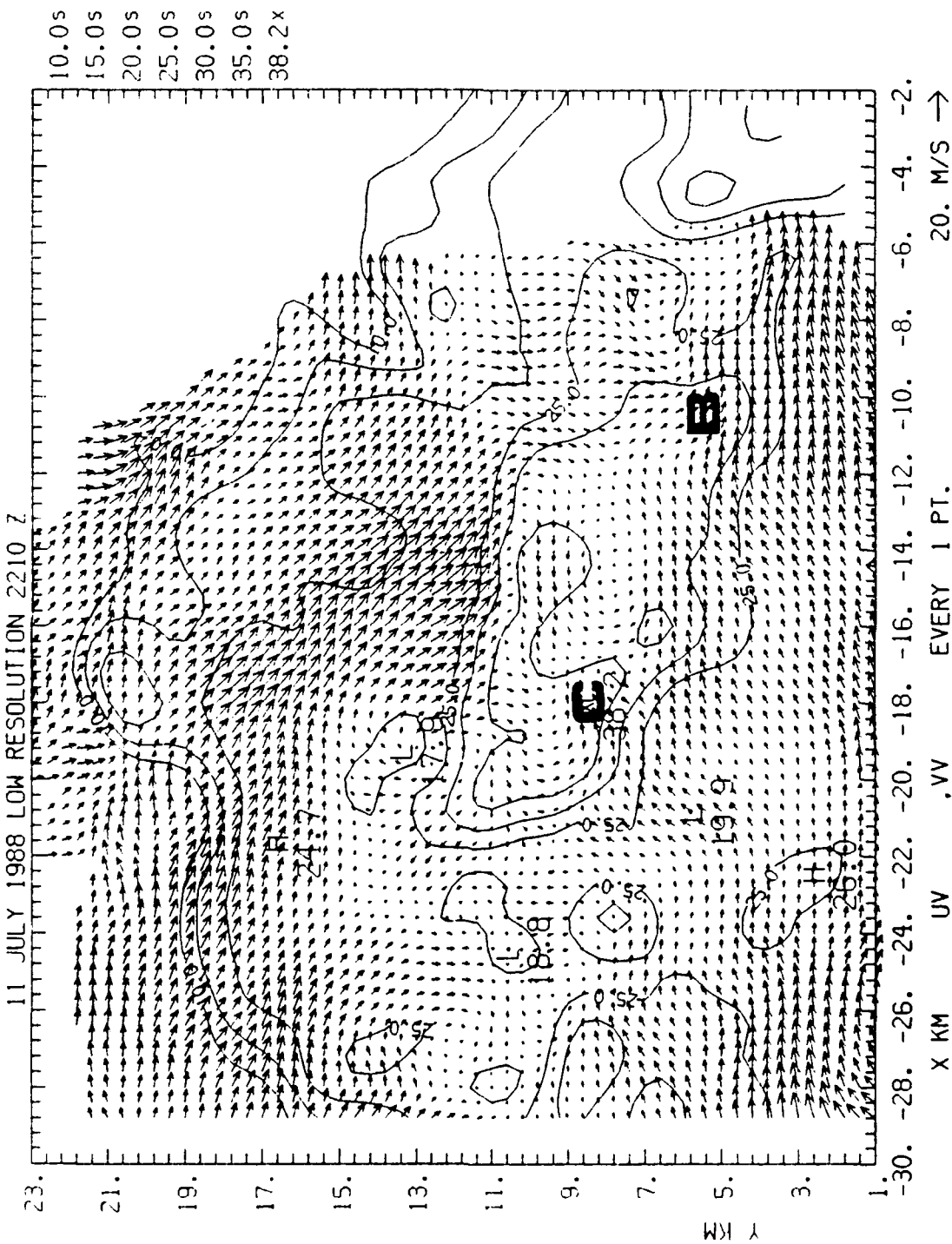
88/ 7/11 22 7 45-22 7 45 COMBIN Z = 7.69 KM 1 DBZ  
 (AS OF 10/04/89) ORIGIN=( 0.00, 0.00) KM X-AXIS= 90.0 DEG



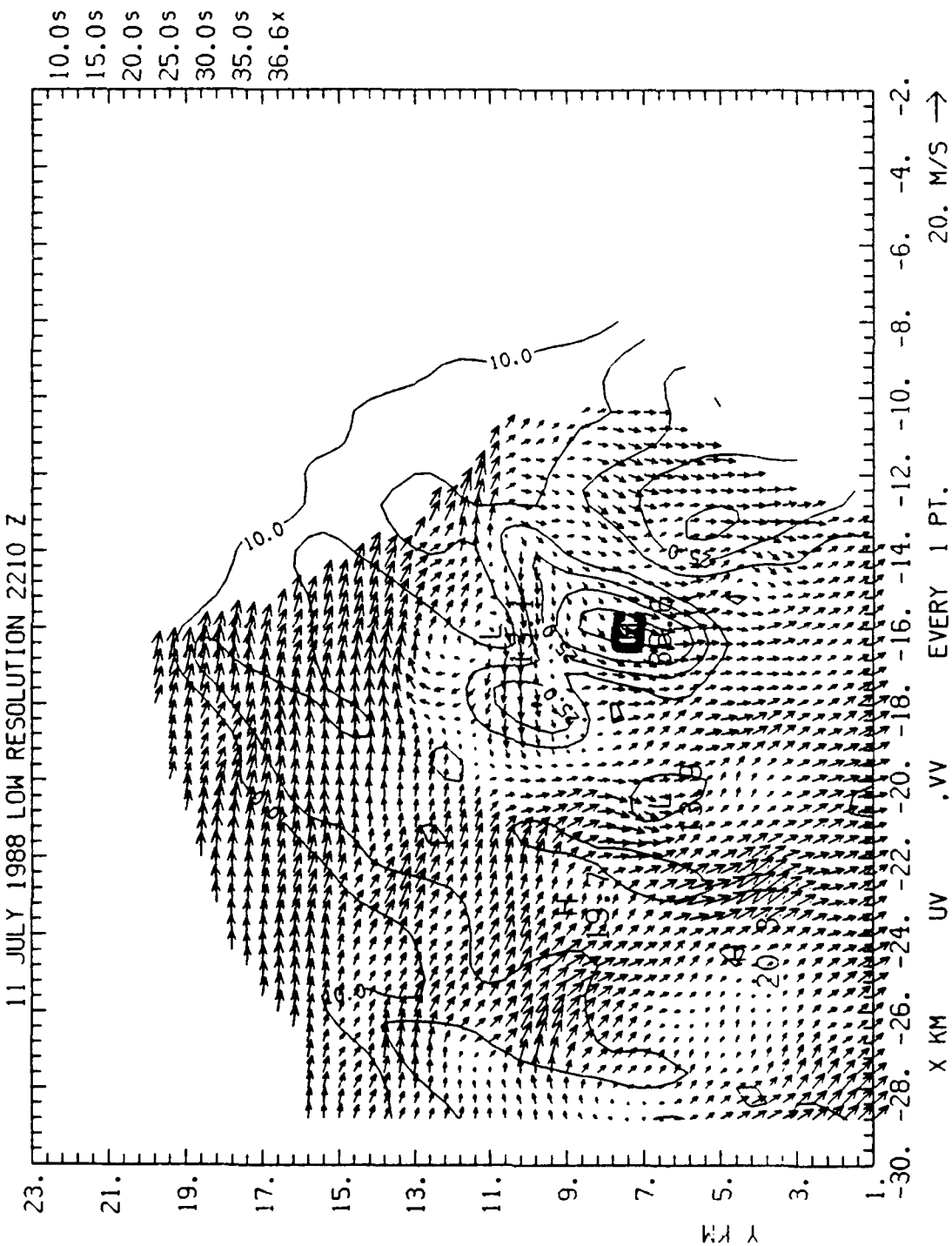
88/ 7/11 22 10 47-22 10 47 COMBIN Z = 0.19 KM DBZ  
 (AS OF 06/23/89) ORIGIN=( 0.00, 0.00) KM X-AXIS= 90.0 DEG



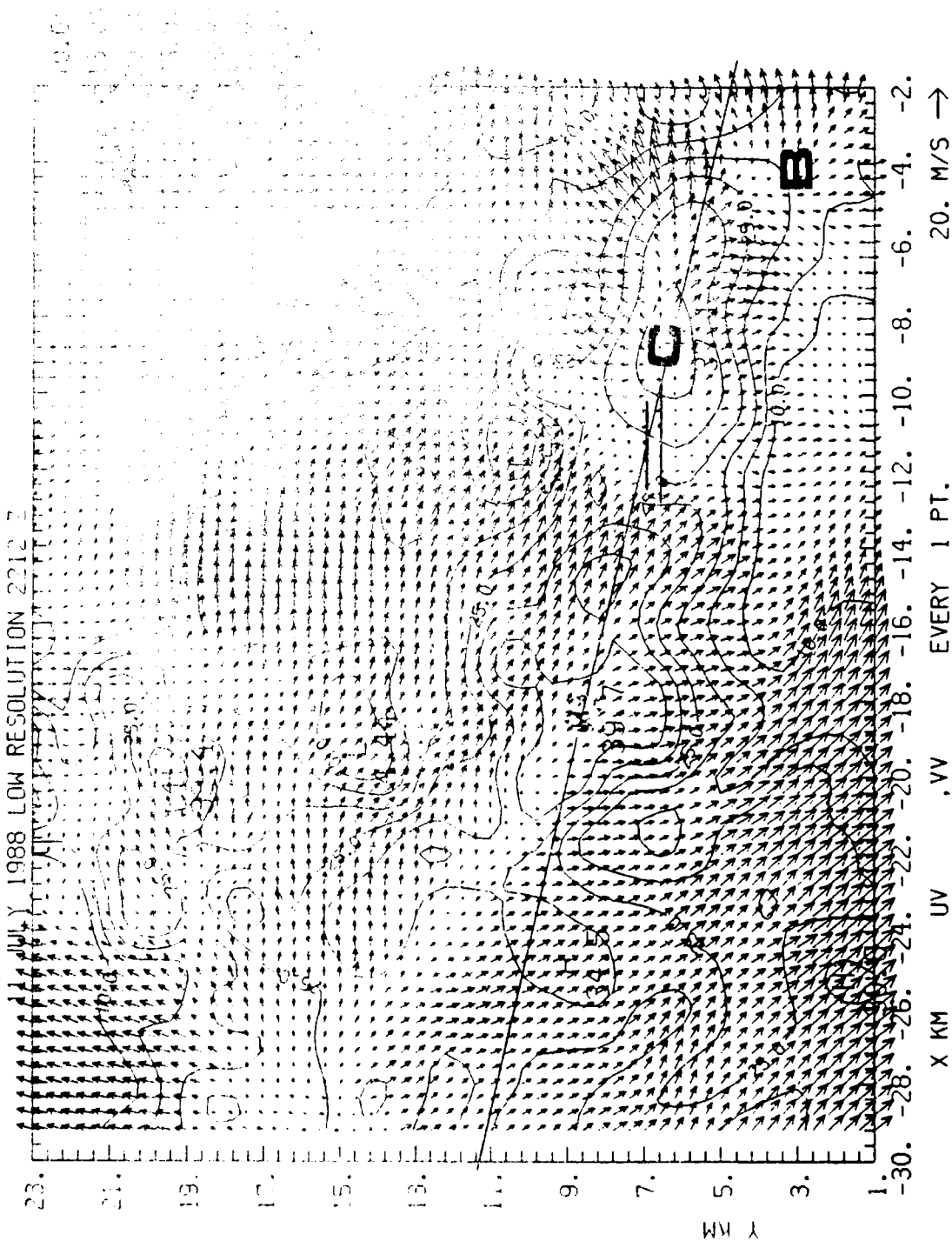
88/ 7/11 22 10 47-22 10 47 COMBIN Z = 4.69 KM DBZ  
 (AS OF 06/23/89) ORIGIN=( 0.00, 0.00) KM X-AXIS= 90.0 DEG



88/ 7/11 22 10 47-22 10 47 COMBIN Z = 7.69 KM DBZ  
 (AS OF 06/23/89) ORIGIN=( 0.00, 0.00) KM X-AXIS= 90.0 DEG



88/ 7/11      22 12 47-22 12 47      COMBIN      Z =    0.19 KM      DBZ  
 (AS OF 06/23/89)      ORIGIN=1    0.00,    0.00) KM    X-AXIS= 90.0 DEG



88/ 7/11 22 12 47-22 12 47 COMBIN Z = 4.69 KM DBZ  
 (AS OF 06/23/89) ORIGIN=( 0.00, 0.00) KM X-AXIS= 90.0 DEG

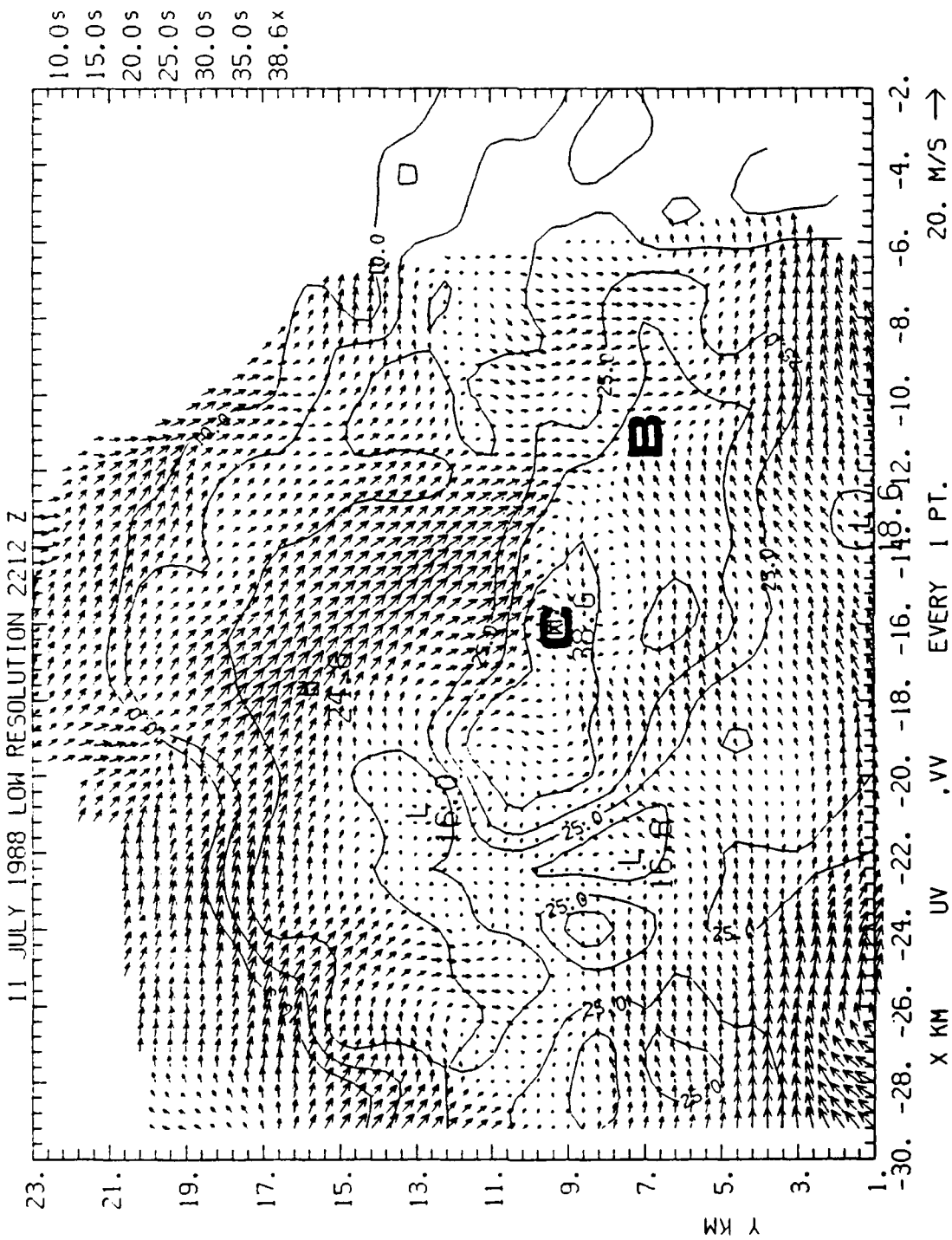
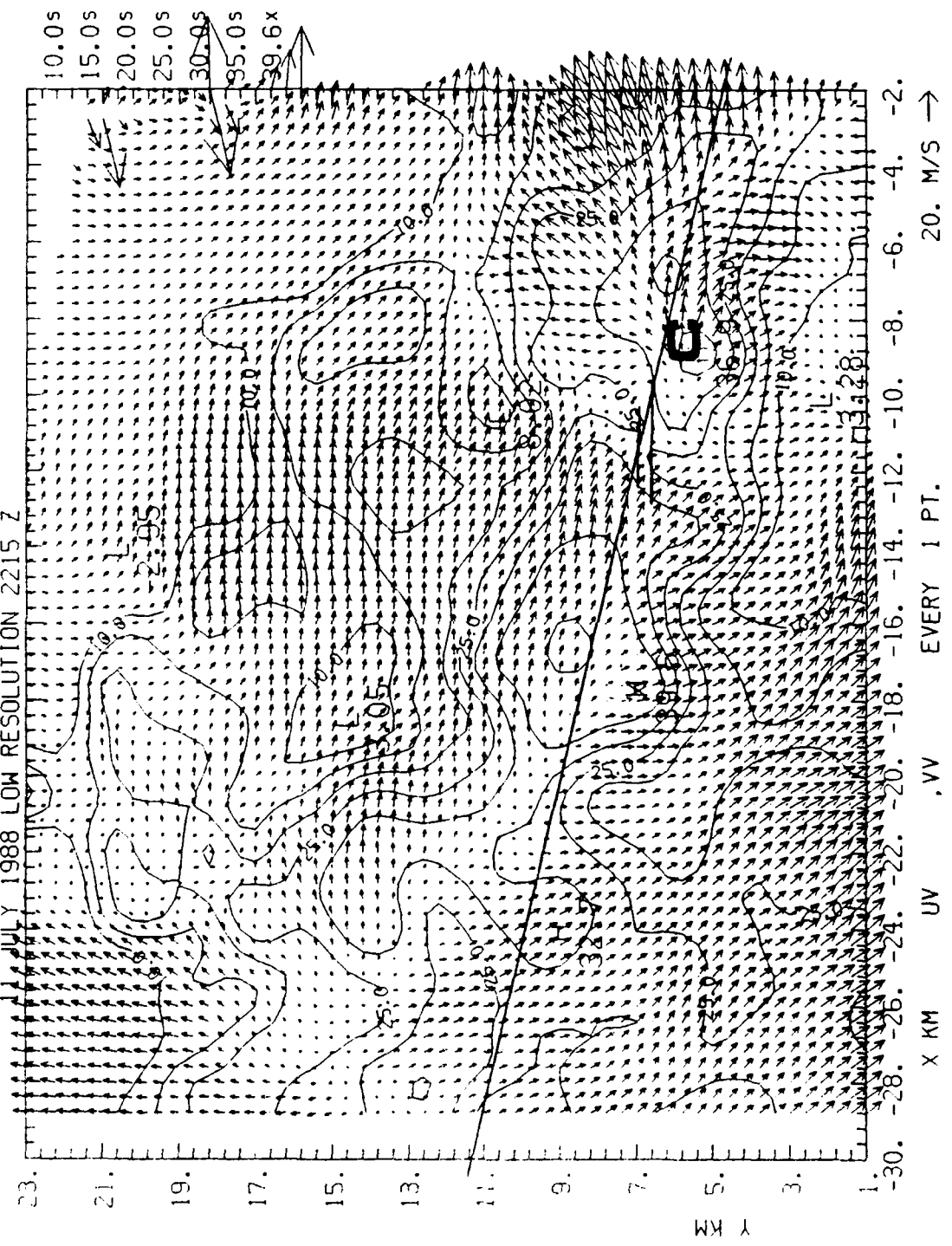


Figure 1 is a map of the North Pacific region, showing the distribution of sea surface temperature (SST) and wind vectors. The map covers the area from 30°N to 10°N latitude and 180° to 150°W longitude. The SST contours are labeled with values such as 10.0, 15.0, 20.0, 25.0, 30.0, and 30.7. The wind vectors are represented by arrows, with a scale of 10 m/s. The map includes a latitude/longitude grid and a title "Figure 1".

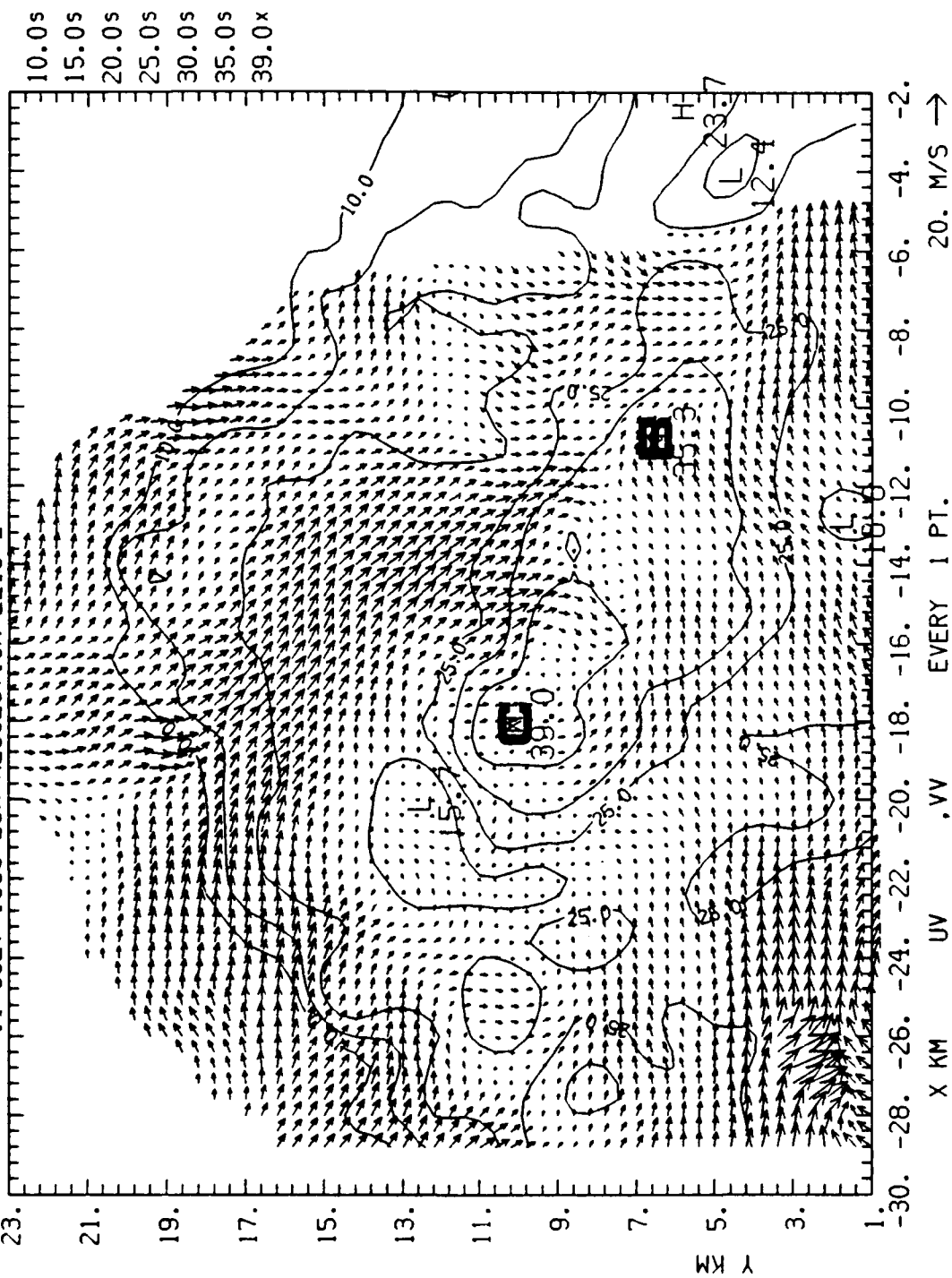
88/ 7/11 22 15 47-22 15 47 COMBIN Z = 0.19 KM DBZ  
 (AS OF 06/23/89) ORIGIN=1 0.00, 0.00) KM X-AXIS= 90.0 DEG



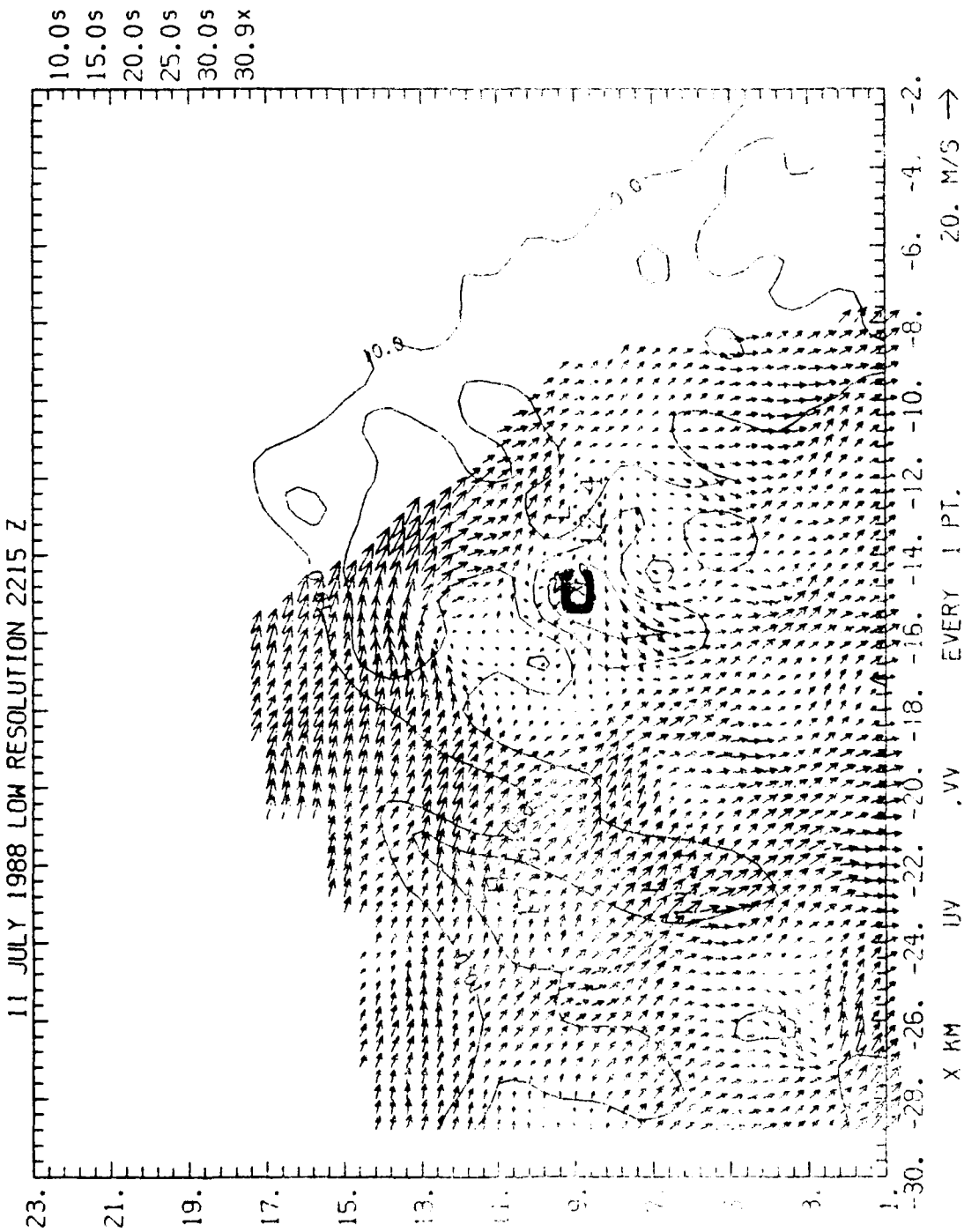


88/ 7/11 22 15 47-22 15 47 COMBIN Z = 4.69 KM DBZ  
(AS OF 06/23/89) ORIGIN={ 0.00, 0.00) KM X-AXIS= 90.0 DEG

11 JULY 1988 LOW RESOLUTION 2215 Z



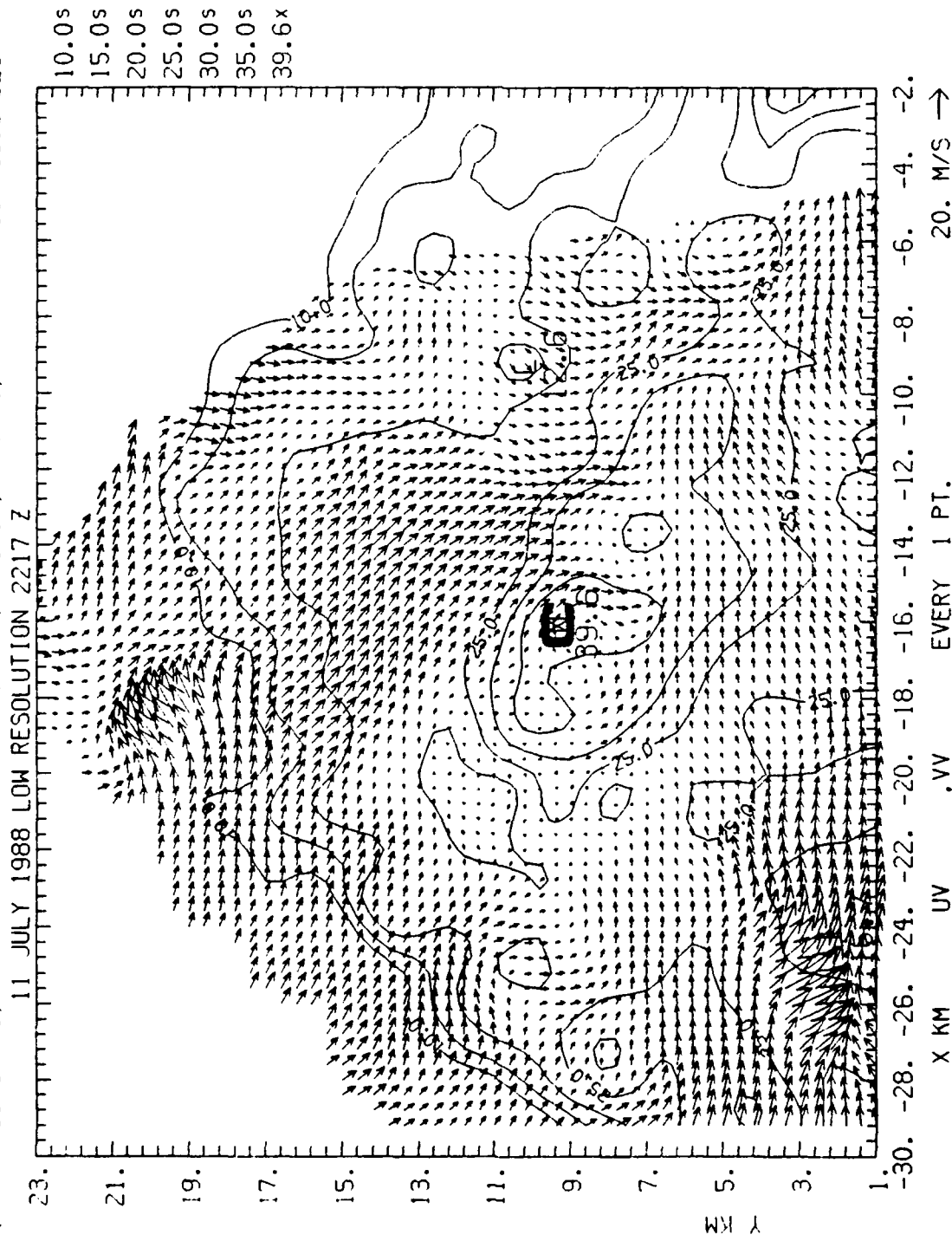
88/ 7/11 22 15 47-22 15 47 COMBIN Z = 7.69 KM DBZ  
(AS OF 06/23/89) ORIGIN=( 0.00, 0.00) KM X-AXIS= 90.0 DEG



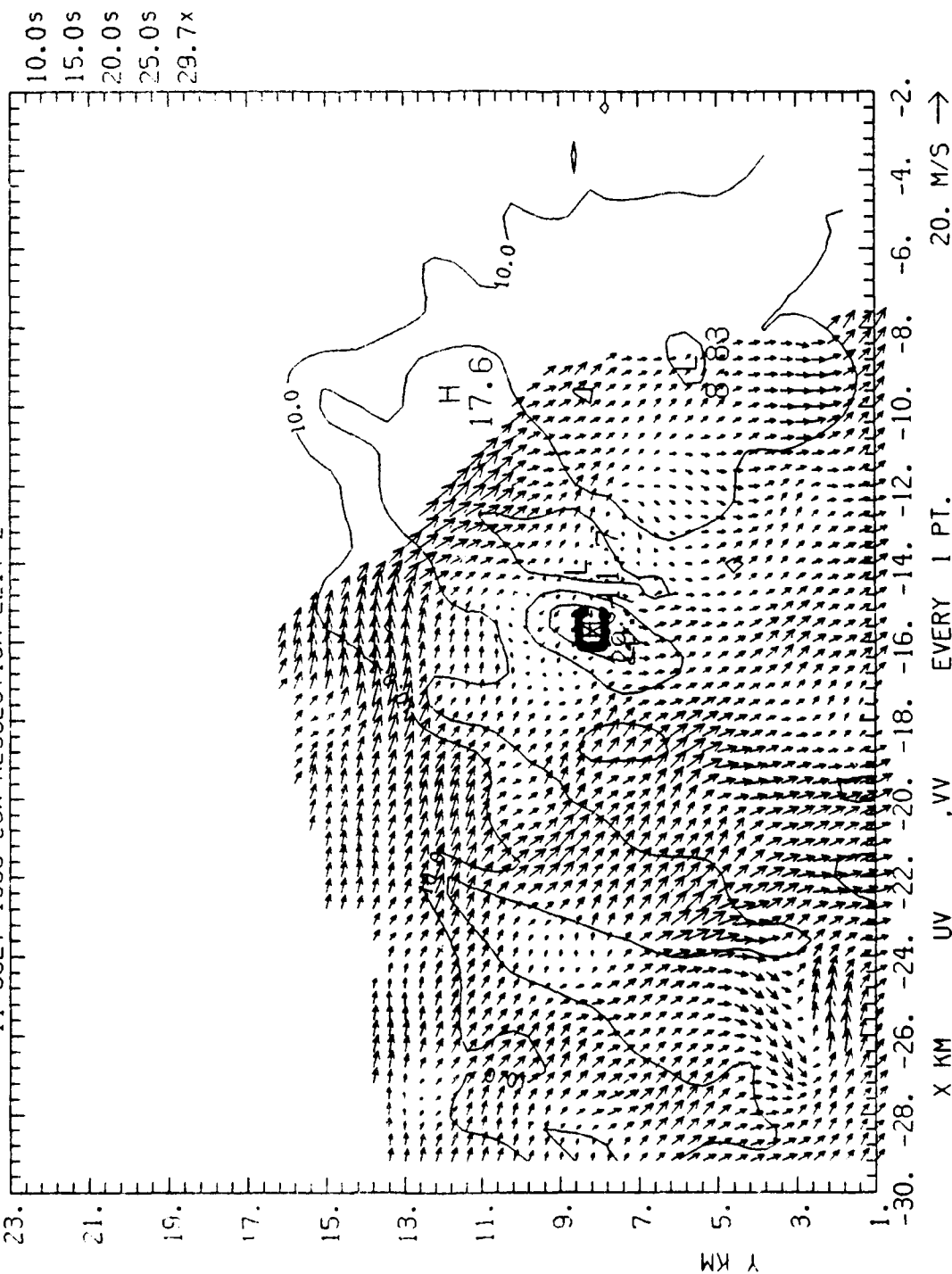
88/ 7/11 22 17 47-22 17 47 COMBIN Z = 0.19 KM DBZ  
 (AS OF 06/23/89) ORIGIN=1 0.00, 0.00) KM X-AXIS= 90.0 DEG



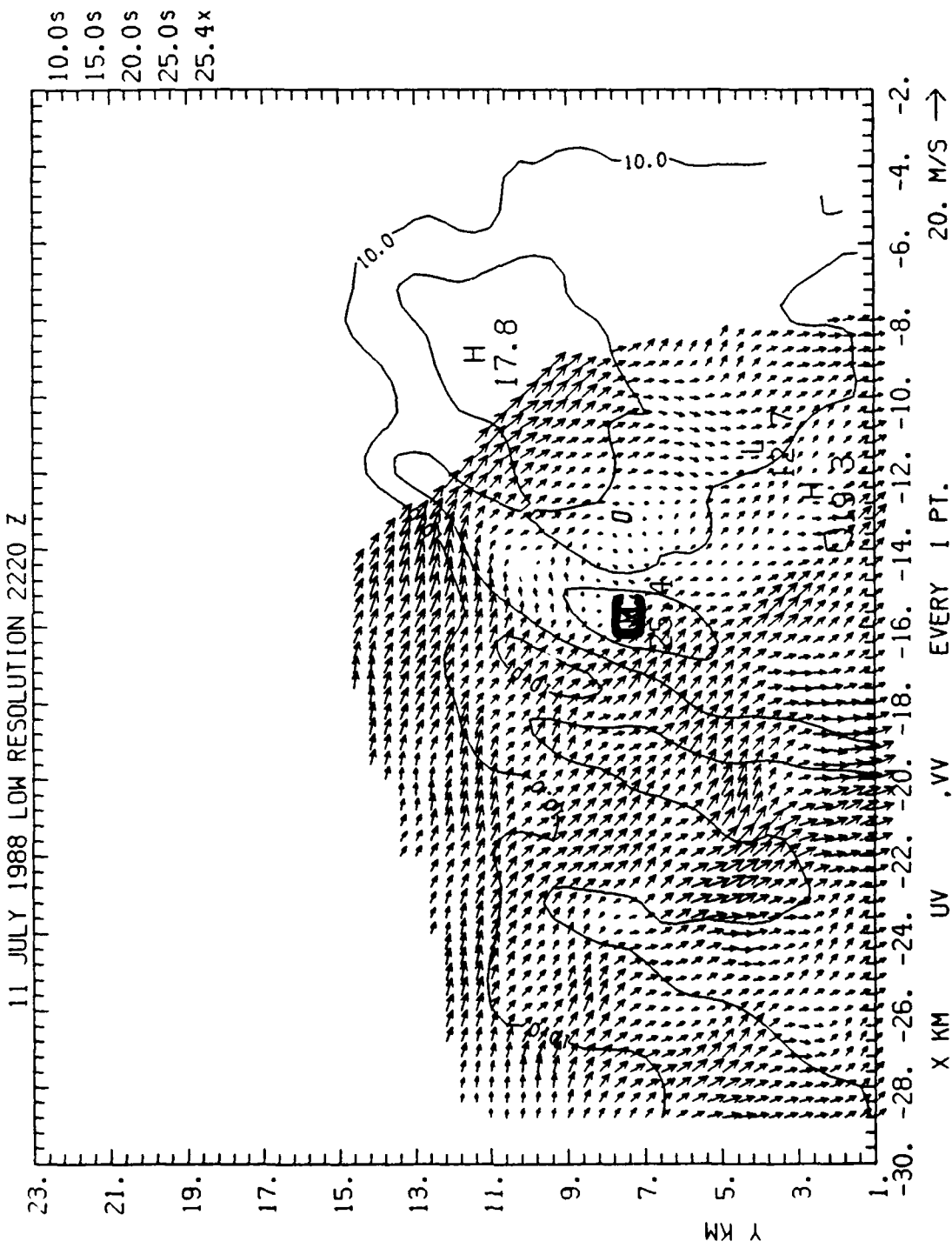
88/ 7/11 22 17 47-22 17 47 COMBIN Z = 4.69 KM DBZ  
 (AS OF 06/23/89) ORIGIN=( 0.00, 0.00) KM X-AXIS= 90.0 DEG



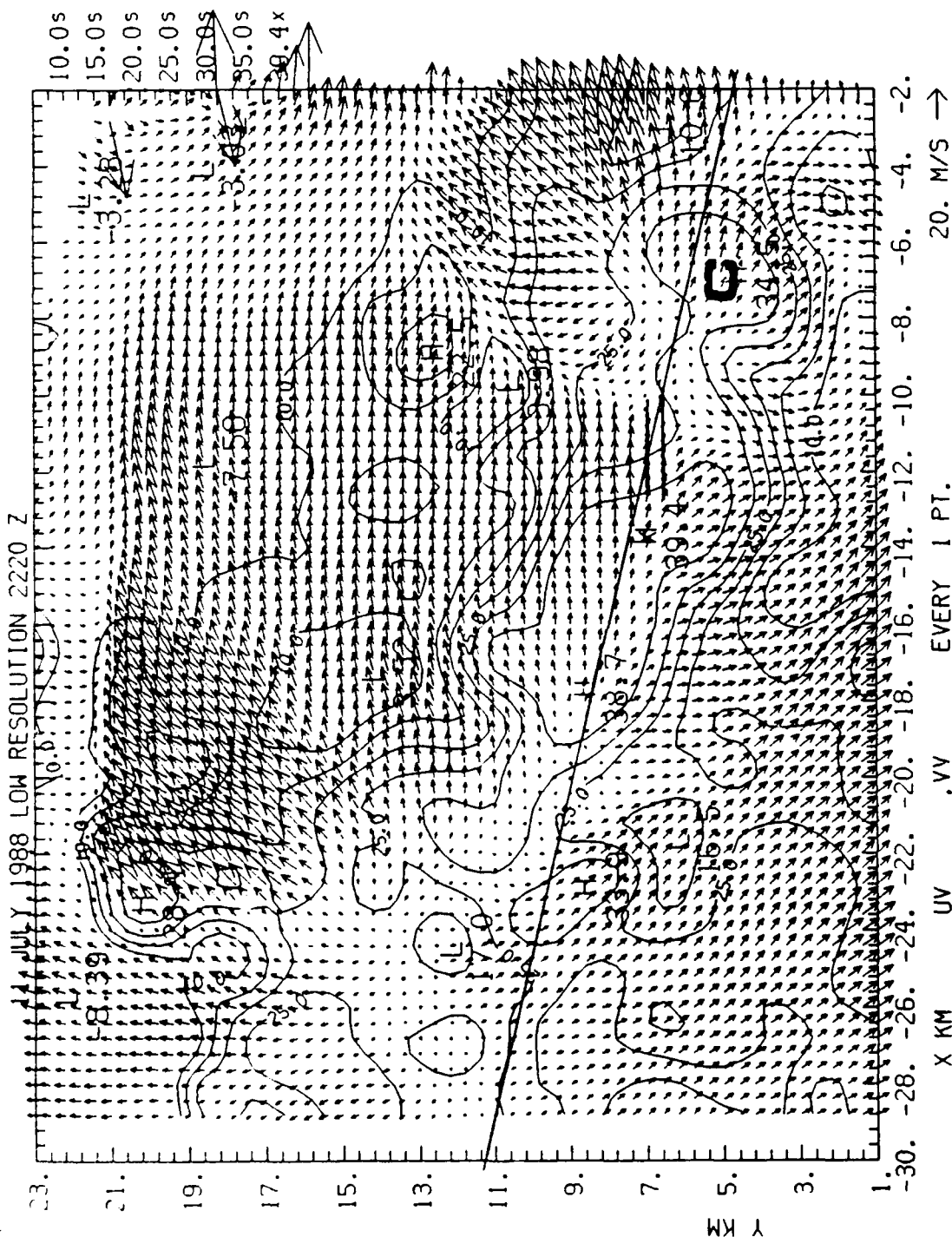
88/ 7/11 22 17 47-22 17 47 COMBIN Z = 7.69 KM DBZ  
 (HS OF 06/23/89) ORIGIN=( 0.00. 0.00) KM X-AXIS= 90.0 DEG  
 11 JULY 1988 LOW RESOLUTION 2217 Z



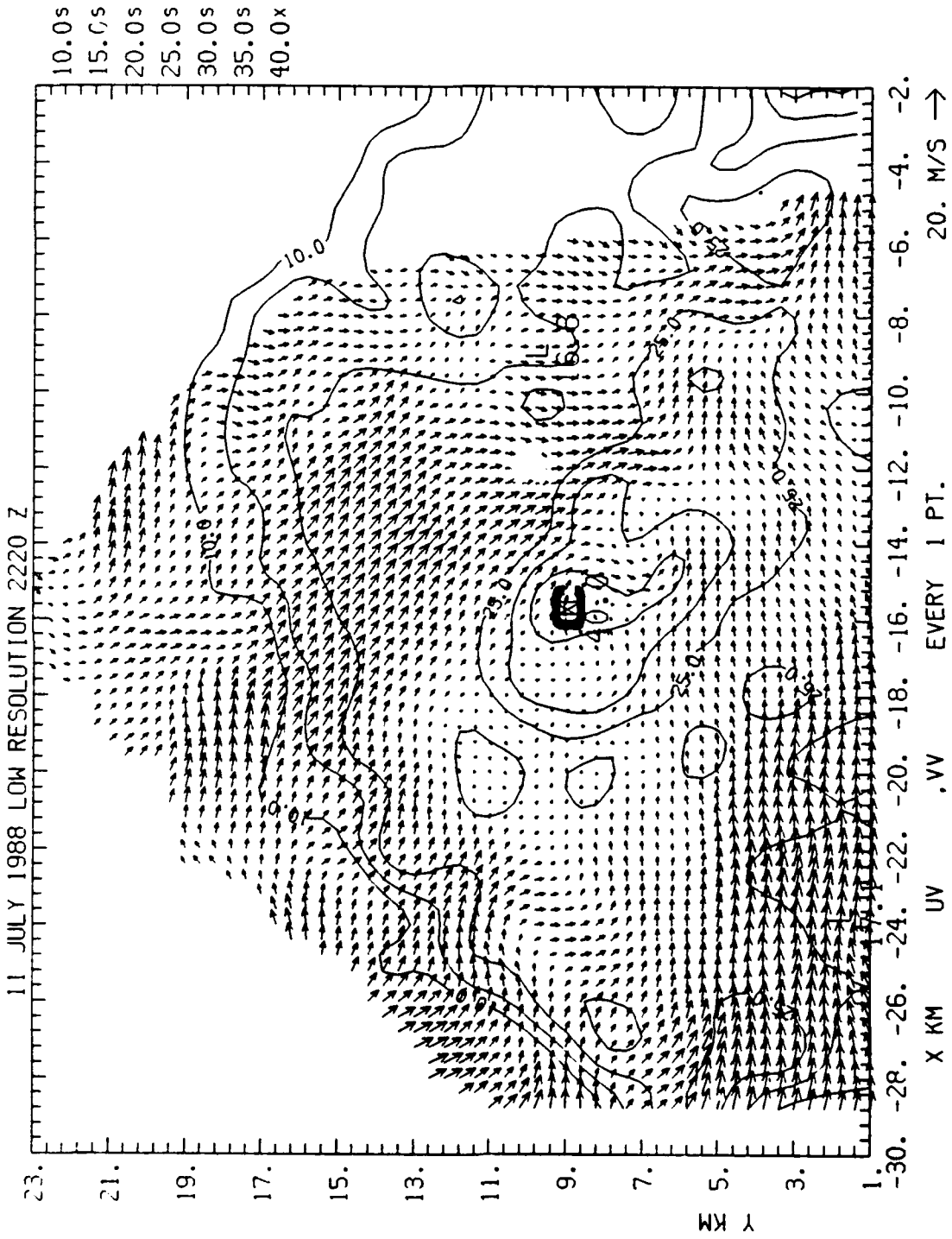
88/ 7/11 22 20 47-22 20 47 COMBIN Z = 7.69 KM DBZ  
 (AS OF 06/23/89) ORIGIN=( 0.00, 0.00) KM X-AXIS= 90.0 DEG



88/ 7/11 22 20 47-22 20 47 COMBIN Z = 0.19 KM DBZ  
 (AS OF 06/23/89) ORIGIN=( 0.00, 0.00) KM X-AXIS= 90.0 DEG



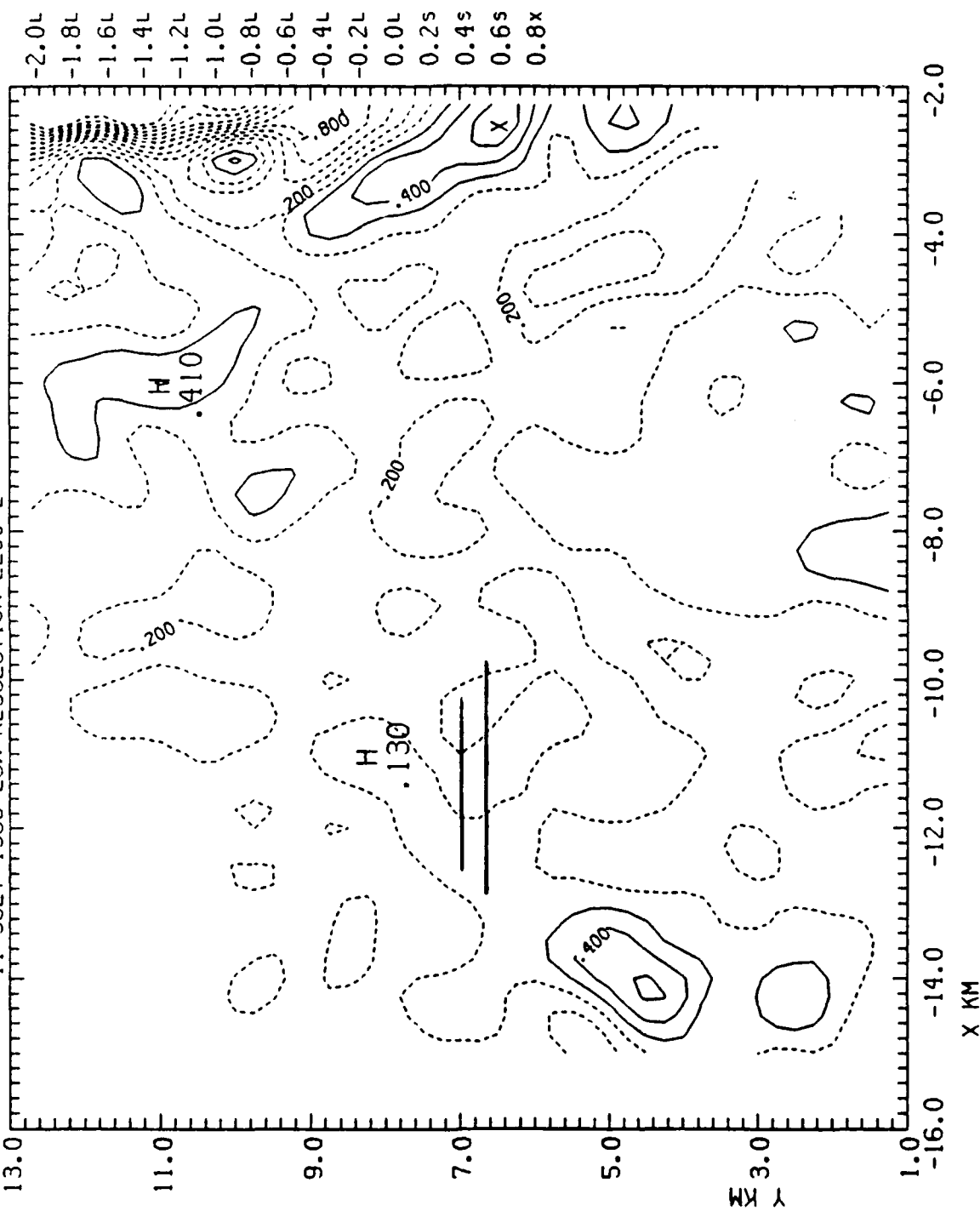
88/ 7/11 22 20 47-22 20 47 COMBIN Z = 4.69 KM DBZ  
 (AS OF 06/23/89) ORIGIN=( 0.00, 0.00) KM X-AXIS= 90.0 DEG







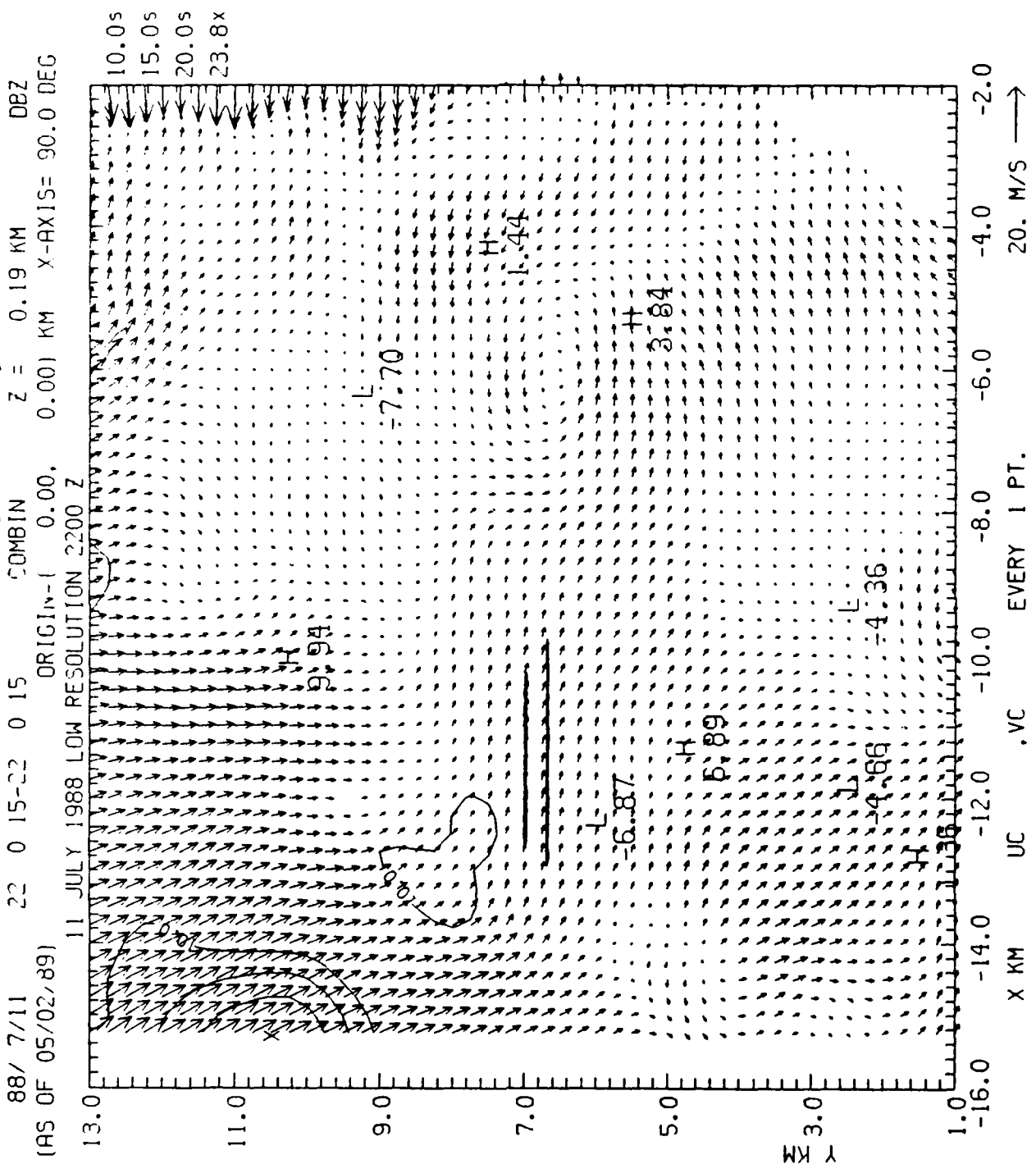
88/ 7/11 22 0 15-22 0 15 COMBIN Z = 0.19 KM F  
 (AS OF 05/02/89) ORIGIN: ( 0.00, 0.00) KM X-AXIS= 90.0 DEG  
 11 JULY 1988 LOW RESOLUTION 2200 Z



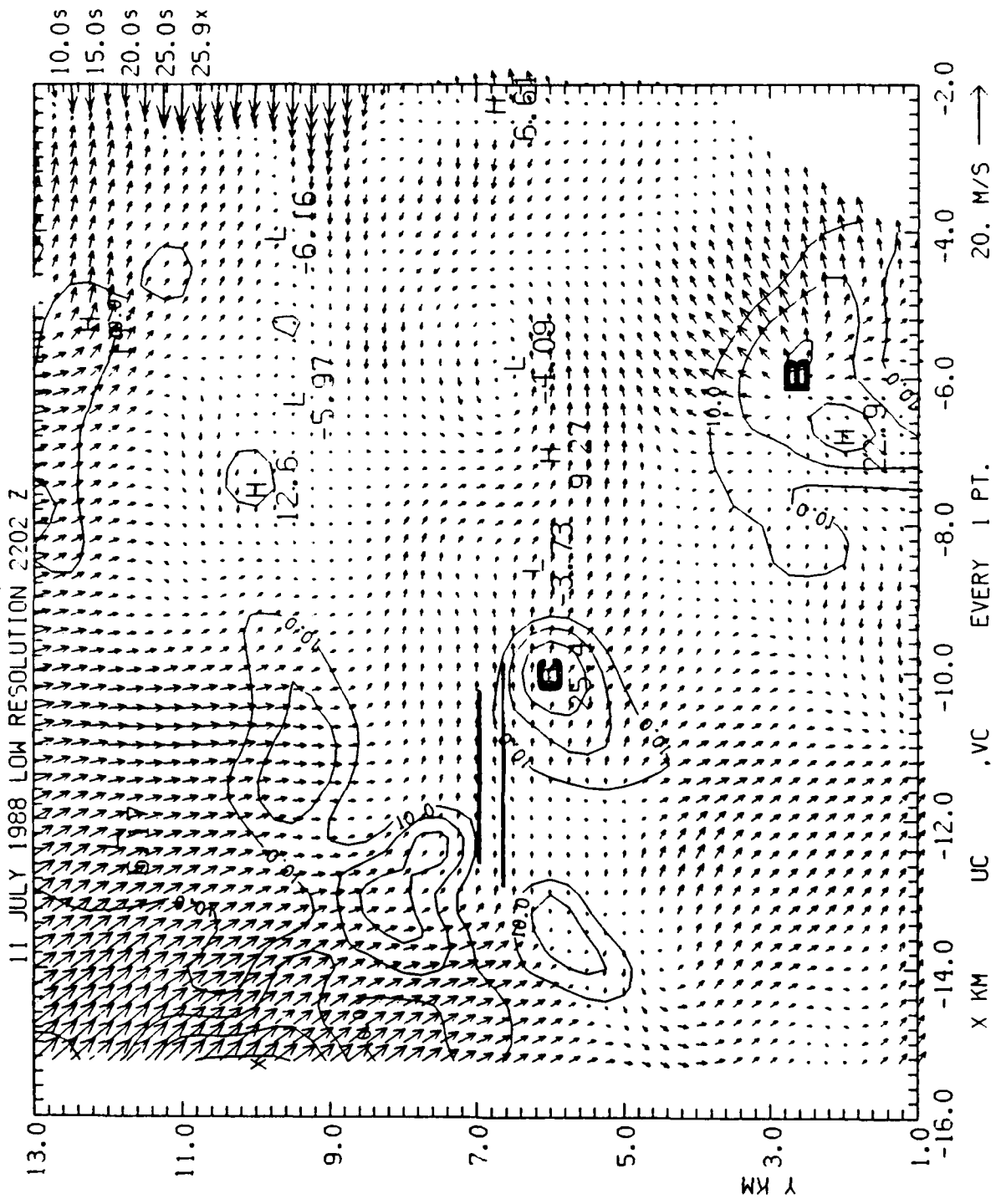
## **Appendix I: Dual Doppler Radar High Resolution Analyses**

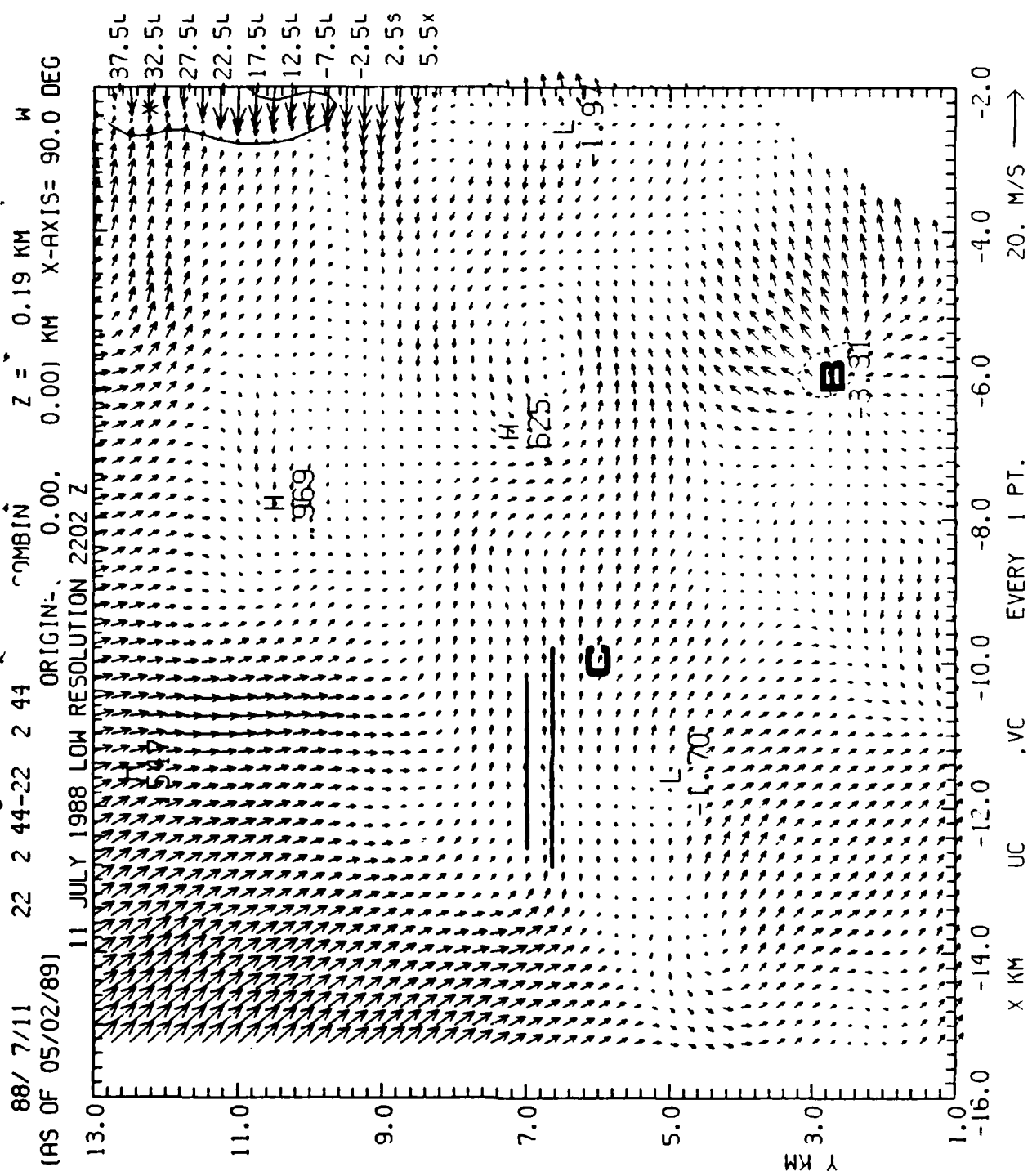
These plots show horizontal wind vectors with radar reflectivity, vertical velocity and east-west F-factor contours overlaid for 0.19 km AGL (1.8 km MSL). X and Y axis labels are in km east and north of the FL2 radar, respectively. The top line above each plot gives the date, time, altitude AGL and overlay field. (Disregard the title 'low resolution' on the third line above the plots.) On the right are the contour levels (values followed by 's') and maximum field value (value followed by 'x'). A scale wind vector is provided in the lower right hand corner. Relative minima ('L') and maxima ('H') of the contoured field are indicated on the diagrams.

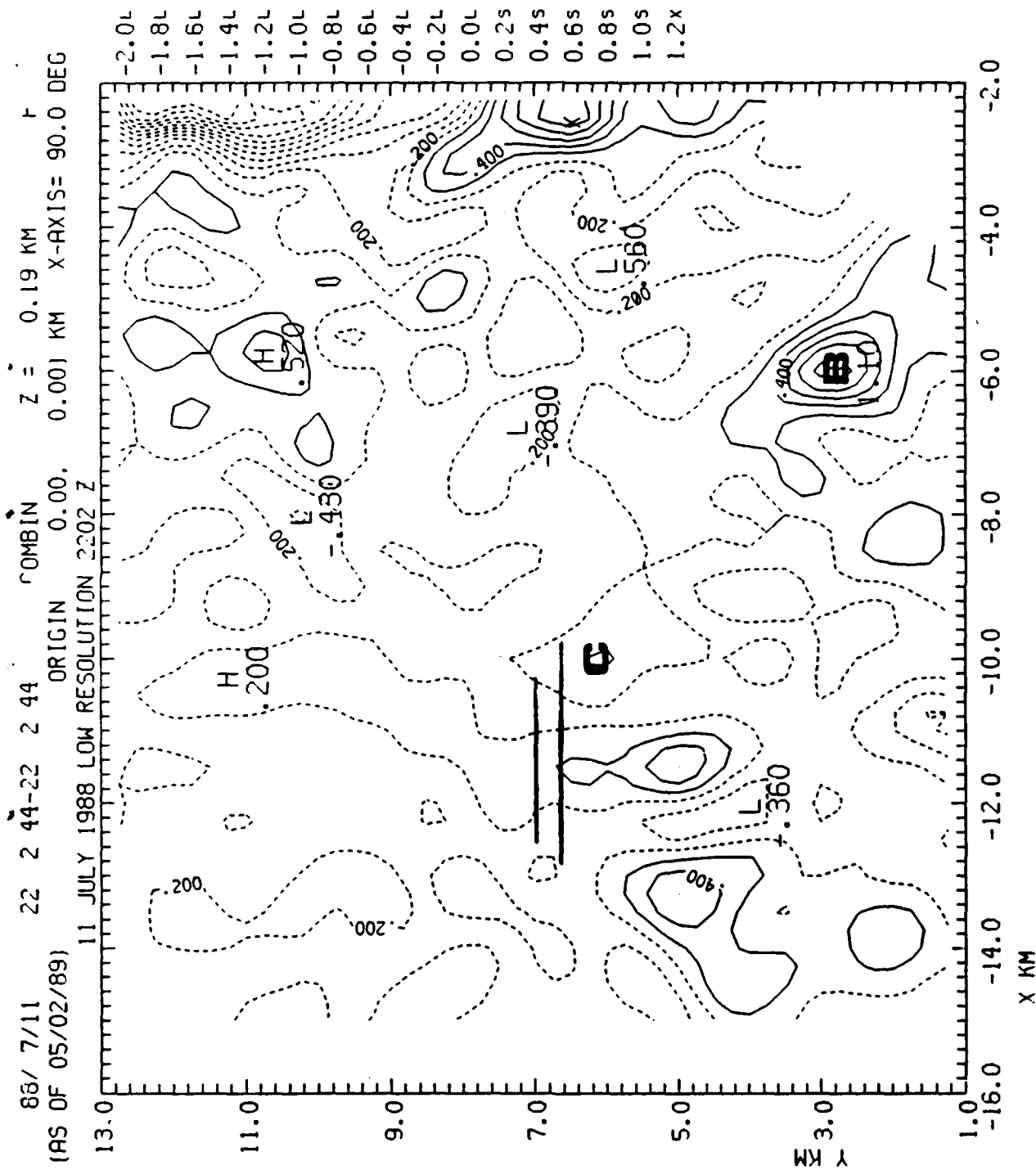
The analysis techniques used to produce these plots are described in the text.

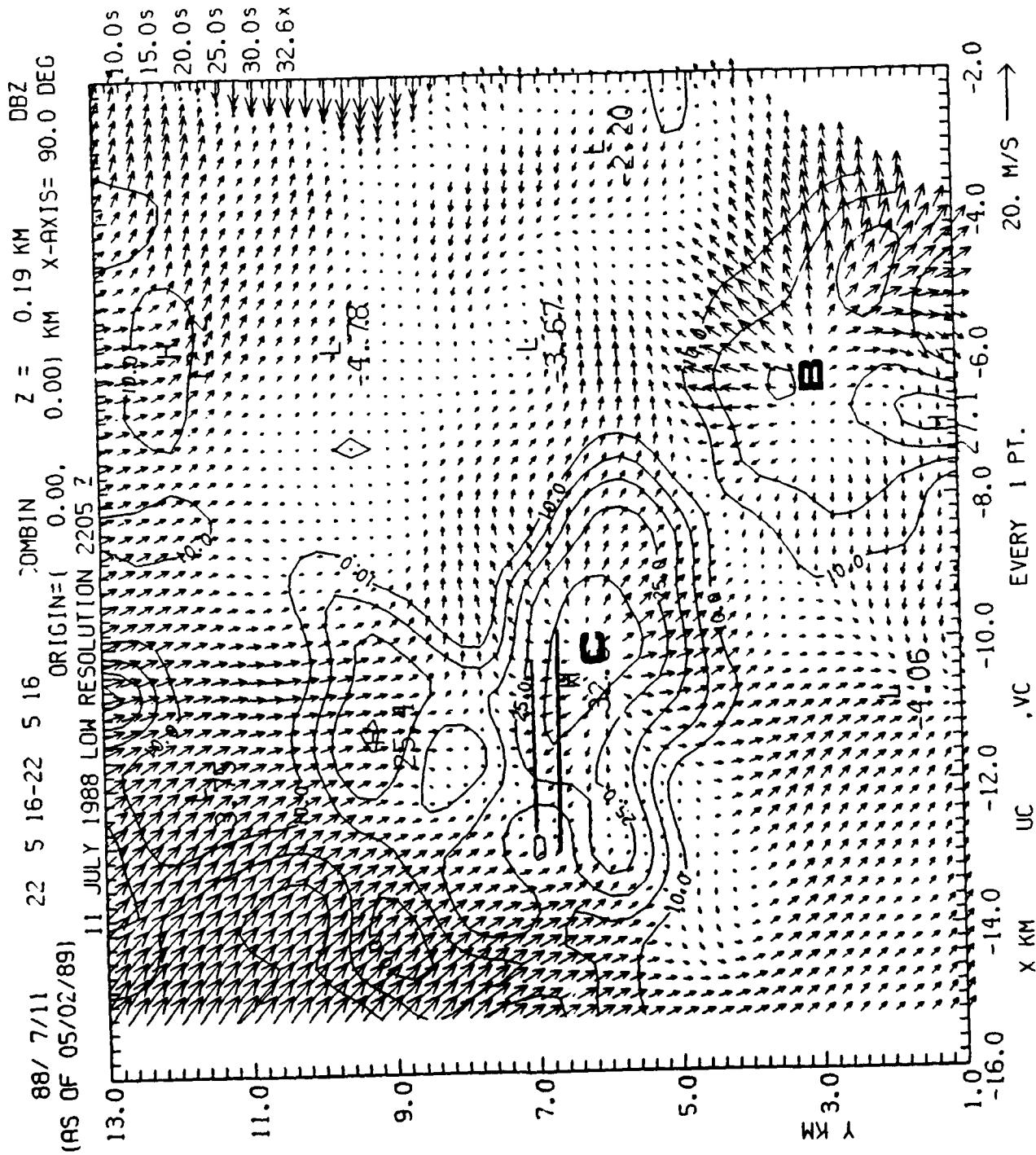


88/ 7/11 22 2 44-22 2 44 COMBIN Z = 0.19 KM DBZ  
 (AS OF 05/02/89) ORIGI ( 0.00, 0.00) KM X-AXIS= 90.0 DEG

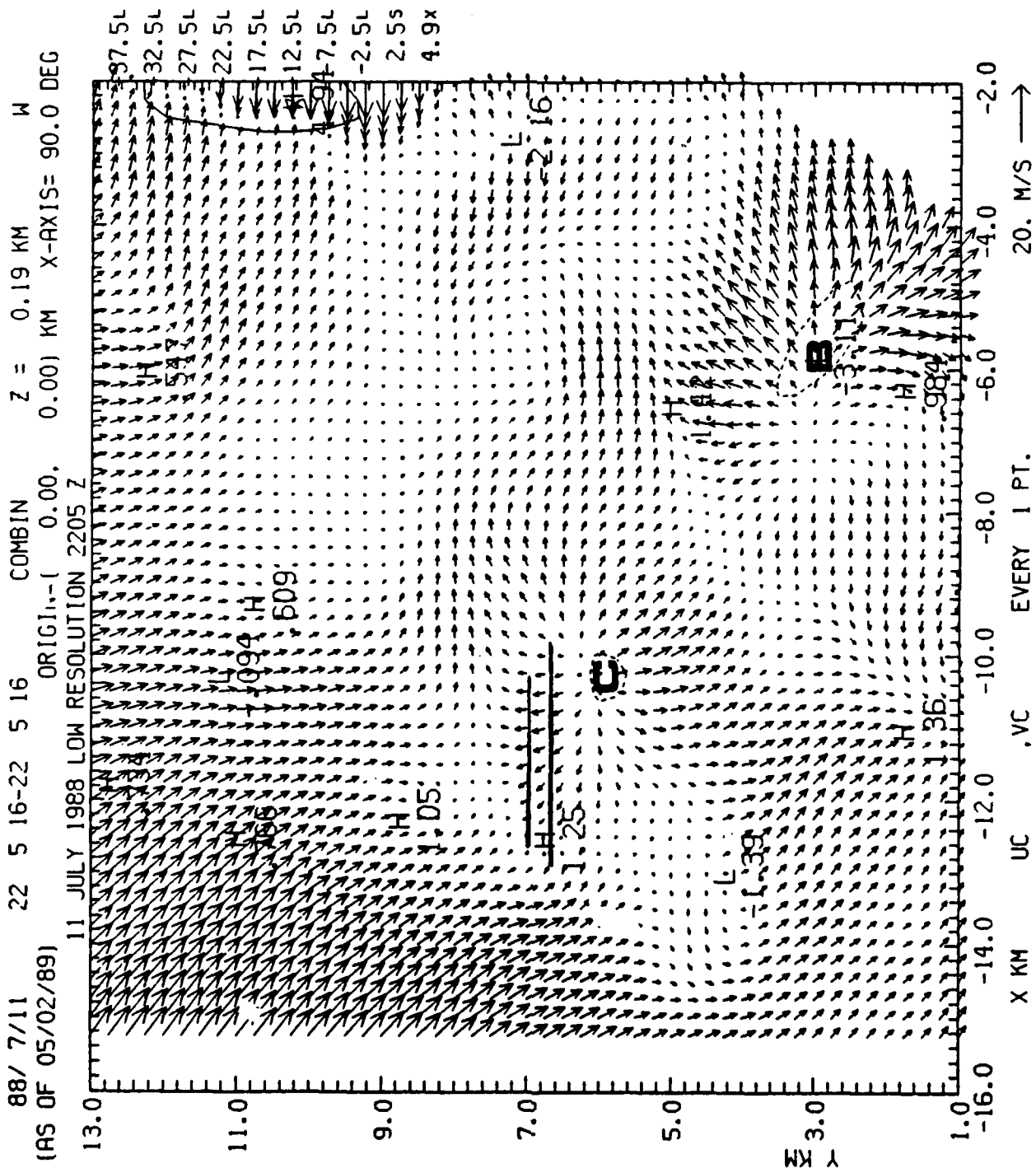




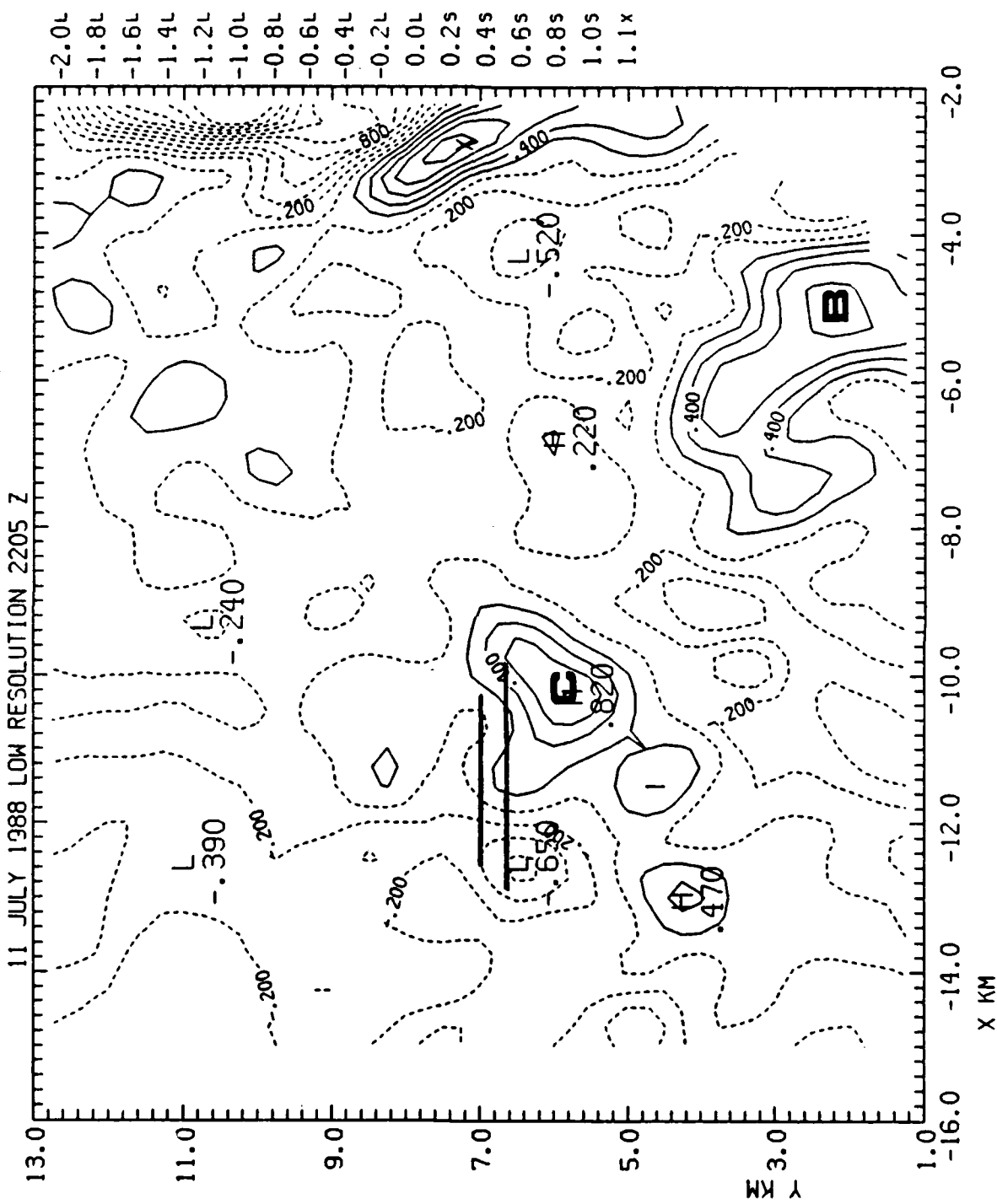




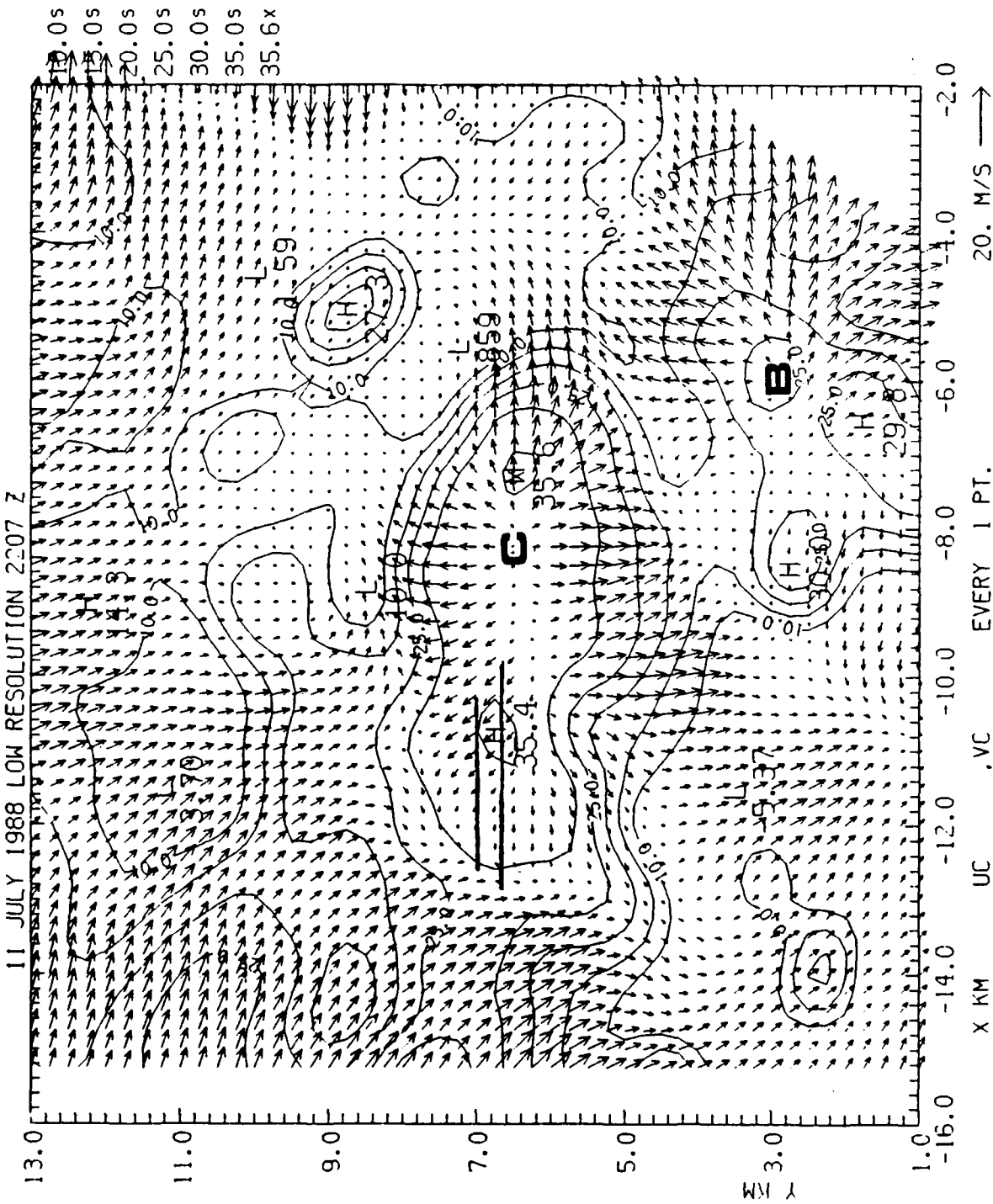




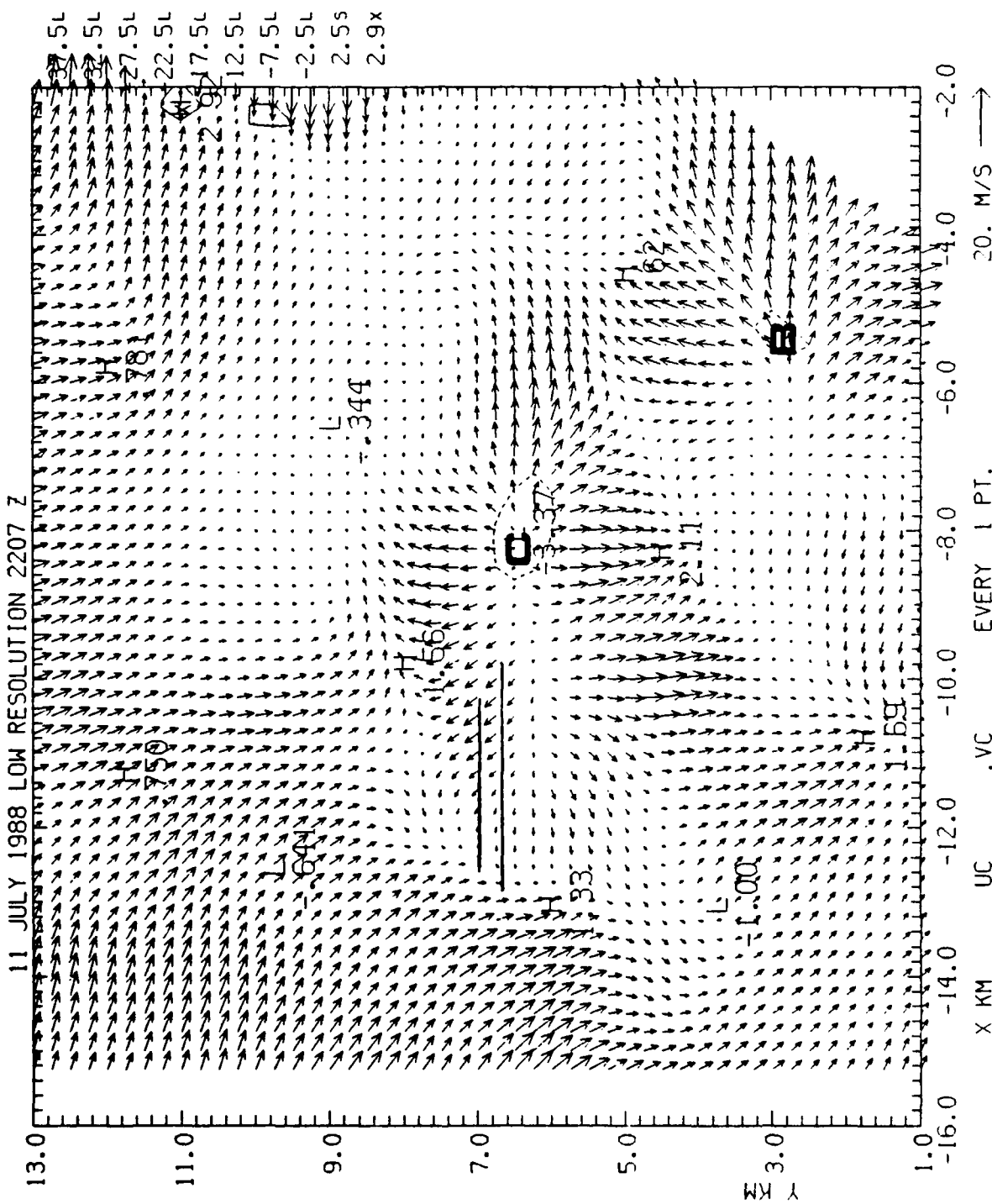
88/ 7/11 22 5 16-22 5 16 COMBIN Z = 0.19 KM F  
 (AS OF 05/02/89) ORIGIN--( 0.00, 0.00) KM X-AXIS= 90.0 DEG

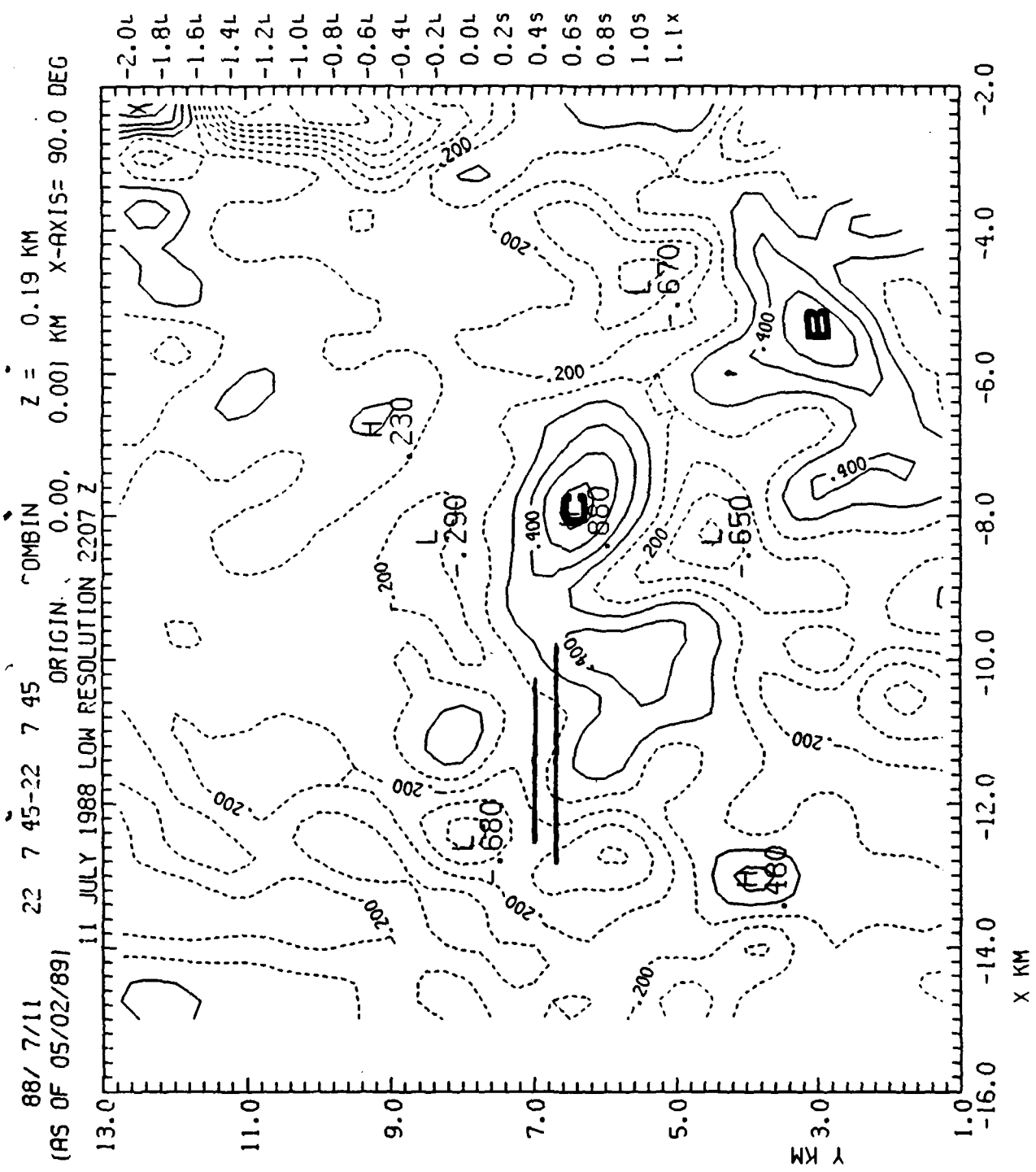


88/ 7/11 22 7 45-22 7 45 COMBIN Z = 0.19 KM DBZ  
 (AS OF 05/02/89) ORIGIN 0.00, 0.00) KM X-AXIS= 90.0 DEG



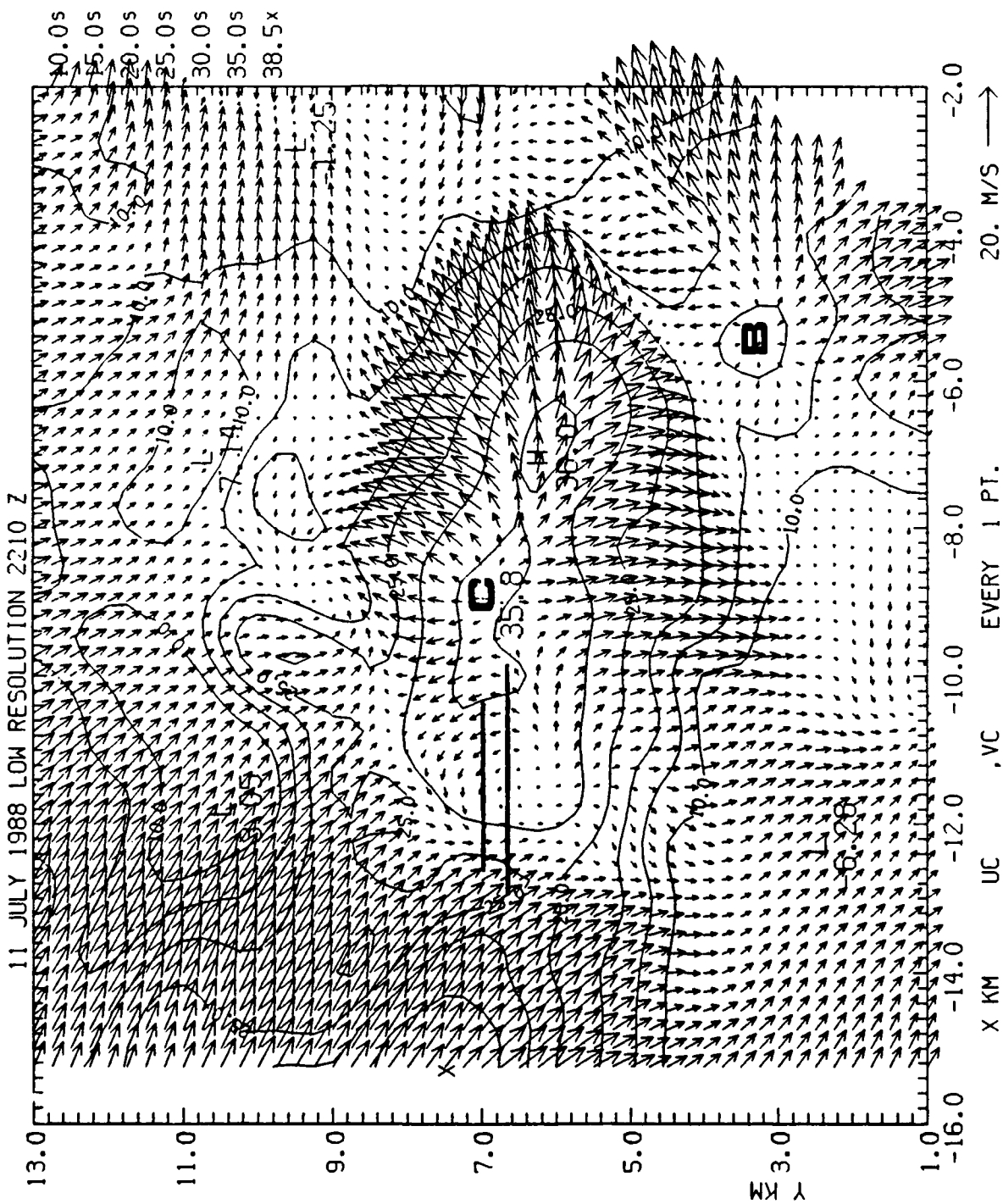
88/ 7/11 22 7 45-22 7 45 0MBIN Z = 0.19 KM W  
(AS OF 05/02/89) ORIGIN = 0.00, 0.00) KM X-AXIS= 90.0 DEG





8.

88/ 7/11 22 10 19-22 10 19 COMBIN Z = 0.19 KM DBZ  
(AS OF 05/02/89) ORIG1...- ( 0.00, 0.00) KM X-AXIS= 90.0 DEG



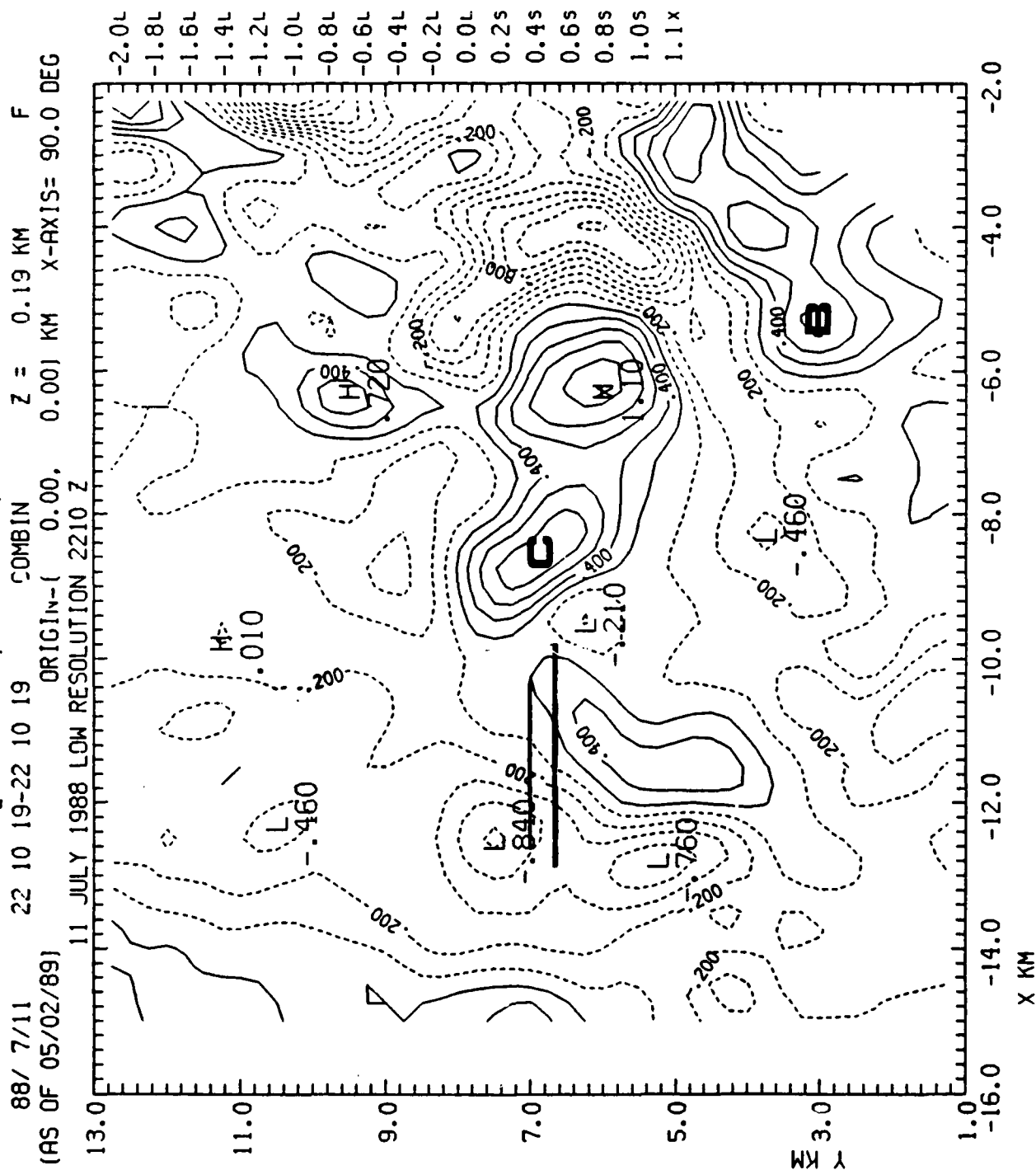
88/ 7/11 22 10 19-22 10 19 COMBIN Z = 0.19 KM W  
(AS OF 05/02/89) ORIGIN-( 0.00, 0.00) KM X-AXIS= 90.0 DEG  
11 JULY 1988 LOW RESOLUTION 2210 Z

13.0 11.0 9.0 7.0 5.0 3.0 1.0  
-16.0 -14.0 -12.0 -10.0 -8.0 -6.0 -4.0 -2.0  
X KM UC ,VC EVERY 1 PT. 20 M/S →

37.5L 32.5L 27.5L 22.5L 17.5L 12.5L 7.5L 2.5L 4.3x  
1.56 1.56 1.56 1.56 1.56 1.56 1.56 1.56 1.56

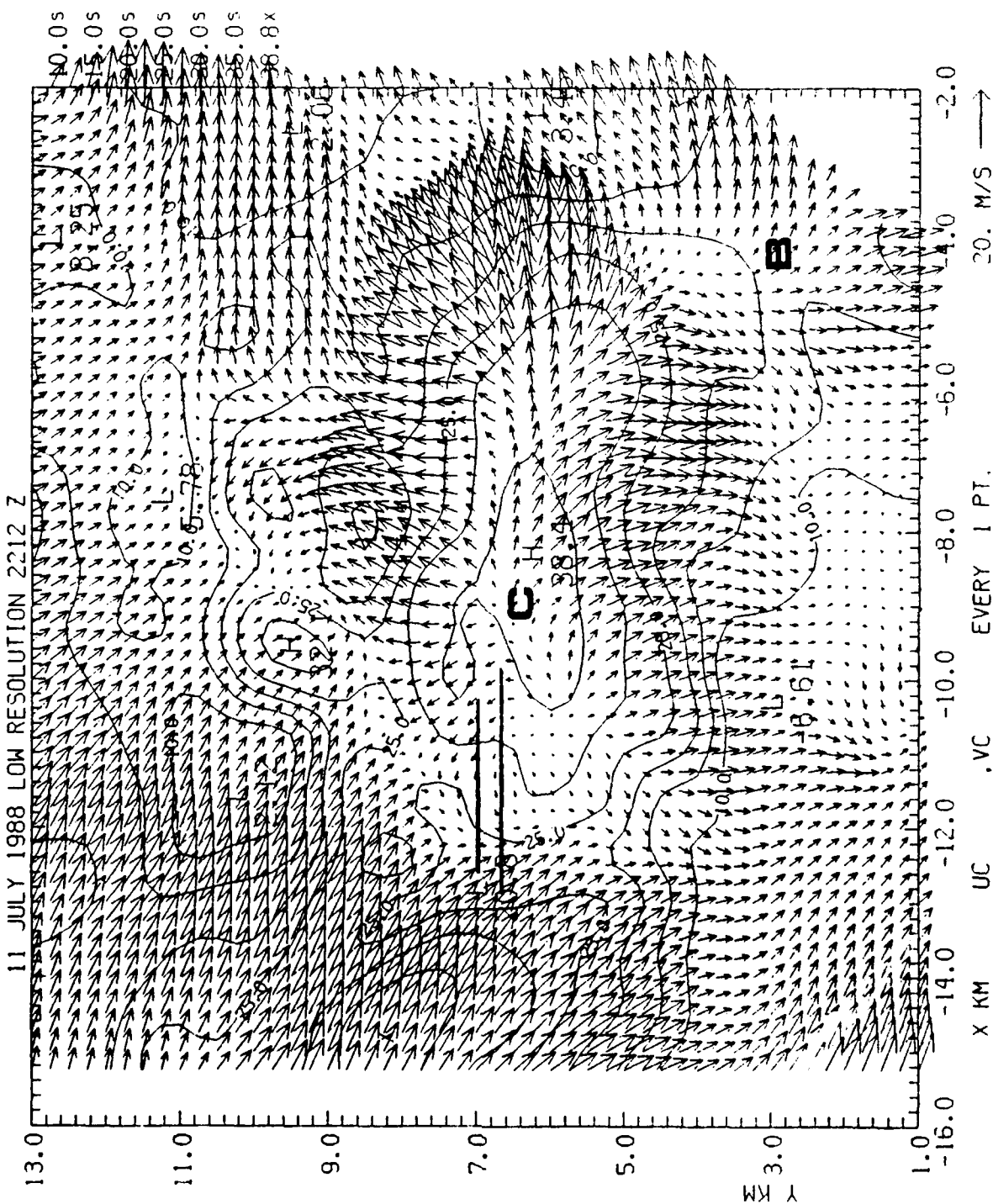
B

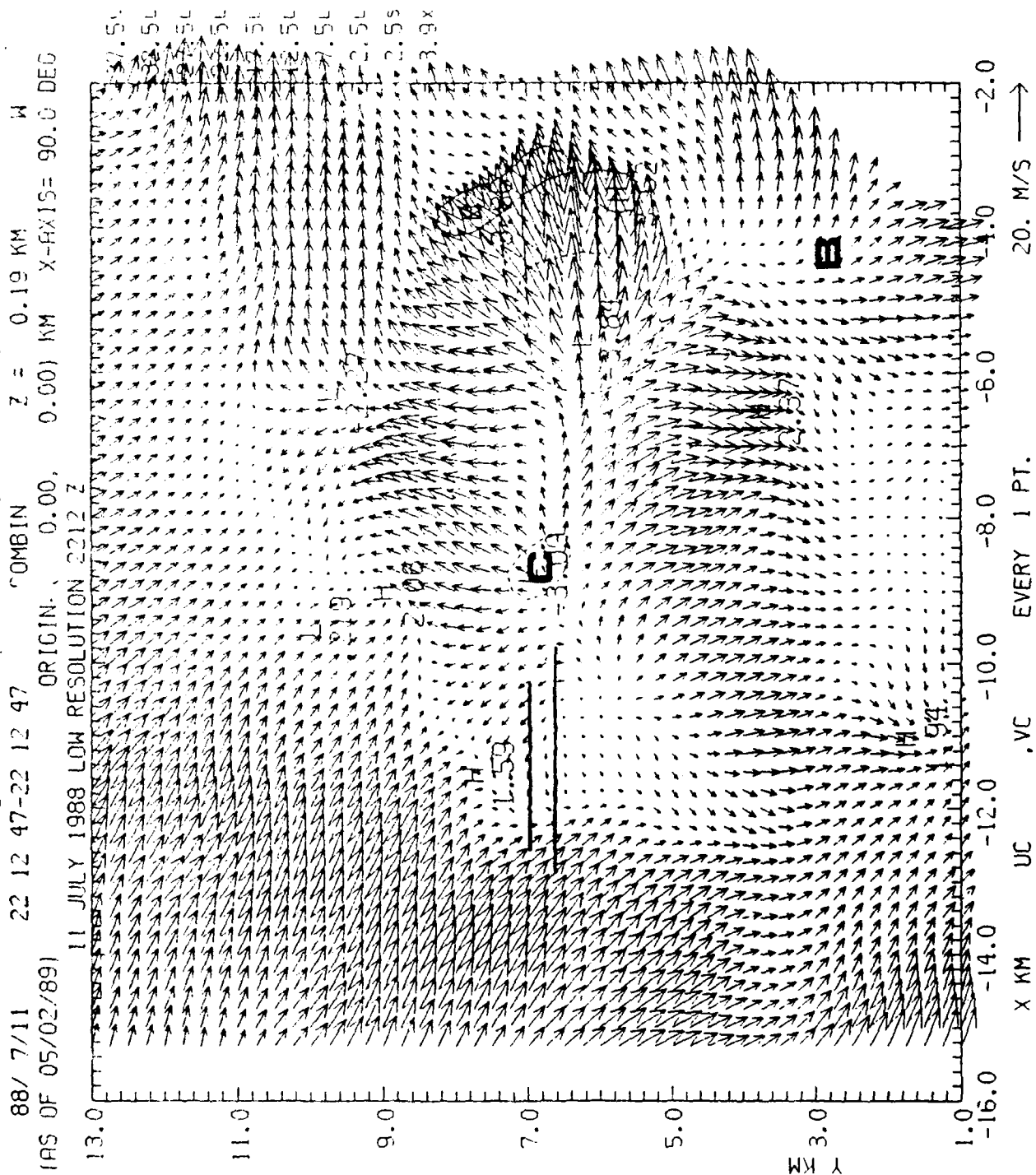
11



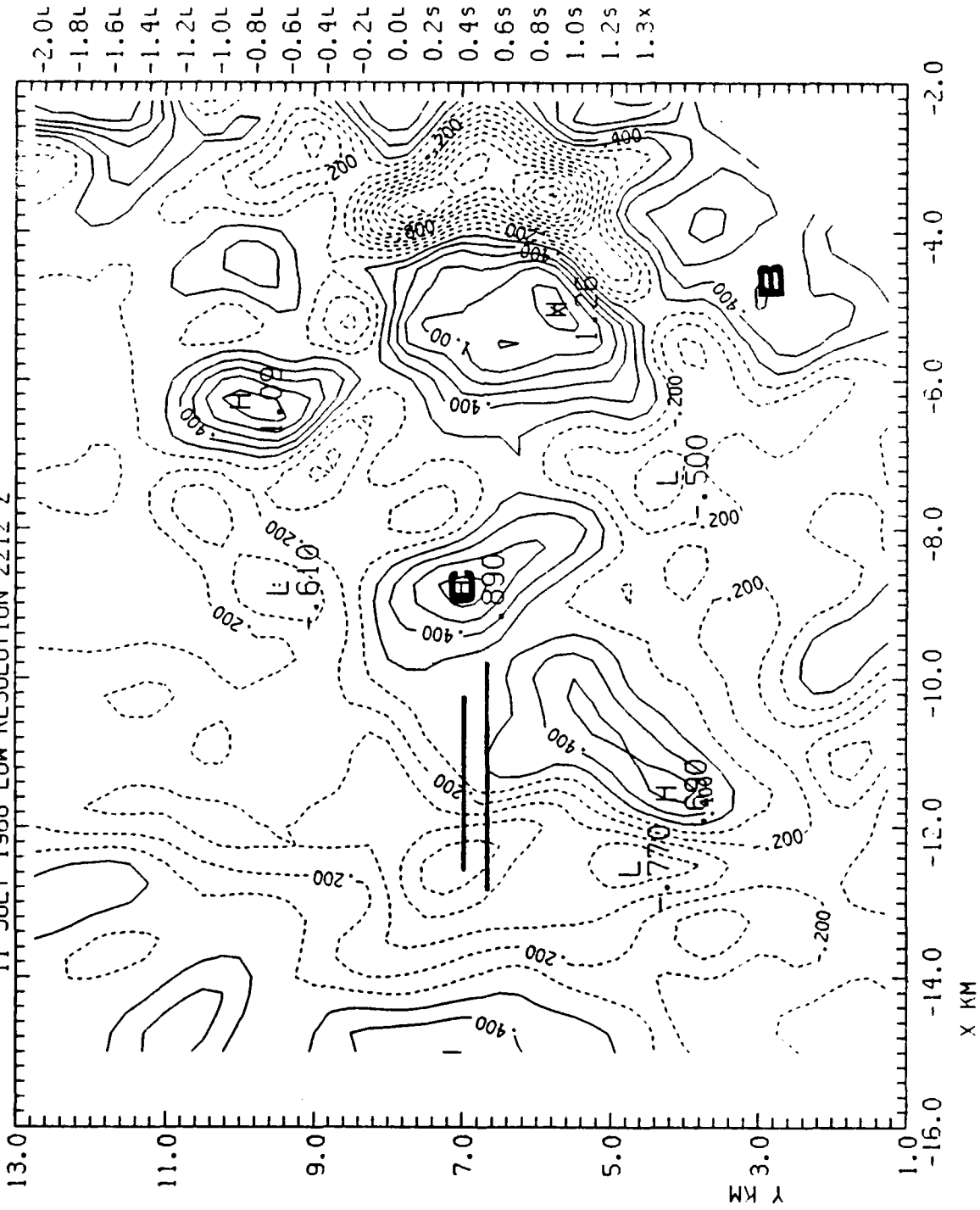


88/ 7/11 22 12 47-22 12 47 7MBIN Z = 0.19 KM DBZ  
 (AS OF 05/02/89) ORIGIN= 0.00. 0.00) KM X-AXIS= 90.0 DEG

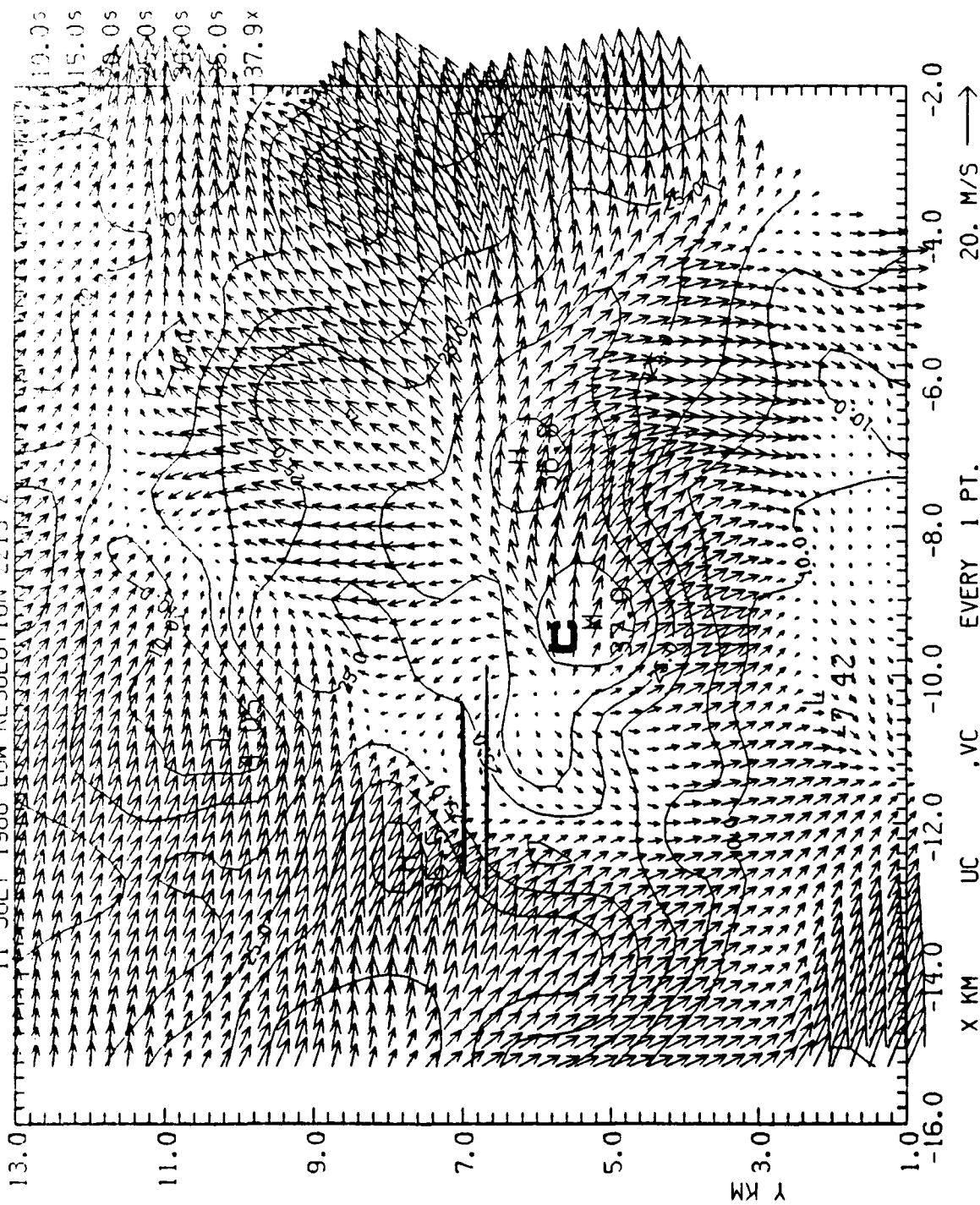




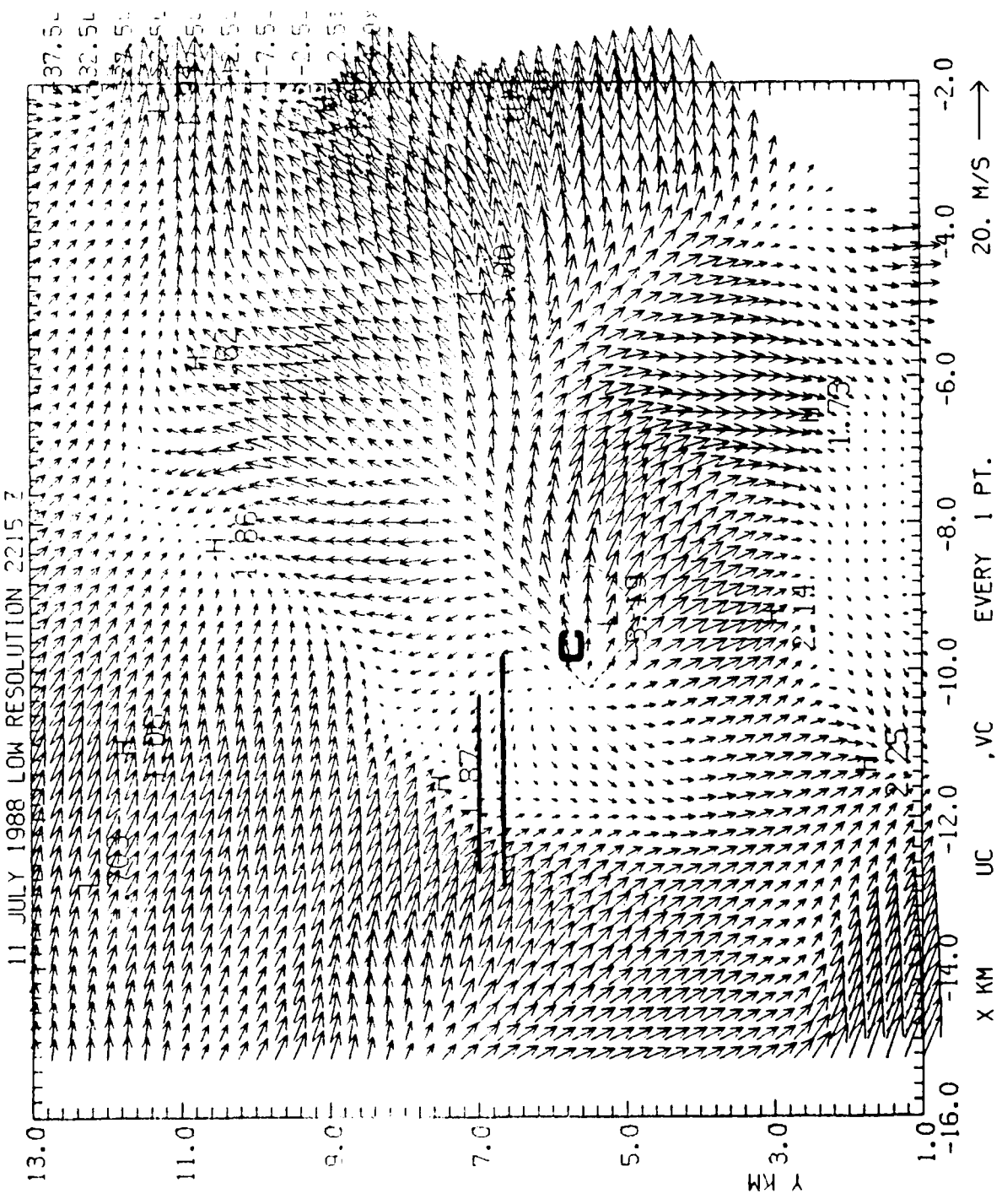
88/ 11 22 12 47-22 12 47 LUMBIN  $\Delta = 0.19$  KM  $\Delta = 0.00$  KM X-AXIS 90.0 DEG  
 (AS OF 05/02/89) ORIGIN 0.00, 0.00) KM X-AXIS 90.0 DEG  
 11 JULY 1988 LOW RESOLUTION 2212 Z



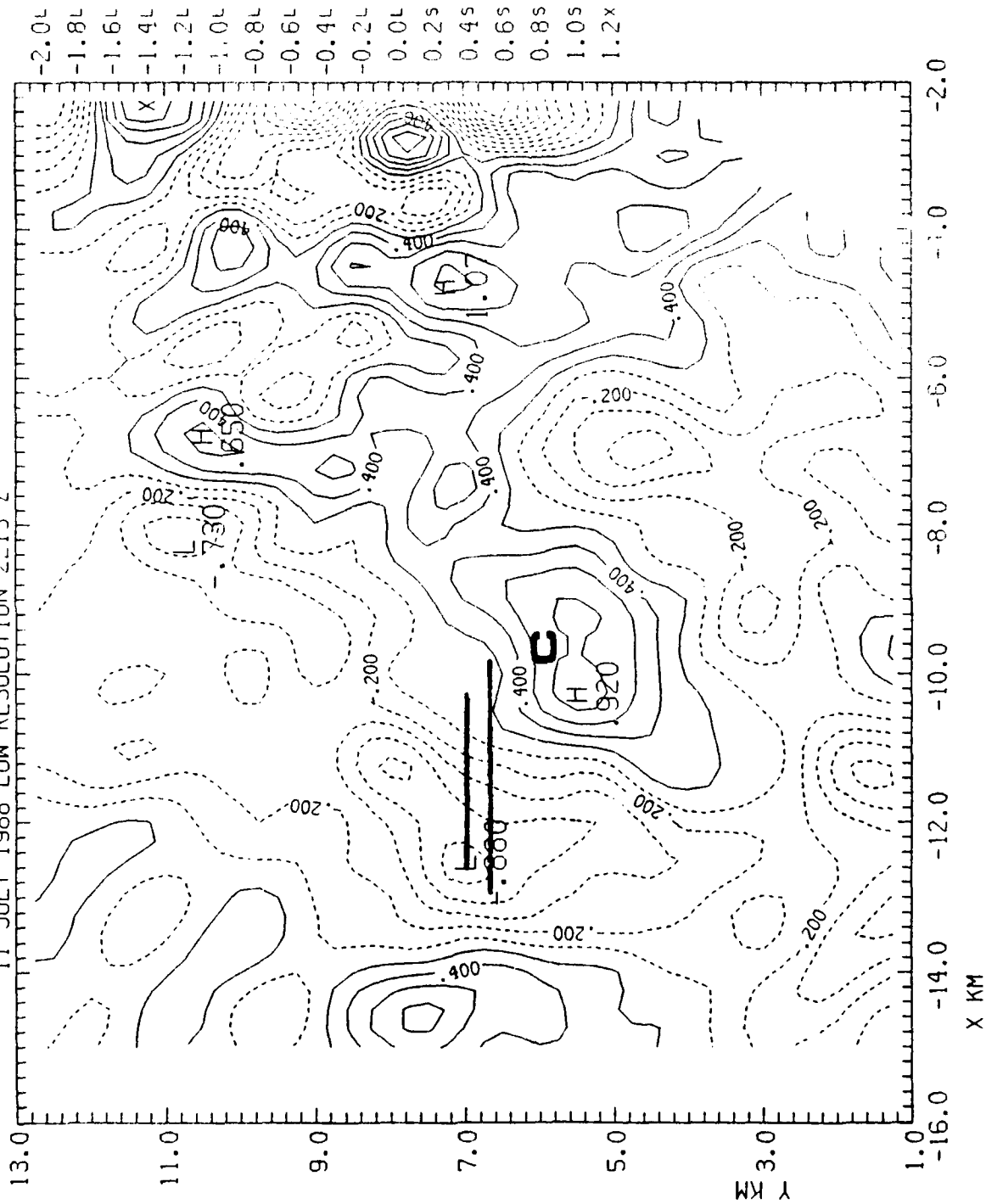
88/ 7/11 22 15 10-22 15 10 COMBIN Z = 0.19 KM DEZ  
 (AS OF 05/02/89) ORIGIN= 0.00, 0.00) KM X-AXIS= 90.0 DEG  
 11 JULY 1988 LOW RESOLUTION 2215 Z



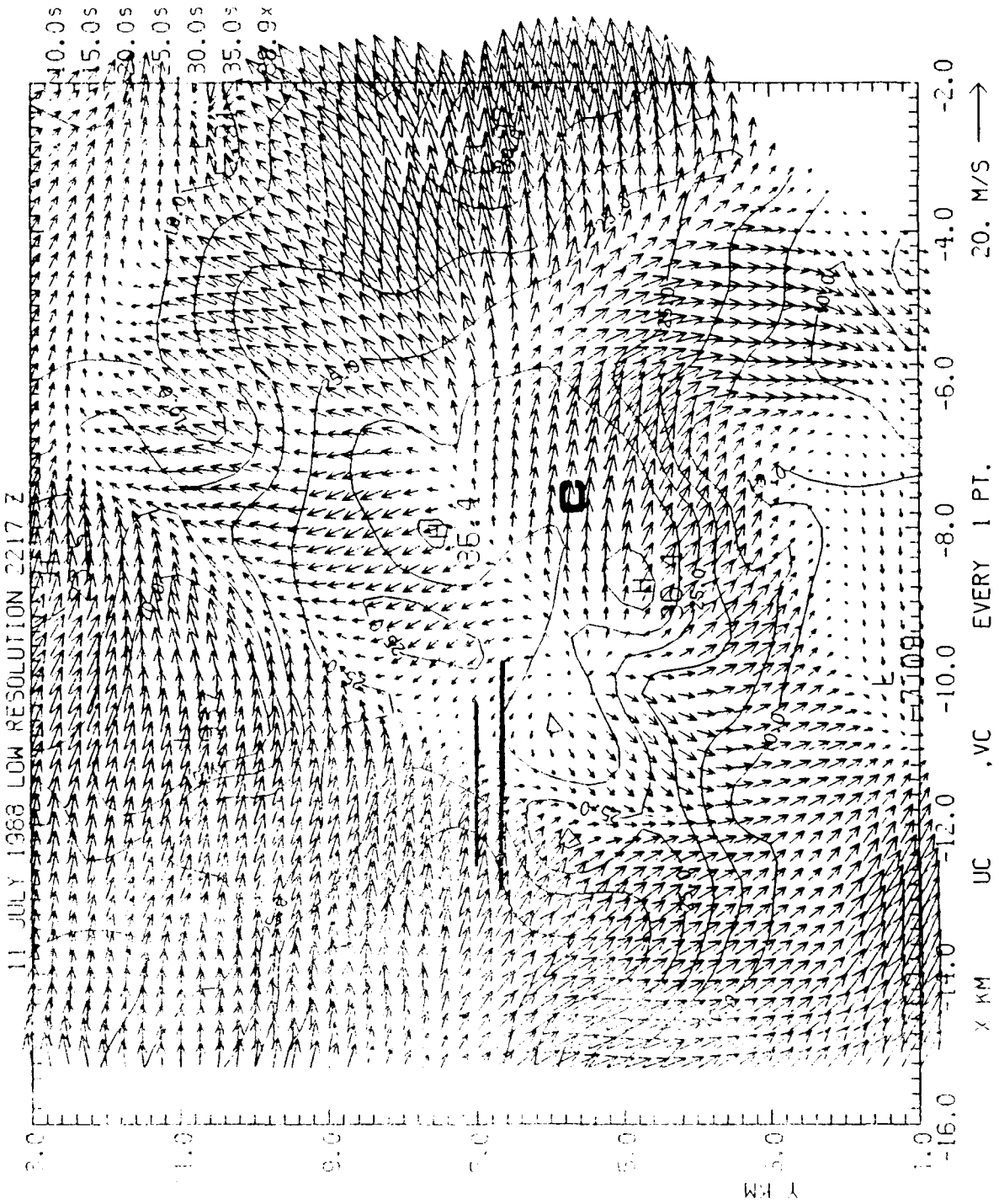
88/ 7/11 22 15 10-22 15 10 COMBIN Z = 0.19 KM W  
(AS OF 05/02/89) ORIGIN=( 0.00, 0.00) KM X-AXIS= 90.0 DEG



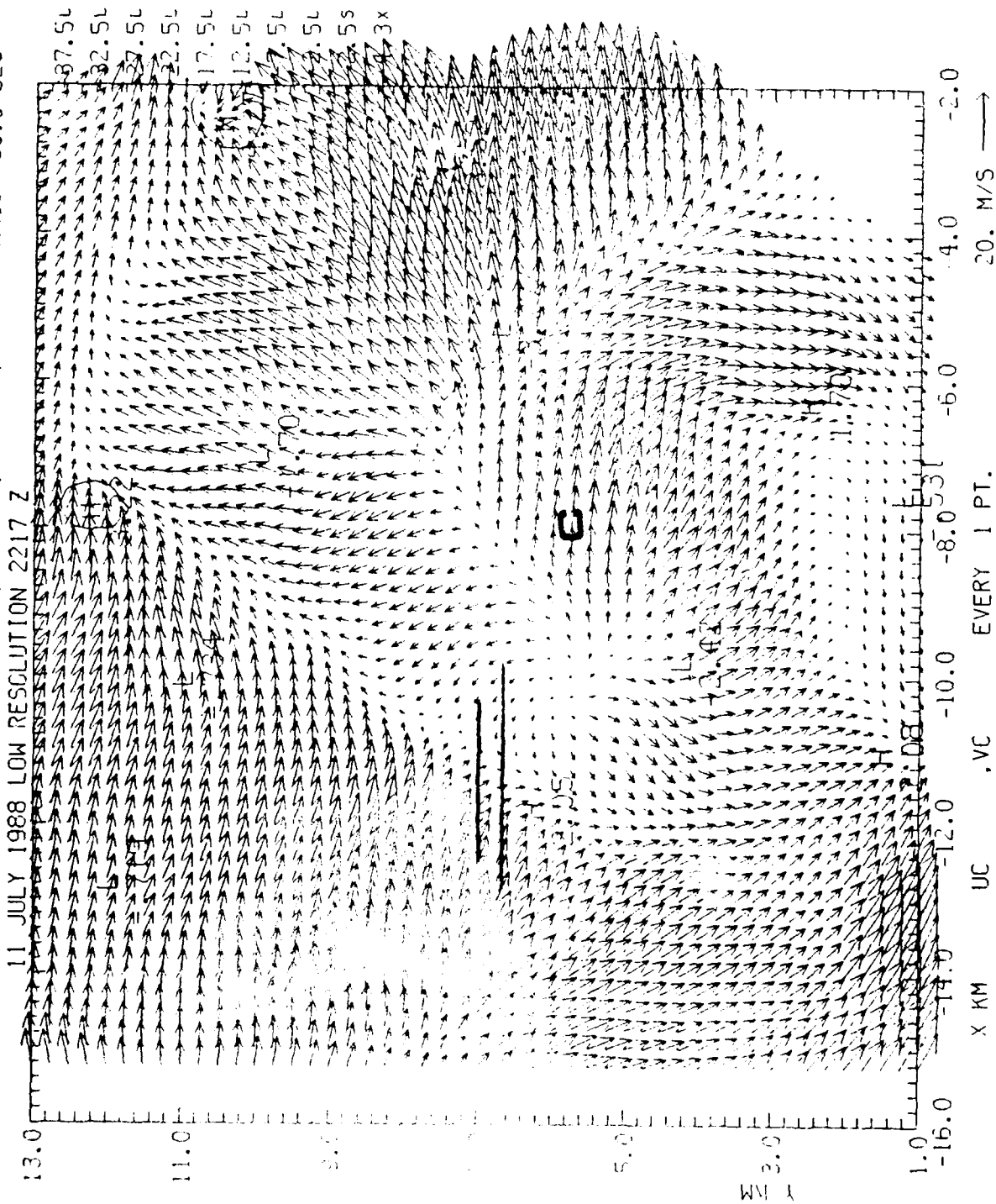
88/ 7/11    22 15 10-22 15 10    COMBIN    Z = 0.19 KM    F  
 (AS OF 05/02/89)    ORIGIN=( 0.00, 0.00) KM    X-AXIS= 90.0 DEG  
 11 JULY 1988 LOW RESOLUTION 2215 Z



88/ 7/11 22 17 47-22 17 47 COMBIN Z = 0.19 KM DBZ  
 (95 OF 05/02 '89) ORIGIN ( 0.00, 0.00) KM X-AXIS= 90.0 DEG

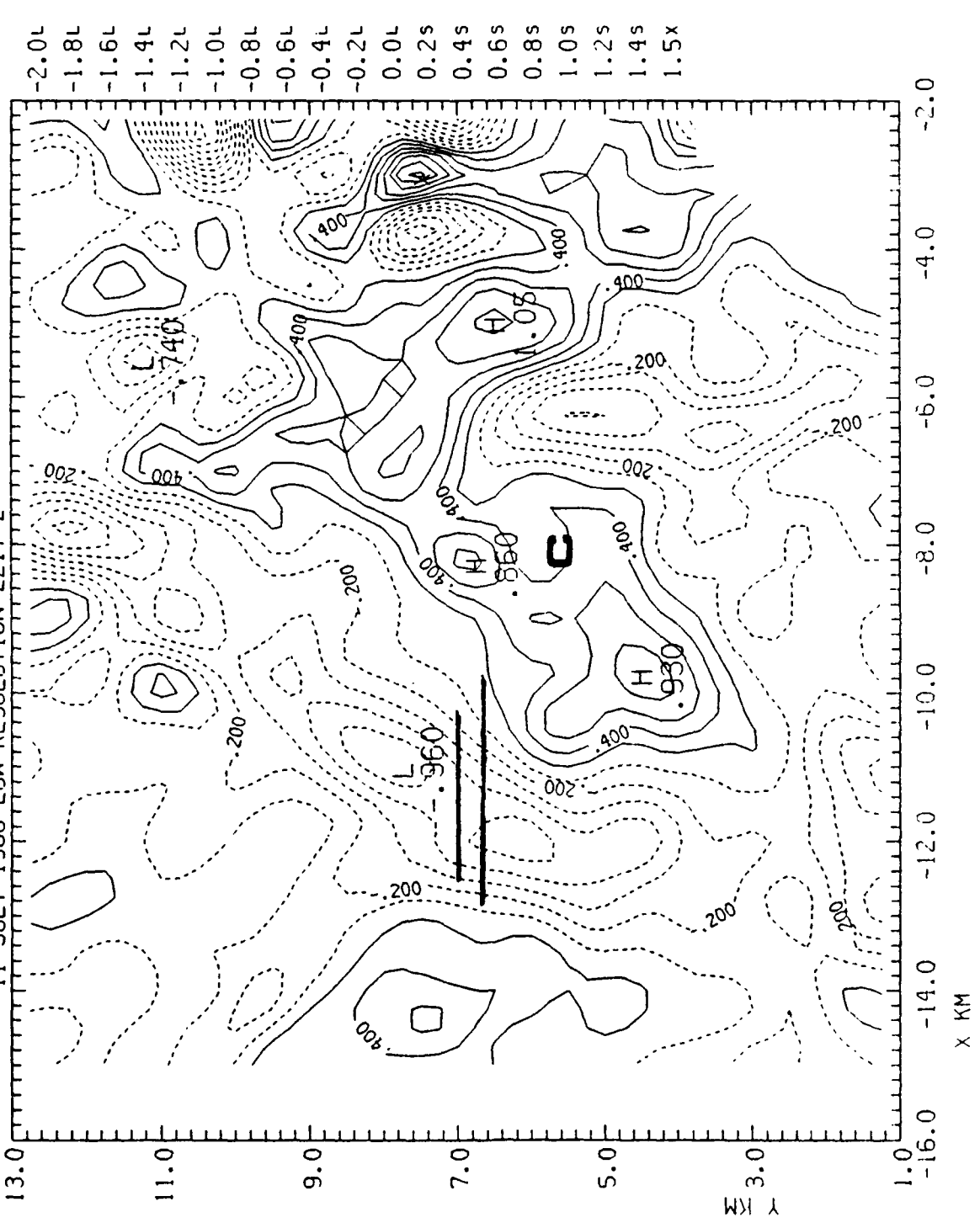


88/ 7/11 22 17 47-22 17 47 COMBIN Z = 0.19 KM W  
 (RS OF 05/02/89) ORIGIN. 0.00. 0.00) KM X-AXIS= 90.0 DEG

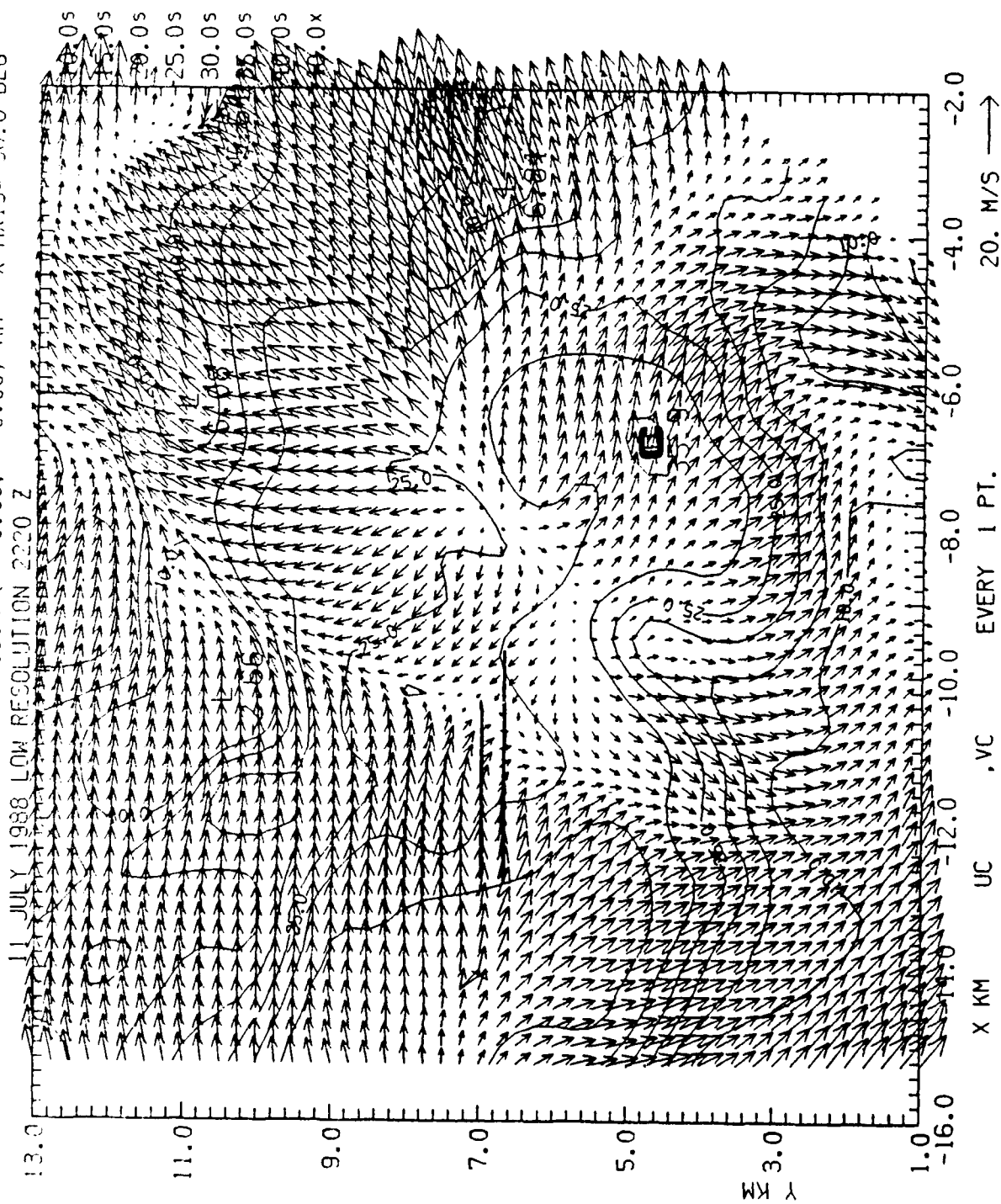


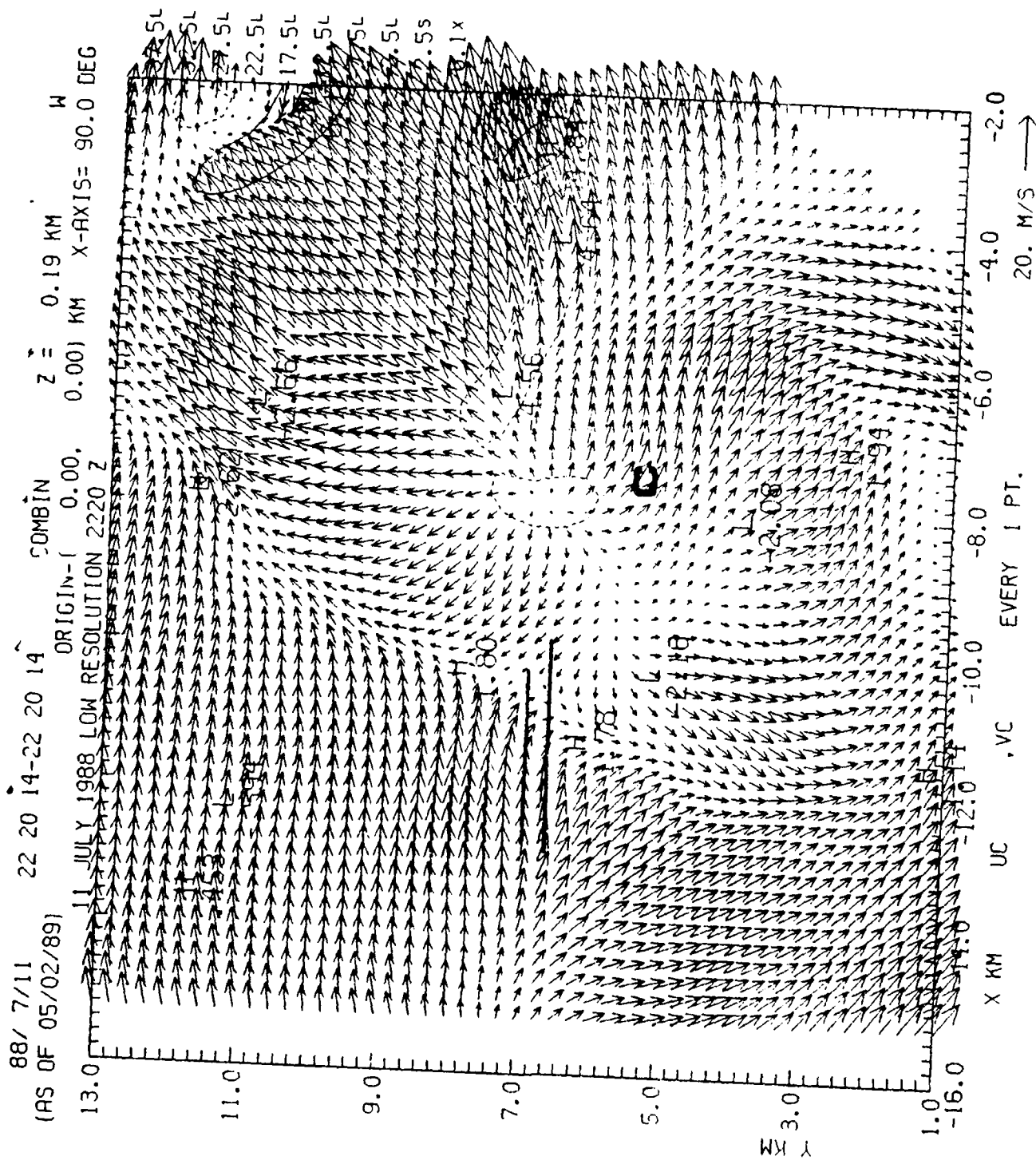


88/ 7/11    22 17 47-22 17 47    COMBIN    Z = 0.19 KM    F  
 (AS OF 05/02/89)    ORIGIN= 0.00, 0.00) KM    X-AXIS= 90.0 DEG  
 11 JULY 1988 LOW RESOLUTION 2217 Z

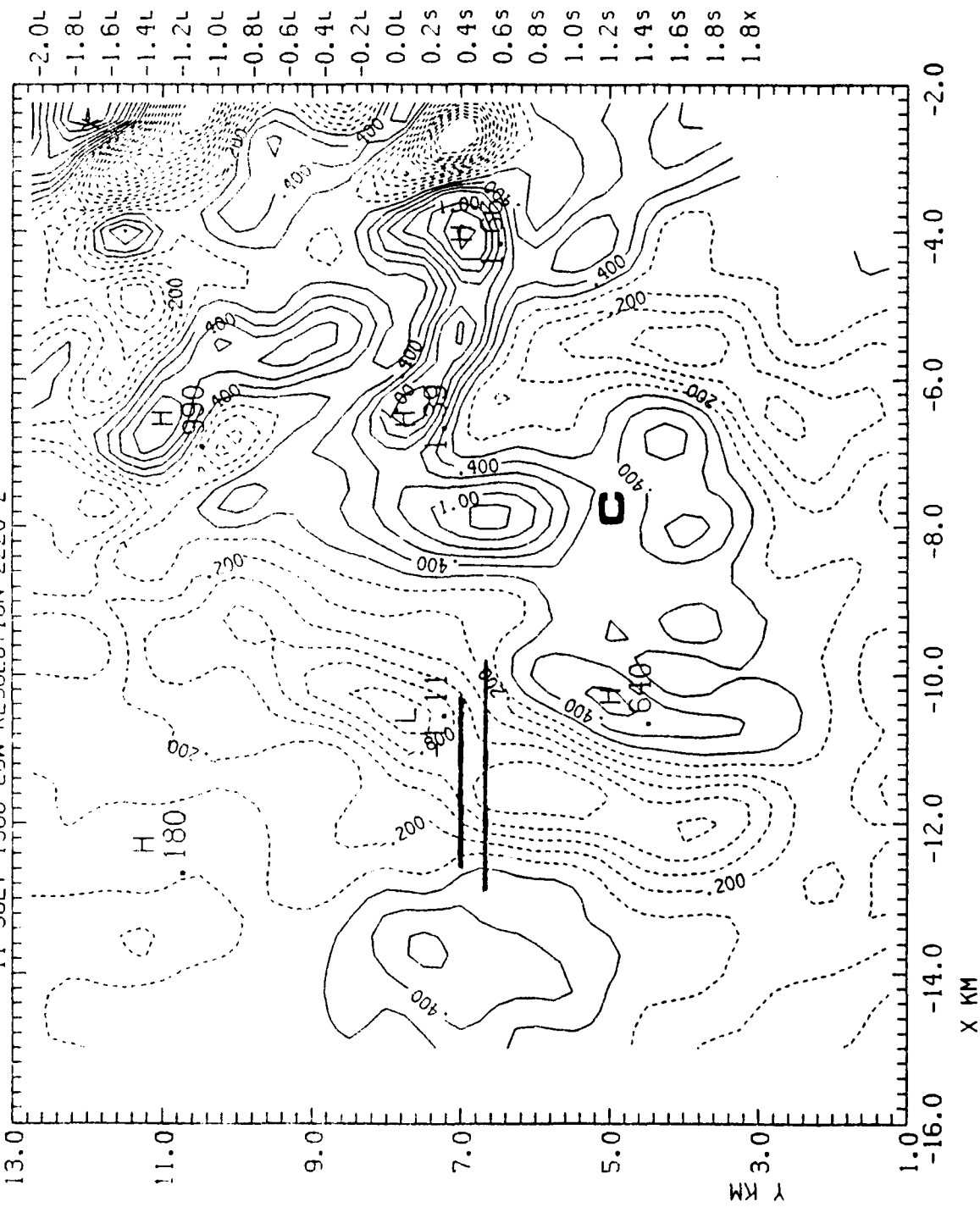


88/ 7/11 22 20 14-22 20 14 COMBIN Z = 0.19 KM DBZ  
 (AS OF 05/02/89) ORIGIN-( 0.00, 0.00) KM X-AXIS= 90.0 DEG





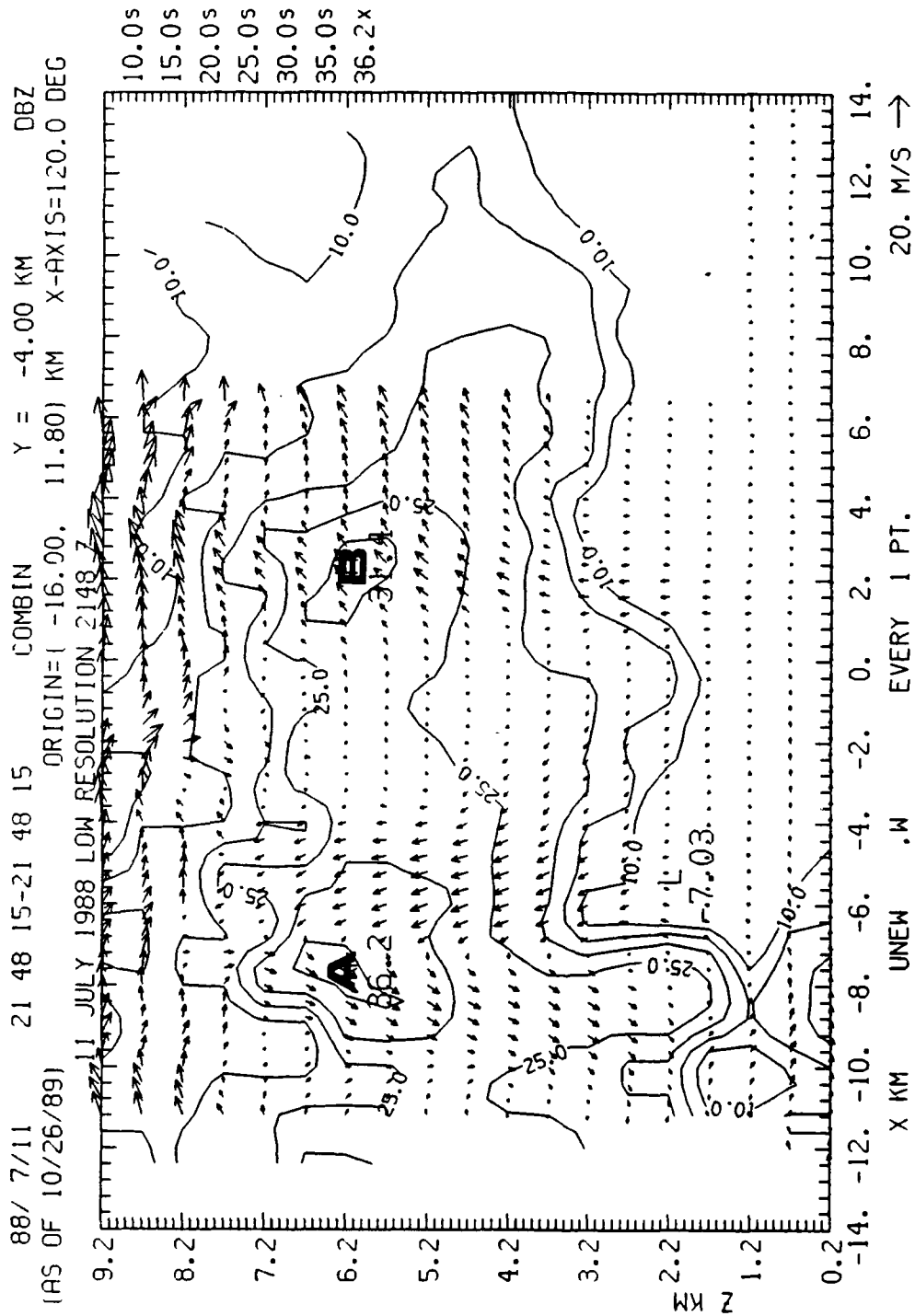
88/ 7/11 22 20 14-22 20 14 COMBIN Z = 0.19 KM F  
 (AS OF 05/02/89) ORIGIN ( 0.00, 0.00) KM X-AXIS= 90.0 DEG  
 11 JULY 1988 LOW RESOLUTION 2220 Z



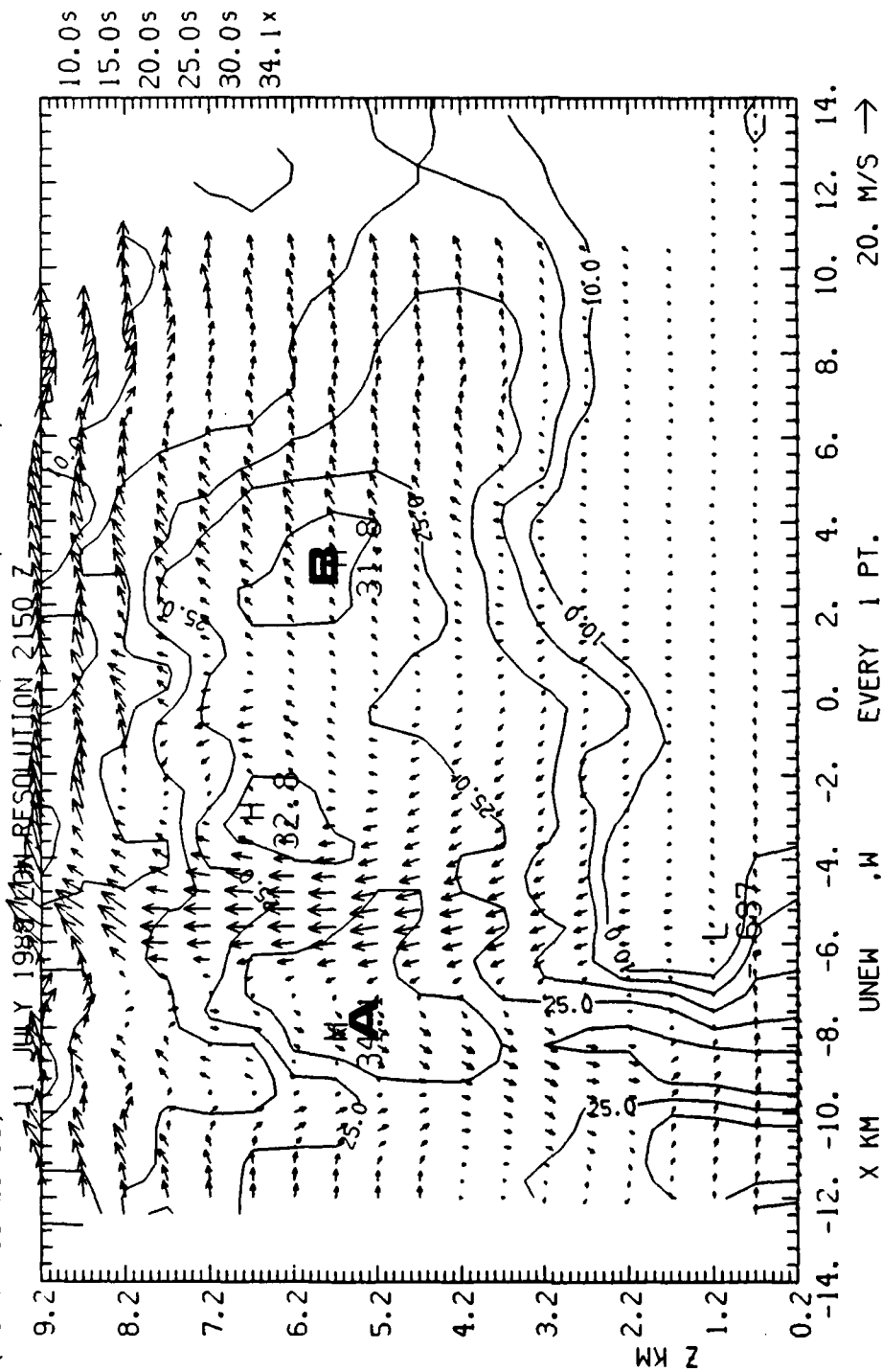
## **Appendix J: Dual Doppler Radar Vertical Cross-sections**

These plots show vertical cross-sections of radar data along the lines indicated on the plots in Appendix H. The plotted wind vectors represent the horizontal and vertical components within the displayed plane. X and Y axis labels are in km east from the centerpoint of the cross-section, and the altitude AGL in km, respectively. The top line above each plot gives the date, time, and overlay field. On the right are the contour levels (values followed by 's') and maximum field value (value followed by 'x'). A scale wind vector is provided in the lower right hand corner. Relative minima ('L') and maxima ('H') for the contoured field are indicated on the diagrams.

The analysis techniques used to produce these plots are described in the text.



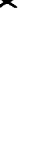
88/ 7/11 21 50 15-21 50 15 COMBIN Y = -4.00 KM DBZ  
(AS OF 10/26/89) ORIGIN=1 -16.00, 11.80) KM X-AXIS=120.0 DEG







OF 10/26.

KM  
X

```

88/ 7/11 21 58 15-21 58 15 COMBIN Y = -3.60 KM DBZ
      (AS OF 10/26/89) ORIGIN=1 -16.00, 11.80 KM X-AXIS=120.0 DEG

```

DBZ

$$Y = -3.60 \text{ KM}$$

COMBIN

21 58 15-21 58 15

88/ 7/11

(AS OF 10/26/89) ORIGIN=( -16.00, 11.80) KM X-AXIS=120.0 DEG

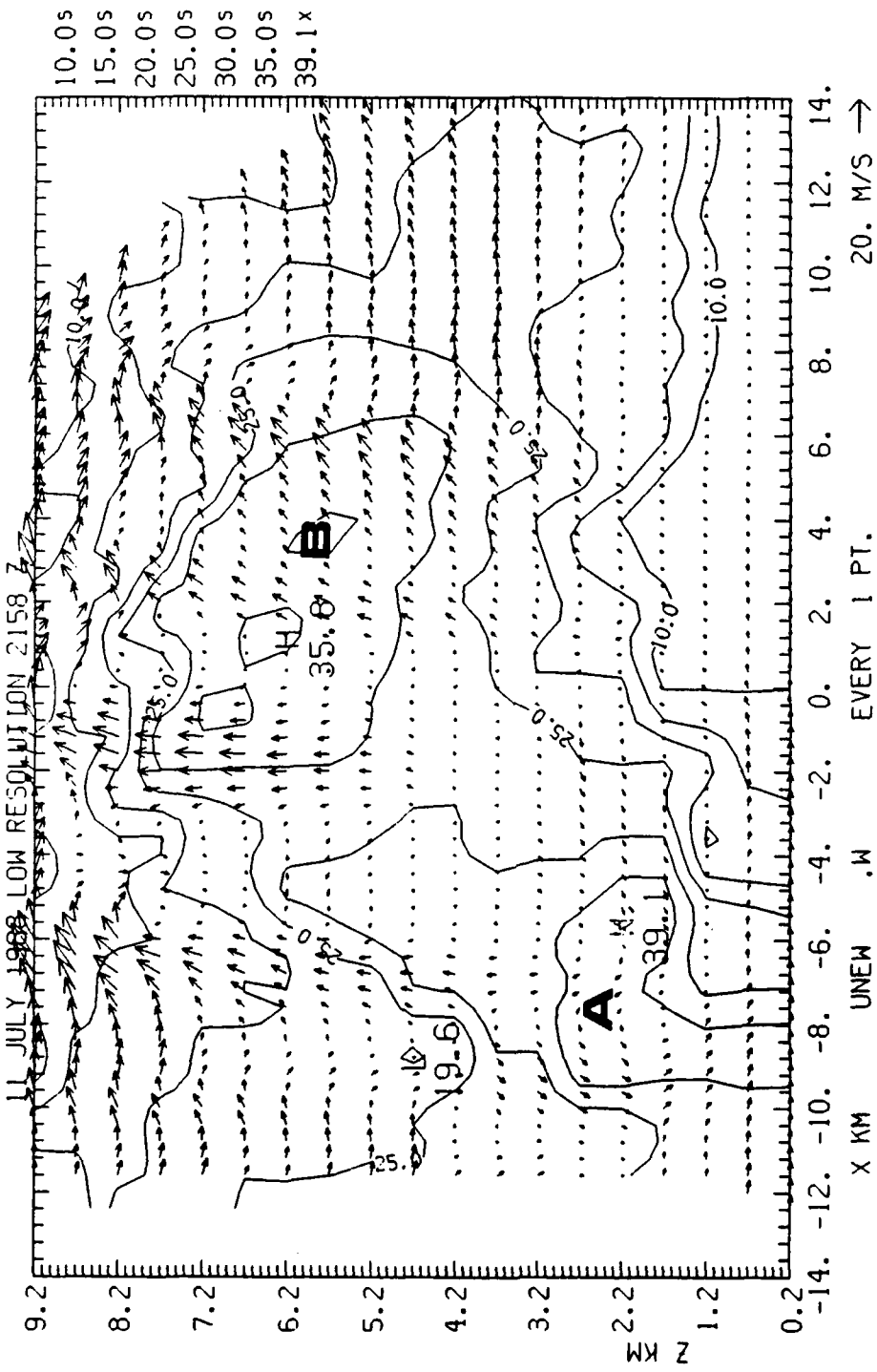
O DE

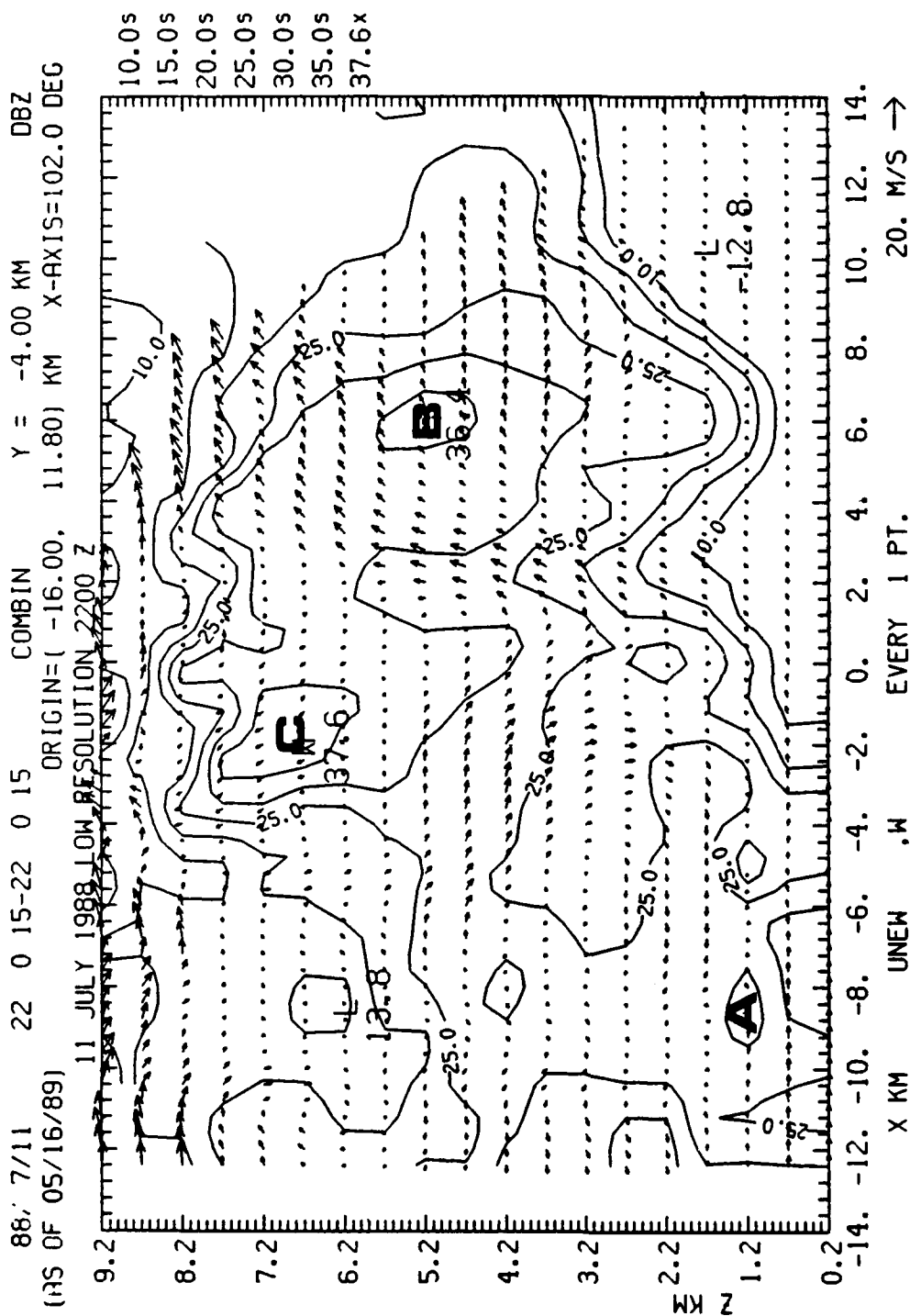
.80) KM X-AX

-16-

U

OF 10/26,





11 JUL 1988

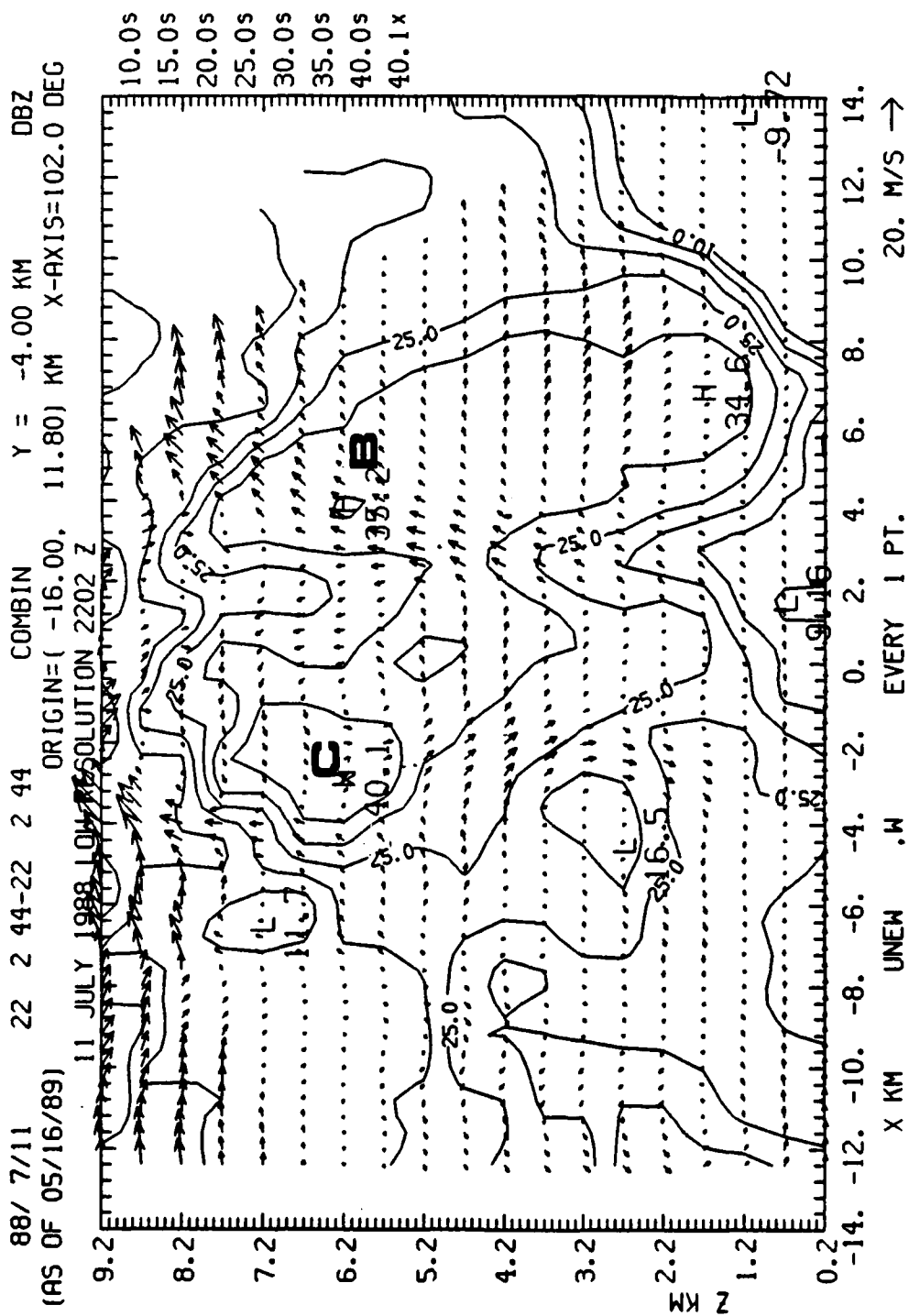


Fig. 33.

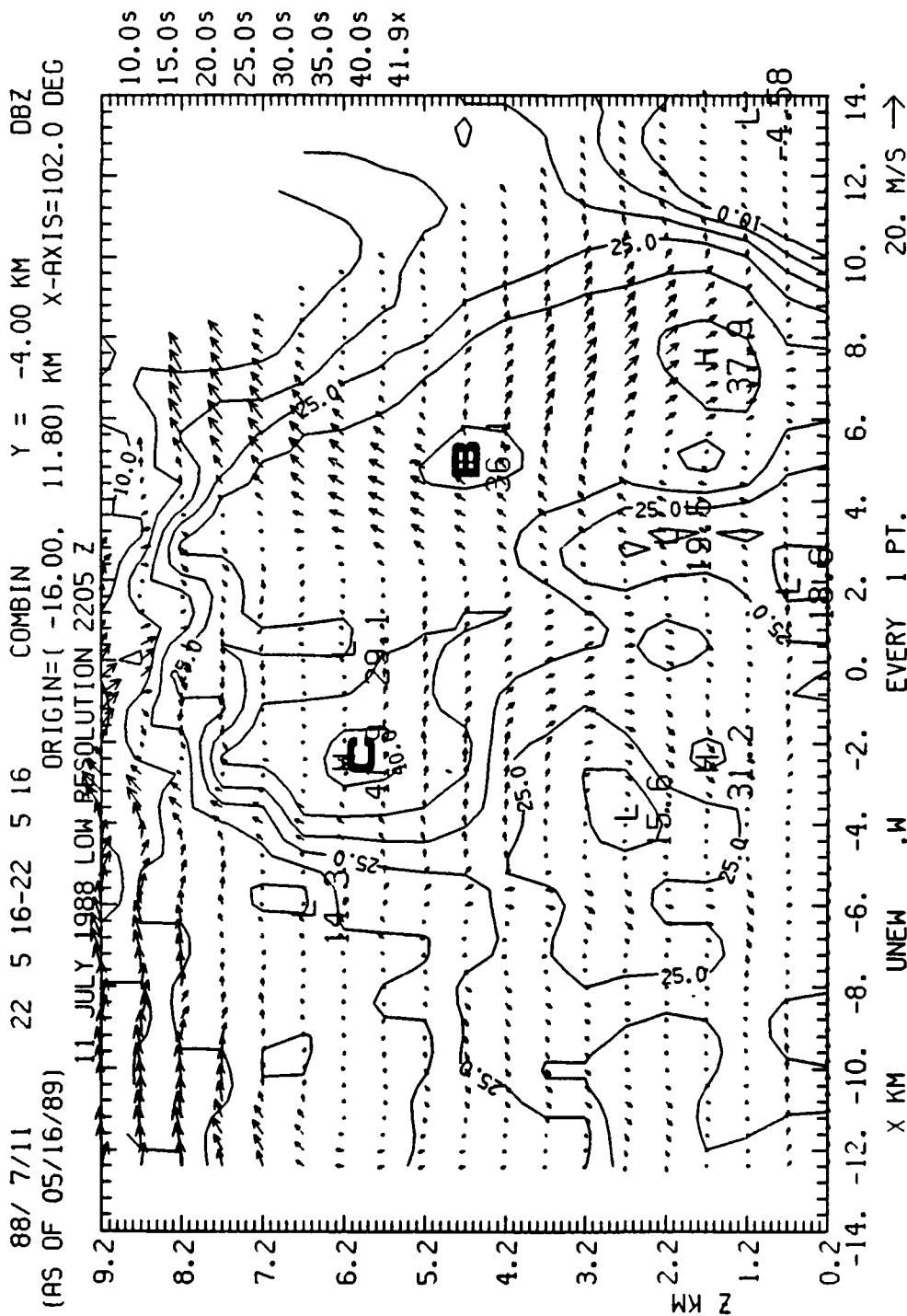
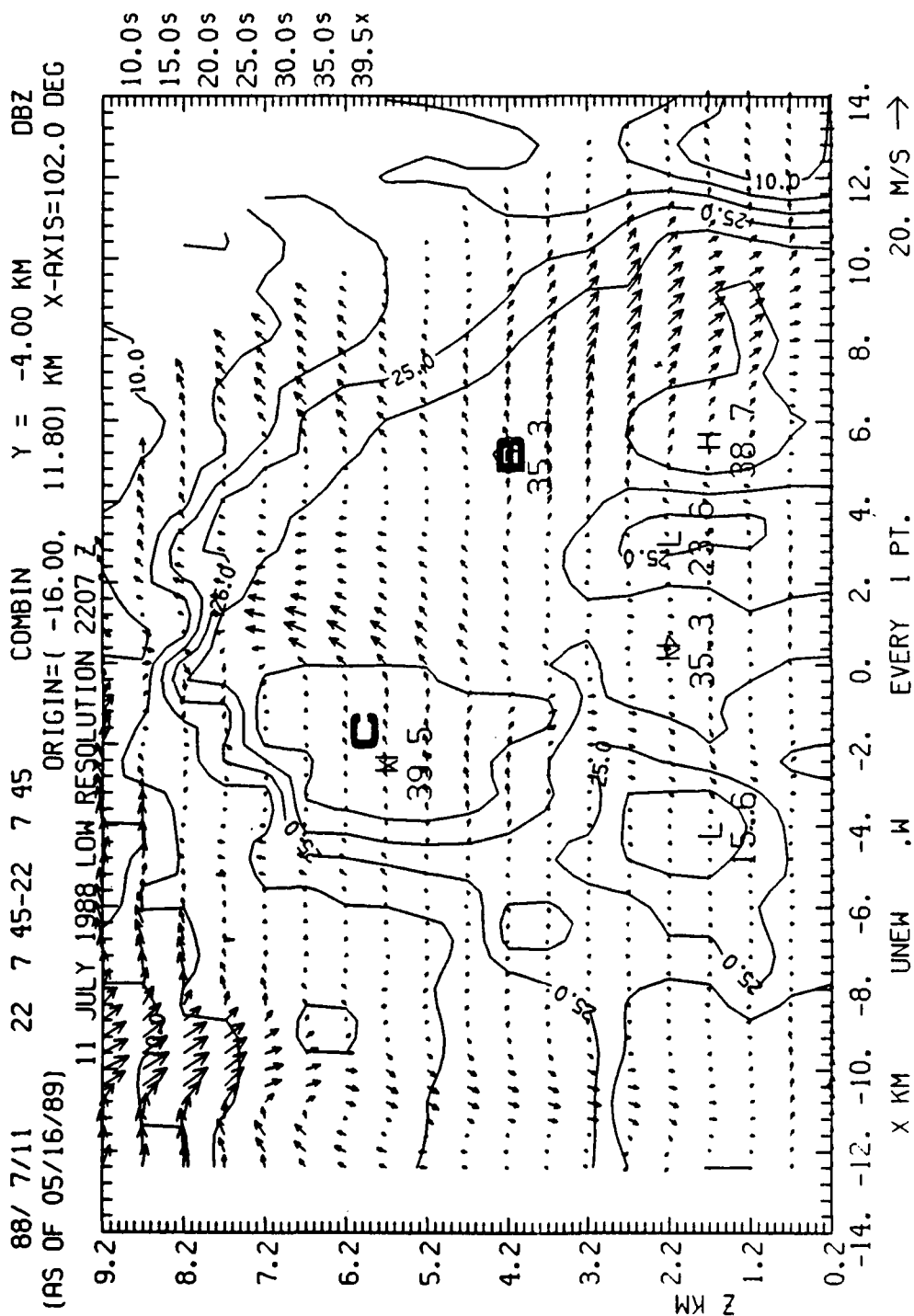


Fig. 2.1



88/ 7/11

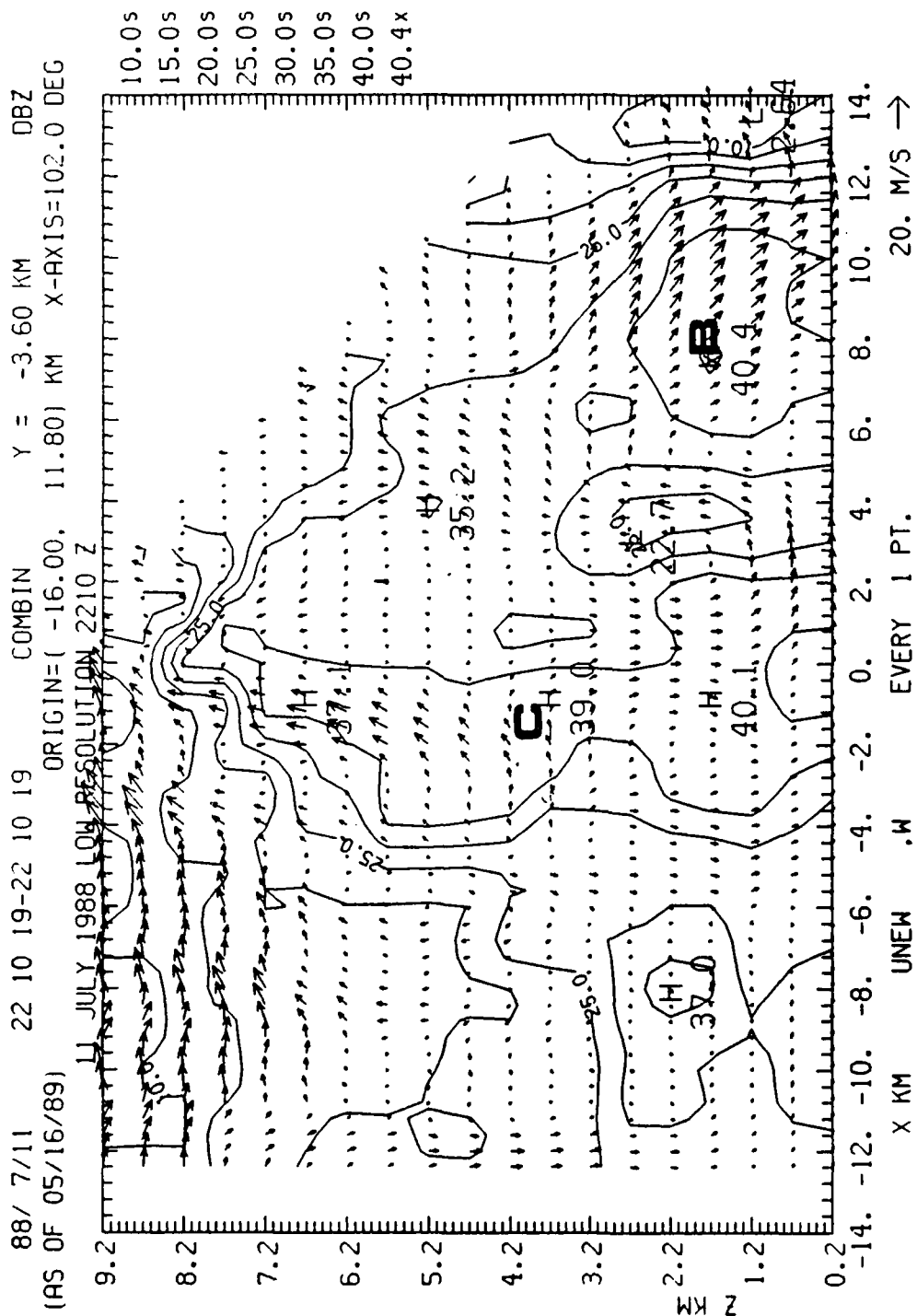


Fig. 36

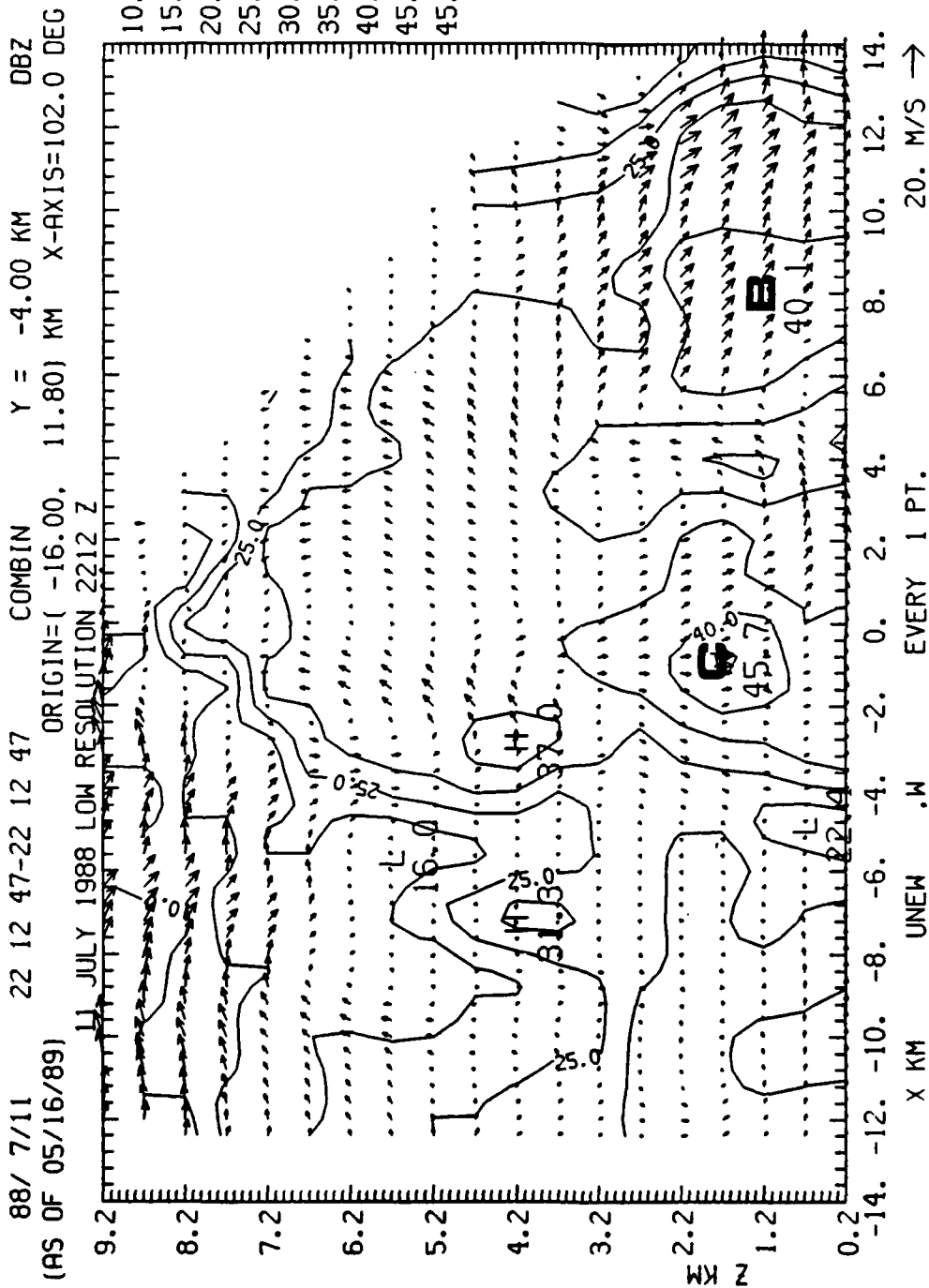


Fig. 3



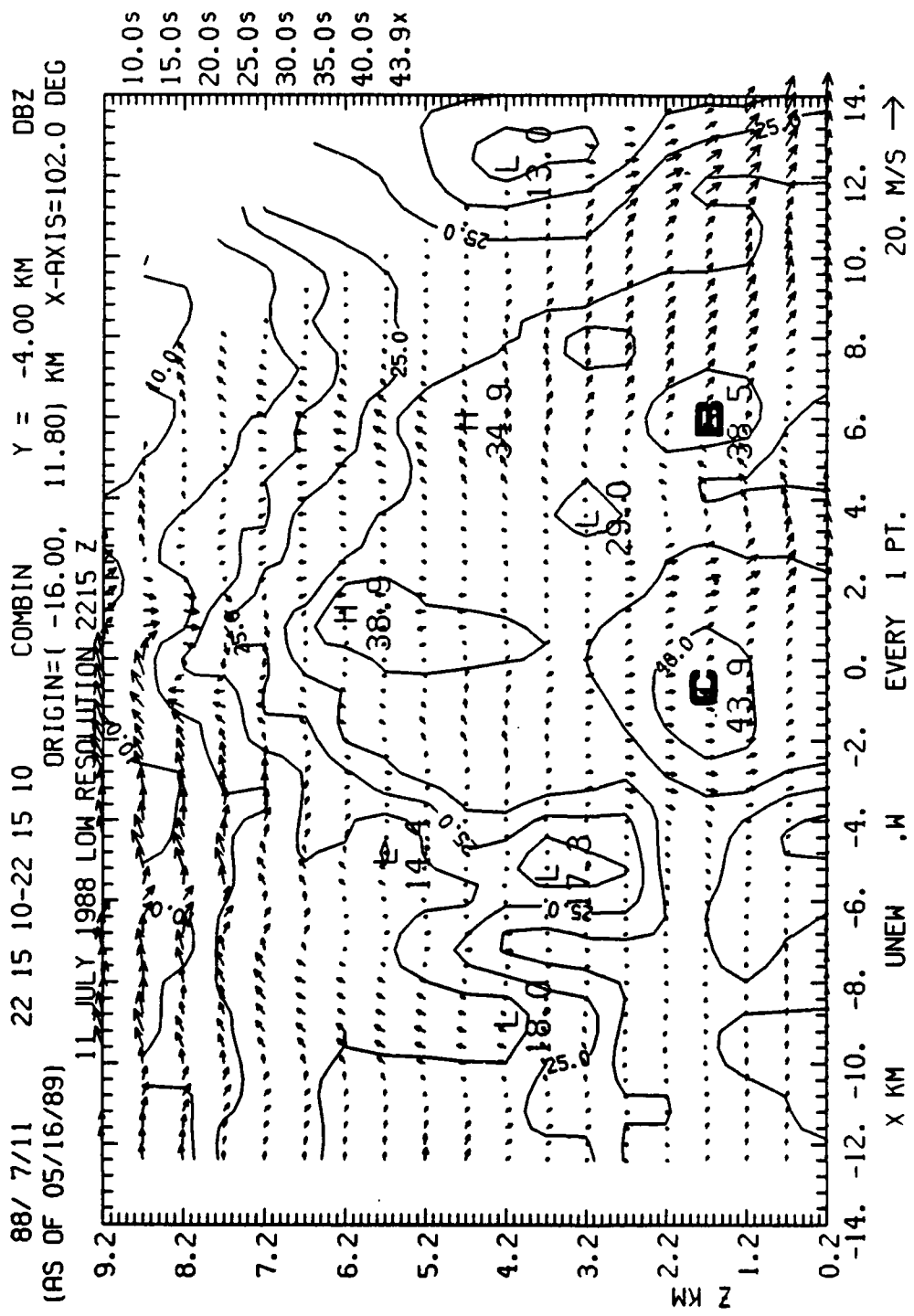


Fig. 38.

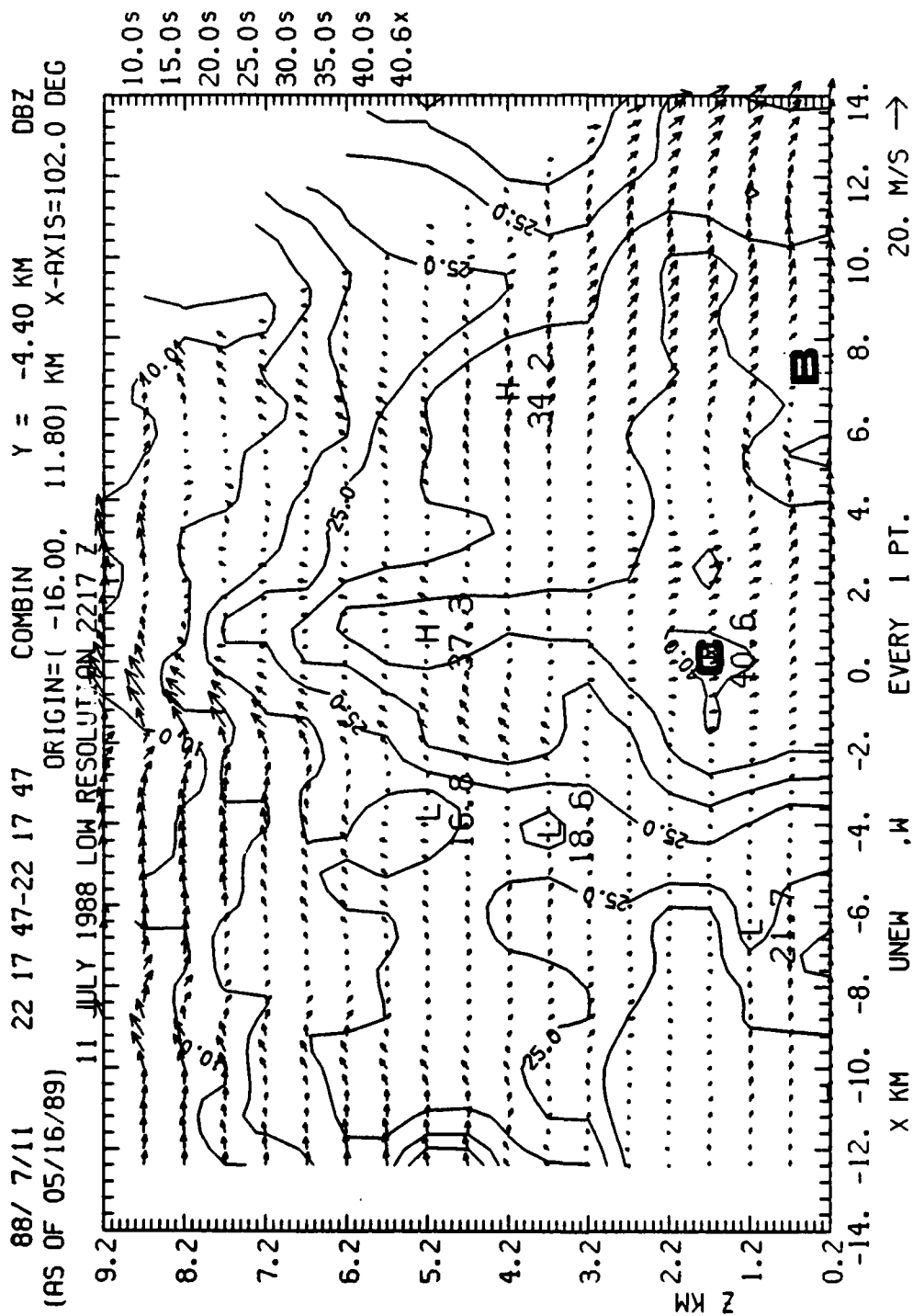


Fig. 3a.

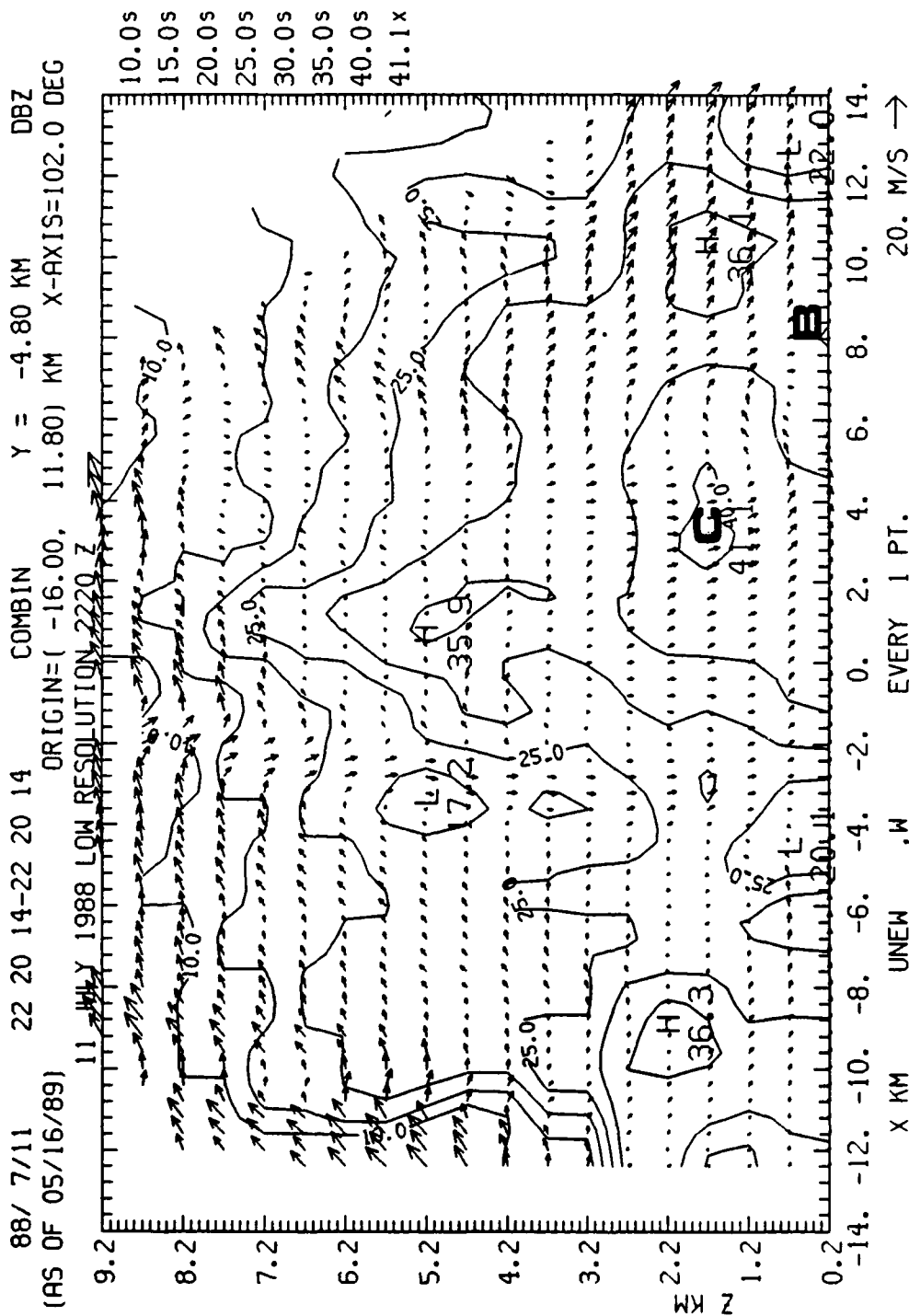


Fig. 40.